Geological Survey of Finland 2018

Development of the Paleoproterozoic Svecofennian orogeny: new constraints from the southeastern boundary of the Central Finland Granitoid Complex

Perttu Mikkola, Pentti Hölttä & Asko Käpyaho (eds)

Bulletin 407 • Special Issue

GTK
gtk.fi

Geological Survey of Finland, Bulletin

The Bulletin of the Geological Survey of Finland publishes the results of scientific research that is thematically or geographically connected to Finnish or Fennoscandian geology, or otherwise related to research and innovation at GTK. Articles by researchers outside GTK are also welcome. All manuscripts are peer reviewed.

Instructions for authors available from the Scientific Editor.

GEOLOGICAL SURVEY OF FINLAND

Bulletin 407

Development of the Paleoproterozoic Svecofennian orogeny: new constraints from the southeastern boundary of the Central Finland Granitoid Complex

by

Perttu Mikkola, Pentti Hölttä and Asko Käpyaho (eds)

Unless otherwise indicated, the figures have been prepared by the authors of the article.

VERTAISARVIOITU
KOLLEGIALT GRANSKAD
PEER-REVIEWED
www.tsv.fi/tunnus

https://doi.org/10.30440/bt407

Received 15 June 2017; Accepted 15 July 2018

Layout: Elvi Turtiainen Oy

Espoo 2018

Mikkola, P., Hölttä, P. & Käpyaho, A. (eds) 2018. Development of the Paleoproterozoic Svecofennian orogeny: new constraints from the southeastern boundary of the Central Finland Granitoid Complex. *Geological Survey of Finland, Bulletin 407,* 221 pages, 107 figures, 16 tables and 2 appendices.

The individual papers of this Bulletin provide data and new interpretations from different geological units and mineralisations present along the southeastern boundary of the Central Finland Granitoid Complex (CFGC) in areas surrounding the city of Jyväskylä. Significant amounts of new field and analytical data (whole-rock geochemistry, age determinations) from this previously little-studied area were collected during a mineral potential estimation project of the Geological Survey of Finland. As the area is the culmination point of several major geological units, these new data allowed a revaluation of previous interpretations and correlations.

The new data confirm earlier tentative suggestions that units belonging to the older Svecofennian magmatic phase (1.93–1.91 Ga) along the boundary with the Karelia Province extend 100 km further southeast than previously known. The paragneiss units present in the area were deposited as greywackes. These units cannot be distinguished on a geochemical basis and display similar detrital zircon patterns, defining ~1.92 Ga as the maximum depositional age for most of the samples. This makes reliable separation of different units difficult, and it is thus likely that the current unit division mainly reflects differences in postdepositional evolution, not in the depositional setting. The eruptive mafic to ultramafic units occurring as interlayers in different paragneiss units represent extensional phases in the development of the depositional basin(s). Ultramafic members are typically picrites with highly variable compositional patterns, whereas the mafic members display E-MORB-like chemical compositions.

The arc-type calc-alkaline volcanism in the area is similar in age (1895–1875 Ma) and composition to that of the classical Tampere group 200 km further west. The voluminous granitoid magmatism took place in two stages, at ca. 1895 and 1885–1875 Ma, and is coeval with less voluminous mafic to ultramafic plutonic activity. The older calc-alkaline phase is present in the vicinity of the contact between the CFGC and the paragneiss units south of it. The oldest calc-alkaline volcanism and plutonism are, based on field observations and compositional data, interlinked. The bulk of the granitoids forming the CFGC crystallized during the younger phase and can be divided into separate units on a compositional basis. The calc-alkaline granitoids display evolution towards more felsic compositions. This probably reflects changes in the pooling level of granitoid magmas due to erosion and uplift, which allowed only the most evolved compositions to reach the present-day erosion surface during the last stages of magmatic activity. The younger calc-alkaline magmas overlap in age with compositionally A-type granitoids that form a bimodal suite with diorites and gabbros. These lower crustal melts rose only locally to the present erosion level via favourable structures.

The highest ore potential in the study area is for Vammala-type magmatic Ni and Cu ores related to ultramafic–mafic intrusions. The potential for orogenic gold ores is related to the crustal-scale Leivonmäki shear zone trending northeast–southwest and transecting the whole study area. This dextral shear zone is interpreted as a conjugate of the Raahe–Ladoga shear zone. Certain indications for relatively late hydrothermal Zn–Pb mineralisations and porphyry-type Cu mineralisations were also identified.

Appendix 1 is available at: http://tupa.gtk.fi/julkaisu/liiteaineisto/bt_407_appendix_1.pdf

Electronic Appendix is available at: http://tupa.gtk.fi/julkaisu/liiteaineisto/bt_407_electronic_appendix.xlsx

Keywords: Paleoproterozoic, Svecofennian, Finland, Central Finland Granitoid Complex, granites, A-type granites, calc-alkalic composition, volcanic rocks, picrite, mid-ocean ridge basalts, paragneiss, greywackes, absolute age

Perttu Mikkola
Geological Survey of Finland
P.O. Box 1237
FI-70211 Kuopio
Finland

E-mail: perttu.mikkola@gtk.fi

Pentti Hölttä and Asko Käpyaho
Geological Survey of Finland
P.O. Box 96
FI-02151 Espoo
Finland

E-mail: pentti.holtta@gtk.fi, asko.kapyaho@gtk.fi

ISBN 978-952-217-397-3 (pdf), ISSN 0367-522X (print), ISSN 2489-639X (online)

CONTENTS

GUEST EDITOR'S PREFACE

This volume presents the results of Geological Survey of Finland's Central Finland's ore potential estimation –project. The motivation to start studying the bedrock along the south-eastern boundary of the Central Finland Granitoid complex in 2011 arose from the Geological Survey's working philosophy of that time: to study areas with limited geological data in order to update geological understanding to a level allowing evaluation of their true ore potential. By doing so, new areas for the private sector to work in could possibly be identified. The idea was not to concentrate on a certain element, or elements, but instead to look for anything with possible economic interest. The study area clearly fulfilled the prerequisite of limited data, as following the initial 1:400 000 bedrock mapping completed in the first years of the 20th century, the limited work carried out had mainly comprised target-scale ore exploration. This activity was either prompted by layman's samples or concentrated on resolving the sources of geophysical anomalies.

As the articles in this volume vary in scope from target-scale studies of mineralisations to the synthesis of the geological development of the area, common denominators other than the location are sparse. However, together they provide an extensive overview of the updated geological knowledge in the area, which is located at the core of the Svecofennian domain in Finland and forms the culmination point of several major geological units. The new data and interpretations presented offer stepping stones for further studies, both economic and scientific. Such studies are needed to further reduce the size of gaps in the geological story of the area. As J.J. Sederholm wrote in the preface to the first systematic study of the area: "It is obvious that all explanations of the Precambrian geology will always be more or less imperfect and full of holes due to the characteristics of the studied material."

It took nearly seven years from the first field visit to the study area in October 2011 to the finalisation of this volume of the Geological Survey of Finland's Bulletin. These seven years have included countless days in the field, office and laboratories for those who participated. The easiest solution would be to simply thank "all those who contributed to this work", but such a generalisation does not give any idea of the number of people involved in such a long-lasting project. At least the following people are to be thanked for making observations, collecting, drilling, preparing and processing samples, taking photos, preparing geochemical figures, running various analytical instruments and measuring geophysics, among other activities: Jarmo Asikainen, Timo Hallikainen, Sini Halonen, Aimo Hartikainen, Matti Haverinen, Lasse Heikkinen, Kai Hyttinen, Jorma Ikonen, Lev Ilyinsky, Kari Jauhiainen, Bo Johansson, Ritva Jokisaari, Veli-Pekka Jutila, Kalervo Jänkälä, Leena Järvinen, Jenni Keränen, Keijo Kinnunen, Tapio Kivijärvi, Heli Kivisaari, Jukka-Pekka Kujasalo, Mira Kyllästinen, Kimmo Kärenlampi, Yann Lahaye, Rauli Lempiäinen, Kerstin Linden, Petri Lippo, Sari Lukkari, Mauri Luukkonen, Esa Marttila, Antti Mäkelä, Tarja Neuvonen, Hugh O'Brien, Lassi Pakkanen, Hannu Pelkonen, Jouko Ranua, Hannu Repo, Timo Saarimäki, Mika Salmela, Reijo Sormunen, Tuomo Stranius, Matti Säkkinen, Urho Tolonen, Riitta Turunen, Tuomo Turunen, Seppo Töllikkö, Esko Virtanen, Maria Vuorio, Martin Whitehouse and the 20 students of the Bedrock Mapping course held in 2012. The above list does not include the authors or the reviewers who kindly contributed their time to improve the final products. Indispensable help was also provided by the GTK personnel working with the unavoidable bureaucratic part of life in a geological survey. I also want to express my gratitude to the two other editors, Asko Käpyaho and Pentti Hölttä, who were responsible for review process of those articles that I had a role as an author. The language of the articles was revised by Roy Siddall and technical editing was carried out by Päivi Kuikka-Niemi.

Kuopio September 14th, 2018

Perttu Mikkola
Guest editor of this Bulletin volume

Development of the Paleoproterozoic Svecofennian orogeny: new constraints from the southeastern boundary of the Central Finland Granitoid Complex
Edited by Perttu Mikkola, Pentti Hölttä and Asko Käpyaho
Geological Survey of Finland, Bulletin 407, 5-27, 2018

GEOLOGICAL EVOLUTION AND STRUCTURE ALONG THE SOUTHEASTERN BORDER OF THE CENTRAL FINLAND GRANITOID COMPLEX

by

Perttu Mikkola[1)], Esa Heilimo[1)], Jouni Luukas[1)], Jukka Kousa[1)], Soile Aatos[1)], Hannu Makkonen[1)], Sami Niemi[1)], Maarit Nousiainen[1)], Marjaana Ahven[1)], Ilona Romu[1)] and Janne Hokka[2)]

Mikkola, P., Heilimo, E., Luukas, J., Kousa, J., Aatos, S., Makkonen, H., Niemi, S., Nousiainen, M., Ahven, M., Romu, I. & Hokka, J. 2018. Geological evolution and structure along the southeastern border of the Central Finland Granitoid Complex. *Geological Survey of Finland, Bulletin 407*, 5–27, 6 figures and 1 table.

The rock record present along the southeastern border of the Central Finland Granitoid Complex provides evidence for the geological evolution of the Paleoproterozoic Svecofennian orogeny from the magmatism of the Savo arc through paragneisses deposited in a passive margin setting to arc volcanism and the collisional final phases. The older Svecofennian magmatic phase (1.93–1.91 Ga) ended when the Savo arc collided with the Archean Karelia craton. After this collision, the greywacke protoliths of the paragneisses, in most cases having maximum deposition ages close to 1.92 Ga, were deposited. Most of the paragneisses have later been migmatised. The local presence of unmigmatised variants in close proximity to the migmatised ones indicates large vertical movements in the late stages of geological evolution. Mafic and ultramafic volcanic units erupted as interbeds during extensional phases of the depositional basins. Subduction and arc-type plutonic and volcanic activity commenced in the area at 1895 Ga and continued until 1875 Ma. The peak of granitoid magmatism in the area took place at 1885–1880 Ma and includes units with calc-alkaline, alkali-calcic and A-type geochemical characteristics. This bipolarity of granitoid compositions requires simultaneous melting of differing source rocks at varying crustal depths. The A-type granitoids are located in close proximity to large-scale faults that provided pathways for ascending magmas in a transtensional setting. Voluminously, the mafic plutonic rocks are minor compared to the granitoids and represent partial melts from the upper mantle. Their composition has been significantly affected by fractional crystallisation and assimilation processes during ascent through the continental crust. In areas dominated by granitoids, the deformation is characterised by faults and shear zones, whereas the supracrustal units display evidence of deformation linked to compression from the southeast at 1.83 Ga.

Keywords: Fennoscandian Shield, Finland, Svecofennian Orogeny, tectonics, Paleoproterozoic, granitoids, batholiths, volcanic rocks, paragneiss

[1)] Geological Survey of Finland, P.O. Box 1237, FI-70211 Kuopio, Finland
[2)] Geological Survey of Finland, P.O. Box 96, FI-02151 Espoo, Finland

VERTAISARVIOITU
KOLLEGIALT GRANSKAD
PEER-REVIEWED
www.tsv.fi/tunnus

https://doi.org/10.30440/bt407.1

Editorial handling by Asko Käpyaho.

Received 5 February 2018; Accepted 9 July 2018

1 INTRODUCTION

The Paleoproterozoic Svecofennian domain, extending from northwestern Russia through Finland to Sweden, is one of the most extensively studied Precambrian accretionary orogens. Due to a research history extending to the 19th century, the overall geological development of the orogeny is well constrained, although discussion of the details continues. Despite extensive research efforts, the basic geological knowledge from certain areas of the Svecofennian domain is outdated. For example, our main study area (Fig. 1) had been systematically studied over a century ago (Frosterus 1903). This is despite the fact that the area represents a junction of several Svecofennian geological units: the Central Finland Granitoid Complex (hereafter CFGC) and voluminous paragneisses of South Finland, as well as older and younger Svecofennian arc magmatism (Fig. 1).

In addition to refining the relationships and boundaries of the different major geological units, the updated data were a prerequisite for being able to reliably estimate the area's true ore potential. Traditionally, the area had been rated as uninteresting with respect to economic geology (e.g. Eilu et al. 2012), and exploration work in the area had mainly comprised target-scale studies. An exception is the more systematic work related to Ni–Cu ores in the southeastern corner of the main study area.

This paper aims at providing a synthesis of the data and conclusions of papers published earlier and in this volume of the Bulletin of the Geological Survey of Finland and provides an updated model for the overall geological development in the area. Additionally, it describes the large-scale structures observed along the southeastern border of the Central Finland Granitoid Complex and sets them in the Svecofennian tectonic framework.

2 GEOLOGICAL UNITS OF THE MAIN STUDY AREA

The following division of the bedrock follows that of Luukas et al. (2017) with respect to the larger scale and that of Mikkola et al. (2016a) at the scale of the study area. The majority of the bedrock in the main study area belongs to the Western Finland Subprovince, and only the areas east of the Mikkeli shear zone (MiSZ) belong to the Southern Finland Subprovince (Fig. 2). The main units of the Western Finland Subprovince in the study area are the CFGC in the north and Pirkanmaa migmatite and intrusive suites, or Pirkanmaa suites collectively, in the south. The boundary between the Pirkanmaa suites and the CFGC is formed by the northeast–southwest-trending sinistral Leivonmäki shear zone (LmSZ, Fig. 2), readily observable in aeromagnetic and gravimetric Bouguer anomaly maps (Fig. 3). The majority of the volcanic rocks in the study area are included in the Makkola suite, forming a discontinuous belt along the LmSZ. In addition to volcanic rocks, the Makkola suite includes a smaller number of sedimentary units and the Lammuste quartz diorite lithodeme, i.e. plutonic rocks directly associated with the volcanic units. Gabbros and ultramafic plutonic rocks intruding into the Pirkanmaa suites belong to the Vammala suite.

The CFGC is dominated by plutonic rocks of the Jyväskylä suite, which comprises Muurame granitoid and Vaajakoski quartz diorite lithodemes. Rocks of the Muurame granitoid lithodeme also intrude into the rocks of Pirkanmaa intrusive suite south of the LmSZ (Fig. 2). The younger bimodal Saarijärvi suite mainly consists of porphyritic granitoids and quartz montzonites, accompanied by less voluminous diorites and gabbros. Intrusions belonging to the Saarijärvi suite are mainly located within the CFGC, although a small number of them are also present south of it. The youngest granitoid suite in the study area is the Oittila granitoid suite, which, like the Saarijärvi suite, is more voluminous within the CFGC, but is also present south of its boundary formed by the LmSZ.

Due to differences in physical properties, the area of the CFGC mainly consisting of felsic plutonic rocks is characterised by faulting. Supracrustal rocks, which are more voluminous south of the LmSZ, and also less competent, more commonly display signs of plastic deformation.

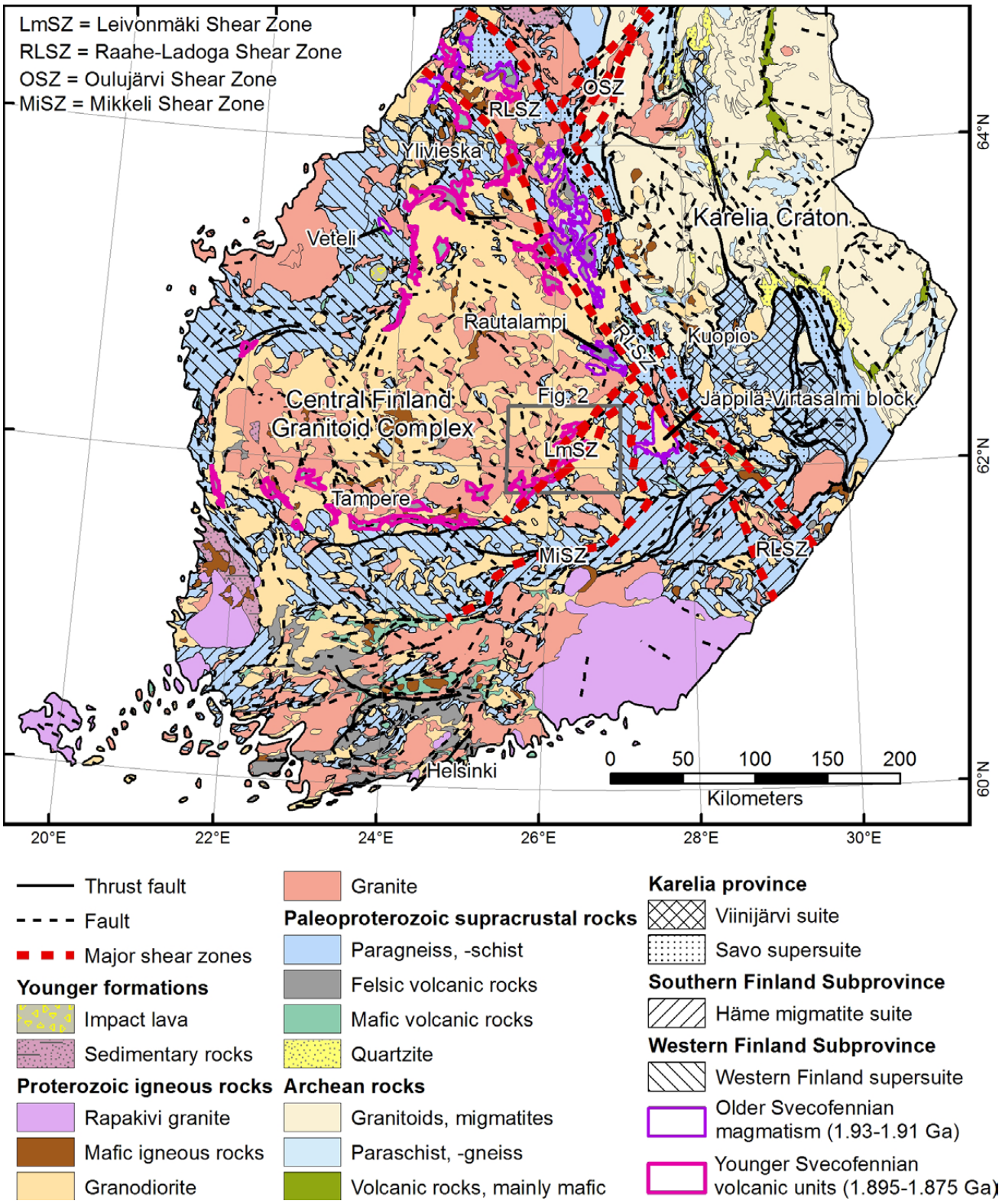

Fig. 1. Geological map of South and Central Finland. Map modified from Nironen et al. (2016) and Bedrock of Finland – DigiKP. Unit division according to Luukas et al. (2017).

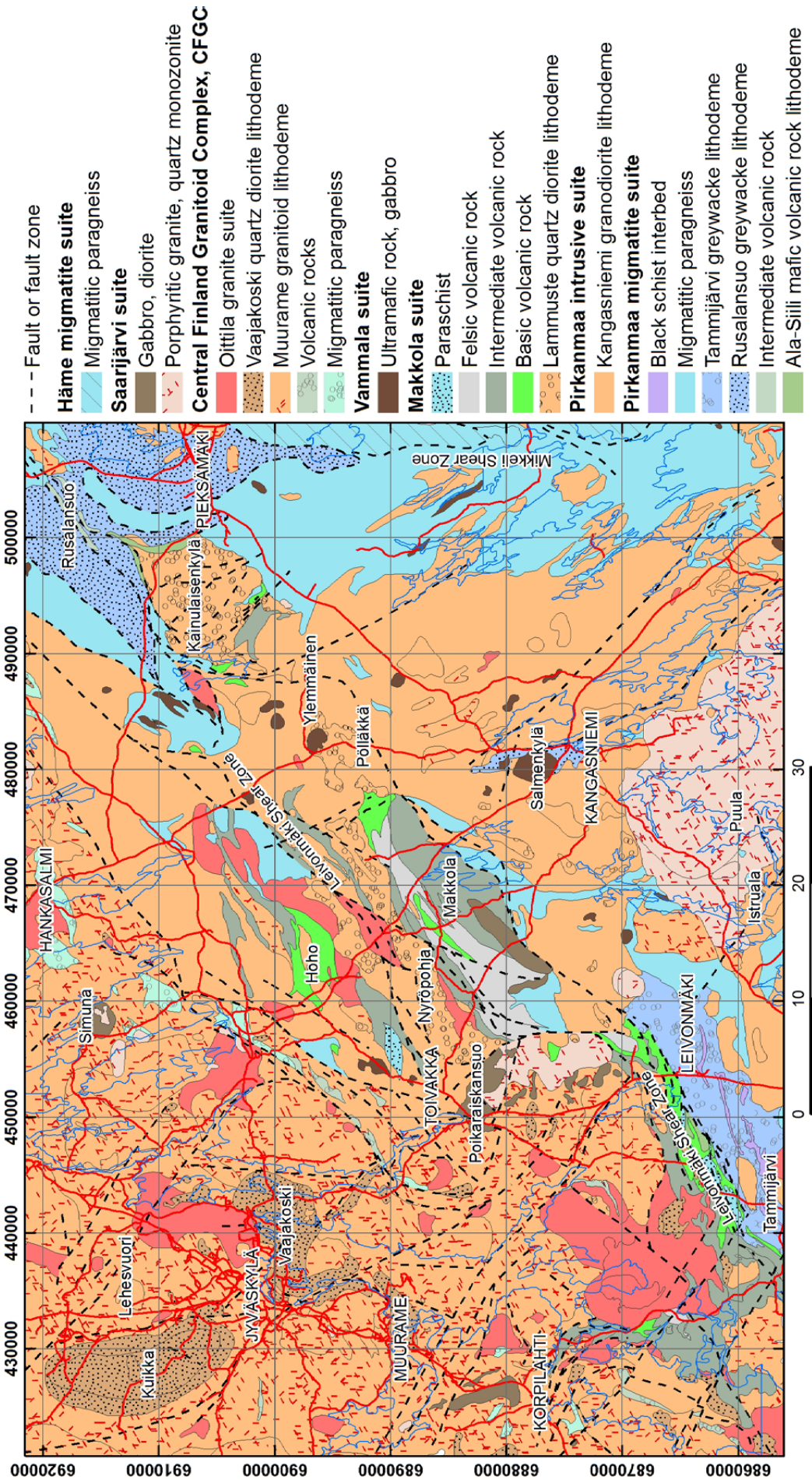

Fig. 2. Geological map of the main study area. Map modified from Mikkola et al. (2016a) and Bedrock of Finland – DigiKP.

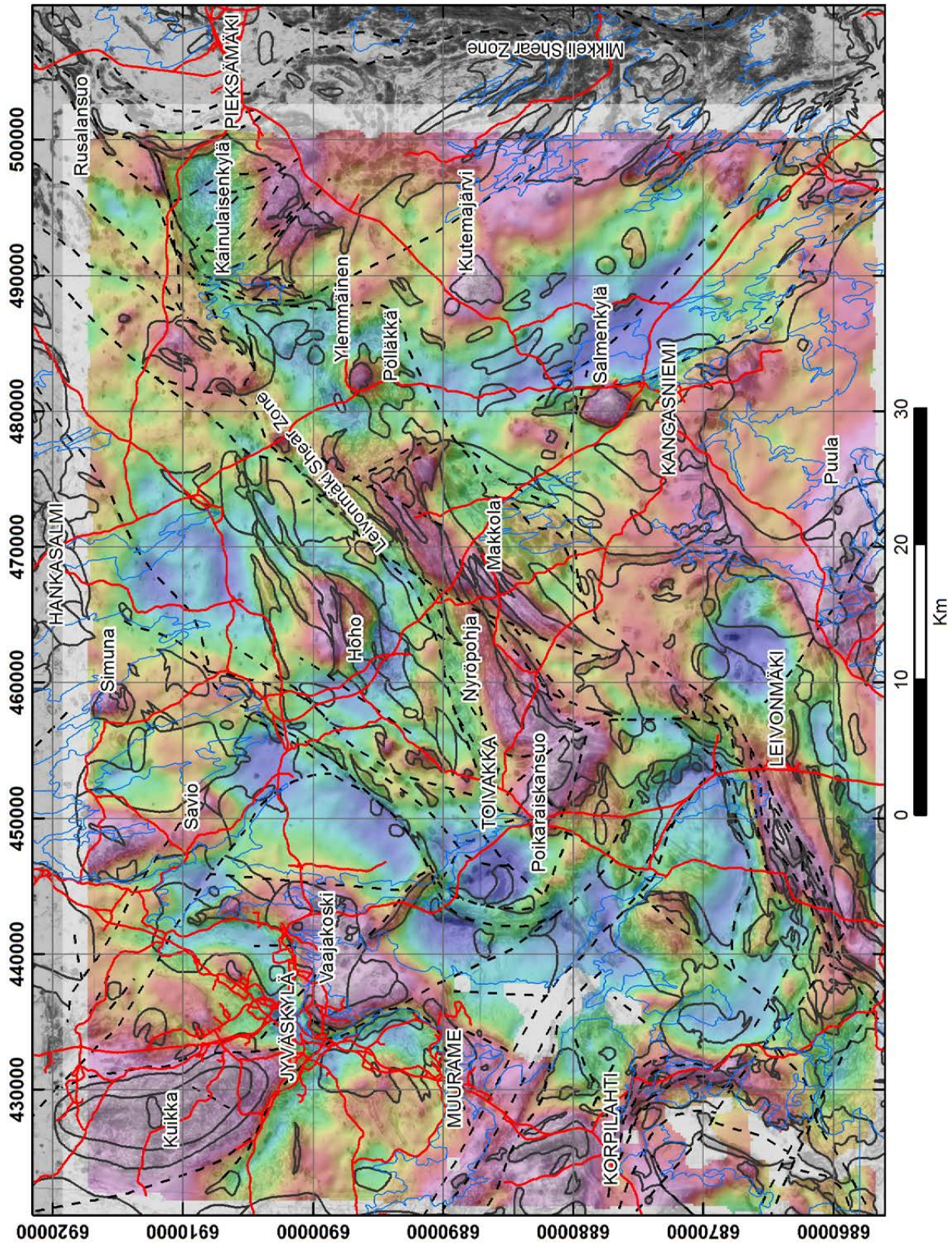

Fig. 3. Combination of aeromagnetic (grey shade: light colour = low values, dark colour = high values) and residual Bouguer anomaly (colour ramp: blue = low values, red = high values) maps of the study area.

3 GRAVITY DATA

The western part of the study area (~2400 km^2) was covered by a regional gravimetric survey in 2012–2016, whereas the eastern part was already measured in the 1980s. On average, there were 4 points per 1 km^2. The majority of the residual gravity anomalies visible in Figure 3 can be explained by the observed surface rocks. The strong, often round positive anomalies, 2–5 km across, are caused by mafic intrusions belonging to either the Vammala suite (e.g. Salmenkylä, Ylemmäinen) or the Saarijärvi suite (e.g. Simuna, Poikaraiskansuo). The rocks of the Vaajakoski lithodeme (mainly diorites and quartz diorites) also cause clear positive anomalies, often larger in area (e.g. Kuikka, Vaajakoski). In some cases, the areal extent of the gravity anomaly is distinctly larger than the observed surface area of the intrusion and/or the magnetic anomaly associated with the intrusion. This suggests that these intrusions broaden below the current erosion surface. For example, the surface width of the Kuikka intrusion, based on both field observations and aeromagnetic data, is six kilometres, but the gravity anomaly associated with it is nine kilometres wide.

In certain areas, the observed gravity anomalies do not correlate with the observed surface geology. For example, north of Savio (Fig. 3), an elongated north–south-trending anomaly can be observed in an area that based on outcrop observations mainly consists of granitoids belonging to the CFGC, in addition to small diorite intrusions belonging to both the Istruala and Vaajakoski lithodemes. The anomaly indicates that the granodiorite is a relatively thin layer covering a larger diorite body. In the Hoho area (Fig. 3), a round-shaped positive gravity anomaly is present in an area where the bedrock, based on both aeromagnetic data and outcrop observations, consists of NE–SW-trending volcanic segments surrounded by granitoids. Based on gravity modelling, the anomaly in this area could be caused by volcanic units dipping to the north and hidden underneath the granitoid cover.

The connection between intrusions belonging to the Lammuste suite and gravity data is not self-evident. The Nyröpohja intrusion flanking the volcanic Makkola segment to the north shows up as a positive anomaly in the gravity data (Fig. 3), while the Pölläkkä intrusion is mainly located in a gravity low. Especially interesting is the Kainulaisenkylä intrusion, which is divided so that the southern half coincides with a positive anomaly and the northern half with a negative anomaly. Based on petrophysical measurements and field observations, this could partly be due to the lower average density of the rocks in the northern half, but it is also possible that the depth extent of the quartz diorite diminishes from south to north.

The large positive anomaly along the eastern edge of the study area is partly caused by paragneisses belonging to the Pirkanmaa migmatite suite and displaying a higher metamorphic degree. However, areas that, based on field observations, mainly consist of granitoids belonging to the Pirkanmaa intrusive suite also fall within this positive anomaly. Thus, it is possible that in addition to the observed small gabbro and diorite areas, there is a larger mafic body hidden below the surface.

The positive Bouguer anomalies along the western contact of the Puula quartz monzonite–granite intrusion are caused by diorite–gabbro intrusions of the Istruala lithodeme. These mafic intrusives, coeval with the granitoid intrusion, are small at the present erosion level, but significantly more voluminous at depth, based on gravity data. Thus, the crustal structure resembles that associated with the classic rapakivi granites in South Finland (Luosto et al. 1990, Elo & Korja 1993).

4 GEOLOGICAL EVOLUTION AND ITS CONNECTION TO THE ROCK UNITS

4.1 Older Svecofennian magmatism

Rocks formed as part of the older Svecofennian magmatism (1.93–1.91 Ga) are mainly present within the Raahe–Ladoga shear zone (RLSZ) between the CFGC and the Archean Karelia craton (Fig. 1, e.g. Ekdahl 1993, Vaasjoki et al. 2003, Kousa et al. 2013). In the current unit classification, these calc-alkaline rocks with arc-type affinity are grouped into the Northern Ostrobothnia supergroup and Venetpalo plutonic suite (Luukas et al. 2017). Earlier, these rocks were interpreted to have a purely linear spatial distribu-

tion in the vicinity of the RLSZ. This view changed when Lahtinen et al. (2016) included the Veteli intrusion (Fig. 1) in this group. The results of Kousa et al. (2018a) broaden the known areal extent of the older Svecofennian units by 65 km to the southeast, as the volcanic and plutonic rocks from the Jäppilä–Virtasalmi block (Viholanniemi volcanic suite, Maavesi Suite, Kousa et al. 2017) are shown to be part of this older succession. The current gap in rocks of these older magmatic units between the Jäppilä–Virtasalmi and Rautalampi areas (Fig. 1) is likely to be an artefact of inconsistent studies. We base this on the field characteristics of tonalites and associated volcanic rocks adjacent to the RLSZ in this area (Mikkola et al. 2016b), from which neither age nor up-to-date geochemical data are available.

In several models, older Svecofennian magmatism, forming the Savo arc, or belt, is linked to subduction towards the southwest and it ends with the collision of the arc with the Karelian craton in the Lapland–Savo orogen at 1.92–1.91 Ga (e.g. Lahtinen et al. 2005, 2009b, Nironen 2017). In certain models, the Savo arc developed at the edge of a small crustal block referred to as Keitele microcontinent (ibid.). The areal extent of this crustal block approximately equalled that of the current CFGC. The existence of this crustal fragment, aged ca. 2.0 Ga, has been interpreted based on Sm–Nd model ages and detrital/inherited zircons (Lahtinen & Huhma 1997, Rämö et al. 2001), as rocks with ages close to 2.0 Ga have not been reported from the area of the CFGC. Alternatively, the Sm–Nd model ages could be a result of mixing between Archean and juvenile sources, but this has been and can be regarded as an unlikely explanation, because reflection seismic data indicate that the Karelia craton ends abruptly at the RLSZ (Kontinen & Paavola 2006, Lahtinen et al. 2009b). The complete reworking of the Keitele microcontinent to what is now the CFGC has been attributed to extensive partial melting and crustal reworking in the culmination stages of the Svecofennian orogeny at 1.88 Ga (e.g. Nikkilä et al. 2016).

In this text, the term ‘Savo arc’, in addition to the older Svecofennian magmatic rocks, also includes the whole area of the CFGC referred to as the Keitele microcontinent in the publications cited above. In our opinion, the separation of the Savo arc and Keitele microcontinent is problematic and most importantly it unnecessarily complicates the tectonic models. The observed isotopic signatures do not require a separate microcontinent; instead, they can be readily explained by variation in the age of the rocks included in the Savo arc itself. For example, the basement of the modern Japanese arc includes voluminous Jurassic rocks representing older phases of the same arc system (e.g. Taira 2001). The collision of such an arc with a continent and nearly complete reworking of it during later stages would result in a situation similar to that in Central Finland, where these older segments are only observable in the isotopic fingerprint of the younger rocks. The preservation of the 1.93–1.91 Ga rocks along the boundary of the Karelia craton, with the exception of the Veteli intrusion (Fig. 1), is a result of later tectonic phases. The dismissal of the Keitele microcontinent becomes especially tempting, as we agree with the terrain wreck model of Lahtinen et al. (2014), in which the originally linear Savo arc (Keitele microcontinent in the reference) transformed into the rounded CFGC close to ~1.87 Ga. The width of the CFGC in its current geometry is ca. 300 km. Thus, its width must have originally been closer to 100–150 km, roughly the same as any modern island arc.

4.2 Paragneisses

The voluminous paragneisses surrounding the CFGC are divided between the Karelia Province and Western Finland supersuite (Fig. 1). In our main study area the latter is represented by the Pirkanmaa migmatite suite (Fig. 2). Paragneisses of the Karelia Province along the northern boundary of the CFGC belong to the Savo supersuite, and further east to the Viinijärvi suite (Fig. 1, Luukas et al. 2017), also known as the Upper Kaleva greywackes (e.g. Lahtinen et al. 2010). Paragneisses east of the main study area belong to the Häme migmatite suite of the Southern Finland Subprovince (Luukas et al. 2017).

Volcanic interlayers in paragneisses of the Pirkanmaa and Häme migmatite suites are mafic to ultramafic in composition and clearly differ from the calc-alkaline arc-type volcanic rocks within, and flanking the CFGC (Kähkönen 2005, Lehtonen et al. 2005, Lahtinen et al. 2017, Kousa et al. 2018b, Mikkola et al. 2018b). On a compositional basis, these mafic to ultramafic (picrites) volcanic rocks can be classified as partial melts of the mantle and

probably represent extensional phase(s) of the basin(s) the paragneisses were deposited in (ibid.). The Enriched Mid-Ocean Ridge Basalt (EMORB)-like lavas of the Haveri formation, the lowermost unit of the Tampere group, have been interpreted in the same way (Kähkönen & Nironen 1994, Kähkönen 2005). In our study area, the majority of the volcanic interlayers (Ala-Siili lithodeme) within the Pirkanmaa intrusive suite are picrites with certain compositional characteristics often associated with rocks formed in volcanic arcs, e.g. Light Rare Earth Element (LREE) enrichment and negative Nb and Ti anomalies (Kousa et al. 2018b). On the other hand, the mafic to ultramafic interbeds (Pahakkala suite) hosted by the Häme migmatite suite display normal MORB affinities, with the exception of samples from one location displaying features similar to the Ala-Siili lithodeme (ibid.). There are most probably multiple causes behind these differences, including variation in the melting depth and temperature, as well as in contamination during ascent. Mikkola et al. (2018b) included a small number of calc-alkaline volcanic rocks in the Pirkanmaa migmatite suite, but as these samples are from highly deformed and poorly exposed areas, this was mainly done on a geographical basis, and further studies could show that these rocks are part of the Makkola suite.

Paragneisses of both the Southern Finland and Western Finland supersuites, as well as the Karelia Province, most often display maximum depositional ages close to 1.92 Ga, and their detrital zircon populations have bimodal distribution patterns with peaks at 2.7 Ga and 2.05–1.92 Ga (Huhma et al. 1991, Lahtinen et al. 2002, 2009a, 2015, Kotilainen et al. 2016, Mikkola et al. 2018a). Despite unit level similarities, there is variation between samples representing the same geological unit, e.g. the proportion of Archean zircons and their age. A classical question with respect to the paragneisses and schists of Central and South Finland is the source of the ~2.0 Ga zircons. One possibility is the Lapland–Kola orogen, culminating close to 1.95 Ga (Daly et al. 2006). Rocks with such ages have also been reported from the vicinity of Moscow, 1000 km to the southeast, hidden below the platform covers (Samsonov et al. 2016). The proposed sources also include the above-discussed Savo arc, with respect to which an interesting phenomenon is the small proportion of zircon grains with ages falling between 1.93 and 1.91 Ga (e.g. Lahtinen et al. 2002, Mikkola et al. 2018a). This is interesting, as the newly formed Lapland–Savo orogen would appear to be a bountiful source for sedimentary input. A possible explanation for the small number of detrital zircons with ages between 1.93 and 1.91 Ga could be a paleogeographic setting that favoured transport from areas other than that hosting the rocks belonging to the older Svecofennian magmatism, or burial of these during the collisional phase. Because most of the paragneiss samples from areas surrounding the CFGC do not contain detrital zircons with 1.90–1.88 Ga ages typical for volcanic rocks within, and surrounding the CFGC (e.g. Kähkönen & Huhma 2012, Nikkilä et al. 2016, Mikkola et al. 2018b), they must have been deposited prior to the onset of active volcanism in the area that later became the CFGC.

Differentiation between the Pirkanmaa and Häme migmatite suites (Fig. 1) has partly been based on the presence of black schist interbeds in the former and their absence from the latter (Luukas et al. 2017). However, especially in the vicinity of our study area, this is not the case, as the Häme migmatite suite also contains abundant black schist interbeds (Bedrock of Finland - DigiKP). In our study area, the boundary between the Pirkanmaa and Häme migmatite suites (Fig. 2) is in the current interpretation formed by the MiSZ. This zone also represents a major change in metamorphic degree from granulite facies of the Pirkanmaa migmatite suite to lower amphibolite facies of the Häme migmatite suite (Korsman et al. 1988). Based on the above and the similarities of the detrital zircon populations displaying peaks at 2.7 and 2.0 Ga (Mikkola et al. 2018a), we agree with Lahtinen et al. (2017), who noted that the two suites might represent protoliths deposited in different parts of the same basin, and the current unit division reflects post-depositional effects.

The question with respect to the unit divisions is also topical in relation to the Tammijärvi greywacke lithodeme in our study area (Fig. 2) and the lowermost unit of the Tampere group, i.e. greywackes of the Myllyniemi formation. Both of these units consist of chemically similar greywackes with conglomerate and metapelite interbeds, as well as mafic to ultramafic volcanic rocks (Kähkönen & Nironen 1994, Kousa et al. 2018b, Mikkola et al. 2018a) interpreted to represent extensional phases in the development of the depositional basins. Both units have detrital zircon populations similar to each other and to the Pirkanmaa migmatite suite (Huhma et al. 1991, Lahtinen et al. 2009a, Mikkola et al. 2018a), and occur in the vicinity of calc-alkaline magmatism aged 1895–1875 Ma. The only significant difference

between the Tammijärvi lithodeme and Myllyniemi formation is the lack of black schist interbeds in the latter (Kähkönen 2005). Despite significant similarities, the Tammijärvi greywackes are included in the Pirkanmaa migmatite suite and the Myllyniemi formation in the Tampere group. This difference in interpretations is partly due to the nature of the contacts. The Tammijärvi greywackes have gradual contacts towards the migmatised members of the Pirkanmaa migmatite suite, whereas the Myllyniemi formation is separated from the Pirkanmaa migmatite suite by a more abrupt change in metamorphic grade, not unlike the Mikkeli shear zone in our study area between the Häme and Pirkanmaa migmatite suites.

The most significant difference between the Savo supersuite and the Häme, Pirkanmaa and Viinijärvi suites is the uniformly unmigmatised character of

Table 1. Timeline of the main geological units and events of the study area.

Time (Ma)	
1920–1910	Magmatism belonging to the older Svecofennian phase in the Jäppilä-Virtasalmi block
	Granitoids and volcanic rocks that can be correlated with those in the Vihanti–Pyhäsalmi area
>1900	Deposition of rocks of the Pirkanmaa migmatite suite and Häme migmatite suite
	Greywackes deposited by turbidites. Most, but not all, were migmatized in later stages. Observed differences in metamorphic degree due to late vertical movements.
	Mafic/ultramafic volcanic rocks erupted on the sediments during extensional phases
~1900	Onset of subduction in the area
1895	Pirkanmaa intrusive suite
	Calc-alkaline granodiorites and tonalites intruding into rocks of the Pirkanmaa migmatite suite.
1895–1875	Makkola suite
	Mainly felsic to intermediate calc-alkaline volcanic rocks, small amounts of associated plutonic rocks and sedimentary rocks. Dykes related to the suite cross-cut the Pirkanmaa intrusive suite.
1885	Vammala suite
	Gabbros and ultramafic plutonic rocks as small intrusions and dykes intruding the Pirkanmaa migmatite and intrusive suites.
1885–1880	Jyväskylä suite
	Porphyritic calc-alkaline granitoids (Muurame lithodeme), smaller amounts of dioritoids (Vaajakoski lithodeme). The majority of the rocks of the Cental Finland Granitoid Complex. Also intrude into Pirkanmaa intrusive and migmatite suites. Partial melts of SOME crust.
~1880	End of subduction in the area
1880–1875	Saarijärvi suite
	Bimodal suite consisting of diorites, granitoids and quartz monzonites. Chemically A-type, felsic members are typically K-feldspar porphyritic.
1875	Oittila suite
	Granitoid dykes and intrusions less than 10 km across, often leucocratic, low degree partial melts of pre-existing crust or last remaining melt fractions from intrsuions below current erosion level.
1830	Thrusting of Pirkanmaa migmatite and intrusive suites from south on top of the Central Finland Granitoid Complex
	Major activity along the Leivonmäki shear zone
	Activity along the southeast-northwest-trending faults within Central Finland Granitoid Complex
1830–1790	Late Svecofennian granites
	Rutalahti peridotites
	Small ultramafic intrusions representing mantle derived melts. Ascent and emplacement controlled by large scale faults. Precise age unknown.
1670–1620	Kuisaari suite
	Subophitic gabbros and diorites, belonging to the Häme dyke swarm of the Southern Finland rapakivi supersuite.

the paragneisses of the last suite. Protoliths of all of these units were deposited as greywackes and all host mafic to ultramafic volcanic interlayers. In the Viinijärvi suite, these are the ophiolites of the Outokumpu assemblage and in the Häme and Pirkanmaa migmatite suites the picrites and MORB affinity rocks (Peltonen 2005a, Lahtinen et al. 2017, Kousa et al. 2018a). Lahtinen et al. (2009a) proposed, based on similar compositions and detrital zircon populations, that the Viinijärvi suite greywackes represent a major source area of the Western Finland supersuite. However, the gradual differences in Ba, Sr, Th/Sc and Ti/Al displayed by rocks of the Pirkanmaa migmatite and Viinijärvi suites, and used by Lahtinen et al. (2009a) for their model, could also result from variation in the mixing ratio from the same source areas. Based on tectonic interpretation and detrital zircon populations, Lahtinen et al. (2015) concluded that the paragneisses of the Savo supersuite northwest of Kuopio (Fig. 1) are part of the Karelia Province and equivalents of the Viinijärvi suite. However, no age data are available from paragneisses of the Savo supersuite southeast of Kuopio and the tectonic setting of the unit is also less well defined. Based on the above, the unit division in areas surrounding the Jäppilä–Virtasalmi block are more or less tentative, as also noted by Luukas et al. (2017). The necessary revision cannot be carried out based on the current material, but would not be an overwhelming task, either.

4.3 Into the active subduction phase, 1895 Ma

Volcanic rocks aged 1895–1875 Ma form a discontinuous belt along the boundary between the CFGC and the paragneisses surrounding it. These volcanic segments have been incorporated in the Central Ostrobothian supergroup (Luukas et al. 2017), which includes, among others, the Tampere group (Fig. 1, Kähkönen 2005) and Ylivieska group (Kousa & Lundqvist 2000). The less extensively studied units are grouped into a number of suites within the Western Finland supersuite. Based on material in Mikkola et al. (2018b), the Makkola suite volcanic rocks correlate with respect to age and composition with the Central Ostrobothnia supergroup and represent the eastern end of the discontinuous volcanic belts of this age. Volcanic and subvolcanic units within the CFGC mainly yield ages close to 1885 Ma (Rämö et al. 2001, Nironen 2003, Nikkilä et al. 2016), although ages close to 1895 Ma are also known (Tiainen & Kähkönen 1994). The genesis of these volcanic rocks has been linked to active subduction along the southern and western edge (current geometry) of the CFGC (Kähkönen 2005, Lahtinen et al. 2009b, Nironen 2017) or alternatively considered to be a result of post-accretional partial melting of crust thickened during the collision of the Savo arc with the Karelia craton (Nikkilä et al 2016). The oldest ages (~1895 Ma) from the volcanic rocks belonging to the Makkola suite (Mikkola et al. 2018b) and Tampere group (Kähkönen & Huhma 2012) are similar to that of the Pirkanmaa intrusive suite (Kallio 1986, authors' unpublished data). As the Pirkanmaa intrusive and Makkola suites display significant compositional similarities in addition to age (Mikkola et al. 2018b, Heilimo et al. 2018), the latter can be regarded as the plutonic equivalent of the volcanic rocks of the former. As rocks belonging to the Pirkanmaa intrusive suite intrude the rocks of the Pirkanmaa migmatite suite, the 1895 Ma age of the former marks the minimum age of the latter. Overall, the observations from our study area support the interpretation of Lahtinen et al. (2009b) and Nironen (2017) concerning the onset of subduction and magmatism related to it in Central Finland close to 1.90 Ga. Weak indications of 1.90 Ga metamorphism given by zircon studies on greywackes (Lahtinen et al. 2009a, Mikkola et al. 2018a) could be linked to this onset of subduction, resulting in the creation of an accretionary prism. The presence of both Archean and Paleoproterozoic detrital zircons in a volcano-sedimentary sample belonging to the Makkola suite (Mikkola et al. 2018b) requires that the volcanism must have taken place in a continental arc setting, as zircons significantly older than the active volcanism are not commonly known from island arcs. Also, the highly evolved chemical characteristics of the volcanic rocks support a continental arc origin for the Makkola suite (Mikkola et al. 2018b).

4.4 Vammala suite

The Svecofennian gabbro and ultramafic intrusions have been intensively studied due to their Ni potential. In our study area, these intrusions are emplaced in the Pirkanmaa suites and thus grouped into the

Vammala suite (Luukas et al. 2017). The mafic to ultramafic interbeds occurring in paragneisses of the Häme migmatite suite belong to the Pahakkala suite (Luukas et al. 2017), although Makkonen and Huhma (2007), for example, concluded that the gabbro and ultramafic intrusions of the Vammala suite are the plutonic equivalents of these volcanic interlayers. However, new data (Lahtinen et al. 2017, Kousa et al. 2018b, Mikkola et al. 2018a) confirm the interpretation of Peltonen (1995) that the mafic to ultramafic volcanic rocks are not co-magmatic with these so-called Ni gabbros. Instead, the volcanic units erupted at 1.91–1.90 Ga on the protoliths of Pirkanmaa and Häme migmatite belts, whereas the ages of the Ni gabbros are 1.89–1.88 Ga (Peltonen 2005b and references therein). In the study area, the minimum age of intrusions is 1875 Ma, defined by the cross-cutting Oittila suite granitoids (Mikkola et al. 2016a, authors' unpublished data). Thus, based on the available age constraints, the youngest Vammala suite intrusions are coeval with the peak of the granitoid magmatism within the CFGC and the oldest ones are roughly of the same age as the oldest volcanism forming the Makkola suite.

Based on the above-described time constraints, the physical location and the overall tectonic setting, we interpret that the Vammala suite intruded during active subduction into tensional structures of the accretionary wedge consisting of the Pirkanmaa suites. This interpretation is in line with that of, for example, Peltonen (1995, 2005b) and Nironen (1997). Due to their syntectonic character, the Ni gabbros were intensively deformed, boudinaged and contaminated by surrounding rocks and fluids over their whole distribution area (Peltonen 2005b, Mikkola et al. 2016a). It should be noted that the Ni gabbros of the coeval Kotalahti suite intruding the Savo supersuite (Fig. 1) were emplaced in a different structural environment, i.e. the transtensional RLSZ between the Savo arc and the Archean craton (Peltonen 2005b).

4.5 Formation of the CFGC at 1885–1875 Ma

The majority of the granitoids forming the CFGC crystallised at 1885–1875 Ma (e.g. Rämö et al. 2001, Nironen 2003, Nikkilä et al. 2016, Kallio et al. 2018). These rocks have earlier been subdivided in variable ways based on either interpreted relationships with kinematics or compositional bases. Nironen (2003) divided these rocks into synkinematic and postkinematic groups and Nikkilä et al. (2016) into three different groups mainly based on their compositional characteristics, interpreted as signs of variation in depth and the degree of melting, as well as in the emplacement depth. The Jyväskylä suite, consisting of porphyritic granitoids accompanied by smaller volumes of dioritoids (Mikkola et al. 2016a, Heilimo et al. 2018), equals the synkinematic group of Nironen (2003) and group 2 of Nikkilä at al. (2016). The bimodal Saarijärvi suite (Luukas et al. 2017, Virtanen & Heilimo 2018) corresponds to the post-kinematic group of Nironen (2003) and group 3 of Nikkilä et al. (2016).

4.5.1 Jyväskylä suite

Based on its chemical characteristics, the Jyväskylä suite represents typical calc-alkaline arc type magmatism. Compositions span from basic to felsic, the majority being relatively felsic porphyritic granodiorites (e.g. Nironen 2003, Nikkilä et al. 2016, Heilimo et al. 2018). Despite compositional similarities with modern arc rocks, Nikkilä et al. (2016) explained the genesis of the Jyväskylä suite granitoids with a model that did not involve active subduction. Instead, these rocks would have been formed due to partial melting of crust thickened in the collision of the Savo arc with the Karelia craton at 1.91 Ga. This model was based on material from the central parts of the CFGC lacking the mafic members of the suite (diorites, quartz diorites), which seem to increase in abundance when moving south from the central parts of the CFGC (Bedrock of Finland - DigiKP). This could possibly be an indication of crustal thickness at the time of emplacement. Diorites originating from the mantle (Heilimo et al. 2018) would have experienced less fractionation and crustal assimilation in areas of thinner crust, i.e. closer to the subduction zone.

4.5.2 Saarijärvi suite

Rocks of the bimodal Saarijärvi suite have been referred to as postkinematic (e.g. Nironen et al. 2000, Nironen 2003), because they are relatively undeformed compared to the rocks of the Jyväskylä suite (ibid. synkinematic). This observation is valid, and the cross-cutting relationships are also clear; the Saarijärvi suite is younger than the Jyväskylä

suite (Nironen et al. 2000, Mikkola et al. 2016a, Virtanen & Heilimo 2018). However, the age determinations of both of these suites yield ages close to 1880 Ma and overlap within error. In the model of Nikkilä et al. (2016), the Saarijärvi suite represents partial melts of the lower crust that were emplaced in an extensional setting, which allowed magmas generated in the lower crust to rise efficiently. Due to the overlap in absolute ages of the Jyväskylä and Saarijärvi suites, this would have meant an extremely rapid transition from a compressional setting to an extensional one. Saarijärvi suite rocks typically occur in, or in the proximity of, large-scale faults, both in our study area (Mikkola et al. 2016a, Virtanen & Heilimo 2018) and in other parts of the CFGC and in its vicinity (Nironen 2003, Kousa & Luukas 2007, Nikkilä et al. 2016). For example, in our study area, the largest intrusions of this suite (Fig. 2, Puula–Viiniperä–Riitalampi–Poikaraiskansuo) form a condensation on a roughly southeast–northwest-trending line, coinciding with the major fault direction within the CFGC. Based on this, it seems that these faults were already active 1880 Ma ago, which is in agreement with the model of Nironen (2017). The transtensional crustal scale faults would have provided pathways for ascending magma created in the lower crust.

Support for the coeval existence of two geochemically differing granitoid melts at 1880 Ma in our study area is given by the observations of Virtanen & Heilimo (2018). They demonstrated that certain samples representing the Saarijärvi suite deviate from an A-type composition due to contamination by arc-type granite melts or rocks (i.e. Jyväskylä suite). Samples representing the Jyväskylä suite also display signs of interaction with the Saarijärvi suite (Heilimo et al. 2018). However, clear observations of magma mixing and mingling have only been reported between the mafic and felsic members of the Saarijärvi suite (e.g. Nironen et al. 2000, Virtanen & Heilimo 2018).

4.5.3 Oittila suite

The Oittila suite, present as intrusions and abundant dykes, represents the youngest granitoid magmatism in the area (~1875 Ma, authors' unpublished data). Often, these granitoids are more leucocratic than those of the Jyväskylä suite and can be distinguished both in the field from cross-cutting relationships and by using geochemistry (Heilimo et al. 2018). However, overlap between these two suites exists and their differentiation is sometimes challenging. The observed compositions of rocks of the Oittila suite can be interpreted in two differing ways: they are either the last remaining melt fractions or result from a low degree of partial melting. As the Oittila suite granitoids display sharp contacts with the rocks they intrude into, and migmatites are rare in our study area outside the Pirkanmaa migmatite suite, the partial melting would have occurred below the current erosion level. However, on a compositional basis, Heilimo et al. (2018) suggested that the Oittila suite represents more evolved intrusions of magma compositionally similar to those of the Jyväskylä suite.

4.5.4 Connection between volcanism and plutonism, building a batholith

The older volcanic activity (~1895 Ma) of both the Makkola suite (Mikkola et al. 2018b) and the Tampere group (Kähkönen & Huhma 2012) is coeval with the Pirkanmaa intrusive suite, whereas younger activity (1885–1875 Ma) is coeval with the Jyväskylä suite plutonic rocks. None of these suites display significant compositional differences (Heilimo et al. 2018, Mikkola et al. 2018b), and they also display similar trace element characteristics, namely those typical for arc-type magmatism. This similarity is demonstrated by the fact that an individual sample from the Pirkanmaa intrusive suite cannot be reliably differentiated from one representing the Jyväskylä suite of the CFGC, and neither can a single sample representing the Makkola suite be separated from a volcanic sample within the CFGC. This should be taken as evidence that the aforementioned suites were all generated in the same processes from roughly similar sources in an arc environment (Heilimo et al. 2018, Mikkola et al. 2018b). It should also be noted that the close spatial association between the CFGC and the Pirkanmaa intrusive suite is not purely a product of later tectonic movements. This is evidenced by the observation that rocks belonging to the CFGC locally intrude in the slightly older Pirkanmaa intrusive suite in a triangle formed by Kangasniemi, Hankasalmi and Leivonmäki (Fig. 2).

Despite strong similarities, there is an overall trend from the tonalite–granodiorite compositions of the Pirkanmaa intrusive suite towards the granodiorite compositions of the Jyväskylä suite and further to the granite compositions of the Oittila suite (Heilimo et al. 2018). Certain trace element ratios

also indicate subtle differences between central parts of the CFGC and its "outer rim". For example, volcanic samples from central parts of the CFGC and Jyväskylä suite granitoids display enrichment in Zr and Th over those of the Makkola and Pirkanmaa intrusive suite, which causes them to plot on differing trends in the classification diagrams of Pearce (1996, 2008, Fig. 4). Such subtle differences are what would be expected during the maturation of the arc. The ca. 5–10 Ma age difference between the Oittila and Jyväskylä suites would equal 5–10 km of crust removed between the emplacement of the two suites if assuming an erosion rate of 1 mm/year, which is typical in the modern-day Alps (Wittmann et al. 2007). Assuming such rates for a Paleoproterozoic orogen in an environment without vegetation and a more acid atmosphere is likely to lead to an underestimate rather than an overestimate. In response to uplift and erosion, the pooling level of granitoid magmas would respectively shift lower in the crust, resulting in more evolved magmas reaching the currently exposed level. This would fit the interpretation of Heilimo et al. (2018), i.e. the Oittila suite represents a more evolved version of Jyväskylä suite magmas. Such a model based solely on the depth of the intrusions would in many ways be the simplest one; it would explain the compositional continuum of the Jyväskylä and Oittila suites without the need for differing melt sources in a geologically brief time period.

Based on the discussion above, we agree with Nironen (2003, 2017), for example, and regard the CFGC as a batholith formed in an active continental arc. The relatively abundant preservation of the volcanic units along the borders of the CFGC is likely to be the result of bulging of the complex during later tectonic movements, resulting in a deeper crustal section being exposed in its central parts. In these areas, volcanic and subvolcanic units have only locally been preserved in areas of down-warped blocks. The current erosion level in the central CFGC coincides with the emplacement level of the main granitoid magmatism. This explains the lack of rocks older than 1.90 Ga that formed the Savo arc. It should also be borne in mind that the inner parts of the CFGC are poorly studied and rocks with such ages could be found in future studies. Rocks of the Pirkanmaa migmatite suite resided at this stage in the accretionary prism, as proposed by Lahtinen et al. (2009a), among others. Fore-arc deposits of this period have been eroded in later stages, and preservation has only locally been possible in

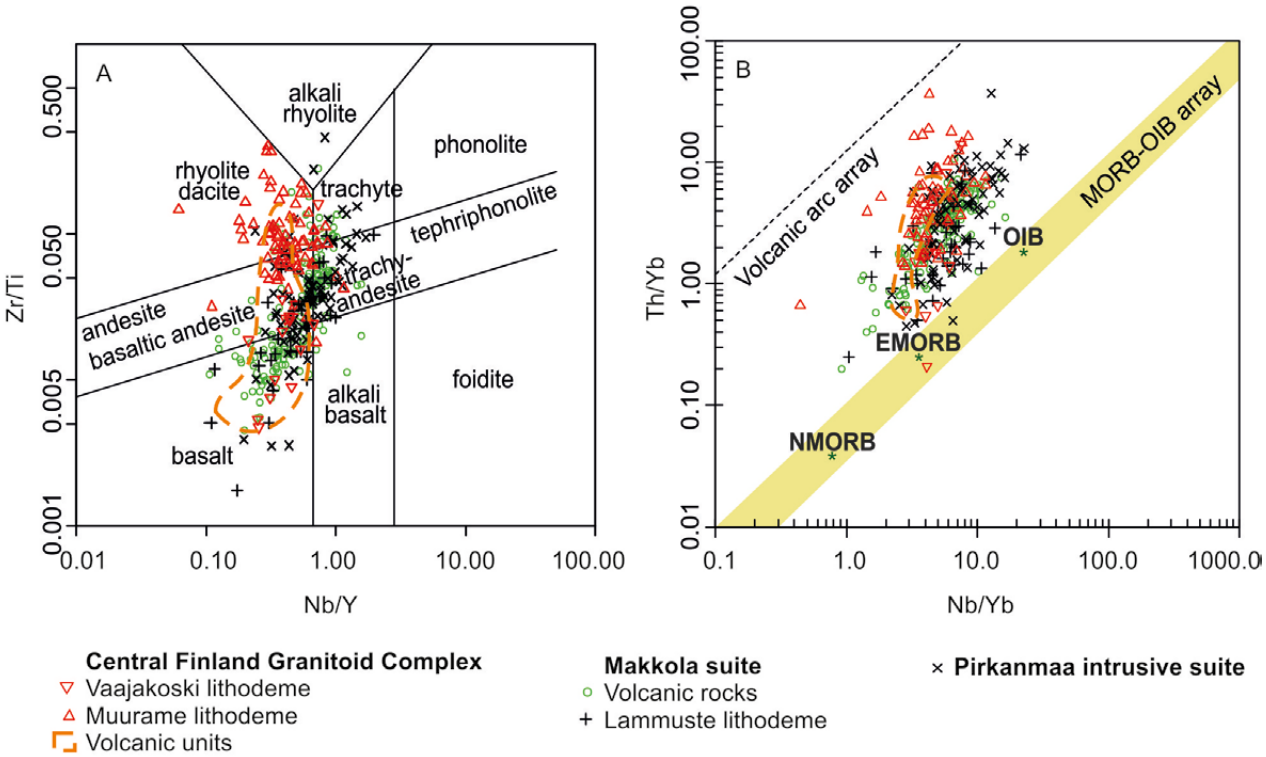

Fig. 4. Comparison between different rock units of the Central Finland Granitoid Complex, Makkola suite and Pirkanmaa intrusive suite. A) Nb/Y vs. Zr/Ti plot of Pearce (1996) and B) Nb/Yb vs. Th/Yb plot of Pearce (2008). Data from Nikkilä et al. (2016), Heilimo et al. (2018) and Mikkola et al. (2018a). Despite overlap, rocks from the CFGC form a trend differing from that defined by samples belonging to the Makkola suite and Pirkanmaa intrusive suite. See the text for further discussion.

structurally favourable locations (e.g. Korsman et al. 1988, Nironen & Mänttäri 2012).

An alternative solution to the active subduction model would be to regard the CFGC as a result of partial melting triggered by thermal relaxation of crust thickened during the accretion of the Savo arc with the Karelia craton close to 1.91 Ga (Nikkilä et al. 2016). The rounded, rather than elongated, shape of the CFGC (Fig. 1), and rock units surrounding it, would seem to favour this post-accretionary partial melting model for its genesis. This is because 180° bends in modern active subduction systems are not at the scale of hundreds, but thousands of kilometres. A solution to this geometrical challenge was proposed by Lahtinen et al. (2014), who argued that the current shape of the CFGC is a result of crustal-scale buckling that bent the originally linear complex, as well as the surrounding units, into their current shape. This would have occurred at 1.88–1.86 Ga, during major activity along the RLSZ, and would have been linked to the dextral rotation of the CFGC (Pajunen et al. 2008) in connection with the collision of the Bergslagen microcontinent from the south (e.g. Lahtinen et al. 2009a, Nironen 2017).

4.5.5 Metamorphism

Most of the age samples from the study area do not provide constraints on the timing of metamorphism, an exception being the relatively precise 1885 Ma age for the anatexis of the Pirkanmaa suite migmatites (Mikkola et al. 2018a). As this age coincides with the main phase of the plutonic activity in the whole study area, it can be assumed that it marks the peak of areal metamorphism in the area, although further to the east, in the vicinity of the Sulkava thermal dome, the metamorphism appears to be somewhat younger, i.e. 1840–1810 Ma (Vaasjoki & Sakko 1988, Kousa et al. 2018b). As the chaotic diatexites rarely show constant deformational structures, correlation with the migmatisation-related deformational phase was not carried out. Based on P-T calculations from migmatitic paragneisses in the study area, the metamorphism of the Pirkanmaa migmatite suite east of Leivonmäki was of the high-T, medium-P type (700–800 °C, 5–6 kbar), suggesting that it was caused by heat transferred to the present erosion level by voluminous magmatism (Romu unpublished data).

4.6 Younger sedimentary phase

A limited number of paragneiss samples from the Pirkanmaa migmatite suite contain detrital zircons that could be coeval with the ca. 1895 Ma active volcanism along the southern boundary of the CFGC (Lahtinen et al. 2009a, Mikkola et al. 2018a). These rocks were named as "fore-arc sediments" by Lahtinen et al. (2009a), who separated them from older greywackes mainly based on Sr contents. Paragneisses with elevated Sr contents were also encountered from the study area, but based on currently available data, they cannot be separated into a different unit (Mikkola et al. 2018a). Furthermore, the possible effects of ancient lead loss must be borne in mind when making interpretations from a limited number of detrital zircons on highly metamorphosed rocks. It is possible that some of the ages now interpreted as detrital in fact result from metamorphic resetting.

Regardless of the above, the Haukivuori conglomerate with granitoid clasts aged 1885 ± 6 Ma (Korsman et al. 1988) represents a later depositional phase in the presently studied area and equals the "fore-arc sediments" of the Pirkanmaa migmatite suite. Its preservation is probably caused by the structural location on a downthrown block, as suggested by the abrupt change in metamorphic grade (ibid.) related to the Mikkeli shear zone. The change in metamorphic grade also correlates with a change on the Bouguer anomaly map.

4.7 Thrusting and folding before the main activity of the LmSZ

Volcanic rocks of the Makkola suite record only one clear folding event prior to the development of the LmSZ (Fig. 5A, B). As rocks belonging to the Pirkanmaa migmatite suite mainly occur as scattered areas between igneous rocks of the Pirkanmaa intrusive suite, their structural history is more difficult to constrain, but their general structural trends are identical to those of the volcanic segments. Thus, it is likely that they have experienced the same compressional deformation as rocks of the Makkola suite. This compression from the southeast resulted in southwest–northeast-trending folding along the edge of the CFGC and later faulting and thrusting of the Pirkanmaa suites and Makkola suite

on top of the CFGC. Major horizontal movements are likely to be associated with this folding and thrusting phase. This is evidenced by the juxtaposition of well-preserved greywackes (Mikkola et al. 2018a) on top of intensively migmatised paragneisses or igneous rocks in several locations. The maximum age of 1885 Ma for these vertical movements is given by paragneisses in the vicinity of Kangasniemi, where the well-preserved greywackes show no signs of the intensive migmatisation of this age characterising their surroundings (Mikkola et al. 2018a). Later activity along the LmSZ has largely obscured the structures related to this phase.

The directions of the fold planes related to this compressional stage are similar to those observed further southeast in the Mikkeli and Sulkava areas and could indicate that the folding is associated with the final stages of Svecofennian development in South Finland (e.g. Pajunen et al. 2008, Nironen 2017). Based on reflection seismic data from the NW parts of the CFGC, Sorjonen-Ward (2006) identified several reflectors dipping at a low angle towards the SE and interpreted them as thrust faults that could be linked to the same event at ~1.83 Ga as the deformation in our study area. However, the timing of the activity along these thrust faults is challenging, and they could also be related to compressional deformation already occurring at 1.88–1.87 Ga (Pajunen et al. 2008, Sorjonen-Ward 2006).

4.8 Leivonmäki shear zone (LmSZ)

The LmSZ is a NE–SW-trending sinistral shear system that differs from the large-scale southeast–northwest-trending fold and fault structures characterising the Raahe–Ladoga shear zone. These fault zones probably developed as a conjugate shear system. The system formed about 1830–1800 Ma ago, probably as a continuation of the previous thrusting and folding phase. The Oulujärvi Shear Zone further north (Fig. 1) represents a similar conjugate of the RLSZ, and the age of the post-orogenic granites (1790 Ma, Kontinen et al. 2013) it deforms can also be tentatively taken as the maximum age of the last major activity along the LmSZ.

The width of the LmSZ in the central part of the main study area is up to 25 km and the total displacement it causes is thus difficult to estimate, but it is in order of tens of kilometres. In the Leivonmäki area, the LmSZ narrows to four kilometres and the shear is distributed in several fault surfaces, forming dextral fault duplexis (Figs 2, 5C). Folding associated with the shearing is the dominant structure of the metasedimentary units in this area (Mikkola & Niemi 2015). The contacts between the Pirkanmaa migmatite suite and the Makkola suite coincide in two places with faults of the LmSZ: south of the Makkola segment, where the Synsiö fault separates the migmatitic paragneisses from the volcanic units, and in Leivonmäki area, where the unmigmatised Tammijärvi greywackes are present south of the shear zone. In both of these locations, the fault also presents a significant change in metamorphic degree.

Due to its large scale and variable outcrop conditions in the study area, the LmSZ can most readily be observed when it affects geological units with varying magnetic properties. For example, the 10 by 10 km Kainulaisenkylä quartz diorite intrusion in the northeastern corner of the study area was rotated, forming a “mega-augen” structure (Fig. 3). Another place where the displacement caused by the LmSZ is easily observable is the volcanic segment at Makkola. Here, one fault transects the volcanic units, displacing them by ca. 2 km, and the western end of the belt is truncated by a fault displacing the western continuum of the suite in the Leivonmäki area by 7 km (Figs 2, 3).

The gold potential in our study area is mainly related to activity along the LmSZ (Luukkonen 1994, Mikkola et al. 2018c). The observed differences between the mineralisations also provide indications of prolonged activity along the LmSZ, which is additionally evidenced by locally intensive signs of brittle activity, in addition to the main plastic deformation phase (Fig. 5D). Observations of the brittle deformation are mainly from drill cores (Fig. 5E, Mikkola & Niemi 2016), as such fault breccias are covered by Quaternary deposits.

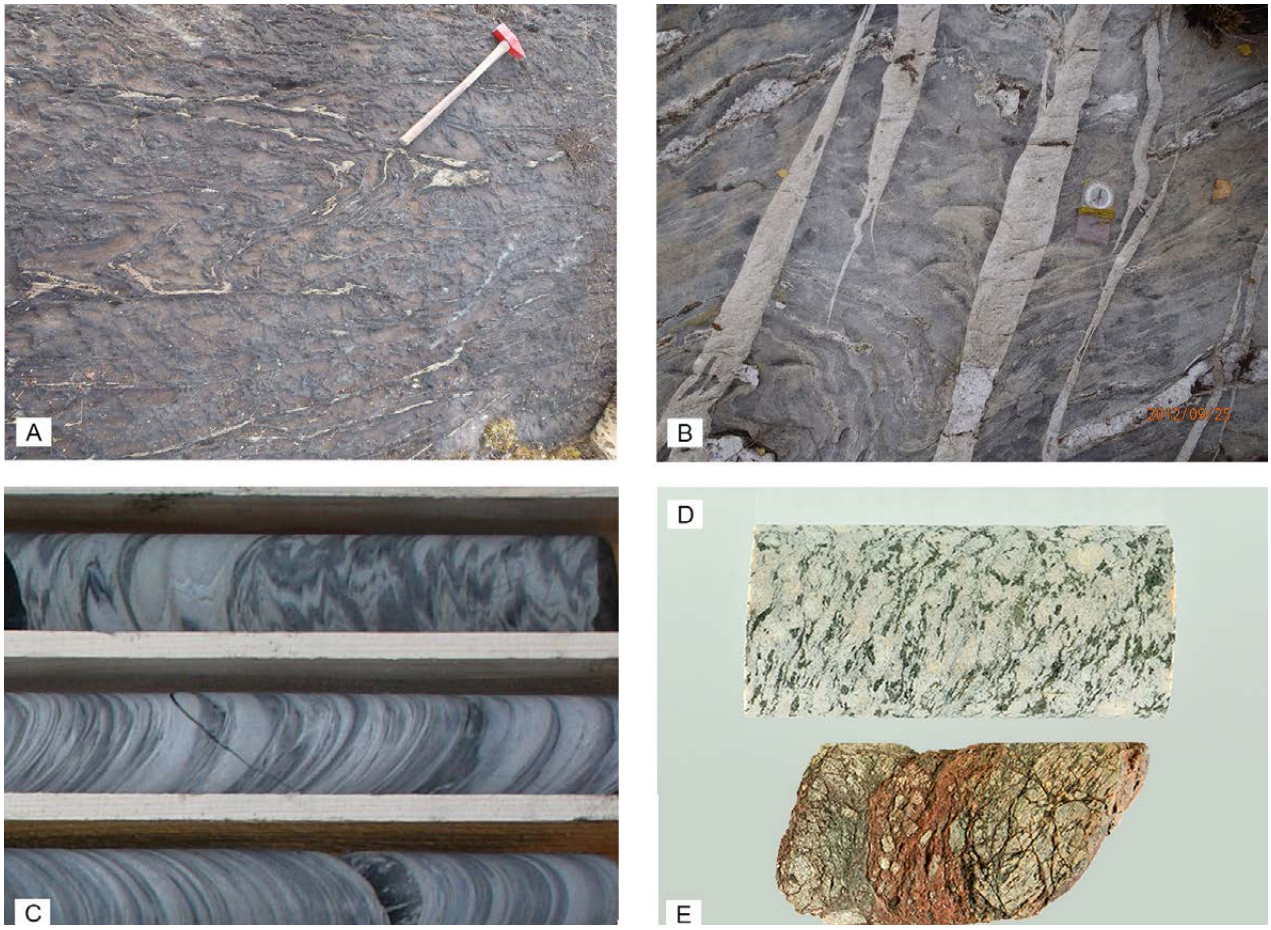

Fig. 5. A) Folded volcanic breccia from central parts of the Makkola segment. The handle of the hammer points to north. Length of the hammer 60 cm. B) Intermediate volcanic rock with folded bedding from the eastern part of the Makkola segment. Length of compass 12 cm. C) Thinly bedded paraschist from the Tammijärvi area displaying locally intensive small-scale left-handed fault duplexing formed during plastic phase of the Leivonmäki shear zone. D) Mylonitised Jyväskylä suite granite from the Leivonmäki shear zone. Drill core from the vicinity of Toivakka. E) Plagioclase porphyrite belonging to the Makkola suite from the vicinity of Toivakka affected by brittle movements along the Leivonmäki shear zone. Diameter of the drill core in all photos 42 mm.

4.9 Later events

Kallio et al. (2018) interpreted that the Suolikko Pb–Zn mineralisation near Muurame is related to hydrothermal alteration caused by magmatism at 1785 Ma. If so, it is evidence for the existence of postorogenic magmatism within the CFGC, in addition to areas surrounding it (e.g. Eklund et al. 1998, Kontinen et al. 2013). Observations from Suolikko also provide ways to estimate the age of the activity along the numerous NW–SE-trending faults. The major ductile phase must have taken place before 1785 Ma, as the mineralisation is controlled by the ductile shear zone, but only affected by the late brittle activity along it.

No absolute age is available for the Rutalahti peridotites, but based on field relationships and magnetic anomaly patterns, they represent relatively young mantle-derived magmatism (Heilimo et al. 2018). They are spatially associated with large SE–NW-trending faults characterising the CFGC, and thus a plausible explanation would be that these faults provided pathways for ascending magmas. What is more difficult to explain is the follow-up question: what triggered the partial melting of the mantle generating these low volume ultramafic intrusions known from various parts of the CFGC (e.g. Salli 1967, Pipping 1972, Pääjärvi 1991)? A possible trigger for the partial melting could be the delamination of the crust thickened during the collisional stages of the Svecofennian orogeny.

Diabase dykes of the Kuisaari suite (Luukas et al. 2017) are likely to be part of the 1670–1620 Ma rapakivi magmatism in Southeast Finland (Rämö &

Haapala 2005). These dykes have the same structural trend as the northwest–southeast faults characterising the CFGC in the study area. This does not imply significant tectonic activity at this stage, but instead it is more probable that the diabase magma intruded into existing crustal weaknesses.

5 SUMMARY

Our interpretation of the geological evolution of CFGC and areas surrounding it during the Svecofennian orogen is summarised in Figure 6. The older Svecofennian magmatism aged 1.93–1.91 Ga and represented by the Savo arc ended with the collision of the arc with the Karelia craton. We interpret the Sm–Nd model ages reported earlier from the CFGC to simply represent the roots of the Savo arc and regard a separate "microcontinent" as an overinterpretation.

After the collision of the Savo arc, the protoliths of the voluminous Svecofennian paragneisses were deposited in a passive margin setting. Locally preserved mafic to ultramafic volcanic rocks represent extensional phases of the depositional basin(s). Subduction below the Savo arc and calc-alkaline magmatism commenced close to 1895 Ma, as witnessed by the oldest volcanic units and the Pirkanmaa intrusive suite. Vammala suite gabbro and ultramafic intrusions represent mantle-derived melts mainly intruding into the accretionary prism. Mantle-derived melts intruding the CFGC further evolved due to the larger crustal thickness, resulting in crustal contamination and fractional crystallisation being more significant. Calc-alkaline magmatism continued until 1875 Ma, peaking in the current erosion level close to 1885–1880 Ma, when the Jyväskylä suite was formed. The chemically A-type Saarijärvi suite was placed in proximity to crustal-scale transtensional faults at ~1880 Ma. Erosion and uplift shifted the pooling level of granitoid magmas to a lower level, resulting in more evolved granitoid magmas reaching the current erosion level at 1875 Ma. This explains the significant compositional similarities displayed by the Jyväskylä and Oittila suites.

After formation, the bedrock of the study area was subjected to deformation in connection with the further development of the Svecofennian orogeny further south. The Leivonmäki shear zone developed as a conjugate system to the Raahe–Ladoga system.

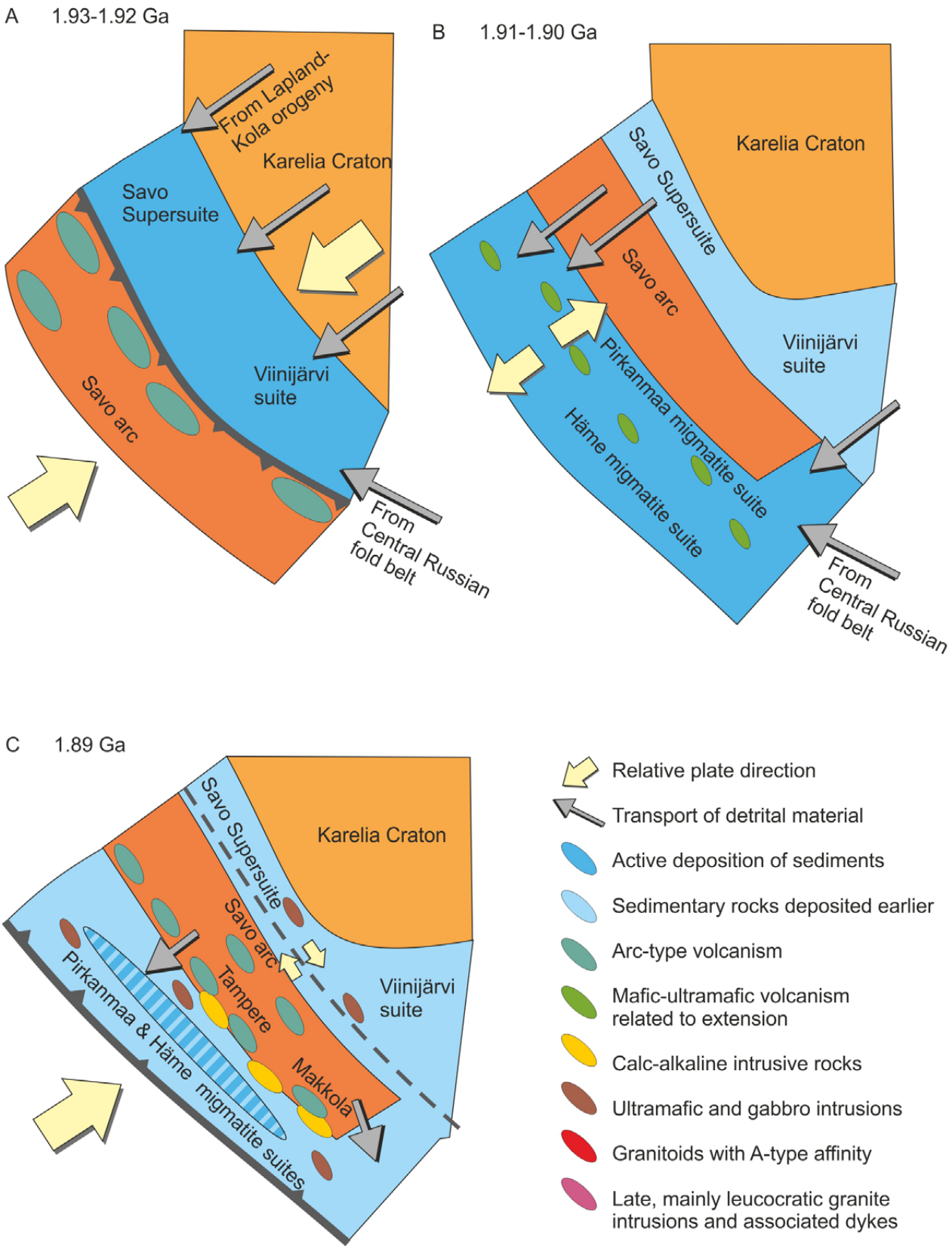

Fig. 6. Revised model for the development of the Svecofennian orogeny in Finland. A) At 1.93–1.91 Ga, the Savo arc is on top of a southwest-directed subduction zone. Paragneisses of the Karelia Province (Viinijärvi and Savo suites) are deposited along the passive margin of the Karelia craton. B) At 1.91 Ga, arc magmatism ends with the collision of the Savo arc and Karelia craton. Following this, the majority of the Svecofennian paragneisses (Häme and Pirkanmaa migmatite suites) are deposited as greywackes by turbidite currents. Local mafic to ultramafic volcanic interbeds represent extensional phases of the depositional basins. C) Close to 1.895 Ga, a subduction zone

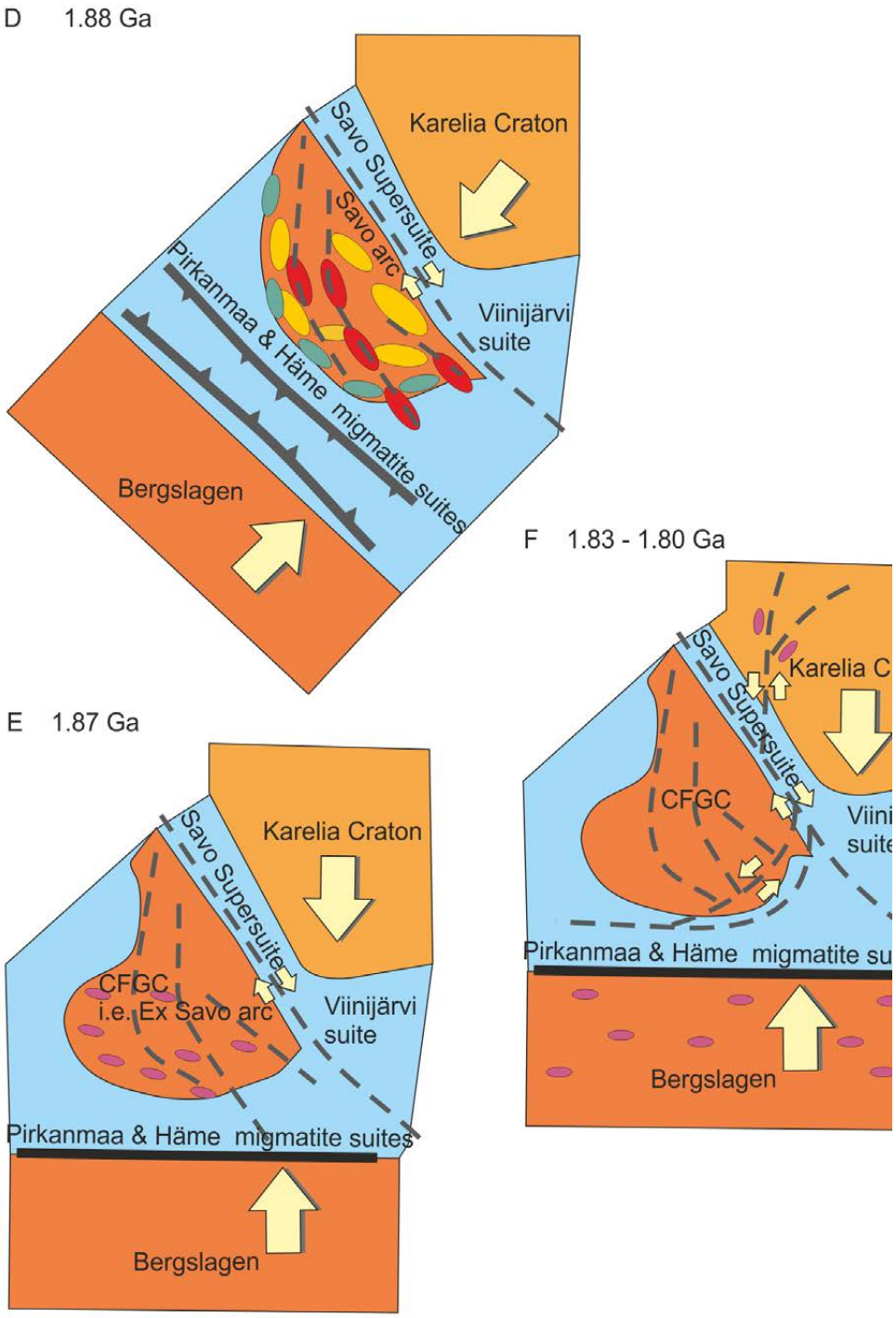

is formed west of the Savo arc and calc-alkaline magmatism commences. Paragneisses deposited before 1.90 Ga form the accretionary prism that is intruded by plutonic equivalents (Pirkanmaa intrusive suite, Vammala suite) of the volcanic units and overlain by fore-arc deposits. D) Plutonic activity forming the CFGC peaks (Jyväskylä suite), while volcanic activity continues. The linear Savo arc starts to round due to the beginning of collision with the Bergslagen block. Transtensional faults are formed within the CFGC, providing pathways for geochemically A-type magmas (Saarijärvi suite) ascending from the lower crust. E) Rounding of the CFGC continues. Uplift and erosion shift the pooling depth of calc-alkaline granitoid magmas below the current erosion level. Therefore, only more evolved melt fractions reach the current erosion level as small intrusions and dykes (Oittila suite). See the text for further discussion. F) Compression from the south–southeast continues and the sinistral Leivonmäki shear zone develops along the southeastern boundary of the CFGC as a conjugate of the Raahe–Ladoga shear zone. A similar conjugate is the Oulujärvi shear zone transecting the Karelia craton.

ACKNOWLEDGEMENTS

Reviews by Drs Matti Kurhila and Alexander Slabunov helped in improving the original manuscript.

REFERENCES

Bedrock of Finland - DigiKP. Digital map database [Electronic resource]. Espoo: Geological Survey of Finland [referred 31.04.2017]. Version 2.0.

Daly, J. S., Balagansky, V. V., Timmerman, M. J. & Whitehouse, M. J. 2006. The Lapland-Kola orogen: Palaeoproterozoic collision and accretion of the northern Fennoscandian lithosphere. In: Gee, D. G. & Stephenson, R. A. (eds) European Lithosphere Dynamics. London: Geological Society, Memoir 32, 561–578.

Eilu, P., Ahtola, T., Äikäs, O., Halkoaho, T., Heikura, P., Hulkki, H., Iljina, M., Juopperi, H., Karinen, T., Kärkkäinen, N., Konnunaho, J., Kontinen, A., Kontoniemi, O., Korkiakoski, E., Korsakova, M., Kuivasaari, T., Kyläkoski, M., Makkonen, H., Niiranen, T., Nikander, J., Nykänen, V., Perdahl, J.-A., Pohjolainen, E., Räsänen, J., Sorjonen-Ward, P., Tiainen, M., Tontti, M., Torppa, A. & Västi, K. 2012. Metallogenic areas in Finland. In: Eilu, P. (ed.) **Mineral deposits and metallogeny of Fennoscandia.** Geological Survey of Finland, Special paper 53, 207–342. Available at: http://tupa.gtk.fi/julkaisu/specialpaper/sp_053.pdf

Ekdahl, E. 1993. Early Proterozoic Karelian and Svecofennian formations and the Evolution of the Raahe-Ladoga Ore Zone, based on the Pielavesi area, central Finland. In: Ekdahl, E. Early Proterozoic Karelian and Svecofennian formations and the Evolution of the Raahe-Ladoga Ore Zone, based on the Pielavesi area, central Finland. Geological Survey of Finland, Bulletin 373, 1–137. Available at: http://tupa.gtk.fi/julkaisu/bulletin/bt_373.pdf

Eklund, O., Konopelko, D., Rutanen, H., Fröjdö, S. & Shebanov, A. D. 1998. 1.8 Ga Svecofennian post-collisional shoshonitic magmatism in the Fennoscandian Shield. Lithos 45, 87–108.

Elo, S. & Korja, A. 1993. Geophysical interpretation of the crustal and upper mantle structure in the Wiborg rapakivi granite area, southeastern Finland. Precambrian Research 64, 273–288.

Frosterus, B. 1903. Mikkeli. General Geological Map of Finland 1:400 000, Explanation to the map of Rocks, Sheet C2. Geological Survey of Finland. 102 p. (in Finnish). Available at: http://tupa.gtk.fi/kartta/kivilajikartta400/kls_c2.pdf

Heilimo, E., Ahven, M. & Mikkola, P. 2018. Geochemical characteristics of the plutonic rock units present at the southeastern boundary of the Central Finland Granitoid Complex. In: Mikkola, P., Hölttä, P. & Käpyaho, A. (eds) Development of the Paleoproterozoic Svecofennian orogeny: new constraints from the southeastern boundary of the Central Finland Granitoid Complex. Geological Survey of Finland, Bulletin 407. (this volume). Available at: https://doi.org/10.30440/bt407.6

Huhma, H., Claesson, S., Kinny, P. D. & Williams, I. S. 1991. The growth of Early Proterozoic crust: new evidence from Svecofennian zircons. Terra Nova 3, 175–179.

Kähkönen, Y. 2005. Svecofennian supracrustal rocks. In: Lehtinen, M., Nurmi, P. & Rämö, O. T. (eds) The Precambrian Bedrock of Finland - Key to the evolution of the Fennoscandian Shield. Elsevier Science B.V., 343–406.

Kähkönen, Y. & Huhma, H. 2012. Revised U-Pb zircon ages of supracrustal rocks of the Paleoproterozoic Tampere Schist Belt, southern Finland. In: Kukkonen, I. T., Kosonen E. M., Oinonen, K., Eklund, O., Korja, A., Korja, T., Lahtinen, R., Lunkka, J. P. & Poutanen, M. (eds) Lithosphere 2012 – Seventh Symposium on the Structure, Composition and Evolution of the Lithosphere in Finland. Programme and Extended Abstracts, Espoo, Finland, November 6-8, 2012. Institute of Seismology, University of Helsinki, Report S-56, 51–54. Available at: http://www.seismo.helsinki.fi/pdf/LITO2012.pdf

Kähkönen, Y. & Nironen, M. 1994. Supracrustal rocks around the Paleoproterozoic Haveri Au-Cu deposit, southern Finland. In: Nironen, M. & Kähkönen, Y. (eds) Geochemistry of Proterozoic supracrustal rocks in Finland: IGCP Project 179 stratigraphic methods as applied to the Proterozoic record and IGCP Project 217 Proterozoic geochemistry. Geological Survey of Finland, Special Paper 19, 101–116. Available at: http://tupa.gtk.fi/julkaisu/specialpaper/sp_019.pdf

Kallio, J. 1986. Joutsan kartta-alueen kallioperä. Summary: Pre-Quaternary Rocks of the Joutsa Map-Sheet area. Geological Map of Finland 1:100 000, Explanation to the Maps of Pre-Quaternary Rocks, Sheet 3122. Geological Survey of Finland. 56 p. Available at: http://tupa.gtk.fi/kartta/kallioperakartta100/kps_3122.pdf

Kallio, V., Mikkola, P., Huhma, H. & Niemi, S. 2018. Suolikko Pb-Zn mineralisation and its country rocks in Muurame, Central Finland. In: Mikkola, P., Hölttä, P. & Käpyaho, A. (eds) Development of the Paleoproterozoic Svecofennian orogeny: new constraints from the southeastern boundary of the Central Finland Granitoid Complex. Geological Survey of Finland, Bulletin 407. (this volume). Available at: https://doi.org/10.30440/bt407.10

Kontinen, A. & Paavola, J. 2006. A preliminary model of the crustal structure of the eastern Finland Archaean complex between Vartius and Vieremä, based on constraints from surface geology and FIRE 1 seismic survey. In: Kukkonen, I. T. & Lahtinen, R. (eds) Finnish Reflection Experiment FIRE 2001-2005. Geological Survey of Finland, Special Paper 43, 223–240. Available at: http://tupa.gtk.fi/julkaisu/specialpaper/sp_043.pdf

Kontinen, A., Huhma, H., Lahaye, Y. & O´Brien, H. 2013. New U-Pb zircon age, Sm-Nd isotope and geochemical data on Proterozoic granitic rocks in the area west of the Oulunjärvi Lake, Central Finland. In: Hölttä, P. (ed.) Current Research: GTK Mineral Potential Workshop, Kuopio, May 2012. Geological Survey of Finland, Report of Investigation 198, 70–74. Available at: http://tupa.gtk.fi/julkaisu/tutkimusraportti/tr_198.pdf

Korsman, K., Niemelä, R. & Wasenius, P. 1988. Multistage evolution of the Proterozoic crust in the Savo schist belt, eastern Finland. In: Korsman, K. (ed.) Tectono-metamorphic evolution of the Raahe-Ladoga zone, eastern Finland. Geological Survey of Finland, Bulletin 343, 89–96. Available at: http://tupa.gtk.fi/julkaisu/bulletin/bt_343.pdf

Kotilainen, A. K., Mänttäri, I., Kurhila, M., Hölttä, P. & Rämö, O. T. 2016. Evolution of a Palaeoproterozoic giant magmatic dome in the Finnish Svecofennian; New insights from U–Pb geochronology. Precambrian Research 272, 39–56.

Kousa, J. & Lundqvist, T. 2000. Svecofennian Domain. In: Lundqvist. T. & Autio, S. (eds) Description to the Bedrock Map of Central Fennoscandia (Mid-Norden). Geological Survey of Finland Special Paper 28, 47-75. Available at: http://tupa.gtk.fi/julkaisu/specialpaper/sp_028_pages_025_075.pdf

Kousa, J. & Luukas, J. 2007. Piippolan ja Rantsilan karttaalueiden kallioperä. Summary: Pre-Quaternary Rocks of the Piippola and Rantsila Map-Sheet Areas. Geological Map of Finland 1:100 000, Explanation to the Maps of Pre-Quaternary Rocks, Sheets 3411 & 3412. Geological Survey of Finland. 53 p. Available at: http://tupa.gtk.fi/kartta/kallioperakartta100/kps_3411_3412.pdf

Kousa, J., Huhma, H., Hokka, J. & Mikkola, P. 2018a. Extension of Svecofennian 1.91 Ga magmatism to the south, results of the reanalysed age determination samples from Joroinen, central Finland. In: Mikkola, P., Hölttä, P. & Käpyaho, A. (eds) Development of the Paleoproterozoic Svecofennian orogeny: new constraints from the southeastern boundary of the Central Finland Granitoid Complex. Geological Survey of Finland, Bulletin 407. (this volume). Available at: https://doi.org/10.30440/bt407.3

Kousa, J., Luukas, J., Huhma, H. & Mänttäri, I. 2013. Paleoproterozoic 1.93-1.92 Ga Svecofennian rock units in the northwestern part of the Raahe-Ladoga zone, central Finland. In: Hölttä, P. (ed.) Current Research: GTK Mineral Potential Workshop, Kuopio, May 2012. Geological Survey of Finland, Report of Investigation 198, 91–96. Available at: http://tupa.gtk.fi/julkaisu/tutkimusraportti/tr_198.pdf

Kousa, J., Mikkola, P. & Makkonen, H. 2018b. Paleoproterozoic mafic and ultramafic volcanic rocks in the South Savo region, eastern Finland. In: Mikkola, P., Hölttä, P. & Käpyaho, A. (eds) Development of the Paleoproterozoic Svecofennian orogeny: new constraints from the southeastern boundary of the Central Finland Granitoid Complex. Geological Survey of Finland, Bulletin 407. (this volume). Available at: https://doi.org/10.30440/bt407.4

Kousa, J., Nousiainen, M. & Niemi, S. 2017. Yksikkökuvausraportti Etelä-Savo. Geological Survey of Finland, archive report 67/2017. 17 p. (in Finnish). Available at: http://tupa.gtk.fi/raportti/arkisto/67_2017.pdf

Lahtinen, R. & Huhma, H. 1997. Isotopic and geochemical constraints on the evolution of the 1.93-1.79 Ga Svecofennian crust and mantle in Finland. Precambrian Research 82, 13–34.

Lahtinen, R., Huhma, H., Kähkönen, Y. & Mänttäri, I. 2009a. Paleoproterozoic sediment recycling during multiphase orogenic evolution in Fennoscandia, the Tampere and Pirkanmaa belts, Finland. Precambrian Research 174, 310–336.

Lahtinen, R., Huhma, H., Kontinen, A., Kohonen, J. & Sorjonen-Ward, P. 2010. New constraints for the source characteristics, deposition and age of the 2.1–1.9 Ga metasedimentary cover at the western margin of the Karelian Province. Precambrian Research 176, 77–93.

Lahtinen, R., Huhma, H. & Kousa, J. 2002. Contrasting source components of the Palaeoproterozoic Svecofennian metasediments: detrital zircon U–Pb, Sm–Nd and geochemical data. Precambrian Research 116, 81–109.

Lahtinen, R., Huhma, H., Lahaye, Y., Kousa, J. & Luukas, J. 2015. Archean-Proterozoic collision boundary in central Fennoscandia: revisited. Precambrian Research 261, 127–165.

Lahtinen, R., Huhma, H., Lahaye, Y., Lode, S., Heinonen, S., Sayab, M. & Whitehouse, M. J. 2016. Paleoproterozoic magmatism across the Archean-Proterozoic boundary in central Fennoscandia: Geochronology, geochemistry and isotopic data (Sm-Nd, Lu-Hf, O). Lithos 262, 507–525.

Lahtinen, R., Huhma, H., Sipilä, P. & Vaarma, M. 2017. Geochemistry, U-Pb geochronology and Sm-Nd data from the Paleoproterozoic Western Finland supersuite – A key component in the coupled Bothnian oroclines. Precambrian Research 299, 264–281.

Lahtinen, R., Johnston, S. T. & Nironen, M. 2014. The Bothnian coupled oroclines of the Svecofennian Orogen: a Palaeoproterozoic terrane wreck. Terra Nova 26, 330–335.

Lahtinen, R., Korja, A. & Nironen, M. 2005. Palaeoproterozoic tectonic evolution of the Fennoscandian Shield. In: Lehtinen, M., Nurmi, P. & Rämö, T. (eds) The Precambrian Bedrock of Finland – Key to the evolution of the Fennoscandian Shield. Amsterdam: Elsevier Science B.V., 418–532.

Lahtinen, R., Korja, A., Nironen, M. & Heikkinen, P. 2009b. Palaeoproterozoic accretionary processes in Fennoscandia. London: Geological Society, Special Publications 318, 237–256.

Lehtonen, M. I., Kujala, H., Kärkkäinen, N., Lehtonen, A., Mäkitie, H., Mänttäri, I., Virransalo, P. & Vuokko, J. 2005. Etelä-Pohjanmaan liuskealueen kallioperä. Summary: Pre-Quaternary rocks of the South Ostrobothnian Schist Belt. Geological Survey of Finland, Report of Investigation 158. 125 p. Available at: http://tupa.gtk.fi/julkaisu/tutkimusraportti/tr_158.pdf

Luosto, U., Tiira, T., Korhonen, H., Azbel, I., Burmin, V., Buyanov, A., Kosminskaya, I., Ionkis, V. & Sharov, N. 1990. Crust and upper mantle structure along the DSS Baltic profile in SE Finland. Geophysical Journal International 101, 89–110.

Luukas, J., Kousa, J., Nironen, M. & Vuollo, J. 2017. Major stratigraphic units in the bedrock of Finland, and an approach to tectonostratigraphic division. In: Nironen, M. (ed.) Bedrock of Finland at the scale 1:1 000 000 - Major stratigraphic units, metamorphism and tectonic evolution. Geological Survey of Finland, Special Paper 60, 9–40. Available at: http://tupa.gtk.fi/julkaisu/specialpaper/sp_060.pdf

Luukkonen, A. 1994. Main geological features, metallogeny and hydrothermal alteration phenomena of certain gold and gold-tin-tungsten prospects in southern Finland. In: Luukkonen, A. Main geological features, metallogeny and hydrothermal alteration phenomena of certain gold and gold-tin-tungsten prospects in southern Finland. Geological Survey of Finland, Bulletin 377, 1–153. Available at: http://tupa.gtk.fi/julkaisu/bulletin/bt_377.pdf

Mikkola, P. & Niemi, S. 2015. Hollan kairaukset Joutsassa 2014. Geological Survey of Finland, archive report 31/2015, 5 p. (in Finnish). Available at: http://tupa.gtk.fi/raportti/arkisto/31_2015.pdf

Mikkola, P. & Niemi, S. 2016. Kairaukset Toivakan Hamperinjoella ja Toivakanlehdossa vuonna 2015. Geological Survey of Finland, archive report 9/2016, 6 p. (in Finnish). Available at: http://tupa.gtk.fi/raportti/arkisto/9_2016.pdf

Mikkola, P., Heilimo, E., Aatos, S., Ahven, M., Eskelinen, J., Halonen, S., Hartikainen, A., Kallio, V., Kousa, J., Luukas, J., Makkonen, H., Mönkäre, K., Niemi, S., Nousiainen, M., Romu, I. & Solismaa, S. 2016a. Jyväskylän seudun kallioperä. Summary: Bedrock of the Jyväskylä area. Geological Survey of Finland,

Report of Investigation 227. 95 p., 6 apps. Available at: http://tupa.gtk.fi/julkaisu/tutkimusraportti/tr_227.pdf

Mikkola, P., Huhma, H., Romu, I. & Kousa, J. 2018a. Detrital zircon ages and geochemistry of the metasedimentary rocks along the southeastern boundary of the Central Finland Granitoid Complex. In: Mikkola, P., Hölttä, P. & Käpyaho, A. (eds) Development of the Paleoproterozoic Svecofennian orogeny: new constraints from the southeastern boundary of the Central Finland Granitoid Complex. Geological Survey of Finland, Bulletin 407. (this volume). Available at: https://doi.org/10.30440/bt407.2

Mikkola, P., Lukkarinen, H. & Luukas, J. 2016b. Suonenjoen kartta-alueen 3241 kallioperä ja kivilajiyksiköt. Geological Survey of Finland, archive report 29/2016. 29 p., 5 apps. (in Finnish). Available at: http://tupa.gtk.fi/raportti/arkisto/29_2016.pdf

Mikkola, P., Mönkäre, K., Ahven, M. & Huhma, H. 2018b. Geochemistry and age of the Paleoproterozoic Makkola suite volcanic rocks in central Finland. In: Mikkola, P., Hölttä, P. & Käpyaho, A. (eds) Development of the Paleoproterozoic Svecofennian orogeny: new constraints from the southeastern boundary of the Central Finland Granitoid Complex. Geological Survey of Finland, Bulletin 407. (this volume). Available at: https://doi.org/10.30440/bt407.5

Mikkola, P, Niskanen, M. & Hokka, J. 2018c. Harjujärvensuo gold mineralisation in Leivonmäki, Central Finland. In: Mikkola, P., Hölttä, P. & Käpyaho, A. (eds) Development of the Paleoproterozoic Svecofennian orogeny: new constraints from the southeastern boundary of the Central Finland Granitoid Complex. Geological Survey of Finland, Bulletin 407. (this volume). Available at: https://doi.org/10.30440/bt407.9

Nikkilä, K., Mänttäri, I., Nironen, M., Eklund, O. & Korja, A. 2016. Three stages to form a large batholith after terrane accretion – An example from the Svecofennian orogen. Precambrian Research 281, 618–638.

Nironen, M. 1997. The Svecofennian Orogen: a tectonic model. Precambrian Research 86, 21–44.

Nironen, M. 2003. Keski-Suomen granitoidikompleksi. Karttaselitys. Summary: Central Finland Granitoid Complex - Explanation to a map. Geological Survey of Finland, Report of Investigation 157. 45 p. Available at: http://tupa.gtk.fi/julkaisu/tutkimusraportti/tr_157.pdf

Nironen, M. 2017. Guide to the Geological Map of Finland – Bedrock 1:1 000 000. In: Nironen, M. (ed.) Bedrock of Finland at the scale 1:1 000 000 - Major stratigraphic units, metamorphism and tectonic evolution. Geological Survey of Finland, Special Paper 60, 41–76. Available at: http://tupa.gtk.fi/julkaisu/specialpaper/sp_060.pdf

Nironen, M. & Mänttäri, I. 2012. Timing of accretion, intra-orogenic sedimentation and basin inversion in the Paleoproterozoic Svecofennian orogen: The Pyhäntaka area, southern Finland. Precambrian Research 192–195, 34–51.

Nironen, M., Elliot, B. A. & Rämö, O. T. 2000. 1.88–1.87 Ga post-kinematic intrusions of the Central Finland Granitoid Complex: a shift from C-type to A-type magmatism during lithospheric convergence. Lithos 53, 37–58.

Nironen, M., Kousa, J., Luukas, J. & Lahtinen, R. (eds) 2016. Geological Map of Finland – Bedrock 1:1 000 000. Espoo: Geological Survey of Finland. Available at: http://tupa.gtk.fi/kartta/erikoiskartta/ek_097_300dpi.pdf

Pääjärvi, A. 1991. Vesannon kartta-alueen kallioperä. Summary: Pre-Quaternary Rocks of the Vesanto Map-Sheet area. Geological Map of Finland 1:100 000, Explanation to the Maps of Pre-Quaternary Rocks, Sheet 3313. Geological Survey of Finland. 64 p. Available at: http://tupa.gtk.fi/kartta/kallioperakartta100/kps_3313.pdf

Pajunen, M., Airo, M-L., Elminen, T., Mänttäri, I., Niemelä, R., Vaarma, M., Wasenius, P. & Wennerström, M. 2008. Tectonic evolution of the Svecofennian crust in southern Finland. In: Pajunen, M. (ed.) Tectonic evolution of the Svecofennian crust in southern Finland - a basis for characterizing bedrock technical properties. Geological Survey of Finland, Special Paper 47, 15-160. Available at: http://tupa.gtk.fi/julkaisu/specialpaper/sp_047.pdf

Peltonen, P. 1995. Petrogenesis of ultramafic rocks in the Vammala Nickel Belt: Implications for crustal evolution of the early Proterozoic Svecofennian arc terrane. Lithos 34, 253–274.

Peltonen, P. 2005a. Ophiolites. In: Lehtinen, M., Nurmi, P. A. & Rämö, O. T. (eds) Precambrian geology of Finland – Key to the evolution of the Fennoscandian Shield. Amsterdam: Elsevier, Developments in Precambrian Geology 14, 237–278.

Peltonen, P. 2005b. Mafic-Ultramafic Intrusions of the Svecofennian Orogen. In: Lehtinen, M., Nurmi, P. A. & Rämö, O. T. (eds) Precambrian geology of Finland – Key to the evolution of the Fennoscandian Shield. Amsterdam: Elvesier, Developments in Precambrian Geology 14, 413–447.

Pipping, F. 1972. Viitasaaren kartta-alueen kallioperä. Summary: Pre-Quaternary Rocks of the Viitasari Map-Sheet area. Geological Map of Finland 1:100 000, Explanation to the Maps of Pre-Quaternary Rocks, Sheet 3311. Geological Survey of Finland. 23 p. Available at: http://tupa.gtk.fi/kartta/kallioperakartta100/kps_3311.pdf

Rämö, O. T. & Haapala, I. 2005. Rapakivi granites. In: Lehtinen, M., Nurmi, P. & Rämö, T. (eds) The Precambrian Bedrock of Finland - Key to the evolution of the Fennoscandian Shield. Elsevier Science B.V., 533–562.

Rämö, O. T., Vaasjoki, M., Mänttäri, I., Elliott, B. A. & **Nironen, M. 2001.** Petrogenesis of the Post-kinematic Magmatism of the Central Finland Granitoid Complex I; Radiogenic Isotope Constraints and Implication for Crustal Evolution. Journal of Petrology 42, 1971–1993.

Salli, I. 1967. Kallioperäkarttojen selitys, Lestijärvi-Reisjärvi. Summary: Pre-Quaternary Rocks of the Lestijärvi-Reisjärvi Map-Sheet area. Geological Map of Finland 1:100 000, Explanation to the Maps of Pre-Quaternary Rocks, Sheets 2341 and 2343. Geological Survey of Finland. 43 p. Available at: http://tupa.gtk.fi/kartta/kallioperakartta100/kps_2341_2343.pdf

Samsonov, A. V., Spiridonov, V. A., Larionova, Y. O. & Larionov, A. N. 2016. The Central Russian fold belt: Paleoproterozoic boundary of Fennoscandia and Volgo-Sarmatia, the East European Craton. In: Abstracts of the 32nd Nordic Geological Winter Meeting. Bulletin of the Geological Society of Finland, Special Volume 162. Available at: http://www.geologinenseura.fi/bulletin/Special_Volume_1_2016/BGSF-NGWM2016_Abstract_Volume.pdf

Sorjonen-Ward, P. 2006. Geological and structural framework and preliminary interpretation of the FIRE 3 and FIRE 3A reflection seismic profiles, central Finland. In: Kukkonen, I. T. & Lahtinen, R. (eds) Finnish Reflection Experiment FIRE 2001–2005. Geological Survey of Finland, Special paper 43, 105–159. Available at: http://tupa.gtk.fi/julkaisu/specialpaper/sp_043.pdf

Taira, A. 2001. Tectonic Evolution of the Japanese Island Arc System. Annual Review of Earth and Planetary Sciences 29, 109–134.

Tiainen, M. & Kähkönen, Y. 1994. Geochemistry of the Paleoproterozoic andesitic to rhyolitic arc-type metavolcanic rocks at Haukkamaa, Kuru, central Finland. In: Nironen, M. & Kähkönen, Y. (eds) Geochemistry of Proterozoic supracrustal rocks in Finland: IGCP Project 179 stratigraphic methods as applied to the Proterozoic record and IGCP Project 217 Proterozoic geochemistry. Geological Survey of Finland, Special Paper 19, 29–44. Available at: http://tupa.gtk.fi/julkaisu/specialpaper/sp_019.pdf

Vaasjoki, M. & Sakko, M. 1988. Evolution of the Raahe–Ladoga zone in Finland: Isotopic constraints. In: Korsman, K. (ed.) Tectono-metamorphic evolution of the Raahe-Ladoga zone, eastern Finland. Geological Survey of Finland, Bulletin 343, 7–31. Available at: http://tupa.gtk.fi/julkaisu/bulletin/bt_343.pdf

Vaasjoki, M., Huhma, H., Lahtinen, R. & Vestin, J. 2003. Sources of Svecofennian granitoids in the light of ion probe U-Pb measurements on their zircons. Precambrian Research 121, 251–262.

Virtanen, V. J. & Heilimo, E. 2018. Petrology of the geochemically A-type Saarijärvi suite: evidence for bimodal magmatism. In: Mikkola, P., Hölttä, P. & Käpyaho, A. (eds) Development of the Paleoproterozoic Svecofennian orogeny: new constraints from the southeastern boundary of the Central Finland Granitoid Complex. Geological Survey of Finland, Bulletin 407. (this volume). Available at: https://doi.org/10.30440/bt407.7

Wittmann, H., von Blanckenburg, F., Kruesmann, T., Norton, K. P. & Kubik, P. 2007. The relation between rock uplift and denudation from cosmogenic nuclides in river sediment in the Central Alps of Switzerland. Journal of Geophysical Research, Earth Surface 112, F04010.

Development of the Paleoproterozoic Svecofennian orogeny: new constraints from the southeastern boundary of the Central Finland Granitoid Complex
Edited by Perttu Mikkola, Pentti Hölttä and Asko Käpyaho
Geological Survey of Finland, Bulletin 407, 28-55, 2018

DETRITAL ZIRCON AGES AND GEOCHEMISTRY OF THE METASEDIMENTARY ROCKS ALONG THE SOUTHEASTERN BOUNDARY OF THE CENTRAL FINLAND GRANITOID COMPLEX

by

Perttu Mikkola[1)], Hannu Huhma[2)], Ilona Romu[1)] and Jukka Kousa[1)]

Mikkola, P., Huhma, H., Romu, I. & Kousa, J. 2018. Detrital zircon ages and geochemistry of the metasedimentary rocks along the southeastern boundary of the Central Finland Granitoid Complex. *Geological Survey of Finland, Bulletin 407*, 28–55, 16 figures and 1 table.

The metasedimentary rocks along the southeastern boundary of the Central Finland Granitoid Complex are variably migmatized greywackes, originally deposited as turbidites. They have been classified into several geological units that cannot be distinguished on a geochemical basis. Six samples were collected for detrital zircon study, five from unmigmatized and one from strongly migmatitic rock. In addition, new data are provided here from two previously studied samples. Most studied samples contained a zircon population typical of the paragneisses of central and southern Finland: a bimodal population with Neoarchean (ca. 2700 Ma) and Paleoproterozoic (2100–1920 Ma) peaks. In addition, some samples also recorded a weak metamorphic overprint at 1900 Ma. The one studied migmatitic sample did not contain Archean detrital material and yielded ca. 1885 Ma as the age of anatexis. Based on the results, the majority, if not all, of the paragneisses in the study area were deposited before the onset of volcanism (1895 Ma) in the study area. The combination of the observed zircon age patterns and abrupt changes in the metamorphic degree would have required large vertical movements in the late stages of geological evolution. The results also warrant further discussion on the unit division of the voluminous Svecofennian paragneisses.

Appendix 1 is available at: hhttp://tupa.gtk.fi/julkaisu/liiteaineisto/bt_407_appendix_1.pdf

Electronic Appendix is available at: http://tupa.gtk.fi/julkaisu/liiteaineisto/bt_407_electronic_appendix.xlsx

Keywords: turbidite, paragneiss, migmatites, metamorphic rocks, Paleoproterozoic, Svecofennian, Finland, zircon, U/Pb, geochronology

[1)] *Geological Survey of Finland, P.O. Box 1237, FI-70211 Kuopio, Finland*
[2)] *Geological Survey of Finland, P.O. Box 96, FI-02151 Espoo, Finland*
E-mail: perttu.mikkola@gtk.fi

VERTAISARVIOITU
KOLLEGIALT GRANSKAD
PEER-REVIEWED
www.tsv.fi/tunnus

https://doi.org/10.30440/bt407.2

Editorial handling by Pentti Hölttä and Asko Käpyaho.

Received 27 June 2017; Accepted 29 June 2018

1 INTRODUCTION

Due to a research history over a century long, the overall development of the Svecofennian orogen covering southern and central Finland, as well as adjacent parts of Sweden and Russian, is relatively well constrained. However, interpretations vary and numerous questions regarding the original relationships between different rock units remain open. One of these open questions concerns the unit division of the voluminous paragneisses (Fig. 1). Single-grain studies on detrital zircons, following the early work of Huhma et al. (1991) and Claesson et al. (1993), have refined our understanding of the Svecofennian depositional history. The majority of the metasedimentary rocks were deposited before the onset of younger Svecofennian volcanism (1895 Ma) and magmatism forming the Central Finland Granitoid Complex (hereafter the CFGC; Lahtinen et al. 2002, 2009, 2010, 2017, Kotilainen et al. 2016). A second intracratonic depositional phase occurred following the main collisional phase of the orogeny, i.e. after 1.88 Ga (Korsman et al. 1988, Bergman et al. 2008, Lahtinen & Nironen 2010, Nironen & Mänttäri 2012). Paragneisses and quartzites belonging to this second depositional phase are known from sporadic localities in southern and central Finland.

This study includes both geochemical and detrital zircon data from the southeastern margin of the CFGC from metasedimentary rocks belonging to various geological units. The results are used to evaluate the origin of, and relationships between, the different geological units, which presently occur in close proximity. In addition, the study aimed at clarifying the relationships between the sedimentary and volcanic rock units in the area and evaluating the possible presence of sedimentary rocks belonging to the younger Svecofennian (<1.88 Ga) depositional phase.

2 GEOLOGICAL SETTING

The CFGC is surrounded by metasedimentary rock units, which are often, but not always, migmatized. Along the northern boundary of the CFGC, these metasedimentary rocks belong to the Savo supersuite (Fig. 1). To the south, the CFGC is bounded by the Pirkanmaa migmatite suite of the Western Finland supersuite, whose other suites form the western boundary of the CFGC (Luukas et al. 2017, Nironen 2017). The Häme migmatite suite, belonging to the Southern Finland supersuite, borders the Pirkanmaa migmatite suite to the south and the east. All of the above-mentioned units mainly consist of greywackes, typically containing black schist interbeds of variable thickness (Matisto 1976, Lahtinen 1996, Kilpeläinen 1998). The volcanic interlayers are scarce, mafic to ultramafic in composition and interpreted to represent extensional phases in the evolution of the sedimentary basin(s) (Lahtinen 1996, Korsman et al. 1997, Lahtinen et al. 2017, Kousa et al. 2018b).

In all of these metasedimentary units, the majority of studied samples contain detrital zircon populations that display roughly similar age distributions with two distinctive peaks: Neoarchean ca. 2.7 Ga and Paleoproterozoic 2.05–1.92 Ga (e.g. Huhma et al. 1991, Lahtinen et al. 2002, 2009, 2017, Kotilainen et al. 2016). A similar distribution is found in the Viinijärvi suite (aka Upper Kaleva, Fig. 1) greywackes further east and interpreted as being deposited on the passive margin of the Karelian craton (Lahtinen et al. 2010). The 1895 Ma Pirkanmaa intrusive suite defines the minimum age for the Pirkanmaa migmatite suite (Kallio 1986, Mikkola et al. 2016, Heilimo et al. 2018).

The lowest formation of the classical Tampere group, i.e. the Myllyniemi formation (Kähkönen & Leveinen 1994), consists of well-preserved greywackes that are similar to the paragneisses of the Pirkanmaa migmatite suite in both whole-rock composition and the detrital zircon population (Lahtinen et al. 2009). In addition to the interpreted geological context, the only significant difference between the Myllyniemi formation and the Pirkanmaa migmatitic paragneisses is the higher metamorphic degree of the latter. Karppanen (1970) interpreted that some of the well-preserved greywackes in our study area could be correlated with the sedimentary members of the Tampere group.

All of the units described above have been interpreted as being deposited in a passive margin setting before the onset of subduction and calc-

alkaline volcanism (1895–1875 Ma) along the southern and western boundary (in current geometry) of the CFGC (Kähkönen 2005, Lahtinen et al. 2009, Kähkönen & Huhma 2012, Mikkola et al. 2018b). Based on similarities in age and geochemistry, Mikkola et al. (2018b) concluded that the mainly volcanic Makkola suite (Fig. 2) in our main study area represents the same phase as the volcanic rocks of the Tampere group, although direct correlation is not possible. One metasedimentary sample from the Pirkanmaa migmatite suite, taken near Tampere, containing zircons that fall into the bracket of the active volcanic phase, was interpreted by Lahtinen et al. (2009) to represent a separate fore-arc unit.

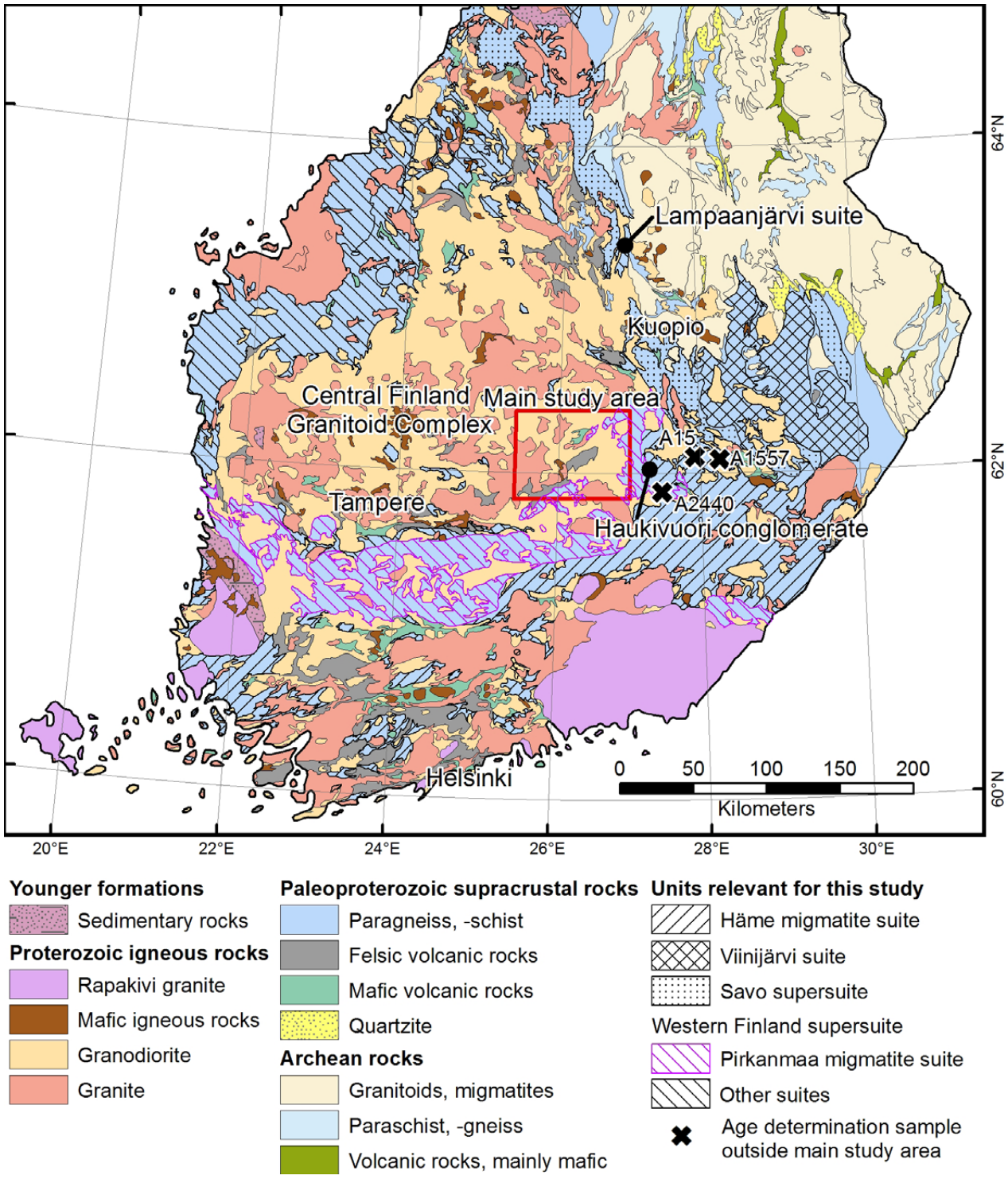

Fig. 1. Bedrock map of southern and central Finland with the geological units relevant for this paper highlighted. Also shown are the locations of the age determination samples outside our main study area. Note that the Myllyniemi formation in the Tampere region cannot be separated on the map due to its small areal extent. Map modified from Nironen et al. (2016) and Bedrock of Finland - DigiKP.

3 METHODS AND MATERIALS

All of the analytical methods are described in Appendix 1. Analytical data from 96 outcrop and drill core samples were used in this study. Five of these originate from Rasilainen et al. (2007) and five have been published by Mikkola et al. (2016). All samples were analysed using XRF for the main and certain trace elements and 49 using ICP-MS for additional trace elements. All of the geochemical data are listed in the Electronic Appendix and representative data are presented in Table 1. The geochemical data were plotted using the Geochemical Data Toolkit (GCDKit) program of Janoušek et al. (2006).

Four age determination samples were taken from selected outcrops and two from drill cores. Single-grain analyses were performed on four of the samples (A2395, A2396, A2397, A2398) using a Cameca IMS 1280 multi-collector ion microprobe at the NORDSIM facility, National Museum of Natural History, Stockholm, Sweden. Two samples (A2440, A2450) were studied in Espoo using a Nu Plasma AttoM single collector ICP-MS. A Nu Plasma HR multicollector ICP-MS was used for additional analyses from two pre-existing age determination samples (A15 & A1557, Lahtinen et al. 2002).

4 RESULTS

4.1 Field observations and petrography

4.1.1 Pirkanmaa migmatite suite

Most of the rocks belonging to the Pirkanmaa migmatite suite have been partially melted, but not all, as two unmigmatized lithodemes were also included in the suite by Mikkola et al. (2016). In addition to metasedimentary rocks, the suite in the study area also includes picritic volcanic rocks (Kousa et al. 2018b).

Undefined migmatitic paragneisses of the Pirkanmaa migmatite suite (hereafter Pirkanmaa paragneisses) form variably sized areas south of the Leivonmäki shear zone (Fig. 2). In addition to larger intact areas, they are typically met as enclaves in the plutonic rocks belonging to the Pirkanmaa intrusive suite (Mikkola et al. 2016). The main minerals of the Pirkanmaa paragneisses are quartz, plagioclase and biotite, and in some samples also K-feldspar and hornblende. Metamorphic index minerals are rarely abundant, the most common ones being garnet and sillimanite, with less common ones being cordierite and orthopyroxene. The leucosome is typically trondhjemitic, although leucogranodiorite variants exist. Locally, the Pirkanmaa paragneisses contain black schist interbeds, represented by two samples in our material.

The Tammijärvi greywacke lithodeme (hereafter Tammijärvi greywackes), belonging to the Pirkanmaa migmatite suite, is located in the southernmost part of the study area (Fig. 2). Their northern contact with the Makkola suite, predominantly consisting of volcanic rocks (Mikkola et al. 2018b), is formed by the Leivonmäki shear zone. The central parts of the lithodeme are intruded by small diorite intrusions. In the south, the greywackes are in contact with variably sized granitoid intrusions. In northern parts, the lithodeme is unmigmatized and does not contain granitoid dykes, while further south the degree of partial melting increases and granitoid dykes related to the intrusives appear, but are not abundant. The contact to the migmatized Pirkanmaa paragneisses is gradual.

The majority of the rocks are greywackes with variable amounts of mineral clasts (plagioclase and quartz) 1–2 mm in size (Fig. 3B). Lithic fragments are scarce and mainly consist of quartz grain aggregates. The groundmass of the greywackes consists of quartz, biotite, plagioclase and K-feldspar present in various proportions. Interbeds of conglomerate and metapelite are locally abundant in the greywackes. Black schist interbeds are rarely observable at outcrops, but can be recognized as magnetic and conductivity anomalies on aerogeophysical maps.

The Rusalansuo greywacke lithodeme (hereafter Rusalansuo greywackes) is present in two locations: in the vicinity of the Kangasniemi parish and in the Rusalansuo-Pieksämäki area in the northeasternmost corner of the main study area. These greywackes differ from the Tammijärvi greywackes

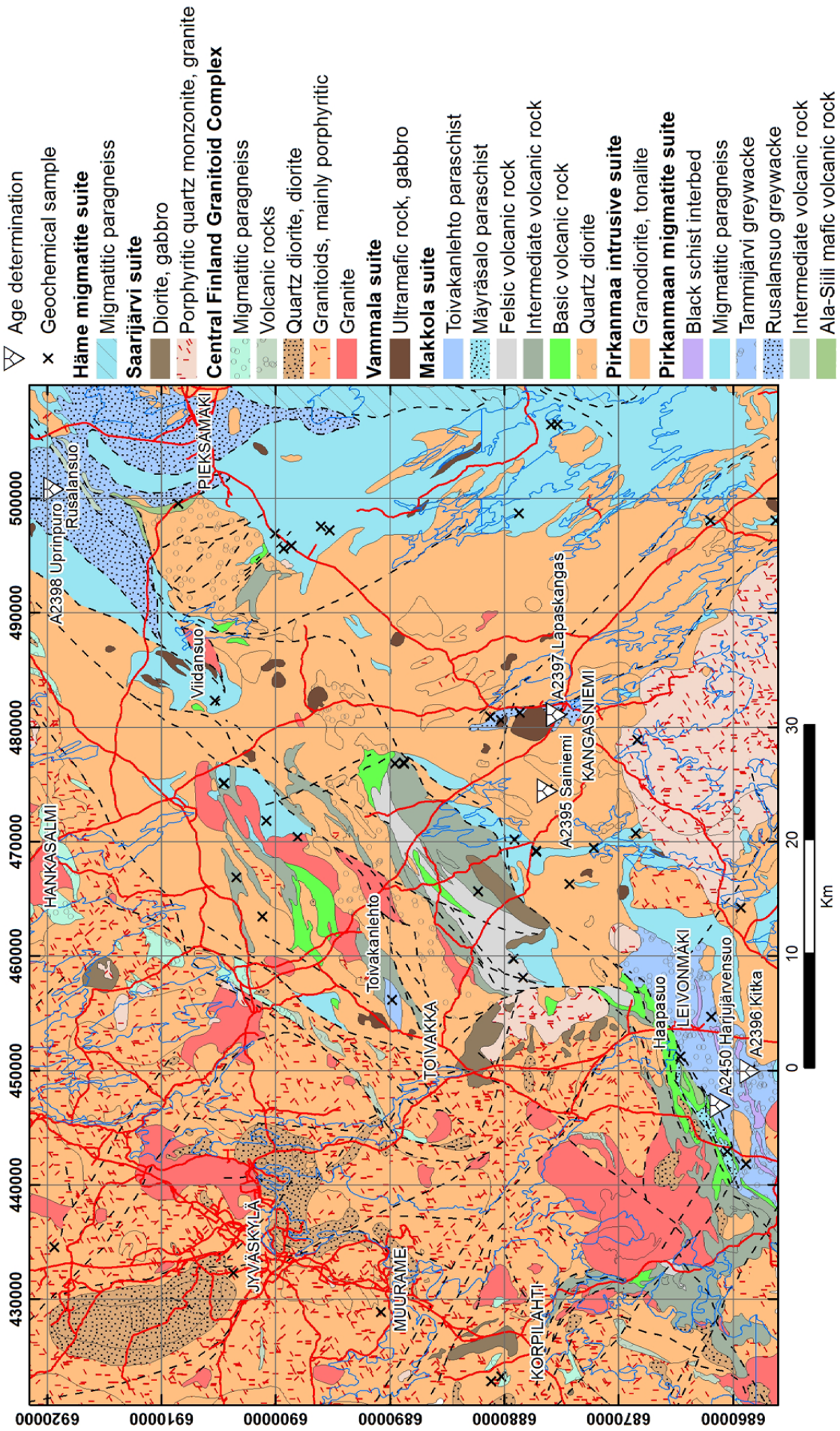

Fig. 2. Bedrock map of the main study area with sample locations. Map modified from Mikkola et al. (2016) and Bedrock of Finland – DigiKP.

by the absence of black schist interbeds. Near Kangasniemi, these relatively homogeneous greywackes lack conglomerate interbeds and are locally weakly migmatized, but significantly less than the Pirkanmaa paragneisses (Fig. 3A vs 3C). This weak anatectic event has been interpreted as contact metamorphism caused by the intrusion of the Salmenkylä gabbro (Mikkola et al. 2016). At Rusalansuo, the greywackes contain quartz pebble conglomerate (Fig. 3D) and intermediate volcanic interbeds. The presence of cordierite in Kangasniemi greywackes indicates either a slightly higher metamorphic grade or higher MgO and Al_2O_3 content in this subarea. Otherwise, Rusalansuo and Kangasniemi greywackes are alike: quartz, biotite, plagioclase and K-feldspar groundmass hosts quartz clasts. In the two areas, the contacts towards the surrounding more intensively metamorphosed rocks are sharp and most likely tectonic.

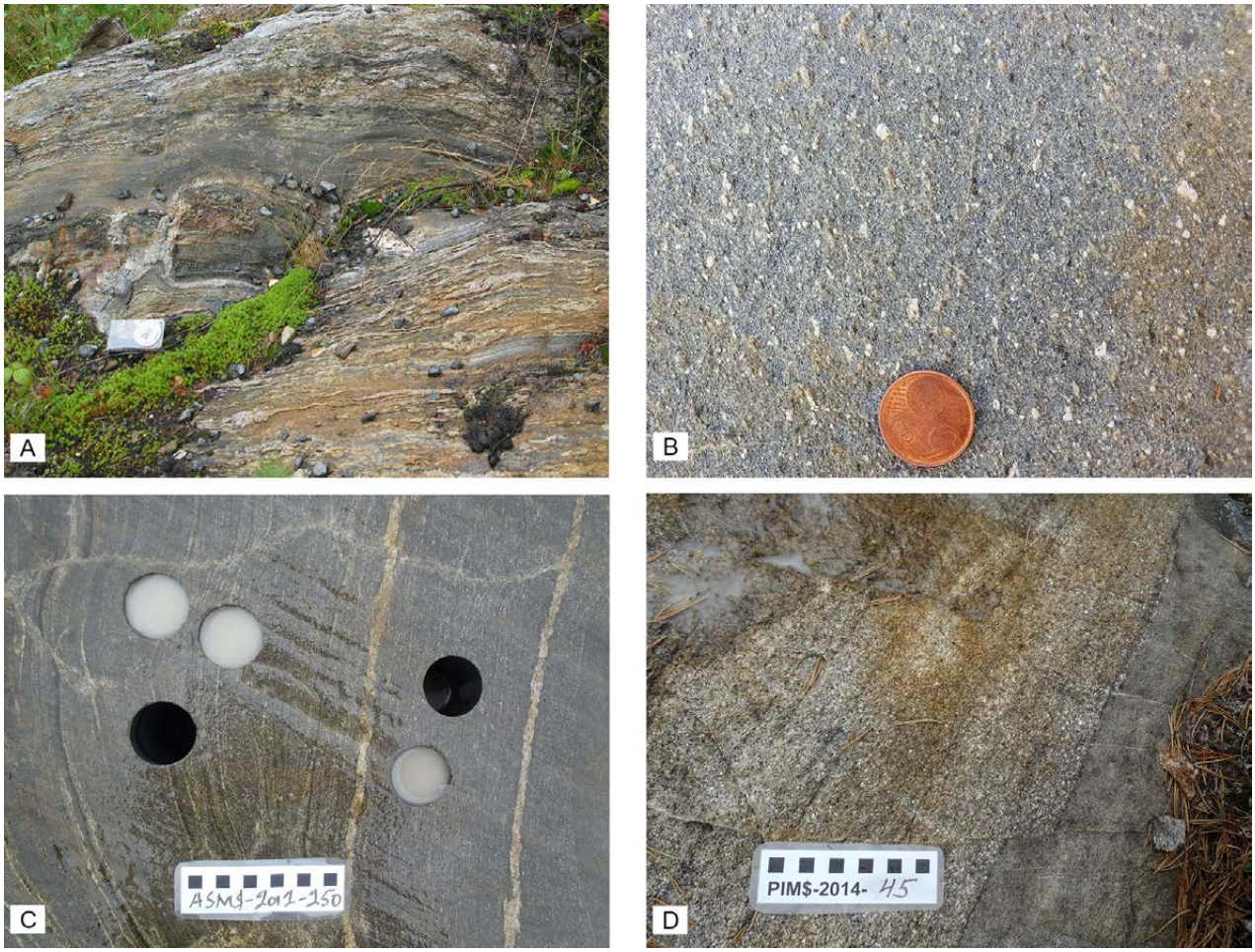

Fig. 3. A) Sample location A2395 Sainiemi, representing the migmatized Pirkanmaa paragneisses occurring in various parts of the study, which occur as large intact areas and variably sized xenoliths in the Pirkanmaa intrusive suite rocks. Length of the compass 12 cm. B) Sample location A2396 Kitka, representing well-preserved Tammijärvi greywackes with mm-scale clasts of plagioclase and quartz. Diameter of the coin 21 mm. C) Weakly migmatized Rusalansuo greywacke from sample location A2397 Lapaskangas. Scale bar with cm division. D) Contact between quartz pebble conglomerate and greywacke from sample location A2398 Rusalansuo. The sample was taken from a greywacke similar in appearance to that on the right in the picture. Scale bar with cm division.

4.1.2 Makkola suite

The Toivakanlehto paraschist lithodeme (hereafter Toivakanlehto paraschists) in the central part of the study area is included in the Makkola suite based on two factors: its location in the vicinity of volcanic units (Fig. 2) and the presence of uralite porphyrite dykes resembling those of the Makkola suite. As the lithodeme name implies, the majority of the rocks are paraschists (Fig. 4A & 4C), and greywackes (Fig. 4B) and calc-silicate rocks are present as interbeds. The fine-grained groundmass of the paraschist consists of variable amounts of quartz, biotite, muscovite and plagioclase. The observed porphyroblasts include K-feldspar and garnet. Muscovite filled pseudomorphs, possibly after andalusite, are also present. The compositional variation of the beds is reflected by the differences in the amount and type of the porphyroblasts.

The Mäyräsalo paraschist lithodeme (hereafter Mäyräsalo paraschists) is present in the southernmost part of the study area, within the Leivonmäki shear zone near the contact of the Tammijärvi greywackes and Makkola suite. The Holla iron formation occurs as an interlayer less than 10 m thick in the Mäyräsalo paraschist. Most of the unit consists of often thinly layered muscovite-biotite paraschist, and coarser grained interbeds are scarce. The observed porphyroblasts are muscovite pseudomorphs, possibly after andalusite, and staurolite.

Black schist beds occurring in the *Teuraanmäki intermediate volcanic rock* lithodeme (hereafter Teuraanmäki black schist) are also included in the material of this study. These black schists occur as relatively thick (<50 m) interbeds in comparatively homogeneous intermediate volcanic rocks.

4.1.3 Central Finland paragneisses

Paragneiss enclaves varying in scale from a few centimetres to a few kilometres are present in the plutonic rocks of the CFGC (Fig. 2). These rocks are hereafter referred to as Central Finland paragneisses. These paragneisses are variably migmatized and do not differ in appearance from Pirkanmaa paragneisses (Fig. 3A vs. 5B).

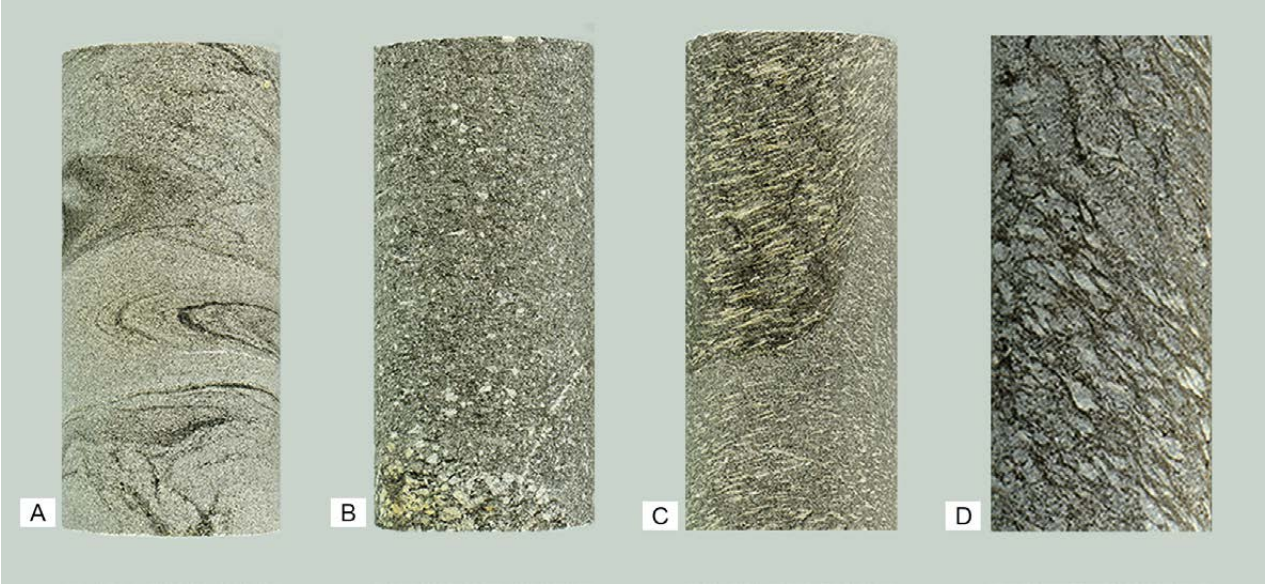

Fig. 4. A) Folded paraschist, B) greywacke and C) paraschist with abundant muscovite filled pseudomorphs from Toivakanlehto. D) Sillimanite-biotite paragneiss from Loukee (A2440). Diameter of drill cores 42 mm.

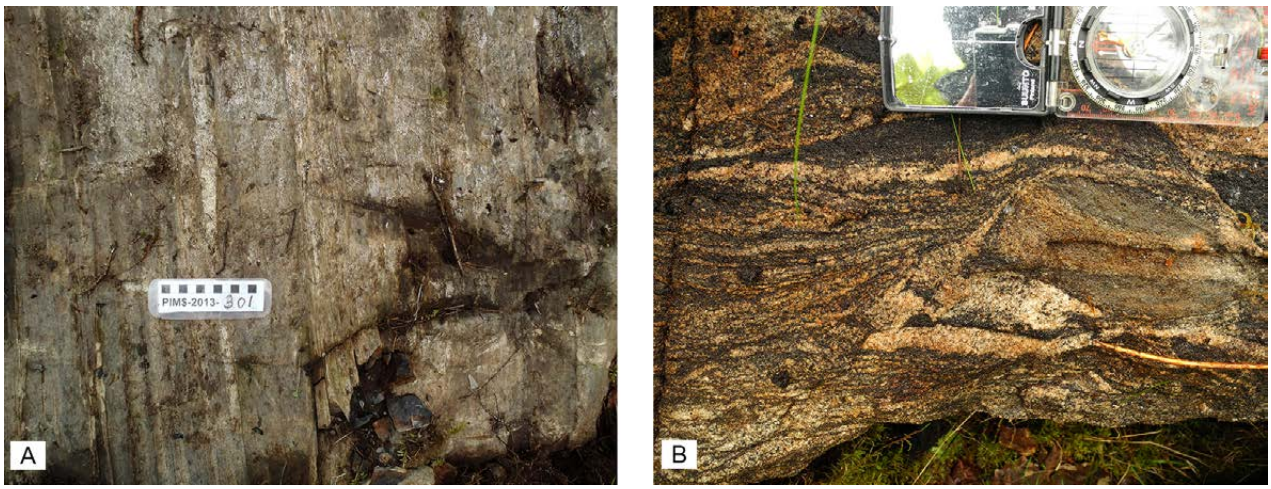

Fig. 5. A) An outcrop of Mäyräsalo paraschist, with variation in grain size and mineralogy of the beds. Scale bar with cm division. B) Migmatitic Central Finland paragneiss. Length of the compass 15 cm.

4.2 Geochemistry

In the sediment type classification diagram, the analysed samples mainly plot in the greywacke field, with a limited number of samples in lithic arenite and arkose fields (Fig. 6A). The compositional variation of the samples is large, as SiO_2 ranges from 46 to 77%. When all of the samples are viewed together, a correlation between SiO_2 and certain elements is observable in the more felsic compositions (e.g. MgO and Al_2O_3), but with respect to most elements, no correlations exist (e.g. Sr and CaO, Fig. 6). When taking the division into lithological units into consideration, the correlations become somewhat stronger, but not significantly in all of the units. Especially the samples representing the Pirkanmaa migmatite suite paragneisses and Mäyräsalo paraschists display significant scatter with respect to practically all elements. In case of the Pirkanmaa paragneisses, the compositionally differing types (e.g. samples with high Sr) do not represent unique subareas. On the other hand, samples deviating from the general trend towards higher MgO contents of the Mäyräsalo paraschist come from the Haapasuo area, but even so, not all samples from this area have high MgO. The samples with high Sr and belonging to the Tammijärvi greywackes come from the Harjujärvensuo area. The Tammijärvi greywackes and Toivakanlehto paraschists partially overlap with the compositional spectrum of the Myllyniemi greywackes, whereas the Mäyräsalo paraschist plots outside the spectrum.

The chondrite-normalized REE patterns of all of the studied units (shown as median values of the samples) display a similar trend, with moderate enrichment in LREE respective to HREE and a weak or missing Eu anomaly (Fig. 7A). Primitive mantle-normalized trace element compositions of the units also display distinctly similar patterns, i.e. negative Nb, P and Ti anomalies. Additionally, the black schists display a positive U anomaly.

Table 1. Representative chemical analyses.

Sample	EPHE-2013-386.1	N4312014R1 22.00-22.95	N4342013R2 46.00-47.00	HEKI-2013-166.1	ASM$-2012-250.2
Rock type	Paragneiss	Paraschist	Black schist	Biotite paragneiss	Greywacke
Suite / complex	Central Finland Granitoid Complex	Makkola suite	Makkola suite	Makkola suite	Pirkanmaa migmatite suite
Lithodeme	undefined migmatitic paragneiss	Mäyräsalo paraschist	Teuraanmäki black schist	Toivakanlehto paraschist	Rusalansuo greywacke
Age sample	---	---	---	---	A2397
SiO_2 %	64.1	61.3	53.2	70.7	67.0
TiO_2	0.79	0.61	0.63	0.48	0.61
Al_2O_3	17.30	17.70	15.50	14.50	13.90
Fe_2O_3t	6.82	7.50	9.10	3.76	5.59
MnO	0.08	0.08	0.03	0.04	0.15
MgO	2.61	3.66	3.30	1.59	2.08
CaO	2.26	2.19	1.74	1.82	7.14
Na_2O	2.40	2.67	2.06	3.20	1.65
K_2O	2.85	3.32	5.43	3.38	1.13
P_2O_5	0.19	0.28	0.12	0.14	0.20
C ppm	<500	<500	51900	1110	1180
Ba	581	856	954	716	n.a.
Cl	186	112	<60	<60	78
Co	n.a.	17.5	23.0	8.9	18.1
Cr	132	355	128	43	181
Ga	24	26	20	21	<20
Hf	n.a.	4.92	3.36	6.67	6.46
Nb	7.0	12.0	11.2	8.4	12.8
Ni	52.0	60	253	31	46
Pb	34	23	48	35	<20
Rb	138.0	102.0	219.0	100.0	54.3
S	310	164	31500	102	1813
Sc	<20	17.4	16.4	8.5	24.5
Sn	<20	20	<20	20	26
Sr	182	250	335	321	402
Ta	n.a.	0.51	0.41	0.61	1.04
Th	31.0	9.3	12.3	10.7	13.3
U	<10	2.56	12.50	2.02	3.43
V	123.0	96.3	669.0	54.7	132.0
Y	35.0	25.7	31.7	15.4	30.6
Zn	117	108	1170	112	70
Zr	165	193	140	171	317
La	<30	43.4	42.1	23.4	43.5
Ce	81.0	88.1	64.2	47.3	88.8
Pr	n.a.	37.1	32.4	17.0	37.8
Nd	n.a.	9.48	8.50	4.71	10.3
Sm	n.a.	6.53	6.08	3.21	6.86
Eu	n.a.	1.23	1.32	0.93	1.34
Gd	n.a.	5.80	5.87	2.92	6.17
Tb	n.a.	0.82	0.84	0.45	0.88
Dy	n.a.	4.85	n.a.	2.80	4.99
Ho	n.a.	0.93	1.08	0.56	0.96
Er	n.a.	2.7	3.4	1.7	2.77
Tm	n.a.	0.39	0.48	0.25	0.41
Yb	n.a.	2.59	3.64	1.71	2.64
Lu	n.a.	0.39	0.53	0.24	0.39

n.a. = not analysed
<30 = below detection limit and the approriate limit

Table 1. Cont.

Sample	PIM$-2014-45.1	PIM$-2013-274.1	N4332013R6 29.40-30.60	ASM$-2012-115.1	N4342015R24 8.75-9.25
Rock type	Greywacke	Greywacke	Black schist	Biotite paragneiss	Paragneiss
Suite / complex	Pirkanmaa migmatite suite	Pirkanmaa migmatite suite	Pirkanmaa migmatite suite	Pirkanmaa migmatite suite	Pirkanmaa migmatite suite
Lithodeme	Rusalansuo greywacke	Tammijärvi greywacke	undefined black schist	undefined migmatitic paragneiss	undefined migmatitic paragneiss
Age sample	A2398	A2396	---	A2395	---
SiO_2 %	76.7	71.4	49.2	62.6	57.9
TiO_2	0.36	0.52	0.57	0.78	0.69
Al_2O_3	11.50	13.90	13.90	17.80	15.90
Fe_2O_3t	3.45	4.23	10.70	7.23	8.74
MnO	0.05	0.05	0.06	0.04	0.11
MgO	0.87	1.62	5.79	3.14	3.51
CaO	1.15	1.86	2.16	1.11	6.39
Na_2O	2.24	3.09	2.49	2.28	3.27
K_2O	3.26	2.88	2.86	4.17	1.77
P_2O_5	0.11	0.14	0.14	0.06	0.26
C ppm	<500	667	70100	3820	707
Ba	739	547	459	643	603
Cl	83	83	65	306	205
Co	5.6	<5	27.6	15.5	n.a.
Cr	43	67	130	138	43
Ga	<20	<20	<20	28	<20
Hf	4.05	5.38	3.02	3.89	n.a.
Nb	6.0	7.1	8.5	10.8	<7
Ni	<20	<20	325	69	<20
Pb	<20	<20	22	<20	<20
Rb	88.0	91.7	141.0	154.0	58.0
S	103	468	41600	2443	21650
Sc	7.4	11.4	15.5	19.8	<20
Sn	<20	<20	26	<20	20
Sr	222	212	174	141	534
Ta	0.56	0.52	0.46	0.50	n.a.
Th	18.0	14.2	11.4	12.3	<30
U	2.63	2.92	15.90	2.61	<10
V	49.9	73.7	765.0	137.0	199.0
Y	19.1	18.0	33.4	22.3	n.a.
Zn	35	55	1760	137	90
Zr	169	233	129	158	114
La	55.9	16.0	34.5	38.7	<30
Ce	116.0	29.1	54.1	77.8	70.0
Pr	41.7	9.9	28.4	33.9	n.a.
Nd	12.10	3.04	7.24	9.38	n.a.
Sm	6.69	2.12	5.81	6.27	n.a.
Eu	1.19	0.95	1.23	1.41	n.a.
Gd	5.40	2.45	5.78	5.35	n.a.
Tb	0.70	0.48	0.89	0.74	n.a.
Dy	4.00	3.32	n.a.	4.41	n.a.
Ho	0.77	0.70	1.19	0.86	n.a.
Er	2.3	2.2	3.8	2.5	n.a.
Tm	0.32	0.30	0.55	0.34	n.a.
Yb	2.19	2.12	4.28	2.38	n.a.
Lu	0.32	0.31	0.61	0.35	n.a.

n.a. = not analysed
<30 = below detection limit and the approriate limit

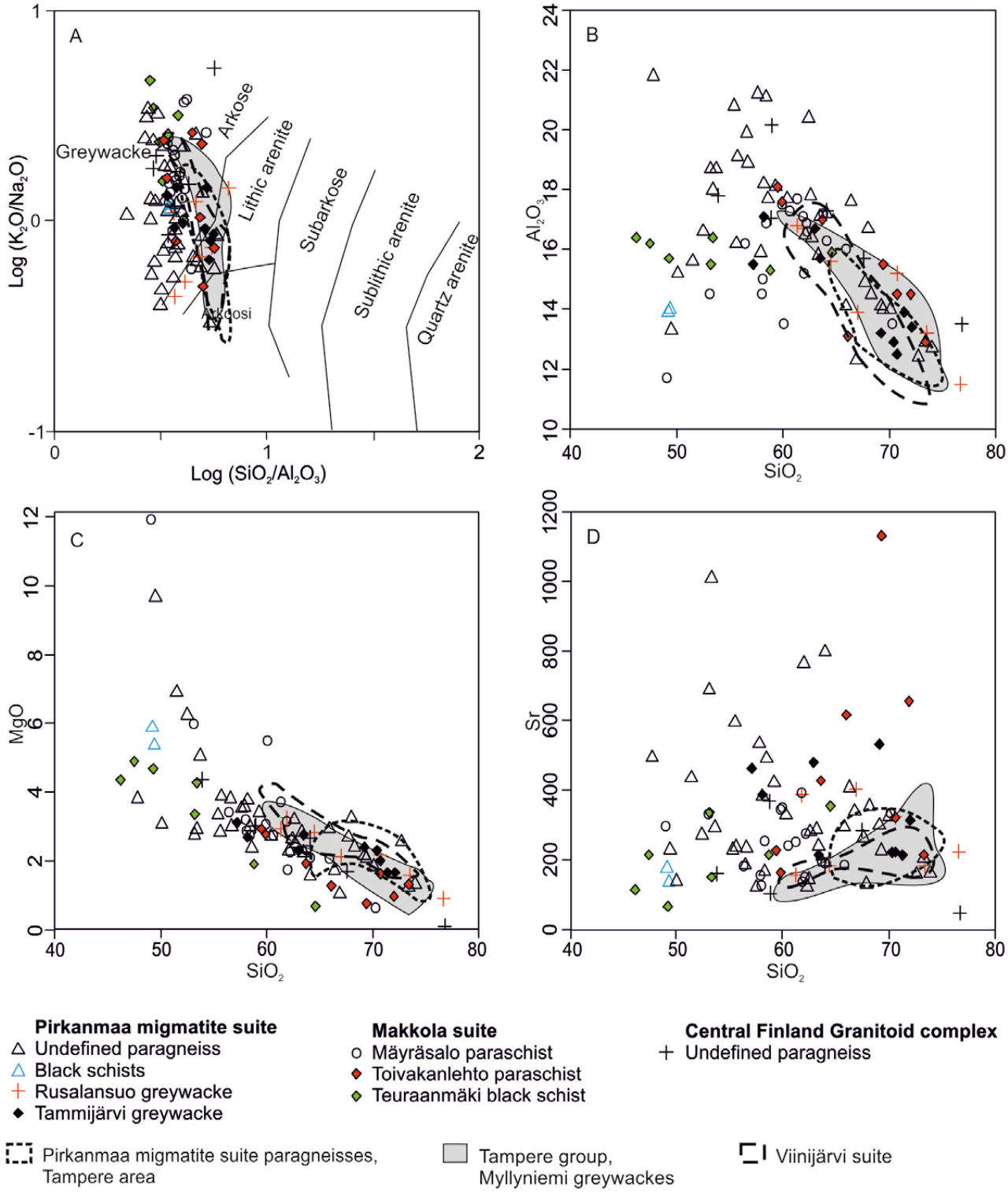

Fig. 6. The studied samples plotted on a sediment type classification diagram (A; Pettijohn et al. 1972, with boundaries modified by Herron 1988) and Harker diagrams (B–D). Reference data (Viinijärvi suite, Myllyniemi formation, Pirkanmaa paragneisses from the Tampere area) from Lahtinen et al. (2009, 2010).

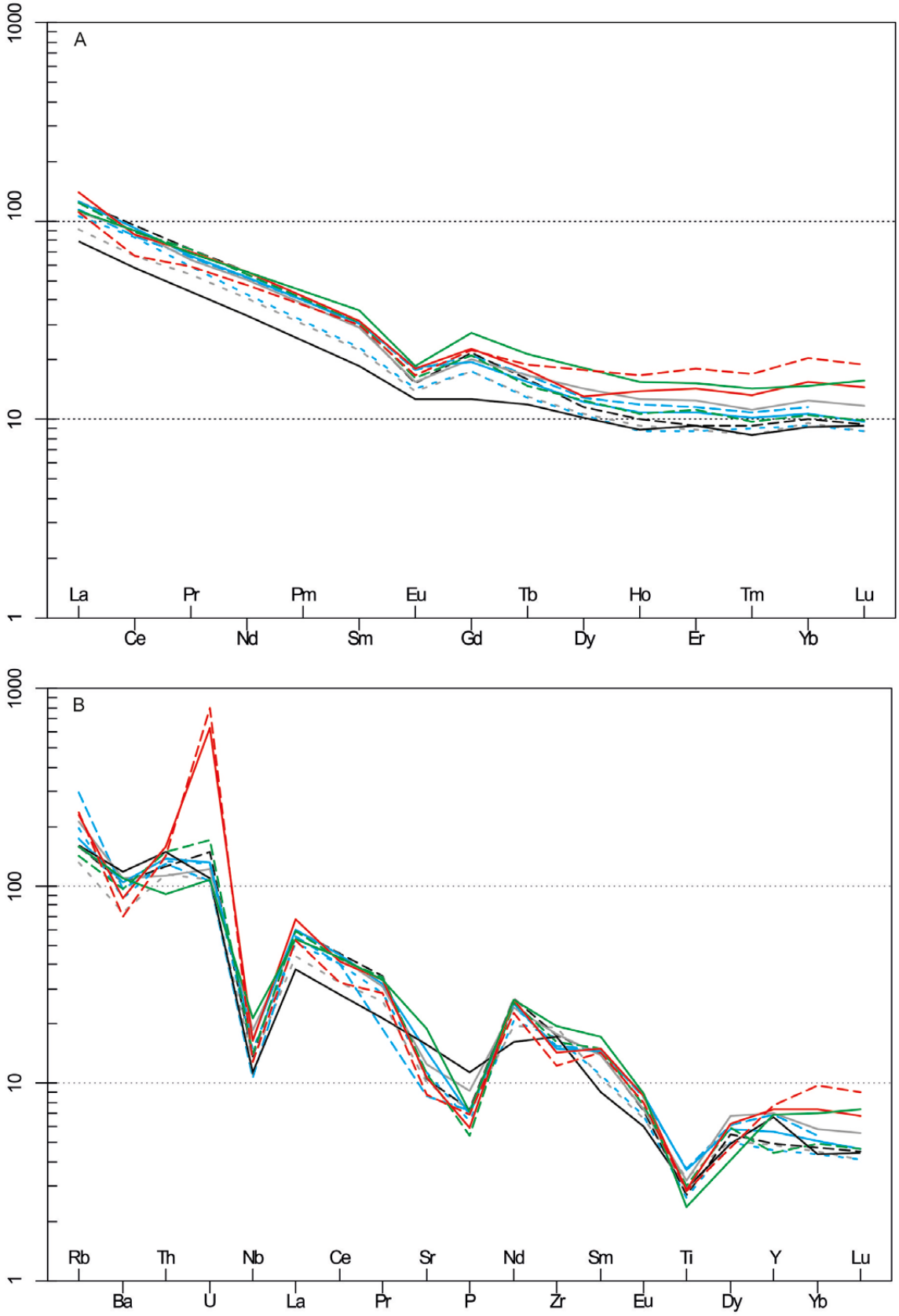

Fig. 7. A) Chondrite-normalized REE values of the studied units. B) Primitive mantle-normalized trace element compositions of the units. The displayed value is the median of each suite. Chondrite values from Boynton (1984) and primitive mantle values from McDonough & Sun (1995). Reference data from Lahtinen et al. (2009, 2010).

4.3 Zircon ages

4.3.1 A2395 Sainiemi

Sample A2395 (Sainiemi) represents the migmatic paragneiss of the study area hosted as variably sized (from cm to km scale) enclaves in the plutonic units of the area (Fig. 2). On the outcrop, the rock is characterized by narrow neosome veining (Fig. 3A). As the veining is so small scaled, no attempt to separate the paleosome from the neosome was made, and a bulk sample was instead taken. Mineralogically, the neosome is trondhjemitic and the paleosome is biotite-rich paragneiss. The zircon population is characterized by two types: homogeneous unzoned grains and grains displaying oscillatory zoned cores with unzoned dark overgrowths (Fig. 8). Altogether, 43 spots were analysed (Electronic Appendix), and out of these, 3 were discarded due to a high level of discordance. All of the spots yield Paleoproterozoic ages ($^{207}Pb/^{206}Pb$ = 1876–2190 Ma, Fig. 9). Dark unzoned grains and overgrowths yield ages younger than 1900 Ma, whereas zoned cores and one light-coloured rim yield $^{207}Pb/^{206}Pb$ ages between 1885 and 2190 Ma, with maxima close to 1900 Ma. We interpret that the dark unzoned grains and rims indicate the migmatization event at 1885 Ma, as discordia calculated using all of these points yields an upper intercept at 1887 ± 6 Ma. Alternatively, a concordia age of 1883 ± 2 Ma using only the concordant analyses (n = 13) can be calculated. In our interpretation, the zoned cores are inherited grains and the nonexisting gap between the metamorphic and youngest inherited ages (1885 Ma) indicates rapid erosion and burial into anatectic conditions. However, the lack of an age gap can partially be an artefact of the lead loss of older crystals during intensive metamorphism.

4.3.2 A2396 Kitka

Sample A2396 (Kitka) represents the well-preserved Tammijärvi greywackes typical of the Leivonmäki area (Fig. 2). On the outcrop scale, the sample is relatively homogeneous and massive with ca. 1 mm clasts (Fig. 3B) in a finer grained groundmass. The majority of the clasts are quartz grains or grain aggregates and a minority are plagioclase grains, whereas lithic fragments are lacking. The zircon population is characterized by rounded grains with strong oscillatory zoning, often displaying homogeneous overgrowths, most of them too narrow for analysis. In cathodoluminescence pictures, the overgrowths form two groups: one is light and the other dark coloured (Fig. 8). The darkness of the cores also varies, but to a lesser extent. The majority of the 35 spots analysed (Electronic Appendix) from 23 different grains are concordant.

Out of the analysed spots, 31 are Paleoproterozoic with $^{207}Pb/^{206}Pb$ ages varying from 1905 to 2090 Ma, and the remaining 4 spots are Neoarchean ($^{207}Pb/^{206}Pb$ =2684–2743 Ma, Fig. 9). All of the Neoarchean cores (n = 3) are relatively dark and show weaker than average zoning, while the one Neoarchean rim is light coloured. The Paleoproterozoic spots do not show any significant correlation between morphology and age. The analysed rims (n = 10), for example, do not define a single metamorphic event; instead, they indicate that they were derived from terrain(s) displaying a range of metamorphic ages. Interpretation of the meaning of the youngest concordant analysis (n5441-23b, 1905 ± 12 Ma) is not self-evident, as the spot is from a weakly zoned rim on an older core (n5441-23a, 2009 ± 12 Ma). If the age of the rim is taken as inherited, it marks the maximum age of deposition, and if taken as metamorphic, it gives the minimum age of deposition for this sample. As the analysis has a low Th/U ratio (0.02) typical for metamorphic zircons (Williams et al. 1996), we prefer the latter interpretation and regard ca. 1.92 Ga as the maximum depositional age of this sample.

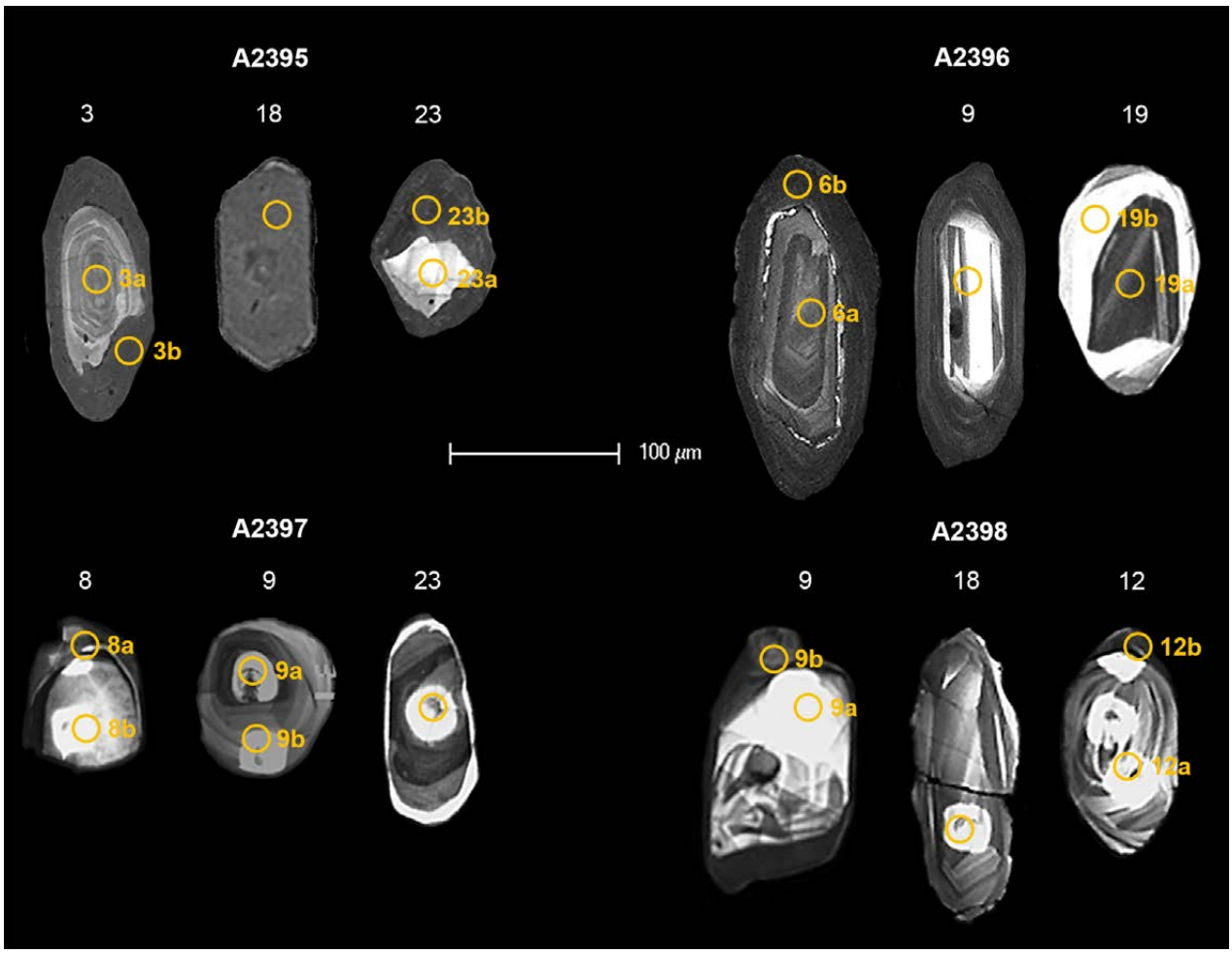

Fig. 8. Representative zircons of the studied samples with analysed spots shown. Note that samples A2397 and A2398 were imaged after the analyses; thus, the rastered area is visible as a light-coloured spot.

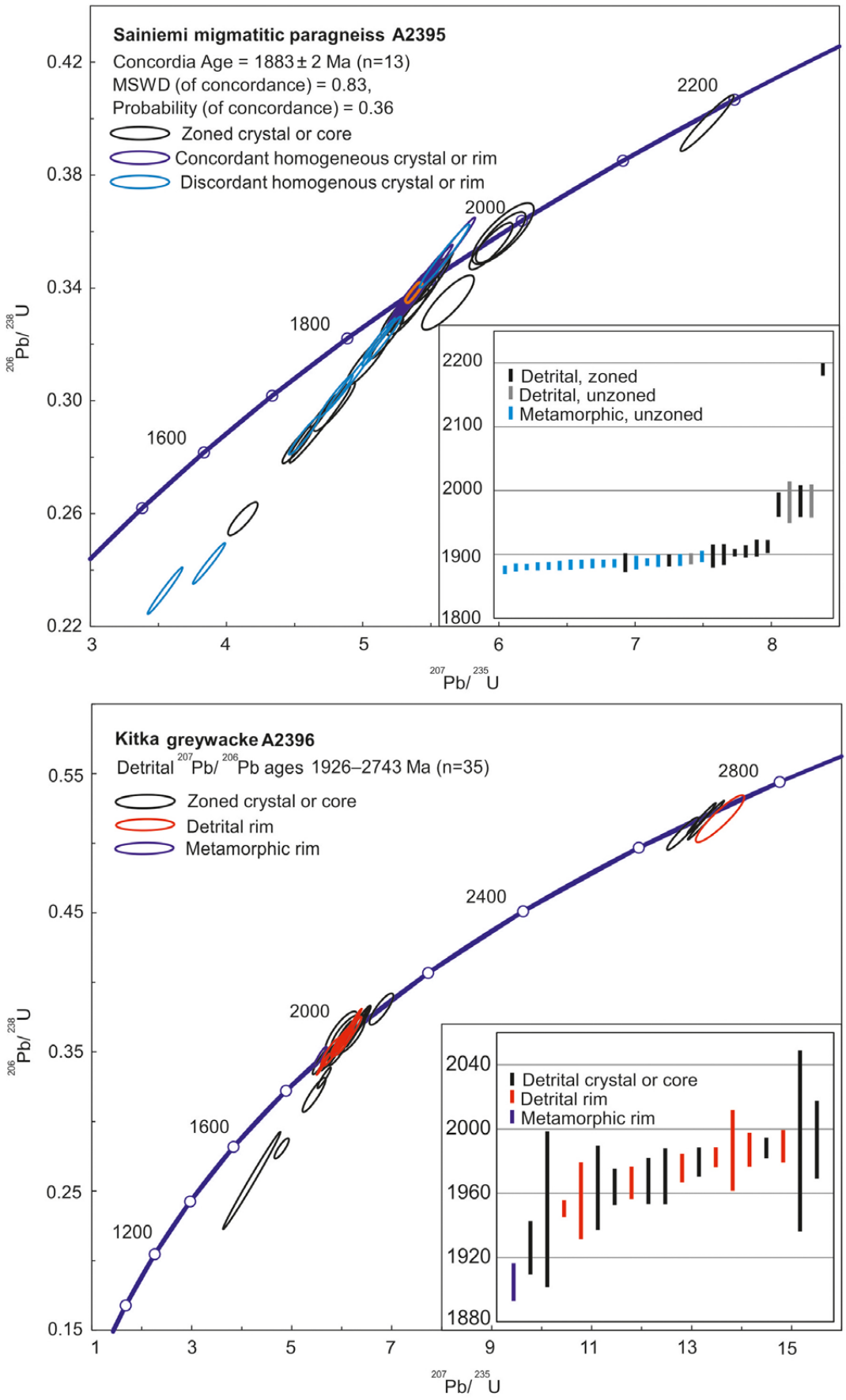

Fig. 9. Concordia diagrams for samples A2395 and A2396. In the insets, the distribution of $^{207}Pb/^{206}Pb$ ages of spots with a discordance of <5%. In A2395 concordia age calculated on basis of spots interpreted as metamorphic shown as orange ellipse. In A2396, only spots with $^{207}Pb/^{206}Pb$ ages younger than 2000 Ma are shown. All data are plotted at the 2σ confidence level.

4.3.3 A2450 Harjujärvensuo

Sample A2450 is from a conglomerate interbed in Tammijärvi greywackes. It was taken from a drilling profile intersecting the Harjujärvensuo Au mineralization (Fig. 2, Mikkola et al. 2018c). The sample represents a conglomerate type referred to as heterogeneous by Mikkola et al. (2018c). It is characterised by variably rounded pebbles up to 5 cm in size. The coarser pebbles are schist fragments and smaller ones are quartz grains or quartz aggregates. This type differs from the typical conglomerate interbeds of the Tammijärvi greywackes, in which the pebbles have on average a more felsic composition and uniform size distribution.

The zircon grains are variably rounded, most display magmatic zoning and some have homogeneous overgrowths. Out of the 51 analyses (Electronic Appendix), from an equal number of grains, most are concordant (Fig. 10). The spread of $^{207}Pb/^{206}Pb$ ages extends from 1905 to 3394 Ma and the population is strongly bimodal with peaks close to 2000 and 2700 Ma. The definition of the maximum depositional age for this sample also depends on the interpretation of the youngest obtained age (1905 ± 14 Ma). As this analysis has a high U concentration (893 ppm), we consider it as being affected by lead loss during metamorphism and regard 1.92 Ga defined by the remaining analysis (Fig. 10) as the best estimation for the maximum depositional age of this sample.

4.3.4 A2397 Lapaskangas

Sample A2397 (Lapaskangas) represents the weakly migmatized greywackes (Fig. 3C) found from a small area near Kangasniemi village (Fig. 2). The outcrop has abundant calc-silicate concretions. The migmatization of this greywacke type clearly differs from the intensive veining displayed by the more common paragneiss type in the area represented in this study by sample A2395 (Fig. 3A). In the case

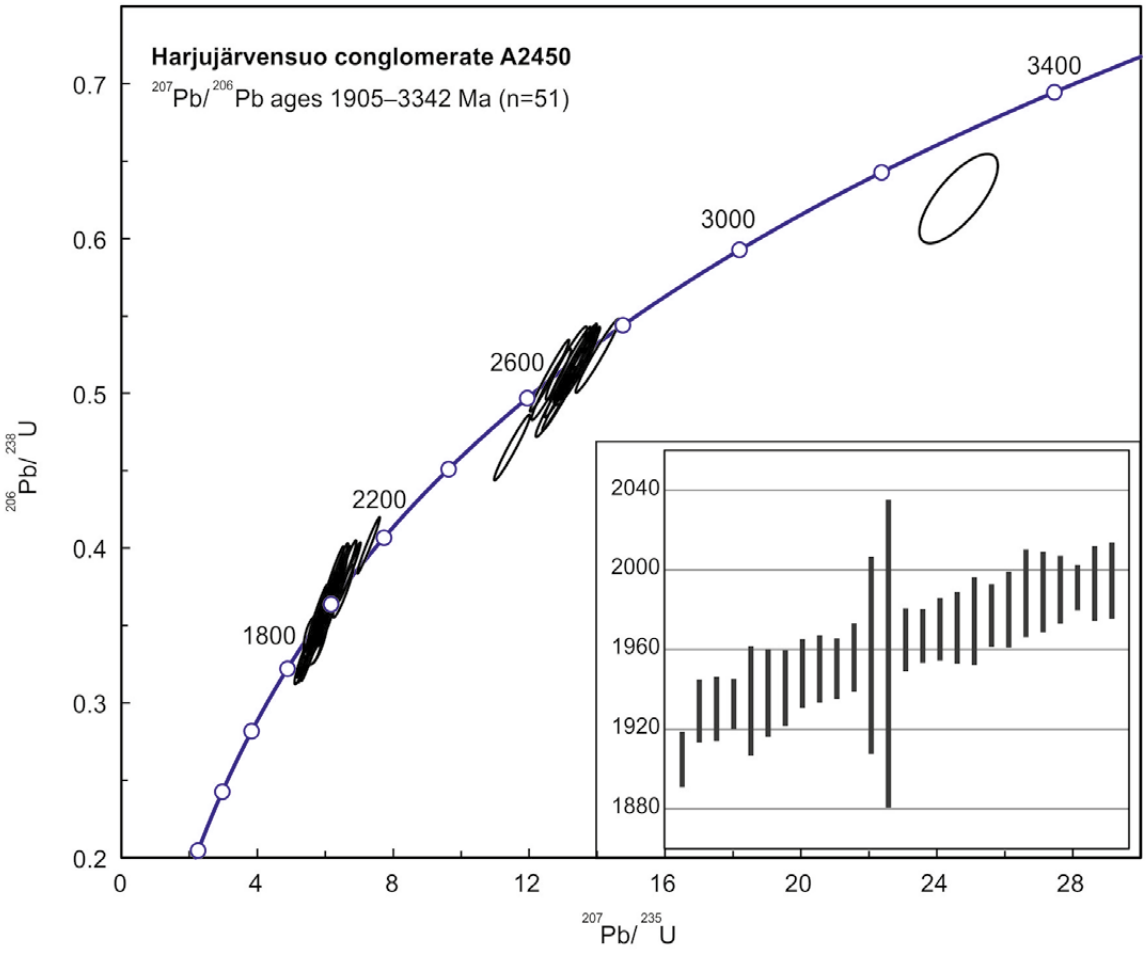

Fig. 10. Concordia diagram of sample A2450. In the inset, the distribution of $^{207}Pb/^{206}Pb$ ages of spots younger than 2000 Ma and with a discordance of <5%. All data are plotted at the 2σ confidence level.

of sample A2397, the migmatization is most likely caused by contact metamorphism related to a large gabbro intrusion in the vicinity of the sample site. Nearly all of the zircons show oscillatory zoning. Two types of rims exist: wider darker coloured and narrower bright ones (Fig. 8). The latter are always too narrow for analysis, as also are most of the former.

Out of the 28 analysed spots from 25 zircons (Electronic Appendix), 22 yielded Paleoproterozoic ages ($^{207}Pb/^{206}Pb$ = 1900–2215 Ma, Fig. 11). The remaining six spots are Archean with $^{207}Pb/^{206}Pb$ ages from 2550 to 2807 Ma. Most of the analyses are concordant. The analysed dark wider rims are interpreted to indicate predepositional metamorphic events, as one yields a $^{207}Pb/^{206}Pb$ age of 2083 Ma and the other one 2807 Ma. The narrow bright rims are interpreted as metamorphic. The youngest age (n5442-13; 1900 ± 22 Ma) is from a morphologically atypical crystal with a low Th/U ratio of 0.03 typical for metamorphic zircons (Williams et al. 1996). Based on these two characteristics, its age is interpreted as metamorphic, therefore marking the minimum age of deposition for this sample. Thus, the maximum depositional age of this sample is ca. 1.92 Ga.

4.3.5 A2398 Uprinpuro

Sample A2398 (Uprinpuro) is an unmigmatized and weakly deformed greywacke from an outcrop with conglomerate interbeds (Fig. 3D). The <1 mm clasts are quartz crystals and aggregates. The zircon population of the sample mostly consists of oscillatory zoned grains (Fig. 8), some of which have dark coloured rims.

Out of the 38 analyses from 34 crystals (Electronic Appendix), two were discarded due to high common lead. Most of the spots are concordant and 23 yield Paleoproterozoic ages ($^{207}Pb/^{206}Pb$ =1903–2083 Ma, Fig. 11). The remaining 13 spots are mainly Neoarchean, but one grain (n5443-12) is Paleoarchean with a $^{207}Pb/^{206}Pb$ age close to 3600 Ma (Fig. 8). This grain also has an unzoned rim that yields a $^{207}Pb/^{206}Pb$ age of 3065 Ma (Fig. 10B). Two out of three spots yielding the youngest ages are from dark unzoned overgrowths and all three have low Th/U ratios typical for metamorphic zircons. Therefore, the ca. 1900 Ma ages given by these three analyses are interpreted as the metamorphic age and the minimum age of deposition for this sample. Based on the above, the best estimation for the maximum depositional age of this sample is ca. 1.91 Ga.

4.3.6 A2440 Loukee

Sample A2440 (Loukee) is outside our main study area (see Figure 1 for sample location). This sillimanite-biotite paragneiss sample (Fig. 4D) represents the Häme migmatite suite flanking the Pirkanmaa migmatite suite to the south and east (Fig. 1). The zircon population of the sample consists of crystals displaying oscillatory zoning, and core-rim structures are observable, but rims are too narrow for dating. Altogether, 25 spots from 19 grains were analysed (Electronic Appendix), and 22 of the spots are concordant (Fig. 12) and display $^{207}Pb/^{206}Pb$ ages from 3382 to 1880 Ma. Five of the grains yield Archean ages (2745–3382 Ma) and the rest are Paleoproterozoic (1880–2166 Ma). No correlation was observed between zircon size, morphology or the U/Th ratio and age. Although the nominal ages of three of the analysed spots are younger than 1900 Ma, their true ages might be over 1900 Ma when errors are taken into account at the 2σ level. Thus, we interpret ca. 1.90 Ga as the maximum depositional age of this sample.

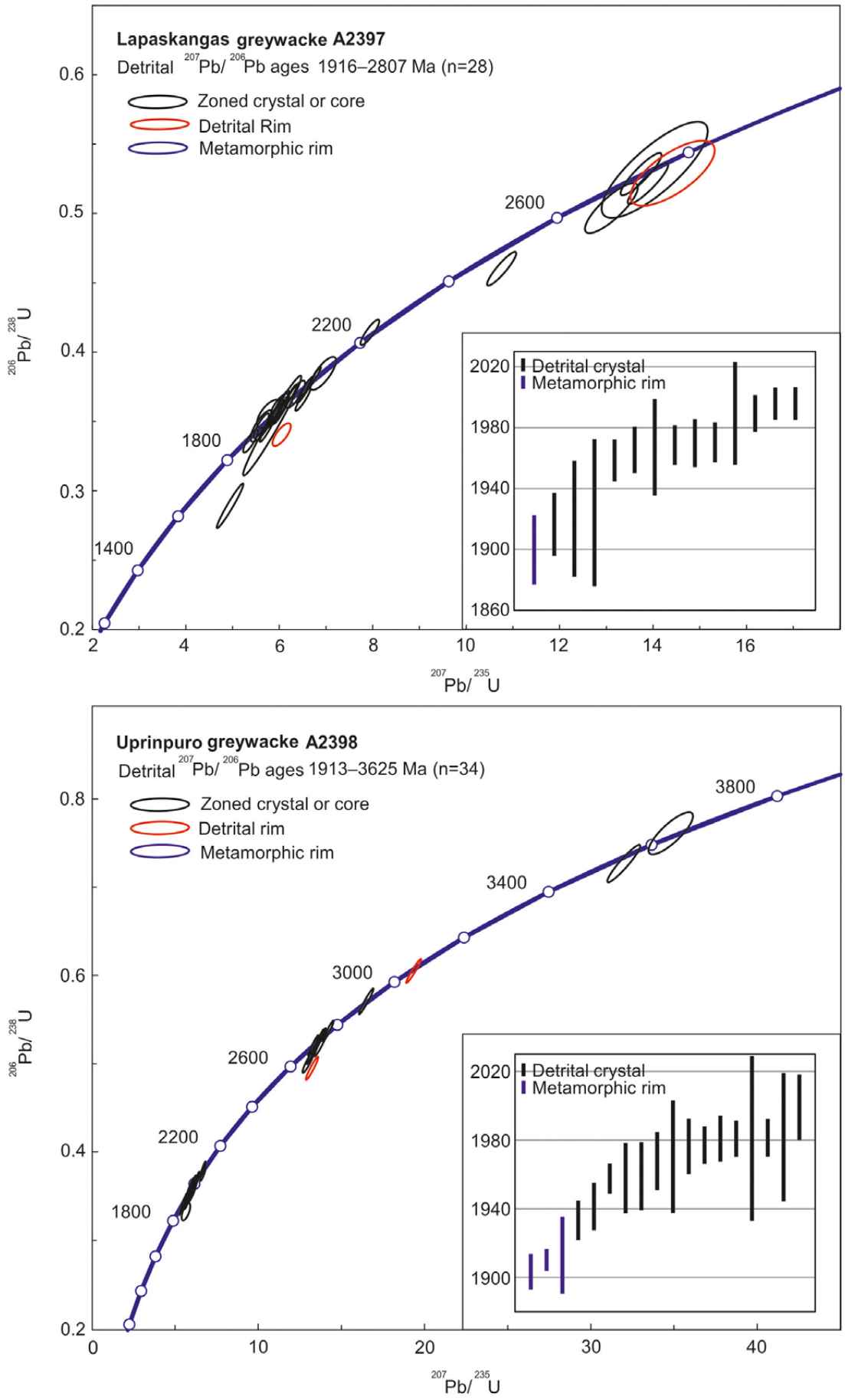

Fig. 11. Concordia diagrams of samples A2397 and A2398. In the insets, the distribution of $^{207}Pb/^{206}Pb$ ages of spots younger than 2000 Ma and with a discordance of <5%. All data are plotted at the 2σ confidence level.

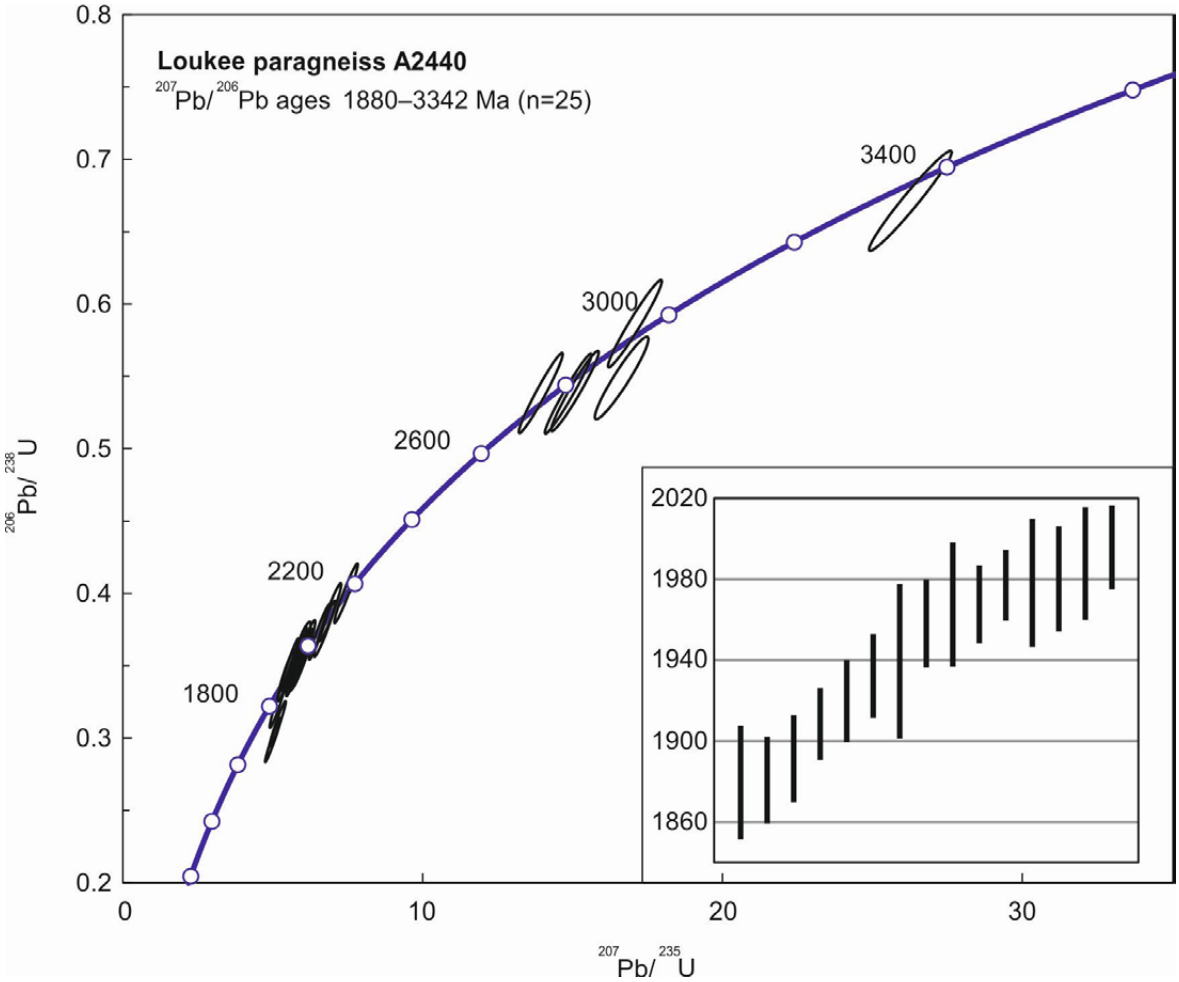

Fig. 12. Concordia diagram of sample A2440. In the insets, the distribution of $^{207}Pb/^{206}Pb$ ages of spots younger than 2000 Ma and with a discordance of <5%. All data are plotted at the 2σ confidence level.

4.3.7 A15 Vuotsinsuo

Metagreywacke sample A15 (Vuotsinsuo), belonging to the Häme migmatite suite, was described by Lahtinen et al. (2002), who published single-grain SIMS analyses of 19 spots representing 18 zircon grains. Out of these analyses, we discarded four based on high common lead and/or a high degree of discordancy. The new data published here consist of 47 analyses from 40 individual zircon grains (Electronic Appendix). Seven of the analyses are discarded due to high common lead. The remaining new analyses are concordant within error. The combined data set includes 12 Archean zircon grains with $^{207}Pb/^{206}Pb$ ages from 2662 to 2741 Ma. Out of the 45 Paleoproterozoic analyses from 38 crystals, 43 yield $^{207}Pb/^{206}Pb$ ages between 1917 and 2085 Ma and the remaining two analyses have $^{207}Pb/^{206}Pb$ ages of 2428 and 1889 Ma. Another analysis from the same morphological domain (Fig. 5 in Lahtinen et al. 2002) as the latter result yielded a $^{207}Pb/^{206}Pb$ age of 1917 Ma. Thus, the significance of this youngest observed age is not self-evident. We consider that the new data confirm the interpretation of Lahtinen et al. (2002), i.e. the phenomenon has either a natural (e.g. small inclusion, lead loss) or analytical cause, and the maximum depositional age of this sample is determined by the bulk of the analyses as ca. 1.92 Ga (Fig. 13).

4.3.8 A1557 Jyrkkäaho

Metapsammite sample A1557 (Jyrkkäaho), belonging to the Häme migmatite suite, was described by Lahtinen et al. (2002). Their dataset included 22 analyses from 20 individual zircon crystals, out of which seven were discarded based on high common lead and/or a high degree of discordancy. We analysed an additional 44 spots from 40 zircon grains (Electronic Appendix), all analyses are concordant

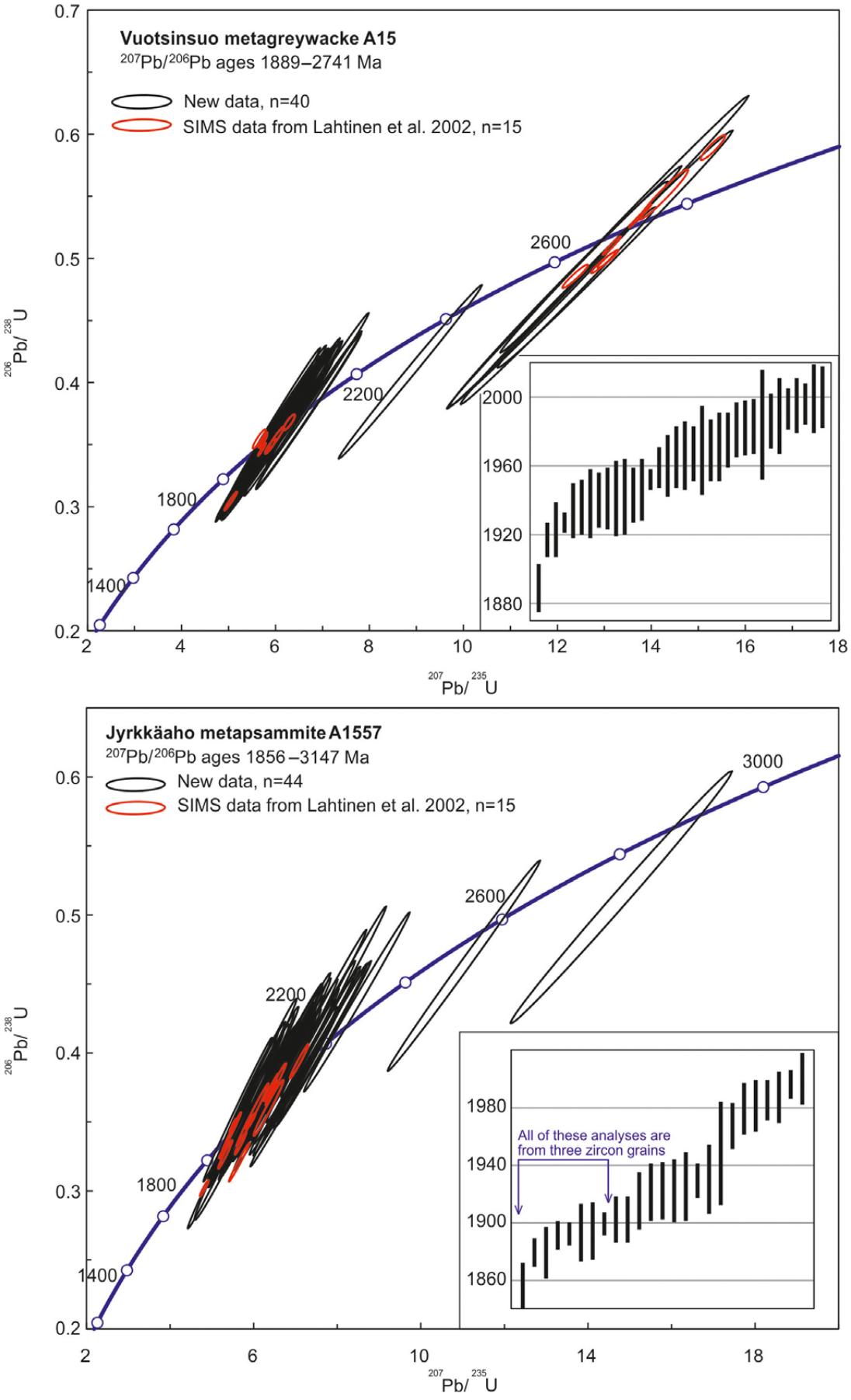

Fig. 13. Concordia diagrams for samples A15 and A1557. In the insets, the distribution of $^{207}Pb/^{206}Pb$ ages of spots younger than 2000 Ma and with a discordance of <5%. Note that the analysis from A1557 yielding a $^{207}Pb/^{206}Pb$ age of 3147 ± 10 Ma plots outside the diagram.

within error. As some of our analyses were carried out on the same zircon grains as the SIMS analyses of Lahtinen et al (2002), the 59 spots represent 43 different crystals. The data set includes only three Archean zircon crystals with $^{207}Pb/^{206}Pb$ ages of 3.15 Ga, 2.90 Ga and 2.58 Ga. The 40 Paleoproterozoic zircons yielded $^{207}Pb/^{206}Pb$ ages from 1856 to 2234 Ma, the majority being in the range 1915–2150 Ma (Fig. 13). Common lead ratios of the two youngest zircon grains are similar to the others and all of them have relatively high U concentrations (>350 ppm in LAMS data), although similar U levels are also present in a small number of analyses yielding older ages. Nevertheless, it is possible that the zircons with higher than average U concentrations have been more prone to post-crystallisation lead loss, resulting in ages younger than the original crystallisation. However definitive conclusions cannot be made, but based on the larger dataset we regard ca. 1.90 Ga as the best estimation for the maximum depositional age of this sample is, i.e. slightly older than the 1.89 Ga proposed earlier by Lahtinen et al. (2002).

5 DISCUSSION

5.1 Composition

All of the analysed samples represent relatively immature metasedimentary rocks, which can be compositionally classified as greywackes and lithic arenites. Based on the preserved graded bedding structures, unsorted textures and conglomerate interbeds, they originated as turbidites (Fig. 3B, D). In this sense, they do not differ from the typical paragneisses of southern and central Finland (e.g. Lahtinen et al. 2002, 2009, 2017, Kotilainen 2016). The different units present in the study area cannot be separated from each other on a compositional basis, and the current division is thus based on their spatial distribution and certain differences in associated rock types and primary structures between the subareas. Further refinement of the units would require detailed isotope studies. The observed LREE enrichment indicates derivation from a relatively felsic source, but does not allow discrimination between, for example, the felsic to intermediate volcanic rocks and granitoids.

The large compositional scatter in our samples from the Pirkanmaa migmatites compared to those of Lahtinen et al. (2009) has several possible explanations. These include the type of the study areas; the samples of this study originate from several small subareas scattered between plutonic rocks, whereas the samples of Lahtinen et al. (2009) represent a single, relatively connected geological domain. However, as even closely spaced samples from our area display significant mutual differences, this is not the sole reason behind the differences. Variation in the degree of migmatization and also the sampling methodology has effects; our samples are on average more strongly migmatized than those of Lahtinen et al. (2009), and as a consequence of this, our samples inevitably contain neosome in varying proportions. The on average lower SiO_2 contents of our samples could partly be an artefact of the segregation of silica-rich melt during anatexis, which would lower the SiO_2 contents of the residue. Overall, the large scatter cannot be explained by sampling alone; it seems to reflect the heterogeneity of the material in the original sedimentary basin(s).

Lahtinen et al. (2009) recognized from the Tampere area a separate fore-arc sedimentary unit that deviated from the other Pirkanmaa paragneisses in both geochemistry (high Sr) and the detrital zircon population. The samples most enriched in Sr from our study area all come from four subareas, but material from one of these areas, Viidansuo, includes only Sr-enriched samples. As no age data are available from the Viidansuo location and it does not differ significantly in texture or structure from other samples of the Pirkanmaa paragneisses, we do not interpret it to represent a separate geological unit.

Out of the described units, the Mäyräsalo paraschists show deviation to lower Al_2O_3 associated with higher MgO and CaO concentrations. This probably reflects proximity to active basic volcanism at the time of deposition, resulting in compositional variation in the sediments deposited during the active eruption phase and between such phases. A number of Pirkanmaa paragneiss samples also show similar compositional deviation to the Mäyräsalo

paraschists and possibly reflect proximity to active volcanism during deposition. The Toivakanlehto paraschist, the other sedimentary unit associated with the Makkola suite, differs in this sense from the Mäyräsalo paraschists, as all samples plot on the same trend with respect to Al_2O_3 and MgO. Instead, some of the samples are enriched in Sr (<1135 ppm, Fig. 6A) and CaO (<11.8%), most likely due to the simultaneous deposition of calc and siliciclastic material.

5.2 Geological unit divisions

5.2.1 Pirkanmaa migmatite suite

At the beginning of this study, the hypothesis was that the three age samples representing the well-preserved Tammijärvi and Rusalansuo greywackes would display maximum depositional ages similar to, or younger than, the active volcanic phase of the Makkola suite (i.e. 1895–1875 Ma, Mikkola et al. 2018b). This would have correlated them with the same phase as the Haukivuori conglomerate or the Lampaanjärvi suite further north (Fig. 1), both of which have maximum depositional ages of ca. 1885 Ma (Korsman et al. 1988, Lahtinen et al. 2015). This would have been in line with the early interpretation of Karppanen (1970), who regarded the Tammijärvi greywackes as an eastern extension of the upper sediments of the Tampere group. This hypothesis was made even more attractive, as it has been confirmed, based on age and geochemistry, that the Makkola suite represents the same magmatic phase as the volcanic rocks of the Tampere group (Mikkola et al. 2018b).

However, contrary to our hypothesis, unmigmatized samples A2396 and A2450 from Tammijärvi displayed similar detrital zircon patterns to the variably migmatized paragneisses surrounding the CFGC (Huhma et al. 1991, Lahtinen et al. 2009, Kotilainen et al. 2016), with a maximum depositional age of ca. 1.92 Ga and a bimodal distribution with peaks at 2.0 and 2.7 Ga. The Myllyniemi formation, the lowermost unit of the Tampere group, also has a similar zircon population and maximum depositional age. Based on these characteristics, the Tammijärvi lithodeme could be correlated with the Myllyniemi formation. However, mainly based on the following two points, we regard the Tammijärvi lithodeme to be part of the Pirkanmaa migmatite suite. The contact between the Makkola suite and the Tammijärvi lithodeme is formed by the Leivonmäki shear zone (Mikkola et al. 2018a), and is not sedimentary, as in Tampere (Kähkönen 2005). The contact between the migmatized members of the Pirkanmaa migmatite suite and the Tammijärvi lithodeme is gradual and interpreted to be a result of a differing metamorphic grade.

The samples (A2397, A2398) from the Rusalansuo lithodeme also have maximum depositional ages close to 1.92 Ga and display bimodal detrital zircon populations, closely resembling that of the sample A2396 from Tammijärvi (Fig. 14). A curiosity worth pointing out is the ca. 3.6 Ga zircon core from sample A2398, which is the oldest zircon dated so far from the Svecofennian domain, the second oldest being a 3.5 Ga grain from the Bothnian Belt (Kotilainen et al. 2016). The contact between the Rusalansuo lithodeme and its surrounding units has been interpreted as tectonic based on an abrupt change in metamorphic degree. In their type area, Rusalansuo greywackes host interlayers of intermediate volcanic rocks of unknown age, which based on the zircon population of the greywackes cannot belong to the Makkola suite. In samples representing Tammijärvi and Rusalansuo greywackes, the timing of the metamorphic event is not self-evident, but all show weak indications of metamorphism and thus a minimum age of deposition of ca. 1.90 Ga. Similar hints of ~1.90 Ga metamorphism were also

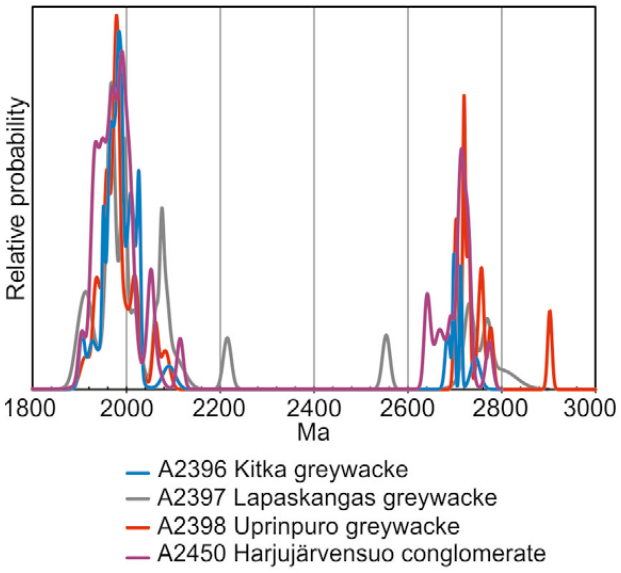

Fig. 14. Probability density plot of $^{207}Pb/^{206}Pb$ ages of spots with a discordance of <5% and interpreted as detrital from samples representing the Tammijärvi and Rusalansuo lithodemes. Note that analyses older than 3000 Ma from sample A2398 and A2450 are not shown.

recognized by Lahtinen et al. (2009) in their samples from near Tampere. The definitive minimum depositional age of these lithodemes is ca. 1885 Ma, as they are intruded by plutonic rocks of this age. Due to the similarities between the Tammijärvi and Rusalansuo lithodemes, we also regard the latter as part of the Pirkanmaa migmatite suite.

The migmatitic sample (A2395) differs from the unmigmatized samples with respect to the zircon population in two ways: the population does not include Archean zircons and youngest detrital zircons are ca. 1885 Ma in age, and thus 30–40 Ma younger than in the unmigmatized samples. The first difference is relatively undisputable, but the significance of the latter can be questioned. The ~1885 Ma ages obtained from zircons displaying magmatic zoning and inferred as detrital could be due to the high degree of metamorphism at that time, resulting in lead loss, resetting the U–Pb system to a younger age. This possibility seems likely, as the granitoids hosting the paragneiss sample are 1895 Ma in age (Kallio 1986, authors' unpublished data). However, if the ages are taken to represent the primary crystallization ages of the zircons, they indicate extremely fast burial to depths and temperatures required for anatexis. In the data of Lahtinen et al. (2009) from the Pirkanmaa migmatite suite further west, one sample contains zircons aged 1900–1890 Ma and was interpreted as representing a younger fore-arc sequence within the Pirkanmaa migmatite suite. The metamorphic age, ~1885 Ma, of sample A2395 is in line with metamorphic zircon ages (1885–1875 Ma, Lahtinen et al. 2009) reported earlier for the Pirkanmaa migmatite suite further west.

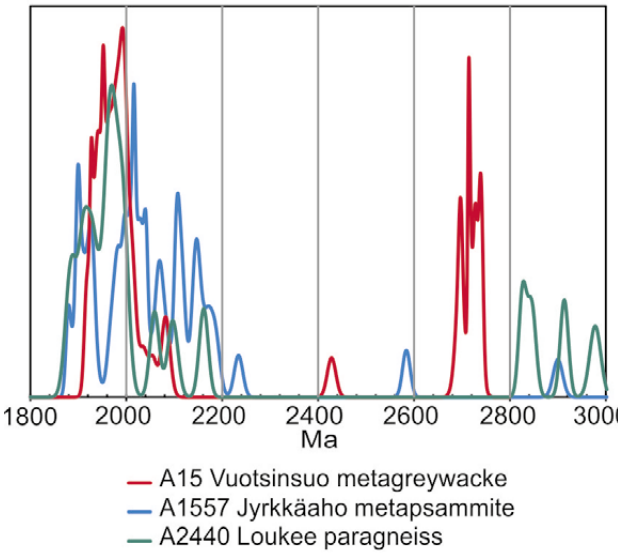

Fig. 15. Probability density plot of the $^{207}Pb/^{206}Pb$ ages of spots with a discordance of <5% and interpreted as detrital from samples representing the Häme migmatite suite. Note that analyses older than 3000 Ma from samples A1557 and A2440 are not shown. For grains with multiple analyses, only the median value was used for constructing the plot.

5.2.2 Häme migmatite suite

The three samples interpreted as part of the Häme migmatite suite (A15, A1557, A2440) and used in this study display differing detrital zircon populations. The maximum depositional age of sample A15 is the one that is best defined, 1.92 Ga. The other two could have marginally younger maximum depositional ages, i.e. 1.90 Ga, although this heavily depends on the significance that is given to the few youngest zircons. An interesting point is the lack of the peak of 2.7 Ga zircons in samples A1557 and A2440 (Fig. 15), shown by sample A15 and data from previously studied samples (Claesson et al. 1993, Lahtinen et al. 2002, Nironen & Mänttäri 2012). Nevertheless, both of these samples contain Archean zircons, but of differing ages and in smaller quantities. However, it should be noted that the amount of data from sample A2440 is too limited to draw definitive conclusions on its detrital zircon population. All three samples from the Häme migmatite suite display a peak in the zircon population close to 2.00 Ga, but some differences in the location of the peak can also be identified; A15 displays a sharp peak between 1.92 and 2.00 Ga, whereas A1557 has a broader distribution from 1.9 to 2.2 Ga (Fig.15).

5.2.3 Demarcation between the various suites

Despite differences between individual samples, all the metasedimentary units within our study area and its vicinity display similar detrital zircon patterns when examined at the unit level (Fig. 16), i.e. all of them contain Archean zircons peaking at ~2.7 Ga in addition to Paleoproterozoic ones peaking at ~2.0 Ga and spanning from 2.2 to 1.9 Ga. The nearly complete lack of grains with ages 2.5–2.2 Ga is also characteristic of all of the units, as noted in earlier studies (e.g. Huhma et al. 1991, Lahtinen et al. 2009, 2010, Kotilainen et al. 2016). The observed Neoarchean (~2.7 Ga) peak coincides with the late magmatic phase of the Karelia Province consisting of granitoids of differing compositions (e.g. Heilimo

et al. 2011, Mikkola et al. 2011). The sources proposed so far for the detrital zircons with ages from 2.05 Ga to 1.95 Ga include the Lapland–Kola orogeny (Lahtinen et al. 2010) and the Keitele microcontinent (Lahtinen et al. 2009), which would have amalgamated with the Karelia Craton at 1.92 Ga. Another possibility could be the Central Russian Fold Belt in the east, which has also been proposed to contain rocks of this age (Samsonov et al. 2016).

The variation shown by individual samples representing the same suite (Figs. 14, 15) and on the other hand the close resemblance of the populations on the suite level (Fig. 16) warrants discussion of the existing geological division of the metasedimentary units in southern and central Finland. Lahtinen et al. (2017) suggested that the protoliths of the Häme and Pirkanmaa migmatite suites could have been deposited in the same basin. Based on our material from the northeastern parts of these units, this model also seems plausible; the age distribution of both suites is nearly identical. The differences individual samples display in the proportion of Archean and Paleoproterozoic zircon grains indicate that variation in the age spectrum of the source area(s) existed either spatially or over time. Lahtinen et al. (2017) additionally pointed out the close resemblance of the Myllyniemi formation of the Tampere group and the two migmatite suites. In our main study area, the Tammijärvi lithodeme is, with respect to the rock types present (Kähkönen 2005) and the zircon population (Fig. 15), identical to the Myllyniemi formation. However, it is interpreted as belonging to the Pirkanmaa migmatite suite instead of the Makkola suite, which is the equivalent of the volcanic formations of the Tampere group (Mikkola et al. 2018b). Thus, it seems that the current unit division in this respect reflects the late tectonic movements and differences in metamorphic degree and not differences in protoliths. Resolving these contradicting interpretations requires additional data from the little studied area between our study area and Tampere.

A likely source for the zircon grains with ages 1.93–1.91 Ga in the studied samples would be the older Svecofennian plutonic and volcanic rocks along the southwestern border of the Karelian Craton (e.g. Lahtinen & Huhma 1997, Vaasjoki et al. 2003, Kousa et al. 2018a), as proposed earlier, for example, by Lahtinen et al. (2002, 2009). An interesting phenomenon with respect to these 1.93–1.91 Ga zircons is their small proportion in the Pirkanmaa and Häme migmatite suites (Fig. 16). These suites, according to the proposed models (e.g. Lahtinen et al. 2017, Nironen 2017), were deposited after the collision of the older Svecofennian arc with the Archean Craton. Such a newly formed orogeny would seem like a bountiful source of detrital material, but the number of zircon crystals of this age is limited. Possible explanations for their unexpectedly small proportion could be paleotransportation in other directions or burial beneath older rocks during collision.

The Viinijärvi suite (Fig. 1), which was deposited before and deformed during the ~1.92 Ga collision (Lahtinen et al. 2010), shares several characteristics with both Pirkanmaa and Häme migmatite suites. All three were deposited as turbidites and host black schist interbeds, albeit in differing proportions. All three have similar zircon populations (Fig. 16) and all three host mafic to ultramafic volcanic sequences related to extensional phases: the Outokumpu ophiolite assemblage in the Viinijärvi suite (Peltonen 2005) and the volcanic rocks with EMORB and picrite affinity in the migmatite suites (Lahtinen et al. 2017, Kousa et al. 2018b). Lahtinen et al. (2009) explained the similarities in geochemistry and detrital zircon populations shown by the Pirkanmaa migmatite suite and the Viinijärvi suite by suggesting that the latter formed a major source area for the former. This interpretation could be correct, but makes reliable separation of these units lacking distinctive characteristics in an intensively deformed area, like the one from where samples A15 and A1557 were taken, difficult, if not impossible. Thus, it is in our opinion possible that the current demarcation between Viinijärvi and the Pirkanmaa and Häme migmatite suites could reflect late deformation phases instead of differences in the time and place of deposition. However, further evaluation of this idea would require additional work, including detrital zircon samples from the paragneisses of the Savo supersuite. This unit extends as a narrow band along the southwestern boundary of the Viinijärvi suite in the current interpretations (Fig. 1), but all available age data from it are north of Kuopio. This lack of data from areas relevant to this study is the reason why we have excluded this unit from discussion.

The lack of detrital zircons with ages similar to the ages of the volcanic rocks of the Makkola suite and the Tampere group (1895–1875 Ma; Kähkönen & Huhma 2012, Mikkola et al. 2018b) either requires that the studied metasedimentary units were deposited before the volcanic activity in the area, or that

in such a location these volcanic rocks were not in their source area. The latter explanation would require late tectonic transportation to their current position, which would mean the complete dismissal of the models previously proposed (e.g. Lahtinen et al. 2017, Nironen 2017 and references therein). Smaller scale tectonic movements are the most likely explanation for the subareas with a lower metamorphic degree but sharing a common origin. The well-preserved rocks of the Tammijärvi and Rusalansuo lithodemes were juxtaposed by vertical movements in the late stages of the Svecofennian evolution with their counterparts that had been metamorphosed to a higher degree.

Evidence for rocks belonging to the younger Svecofennian sedimentation phase (1.88–1.83 Ga; Korsman et al. 1988, Bergman et al. 2008, Nironen & Mänttäri 2012, Lahtinen et al. 2015) known from a number of locations in southern and central Finland was not found from our main study area. Their existence cannot be completely ruled out due to locally extensive Quaternary coverage, but their presence seems unlikely.

The significance of the presented data for the overall geological development and structure of the study area and its surroundings is further discussed in the article of Mikkola et al. (2018a).

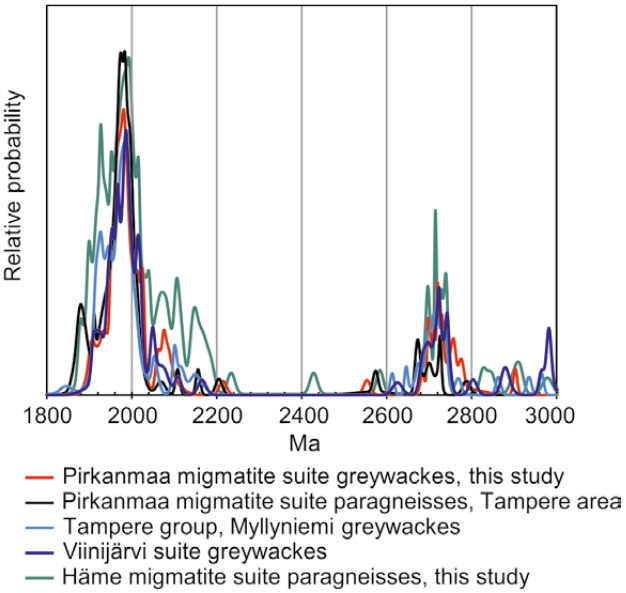

Fig. 16. Comparison of detrital zircon populations from the unmigmatized greywackes of the study area, samples representing the eastern end of the Häme migmatite suite, the Pirkanmaa migmatite suite in the Tampere area, Myllyniemi greywackes of the Tampere group and Viinijärvi suite greywackes. Data for the last three are from Lahtinen et al. (2009, 2010).

6 CONCLUSIONS

Metasedimentary units on the southeastern flank of Central Finland Granitoid Complex were deposited as turbidites before the onset of the main phase of volcanic activity in the area.

The maximum depositional ages of the studied metasedimentary samples vary between 1.92 and 1.90 Ga. In the majority of the samples, detrital zircon populations display age distribution patterns with Neoarchean (~2.7 Ga) and Paleoproterozoic (2.00–1.92 Ga) peaks. Thus, the populations are similar to the majority of the paragneiss samples from central and southern Finland.

Our data support the earlier presented idea that the Häme migmatite suite and Pirkanmaa migmatite suite were deposited in the same sedimentary basin. The material in the basin was heterogeneous, which is reflected in the large scatter in chemical composition of the analysed samples. The different stratigraphic units could not be distinguished on a geochemical basis.

The present unit division in southern and central Finland reflects the original differences in the depositional environment, but the boundaries result from tectonic movements. Thus, the current unit division should be re-evaluated on a tectonostratigraphic basis.

ACKNOWLEDGEMENTS

Jouko Ranua is thanked for the drill core pictures used for Figure 4. Dr Raimo Lahtinen is acknowledged for the data from samples A15 and A1557. The staff of the isotope laboratory of the Geological Survey of Finland are thanked for the separation and preparation of the age samples, as well as keeping the machines running. Uranium–lead isotopes were studied with the help from Martin Whitehouse, Lev Ilyinsky and Kerstin Linden in the NORDSIM laboratory in Stockholm. The NORDSIM facility is supported by the Research Councils of Denmark, Norway and Sweden, the Geological Survey of Finland and the Swedish Museum of Natural History. This is NORDSIM contribution number 553. Reviewers Kari Strand and Mikko Nironen provided numerous comments that helped in improving the original manuscript.

REFERENCES

Bedrock of Finland - DigiKP. Digital map database [Electronic resource]. Espoo: Geological Survey of Finland [referred 31.04.2017]. Version 2.0.

Bergman, S., Högdahl, K., Nironen, M., Ogenhall, E., Sjöström, H., Lundqvist, L. & Lahtinen, R. 2008. Timing of Palaeoproterozoic intra-orogenic sedimentation in the central Fennoscandian Shield; evidence from detrital zircon in metasandstone. Precambrian Research 161, 231–249.

Boynton, W. V. 1984. Cosmochemistry of the rare earth elements; meteorite studies. In: Henderson, P. (ed.) Rare earth element geochemistry. Amsterdam: Elsevier, 63–114.

Claesson, S., Huhma, H., Kinny, P. D. & Williams, I. S. 1993. Svecofennian detrital zircon ages—implications for the Precambrian evolution of the Baltic Shield. Precambrian Research 64, 109–130.

Heilimo, E., Ahven, M. & Mikkola, P. 2018. Geochemical characteristics of the plutonic rock units present at the southeastern boundary of the Central Finland Granitoid Complex. In: Mikkola, P., Hölttä, P. & Käpyaho, A. (eds) Development of the Paleoproterozoic Svecofennian orogeny: new constraints from the southeastern boundary of the Central Finland Granitoid Complex. Geological Survey of Finland, Bulletin 407. (this volume). Available at: https://doi.org/10.30440/bt407.6

Heilimo, E., Halla, J. & Huhma, H. 2011. Single-grain zircon U–Pb age constraints of the western and eastern sanukitoid zones in the Finnish part of the Karelian Province. Lithos 121, 87–99.

Herron, M. M. 1988. Geochemical classification of terrigenous sands and shales from core or log data. Journal of Sedimentary Petrology 58, 820–829.

Huhma, H., Claesson, S., Kinny, P. D. & Williams, I. S. 1991. The growth of Early Proterozoic crust: new evidence from Svecofennian zircons. Terra Nova 3, 175–179.

Janoušek, V., Farrow, C. M. & Erban, V. 2006. Interpretation of whole-rock geochemical data in igneous geochemistry: introducing Geochemical Data Toolkit (GCDkit). Journal of Petrology 47, 1255–1259.

Kähkönen, Y. 2005. Svecofennian supracrustal rocks. In: Lehtinen, M., Nurmi, P. & Rämö, O. T. (eds) The Precambrian Bedrock of Finland—Key to the evolution of the Fennoscandian Shield. Elsevier Science B.V., 343–406.

Kähkönen, Y. & Huhma, H. 2012. Revised U-Pb zircon ages of supracrustal rocks of the Paleoproterozoic Tampere Schist Belt, southern Finland. In: Kukkonen, I. T., Kosonen E. M., Oinonen, K., Eklund, O., Korja, A., Korja, T., Lahtinen, R., Lunkka, J. P. & Poutanen, M. (eds) Lithosphere 2012 – Seventh Symposium on the Structure, Composition and Evolution of the Lithosphere in Finland. Programme and Extended Abstracts, Espoo, Finland, November 6–8, 2012. Institute of Seismology, University of Helsinki, Report S-56, 51–54. Available at: http://www.seismo.helsinki.fi/pdf/LITO2012.pdf

Kähkönen, Y. & Leveinen, J. 1994. Geochemistry of metasedimentary rocks of the Paleoproterozoic Tampere schist belt, southern Finland. In: Nironen, M. & Kähkönen, Y. (eds) Geochemistry of Proterozoic supracrustal rocks in Finland. Geological Survey of Finland, Special Paper 19, 117–136. Available at: http://tupa.gtk.fi/julkaisu/specialpaper/sp_019.pdf

Kallio, J. 1986. Joutsan kartta-alueen kallioperä. Summary: Pre-Quaternary rocks of the Joutsa Map-Sheet area. Geological Map of Finland 1:100 000, Explanation to the Maps of Pre-Quaternary Rocks, Sheet 3122. Geological Survey of Finland. 56 p. Available at: http://tupa.gtk.fi/kartta/kallioperakartta100/kps_3122.pdf

Karppanen, T. 1970. Tampereen liuskejakson geologiaa Luhangan Tammijärvellä. Unpublished master's thesis, University of Helsinki, Department of Geology and Mineralogy. 75 p. (in Finnish)

Kilpeläinen, T. 1998. Evolution and 3D modelling of structural and metamorphic patterns of the Palaeoproterozoic crust in the Tampere-Vammala area, southern Finland. In: Kilpeläinen, T. Evolution and 3D modelling of structural and metamorphic patterns of the Palaeoproterozoic crust in the Tampere-Vammala area, southern Finland. Geological Survey of Finland, Bulletin 397, 1–124. Available at: http://tupa.gtk.fi/julkaisu/bulletin/bt_397.pdf

Korsman, K., Koistinen, T., Kohonen, J., Wennerström, M., Ekdahl, E., Honkamo, M., Idman, H. & Pekkala, Y. (eds) 1997. Suomen kallioperäkartta - Berggrundskarta över Finland - Bedrock map of Finland 1:1,000,000. Espoo: Geological Survey of Finland.

Korsman, K., Niemelä, R. & Wasenius, P. 1988. Multistage evolution of the Proterozoic crust in the Savo schist belt, eastern Finland. In: Korksman, K. (ed.) Tectono-metamorphic evolution of the Raahe-Ladoga zone, eastern Finland. Geological Survey of Finland, Bulletin 343, 89–96. Available at: http://tupa.gtk.fi/julkaisu/bulletin/bt_343.pdf

Kotilainen, A. K., Mänttäri, I., Kurhila, M., Hölttä, P. & Rämö, O. T. 2016. Evolution of a Palaeoproterozoic giant magmatic dome in the Finnish Svecofennian; New

insights from U–Pb geochronology. Precambrian Research 272, 39–56.

Kousa, J., Huhma, H., Hokka, J. & Mikkola, P. 2018a. Extension of Svecofennian 1.91 Ga magmatism to the south, results of the reanalysed age determination samples from Joroinen, central Finland. In: Mikkola, P., Hölttä, P. & Käpyaho, A. (eds) Development of the Paleoproterozoic Svecofennian orogeny: new constraints from the southeastern boundary of the Central Finland Granitoid Complex. Geological Survey of Finland, Bulletin 407. (this volume). Available at: https://doi.org/10.30440/bt407.3

Kousa, J., Mikkola, P. & Makkonen, H. 2018b. Paleoproterozoic mafic and ultramafic volcanic rocks in the South Savo region, eastern Finland. In: Mikkola, P., Hölttä, P. & Käpyaho, A. (eds) Development of the Paleoproterozoic Svecofennian orogeny: new constraints from the southeastern boundary of the Central Finland Granitoid Complex. Geological Survey of Finland, Bulletin 407. (this volume). Available at: https://doi.org/10.30440/bt407.4

Lahtinen, R. 1996. Geochemistry of Palaeoproterozoic supracrustal and plutonic rocks in the Tampere-Hämeenlinna area, southern Finland. In: Lahtinen, R. Geochemistry of Palaeoproterozoic supracrustal and plutonic rocks in the Tampere-Hämeenlinna area, southern Finland. Geological Survey of Finland, Bulletin 389, 1–113. Available at: http://tupa.gtk.fi/julkaisu/bulletin/bt_389.pdf

Lahtinen, R. & Huhma, H. 1997. Isotopic and geochemical constraints on the evolution of the 1.93–1.79 Ga Svecofennian crust and mantle. Precambrian Research 82, 13–34.

Lahtinen, R. & Nironen, M. 2010. Paleoproterozoic lateritic paleosol–ultra-mature/mature quartzite–meta-arkose successions in southern Fennoscandia—intra-orogenic stage during the Svecofennian orogeny. Precambrian Research 183, 770–790.

Lahtinen, R., Huhma, H., Kähkönen, Y. & Mänttäri, I. 2009. Paleoproterozoic sediment recycling during multiphase orogenic evolution in Fennoscandia, the Tampere and Pirkanmaa belts, Finland. Precambrian Research 174, 310–336.

Lahtinen, R., Huhma, H., Kontinen, A., Kohonen, J. & Sorjonen-Ward, P. 2010. New constraints for the source characteristics, deposition and age of the 2.1–1.9 Ga metasedimentary cover at the western margin of the Karelian Province. Precambrian Research 176, 77–93.

Lahtinen, R., Huhma, H. & Kousa, J. 2002. Contrasting source components of the Palaeoproterozoic Svecofennian metasediments: detrital zircon U–Pb, Sm–Nd and geochemical data. Precambrian Research 116, 81–109.

Lahtinen, R., Huhma, H., Lahaye, Y., Kousa, J. & Luukas, J. 2015. Archean-Proterozoic collision boundary in central Fennoscandia: revisited. Precambrian Research 261, 127–165.

Lahtinen, R., Huhma, H., Sipilä, P. & Vaarma, M. 2017. Geochemistry, U-Pb geochronology and Sm-Nd data from the Paleoproterozoic Western Finland supersuite – A key component in the coupled Bothnian oroclines. Precambrian Research 299, 264–281.

Luukas, J., Kousa, J., Nironen, M. & Vuollo, J. 2017. Major stratigraphic units in the bedrock of Finland, and an approach to tectonostratigraphic division. In: Nironen, M. (ed.) Bedrock of Finland at the scale 1:1 000 000 - Major stratigraphic units, metamorphism and tectonic evolution. Geological Survey of Finland, Special Paper 60, 9–40. Available at: http://tupa.gtk.fi/julkaisu/specialpaper/sp_060.pdf

Matisto, A. 1976. Kangasalan kartta-alueen kallioperä. Summary: Pre-Quaternary rocks of the Kangasala Map-Sheet area. Geological Map of Finland 1:100 000, Explanation to the Maps of Pre-Quaternary Rocks, Sheet 2141. Geological Survey of Finland. 27 p. Available at: http://tupa.gtk.fi/kartta/kallioperakartta100/kps_2141.pdf

McDonough, W. F. & Sun, S.-S. 1995. Composition of the Earth. Chemical Geology 120, 223–253.

Mikkola, P., Heilimo, E., Aatos, S., Ahven, M., Eskelinen, J., Halonen, S., Hartikainen, A., Kallio, V., Kousa, J., Luukas, J., Makkonen, H., Mönkäre, K., Niemi, S., Nousiainen, M., Romu, I. & Solismaa, S. 2016. Jyväskylän seudun kallioperä. Summary: Bedrock of the Jyväskylä area. Geological Survey of Finland, Report of Investigation 227. 95 p., 6 apps. Available at: http://tupa.gtk.fi/julkaisu/tutkimusraportti/tr_227.pdf

Mikkola, P., Heilimo, E., Luukas, J., Kousa, J., Aatos, S., Makkonen, H., Niemi, S., Nousiainen, M., Ahven, M., Romu, I. & Hokka, J. 2018a. Geological evolution and structure along the southeastern border of the Central Finland Granitoid Complex. In: Mikkola, P., Hölttä, P. & Käpyaho, A. (eds) Development of the Paleoproterozoic Svecofennian orogeny: new constraints from the southeastern boundary of the Central Finland Granitoid Complex. Geological Survey of Finland, Bulletin 407. (this volume). Available at: https://doi.org/10.30440/bt407.1

Mikkola, P., Huhma, H., Heilimo, E. & Whitehouse, M. 2011. Archean crustal evolution of the Kianta Complex, Karelia; constraints from geochemistry and isotopes of granitoids from Suomussalmi, Finland. Lithos 125, 287-307.

Mikkola, P., Mönkäre, K., Ahven, M. & Huhma, H. 2018b. Geochemistry and age of the Paleoproterozoic Makkola suite volcanic rocks in central Finland. In: Mikkola, P., Hölttä, P. & Käpyaho, A. (eds) Development of the Paleoproterozoic Svecofennian orogeny: new constraints from the southeastern boundary of the Central Finland Granitoid Complex. Geological Survey of Finland, Bulletin 407. (this volume). Available at: https://doi.org/10.30440/bt407.5

Mikkola, P, Niskanen, M. & Hokka, J. 2018c. Harjujärvensuo gold mineralisation in Leivonmäki, Central Finland. In: Mikkola, P., Hölttä, P. & Käpyaho, A. (eds) Development of the Paleoproterozoic Svecofennian orogeny: new constraints from the southeastern boundary of the Central Finland Granitoid Complex. Geological Survey of Finland, Bulletin 407. (this volume). Available at: https://doi.org/10.30440/bt407.9

Nironen, M. 2017. Guide to the Geological Map of Finland – Bedrock 1:1 000 000. In: Nironen, M. (ed.) Bedrock of Finland at the scale 1:1 000 000 - Major stratigraphic units, metamorphism and tectonic evolution. Geological Survey of Finland, Special Paper 60, 41–76. Available at: http://tupa.gtk.fi/julkaisu/specialpaper/sp_060.pdf

Nironen, M. & Mänttäri, I. 2012. Timing of accretion, intra-orogenic sedimentation and basin inversion in the Paleoproterozoic Svecofennian orogen: The Pyhäntaka area, southern Finland. Precambrian Research 192–195, 34–51.

Nironen, M., Kousa, J., Luukas, J. & Lahtinen, R. (eds) 2016. Geological Map of Finland – Bedrock 1:1 000 000. Espoo: Geological Survey of Finland. Available at: http://tupa.gtk.fi/kartta/erikoiskartta/ek_097_300dpi.pdf

Pettijohn, F. J., Potter, P. E. & Siever, R. 1972. Sand and Sandstone. Berlin: Springer-Verlag. 600 p.

Rasilainen, K., Lahtinen, R. & Bornhorst, T. J. 2007. The Rock Geochemical Database of Finland Manual. Geological Survey of Finland, Report of Investigation 164. 38 p. Available at: http://tupa.gtk.fi/julkaisu/tutkimusraportti/tr_164.pdf

Samsonov, A. V., Spiridonov, V. A., Larionova, Y. O. & Larionov, A. N. 2016. The Central Russian fold belt: Paleoproterozoic boundary of Fennoscandia and Volgo-Sarmatia, the East European Craton. In: Abstracts of the 32nd Nordic Geological Winter Meeting. Bulletin of the Geological Society of Finland, Special Volume 162. Available at: http://www.geologinenseura.fi/bulletin/Special_Volume_1_2016/BGSF-NGWM2016_Abstract_Volume.pdf

Vaasjoki, M., Huhma, H., Lahtinen, R. & Vestin, J. 2003. Sources of Svecofennian granitoids in the light of ion probe U-Pb measurements on their zircons. Precambrian Research 121, 251–262.

Williams, I. S., Buick, I. S. & Cartwright, I. 1996. An extended episode of early Mesoproterozoic metamorphic fluid flow in the Reynolds Range, central Australia. Journal of Metamorphic Geology 14, 29–47.

Development of the Paleoproterozoic Svecofennian orogeny: new constraints from the southeastern boundary of the Central Finland Granitoid Complex
Edited by Perttu Mikkola, Pentti Hölttä and Asko Käpyaho
Geological Survey of Finland, Bulletin 407, 56-62, 2018

EXTENSION OF SVECOFENNIAN 1.91 GA MAGMATISM TO THE SOUTH, RESULTS OF THE REANALYSED AGE DETERMINATION SAMPLES FROM JOROINEN, CENTRAL FINLAND

by

Jukka Kousa[1)], Hannu Huhma[2)], Janne Hokka[2)] and Perttu Mikkola[1)]

Kousa, J., Huhma, H., Hokka, J. & Mikkola, P. 2018. Extension of Svecofennian 1.91 Ga magmatism to the south, results of the reanalysed age determination samples from Joroinen, central Finland. *Geological Survey of Finland, Bulletin 407*, 56–62, 3 figures.

New analyses from three old age determination samples conducted on coeval volcanic and plutonic rocks from Viholanniemi in central Finland yielded ages from 1914 ± 3 Ma to 1908 ± 2 Ma. Based on the new and pre-existing isotope data, they can be regarded as part of the older Svecofennian magmatic stage aged 1.93–1.91 Ga, predating the main phase of crustal growth in central Finland by 20 Ma. The updated data extend the known area of the older Svecofennian magmatic stage 100 km to the southeast.

Appendix 1 is available at: http://tupa.gtk.fi/julkaisu/liiteaineisto/bt_407_appendix_1.pdf

Electronic Appendix is available at: http://tupa.gtk.fi/julkaisu/liiteaineisto/bt_407_electronic_appendix.xlsx

Keywords: volcanic rocks, granites, Paleoproterozoic, Svecofennian, Finland, absolute age, zircon, U/Pb, geochronology

[1)] *Geological Survey of Finland, P.O. Box 1237, FI-70211 Kuopio, Finland*
[2)] *Geological Survey of Finland, P.O. Box 96, FI-02151 Espoo, Finland*
E-mail: janne.hokka@gtk.fi

VERTAISARVIOITU
KOLLEGIALT GRANSKAD
PEER-REVIEWED
www.tsv.fi/tunnus

https://doi.org/10.30440/bt407.3

Editorial handling by Pentti Hölttä.

Received 15 June 2017; Accepted 1 June 2018

1 INTRODUCTION

The Svecofennian magmatic rocks in central Finland form two distinct age groups: an older 1.93–1.91 Ga (Helovuori 1979, Ekdahl 1993, Lahtinen 1994, Vaasjoki et al. 2003, Kousa et al. 1994, 2004, Lahtinen et al. 2016) and a younger 1.895–1.875 Ga group (e.g. Vaasjoki et al. 2003, Kähkönen & Huhma 2012, Mikkola et al. 2018b). The older age group is documented as the Northern Ostrobothnia supergroup, comprising metavolcanic rocks of the Pyhäsalmi and Vihanti groups and the tonalitic

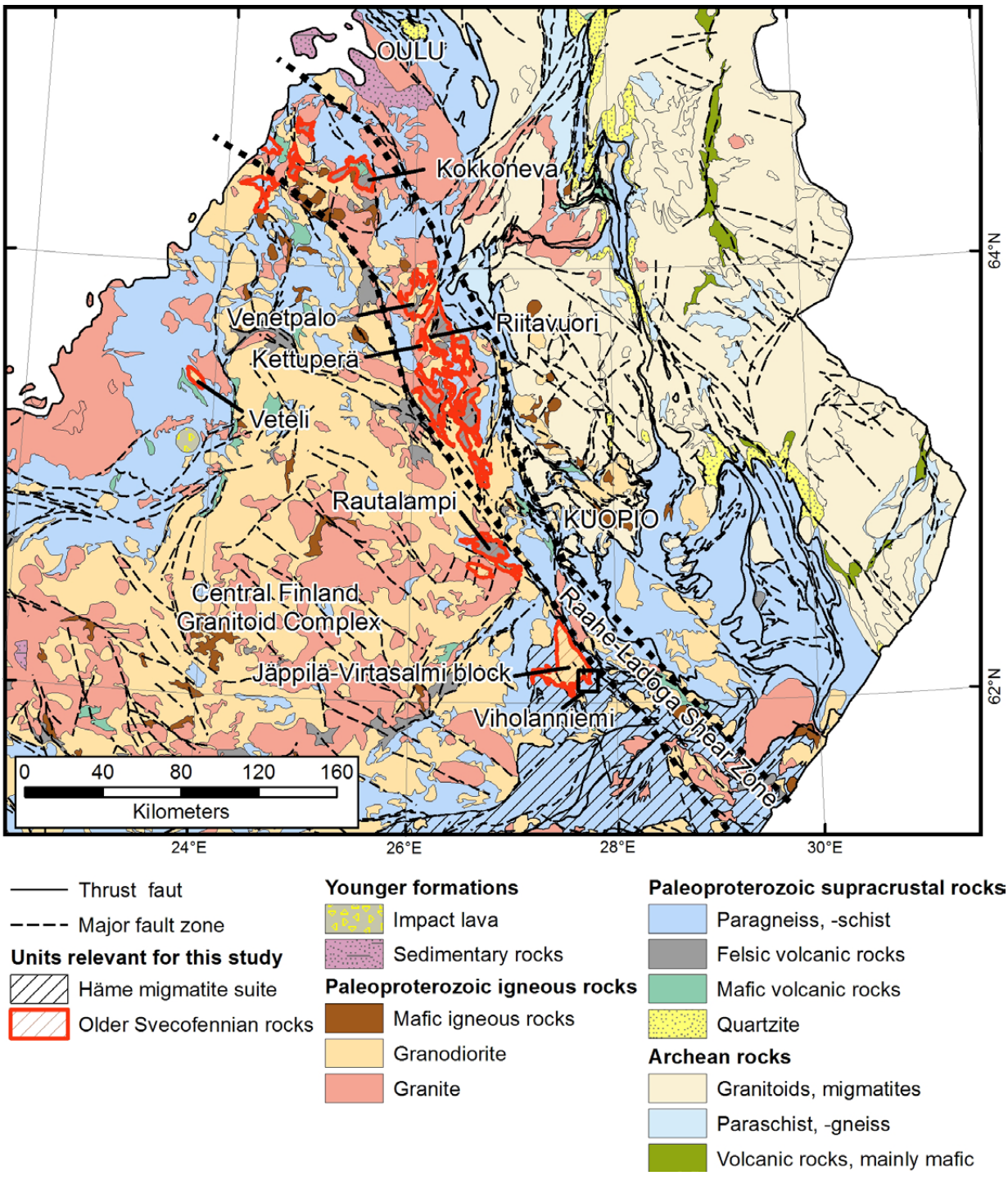

Fig. 1. Geological map of central Finland with rock units and locations relevant for this study highlighted. References for the age determinations of older Svecofennian succession: Kokkoneva 1926 ± 3 Ma, Venetpalo 1917 ± 5 Ma, Kettuperä 1924 ± 3 Ma (Kousa et al. 2013), Riitavuori 1921 ± 2 Ma (Kousa et al. 1994), Rautalampi (Rastinpää 1920 ± 6 Ma, Pyöreänsuonvuori 1914 ± 5 Ma, Vaasjoki et al. 2003) and Veteli 1921 ± 5 Ma (Lahtinen et al. 2016). Map modified from Nironen et al. (2016) and Bedrock of Finland - DigiKP.

intrusions of the Venetpalo suite (Luukas et al. 2017). These units form small scattered occurrences within the Raahe–Ladoga Shear Zone along the western boundary of the Archean Karelian craton (Fig. 1), the exception being the Veteli intrusion located further west. This older succession has been interpreted to represent a distinct phase of arc-type magmatism that ended when the Keitele microcontinent, roughly equalling the current Central Finland Granitoid Complex (CFGC), collided with the Archean craton at 1.92–1.91 Ga and the Lapland-Savo orogen was formed (e.g. Lahtinen 2014 and references therein). As several VHMS-type ores, including the Pyhäsalmi Cu–Zn mine and the Vihanti Zn mine (Helovuori 1979, Mäki et al. 2015), are hosted by the older Svecofennian volcanic succession, its spatial extent is important for evaluating the areal ore potential and guiding exploration activities. Currently, the southernmost known location of magmatic rocks of the older succession is in Rautalampi (Vaasjoki et al. 2003, Mikkola et al. 2016).

In this paper, we present new U–Pb zircon analyses from three previously dated samples from the Viholanniemi area in Joroinen (Huhma 1986, Vaasjoki & Sakko 1988). These samples originally yielded age results close to 1905 Ma, which seemed to fall between the two major Svecofennian age groups. The main motivation for this study was to either confirm or refute this with additional analyses. The obtained results are used to discuss the geological correlation of the Viholanniemi area and Jäppilä-Virtasalmi block in general.

2 GEOLOGICAL SETTING

The Viholanniemi area, about 5 km southwest of the village of Joroinen, forms the south-easternmost corner of the Jäppilä-Virtasalmi block formed by rocks belonging to the Maavesi suite (Bedrock of Finland – DigiKP). This suite is formed by gneissose rock types intruded by granitoids, mainly granodiorites and tonalites. These relatively leucocratic plutonic rocks are mainly composed of quartz, plagioclase and biotite with rare hornblende and potassium feldspar, and have intrusive contacts with the volcanic rocks flanking the block (Pekkarinen 2002). The Viholanniemi volcanic suite includes rhyolitic quartz feldspar porphyries, intermediate pyroclastic rocks and lavas with locally more mafic beds and minor carbonate rock interlayers (Korsman 1973, Makkonen 1991, Zhang 2000, Kousa 2009). On average, the volcanic units of the Viholanniemi volcanic suite are more felsic than those surrounding the Jäppilä-Virtasalmi block. The latter, locally pillowed lavas are classified into the Virtasalmi suite and are present in southern part(s) of the study area (Fig. 2).

The contact between the Viholanniemi volcanic suite and the metagreywackes of the Häme migmatite suite (Fig. 2) is covered by Quaternary deposits, and their stratigraphic relationship thus remains uncertain. Based on indirect interpretation, these greywackes could have been deposited contemporaneously with the Viholanniemi volcanic rocks (Kousa 2009). The maximum depositional age of a metasedimentary sample belonging to the Häme migmatite suite in the proximity of Viholanniemi is close to 1.92 Ga (Mikkola et al. 2018a, sample A15).

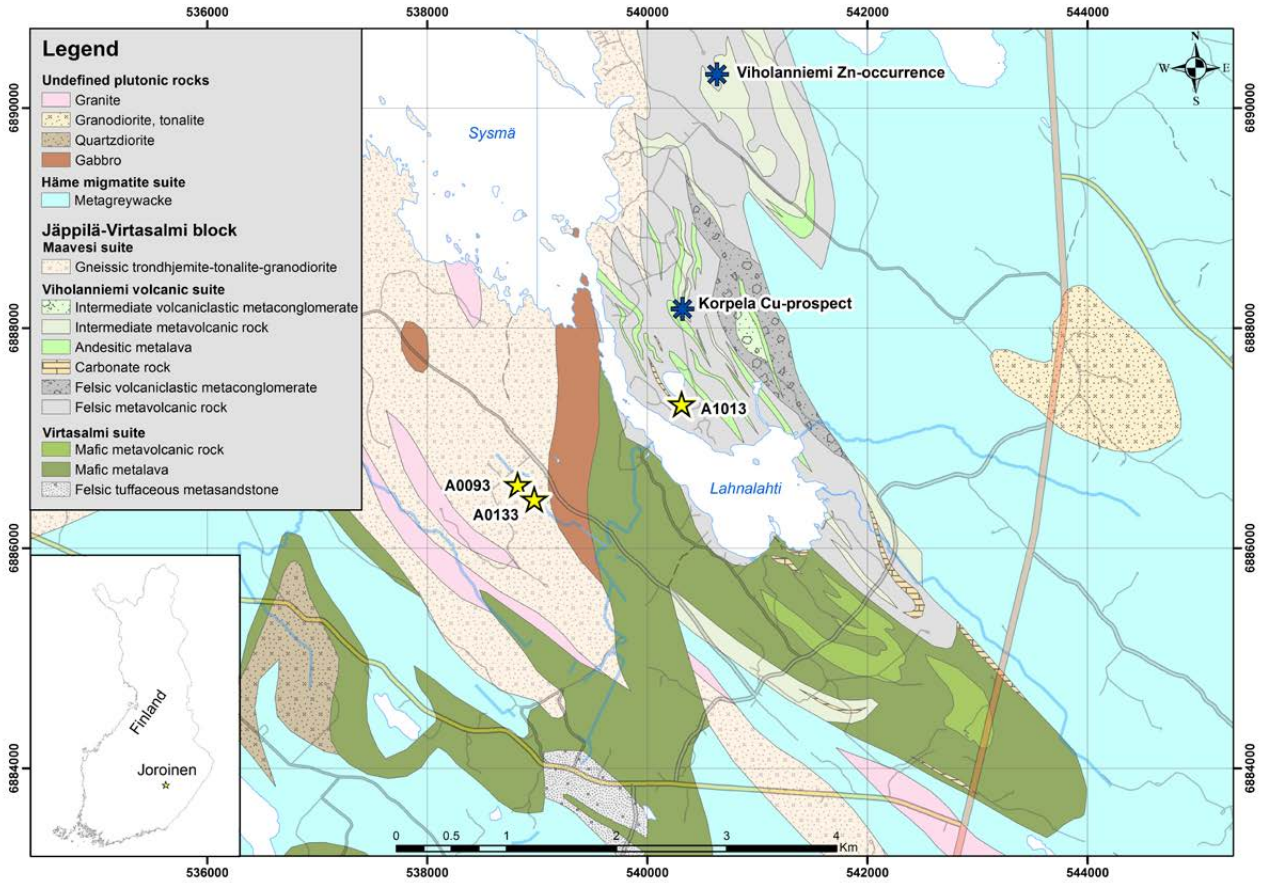

Fig. 2. Bedrock map of the study area, with the locations of the age determination samples and mineralisations shown. Map modified from Bedrock of Finland – DigiKP. Base map © National Land Survey of Finland.

3 AGE DETERMINATIONS

For this study, zircons from the old age determination samples (Huhma 1986, Vaasjoki & Sakko 1988) were reanalysed in the isotope laboratory of the Geological Survey of Finland (GTK) in Espoo using a VG Sector 54 TIMS (thermal ionisation decoupled multicollector mass spectrometer). The zircons were treated using the chemical abrasion (CA) method of Mattinson (2005). See Appendix 1 for a more detailed description of the method and the Electronic Appendix for the results, including the previously published ones.

3.1 A93 Saunakangas trondhjemite

Sample A93 is a foliated trondhjemite that has been interpreted to belong to the Maavesi suite granitoids cross-cutting the volcanic rocks of the Viholanniemi suite. The data published by Huhma (1986) for this sample are scattered, most likely due to analytical problems. The multi-grain CA-TIMS analysis (D) is concordant and yields a $^{207}Pb/^{206}Pb$ age of 1908 ± 2 Ma (Electronic Appendix, Fig. 3), which we consider as the best estimate for the crystallisation age of sample A93.

3.2 A133 Saunakangas granodiorite

Sample A133 Saunakangas granodiorite represents the same Maavesi suite as sample A93. Based on three variably discordant zircon U–Pb analyses, Huhma (1986) obtained an upper intercept age of 1903 ± 10 Ma, which was interpreted as the age of this rock. The scattered data from A93 were consistent with this interpretation (Fig. 3). The CA analysis (D) is concordant and yields a $^{207}Pb/^{206}Pb$ age of 1911 ± 2 Ma, which is within error similar to the result obtained from sample A93. If all four fractions analysed from A133 are used, an upper intercept of 1912 ± 3 Ma is obtained, which we consider as the best estimate for the age of zircon in and the crystallisation of sample A133.

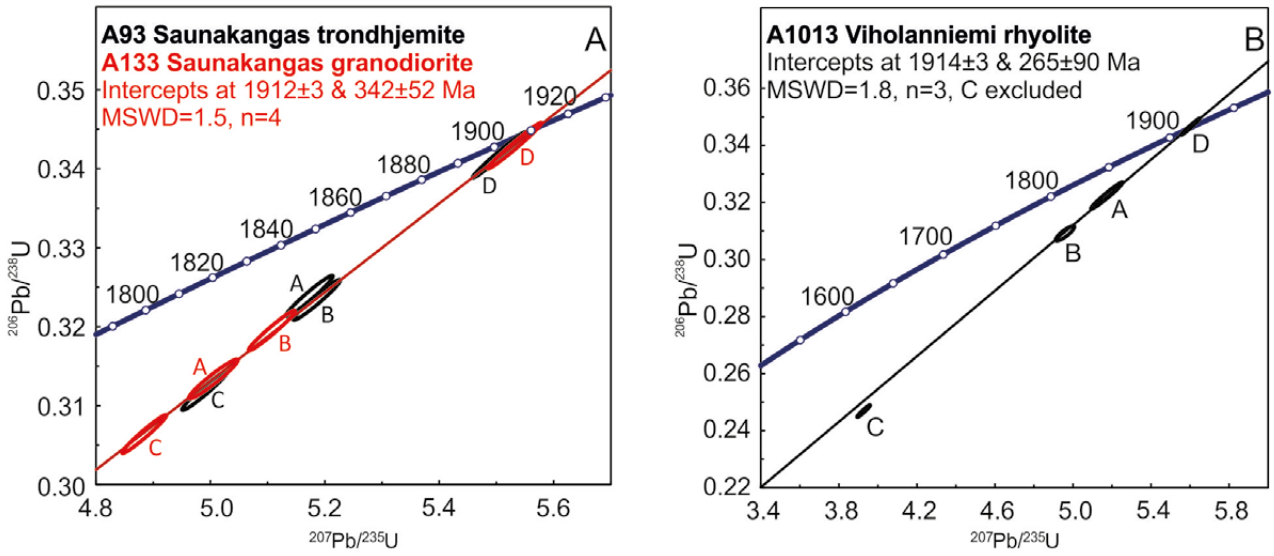

Fig. 3. Concordia diagram for samples A93 and A133 (A) and A1013 (B). See the text for more details. Error ellipses plotted at the 2σ level.

3.3 A1013 Viholanniemi rhyolite

Based on three discordant zircon U–Pb analyses, Vaasjoki & Sakko (1988) obtained an age of 1906 ± 4 Ma for sample A1013, representing the felsic volcanic rocks hosting the Viholanniemi Zn–Ag–Au mineralisation. Texturally, this rhyolite is a feldspar porphyritic quartz-feldspar schist. The CA analysis (D) is concordant with a $^{207}Pb/^{206}Pb$ age of 1914 ± 2 Ma. If the highly discordant low-density fraction (C) is discarded, an upper intercept age of 1914 ± 3 Ma can be calculated (Fig. 3). We interpret this as the best estimate for the crystallisation age of this rock.

4 DISCUSSION

Based on our new CA-TIMS results, all three of the age determination samples from the Viholanniemi area are slightly older than previously thought (Huhma 1986, Vaasjoki & Sakko 1988). The felsic metavolcanic rock (A1013) yielded the oldest absolute age of 1914 ± 3 Ma, but granodiorite sample A133 is similar within error (1912 ± 3 Ma). This age for the granodiorite is supported by the CA-TIMS analysis conducted on sample A93, which, however, shows a slightly higher amount of common lead ($^{206}Pb/^{204}Pb$ 5671 vs. 21986).

The new age data confirm that the first magmatic activity in the Viholanniemi area took place well before the onset of magmatic activity along the southern boundary of the CFGC, i.e. 1895 Ma (Kallio 1986, Kähkönen & Huhma 2012, Mikkola et al. 2018b). The ages from the Viholanniemi area, clustering close to 1910 Ma, are within error similar to the youngest ages reported for magmatic rocks belonging to the older Svecofennian group (e.g. Ekdahl 1993, Vaasjoki et al. 2003, Kousa et al. 2013).

Published Sm–Nd analyses of samples A93 and A113 yielded initial ε_{Nd} values of 3.3 ± 0.5 and 3.4 ± 0.4, respectively, which suggest a depleted mantle source (Huhma 1986, Lahtinen & Huhma 1997). These results are similar to those obtained from older Svecofennian rocks elsewhere (Fig. 1, Lahtinen & Huhma 1997).

The lead isotopic composition of the Viholanniemi Zn–Cu–Ag–Au mineralisation is intermediate between the CFGC (cf. Vaasjoki 1981) and the older Svecofennian rocks (Vaasjoki & Sakko 1988). Makkonen (1991) and Zhang (2000) noted that the Viholanniemi mineralisation is not a typical VHMS deposit, but the mineralisation is hosted by quartz-carbonate veins in a volcanic environment. Therefore, it is possible that the lead isotope values obtained from Viholanniemi are a result of a hydrothermal ore-forming process younger than the crystallisation ages of the Viholanniemi volcanic suite. However, as there are also indications for VHMS-type Cu–Zn deposits in the area

(Korpela in Fig. 2, Hokka et al. 2014), additional studies are needed to identify the timing of mineralisation event(s) in Viholanniemi.

Based on the updated age data and discussion above, it can be concluded that the magmatism in Viholanniemi is part of the older Svecofennian sequence. Therefore, the plutonic rocks in the area can be correlated with the Venetpalo plutonic suite further north (Nironen et al. 2016, Luukas et al. 2017) and the volcanic rocks with the Vihanti group (Luukas et al. 2017). This was already proposed by Ekdahl (1993), who suggested that Viholanniemi is the eastern end point of the "Pyhäsalmi arc". However, the so far spatially constrained linear form of the rocks belonging to the older Svecofennian magmatic phase has been scrapped following interpretation that the Veteli tonalite belongs to this group (Lahtinen et al. 2016).

Detrital zircon grains in the paragneisses belonging to the Häme migmatite suite and surrounding Viholanniemi, and the whole Virtasalmi-Jäppilä block, are mostly older than the presently studied samples (Lahtinen et al. 2002, Mikkola et al. 2018a). Only a limited number of detrital zircons in the paragneisses have ages between 1.92 and 1.90 Ga. The difficulties in reliably excluding the younging effects due to postdepositional alteration also have to be borne in mind. Therefore, despite the current spatial proximity, neither the Virtasalmi-Jäppilä block nor other parts of the older Svecofennian magmatic succession were the main source for the sediments of the Häme migmatite suite. Hence, the contacts between the larger geological units in the area are likely to be tectonic in origin.

5 CONCLUSIONS

The volcanic and plutonic rocks from the Viholanniemi area are roughly coeval, yielding ages from 1914 ± 3 to 1908 ± 2 Ma.

The Jäppilä-Virtasalmi block forms the south-eastern end point of the older Svecofennian magmatic rocks.

ACKNOWLEDGEMENTS

The authors would like to acknowledge the work by the staff of Geological Survey of Finland's isotope laboratory during sample preparation and analysis. Reviews by Dr Markku Väisänen and Dr Jukka Reinikainen clarified the manuscript.

REFERENCES

Bedrock of Finland – DigiKP. Digital map database [Electronic resource]. Espoo: Geological Survey of Finland [referred 31.04.2017]. Version 2.0.

Ekdahl, E. 1993. Early Proterozoic Karelian and Svecofennian formations and the Evolution of the Raahe-Ladoga Ore Zone, based on the Pielavesi area, central Finland. In: Ekdahl, E. Early Proterozoic Karelian and Svecofennian formations and the Evolution of the Raahe-Ladoga Ore Zone, based on the Pielavesi area, central Finland. Geological Survey of Finland, Bulletin 373, 1–137. Available at: http://tupa.gtk.fi/julkaisu/bulletin/bt_373.pdf

Helovuori, O. 1979. Geology of the Pyhäsalmi ore deposit, Finland. Economic Geology 74, 1084–1101.

Hokka, J., Niemi, S. & Kousa, J. 2014. The Korpela Cu-Zn mineralization, a new VMS potential target in the Palaeoproterozoic Viholanniemi volcanic suite in Joroinen, southeastern Finland. In: Lauri, L. S., Heilimo, E., Leväniemi, H., Tuusjärvi, M., Lahtinen, R. & Hölttä, P. (eds) Current Research: 2nd GTK Mineral Potential Workshop, Kuopio, Finland, 6–7 May 2014. Geological Survey of Finland, Report of Investigation 207, 35–38. Available at: http://tupa.gtk.fi/julkaisu/tutkimusraportti/tr_207.pdf

Huhma, H. 1986. Sm-Nd, U-Pb and Pb-Pb isotopic evidence for the origin of the Early Proterozoic Svecokarelian crust in Finland. Geological Survey of Finland, Bulletin 337. 48 p. Available at: http://tupa.gtk.fi/julkaisu/bulletin/bt_337.pdf

Kähkönen, Y. & Huhma, H. 2012. Revised U-Pb zircon ages of supracrustal rocks of the Paleoproterozoic Tampere Schist Belt, southern Finland. In: Kukkonen, I. T., Kosonen E. M., Oinonen, K., Eklund, O., Korja, A., Korja, T., Lahtinen, R., Lunkka, J. P. & Poutanen, M. (eds) Lithosphere 2012 – Seventh Symposium on the Structure, Composition and Evolution of the Lithosphere in Finland. Programme and Extended Abstracts, Espoo, Finland, November 6–8, 2012. Institute of Seismology, University of Helsinki, Report S-56, 51–54. Available at: http://www.seismo.helsinki.fi/pdf/LITO2012.pdf

Kallio, J. 1986. Joutsan kartta-alueen kallioperä. Summary: Pre-Quaternary rocks of the Joutsa Map-Sheet area. Geological Map of Finland 1:100 000, Explana-

tion to the Maps of Pre-Quaternary Rocks, Sheet 3122. Geological Survey of Finland. 56 p. Available at: http://tupa.gtk.fi/kartta/kallioperakartta100/kps_3122.pdf

Korsman, K. 1973. Rantasalmi. Geological Map of Finland 1:100 000, Pre-Quaternary Rocks, Sheet 3233. Geological Survey of Finland. Available at: http://tupa.gtk.fi/kartta/kallioperakartta100/kp_3233.pdf

Kousa, J. 2009. Joroisten Viholanniemen-Lahnalahden alueen kairaukset ja kallioperäkartoitus 2008. Geological Survey of Finland, archive report M19/2009/60. 27 p. (in Finnish). Available at: http://tupa.gtk.fi/raportti/arkisto/m19_2009_60.pdf

Kousa, J., Huhma, H. & Vaasjoki, M. 2004. U-Pb –ajoitukset eräistä magmasyntyisistä kivistä Pohjois-Pohjanmaalta, Raahe-Laatokka –vyöhykkeen luoteisosasta. In: Kousa, J. & Luukas, J. (eds) Vihannin ympäristön kallioperä- ja malmitutkimukset vuosina 1992-2003. Geological Survey of Finland, archive report M10.4/2004/2. 142 p. (in Finnish). Available at: http://tupa.gtk.fi/raportti/arkisto/m10_4_2004_2.pdf

Kousa, J., Luukas, J., Huhma, H. & Mänttäri, I. 2013. Paleoproterozoic 1.93-1.92 Ga Svecofennian rock units in the northwestern part of the Raahe-Ladoga zone, central Finland. In: Hölttä, P. (ed.) Current Research: GTK Mineral Potential Workshop, Kuopio, May 2012. Geological Survey of Finland, Report of Investigation 198, 91–96. Available at: http://tupa.gtk.fi/julkaisu/tutkimusraportti/tr_198.pdf

Kousa, J., Marttila, E. & Vaasjoki, M. 1994. Petrology, geochemistry and dating of Paleoproterozoic metavolcanic rocks in the Pyhäjärvi area Central Finland. In: Nironen, M. & Kähkönen, Y. (eds) Geochemistry of Proterozoic Supracrustal Rocks in Finland. Geological Survey of Finland Special Paper 19, 7–27. Available at: http://tupa.gtk.fi/julkaisu/specialpaper/sp_019.pdf

Lahtinen, R. 1994. Crustal evolution of the Svecofennian and Karelian domains during 2.1-1.79 Ga, with special emphasis on the geochemistry and origin of 1.93-1.91 Ga gneissic tonalities and associated supracrustal rocks in the Rautalampi area, central Finland. In: Lahtinen, R. Crustal evolution of the Svecofennian and Karelian domains during 2.1-1.79 Ga, with special emphasis on the geochemistry and origin of 1.93-1.91 Ga gneissic tonalites and associated supracrustal rocks in the Rautalampi area, central Finland. Geological Survey of Finland, Bulletin 378, 1–128. Available at: http://tupa.gtk.fi/julkaisu/bulletin/bt_378.pdf

Lahtinen, R. & Huhma, H. 1997. Isotopic and geochemical constraints on the evolution of the 1.93–1.79 Ga Svecofennian crust and mantle. Precambrian Research 82, 13–34.

Lahtinen, R., Huhma, H., Lahaye, Y., Lode, S., Heinonen, S., Sayab, M. & Whitehouse, M. J. 2016. Paleoproterozoic magmatism across the Archean-Proterozoic boundary in central Fennoscandia: Geochronology, geochemistry and isotopic data (Sm-Nd, Lu-Hf, O). Lithos 262, 507–525.

Lahtinen, R., Johnston, S. T. & Nironen, M. 2014. The Bothnian coupled oroclines of the Svecofennian Orogen: a Palaeoproterozoic terrane wreck. Terra Nova 26, 330–335.

Luukas, J., Kousa, J., Nironen, M. & Vuollo, J. 2017. Major stratigraphic units in the bedrock of Finland, and an approach to tectonostratigraphic division. In: Nironen, M. (ed.) Bedrock of Finland at the scale 1:1 000 000 - Major stratigraphic units, metamorphism and tectonic evolution. Geological Survey of Finland, Special Paper 60, 9–40. Available at: http://tupa.gtk.fi/julkaisu/specialpaper/sp_060.pdf

Mäki, T., Imaña, M., Kousa, J. & Luukas, J. 2015. The Vihanti-Pyhäsalmi VMS Belt. In: Maier, W. D., Lahtinen, R. & O'Brien, H. 2015 (eds) Mineral Deposits of Finland. Amsterdam: Elsevier Inc., 507–530.

Makkonen, H. 1991. Viholanniemen Zn-esiintymän tutkimukset Joroisissa vuosina 1984-1988. Geological Survey of Finland, archive report M19/3234/-91/1/10. 25 p. (in Finnish). Available at: http://tupa.gtk.fi/raportti/arkisto/m19_3234_91_1_10.pdf

Mattinson, J. M. 2005. Zircon U-Pb chemical abrasion ("CA-TIMS") method: Combined annealing and multi-step partial dissolution analysis for improved precision and accuracy of zircon ages. Chemical Geology 220, 47–66.

Mikkola, P., Huhma, H., Romu, I. & Kousa, J. 2018a. Detrital zircon ages and geochemistry of the metasedimentary rocks along the southeastern boundary of the Central Finland Granitoid Complex. In: Mikkola, P., Hölttä, P. & Käpyaho, A. (eds) Development of the Paleoproterozoic Svecofennian orogeny: new constraints from the southeastern boundary of the Central Finland Granitoid Complex. Geological Survey of Finland, Bulletin 407. (this volume). Available at: https://doi.org/10.30440/bt407.2

Mikkola, P., Lukkarinen, H. & Luukas, J. 2016. Suonenjoen kartta-alueen 3241 kallioperä ja kivilajiyksiköt. Geological Survey of Finland, archive report 29/2016. 29 p., 5 apps. (in Finnish). Available at: http://tupa.gtk.fi/raportti/arkisto/29_2016.pdf

Mikkola, P., Mönkäre, K., Ahven, M. & Huhma, H. 2018b. Geochemistry and age of the Paleoproterozoic Makkola suite volcanic rocks in central Finland. In: Mikkola, P., Hölttä, P. & Käpyaho, A. (eds) Development of the Paleoproterozoic Svecofennian orogeny: new constraints from the southeastern boundary of the Central Finland Granitoid Complex. Geological Survey of Finland, Bulletin 407. (this volume). Available at: https://doi.org/10.30440/bt407.5

Nironen, M., Kousa, J., Luukas, J. & Lahtinen, R. (eds) 2016. Geological Map of Finland – Bedrock 1:1 000 000. Espoo: Geological Survey of Finland. Available at: http://tupa.gtk.fi/kartta/erikoiskartta/ek_097_300dpi.pdf

Pekkarinen, L. 2002. Haukivuoren ja Pieksämäen kartta-alueiden kallioperä. Summary: Pre-Quaternary Rocks of the Haukivuori and Pieksämäki Map-Sheet areas. Geological Map of Finland 1:100 000, Explanation to the Maps of Pre-Quaternary Rocks, Sheets 3231, 3232. Geological Survey of Finland. 98 p. Available at: http://tupa.gtk.fi/kartta/kallioperakartta100/kps_3231_3232.pdf

Vaasjoki, M. 1981. The lead isotopic composition of some Finnish galenas. Geological Survey of Finland, Bulletin 316. 25 p. + 1 app. Available at: http://tupa.gtk.fi/julkaisu/bulletin/bt_316.pdf

Vaasjoki, M. & Sakko, M. 1988. Evolution of the Raahe–Ladoga zone in Finland: Isotopic constraints. In: Korsman, K. (ed.) Tectono-metamorphic evolution of the Raahe-Ladoga zone, eastern Finland. Geological Survey of Finland, Bulletin 343, 7–31. Available at: http://tupa.gtk.fi/julkaisu/bulletin/bt_343.pdf

Vaasjoki, M., Huhma, H., Lahtinen, R. & Vestin, J. 2003. Sources of Svecofennian granitoids in the light of ion probe U-Pb measurements on their zircons. Precambrian Research 121, 251–262.

Zhang, X. 2000. Geochemical exploration for polymetallic ores in volcano-sedimentary rocks: studies in China and Finland. Acta Universitatis Ouluensis. A, Scientiae rerum naturalium 352. 140 p. Available at: http://jultika.oulu.fi/files/isbn9514257871.pdf

Development of the Paleoproterozoic Svecofennian orogeny: new constraints from the southeastern boundary of the Central Finland Granitoid Complex
Edited by Perttu Mikkola, Pentti Hölttä and Asko Käpyaho
Geological Survey of Finland, Bulletin 407, 63-84, 2018

PALEOPROTEROZOIC MAFIC AND ULTRAMAFIC VOLCANIC ROCKS IN THE SOUTH SAVO REGION, EASTERN FINLAND

by

Jukka Kousa, Perttu Mikkola and Hannu Makkonen

Kousa, J., Mikkola, P. & Makkonen, H. 2018. Paleoproterozoic mafic and ultramafic volcanic rocks in the South Savo region, eastern Finland. *Geological Survey of Finland, Bulletin 407*, 63–84, 11 figures and 1 table.

Ultramafic and mafic volcanic rocks are present as sporadic interlayers in the Paleoproterozoic Svecofennian paragneiss units in the South Savo region of eastern Finland. These elongated volcanic bodies display locally well-preserved primary structures, have a maximum thickness of ca. 500 m and a maximum length of several kilometres. Geochemically, the ultramafic variants are picrites, whereas the mafic members display EMORB-like chemical compositions. The picrites, in particular, display significant compositional variation in both major and trace elements (light rare earth and large-ion lithophile elements). These differences may have been caused by differences in their magma source, variable degrees of crustal contamination and post-magmatic alteration, as well as crystal accumulation and fractionation processes. The volcanic units are interpreted to represent extensional phase(s) in the development of the sedimentary basin(s) where the protoliths of the paragneisses were deposited. The eruption age of the volcanic units is interpreted to be 1.91–1.90 Ga.

Appendix 1 is available at: http://tupa.gtk.fi/julkaisu/liiteaineisto/bt_407_appendix_1.pdf

Electronic Appendix is available at: http://tupa.gtk.fi/julkaisu/liiteaineisto/bt_407_electronic_appendix.xlsx

Keywords: volcanic rocks, picrite, ultramafic composition, mid-ocean ridge basalts, extension tectonics, Paleoproterozoic, Svecofennian, Finland

Geological Survey of Finland, P.O. Box 1237, FI-70211 Kuopio, Finland
E-mail: perttu.mikkola@gtk.fi

VERTAISARVIOITU
KOLLEGIALT GRANSKAD
PEER-REVIEWED
www.tsv.fi/tunnus

https://doi.org/10.30440/bt407.4

Editorial handling by Pentti Hölttä and Asko Käpyaho.

Received 30 July 2017; Accepted 29 June 2018

1 INTRODUCTION

Picrite is a variety of high-magnesium basalt rich in olivine phenocrysts, which can make up to 40% of the rock, such as in arc picrites from Solomon Islands (Schuth et al. 2004). Svecofennian (meta) picrites have been described around the Central Finland Granitoid Complex (e.g., Lehtonen et al. 2005), southern Finland (Nironen et al. 2016b) and in Sweden from the Skellefte area (Berge 2013 and references therein). The nomenclature used for these ultramafic rocks varies considerably, including at least the following: cortlandite, ultramafic rock/lava/volcanic rock, metaperidotite, metapicrite and komatiite.

The presence of ultramafic volcanic rocks in South Savo has been known since the early 1970s, when Korsman (1973) and his bedrock mapping group found ultramafic olivine-bearing rocks among the more common amphibolites. A volcanic origin both for the amphibolites and some of the ultramafic rocks was evident from their locally well-preserved pillow lava structures (Pääjärvi 1975, Kousa 1985). Gaál and Rauhamäki (1971) also observed ultramafic lavas at the same time near Savonlinna, approximately 30 km east of Rantasalmi. Since their initial discovery, most of the ultramafic volcanic units have received little attention, with the exception of some of the occurrences that have been involved in target-scale ore exploration, e.g., the Ni mineralisation at Rantala (Makkonen 1984) and Ylänne (Laitakari 1985).

This article provides a brief overview of the different occurrences of picrites and associated mafic volcanic rocks in the South Savo region, focusing on geochemical data that have been accumulated over the last 30 years in various research projects. The data also include the results of two single-grain age determinations. In addition, we discuss the possible stratigraphic significance of these volcanic units and their tectonic implications.

2 GEOLOGICAL SETTING

The bedrock of the South Savo region is located on the southeast flank of the Central Finland Granitoid Complex and mainly consists of Paleoproterozoic Svecofennian paragneisses, which are divided into two major units: the Pirkanmaa migmatite suite of the Western Finland supersuite and the Häme migmatite suite of the Southern Finland supersuite (Luukas et al. 2017). The latter unit in the study area has also been referred to as the Saimaa area (Kähkönen 2005). The contact between the Pirkanmaa and Häme migmatite suites in the South Savo region is tectonic and marked by the Mikkeli shear zone, which also represents a step-like change in the degree of metamorphism (Korsman et al. 1988, Mikkola et al. 2018a). In addition to the main domain in the western part of the study area, rocks belonging to the Pirkanmaa migmatite suite are also present within the Häme migmatite suite as smaller segments bound by fault and thrust contacts (Fig. 1).

Protoliths of the paragneisses have been interpreted as turbiditic greywackes deposited in a passive margin setting following the collision of the older Svecofennian arc system at 1.91 Ga with the Karelian craton. The maximum depositional ages of paragneisses vary from 1.92 to 1.90 Ga (e.g. Huhma et al. 1991, Lahtinen et al. 2002, 2009, 2017, Mikkola et al. 2018b). Both of the migmatite suites locally contain mafic to ultramafic volcanic rocks (Fig. 1), which have been interpreted to represent extensional stages in the development of the depositional basin (e.g. Lahtinen et al. 2009, 2017). In the study area, the ultramafic variants are assigned to the Pahakkala suite when occurring in the Häme migmatite suite and the Ala-Siili lithodeme when found in the Pirkanmaa migmatite suite. Based on the locally well-preserved pillow and lava breccia structures (Korsman 1973, Pääjärvi 1975, Kousa 1985, Viluksela 1988, Pekkarinen 2002), the suites are thought to represent submarine eruptions, although according to Makkonen (1996), some of the ultramafic bodies are probably subvolcanic sills.

The Jäppilä–Virtasalmi block (Fig. 1, Pekkarinen 2002), also known as the Pieksämäki block (Korsman et al. 1988), shows up as a distinct anomaly pattern on both aeromagnetic and electromagnetic maps. This complex migmatite block has been regarded as a part of the Southern Finland plutonic suite (Luukas et al. 2017), but based on new age

data (~1910 Ma) it can be correlated with the older Svecofennian magmatic rocks occurring along the margin of the Archean Karelian Craton (Kousa et al. 2018). The rock types in the Jäppilä–Virtasalmi block consist of hornblende gneisses, amphibolites and paragneisses, in addition to a complex collection of originally intrusive, but intensively deformed, often migmatized gneisses varying in composition from granodiorite to gabbro (Vorma 1971, Fig. 1). In this paper, the unit name Maavesi suite is used to cover the entirety of the rock types in the Jäppilä–Virtasalmi block (Fig. 1). This name will also be used in the Bedrock of Finland - DigiKp map database and the associated Finstrati database for geological units. The contact zone between the Maavesi suite and the paragneisses of the Häme migmatite suite typically hosts amphibolites, often diopside banded, carbonate rocks, calc-silicate-bearing quartz feldspar gneisses and intermediate metavolcanic rocks forming the Virtasalmi suite (Vorma 1971, Pekkarinen & Hyvärinen 1984, Pekkarinen 2002, Luukas et al. 2017). Volcano-sedimentary rocks interpreted as part of the Virtasalmi suite are also present within the paragneisses as smaller tectonic slivers.

The paragneisses are intruded by granodiorites and quartz diorites belonging to the Central Finland Granitoid Complex and Southern Finland Plutonic suite. The ~1885 Ma age of these intrusions defines a minimum age for the deposition of the paragneiss protoliths and eruption of the volcanic interlayers within them (Korsman et al. 1984, Vaasjoki & Kontoniemi 1991, Pekkarinen 2002). Rocks of the Pirkanmaa migmatite suite also host smaller, less evolved intrusions varying in composition from ultramafic to diorite and being potentially prospective for Ni and Cu ores (Makkonen 1996, Barnes et al. 2009).

Evidence for the existence of a younger sedimentation phase in the area is provided by the 1885 ± 6 Ma age obtained for a granitoid clast in the Haukivuori conglomerate (Korsman et al. 1988). This now spatially limited unit has been preserved on top of a down-warped bedrock block (ibid.), although originally, the unit was presumably significantly wider.

3 METHODS AND MATERIAL

Analytical data from a total of 180 outcrop and drill core samples were utilized in this study. These data are listed in the Electronic Appendix, and representative chemical compositions of volcanic rocks from each subarea are presented in Table 1. Due to the extended period of data gathering, the analyses were carried out using several analytical methods and laboratories. The main elements were in all cases determined using X-ray fluorescence (XRF), and for most samples, inductively coupled plasma mass spectrometry (ICP-MS) was used for REE and other trace elements. The analytical methods are described in Appendix 1, and the analytical method applied to each sample is indicated in the Electronic Appendix.

Two single-grain age determinations were performed using a Nu Plasma AttoM single collector LA-ICP-MS in GTK's isotope laboratory in Espoo. The method is described Appendix 1.

4 RESULTS

4.1 Field observations and petrography

4.1.1 Ala-Siili lithodeme

4.1.1.1 Ala-Siili

The type area of the Ala-Siili lithodeme of the Pirkanmaa suite (Mikkola et al. 2016) is poorly exposed and practically all of the material used in this study is from a single drilling profile targeting a N–S-trending positive Bouguer and magnetic anomaly (Mikkola et al. 2014). Based on the geophysical data, the volcanic sequence in the area is approximately 5 km long and 500 m wide. As the drilling profile only transected the eastern contact, only a minimum thickness of 350 m can be deduced from it. The volcanic sequence is located

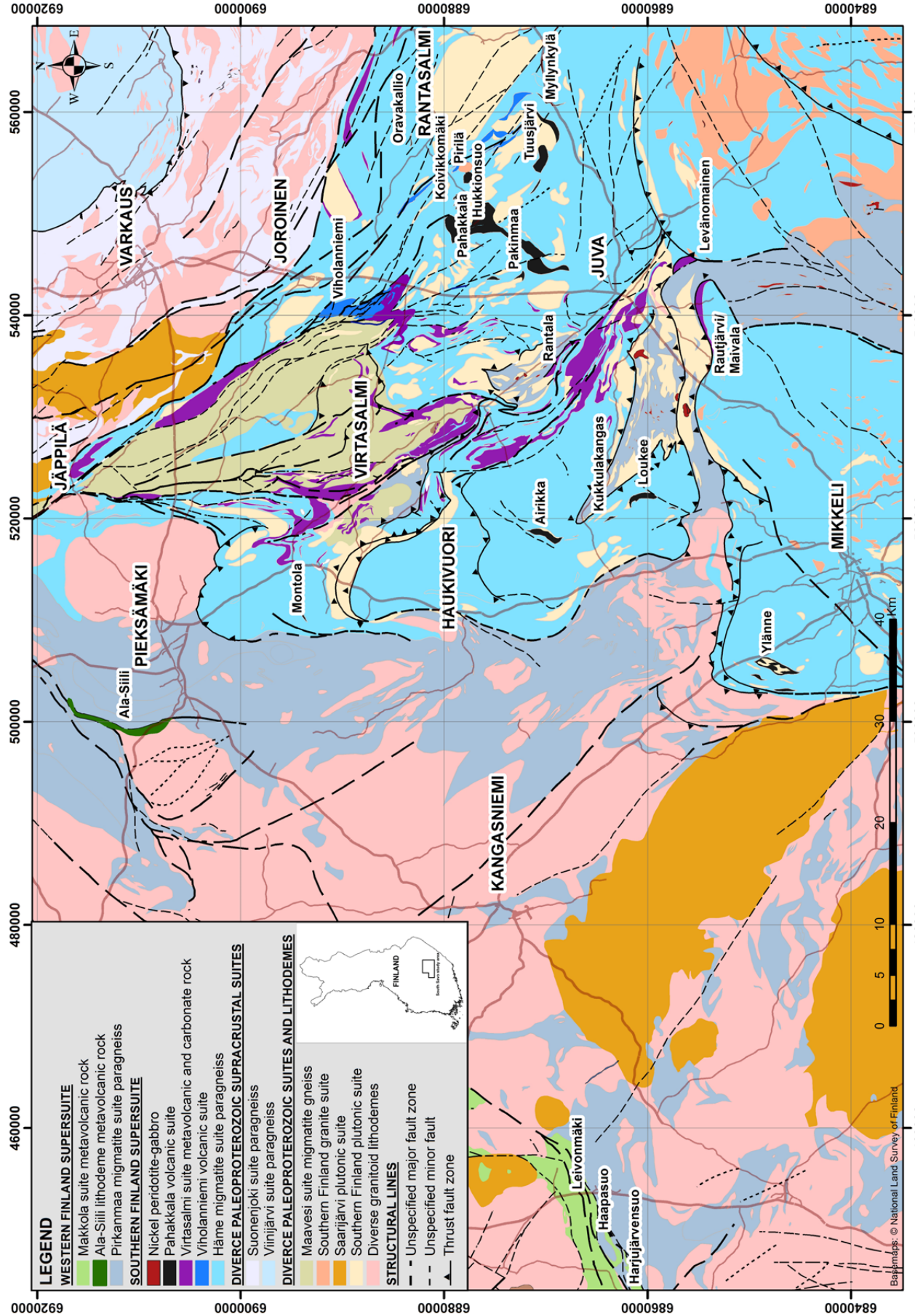

Fig. 1. Bedrock map of South Savo with the locations described in this study. Map modified from Bedrock of Finland – DigiKP.

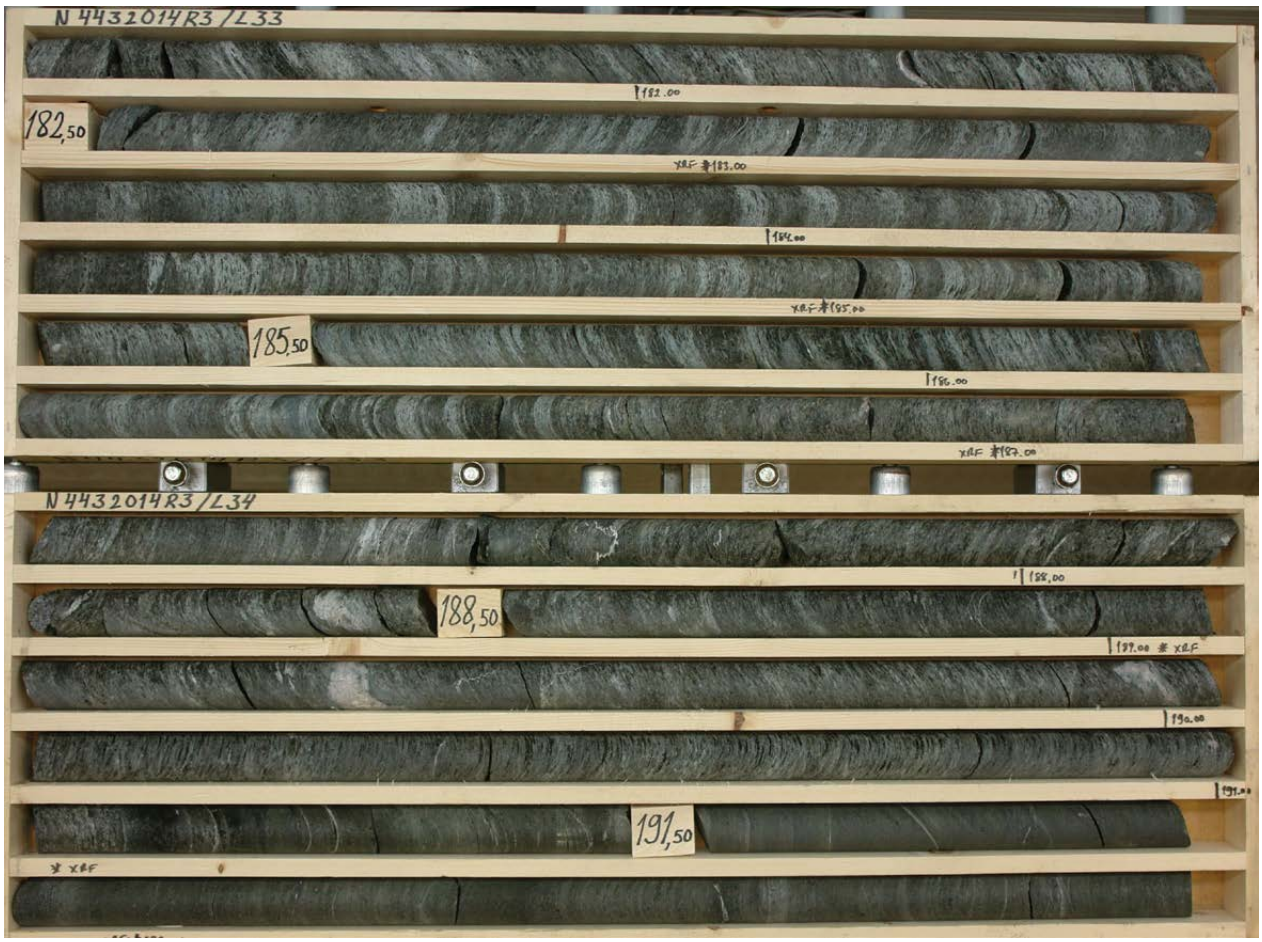

Fig. 2. A drill core from the Ala-Siili area displaying compositional variation, which suggests a supracrustal origin, despite intensive deformation and alteration. Box width 1 m.

in a sheared contact zone of a quartz diorite intrusion in the west and Pirkanmaa migmatite suite paragneisses in the east (Fig. 1).

The Ala-Siili lithodeme consists of picritic volcanic rocks that are intensively sheared and altered. Thus, most of the primary structures have been destroyed, but locally, volcaniclastic features can be observed. Small-scale mineralogical variation, probably representing original layering, can also be seen (Fig. 2), suggesting a supracrustal, rather than subvolcanic, origin. Mineralogically, the picrites are typically lepidoblastic biotite-amphibole schists, locally with abundant chlorite and epidote. Tshermakite is the most common amphibole, with cummingtonite occurring in some of the samples. Drill cores also intersect interlayers of serpentinite (<5 m) and intermediate volcanic rock (<20 m).

1.1.1.2 *Leivonmäki*

In the Leivonmäki area, picrites have been observed in two drilling profiles and a few outcrops, although this area is also mostly poorly exposed. The picrites are located near the contact between the Pirkanmaa migmatite suite in the south and the volcanic rocks of the Makkola suite in the north. The contact coincides with the Leivonmäki shear zone (Mikkola et al. 2018a). Mikkola et al. (2016) assigned the picrites of this area to the Ala-Siili mafic volcanic lithodeme.

Picrites in the Haapasuo profile (Mikkola & Niemi 2015) occur among the metasediments of the Tammijärvi greywacke lithodeme. Although strongly serpentinized (Fig. 3), compositional and structural variations indicate that they were originally volcanic rocks. In addition to serpentine, most of the serpentinites contain olivine as a main mineral together with various proportions of talc, actinolite, biotite, and chlorite.

In the outcrops west of Haapasuo and in the Harjujärvensuo profile, the picrites are variably sheared uralite porphyrites (Fig. 4), which are interpreted as supracrustal in origin based on textural variations (Mikkola et al. 2018d). The main minerals are hornblende, biotite, and plagioclase, and the porphyritic texture is typically caused by the presence of rounded biotite-hornblende aggregates.

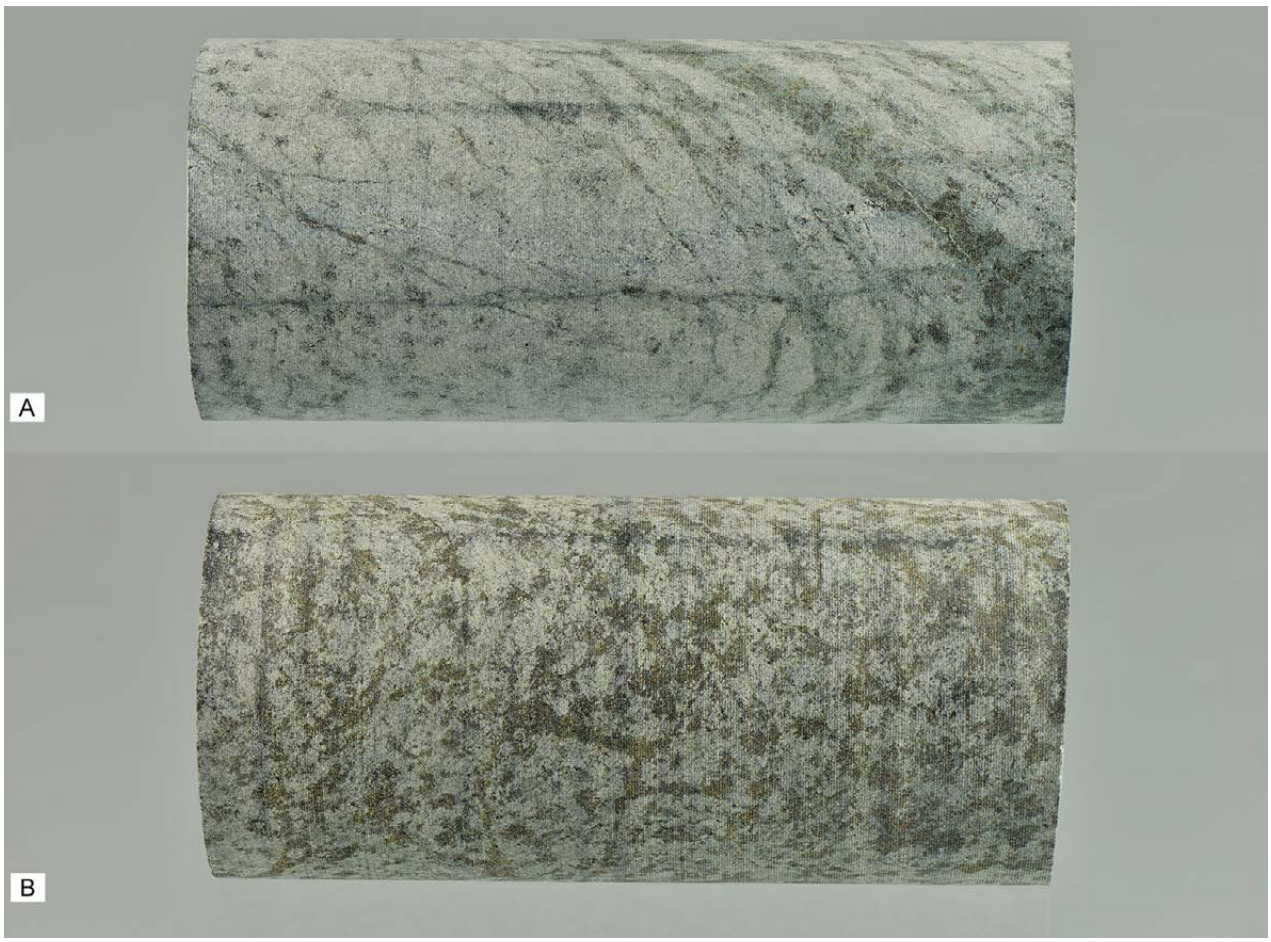

Fig. 3. A) and B) Drill core samples of serpentinized picrites from the Haapasuo drilling profile. Core diameter 42 mm.

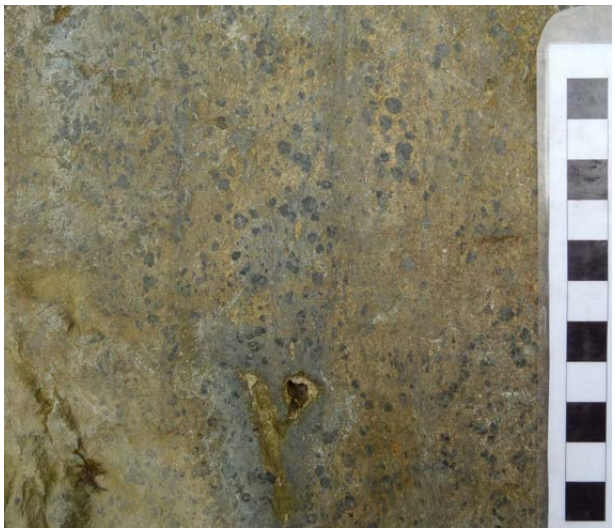

Fig. 4. Uralite porphyrite from the Leivonmäki area. Scale bar with cm scale.

4.1.2 Pahakkala suite metavolcanic rocks

4.1.2.1 Loukee–Airikka area

The Loukee–Airikka metavolcanic formation is formed by a ca. 14-km-long and less than 1-km-wide, N–S-trending, discontinuous chain of mafic-ultramafic bodies in paragneisses of the Häme migmatite suite, forming part of the Pahakkala suite (Fig. 1). From north to south, the separate bodies are named Airikka, Kukkulakangas and Loukee. Pekkarinen (2002) used the name Halmelampi for the last one. In addition to outcrops, the volcanic rocks are accessible in drill cores from a profile at Loukee, consisting of three holes transecting the ca. 400-m-thick metavolcanic formation.

The main rock type of these bodies is dark green, usually more or less schistose amphibolite composed of hornblende and plagioclase with occasional diopside- and epidote-bearing bands and nodes. In places, amphibolite is garnet bearing. Locally preserved lava breccia and pillow lava structures

Fig. 5. Drill core samples of variably altered and deformed picrites from the Loukee area. Core diameter 42 mm.

indicate a primary submarine volcanic nature for the amphibolites.

Approximately one-third of the Airikka–Loukee formation is composed of picrites with green to pale green clinoamphibole (tremolite-actinolite), chlorite, and serpentine as the main minerals. Locally, biotitization is intensive. Secondary alteration and deformation have generally resulted in highly variable mineral assemblages and structures of the picrites, as demonstrated in Figure 5. A common diagnostic feature of this rock type is the presence of partly serpentinized olivine porphyroblasts up to 1 cm in size. In most cases, the ultramafic rock is homogeneous, fine grained and massive, especially in the Airikka area. Locally in the Kukkulakangas area, the ultramafic rock type shows pillow lava structures and in the Loukee area, lapilli-sized fragments and amygdales can be observed in a few outcrops. The southernmost observations of the highly schistose picrite-amphibolite association intruded by granites are from the Ylänne area approximately 15 km southwest of Loukee (Fig. 1).

Based on drill core observations from Loukee, the paragneisses represent the original eruptional environment of the picrites. In addition to tuffite interbeds, the picrites contain calcite-rich interbeds, further supporting a submarine eruption environment. The picrites are cut by amphibolite and fluorite granite dykes and quartz veins.

4.1.2.2 Rantasalmi–Juva area

Several mafic and ultramafic metavolcanic rock bodies surrounded by, or intercalated with, metapelites and metapsammites of the Häme migmatite suite are known to occur in the Rantasalmi and Juva areas (Fig. 1, Korsman 1973). Well-preserved pillow lava and volcanic breccia structures exist, especially in outcrops of the Hukkionsuo, Koivikkomäki and Pirilä areas (Pääjärvi 1975, Kousa 1985, Viluksela 1988, Makkonen & Ekdahl 1988). The mineral compositions of the Rantasalmi amphibolites and picrites are almost identical to those in the Loukee–Airikka area. In spite of the good exposure in some areas, the contacts between the Pahakkala suite and the surrounding metagreywackes are mostly covered by glacial overburden.

The mafic metavolcanic rocks are fine-grained, usually dark green, fragmented lavas, locally showing pillow or pillow breccia structures and their deformed variants. Mineralogical variation exists according to the metamorphic grade. Mafic pillow lavas and their highly deformed banded variants have an amphibolitic mineral composition with green or brownish green hornblende, some pale tremolite-actinolite, and granular andesine plagioclase as the main constituents. The pale green bands and cavity fillings are mainly composed of diopside and plagioclase. Sphene, epidote, apatite, chlorite, carbonate and opaque minerals are common accessory minerals. Rare tourmaline, zircon and scapolite are also present (Viluksela 1988).

Picrites occur as greyish green, fine-grained, conformal lava flows among the amphibolites or sometimes as obvious dykes intersecting them. The thickness of the lava flows and dykes is typically several metres. Picrites are commonly fragmented. Some massive beds in the Koivikkomäki area show both bottom and top breccia structures, indicating

an extrusive origin. In outcrops of the Pahakkala area, pillow structures have also been observed (Kousa 1985). The presence of reddish brown olivine porphyroblasts is a reliable distinguishing feature of the picrites in the field. These porphyroblasts attain a diameter of 10 mm in the most magnesium-rich lavas. Spinifex-like pseudofeatures have been observed in some Pahakkala and Ylänne outcrops, but indisputable spinifex textures have not been recognized. Variation in the whole-rock chemistry of picrites results in mineralogical differences within single lava beds, such as differences in the amount of pale green tremolite-actinolite and green hornblende.

Other occurrences of picrites in the Juva area include those of Levänomainen, Myllynkylä, Pakinmaa, Rantala and Rautjärvi (Makkonen 1996). The Rautjärvi picrite is composed of a distinctly layered ultramafic rock. Six separate layers can be distinguished in outcrop, varying in thickness from 0.4 m to more than 10 m. The observed mineralogy is totally metamorphic (mainly orthopyroxene, clinoamphibole, olivine). The textures varying from harrisitic to cumulate coupled with chemical and mineral compositional variations (whole-rock MgO, FeO and En of orthopyroxene; Makkonen 1992) suggest multiple lava flows or magma injections.

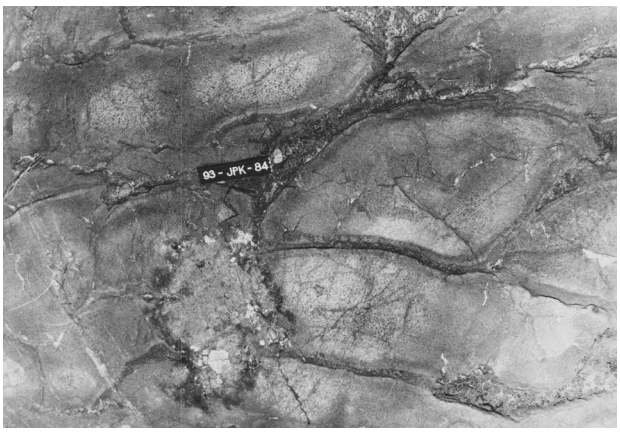

Fig. 6. Well-preserved pillow lava structures in the Pahakkala type area. Length of the scale bar 12 cm.

4.2 Geochemistry

Table 1 presents representative analyses of 12 volcanic rock samples from the studied locations. All analyses are listed in the Electronic Appendix. According to the IUGS classification (Le Bas 2000), picrite is a volcanic rock with SiO_2 <52 wt%, MgO >18 wt% and Na_2O+K_2O = 2–3 wt% or if MgO is 12–18 wt%, Na_2O+K_2O must be <3 wt%. Of these, we have only applied the volatile free SiO_2 and MgO contents of analyses normalised to 100 wt%, because locally intensive biotitization has affected the K_2O contents of our samples. This alteration is especially evident in several samples from the Ala-Siili lithodeme. Of the 180 samples, 106 are consistent with the picrite classification in terms of SiO_2 and MgO (Fig. 7). A subset of twenty-four samples from several locations also meet the definition of komatiite, having SiO_2 <52 wt%, MgO >18 wt%, TiO_2 <1 wt%, and Na_2O+K_2O <1 wt% (Le Bas 2000).

When plotted against MgO, most of the elements form variably well-defined differentiation trends (Fig. 7), and certain differences between the studied units can be observed. Picrite samples representing the Ala-Siili lithodeme display lower FeOt, CaO, TiO_2 and Ni concentrations than the samples from the Pahakkala suite, although overlap exists. Picrites from Ala-Siili display on average higher P_2O_5 concentrations than those from the Pahakkala suite, and the most effective plot for distinguishing the two suites is TiO_2 vs. P_2O_5 (Fig. 7F). As the Al_2O_3 concentrations are similar in both suites, the lower TiO_2 concentration of the Ala-Siili lithodeme results in it having a significantly higher Al_2O_3/TiO_2 ratio. An exception to the above are the four samples from Oravakallio (1 picrite, 3 mafic volcanic rocks), which consistently plot in the area occupied by samples from the Ala-Siili lithodeme. Picrites and the mafic volcanic rocks of the Pahakkala suite follow the same differentiation trend.

On the R_1-R_2 plot of De la Roche et al. (1980), the picrite samples of the Pahakkala suite plot along the boundary between tholeiite and picritic rock fields and the Ala-Siili samples predominantly plotting in the tholeiite field (Fig. 8A). The samples of mafic volcanic rocks mainly classify as basalts on the same diagram. On the TAS diagram (Fig. 8B), the samples mainly plot in the basalt field. On the classification diagram of Hanski et al. (2001), the differences in Al_2O_3/TiO_2 ratio result in the majority of the samples from the Ala-Siili lithodeme and Oravakallio locality plotting in the Al-undepleted komatiite field, whereas those from the Pahakkala suite mainly plot in the Ti-enriched komatiite field and partly in the picrite field (Fig. 8C). A small number of samples, mainly from the

Loukee–Airikka area, have higher TiO_2 values than the main group. On the Jensen cation plot of Fig. 8D, the picrite samples fall in the komatiite and komatitic basalt fields, whereas the mafic volcanic rocks are tholeiitic basalts. The samples from the Ala-Siili lithodeme and the Oravakallio locality form a slightly Mg-richer trend than the majority of the samples from the Pahakkala suite. On the Zr vs. Ti classification plot (Pearce 1982), the samples from the Pahakkala suite mainly plot in the MORB field, whereas those from Ala-Siili lithodeme plot in the island arc field or below it (Fig. 8E). The exceptions are again the Oravakallio samples, which plot in the same group with the Ala-Siili lithodeme samples. On the diagram of Wood (1980), the samples from the Ala-Siili lithodeme plot in the field of continental arc basalts, whereas the samples representing the Pahakkala suite mainly plot in the EMORB field, with the most significant exception again being the Oravakallio samples.

Chondrite-normalized REE patterns of the samples from the Pahakkala suite show mainly weak LREE enrichment and relatively unfractionated REE patterns (Fig. 9). On average, the mafic volcanic rocks have higher REE abundances than the picrites. Two samples from Loukee display higher and more strongly fractionated REE patterns, but do not significantly differ in other chemical aspects from the other samples. Three samples from Porttiaho location display higher REE abundances, but like the anomalous samples from Loukee do not differ significantly in other respects from the main population. The samples representing the Ala-Siili lithodeme have on average a more fractionated REE distribution and higher LREE levels, and some of them display negative Eu anomalies. It should be noted that the data set does not include REE data from the Oravakallio locality.

In the primitive mantle-normalized spidergram (Fig. 10), the samples from the Pahakkala suite do not display significant anomalies that would characterize the whole group, but on average, the mafic volcanic samples display higher concentrations of trace elements than the picrites. The samples from the Ala-Siili lithodeme have significantly higher Th and U concentrations, although enrichment of the latter can partly be due to alteration. Clear negative Nb anomalies and small Ti anomalies are observable in most of the samples from Ala-Siili. Some of the samples from the Ala-Siili location display strong positive Sr anomalies, but the lithodeme also includes samples with negative Sr anomalies.

Table 1. Representative analyses from the studied locations. All chemical data are listed in the Electronic Appendix.

Sample	N4432014R1 105.00-106.00	N4312015R4 99.00-100.00	JPK1-1984-88.5	PHK1-1	PR03-1	PR08-1
Rock type	Chlorite-biotite-amphibole schist	Antophyllite-hornblende schist	Plagioclase porphyrite	Ultramafic volcanic rock	Ultramafic volcanic rock	Mafic volcanic rock
Unit	Ala-Siili	Ala-Siili	Pahakkala suite	Pahakkala suite	Pahakkala suite	Pahakkala suite
Area	Ala-Siili	Leivonmäki	Pahakkala	Pahakkala	Pirilä	Pirilä
SiO_2 %	48.60	46.40	47.54	44.61	39.57	46.95
TiO_2	0.51	0.45	1.97	0.81	0.52	1.49
Al_2O_3	9.38	9.54	17.00	8.38	5.97	12.73
Fe_2O_3t	9.06	9.82	13.45	10.25	11.91	15.47
MnO	0.13	0.14	0.17	0.18	0.17	0.24
MgO	20.30	19.30	4.89	14.92	19.19	9.83
CaO	6.02	5.63	9.07	15.53	14.06	8.97
Na_2O	0.96	0.78	5.21	0.59	0.03	2.42
K2O	2.08	1.68	0.23	0.14	0.02	0.10
P_2O_5	0.18	0.14	0.17	0.06	0.05	0.14
C ppm	912	n.a.	7900	n.a.	n.a.	n.a.
Ba	458	425	190	811	n.a.	17
Cl	95	163	n.a.	n.a.	n.a.	n.a.
Co	58.2	62.3	n.a.	70.0	85.0	64.0
Cr	1499	2389	140	1698	2169	372
Cu	n.a.	40	180	106	117	70
Hf	1.3	1.2	n.a.	1.4	0.9	2.7
Nb	3.6	4.3	n.a.	4.2	2.7	7.1
Ni	873	656	150	807	892	240
Rb	65.3	53.2	n.a.	n.a.	n.a.	n.a.
S	n.a.	98	400	663	16412	97
Sc	20.5	27.7	n.a.	n.a.	n.a.	n.a.
Sr	93	36	280	327	30	160
Ta	0.22	n.a.	n.a.	0.20	0.20	0.41
Th	2.4	2.0	n.a.	0.3	0.1	0.5
U	0.5	0.7	n.a.	0.2	0.1	0.2
V	141.0	162.0	420.0	188.0	129.0	292.0
Y	10.1	10.9	40.0	16.0	10.0	29.0
Zn	79	81	110	94	653	104
Zr	59.2	52.2	120.0	40.0	27.0	86.0
La	12.8	9.4	8.8	4.2	1.3	6.3
Ce	26.0	20.9	23.0	9.7	3.9	15.9
Pr	3.2	2.6	n.a.	1.5	0.7	2.5
Nd	12.60	9.97	16.20	6.65	3.34	11.60
Sm	2.59	2.13	4.60	1.91	0.99	3.53
Eu	0.79	0.50	1.64	0.81	0.29	1.42
Gd	2.39	2.08	n.a.	2.39	1.27	4.41
Tb	1.96	1.79	7.30	2.46	1.35	4.77
Dy	0.34	0.29	0.89	0.42	0.22	0.78
Ho	0.39	0.35	n.a.	0.55	0.30	1.07
Er	1.14	1.03	n.a.	1.43	0.80	2.91
Tm	0.15	0.15	n.a.	0.21	0.11	0.45
Yb	1.05	0.93	2.50	1.30	0.72	2.70
Lu	0.15	0.14	0.28	0.19	0.11	0.43

n.a. = not analysed

Table 1. Cont.

Sample	10.5-JPK-87	N5112015R8 125.00-126.00	N5112015R8 158.00-159.00	MIK-2.1	MIK-3.3	Porttiaho
Rock type	Ultramafic volcanic rock	Mafic lava	Ultramafic lava	Mafic volcanic rock	Ultramafic volcanic rock	Mafic lava
Unit	Pahakkala suite	Pahakkala suite	Pahakkala suite	Pahakkala suite	Pahakkala suite	Pahakkala suite
Area	Oravikallio	Loukee-Airikka	Loukee-Airikka	Mikkeli	Mikkeli	Other
SiO_2 %	48.60	46.40	43.30	47.75	45.09	45.72
TiO_2	0.54	3.32	0.89	1.77	0.87	1.39
Al_2O_3	9.09	14.10	9.98	14.03	9.53	9.23
Fe_2O_3t	9.07	14.90	11.70	16.17	12.70	12.30
MnO	0.16	0.14	0.17	0.22	0.19	0.20
MgO	17.00	5.12	15.60	6.17	20.38	14.19
CaO	6.54	8.04	10.04	10.56	8.23	10.39
Na_2O	0.89	2.98	1.50	2.54	0.94	1.63
K2O	1.92	0.78	0.45	0.36	0.09	1.59
P_2O_5	0.21	0.72	0.07	0.16	0.07	0.45
C ppm	400	3600	1700	400	300	n.a.
Ba	540	294	30	60	n.a.	455
Cl	n.a.	148	67	n.a.	n.a.	n.a.
Co	n.a.	33.4	68.7	n.a.	n.a.	53.0
Cr	2070	68	1432	120	2030	1261
Cu	70	278	164	170	120	32
Hf	n.a.	5.2	1.2	n.a.	n.a.	5.3
Nb	n.a.	21.1	3.8	n.a.	n.a.	20.2
Ni	540	38	678	90	1110	195
Rb	n.a.	19.9	10.2	n.a.	n.a.	75.0
S	580	3048	9222	130	340	n.a.
Sc	n.a.	60.3	44.3	n.a.	n.a.	n.a.
Sr	150	399	177	220	30	161
Ta	n.a.	0.94	<0.2	n.a.	n.a.	1.34
Th	n.a.	1.4	<0.5	n.a.	n.a.	8.1
U	n.a.	0.8	<0.2	n.a.	n.a.	3.2
V	160.0	521.0	215.0	400.0	250.0	250.0
Y	n.a.	43.4	13.1	20.0	10.0	26.0
Zn	90	182	79	110	80	114
Zr	90.0	222.0	44.1	130.0	60.0	227.0
La	n.a.	22.7	3.8	n.a.	n.a.	42.8
Ce	n.a.	54.9	9.1	n.a.	n.a.	93.8
Pr	n.a.	7.5	1.3	n.a.	n.a.	14.4
Nd	n.a.	34.80	6.42	n.a.	n.a.	58.69
Sm	n.a.	8.51	1.95	n.a.	n.a.	11.98
Eu	n.a.	2.65	0.69	n.a.	n.a.	3.45
Gd	n.a.	9.29	2.45	n.a.	n.a.	9.91
Tb	n.a.	8.99	2.77	n.a.	n.a.	6.48
Dy	n.a.	1.46	0.42	n.a.	n.a.	1.37
Ho	n.a.	1.74	0.57	n.a.	n.a.	1.17
Er	n.a.	4.80	1.59	n.a.	n.a.	2.69
Tm	n.a.	0.65	0.22	n.a.	n.a.	0.36
Yb	n.a.	4.19	1.43	n.a.	n.a.	2.04
Lu	n.a.	0.61	0.20	n.a.	n.a.	0.31

n.a. = not analysed

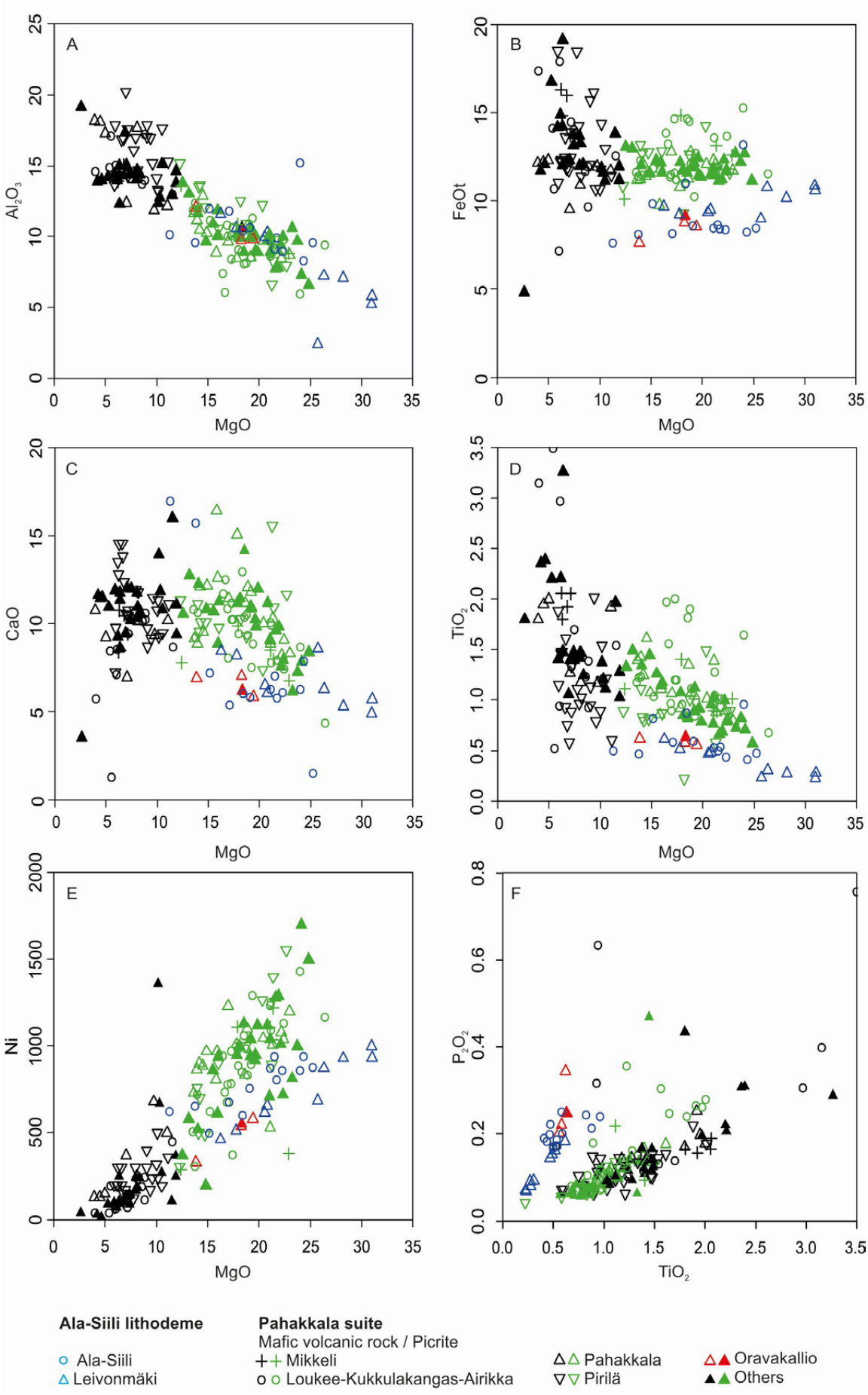

Fig. 7. Plots of MgO versus selected elements (A–E) and TiO_2 vs. P_2O_5 plot (F). Main elements normalised to 100% on a volatile-free basis.

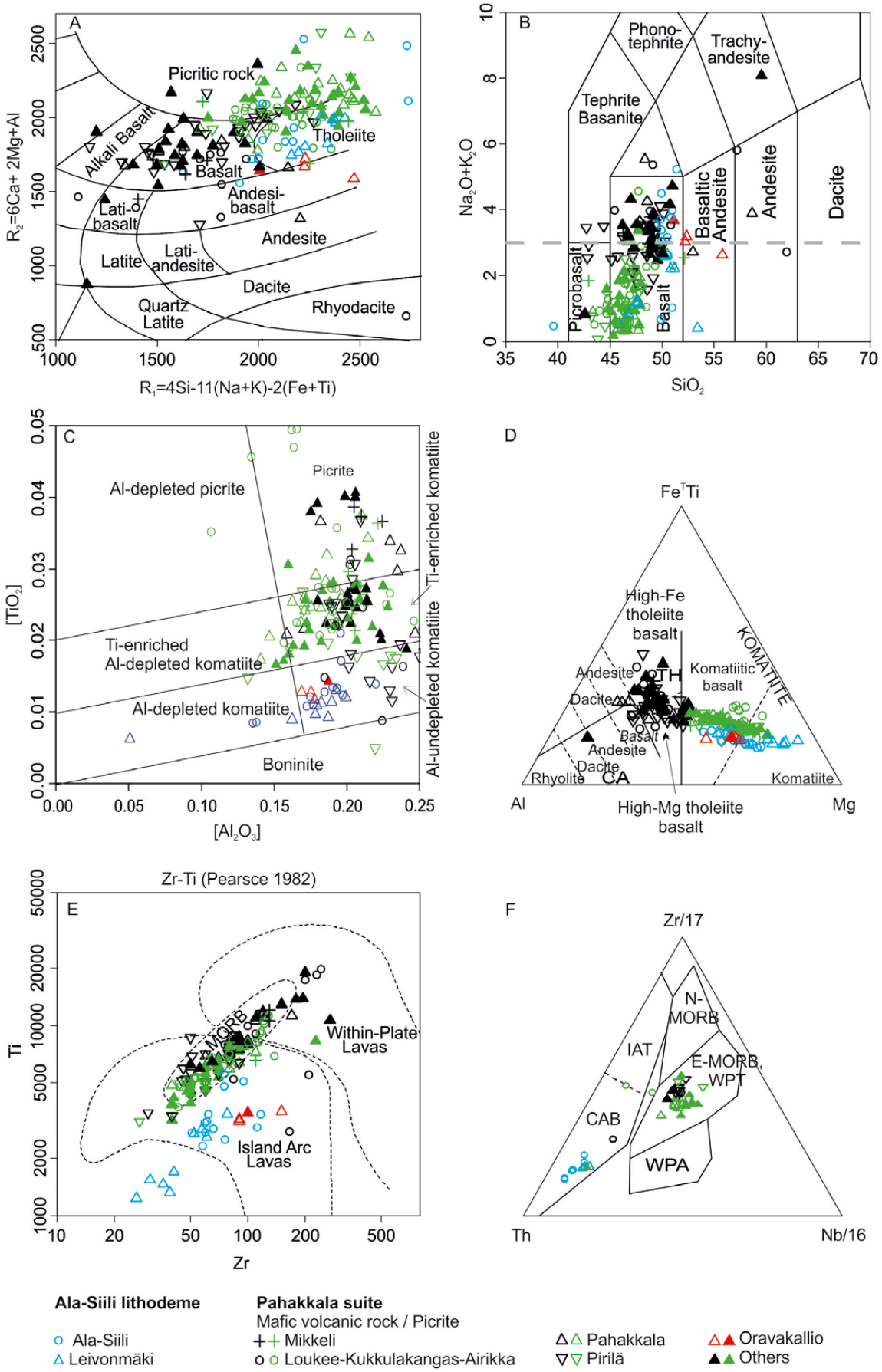

Fig. 8. Chemical classification diagrams applied to volcanic rocks from South Savo. A) R_1-R_2 plot of De la Roche et al. (1980), B) TAS (total alkali silica) diagram of Le Bas et al. (1986), C) Al_2O_3 vs. TiO_2 diagram of Hanski et al. (2001), D) Jensen cation plot (Jensen 1976), E) Zr vs. Ti plot of Pearce (1982), F) Zr/117-Nb/16-Th diagram of Wood (1980).

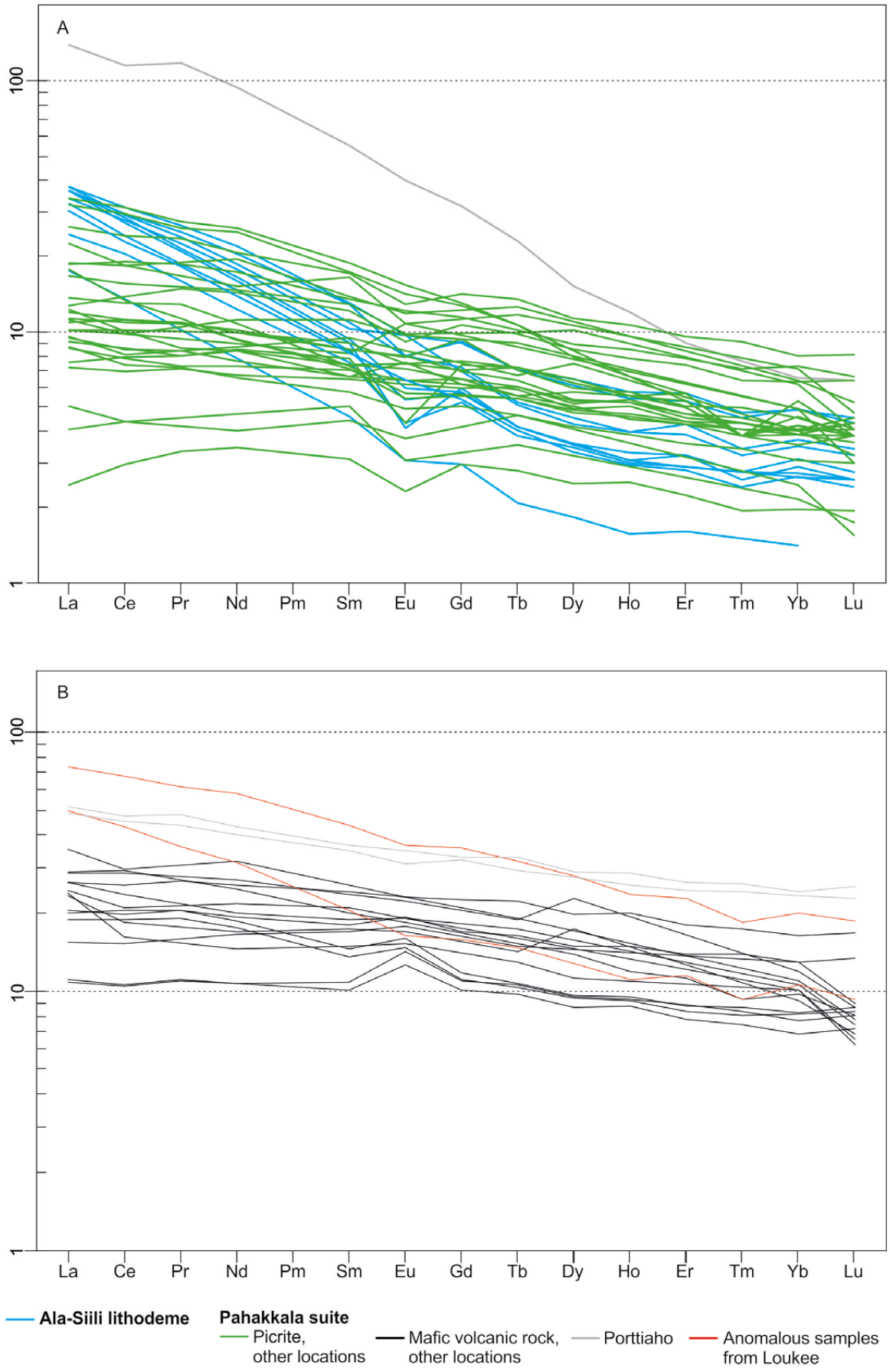

Fig. 9. Chondrite-normalised REE diagram for A) picrite samples and B) mafic volcanic rocks. Anomalous samples from Porttiaho and Loukee locations are separated from the Pahakkala suite, for which the main population is shown as "Other locations". Normalization values for chondrite from Boynton (1984).

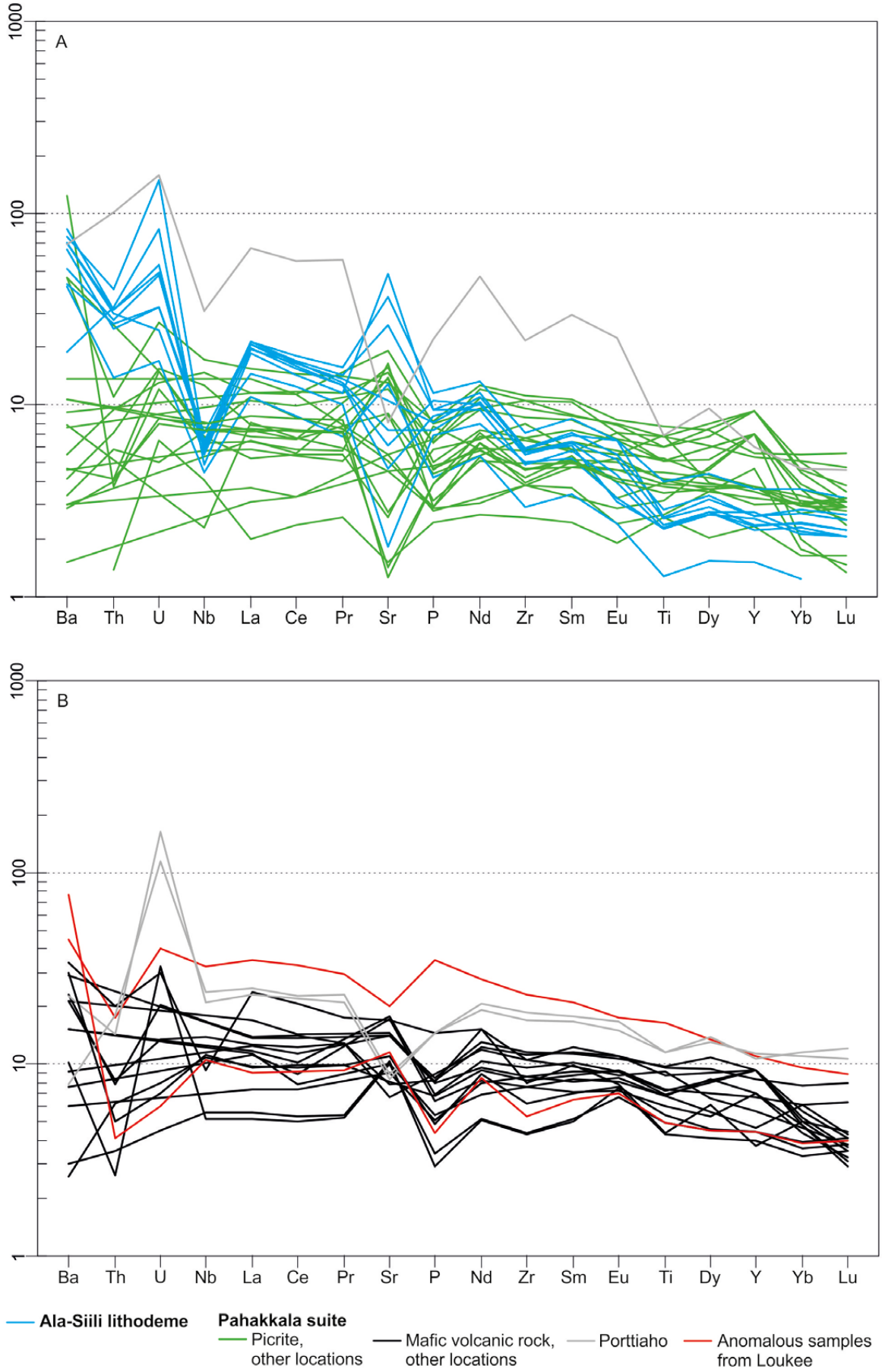

Fig. 10. Primitive mantle-normalised spidergram for A) picrite samples and B) mafic volcanic rocks. Anomalous samples from Porttiaho and Loukee locations are separated from the Pahakkala suite, for which the main population is shown as "Other locations". Normalization values for primitive mantle from McDonough & Sun (1995).

5 AGE DETERMINATIONS

Sample HVM-83-1.5 is a picrite from the Maivala location (Makkonen 1992, 1996). Atypically for ultramafic rocks, the sample contains relatively abundant zircon, which was utilized for *in situ* isotope analysis from a thin section. Eleven spots from 10 zircon grains were analysed, but one spot was discarded due to its high common lead content (Fig. 11). Two analyses from a large zircon grain yielded $^{207}Pb/^{206}Pb$ ages of 2083 and 2031 Ma, with the latter being discordant. Eight analyses from smaller crystals are concordant and the obtained ages cluster at 1840 Ma, yielding a weighted average of 1841 ± 18 Ma. The analysed large crystal probably represents xenocrystic material captured from the sediments on which the lava erupted. The younger ages are interpreted as metamorphic.

Sample A2438 is from an 8-m-wide amphibolite dyke cutting picrites at Loukee. Mineral separation only produced a limited amount of zircon. Eight spots from seven zircon grains were analysed. Two of the analyses were discarded due to high common lead. One of the analyses yielded a Neoarchean age ($^{207}Pb/^{206}Pb$ = 2744 ± 24 Ma), whereas the remaining five analyses gave $^{207}Pb/^{206}Pb$ –ages from 1718 to 1809 Ma (Fig. 11). These five spots contain high concentrations of both Th (407–12089 ppm) and U (774–6088 ppm). The Neoarchean crystal is interpreted as being captured from the paragneisses in the area during the emplacement of the dyke, as its age is similar to those obtained for zircon from the surrounding paragneisses (Mikkola et al. 2018b). The younger ages represent metamorphic event(s), but the small number of analyses together with their large scatter prevents further interpretations.

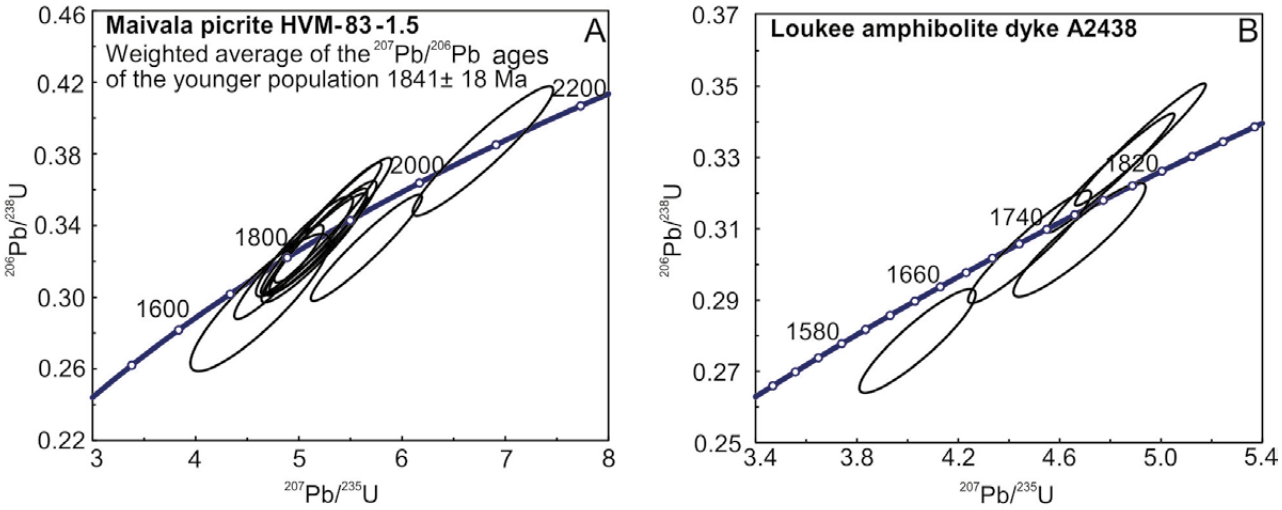

Fig. 11. Concordia diagrams for zircon from samples HVM-83-1.5 (A) and A2438 (B). Note that the two oldest dates from sample HVM-83-1.5 are from the same zircon crystal and the single Neoarchean age obtained from sample A2438 is not shown. Errors drawn at the 2σ level.

6 DISCUSSION

6.1 Geochemistry

The scatter in chemical composition displayed by the studied volcanic rocks has several possible explanations. Post-crystallization alteration is evident, especially in the case of the Ala-Siili location, as strong biotite alteration is clearly reflected in elevated K_2O concentrations. Evidence for contamination during ascent or emplacement is provided by the inherited zircon grains in the samples used in dating, which most likely originated from the sediments on which the lavas erupted. In the case of mafic and ultramafic magmas, cumulation processes have to be taken into account. For example,

the Sr-enriched samples from the Ala-Siili location have higher than average CaO concentrations, suggesting the accumulation of clinopyroxene. It is possible that some of the picrite samples are cumulates from a basaltic magma (e.g. Makkonen 1996, Barnes et al. 2009), while some of the basic volcanic samples are fractionated members of a picritic magma (Nironen 2017). Moreover, the observed difference in the MgO/FeOt ratio of the picrites of the two suites (Fig. 7C) could be a result of olivine fractionation and accumulation from a single parental magma.

Especially the samples of the Pahakkala suite display rather typical EMORB-type trace element characteristics, indicating formation in an extensional environment. The initial ε_{Nd} values for the Pahakkala suite samples are close to +4, suggesting a depleted mantle source for the parental magma (Makkonen & Huhma 2007). Certain compositional characteristics of the Ala-Siili lithodeme, e.g. the negative Nb and Ti anomalies, Zr/Ti ratio and fractionated REE pattern, point to arc-type magmatism. These rocks are not included in the calc-alkaline Makkola suite (Mikkola et al. 2018c), as, based on drill core observations, the rocks of the Ala-Siili lithodeme erupted on the paragneisses of the Pirkanmaa migmatite suite (Mikkola et al. 2018d) and the contact between the Pirkanmaa migmatite and Makkola suites has been interpreted to be tectonic (Mikkola et al. 2018a). As indirect evidence, the lack of similar compositions in the Makkola suite favours the current interpretation of the Ala-Siili lithodeme as part of the Pirkanmaa migmatite suite.

Based on field observations, the mafic to ultramafic volcanic rocks erupted on the protoliths of the paragneisses on the sea bottom. A plausible explanation is that they represent extensional phase(s) in the development of the sedimentary basins in which the paragneisses were deposited. One possible explanation for the compositional differences is that the Pahakkala suite represents a purely extensional phase and the Ala-Siili lithodeme marks a transition to arc-type magmatism. However, it should be noted that claiming that the Ala-Siili lithodeme formed in an arc setting would mark the discovery of a completely new episode of arc magmatism between the older (1930–1910 Ga) and younger (1895–1875 Ma) Svecofennian magmatism (Kähkönen & Huhma 2012, Kousa et al. 2018, Mikkola et al. 2018c and references therein) due to the time constraints for the eruption of the picrites (see below). A partial analogue to the units studied here is the 1877–1852 Ma magmatism in the Skellefte district, where LREE-enriched, Al-undepleted, continental arc-type mafic to ultramafic volcanic rocks erupted contemporaneously with mafic to ultramafic rocks with a MORB affinity (Berge 2013). Berge (2013) proposed a model where the REE and Al enrichment as well as the overall continental arc signature was superimposed on "normal" Al-depleted ultramafic magma by contamination with felsic crustal material. This model could explain certain compositional features of the Ala-Siili lithodeme, e.g., the LILE, LREE enrichment and negative Nb anomalies. However, contamination alone cannot modify the Pahakkala-type picrites into Ala-Siili-type picrites, as the latter have, for instance, higher Mg# and P_2O_5. Both of these would be lower if the magma had been contaminated with felsic material. Thus, differences in the melting depth and temperature are required, in addition to different degrees of contamination, to explain the compositional differences between the Ala-Siili lithodeme and Pahakkala suite. It is also possible that magmas forming the Ala-Siili lithodeme originated from lithospheric mantle enriched during an earlier subduction event.

Comparison with the mafic volcanic rocks from other parts of the Western Finland supersuite reveals that the picrites relatively abundant in our study area are a rarity further west (Lahtinen at al. 2017). Only one locality in central parts of the Pirkanmaa migmatite suite in the data set of Lahtinen et al. (2017) contains rocks with picrite compositions, whereas the remaining are tholeiitic basalts variably displaying within-plate basalt and MORB affinities. More abundant picrite observations have been reported from the Western Finland supersuite further west, where narrow interbeds exist in both mafic metavolcanic rocks and paragneisses (Lehtonen et al. 2005, Kousa & Lundqvist 2000, Kontoniemi & Mursu 2006). The picrites from the Salittu area (Nironen 2017) in South Finland resemble those from the Pahakkala lithodeme, e.g. FeOt >10%, high CaO, TiO_2 and Ni, low P_2O_5 and weakly fractioned REE patterns. Additionally, on the classification diagram of Hanski et al. (2001), samples from Salittu plot in the picrite field, the majority close to the boundary of the Ti-enriched komatiite field, and on the diagram of Pearce (1982) in the MORB field, akin to the samples from the Pahakkala suite.

6.2 Age of the picrites

Due to their ultramafic metamorphic mineral assemblages, the picrites do not contain minerals suitable for dating them directly. When zircon is present, it is either metamorphic or inherited, as demonstrated by the samples of this study used for dating. The maximum depositional age of the paragneisses, 1900–1920 Ma (Lahtinen et al. 2002, 2017, Mikkola et al. 2018b), is also the maximum eruption age of the picrites. The age is further constrained by the observation that the paragneisses do not contain zircon grains derived from the active arc volcanic phase in the vicinity of the study area, which is dated at 1895–1875 Ma (Mikkola et al. 2018c), and hence 1900–1910 Ma probably represents the approximate age of deposition. An indisputable minimum age for the deposition of the paragneisses and eruption of the picrites is given by the granitoid intrusions at ~1885 Ma (Vaasjoki & Kontoniemi 1991, Pekkarinen 2002), thus all ages younger than this must be regarded as metamorphic.

The synorogenic 1885 Ma gabbros and peridotites occurring in South Savo area have been studied in detail due to their Ni and Cu sulphide ore potential (see references in Peltonen 2005). The picrites and associated metatholeiites in the South Savo region have earlier been interpreted to represent extrusive counterparts of these intrusions (Makkonen 1992, 1996, 2015, Makkonen & Huhma 2007). Hill et al. (2005) and Barnes et al. (2009) concluded that the parent magmas to the intrusions and the extrusive picrites had a common mantle source, but the magmas ascended through different routes into the upper crust and the intrusive phases were more contaminated by crustal material than the extrusive phases. This interpretation is supported by the initial ε_{Nd} values of the picrites and associated mafic volcanic rocks being close to that of depleted mantle and differing distinctly from those of the gabbro intrusions (Makkonen & Huhma 2007). However, the now available age constraints on the South Savo picrites suggest that they predate the emplacement of the above-mentioned intrusions more clearly than previously interpreted (Hill et al. 2005). Similar ~1.91 Ga eruption ages have been interpreted for mafic volcanic rocks interbedded with paragneisses in other parts of the Western Finland Supersuite (Lahtinen et al. 2017).

6.3 Implications for areal geology and stratigraphy

The division of the metasedimentary units in our study area has been ongoing since the tectono-metamorphic interpretation of Korsman et al. (1988), who recognized a fundamental difference between the northern and southern parts of the "Savo schist belt". The northern part consists of many fault-separated blocks along the Raahe–Ladoga shear zone, where the metamorphic peak conditions were reached at about 1880 Ma, whereas the southern part, the Rantasalmi–Sulkava area, is characterized by zones of progressive metamorphism with its peak at 1830–1810 Ma. In the current unit division (Nironen et al. 2016a, Luukas et al. 2017), the Savo schist belt is divided into the Savo supersuite in the north, the Pirkanmaa migmatite suite in the west and southwest, and the Häme migmatite suite in the south, with the last one roughly corresponding to the Rantasalmi–Sulkava area of Korsman et al. (1988). The metamorphic ages obtained for zircon in this study, despite a significant scatter, are in line with the areal metamorphism of this subarea. The chemical differences displayed by the picrites of the Pahakkala suite and the Ala-Siili lithodeme could be used as an argument for separating the Häme and Pirkanmaa migmatite suites, despite the fact that the paragneisses do not differ significantly from each other in their composition or depositional age (Lahtinen et al. 2002, 2009, Mikkola et al. 2018b). This interpretation would also require dismissing the Ala-Siili-type chemical characteristics of the samples from Oravakallio locality, which is located clearly within the Häme migmatite suite (Fig. 1) and thus belongs to the Pahakkala suite. Furthermore, as the compositional differences at least partly result from a variable degree of crustal contamination and fractional crystallization, the separation or fusing of these units is not possible without further studies.

Our interpretation of the eruption age of the picrites does not differ significantly from the ages obtained for the tonalites and associated volcanic units from the Viholanniemi area in the Jäppilä–Virtasalmi block (Fig. 1, 1.91 Ga; Kousa et al. 2018). According to Pekkarinen (2002), these tonalites cut the amphibolites of the Jäppilä–Virtasalmi block, which have been interpreted as volcanic in

origin. Ultramafic rocks have not been reported in connection with these amphibolites and similar tonalites have not been reported from the Häme migmatite suite. Thus, the amphibolites of the Jäppilä–Virtasalmi block and the picrites of this study seem to represent different tectonic stages, with the former being associated with the latest activity of the Savo arc (Kousa et al. 2018) and the latter representing a slightly younger extensional phase before the onset of calc-alkaline volcanism and magmatism at 1895 Ma (Kähkönen & Huhma 2012, Mikkola et al. 2018c). Thus, our interpretation is the same as that of Lahtinen et al. (2017) made from areas further west.

Several interpretations of the stratigraphy in the South Savo region have been offered over the years. In the Virtasalmi area, including the Loukee–Airikka area, Hyvärinen (1969) regarded mica schists and intercalated black schists as the oldest, being overlain by quartz-feldspar gneisses, diopside gneisses, carbonate rocks and amphibolites, which are topped again by mica schists. According to Simonen (1982), the stratigraphic sequence in the Mikkeli area starts with diopside amphibolites and quartz-feldspar gneisses, which are followed by mica schists, whereas Gaál and Rauhamäki (1971) proposed that the mafic and ultramafic volcanic rocks in the Haukivesi–Savonlinna area were deposited between two separate sedimentary units, i.e. they are underlain by metapelites and overlain by metagreywackes. Makkonen and Ekdahl (1988) suggested a stratigraphic succession for the Pirilä area, in which the rock units are, from oldest to youngest, mica schists, iron formations, felsic volcanic rocks, intermediate volcanic rocks, mafic volcanic rocks and picrites.

The different locations of the mafic and ultramafic units in the above-mentioned stratigraphic interpretations seem confusing at first, but it must be taken into account that each of them is based on studies in relatively small areas. Nevertheless, it is possible that mafic to ultramafic volcanism occurred several times during the evolution of the sedimentary basin(s). We suggest that the picrite units in the South Savo region do not represent a distinct marker horizon, which could be used to solve the stratigraphy of the associated sedimentary rocks. This is even more evident when the ultramafic and mafic intrusive rocks showing chemical similarities to the picrites of this study, but ca. 20 Ma younger in age (Makkonen 1996, Hill et al. 2005), are taken into account. Furthermore, Salittu picrites from South Finland have been interpreted as 1.88–1.87 Ga old (Nironen et al. 2016b), i.e. postdating the peak of the Svecofennian orogeny in Finland at 1.88 Ga. It is thus evident that mantle-derived mafic to ultramafic melts were generated in at least three stages during the development of the Svecofennian orogeny in Finland.

7 CONCLUSIONS

Volcanic rocks displaying picritic chemical compositions are widespread but low-volume constituents in the paragneiss dominating the bedrock of the South Savo region.

These ultramafic rocks are spatially associated with mafic volcanic rocks displaying EMORB-like chemical affinities.

Based on locally observable pillow lava, lava breccia and amygdale structures, some of the picrites are volcanic rocks, whereas cross-cutting relationships with surrounding rocks indicate that the some of them originated as subvolcanic dykes.

Compositional differences in the here-studied volcanic rocks in both major and trace elements (light rare earth and large-ion lithophile elements) can be explained by differences in their magma source, degree of crustal contamination, post-magmatic alteration and accumulation and fractionation processes.

The picrites were erupted during the extensional phase(s) of the basin(s) that the surrounding paragneisses were deposited in.

The best estimation for the eruption age of the picrites is 1.91–1.90 Ga.

ACKNOWLEDGEMENTS

Mauri Luukkonen is acknowledged for Figure 2 and Jouko Ranua for Figures 3 and 5. Hannu Huhma and the whole staff of GTK's isotope laboratory are thanked for the work on the age determination samples. Reviews by Dr Tuomo Törmänen and Professor Eero Hanski helped in the overall improvement of the original manuscript.

REFERENCES

Barnes, S. J., Makkonen, H. V., Dowling, S. E., Hill, R. E. T. & Peltonen, P. 2009. The 1.88 Ga Kotalahti and Vammala nickel belts, Finland: geochemistry of the mafic and ultramafic metavolcanic rocks. Bulletin of the Geological Society of Finland 81, 103–141. Available at: https://doi.org/10.17741/bgsf/81.2.002

Bedrock of Finland - DigiKP. Digital map database [Electronic resource]. Espoo: Geological Survey of Finland [referred 31.04.2017]. Version 2.0.

Berge, J. 2013. Likely "mantle plume" activity in the Skellefte district, Northern Sweden. A reexamination of mafic/ultramafic magmatic activity: Its possible association with VMS and gold mineralization. Ore Geology Reviews 55, 64–79.

Boynton, W. V. 1984. Cosmochemistry of the rare earth elements; meteorite studies. In: Henderson, P. (ed.) Rare earth element geochemistry. Amsterdam: Elsevier, 63–114.

De La Roche, H., Leterrier, P., Crandclaude, P. & Marchal, M. 1980. A classification of volcanic and plutonic rocks using the RI-R2 diagram and major element analyses. Its relationships with current nomenclature. Chemical Geology 29, 183–210.

Gaál, G. & Rauhamäki, E. 1971. Petrological and structural analysis of the Haukivesi area between Varkaus and Savonlinna, Finland. Bulletin of the Geological Society of Finland 43, 265–337. Available at: https://doi.org/10.17741/bgsf/43.2.010

Hanski, E., Huhma, H., Rastas, P. & Kamenetsky, V. S. 2001. The Palaeoproterozoic Komatiite–Picrite Association of Finnish Lapland. Journal of Petrology 42, 855–876.

Hill, R., Barnes, S., Dowling, S., Makkonen, H. & Peltonen, P. 2005. Chalcophile element distribution in mafic and ultramafic metavolcanic rocks of the Svecofennian Kotalahti and Vammala Nickel Belts Finland – A test for a geochemical signature of subvolcanic magmatic ore forming processes. Regional area selection criteria for intrusive Ni/Cu sulfide ore deposits. Final report, CSIRO, GTK. Geological Survey of Finland, archive report, M10.4/2005/2. 217 p. Available at: http://tupa.gtk.fi/raportti/arkisto/m10_4_2005_2.pdf

Huhma, H., Claesson, S., Kinny, P. D. & Williams, I. S. 1991. The growth of Early Proterozoic crust: new evidence from Svecofennian zircons. Terra Nova 3, 175–179.

Hyvärinen, L. 1969. On the geology of the copper ore field in the Virtasalmi area, eastern Finland. Geological Survey of Finland, Bulletin 240. 82 p. Available at: http://tupa.gtk.fi/julkaisu/bulletin/bt_240.pdf

Jensen, L. S. 1976. A new cation plot for classifying subalkalic volcanic rocks. Ontario Geological Survey Miscellaneous Paper 66. 22 p.

Kähkönen, Y. 2005. Svecofennian supracrustal rocks. In: Lehtinen, M., Nurmi, P. & Rämö, O. T. (eds) The Precambrian Bedrock of Finland—Key to the evolution of the Fennoscandian Shield. Elsevier Science B.V., 343–406.

Kähkönen, Y. & Huhma, H. 2012. Revised U-Pb zircon ages of supracrustal rocks of the Paleoproterozoic Tampere Schist Belt, southern Finland. In: Kukkonen, I. T., Kosonen E. M., Oinonen, K., Eklund, O., Korja, A., Korja, T., Lahtinen, R., Lunkka, J. P. & Poutanen, M. (eds) Lithosphere 2012 – Seventh Symposium on the Structure, Composition and Evolution of the Lithosphere in Finland. Programme and Extended Abstracts, Espoo, Finland, November 6-8, 2012. Institute of Seismology, University of Helsinki, Report S-56, 51–54. Available at: http://www.seismo.helsinki.fi/pdf/LITO2012.pdf

Kontoniemi, O. & Mursu, J. 2006. Hirsikangas gold prospect in Himanka, western Finland. Geological Survey of Finland, archive report M19/2413/2006/1/10. 30p + 6 app. Available at: http://tupa.gtk.fi/raportti/arkisto/m19_2413_2006_1_10.pdf

Korsman, K. 1973. Rantasalmi. Geological Map of Finland 1:100 000, Pre-Quaternary Rocks, Sheet 3233. Geological Survey of Finland. Available at: http://tupa.gtk.fi/kartta/kallioperakartta100/kp_3233.pdf

Korsman, K., Hölttä, P., Hautala, T. & Wasenius, P. 1984. Metamorphism as an indicator of evolution and structure of the crust in Eastern Finland. In: Korsman, K.,Hölttä, P., Hautala, T. & Wasenius, P. Metamorphism as an indicator of evolution and structure of the crust in Eastern Finland. Geological Survey of Finland, Bulletin 328, 1–40. Available at: http://tupa.gtk.fi/julkaisu/bulletin/bt_328.pdf

Korsman, K., Niemelä, R. & Wasenius, P. 1988. Multistage evolution of the Proterozoic crust in the Savo schist belt, eastern Finland. In: Korsman, K. (ed.) Tectono-metamorphic evolution of the Raahe-Ladoga zone, eastern Finland. Geological Survey of Finland, Bulletin 343, 89–96. Available at: http://tupa.gtk.fi/julkaisu/bulletin/bt_343.pdf

Kousa, J. 1985. Rantasalmen tholeiittisista ja komatiittisista vulkaniiteista. Geologi 37, 18–21. (in Finnish)

Kousa, J. & Lundqvist, Th. 2000. Proterozoic crystalline rocks, Svecofennian Domain. In: Lundqvist, Th. & Autio, S. (eds) Description to the bedrock map of central Fennoscandia (Mid-Norden). Geological Survey of Finland, Special Paper 28, 47-75. Available at: http://tupa.gtk.fi/julkaisu/specialpaper/sp_028.pdf

Kousa, J., Huhma, H., Hokka, J. & Mikkola, P. 2018. Extension of Svecofennian 1.91 Ga magmatism to the south, results of the reanalysed age determination samples from Joroinen, central Finland. In: Mikkola, P., Hölttä, P. & Käpyaho, A. (eds) Development of the Paleoproterozoic Svecofennian orogeny: new constraints from the southeastern boundary of the Central Finland Granitoid Complex. Geological Survey of Finland, Bulletin 407. (this volume). Available at: https://doi.org/10.30440/bt407.3

Lahtinen, R., Huhma, H., Kähkönen, Y. & Mänttäri, I. 2009. Paleoproterozoic sediment recycling during multiphase orogenic evolution in Fennoscandia, the

Tampere and Pirkanmaa belts, Finland. Precambrian Research 174, 310–336.

Lahtinen, R., Huhma, H. & Kousa, J. 2002. Contrasting source components of the Palaeoproterozoic Svecofennian metasediments: detrital zircon U–Pb, Sm–Nd and geochemical data. Precambrian Research 116, 81–109.

Lahtinen, R., Huhma, H., Sipilä, P. & Vaarma, M. 2017. Geochemistry, U-Pb geochronology and Sm-Nd data from the Paleoproterozoic Western Finland supersuite – A key component in the coupled Bothnian oroclines. Precambrian Research 299, 264–281.

Laitakari, A. J. 1985. Tutkimustyöselostus Mikkelin mlk:ssa valtausalueilla Korpijärvi 1, kaiv.rek.n:o 2978/1 sekä Iso-Mietiäinen 1, kaiv.rek.n:o 2978/2 ja Iso-Mietiäinen 2, kaiv.rek.n:o 2978/3 suoritetuista tutkimuksista. Geological Survey of Finland, archive report M06/3142/-85/1. 8 p., 21 apps. (in Finnish). Available at: http://tupa.gtk.fi/raportti/valtaus/m06_3142_85_1.pdf

Le Bas, M. J. 2000. IUGS reclassification of the high-Mg and picritic volcanic rocks. **Journal of Petrology** 41, 1467–1470.

Le Bas, M. J., Le Maitre, R. W., Streckeisen, A. & Zanettin, B. A. 1986. Chemical classification of volcanic rocks based on the total alkali-silica diagram. Journal of Petrology 27, 745–750.

Lehtonen, M. I., Kujala, H., Kärkkäinen, N., Lehtonen, A., Mäkitie, H., Mänttäri, I., Virransalo, P. & Vuokko, J. 2005. Etelä-Pohjanmaan liuskealueen kallioperä. Summary: Pre-Quaternary rocks of the South Ostrobothnian Schist Belt. Geological Survey of Finland, Report of Investigation 158, 125 p. Available at: http://tupa.gtk.fi/julkaisu/tutkimusraportti/tr_158.pdf

Luukas, J., Kousa, J., Nironen, M. & Vuollo, J. 2017. Major stratigraphic units in the bedrock of Finland, and an approach to tectonostratigraphic division. In: Nironen, M. (ed.) Bedrock of Finland at the scale 1:1 000 000 - Major stratigraphic units, metamorphism and tectonic evolution. Geological Survey of Finland, Special Paper 60, 9-40. Available at: http://tupa.gtk.fi/julkaisu/specialpaper/sp_060.pdf

Makkonen, H. 1984. Tutkimustyöselostus Juvan kunnassa valtausalueella Rantala 1, kaiv. rek. n:o 3401 suoritetuista tutkimuksista. Geological Survey of Finland, archive report M06/3231/-84/2/10. 4 p. (in Finnish). Available at: http://tupa.gtk.fi/raportti/valtaus/m06_3231_84_2_10.pdf

Makkonen, H. 1992. 1.9 Ga tholeiittinen magmatismi ja siihen liittyvä Ni-Cu-malminmuodostus Juvan alueella, Kaakkois-Suomessa. Unpublished licentiate thesis, University of Oulu, Department of Geology. 200 p. (in Finnish)

Makkonen, H. 1996. 1.9 Ga tholeiitic magmatism and related Ni-Cu deposition in the Juva area, SE Finland. In: Makkonen, H. V. 1.9 Ga tholeiitic magmatism and related Ni-Cu deposition in the Juva area, SE Finland. Geological Survey of Finland, Bulletin 386, 1–101. Available at: http://tupa.gtk.fi/julkaisu/bulletin/bt_386.pdf

Makkonen, H. V. 2015. Nickel deposits of the 1.88 Ga Kotalahti and Vammala belt. In: Maier, W. D., O'Brien, H. & Lahtinen, R. (eds) Mineral Deposits of Finland. Elsevier, 253–290.

Makkonen, H. & Ekdahl, E. 1988. Petrology and structure of the early Proterozoic Pirilä gold deposit in southeastern Finland. Bulletin of the Geological Society of Finland 60, 55–66. Available at: https://doi.org/10.17741/bgsf/60.1.004

Makkonen, H. & Huhma, H. 2007. Sm-Nd data for mafic-ultramafic intrusions in the Svecofennian (1.88 Ga) Kotalahti Nickel Belt, Finland – implications for crustal contamination at the Archaean/Proterozoic boundary. Bulletin of the Geological Society of Finland 79, 175–201. Available at: https://doi.org/10.17741/bgsf/79.2.003

McDonough, W. F. & Sun, S.-S. 1995. Composition of the Earth. Chemical Geology 120, 223–253.

Mikkola, P. & Niemi, S. 2015. Haapasuon kairaukset Joutsassa vuonna 2015. Geological survey of Finland, archive report 79/2015. 6 p. (in Finnish). Available at: http://tupa.gtk.fi/raportti/arkisto/79_2015.pdf

Mikkola, P., Heilimo, E., Aatos, S., Ahven, M., Eskelinen, J., Halonen, S., Hartikainen, A., Kallio, V., Kousa, J., Luukas, J., Makkonen, H., Mönkäre, K., Niemi, S., Nousiainen, M., Romu, I. & Solismaa, S. 2016. Jyväskylän seudun kallioperä. Summary: Bedrock of the Jyväskylä area. Geological Survey of Finland, Report of Investigation 227. 95 p., 6 apps. Available at: http://tupa.gtk.fi/julkaisu/tutkimusraportti/tr_227.pdf

Mikkola, P., Heilimo, E., Luukas, J., Kousa, J., Aatos, S., Makkonen, H., Niemi, S., Nousiainen, M., Ahven, M., Romu, I. & Hokka, J. 2018a. Geological evolution and structure along the southeastern border of the Central Finland Granitoid Complex. In: Mikkola, P., Hölttä, P. & Käpyaho, A. (eds) Development of the Paleoproterozoic Svecofennian orogeny: new constraints from the southeastern boundary of the Central Finland Granitoid Complex. Geological Survey of Finland, Bulletin 407. (this volume). Available at: https://doi.org/10.30440/bt407.1

Mikkola, P., Huhma, H., Romu, I. & Kousa, J. 2018b. Detrital zircon ages and geochemistry of the metasedimentary rocks along the southeastern boundary of the Central Finland Granitoid Complex. In: Mikkola, P., Hölttä, P. & Käpyaho, A. (eds) Development of the Paleoproterozoic Svecofennian orogeny: new constraints from the southeastern boundary of the Central Finland Granitoid Complex. Geological Survey of Finland, Bulletin 407. (this volume). Available at: https://doi.org/10.30440/bt407.2

Mikkola, P., Mönkäre, K., Ahven, M. & Huhma, H. 2018c. Geochemistry and age of the Paleoproterozoic Makkola suite volcanic rocks in central Finland. In: Mikkola, P., Hölttä, P. & Käpyaho, A. (eds) Development of the Paleoproterozoic Svecofennian orogeny: new constraints from the southeastern boundary of the Central Finland Granitoid Complex. Geological Survey of Finland, Bulletin 407. (this volume). Available at: https://doi.org/10.30440/bt407.5

Mikkola, P., Niemi, S. & Ruotsalainen, R. 2014. Ala-Siilin kairaukset Pieksämäellä 2014. Geological survey of Finland, archive report 85/2014. 4 p. (in Finnish). Available at: http://tupa.gtk.fi/raportti/arkisto/85_2014.pdf

Mikkola, P, Niskanen, M. & Hokka, J. 2018d. Harjujärvensuo gold mineralisation in Leivonmäki, Central Finland. In: Mikkola, P., Hölttä, P. & Käpyaho, A. (eds) Development of the Paleoproterozoic Svecofennian orogeny: new constraints from the southeastern boundary of the Central Finland Granitoid Complex. Geological Survey of Finland, Bulletin 407. (this volume). Available at: https://doi.org/10.30440/bt407.9

Nironen, M. 2017. The Salittu Formation in southwestern Finland, part II: Picritic-basaltic volcanism in mature arc environment. Bulletin of the Geological Society of Finland 89, 5–19. Available at: https://doi.org/10.17741/bgsf/89.1.001

Nironen, M., Kousa, J., Luukas, J. & Lahtinen, R. (eds) 2016a. Geological Map of Finland – Bedrock 1:1 000 000. Espoo: Geological Survey of Finland.

Available at: http://tupa.gtk.fi/kartta/erikoiskartta/ek_097_300dpi.pdf

Nironen, M., Mänttäri, I. & Väisänen, M. 2016b. The Salittu Formation in southwestern Finland, part I: Structure, age and stratigraphy. Bulletin of the Geological Society of Finland 88, 85–103. Available at: https://doi.org/10.17741/bgsf/88.2.003

Pääjärvi, A. 1975. Tuusmäen tyynylaava. Unpublished bachelor's thesis, University of Oulu, Department of Geology. 16 p. (in Finnish)

Pearce, J. A. 1982. Trace element characteristics of lavas from destructive plate boundaries. In: Thorp, R. S. (ed.) Andesites: Orogenic Andesites and Related Rocks. New York: John Wiley and Sons, 525–548.

Pekkarinen, L. 2002. Haukivuoren ja Pieksämäen kartta-alueiden kallioperä. Summary: Pre-Quaternary rocks of the Haukivuori and Pieksämäki Map-Sheet areas. Geological Map of Finland 1:100,000, Explanation to the Maps of Pre-Quaternary Rocks, Sheets 3231, 3232. Geological Survey of Finland. 98 p. Available at: http://tupa.gtk.fi/kartta/kallioperakartta100/kps_3231_3232.pdf

Pekkarinen, L. J. & Hyvärinen, L. 1984. Haukivuori. Geological Map of Finland 1:100 000, Pre-Quaternary Rocks, Sheet 3231. Geological Survey of Finland. Available at: http://tupa.gtk.fi/kartta/kallioperakartta100/kp_3231.pdf

Peltonen, P. 2005. Mafic-Ultramafic Intrusions of the Svecofennian Orogen. In: Lehtinen, M., Nurmi, P. A. & Rämö, O. T. (eds) Precambrian geology of Finland – Key to the evolution of the Fennoscandian Shield. Developments in Precambrian. Geology 14, 413–447.

Schuth, S., Rohrbach, A., Münker, C., Ballhaus, C., Garbe-Schönberg D. & Qopoto, C. 2004. Geochemical constraints on the petrogenesis of arc picrites and basalts, New Georgia Group, Solomon Islands. Contributions to Mineralogy and Petrology 148, 288–304.

Simonen, A. 1982. Mäntyharjun ja Mikkelin kartta-alueiden kallioperä. Summary: Pre-Quaternary Rocks of the Mäntyharju and Mikkeli Map-Sheet areas. Geological Map of Finland 1:100 000, Explanation to the Maps of Pre-Quaternary Rocks, Sheets 3123, 3142. Geological Survey of Finland. 36 p. Available at: http://tupa.gtk.fi/kartta/kallioperakartta100/kps_3123_3142.pdf

Vaasjoki, M. & Kontoniemi, O. 1991. Isotopic studies from the Proterozoic Osikonmäki gold prospect at Rantasalmi, southeastern Finland. In: Autio, S. (ed.) Current Research 1989-1990. Geological Survey of Finland, Special Paper 12, 53–57. Available at: http://tupa.gtk.fi/julkaisu/specialpaper/sp_012.pdf

Viluksela, A. 1988. Rantasalmen ja Parikkalan-Punkaharjun vulkaniittien petrografia, geokemia ja tektonomagmaattinen luonne. Unpublished Master's thesis, University of Helsinki, Deparment of Geology and Mineralogy. 96 p. (in Finnish)

Vorma, A. 1971. Pieksämäki. Geological Map of Finland 1:100 000, Pre-Quaternary Rocks, Sheet 3232. Geological Survey of Finland. Available at: http://tupa.gtk.fi/kartta/kallioperakartta100/kp_3232.pdf

Wood, D. A. 1980. The application of a Th-Hf-Ta diagram to problems of tectonomagmatic classification and to establish the nature of crustal contamination of basaltic lavas of the British Tertiary Volcanic Province. Earth and Planetary Science Letters 50, 11–30.

Development of the Paleoproterozoic Svecofennian orogeny: new constraints from the southeastern boundary of the Central Finland Granitoid Complex
Edited by Perttu Mikkola, Pentti Hölttä and Asko Käpyaho
Geological Survey of Finland, Bulletin 407, 85-105, 2018

GEOCHEMISTRY AND AGE OF THE PALEOPROTEROZOIC MAKKOLA SUITE VOLCANIC ROCKS IN CENTRAL FINLAND

by

Perttu Mikkola[1)], Krista Mönkäre[2)], Marjaana Ahven[1)] and Hannu Huhma[3)]

Mikkola, P., Mönkäre, K., Ahven, M. & Huhma, H. 2018. Geochemistry and age of the Paleoproterozoic Makkola suite volcanic rocks in central Finland. *Geological Survey of Finland, Bulletin 407*, 85–105, 8 figures and 2 tables.

The Paleoproterozoic volcanic rocks of the Makkola suite form a discontinuous belt along the southeastern border of the Central Finland Granitoid Complex. Based on single-grain age determinations from four samples, the ages of these volcanic rocks and associated dykes vary from 1895 to 1875 Ma. One volcanogenic-sedimentary sample has a dominant zircon population aged 1885 Ma, the remaining ages varying from 1.98 to 3.09 Ga. The majority of the rocks are intermediate to acid and display enrichment in light rare earth elements and negative Nb, Ti and Zr anomalies on spider diagrams normalized with primitive mantle. Overall, these rocks are typical representatives of calc-alkaline continental arc type magmatism related to subduction during the Svecofennian orogeny. Primary textures are locally well preserved and vary from coarse volcanic breccias to thin layered tuffs and tuffites. Massive tuffs and subvolcanic plagioclase porphyrites are common and differentiation between these two rock types is difficult. Based on similarities in both age and composition, the Makkola suite can be considered as the eastern equivalent of the classical Tampere group volcanic rocks located 100 km to the west.

Appendix 1 is available at: http://tupa.gtk.fi/julkaisu/liiteaineisto/bt_407_appendix_1.pdf

Electronic Appendix is available at: http://tupa.gtk.fi/julkaisu/liiteaineisto/bt_407_electronic_appendix.xlsx

Keywords: volcanic rocks, volcanic belts, calc-alkalic composition, U/Pb, absolute age, zircon, Svecofennian, Paleoproterozoic, Finland

[1)] *Geological Survey of Finland, P.O. Box 1237, FI-70211 Kuopio, Finland*
[2)] *Department of Geography and Geology, University of Turku, FI-20014 Turku, Finland*
[3)] *Geological Survey of Finland, P.O. Box 96, FI-02151 Espoo, Finland*
E-mail: perttu.mikkola@gtk.fi

VERTAISARVIOITU
KOLLEGIALT GRANSKAD
PEER-REVIEWED
www.tsv.fi/tunnus

https://doi.org/10.30440/bt407.5

Editorial handling by Pentti Hölttä and Asko Käpyaho.

Received 30 June 2017; Accepted 25 June 2018

1 INTRODUCTION

The Paleoproterozoic bedrock of southern and central Finland, as well as that in adjacent areas of Sweden and Russia, was formed in accretionary and collisional processes of the collisional Paleoproterozoic Svecofennian orogeny around 1.9 Ga (Lahtinen et al. 2016, 2017, Nironen 2017 and references therein). The majority of the bedrock is formed by granitoids and variably migmatized paragneisses, whereas volcanic rocks are volumetrically less significant and present as narrow elongated belts (Fig. 1). Various models for the overall geological evolution of the Svecofennian orogeny have been proposed (e.g. Rutland et al. 2004, Williams et al. 2008, Lahtinen et al. 2009, 2017), and although they differ in detail, they concur in the main features. As a whole the Svecofennian domain provides an excellent example for studying and understanding the deeply eroded Paleoproterozoic collisional orogeny. Although the overall development of the orogeny is well constrained due to a research history extending back to the 19th century, the amount of data varies significantly from one area to another. For example, the calc-alkaline ~1.89 Ga volcanic succession of the Tampere group along the southern boundary of the Central Finland Granitoid Complex (CFGC, Fig. 1) has been extensively studied (e.g. Seitsaari 1951, Simonen 1953, Kähkönen 1987, 1999, 2005, Nironen 1989) since the early work by Sederholm

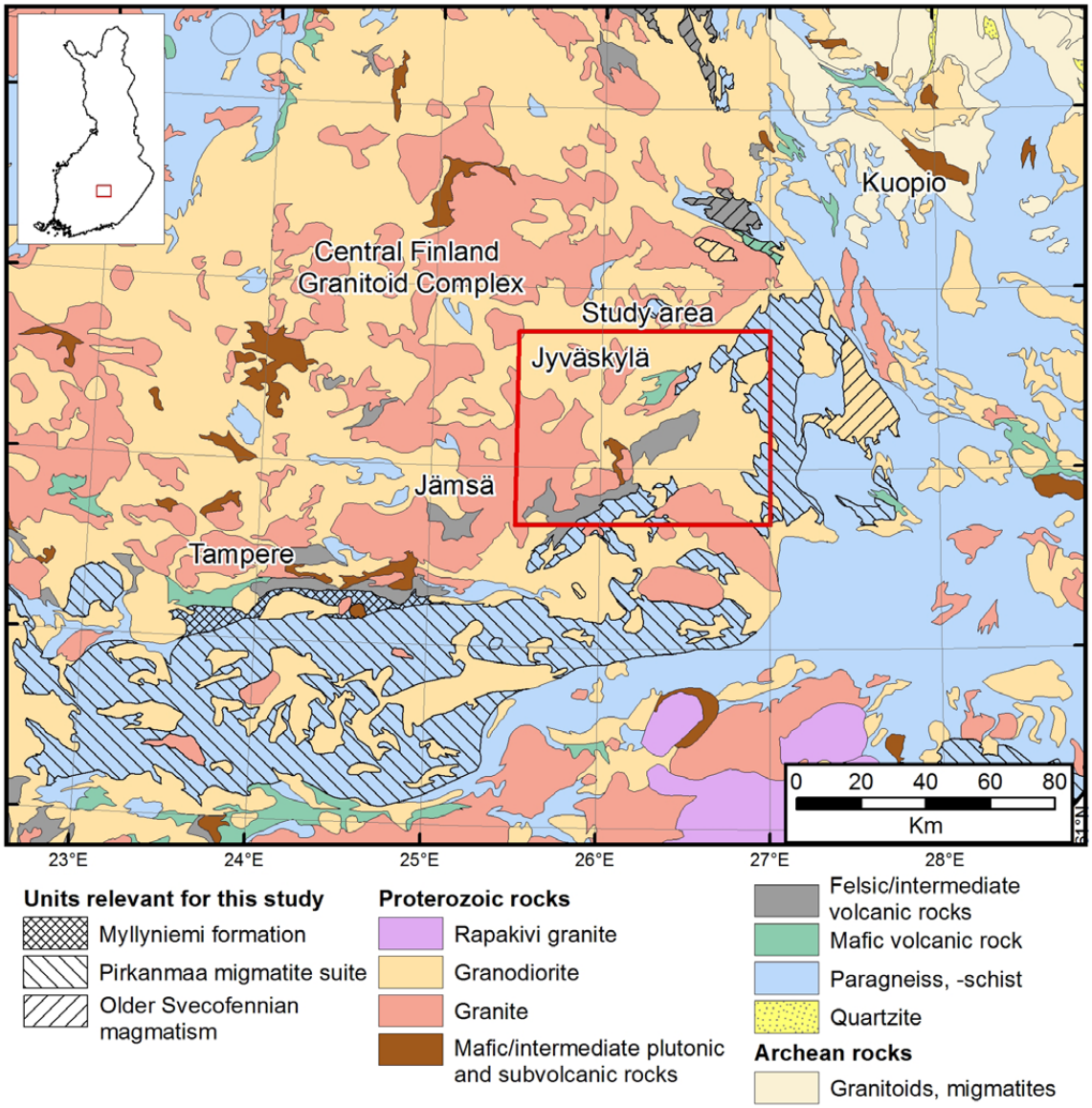

Fig. 1. The location of the study area on an index map and on the geological map of central Finland. Relevant geological units as raster on top of lithological map. Map modified from Nironen et al. (2016) and Bedrock of Finland - DigiKP.

(1897). At the same time, its extensions to the east have been the subject of a limited number of unpublished Master's theses (Karppanen 1970, Ikävalko 1981, Heikura 2017).

This paper describes the field and geochemical characteristics of the volcanic rocks belonging to the previously little studied Makkola suite located along the southeast boundary of CFGC and consisting mainly of intermediate volcanic rocks. Results from single-grain U–Pb zircon age determinations from volcanic units and associated dykes and volcanogenic-sedimentary rock are also presented. The data are used to evaluate the genesis of the Makkola suite, with emphasis on the differences and similarities compared with the classical Tampere group volcanic rocks in order to either confirm or refute the preliminary interpretations of the Makkola suite as a eastern extension of the Tampere group (Karppanen 1970, Ikävalko 1981, Kähkönen 2005).

2 GEOLOGICAL SETTING

The Svecofennian domain in Finland has been divided into Southern and Western Finland Subprovinces (Nironen et al. 2016). Core of the latter is formed by the CFGC, which is surrounded by narrow intermittent volcanic belts and voluminous, often migmatitic paragneisses (Fig.1). In our study area these paragneisses belong to the Pirkanmaa migmatite belt (Luukas et al. 2017).

The oldest Svecofennian magmatic rocks are the 1.93–1.91 Ga volcanic units (Fig. 1) and their plutonic counterparts, which were formed in a primitive arc setting and occur along the boundary of the Archean Karelian Craton (e.g. Vaasjoki et al. 2003, Kousa et al. 2004, 2018a). This older Svecofennian magmatism ended when the arc collided with the Archean continent (e.g. Lahtinen et al. 2014).

Protoliths of the Pirkanmaa migmatite suite (Fig. 1) were deposited as greywackes immediately after, or partly coevally with the first collisional stage, as their maximum depositional ages are typically close to 1.92 Ga (Lahtinen et al. 2009, 2017, Mikkola et al. 2018b). Ultramafic and mafic volcanic rocks belonging to the Pirkanmaa migmatite suite have been interpreted to represent 1.91–1.90 Ga extensional phases of the depositional basin(s) (e.g. Lahtinen 1996, Lahtinen et al. 2017, Kousa et al. 2018b). A small number of more intermediate volcanic rocks from small areas or narrow interbeds have also been included in the Pirkanmaa migmatite suite. These are located in southern and eastern parts of our study area. In all locations, these rocks are intensively deformed and do not display clear primary structures. Their classification as volcanic rocks is mainly based on their small grain size and mineralogy. Most of the paragneisses of the Pirkanmaa migmatite suite are, as the name implies, variably migmatitic, but are locally of a lower metamorphic grade, and well-preserved primary structures are observable, for example, in the Tammijärvi area (Fig. 2, Mikkola et al. 2018b).

The ca. 1895 Ma plutonic rocks of the Pirkanmaa intrusive suite intrude into the Pirkanmaa migmatite suite and mainly consist of granodiorites, with smaller areas of tonalites and diorites (Kallio 1986, Heilimo et al. 2018). The plutonic rocks of the CFGC forming the majority of the bedrock north of the Makkola suite rocks are typically porphyritic granodiorites and granites, yielding zircon ages between 1885 and 1875 Ma (Rämö et al. 2001, Lahtinen et al. 2016, Nikkilä et al. 2016, Heilimo unpublished data). The small areas of volcanic rocks north of the Leivonmäki shear zone in our study area have been classified as belonging to the CFGC (Fig. 2, Mikkola et al. 2016). These rocks have not been correlated with the units of the Makkola suite due to their scattered nature, although they do not display significant differences from them in the field. Due to later deformation, primary textures are only locally observable in these rocks, varying mineralogically from amphibolites to hornblende-biotite–quartz–feldspar gneisses. The volcanic and subvolcanic areas within the central parts of the CFGC are aged between 1890 and 1886 Ma (Nikkilä et al. 2016). Calc-alkaline magmatic rocks of Tampere group, its equivalents and the majority of the CFGC have been interpreted as originating in a subduction setting (e.g. Kähkönen 2005, Lahtinen et al. 2017) or alternatively as a result of partial melting of island arc crust thickened in the 1.91 Ga collision of the Archean craton and the older Svecofennian arc (Nikkilä et al. 2016). All of the above-mentioned rock units in the study area are cross-cut by granite intrusions and veins belonging to the Oittila suite, with an age of ca. 1875 (Heilimo unpublished data),

which also defines the minimum age of the Makkola suite.

The rocks of the here-studied Makkola suite are located in the border zone between the CFGC and Pirkanmaa migmatite and intrusive suites, where they occur as several elongated belts separated by both faulting and intrusive units (Fig. 2). The largest intact segment is 25 by 9 km in size, whereas the smallest fragments are inclusions less than 50 cm across in the surrounding plutonic rocks. The same general structure of scattered volcanic belts between the often migmatitic paragneisses and the CFGC is evident along the whole length of the CFGC border (Fig. 1).

3 MAKKOLA SUITE

Based on geological setting and field observations the volcanic rocks of the Makkola suite have been tentatively considered as an eastern continuation of the Tampere group (Karppanen 1970, Ikävalko 1981, Kähkönen 2005). The lowermost unit of the Tampere group, the Haveri formation, with its EMORB affinity, has been interpreted to represent early extensional phases (Kähkönen 2005) followed by the deposition of greywackes of the Myllyniemi Formation, having maximum depositional ages close to 1.91 Ga (Huhma et al. 1991, Claesson et al. 1993, Lahtinen et al. 2009). The volcanic units in the Tampere area display zircon ages between 1895 and 1880 Ma and calc-alkaline arc type geochemistry (Kähkönen 2005 and references therein, Kähkönen & Huhma 2012). Heikura (2017) concluded that the volcanic rocks in the Jämsä area (Fig. 1) are similar in composition to those of the Tampere group, but the material did not include age determinations.

Due to the combination of often poor exposure and intensive deformation, no attempt at a stratigraphic approach has been made and the Makkola suite has been divided into lithodemes (Mikkola et al. 2016). A brief description of these lithodemes is given in Table 1 and below. More detailed descriptions can be found from Mikkola et al. (2016). In addition to more specifically described lithodemes, the suite also contains "undefined volcanic rock" lithodemes, which include rocks from certain areally small segments that cannot be correlated with a specific lithodeme.

The preservation of primary textures in the Makkola suite is highly variable, and in most parts these have been destroyed by deformation. However, especially the central parts of the Makkola area display well-preserved depositional structures (Fig. 3A). The main deformation in the area is related to the sinistral Leivonmäki shear zone trending from northeast to southwest (Mikkola et al. 2018a, Fig. 2). Rocks of the Makkola suite have been metamorphosed in low amphibolite facies (Hölttä & Heilimo 2018). The majority of the volcanic rocks, especially in the Makkola area and in smaller segments north of it, are relatively felsic tuffs (Teuraanmäki and Mesiänmäki lithodemes) and tuffites (Myllypelto and Keijupelto lithodemes). In some places, these rocks show thin bedding or pyroclastic features, but more commonly they are massive and lack clear primary features (Fig. 3B). In Korospohja, large areas consist of homogeneous, weakly oriented, intermediate uralite-plagioclase porphyrites and plagioclase porphyrites (Töppöspohja and Kieroselkä lithodemes). Based on locally observable cross-cutting relationships, these rocks can be interpreted as subvolcanic (Fig. 3C). Both tuffs and subvolcanic intrusives have a common texture where uralite and plagioclase phenocrysts few millimetres in size are hosted by a finer grained, typically plagioclase-rich ground mass.

Paraschist units interpreted to belong to the Makkola suite are known from two locations (Toivakanlehto and Mäyräsalo lithodemes). This interpretation is based on the close spatial association these rocks display with the volcanic units. Another feature distinguishing between the well-preserved lithodemes of Pirkanmaa migmatite suite (Mikkola et al. 2018b) and the sedimentary units of the Makkola suite is the smaller proportion or lack of greywackes of the latter. Closely related to the Mäyräsalo lithodeme is an iron formation (Holla lithodeme), which is also present as enclaves in the adjacent granitoids.

Mafic units (Oralanmäki, Orala and Kivisuo lithodemes) are less voluminous and occur as both larger areas and interbeds or dykes in the more felsic units. The uralite and plagioclase porphyritic dykes are usually concordant or nearly concordant with the bedding, thus their separation from lava interbeds in poorly exposed areas is difficult. Texturally similar dykes cross-cut the surrounding plutonic rocks (Fig. 3D), especially in the area between Makkola and Halttula (Fig. 2).

Table 1. Summary table of the lithodemes forming the Makkola suite.

Lithodeme	Areal extent	Lithology	Geochemistry
Toivakanlehto paraschist, Mikkola et al. 2017a	In the Halttula area, extent poorly constrained, thickness at least 800 metres.	Paraschist with greywacke and calc-silicate rock interbeds.	----
Keijupelto felsic volcanogenic sedimentary rock	Two small areas in the Korospohja area.	Small grained quartz rich rock, no preserved primary structures, locally weak signs of anatexis	SiO2=63–65%, Trachydacite, dacite
Myllypelto tuffite	Small segments in the Makkola and Halttula area. Sporadic observations also from Korospohja area. Not shown in Figure 2.	Laminar felsic rock, with graded bedding, cross-bedding also often visible.	SiO2=61–71%, Andesite, dacite
Orala mafic volcanic rock	200–400 m wide and 3–7 km long sections. Most common in Makkola area, but present in all subareas.	Fine grained tuff, often with pyroclastic fragments alternating with laminary layers.	SiO2=47–51%, Basalt, basaltic andesite
Mesiänmäki felsic volcanic rock	20 km long and 1–5 km wide section in the Makkola area. Lacking from other parts.	Relatively massive, ejected fragments locally observable.	SiO2=58–74%, Rhyolite, dacite
Teuraanmäki intermediate volcanic rock	Most voluminous lithodeme of the suite. Present in all subareas.	Variably preserved tuffs, variation from massive type to crystal tuffs displaying layering. Larger ejecta fragments scarce.	SiO2=50–72%, Basaltic andesite to trachyte
Oralanmäki uralite porphyrite	Separated areas less than 4 km in length from Korospohja to Makkola	Massive rocks with porphyritic structure caused by clinopyroxene phenocrysts completely altered to amphibole.	SiO2=47–56%, Basalt, basaltic andesite
Kieroselkä plagioclase porphyrite	Dykes/sills in Makkola area intruding both the volcanic segment and surrounding plutonic rocks.	Massive rocks with variable amounts of porphyritic plagioclase crystals.	SiO2=54–67%, Basaltic andesite to dacite
Töppöspohja intermediate subvolcanic rock	Dominant rock type in the Korospohja area. Smaller segements also in Halttula area.	Homogeneous in outcrop scale, in larger scale variable amounts of plagioclase phenocrysts and/or amphibole-biotite agglomerates 2–4 across.	SiO2=56–65%, Trachyandesite, trachyte
Holla iron formation, Mikkola et al. 2016	As less than 10 m thick interbed in Mäyräsalo parachist, also as enclaves in granitoids	Laminar silicate facies iron formation.	Fe2O3=22–47%, Al2O3=1–12%
Mäyräsalo paraschist, Mikkola et al. 2017a	In the proximity of Kivisuo mafic volcanic rock in the contact zone between Makkola suite and Pirkanmaa migmatite suite in the Leivonmäki area	Paraschist, often displaying laminar bedding.	----
Kivisuo mafic volcanic rock	Dominant rock type in the contact zone between Makkola suite and Pirkanmaa migmatite suite.	Lava structures typical, only locally tuff and pyroclastic interbeds. Calc-silicate interbeds common.	SiO2=43–54%, Basalt, basaltic andesite

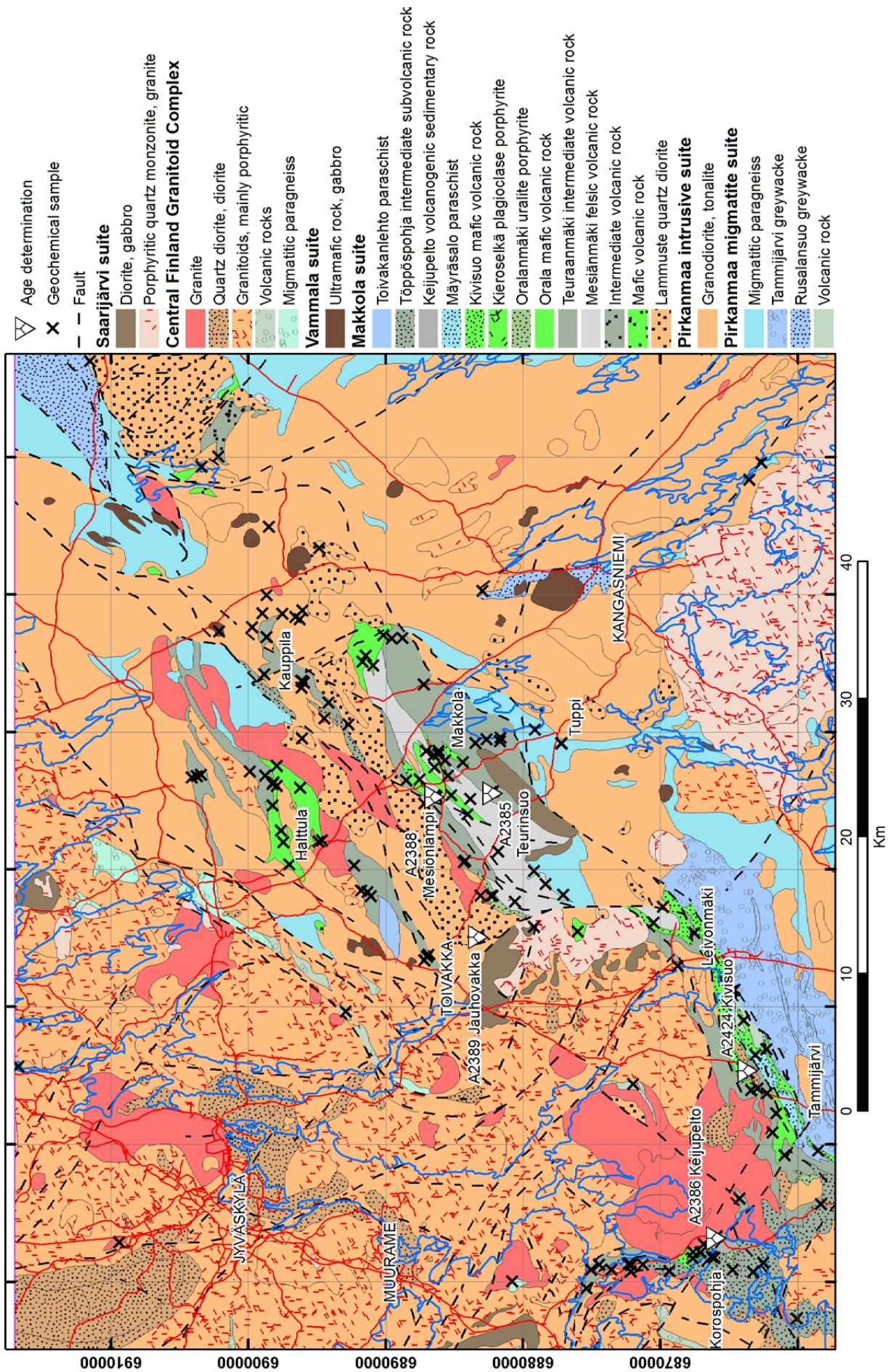

Fig. 2. Sample locations on the geological map modified from Mikkola et al. (2016). The location of the study area is indicated in Figure 1.

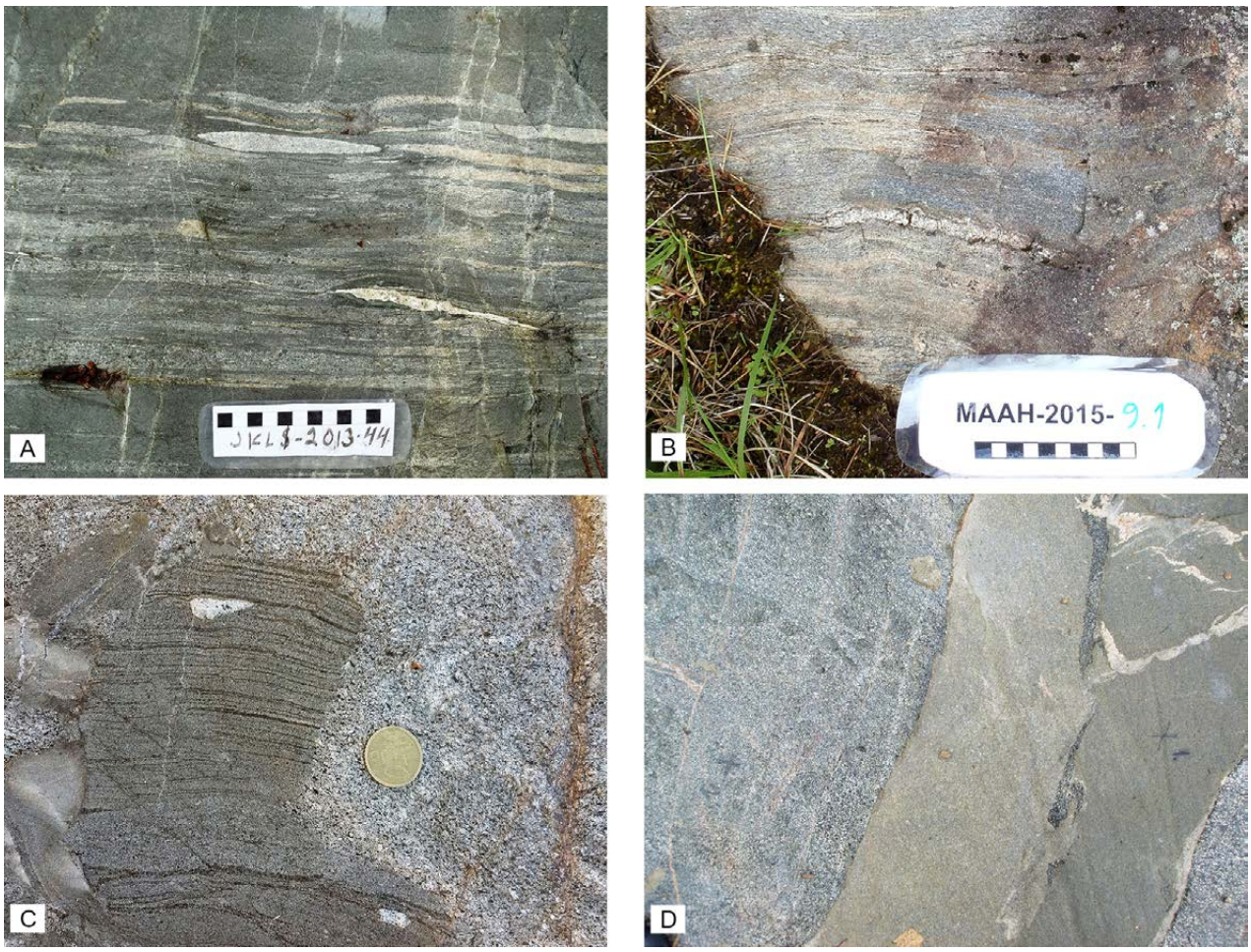

Fig. 3. A) Volcanic breccia, with felsic volcanic rock fragments and more mafic groundmass. Scale bar with cm scale. B) Felsic volcanic rock displaying secondary banding and lacking clear primary features. Scale bar with cm scale. C) Subvolcanic plagioclase porphyrite hosting fragments of sedimentary rocks. Diameter of the coin 24 mm. D) Two parallel weakly plagioclase porphyrite dykes cross-cutting diorite. The width of the dykes is ca. 30 cm.

4 ANALYTICAL METHODS AND SAMPLE MATERIAL

Altogether, 213 analyses from outcrops and drill cores were selected for analysis. In addition to new samples, five previously published analyses from Rasilainen et al. (2007) were included in the material, making the total number of used samples 218. In this study, the compositions of the samples are classified based on their interpreted lithodeme and the locations are not taken into account, as Mönkäre (2016) demonstrated that compositional differences between the different volcanic segments making up the Makkola suite are insignificant. Out of the 218 samples, 187 represent volcanic or subvolcanic units of the Makkola suite, 17 are porphyrite dykes cross-cutting the surrounding plutonic rocks. Six samples represent the volcanic units of the Pirkanmaa migmatite suite and seven samples from volcanic units of the CFGC are also included for comparison. All analytical results are listed in the Electronic Appendix and representative ones are presented in Table 2. All of the new samples were analysed by Labtium Oy using XRF (Labtium code 175X) for major elements and certain trace elements. Additional trace elements were analysed from 167 samples using ICP-MS (Labtium code 308 PM). A description of the analytical methods and list of elements is provided in Appendix 1. The geochemical data were plotted using the Geochemical Data Toolkit (GCDKit) program of Janoušek et al. (2006).

For age determinations, five samples (5 to 10 kg each) representing different lithodemes and subareas were taken from selected outcrops or drill holes. Four of the samples were dated using a Nu

Plasma HR multicollector ICP-MS and one using a Nu Plasma AttoM single collector ICP-MS. The analytical methods are described in Appendix 1 and data are listed in the Electronic Appendix.

5 RESULTS

5.1 Geochemistry

5.1.1 Makkola suite

Compositionally, the Makkola suite forms a continuum from basic to acid compositions, the majority of the samples being intermediate to acid (Fig. 4). CaO and Fe_2O_3 display a good correlation with SiO_2, whereas the other major elements are scattered. In the case of P_2O_5, Al_2O_3, MgO and TiO_2, the scatter concentrates in the compositions with low SiO_2 and is likely to be caused by fractional crystallization processes. The Kivisuo and Orala mafic volcanic rocks especially display this type of scatter.

With respect to alkalies, the scatter is present regardless of the SiO_2 concentrations and is likely to be caused by variable alteration of the original compositions. Thus, the TAS diagram in Figure 5A, in which the samples mainly plot in the subalkaline/tholeiitic field, should be treated as only tentative. However, in the plot of Ishikawa's alteration index (Ishikawa et al. 1976) against the chlorite-carbonate-pyrite index, samples mainly plot within the box of least altered composition of Large et al. (2001) (Fig. 5B). On diagrams based on less mobile elements, the scatter is significantly less than on those involving alkalies. In the Nb/Y vs. Zr/Ti plot, the samples are mainly subalkaline and only the most evolved samples transect the field of alkaline compositions. In Th vs. Co classification diagram of Hastie et al. (2007), the samples plot on both sides of the boundary between calc-alkaline and high-K calc-alkaline fields (Fig. 5D). Most of the samples form a tight group in the volcanic arc array on Pearce's (2008) classification diagram (Fig. 5E).

On chondrite-normalized REE diagrams (Fig. 6), all units display similar trends and the variation in absolute values is mainly related to the main element compositions of the samples. The mafic units have lower LREE concentrations and thus weaker REE fractionation than the more felsic units, as the HREE levels do not vary significantly. Eu anomalies of the units vary from non-existent to weakly negative.

On spider diagrams (Fig. 6), the differences in LILE concentrations are one order of magnitude, and like the LREE concentrations, they correlate with the SiO_2 concentrations, as the more mafic units display lower concentrations. All units display negative Nb, Ti and Zr anomalies, the exception being the Myllypelto lithodeme, which lacks a Zr anomaly. In most of the units, Sr and Nd form positive anomalies.

Most of the porphyrite dykes cross-cutting the plutonic rocks are intermediate in composition, although SiO_2 concentrations vary from 46.8 to 71.4 wt%. With respect to the main elements, they are compositionally similar to the volcanic units. At the basic end of the compositional spectrum, they also display a similar compositional scatter with respect to Al_2O_3, MgO, P_2O_5 and TiO_2 as the volcanic units (Fig. 4). On the classification diagrams, the samples also plot in the same fields as the volcanic rock samples (Fig. 5). Furthermore, they also display similar trends in REE and spider diagrams (Fig. 6), with the same negative Nb, Zr and Ti anomalies along positive ones in Sr and Nd.

5.1.2 Volcanic rocks of the Central Finland Granitoid Complex

The seven samples representing the variably sized volcanic xenoliths within the granitoids of the CFGC vary from basic to acid in composition (SiO_2 = 45.0–65.5%) and display similar compositional characteristics to the samples from the Makkola suite with respect to both main (Fig. 4) and trace elements (Fig. 6).

Table 2. Representative analyses from the studied volcanic units.

Sample	PIM$-2013-24.1	KK4$-2012-900.1	HEKI-2012-271.2	KK4$-2012-802.1	N4342013R1 32.00-32.80	PIM$-2013-300.1	N4342014R13 177.05-177.75
Rock type	Felsic volcanic rock	Felsic tuffite	Uralite porphyrite	Felsic volcanic rock	Intermediate volcanic rock	Plagioclase porphyrite	Uralite porphyrite
Suite / complex	Makkola suite	Makkola suite	Makkola suite	Makkola suite	Makkola suite	Makkola suite	Makkola suite
Lithodeme	Keijupelto volcanogenic sedimentary rock	Myllypelto tuffite	Orala mafic volcanic rock	Mesiänmäki felsic volcanic rock	Teuraanmäki intermediate volcanic rock	Teuraanmäki intermediate volcanic rock	Oralanmäki uralite porphyrite
Occurrence type	Main rock	Main rock	Main rock	Main rock	Main rock	Main rock	Main rock
Age sample	A2386	----	----	A2388	A2385	A2424	----
SiO_2 wt. %	65.20	68.30	50.80	69.10	59.50	61.23	50.10
TiO_2	0.27	0.67	0.82	0.31	0.62	0.74	0.50
Al_2O_3	17.90	15.60	14.00	15.80	18.80	17.95	14.50
Fe_2O_3t	3.02	4.57	11.60	3.84	6.61	6.51	9.58
MnO	0.06	0.07	0.19	0.07	0.13	0.08	0.15
MgO	1.13	1.35	7.27	0.93	1.65	2.31	7.12
CaO	2.35	2.99	8.57	3.06	3.71	3.77	10.81
Na_2O	4.93	3.66	2.63	4.18	5.44	2.87	1.91
K_2O	4.06	2.16	2.17	2.19	2.82	3.11	1.29
P_2O_5	0.15	0.20	0.25	0.11	0.23	0.28	0.23
C ppm	n.a.	<500	<500	1240	1610	<500	760
Ba	1530	641	864	1011	1490	1110	395
Cl	0	<60	<60	90	167	300	233
Co	6.6	10.8	31.4	4.3	10.8	12.8	39.7
Cr	13	118	289	<20	5	140	444
Ga	<20	27	<20	22	24	<30	<20
Hf	2.2	10.6	1.6	4.4	3.5	5.1	1.0
Nb	5.1	11.0	4.7	10.3	11.8	12.4	5.2
Pb	32	<20	<20	<20	<20	40	<20
Rb	107.0	90.3	41.9	38.1	60.5	110.0	38.7
S	120	<60	<60	61	944	700	127
Sc	4.4	11.7	31.8	5.7	12.9	13.4	37.7
Ta	<0.2	1.78	0.33	0.45	0.40	0.50	<0.2
Th	5.2	19.7	2.9	7.2	4.1	7.7	2.2
U	1.7	3.9	1.1	2.0	1.7	3.9	0.8
V	36.9	69.7	n.a.	24.9	68.8	91.4	197.0
Y	9.3	26.1	13.5	16.9	19.4	19.8	12.8
Zn	87	60	106	50	190	90	107
Zr	103.0	336.0	60.4	164.0	174.0	183.0	50.3
La	24.0	41.0	14.2	43.6	38.9	31.0	15.6
Ce	37.2	87.2	29.4	85.0	69.5	61.5	25.1
Pr	13.6	36.0	14.7	34.8	34.3	27.5	11.3
Nd	3.79	9.54	3.65	9.33	8.44	7.20	3.13
Sm	1.77	6.76	3.12	5.71	6.22	5.10	2.46
Eu	0.34	1.44	0.88	1.41	1.93	1.40	0.78
Gd	1.52	5.90	3.24	4.55	5.36	4.60	2.51
Tb	<0.1	0.87	0.45	0.58	0.68	0.70	0.39
Dy	1.13	5.09	2.60	3.33	n.a.	n.a.	2.29
Ho	<0.1	1.00	0.50	0.63	0.73	0.80	0.46
Er	0.56	3.00	1.40	1.90	2.09	2.30	1.35
Tm	<0.1	0.46	0.20	0.28	0.29	0.30	0.21
Yb	0.72	3.12	1.35	1.90	2.11	2.20	1.36
Lu	<0.1	0.50	0.19	0.31	0.29	0.30	0.19

n.a. = not analysed
<30 = below detection limit and the approriate limit

Table 2. Cont.

Sample	ASM$-2013-259.1	HEKI-2012-26.1	KOROS-POHJA-SK-007 39.00-40.00	ASM$-2012-360.1	MAAH-2012-177.2	PIM$-2014-266.1	N4332013R2 70.40-70.55
Rock type	Plagioclase porphyrite	Plagioclase porphyrite	Plagioclase porphyrite	Mafic volcanic rock	Intermediate volcanic rock	Plagioclase porphyrite	Garnet amphibolite
Suite / complex	Makkola suite	Makkola suite	Makkola suite	Makkola suite	Makkola suite	Central Finland Granitoid Complex	Pirkanmaa migmatite suite
Lithodeme	Kieroselkä plagioclase porphyrite	Kieroselkä plagioclase porphyrite	Töppöspohja intermediate subvolcanic rock	Kivisuo mafic volcanic rock	undefined volcanic rock	undefined volcanic rock	undefined volcanic rock
Occurrence type	Porphyrite dyke in plutonic rock	Porphyrite dyke in plutonic rock	Main rock	Main rock	Enclave in plutonic rock	Main rock	Interbed / Dyke
Age sample	A2389	----	----	----	----	----	----
SiO_2 wt. %	71.40	57.80	58.20	50.30	53.10	52.20	55.20
TiO_2	0.22	0.77	0.57	2.86	0.91	1.29	1.10
Al_2O_3	15.10	15.30	17.40	16.30	18.90	17.50	18.20
Fe_2O_3t	2.54	7.57	6.18	8.67	8.49	8.98	10.50
MnO	0.05	0.09	0.18	0.10	0.12	0.12	0.14
MgO	0.49	4.68	3.15	4.15	3.74	5.02	3.30
CaO	2.63	6.39	4.58	6.00	6.55	8.83	5.97
Na_2O	3.63	3.42	2.93	3.10	4.33	3.04	1.65
K_2O	3.37	2.14	4.37	4.40	1.64	1.90	2.96
P_2O_5	0.05	0.23	0.32	1.36	0.41	0.58	0.35
C ppm	<500	<500	608	821	587	614	1000
Ba	2254	1412	1160	n.a.	890	772	813
Cl	156	205	307	350	215	432	332
Co	2.9	18.6	15.6	28.1	17.8	35.3	27.4
Cr	<20	103	60	55	71	128	18
Ga	<20	25	22	30	<20	22	26
Hf	3.1	2.3	3.2	6.0	1.4	3.4	4.9
Nb	6.3	7.7	8.9	31.0	8.2	11.0	11.0
Pb	<20	<20	66	22	<20	<20	22
Rb	58.9	43.2	178.0	129.0	42.0	58.0	116.0
S	245	<60	1890	1517	219	213	748
Sc	1.9	18.2	17.1	22.9	17.1	24.1	15.8
Ta	0.46	0.47	<0.2	1.64	0.41	0.58	1.42
Th	10.2	2.6	6.5	2.5	0.6	3.1	6.9
U	3.3	1.4	3.2	1.2	0.5	1.0	2.4
V	14.9	174.0	94.5	208.0	n.a.	170.0	140.0
Y	6.7	10.8	14.4	19.9	13.2	19.5	24.4
Zn	39	71	219	137	102	102	182
Zr	128.0	74.1	133.0	341.0	59.4	116.0	148.0
La	35.5	14.9	32.4	68.3	20.9	24.5	42.9
Ce	57.9	31.4	54.6	148.0	41.5	57.7	67.5
Pr	18.3	15.6	24.3	68.6	19.8	29.8	32.7
Nd	5.73	3.76	6.37	18.50	4.99	7.52	8.13
Sm	2.26	3.00	4.22	10.20	3.52	5.74	6.11
Eu	0.95	0.92	1.09	2.91	1.42	1.58	1.68
Gd	1.68	2.85	3.56	7.49	3.57	5.02	5.81
Tb	0.21	0.40	0.51	0.90	0.48	0.65	0.79
Dy	1.11	2.22	2.87	4.06	2.62	3.75	n.a.
Ho	0.22	0.42	0.57	0.65	0.49	0.78	0.85
Er	0.76	1.18	1.70	1.62	1.32	2.10	2.44
Tm	0.12	0.17	0.23	0.21	0.18	0.32	0.33
Yb	0.95	1.08	1.68	1.31	1.23	1.87	2.50
Lu	0.15	0.17	0.23	0.19	0.17	0.27	0.33

n.a. = not analysed
<30 = below detection limit and the approriate limit

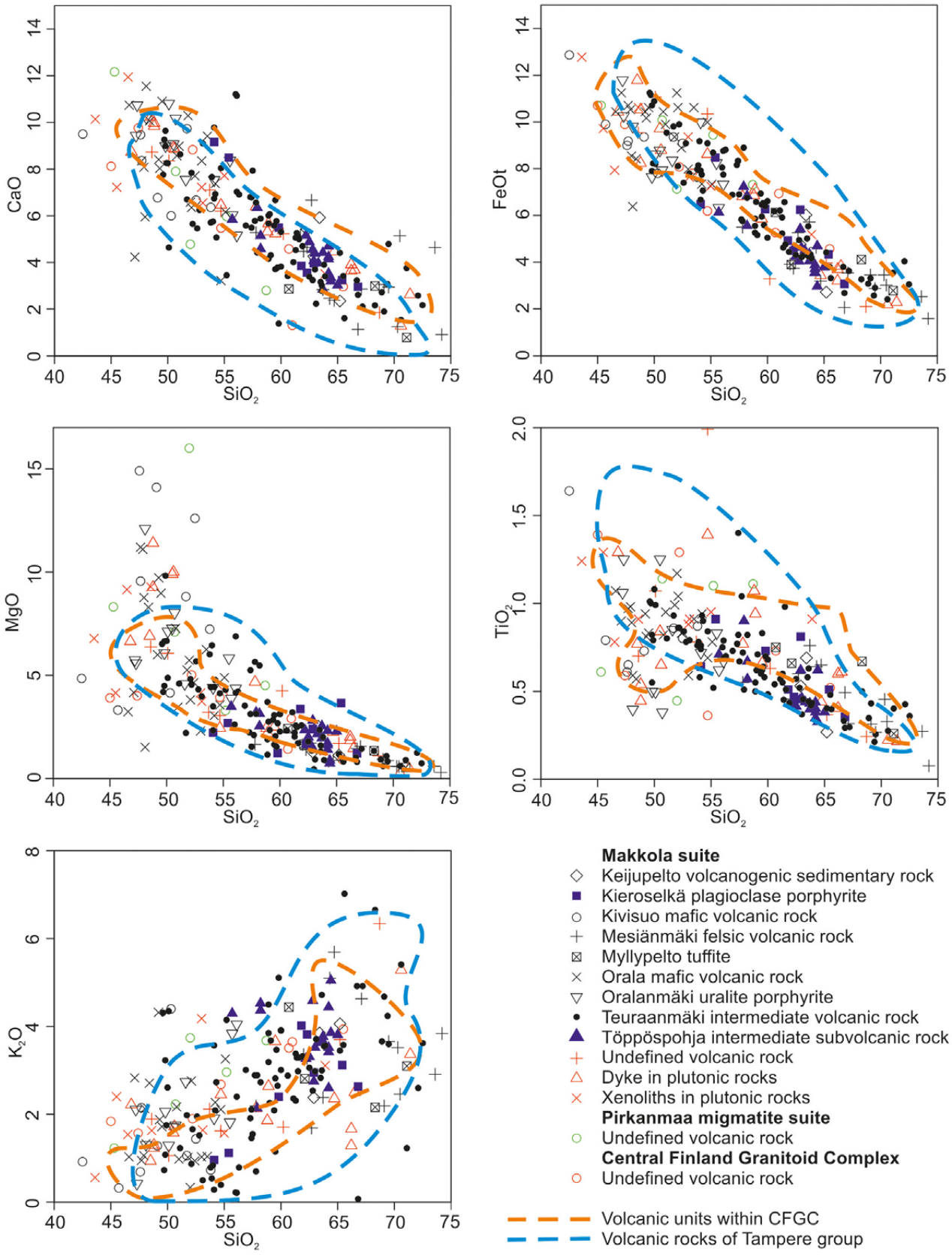

Fig. 4. The studied samples plotted on Harker diagrams. Data for the Tampere group (Kähkönen 1989, unpublished material) and volcanic rocks from central parts of the Central Finland Granitoid Complex (CFGC, Nikkilä et al. 2016) are shown for reference.

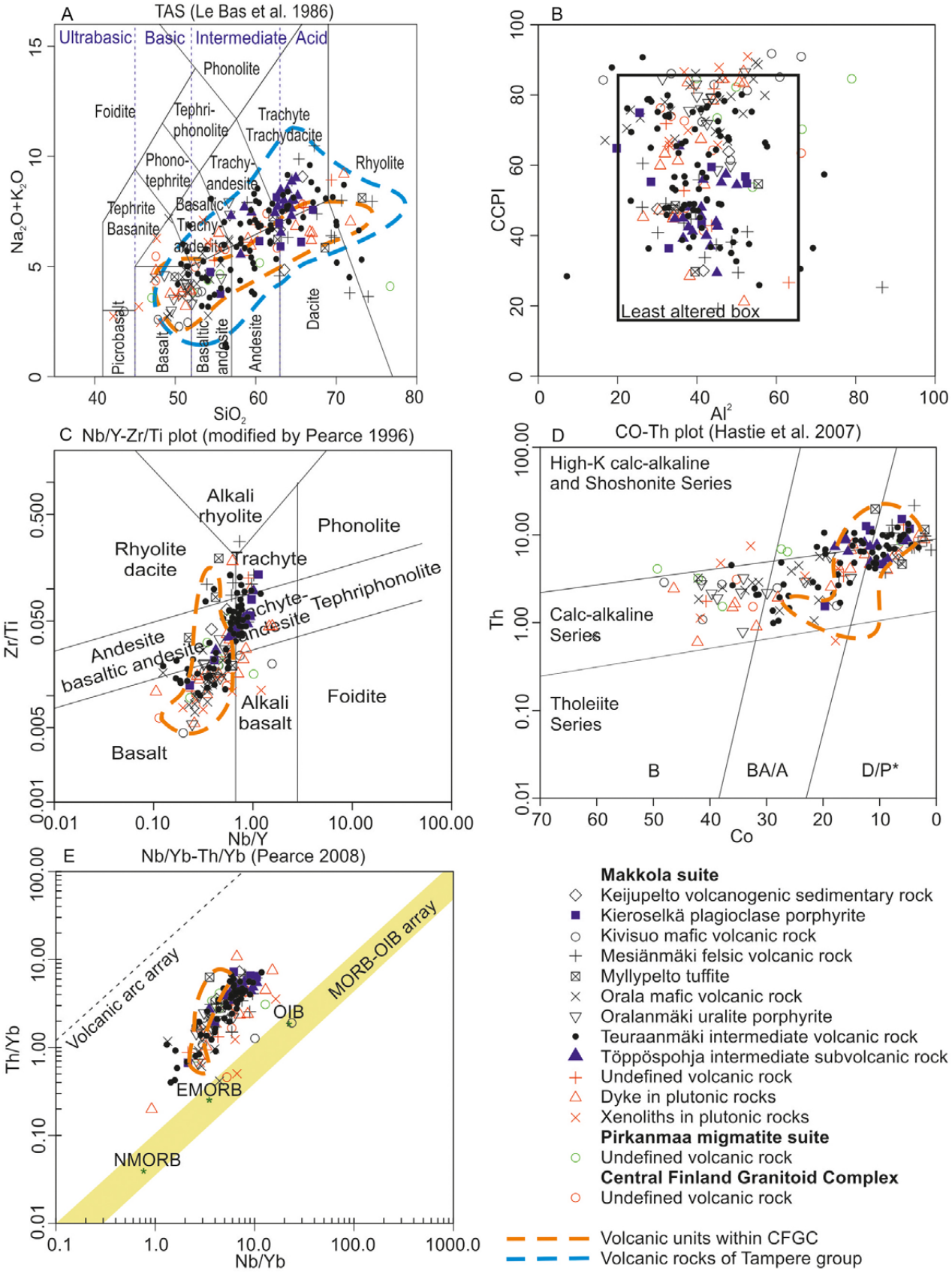

Fig. 5. The studied samples plotted on A) a TAS diagram (Le Bas et al. 1986), B) Ishikawa's alteration index (AI = 100*(K_2O+MgO)/(K_2O+MgO+Na2O+CaO), (Ishikawa et al. 1976) plotted against the chlorite-carbonate-pyrite index (CCPI = 100(MgO+FeO)/(MgO+FeO+Na_2O+K_2O), least altered box according to Large et al. (2001), C) Nb/Y vs Zr/Ti diagram (Pearce 1996), D) Co vs. Th (Hastie et al. 2007) and E) Nb/Yb vs. Th/Yb diagram (Pearce 2008). Data for the Tampere group (in A, Kähkönen 1989, unpublished material) and volcanic rocks from central parts of the Central Finland Granitoid Complex (CFGC, in A, C, D, E. Nikkilä et al. 2016) are shown for reference.

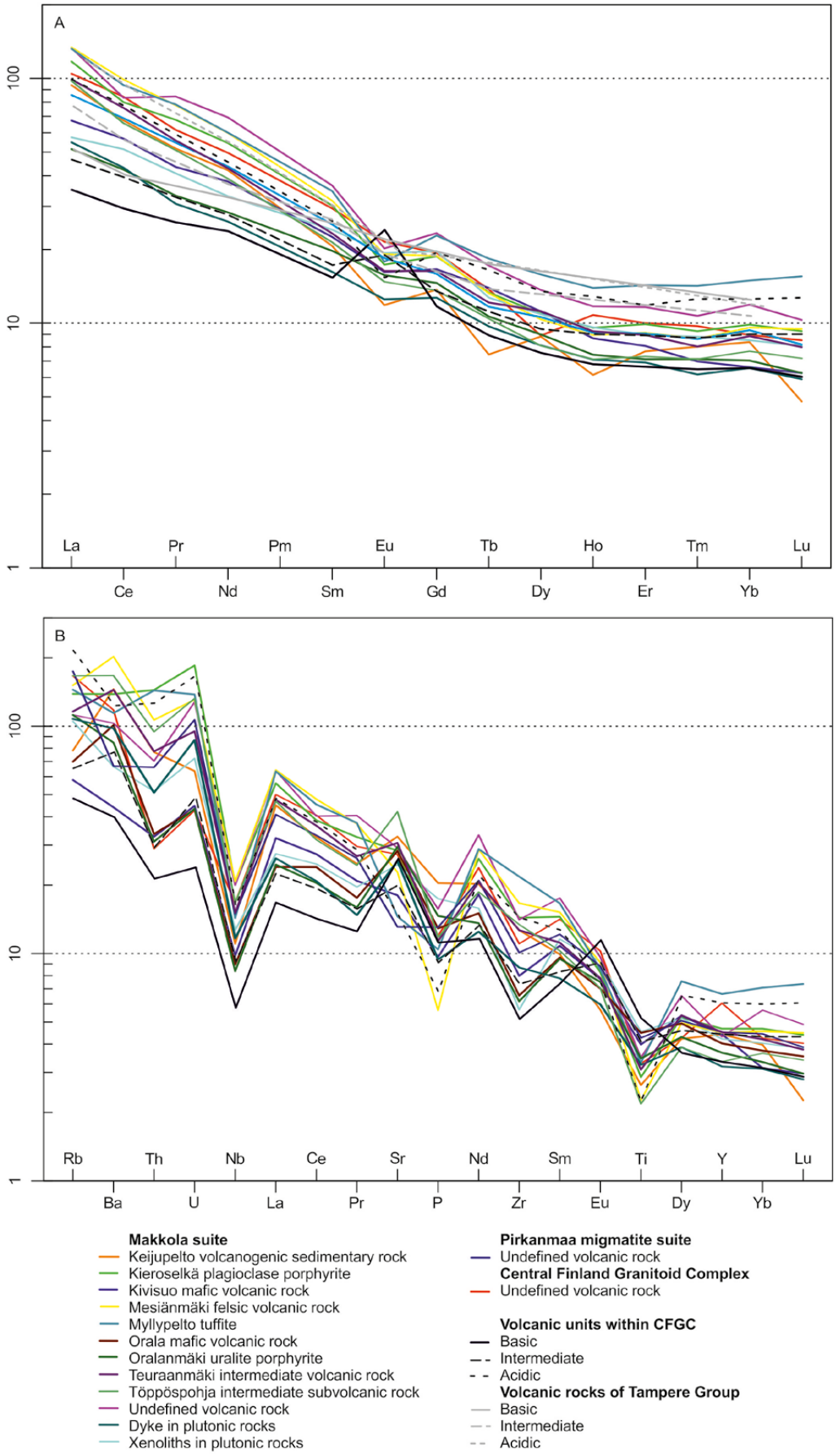

Fig. 6. Median values of each volcanic unit plotted on a chondrite-normalized REE diagram (A) and spider diagram normalized with primitive mantle (B). Chondrite values from Boynton (1984) and primitive mantle values from McDonough & Sun (1995).

5.1.3 Volcanic rocks of the Pirkanmaa migmatite suite

The volcanic samples interpreted as representing the Pirkanmaa migmatite suite are on average more basic than those from the Makkola suite, as SiO_2 varies from 45.3 to 58.7%, excluding an altered sample with 76.4% SiO_2. In other respects, the samples of the Pirkanmaa migmatite suite do not deviate from the samples of the Makkola suite, but the reader should note that the picritic Ala-Siili mafic volcanic rock lithodeme is dealt with in a separate paper (Kousa et al. 2018).

5.2 Age results

5.2.1 Teurinsuo intermediate volcanic rock, sample A2385

The Teurinsuo sample is an intermediate, homogeneous, grey and weakly bedded tuff from the best-preserved part of the Makkola suite. The zircons are mostly subhedral to euhedral (prismatic 100–150 µm long) and lack visible zoning or inherited cores. They contain numerous inclusions, although metamictisation is minor. All 14 analysed spots constitute a concordia age of 1894 ± 4 Ma (Fig. 7). The homogeneity of the zircons supports a volcanic origin for the Teurinsuo intermediate tuff, distinguishing it from the intermediate volcanogenic sediments.

5.2.2 Mesiänlampi acid tuff, sample A2388

The Mesiänlampi acid tuff sample is foliated, displays primary bedding and contains small ellipsoid shapes of quartz and calcite, interpreted as filled pore spaces or amygdales. The zircons from the Mesiänlampi acid tuff are small (<100 µm), euhedral, rounded, inclusion rich and display magmatic oscillatory zoning. Some grains have strongly metamict inner domains and some weakly developed zoning, or no zoning at all. Altogether, 14 spots were analysed from the intact cores and rims, and a concordia age of 1891 ± 4 Ma (Fig. 7) can be calculated for them. The homogeneity of the zircons confirms the origin of the Mesiänlampi tuff as volcanic, although it occurs on the same outcrop group as laminar, clearly sedimentary rocks.

5.2.3 Jauhovakka dyke, sample A2389

The Jauhovakka dacitic plagioclase porphyrite dyke cross-cuts a diorite 3 km northwest of the Makkola volcanic belt. The plagioclase porphyrite is similar to the porphyries in the Korospohja area, as well as to the porphyries in the northeast Kauppila area. Zircons from the porphyrite display weak oscillatory zoning and are rounded, but euhedral, with minor metamictization on the rims. Inclusions are a typical feature. The length of the grains is ≤150 µm. Altogether, 12 spot analyses were executed. The analysed inner domains and rims of the same zircon (n = 2) are of the same age within error limits. All data point error ellipses are concordant and define a concordant age of 1894 ± 4 Ma (Fig. 7). The obtained age shows that the dyke is coeval with the Makkola volcanic suite magmatism.

5.2.4 Keijupelto acid volcanogenic sedimentary rock, sample A2386

The Keijupelto sample is a strongly recrystallized sedimentary quartz-rich rock. The zircons are eroded (rounded and fragmented) and display mostly well-developed magmatic oscillatory zoning. A small number of crystals have metamict cores. The size of the grains is ≥100 µm, which is larger than in most of the studied samples. Altogether, 21 spots from 16 zircons were analysed, and of these, 9 define a concordia age of 1888 ± 5 Ma (MSWD = 4.7, probability of concordance 0.030, Fig. 8). Out of the remaining spots, seven yield $^{207}Pb/^{206}Pb$ ages between 2095–1979 Ma, three are Archean (3092–2700 Ma) and one plots near the Archean–Proterozoic transition (2488 Ma). The rim on one of the zircons yields a slightly younger $^{207}Pb/^{206}Pb$ age (1863 Ma), possibly reflecting metamorphic effects. Otherwise, the morphology of the zircon grains does not show any age-dependent differences. We interpret that the concordia age of 1888 ± 5 Ma represents the maximum age of deposition of this volcano-sedimentary unit. The presence of detrital zircons, with both Archean and ~2000 Ma ages, is typical for the sedimentary units surrounding the CFGC (Lahtinen et al. 2009, 2017, Mikkola et al. 2018b), although the occurrence of ca. 2000 Ma rocks is not known from the vicinity.

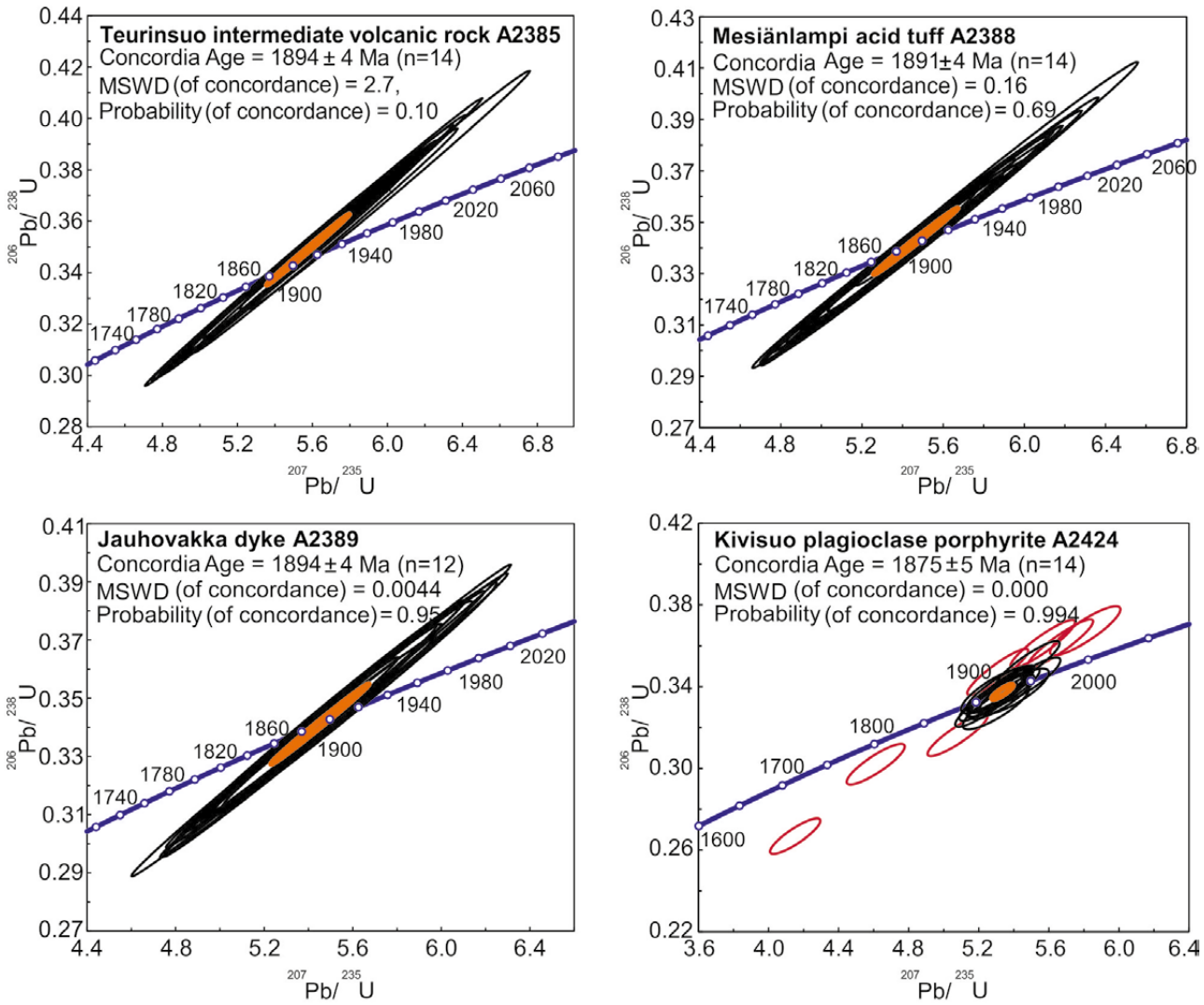

Fig. 7. Concordia diagrams of samples A2388, A2385, A2389 and A2424. All data plotted at the 2σ confidence level.

5.2.5 Kivisuo plagioclase porphyrite A2424

The Kivisuo plagioclase porphyrite sample consists of plagioclase porphyritic ground mass hosting ca. 5% of paraschist fragments up to 20 cm in size. Based on locally observable weak layering, most likely original bedding, the plagioclase porphyrite has been interpreted as a massive tuff or tuffite containing older sediment fragments. The bulk sample was crushed, because the sedimentary fragments could not be reliably removed due to their small size. Most of the zircons are elongated and euhedral, metamict domains are common and magmatic zoning is commonly visible. Out of the 21 analysed spots, 3 were discarded due to high common lead or high uranium contents. The remaining 18 spots are scattered and yield $^{207}Pb/^{206}Pb$ ages between 1852 and 1902 Ma (Fig. 7). Two of the spots are reversely discordant and two are normally discordant. The 14 concordant spots define a concordia age of 1875 ± 5 Ma, which is interpreted as best estimation for the age of this sample. Despite the scatter, it is evident that the sedimentary fragments do not contain significantly older zircons than the plagioclase porphyrite hosting them.

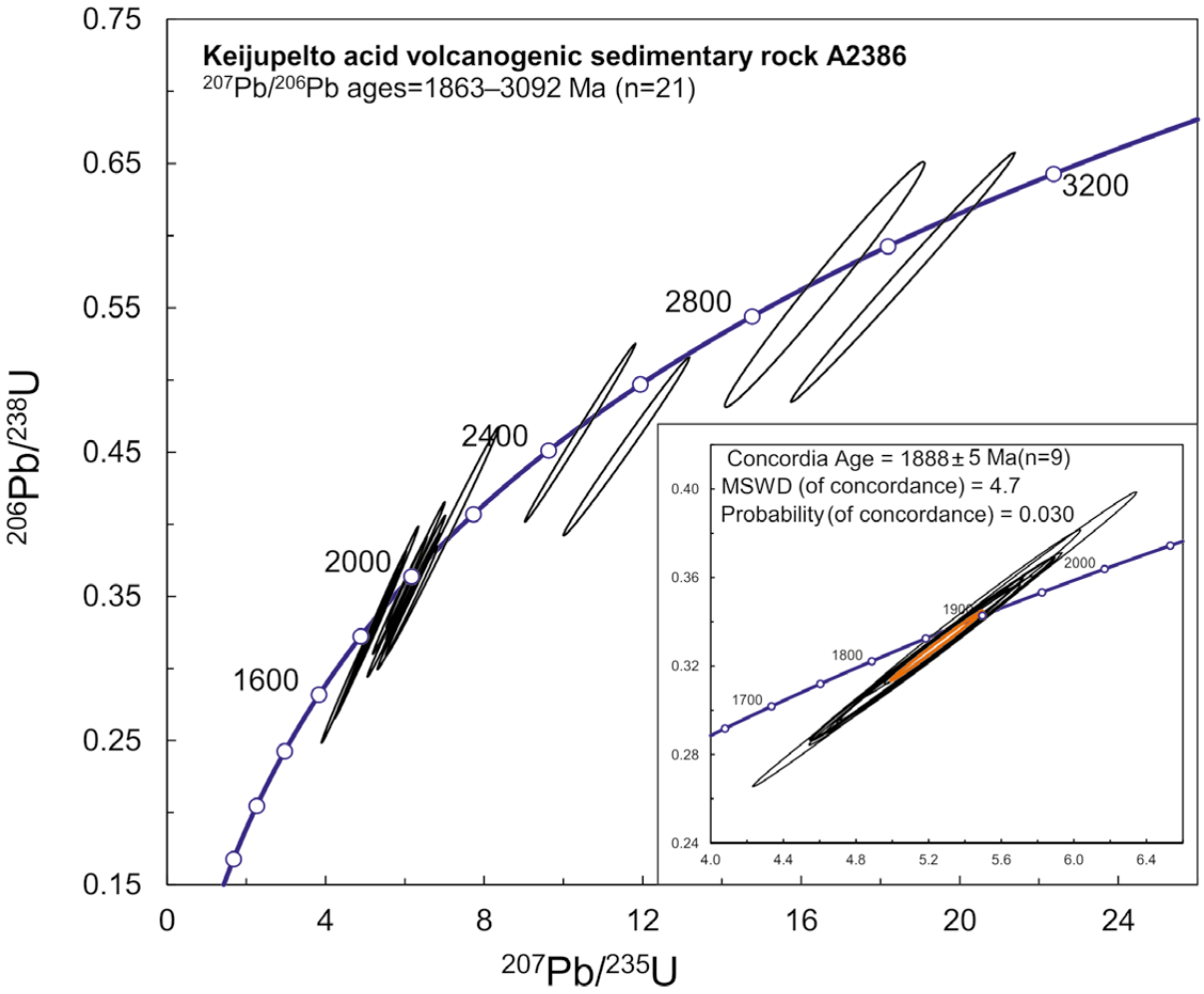

Fig. 8. Concordia diagram of sample A2386. In the inset, a close-up of the analyses with $^{207}Pb/^{206}Pb$ ages between 1875 and 1895 Ma and the concordia age calculated based on them. All data plotted at the 2σ confidence level.

6 DISCUSSION

6.1 Makkola suite

The volcanic rocks of the Makkola suite form continuous trends on Harker diagrams, excluding a certain amount of scatter, e.g. MgO and TiO_2, in basic compositions. The latter is likely to be due to fractional processes operating more efficiently in less viscous magmas. As the patterns on both REE and spider diagrams also display similar shapes, the suite can be interpreted as comagmatic. Geochemistry of the volcanic rocks suggest that they were formed in arc type setting. Distinct negative Ti and Nb anomalies, as well as enrichment of large-ion lithophile elements over high-field strength elements can be interpreted as signs of a subduction source (e.g. Turner et al. 1996, Wang et al. 2006). The observed Ta/Yb ratios between 0.10 and 1.00 suggest continental arc-type affinity (Pearce 1983). The relatively high Al_2O_3 concentrations of the Makkola suite are also a typical feature for volcanic rocks formed in a mature continental arc setting (e.g. Condie 1997), as is the dominance of intermediate and acid compositions. The observed elevated K_2O concentrations are also characteristic for continental arcs, but in the case of the Makkola suite, this can be partially caused by alteration, as the values display a large amount of scatter. Based on the above, we conclude that the Makkola suite originated in an active continental margin setting.

Based on the similarities of the age and composition, the hypabyssal porphyrite dykes cross-cutting the plutonic rocks in the study area are interpreted to be part of the Makkola suite. This indicates that the volcanic segments and the plutonic rocks

surrounding them originated in close proximity and do not represent significantly differing erosion levels. This has implications for the ore potential of the study area, as it supports the possibility for porphyry-type deposits in the area, for which the mineralisation condensation of the Hiekkapohja area (Halonen 2015) gives additional evidence.

Excluding the zircons younger than 1900 Ma, the zircon population of the volcano-sedimentary Keijupelto sample is similar to that of the Svecofennian metasedimentary units surrounding the CFGC (Lahtinen et al. 2009. 2017, Kotilainen et al. 2016, Mikkola et al. 2018b). The Keijupelto sample, containing zircons with Archean ages, and active volcanism in the area is one constrain in respect to the overall tectonic scenario. The depositional environment was most likely a continental arc, as the transportation of Archean detrital zircons into a juvenile island arc environment seems unlikely. The Keijupelto sample also contains a zircon population aged ca. 2000 Ma. The well-recognized but unresolved problem with the 2000 Ma zircons is their source; felsic rocks of this age are scarce in the Fennoscandian Shield, but zircons are abundant (e.g. Lahtinen et al. 2009, 2010). Possible explanations for their source include the hypothetical Keitele microcontinent, which would have been completely destroyed at least at the current erosion level during the culmination of the Svecofennian orogeny, or transportation from the Lapland–Kola orogeny (Lahtinen et al. 2009). An additional possible source could be the Central Russian fold belt near Moscow, containing ca. 2000 Ma juvenile volcanic and sedimentary units (Samsonov et al. 2016).

Based on the age determinations from our study area, it seems that the volcanic rocks from the Makkola area are older than those further to the southwest; 1895–1890 Ma vs. 1885–1875 Ma. Verification of this difference would require a number of additional age determinations, as the subareas of the Makkola suite cannot be differentiated on a geochemical (Mönkäre 2016, this study) or petrographical basis. The older ages are clearly similar to those of the Pirkanmaa igneous suite, whereas the latter are more akin in age to the main phase of plutonic activity of the CFGC (e.g. Nikkilä et al. 2016). It should be noted that the youngest volcanic activity is within error margins coeval with three of the four granitoid suites in the area: Oittila, Saarijärvi and Muurame (1885–1875 Ma, Heilimo et al. 2018). The close proximity of rock suites with differing geochemical characteristics but overlapping ages further emphasizes the rapid geological evolution of the area.

6.2 Relationship of the Pirkanmaa migmatite and Makkola suites

The majority of the samples from the metasedimentary units of the Pirkanmaa migmatite suite bounding the volcanic units to the south, both in the current study area (Mikkola et al. 2018b) and further west (Lahtinen et al. 2009, 2017), do not contain detrital zircons with ages similar to those of the here-studied volcanic units. Therefore, they were most likely deposited prior to the active volcanic phase. The age distribution of the detrital zircons, and thus the maximum age of the well-preserved greywackes within the Pirkanmaa suite (Tammijärvi and Rusalansuo lithodemes, Fig. 2) in the study area, is approximately similar to that of the lowest sedimentary members of the Tampere group (Myllyniemi formation, Huhma et al. 1991, Claesson et al. 1993, Mikkola et al. 2018b). However, the well-preserved greywackes of the Tammijärvi lithodeme have not been interpreted as equivalent to the Myllyniemi formation and the depositional basement of the Makkola suite. The main reason is that the contact between the Makkola suite and the Tammijärvi lithodeme is formed by the large-scale southwest-trending Leivonmäki shear zone (Mikkola et al. 2018a).

Typical volcanic rocks in the Pirkanmaa migmatite suite show MORB or picritic compositions in the study area, as well as further west (e.g. Peltonen 1995, Kähkönen 2005, Kousa et al 2018b, Lahtinen et al. 2017). However, six samples interpreted as volcanic in origin from three different locations and included in the Pirkanmaa migmatite suite do not show significantly differing chemical compositions from those of the Makkola suite. Due to limited exposure in these areas, this observation has to be treated with prudence; for example, half of these samples originate from drill cores from Tuppi (Fig. 2), and they were taken from narrow sections interpreted as volcanic interbeds in migmatitic paragneisses. Nevertheless, it is not inconceivable that they could be narrow veins similar to those sampled cross-cutting the plutonic rocks in the vicinity of Makkola. These samples also originate from the same area as a paragneiss sample with detrital zircon population differing from that

typical for the Pirkanmaa migmatite suite (Mikkola et al. 2018b), i.e. it lacks Archean zircons and contains detrital grains that could be coeval with the magmatic activity of the Makkola suite. Therefore, it is not unfeasible that some of the paragneisses included in Pirkanmaa migmatite suite could belong to the Makkola suite, but further evaluation of this would require additional age determination samples, both from these small volcanic units and the paragneisses in their vicinity.

6.3 Comparison with the Tampere group and volcanic units within the CFGC

Geochemically, the volcanic rocks of the Tampere group are similar to those of the Makkola suite (Figs. 4, 5). The rock types present in the two units also show strong similarities; plagioclase and uralite porphyrites are typical, although sedimentary rocks are more abundant in Tampere group than in the Makkola suite. Despite strong similarities, a direct correlation of the various subunits cannot be achieved due to the scattered nature of the volcanic belts, extending over 200 km along strike, and the often poor exposure of the units. The age results from the Makkola suite are similar to those reported from the Tampere group, the oldest samples from both locations yielding ages from 1895 to 1890 Ma (Kähkönen et al. 1989, Kähkönen 2005, Kähkönen & Huhma 2012), and our younger Kivisuo sample (1875 ± 5 Ma) coincides in error limits with the younger ca. 1880 Ma activity in Tampere (ibid). Based on the above, the Makkola suite can be regarded as the eastern equivalent of the Tampere group. The main difference between Makkola suite and the Tampere group is the Haveri and Myllyniemi formations of the latter, which have no analogue in the former. The Haveri formation, with its EMORB affinity, has been interpreted to represent the initial rifting stages, followed by deposition of the greywackes of the Myllyniemi formation, and later transition to arc-type volcanism (Kähkönen 2005). In our study area, the analogues for the Haveri and Myllyniemi formations are the mafic volcanic rocks of the Ala-Siili lithodeme and greywackes of the Tammijärvi lithodeme, which are interpreted as belonging to the Pirkanmaa migmatite suite (Kousa et al. 2018b, Mikkola et al. 2018b).

The volcanic samples of this study interpreted as belonging to volcanic units within the CFGC do not show any geochemical differences from the Makkola suite. This could, however, be a result of the limited number of samples, as when the compositions of the Makkola suite are compared with the larger data set from the central part of the CFGC (Nikkilä et al. 2016), certain small differences are apparent, such as the lower TiO_2 concentrations of the Makkola suite at the acidic end of the compositional spectrum and the lower trend of the samples from the central CFGC on the TAS diagram (Fig. 5). On the Nb/Y versus Zr/Ti plot, intermediate and acid volcanic rocks in the two groups also deviate, as the samples from the central CFGC, due to slightly higher Y concentrations (Fig. 6B) display lower Nb/Y ratios at higher Zr/Ti ratios. On the Nb/Yb versus Th/Yb plot, the two groups also show different patterns, as the samples of the Makkola suite form a trend towards a lower angle with respect to the volcanic and subvolcanic samples from the central CFGC. This is caused by the higher variation in Th concentrations of the latter group (Fig. 6), as the Yb concentrations and their variation are similar. The same difference in the Nb/Yb versus Th/Yb plot is also observable between the Pirkanmaa intrusive suite and granitoids of the CFGC (Mikkola et al. 2018a). Both the basic and intermediate volcanic rocks from the CFGC display a positive Eu anomaly, which is not found in any of the lithodemes making up the Makkola suite (or in individual samples). This could indicate melting in higher pressure, i.e. outside the stability field of plagioclase, in central parts of the CFGC. On the spider diagram, the basic samples from the central CFGC lack the negative Ti anomaly that is present in all of the other groups (Fig. 6).

The subtle compositional differences shown by the volcanic rocks within CFGC and those flanking it to the south indicate certain differences in magma genesis. Nikkilä et al. (2016) suggested that the main plutonic activity between 1890 and 1880 Ma forming the CFGC (ibid, Rämö et al. 2001, authors' unpublished data) is not directly related to subduction, as the plutonic rocks have crustal affinity. They interpreted that the magma genesis was mainly a consequence of partial melting due to heating caused by radioactive decay in a thickened crust during and after terrain accretion with the Karelian craton. However, the onset of the plutonic main phase after 1890 Ma within the CFGC coincides with continuing active volcanism along the southern boundary of it. This volcanism, forming younger parts of both the Tampere group and Makkola suite,

has been interpreted as being related to active subduction (Lahtinen et al. 2009, Kähkönen & Huhma 2012, this study). Taking into account the overlap in ages, compositional similarities and the geologically small areal extent of the CFGC, it is reasonable to presume that volcanism within, and south of, the CFGC was a result of the same process(es). The last point is especially true if the orocline model of Lahtinen et al. (2014) is taken into account, and the now rounded shape of CFGC is a result of the deformation of an originally narrower linear belt. The small compositional differences most likely reflect a variable distance from the trench and in crustal thickness. The overall geological evolution of the study area is further discussed in Mikkola et al. (2018a) in this volume.

7 CONCLUSIONS

The age span of volcanism of the Makkola suite extends from 1895 to 1875 Ma.

Compositionally, the volcanic rocks forming the Makkola suite represent typical calc-alkaline arc-type magmas.

As subvolcanic dykes locally cutting the plutonic rocks are compositionally akin to the Makkola suite volcanic rocks and coeval with them, they can be regarded as part of the same suite.

Based on the resemblance of the volcanic rocks of the Tampere group and the Makkola suite in both age and composition, the latter can be regarded as representing the same phase of arc magmatism. However, a direct correlation of the geological subunits is not possible due to deformation, locally poor exposure and the strike length of the volcanic belt extending over 200 km.

ACKNOWLEDGEMENTS

The staff of GTK's isotope laboratory in Espoo are thanked for sample preparation and assistance in analytical work. Reviews by Drs Elina Lehtonen and Kaisa Nikkilä helped in focusing and clarifying the manuscript. Yrjö Kähkönen kindly allowed the use of unpublished data from Tampere as reference material.

REFERENCES

Bedrock of Finland - DigiKP. Digital map database [Electronic resource]. Espoo: Geological Survey of Finland [referred 31.04.2017]. Version 2.0.

Boynton, W. V. 1984. Cosmochemistry of the rare earth elements; meteorite studies. In: Henderson, P. (ed.) Rare earth element geochemistry. Amsterdam: Elsevier, 63–114.

Claesson, S., Huhma, H., Kinny, P. D. & Williams, I. S. 1993. Svecofennian detrital zircon ages—implications for the Precambrian evolution of the Baltic Shield. Precambrian Research 64, 109–130.

Condie, K. C. 1997. Tectonic settings. In: Plate tectonics and crustal evolution. 4th ed. Butterworth-Heinemann. 70–109.

Halonen, S. 2015. Keski-Suomen granitoidikompleksin malmiviitteet Hiekkapohjan alueella. Unpublished master's thesis, University of Oulu, Oulu Mining School. 100 p. (in Finnish). Available at: http://jultika.oulu.fi/files/nbnfioulu-201511242172.pdf

Hastie, A. R., Kerr, A. C., Pearce, J. A. & Mitchell, S. F. 2007. Classification of altered island arc rocks using immobile trace elements: development of the Th–Co discrimination diagram. Journal of Petrology 48, 2341–2357.

Heikura, A. 2017. The volcanic rocks of the Länkipohja-Jämsä area in the southern part of the Central Finland Granitoid Complex. Unpublished master's thesis, University of Oulu, Oulu Mining School. 81 p. Available at: http://tupa.gtk.fi/opinnayte/heikura_antti_gradu.pdf

Heilimo, E., Ahven, M. & Mikkola, P. 2018. Geochemical characteristics of the plutonic rock units present at the southeastern boundary of the Central Finland Granitoid Complex. In: Mikkola, P., Hölttä, P. & Käpyaho, A. (eds) Development of the Paleoproterozoic Svecofennian orogeny: new constraints from the southeastern boundary of the Central Finland Granitoid Complex. Geological Survey of Finland, Bulletin 407. (this volume). Available at: https://doi.org/10.30440/bt407.6

Heilimo, E., Mikkola, P., Niemi, S., Luukas, J. & Halonen, S. 2017. Hiekkapohja ore showings in Paleoproterozoic Central Finland Granitoid Complex - a hydrothermal system? Proceedings of the 14th SGA Biennial Meeting, 20-23 August 2017, Québec City, Canada, 359–362.

Hölttä, P. & Heilimo, E. 2017. Metamorphic map of Finland. In: Nironen, M. (ed.) Bedrock of Finland at the scale 1:1 000 000 - Major stratigraphic units, metamorphism and tectonic evolution. Geological Survey of Finland, Special Paper 60, 77–128. Available at: http://tupa.gtk.fi/julkaisu/specialpaper/sp_060.pdf

Huhma, H., Claesson, S., Kinny, P. D. & Williams, I. S. 1991. The growth of Early Proterozoic crust: new evidence from Svecofennian zircons. Terra Nova 3, 175–179.

Ikävalko, O. 1981. Makkolan-Kokonkylän suprakrustinen vyöhyke. Unpublished master's thesis, University of Helsinki, Department of Geology and Mineralogy. 119 p. (in Finnish)

Ishikawa, Y., Sawaguchi, T., Iwaya, S. & Horiuchi, M. 1976. Delineation of prospecting targets for kuroko deposits based on models of volcanism of underlying dacite and alteration halos. Mining Geology 26, 103–117.

Janoušek, V., Farrow, C. M. & Erban, V. 2006. Interpretation of whole-rock geochemical data in igneous geochemistry: introducing Geochemical Data Toolkit (GCDkit). Journal of Petrology 47, 1255–1259.

Kähkonen, Y. 1987. Geochemistry and tectonomagrnatic affinities of the metavolcanic rocks of the early Proterozoic Tampere Schist Belt, southern Finland. Precambrian Research 35, 295–311.

Kähkönen, Y. 1989. Geochemistry and petrology of the metavolcanic rocks of the early Proterozoic Tampere Schist Belt, southern Finland. In: Kähkönen, Y. Geochemistry and petrology of the metavolcanic rocks of the early Proterozoic Tampere Schist Belt, southern Finland. Geological Survey of Finland, Bulletin 345, 1–104. Available at: http://tupa.gtk.fi/julkaisu/bulletin/bt_345.pdf

Kähkönen, Y. 1999. Stratigraphy of the central parts of the Palaeoproterozoic Tampere Schist Belt, southern Finland: review and revision. Bulletin of the Geological Society of Finland 71, 13–29. Available at: https://doi.org/10.17741/bgsf/71.1.002

Kähkönen, Y. 2005. Svecofennian supracrustal rocks. In: Lehtinen, M., Nurmi, P. & Rämö, O. T. (eds.) The Precambrian Bedrock of Finland—Key to the evolution of the Fennoscandian Shield. Elsevier Science B.V., 343–406.

Kähkönen, Y. & Huhma, H. 2012. Revised U-Pb zircon ages of supracrustal rocks of the Paleoproterozoic Tampere Schist Belt, southern Finland. In: Kukkonen, I. T., Kosonen E. M., Oinonen, K., Eklund, O., Korja, A., Korja, T., Lahtinen, R., Lunkka, J. P. & Poutanen, M. (eds.). Lithosphere 2012 – Seventh Symposium on the Structure, Composition and Evolution of the Lithosphere in Finland. Programme and Extended Abstracts, Espoo, Finland, November 6-8, 2012. Institute of Seismology, University of Helsinki, Report S-56, 51–54. Available at: http://www.seismo.helsinki.fi/pdf/LITO2012.pdf

Kähkönen, Y., Huhma, H. & Aro, K. 1989. U-Pb zircon ages and Rb-Sr whole-rock isotope studies of Early Proterozoic volcanic and plutonic rocks near Tampere, southern Finland. Precambrian Research 45, 27–43.

Kallio, J. 1986. Joutsan kartta-alueen kallioperä. Summary: Pre-Quaternary rocks of the Joutsa Map-Sheet area. Geological Map of Finland 1:100 000, Explanation to the Maps of Pre-Quaternary Rocks, Sheet 3122. Geological Survey of Finland. 56 p. Available at: http://tupa.gtk.fi/kartta/kallioperakartta100/kps_3122.pdf

Karppanen, T. 1970. Tampereen liuskejakson geologiaa Luhangan Tammijärvellä. Unpublished master's thesis, University of Helsinki, Department of Geology and Mineralogy. 75 p. (in Finnish)

Kotilainen, A. K., Mänttäri, I., Kurhila, M., Hölttä, P. & Rämö, O. T. 2016. Evolution of a Palaeoproterozoic giant magmatic dome in the Finnish Svecofennian; New insights from U–Pb geochronology. Precambrian Research 272, 39–56.

Kousa, J., Huhma, H., Hokka, J. & Mikkola, P. 2018a. Extension of Svecofennian 1.91 Ga magmatism to the south, results of the reanalysed age determination samples from Joroinen, central Finland. In: Mikkola, P., Hölttä, P. & Käpyaho, A. (eds) Development of the Paleoproterozoic Svecofennian orogeny: new constraints from the southeastern boundary of the Central Finland Granitoid Complex. Geological Survey of Finland, Bulletin 407. (this volume). Available at: https://doi.org/10.30440/bt407.3

Kousa, J., Huhma, H. & Vaasjoki, M. 2004. U-Pb –ajoitukset eräistä magmasyntyisistä kivistä Pohjois-Pohjanmaalta, Raahe-Laatokka –vyöhykkeen luoteisosasta. In: Kousa, J. & Luukas, J. (eds) Vihannin ympäristön kallioperä- ja malmitutkimukset vuosina 1992-2003. Geological Survey of Finland, archive report M10.4/2004/2. 142 p. (in Finnish). Available at: http://tupa.gtk.fi/raportti/arkisto/m10_4_2004_2.pdf

Kousa, J., Mikkola, P. & Makkonen, H. 2018b. Paleoproterozoic mafic and ultramafic volcanic rocks in the South Savo region, eastern Finland. In: Mikkola, P., Hölttä, P. & Käpyaho, A. (eds) Development of the Paleoproterozoic Svecofennian orogeny: new constraints from the southeastern boundary of the Central Finland Granitoid Complex. Geological Survey of Finland, Bulletin 407. (this volume). Available at: https://doi.org/10.30440/bt407.4

Lahtinen, R. 1996. Geochemistry of Palaeoproterozoic supracrustal and plutonic rocks in the Tampere-Hämeenlinna area, southern Finland. In: Lahtinen, R. Geochemistry of Palaeoproterozoic supracrustal and plutonic rocks in the Tampere-Hämeenlinna area, southern Finland. Geological Survey of Finland, Bulletin 389, 1–113. Available at: http://tupa.gtk.fi/julkaisu/bulletin/bt_389.pdf

Lahtinen, R., Huhma, H., Kähkönen, Y. & Mänttäri, I. 2009. Paleoproterozoic sediment recycling during multiphase orogenic evolution in Fennoscandia, the Tampere and Pirkanmaa belts, Finland. Precambrian Research 174, 310–336.

Lahtinen, R., Huhma, H., Lahaye, Y., Lode, S., Heinonen, S., Sayab, M. & Whitehouse, M. J. 2016. Paleoproterozoic magmatism across the Archean-Proterozoic boundary in central Fennoscandia: Geochronology, geochemistry and isotopic data (Sm-Nd, Lu-Hf, O). Lithos 262, 507–525.

Lahtinen, R., Huhma, H., Sipilä, P. & Vaarma, M. 2017. Geochemistry, U-Pb geochronology and Sm-Nd data from the Paleoproterozoic Western Finland supersuite – A key component in the coupled Bothnian oroclines. Precambrian Research 299, 264–281.

Lahtinen, R., Johnston, S. T. & Nironen, M. 2014. The Bothnian coupled oroclines of the Svecofennian Orogen: a Palaeoproterozoic terrane wreck. Terra Nova 26, 330–335.

Large, R. R., Gemmel, J. B., Paulick, H. & Huston, D. L. 2001. The Alteration Box Plot: A Simple Approach to Understanding the Relationship between Alteration Mineralogy and Lithogeochemistry Associated with Volcanic-Hosted Massive Sulfide Deposits. Economic Geology 96, 957–971.

Le Bas, M. J., Le Maitre, R. W., Streckeisen, A. & Zanettin, B. A. 1986. Chemical classification of volcanic rocks based on the total alkali-silica diagram. Journal of Petrology 27, 745–750.

Luukas, J., Kousa, J., Nironen, M. & Vuollo, J. 2017. Major stratigraphic units in the bedrock of Finland, and an approach to tectonostratigraphic division. In: Nironen, M. (ed.) Bedrock of Finland at the scale 1:1 000 000 – Major stratigraphic units, metamorphism and tectonic evolution. Geological Survey of Finland, Special Paper 60, 9–40. Available at: http://tupa.gtk.fi/julkaisu/specialpaper/sp_060.pdf

McDonough, W. F. & Sun, S.-S. 1995. Composition of the Earth. Chemical Geology 120, 223–253.

Mikkola, P., Heilimo, E., Aatos, S., Ahven, M., Eskelinen, J., Halonen, S., Hartikainen, A., Kallio, V., Kousa, J., Luukas, J., Makkonen, H., Mönkäre, K., Niemi, S., Nousiainen, M., Romu, I. & Solismaa, S. 2016. Jyväskylän seudun kallioperä. Summary: Bedrock of the Jyväskylä area. Geological Survey of Finland, Report of Investigation 227. 95 p., 6 apps. Available at: http://tupa.gtk.fi/julkaisu/tutkimusraportti/tr_227.pdf

Mikkola, P., Heilimo, E., Luukas, J., Kousa, J., Aatos, S., Makkonen, H., Niemi, S., Nousiainen, M., Ahven, M., Romu, I. & Hokka, J. 2018a. Geological evolution and structure along the southeastern border of the Central Finland Granitoid Complex. In: Mikkola, P., Hölttä, P. & Käpyaho, A. (eds) Development of the Paleoproterozoic Svecofennian orogeny: new constraints from the southeastern boundary of the Central Finland Granitoid Complex. Geological Survey of Finland, Bulletin 407. (this volume). Available at: https://doi.org/10.30440/bt407.1

Mikkola, P., Huhma, H., Romu, I. & Kousa, J. 2018b. Detrital zircon ages and geochemistry of the metasedimentary rocks along the southeastern boundary of the Central Finland Granitoid Complex. In: Mikkola, P., Hölttä, P. & Käpyaho, A. (eds) Development of the Paleoproterozoic Svecofennian orogeny: new constraints from the southeastern boundary of the Central Finland Granitoid Complex. Geological Survey of Finland, Bulletin 407. (this volume). Available at: https://doi.org/10.30440/bt407.2

Mönkäre, K. 2016. Geochemistry of volcanic rocks from the southeast of the Central Finland Granitoid Complex. Unpublished master's thesis, University of Turku, Department of Geography and Geology. 76 p. Available at: http://tupa.gtk.fi/opinnayte/monkare_krista_gradu.pdf

Nikkilä, K., Mänttäri, I., Nironen, M., Eklund, O. & Korja, A. 2016. Three stages to form a large batholith after terrane accretion – An example from the Svecofennian orogen. Precambrian Research 281, 618–638.

Nironen, M. 1989. The Tampere schist belt: structural style within an early Proterozoic volcanic arc system in southern Finland. Precambrian Research 43, 23–40.

Nironen, M. 2017. Guide to the Geological Map of Finland – Bedrock 1:1 000 000. In: Nironen, M. (ed.) Bedrock of Finland at the scale 1:1 000 000 - Major stratigraphic units, metamorphism and tectonic evolution. Geological Survey of Finland, Special Paper 60, 41–76. Available at: http://tupa.gtk.fi/julkaisu/specialpaper/sp_060.pdf

Nironen, M., Kousa, J., Luukas, J. & Lahtinen, R. (eds) 2016. Geological Map of Finland – Bedrock 1:1 000 000. Espoo: Geological Survey of Finland. Available at: http://tupa.gtk.fi/kartta/erikoiskartta/ek_097_300dpi.pdf

Pearce, J. A. 1983. Role of the sub-continental lithosphere in magma genesis at active continental margins. In: Hawkesworth, C. J. & Norry, M. J. (eds) Continental Basalts and Mantle Xenoliths. Cambridge, Mass.: Shiva Publishing Ltd., 230–249.

Pearce, J. A. 1996. A user's guide to basalt discrimination diagrams. Geological Association of Canada, Short Course Notes 12, 79–113.

Pearce, J. A. 2008. Geochemical fingerprinting of oceanic basalts with applications to ophiolite classification and the search for Archean oceanic crust. Lithos 100, 14–48.

Peltonen, P. 1995. Magma-country rock interaction and the genesis of Ni-Cu deposits in the Vammala Nickel Belt, SW Finland. Mineralogy and Petrology 52, 1–24.

Rämö, O. T., Vaasjoki, M., Mänttäri, I., Elliott, B. A. & Nironen, M. 2001. Petrogenesis of the post-kinematic magmatism of the Central Finland granitoid complex; I, Radiogenic isotope constraints and implications for crustal evolution. Journal of Petrology 42, 1971–1993.

Rasilainen, K., Lahtinen, R. & Bornhorst, T. J. 2007. The Rock Geochemical Database of Finland Manual. Geological Survey of Finland, Report of Investigation 164. 38 p. Available at: http://tupa.gtk.fi/julkaisu/tutkimusraportti/tr_164.pdf

Rutland, R. W. R., Williams, I. S. & Korsman, K. 2004. Pre-1. 91 Ga deformation and metamorphism in the Palaeoproterozoic Vammala Migmatite Belt, southern Finland, and implications for Svecofennian tectonics. Bulletin of the Geological Society of Finland 76, 93–140. Available at: https://doi.org/10.17741/bgsf/76.1-2.005

Samsonov, A. V., Spiridonov, V. A., Larionova, Y. O. & Larionov, A. N. 2016. The Central Russian fold belt: Paleoproterozoic boundary of Fennoscandia and Volgo-Sarmatia, the East European Craton. In: Abstracts of the 32nd Nordic Geological Winter Meeting, Bulletin of the Geological Society of Finland, Special Volume, 162. Available at: http://www.geologinenseura.fi/bulletin/Special_Volume_1_2016/BGSF-NGWM2016_Abstract_Volume.pdf

Sederholm, J. J. 1897. Über eine archäische Sedimentformation im südwestlichen Finnland und ihre Bedeutung für die Erklärung der Entstehungsweise des Grundgebirges. Bulletin de la Commission Géologique de Finlande 6. 254 p. Available at: http://tupa.gtk.fi/julkaisu/bulletin/bt_006.pdf

Seitsaari, J. 1951. The schist belt Northeast of Tampere in Finland. Bulletin de la Commission Géologique de Finlande 153. 120 p. Available at: http://tupa.gtk.fi/julkaisu/bulletin/bt_153.pdf

Simonen, A. 1953. Stratigraphy and sedimentation of the Svecofennidic, early Archean supracrustal rocks in southwestern Finland. Bulletin de la Commission Géologique de Finlande 153. 64 p. Available at: http://tupa.gtk.fi/julkaisu/bulletin/bt_160.pdf

Turner, S., Arnaud, N., Liu, J., Rogers, N., Hawkesworth, C., Harris, N., Kelley, S., van Calsteren, P. & Deng, W. 1996. Post-collision, Shoshonitic Volcanism on the Tibetan Plateau: Implications for Convective Thinning of the Lithosphere and the Source of Ocean Island Basalts. Journal of Petrology 37, 45-71.

Vaasjoki, M., Huhma, H., Lahtinen, R. & Vestin, J. 2003. Sources of Svecofennian granitoids in the light of ion probe U-Pb measurements on their zircons. Precambrian Research 121, 251–262.

Wang, Q., Wyman, D. A., Xu, J. F., Zhao, Z. H., Jian, P., Xiong, X. L., Bao, Z. W. & Li, C. F. 2006. Petrogenesis of Cretaceous adakitic and shoshonitic igneous rocks in the Luzong area, Anhui Province (eastern China): Implications for geodynamics and Cu–Au mineralization. Lithos 89, 424-446.

Williams, I. S., Rutland, R. W. R. & Kousa, J. 2008. A regional 1.92 Ga tectonothermal episode in Ostrobothnia, Finland: Implications for models of Svecofennian accretion. Precambrian Research 165, 15–36.

Development of the Paleoproterozoic Svecofennian orogeny: new constraints from the southeastern boundary of the Central Finland Granitoid Complex
Edited by Perttu Mikkola, Pentti Hölttä and Asko Käpyaho
Geological Survey of Finland, Bulletin 407, 106–129, 2018

GEOCHEMICAL CHARACTERISTICS OF THE PLUTONIC ROCK UNITS PRESENT AT THE SOUTHEASTERN BOUNDARY OF THE CENTRAL FINLAND GRANITOID COMPLEX

by

Esa Heilimo, Marjaana Ahven and Perttu Mikkola

Heilimo, E., Ahven, M. & Mikkola, P. 2018. Geochemical characteristics of the plutonic rock units present at the southeastern boundary of the Central Finland Granitoid Complex. *Geological Survey of Finland, Bulletin 407*, 106–129, 10 figures and 1 table.

The voluminous Paleoproterozoic granitoids and coeval mafic intrusions that were formed during the Svecofennian orogeny have been studied for decades in Finland. Based on field observations, geochemistry and geochronological data from the southeastern corner of the Central Finland Granitoid Complex (CFGC), we propose a refined division of these plutonic rocks into several suites. The oldest plutonic rocks (ca. 1895 Ma) belong to the Pirkanmaa igneous suite, which occurs on the southeastern side of the Central Finland Granitoid Complex (CFGC) along with coeval volcanic units. The bulk of the CFGC consists of the Jyväskylä suite (ca. 1885–1880 Ma), which displays variation in rock type and chemical composition from diorites to porphyritic granitoids. Geochemically, they vary between alkaline-calcic and calc-alkalic. Mantle-derived ultramafic–mafic intrusions of the Vammala suite are temporally coeval with the magmatic peak within the CFGC units and are located south of it. The bimodal Saarijärvi suite (ca. 1880–1875 Ma) intruded into both the CFGC and units south of it. The youngest voluminous granitoid suite is the commonly leucocratic Oittila suite (ca. 1875 Ma), which occurs as smaller intrusions and locally abundant dykes. Based on geochemical data, the majority of the igneous rocks display a continuous trend and characteristics typical of calc-alkaline rocks formed in a continental arc setting. Only the Saarijärvi suite is clearly set apart from the others, for example in having higher K_2O, Ba and Zr contents at a given SiO_2 level. As the observed differences between the suites are most often small and gradual, we interpret them as representing a 20 Ma period of continuous geological evolution along an active continental margin during active subduction. Field relationships, age data and compositional characteristics emphasize contributions from, and the interaction of, mantle-derived and crustal magmas during this phase.

Appendix 1 is available at: http://tupa.gtk.fi/julkaisu/liiteaineisto/bt_407_appendix_1.pdf

Electronic Appendix is available at: http://tupa.gtk.fi/julkaisu/liiteaineisto/bt_407_electronic_appendix.xlsx

Keywords: plutonic rocks, calc-alkalic composition, granites, diorites, gabbros, peridotites, Svecofennian, Paleoproterozoic, Finland

Geological Survey of Finland, P.O. Box 1237, FI-70211 Kuopio, Finland
E-mail: esa.heilimo@gtk.fi

VERTAISARVIOITU
KOLLEGIALT GRANSKAD
PEER-REVIEWED
www.tsv.fi/tunnus

https://doi.org/10.30440/bt407.6

Editorial handling by Asko Käpyaho.

Received 30 January 2018; Accepted 18 June 2018

1 INTRODUCTION

The formation of the Paleoproterozoic Svecofennian crust took place by progressive accretion of arc complexes to the Archean craton and subduction-related magmatism (e.g. Nironen 1997, Lahtinen et al. 2017). The peak of the orogeny took place between 1.91–1.87 Ga. The core of the Svecofennian orogen in Finland, the Central Finland Granitoid Complex (hereafter CFGC), is dominated, as the name alludes, by felsic plutonic rocks. The CFGC is surrounded by voluminous paragneisses (Fig. 1) interpreted to have been deposited mainly before the peak of magmatic activity within and around the CFGC, i.e. 1895–1875 Ma (e.g. Huhma et al. 1991, Lahtinen et al. 2009, Kotilainen et al. 2016, Nikkilä et al. 2016, Mikkola et al. 2018c).

The voluminous Svecofennian granitoids have a long history of research in Finland, and several classification schemes have been proposed over the years (e.g. Eskola 1932, Simonen 1960, 1980). Nironen (2005) divided the Svecofennian granitoids based on their relationship with the orogenic stages into four groups: preorogenic (1.95–1.91 Ga), syn-orogenic (1.89–1.86 Ga), late orogenic (1.84–1.80 Ga) and postorogenic (1.81–1.77 Ga). The granitoids and volcanic rocks within and surrounding the CFGC are mainly synorogenic. Their genesis has been interpreted in two fundamentally differing ways: subduction-related arc magmatism (e.g. Nironen 2005, 2017, Lahtinen et al. 2009, 2017) or partial melting of crust thickened in the collision of exotic terranes with the Karelia craton at ~1.91 Ga (Nikkilä et al. 2016).

Within the CFGC, and the whole Svecofennian domain, mafic and ultramafic igneous rocks are sparser than granitoids, but can be found in most areas. Economic interest in the intrusions within the paragneiss domains surrounding CFGC is driven by their Ni–Cu ore potential (Makkonen 2015). Based on proposed ore models, segregation of sulphide melt occurred due to the assimilation of sulphur from country rocks during ascent and emplacement of mantle-derived magmas (e.g. Peltonen 2005, Makkonen 2015 and references therein). The mafic intrusions within the CFGC have received considerably less attention, and their relationship with the intrusions of the surrounding areas still provides challenges. In this paper, we present an extensive geochemical data set collected from the plutonic rocks in the southeastern CFGC and the surrounding unit. The data are used to describe the geochemical affinities of the units and provide additional insight into the processes of crustal formation during the culmination of the Svecofennian orogeny in the study area.

2 GEOLOGICAL SETTING

Our study area is located in the core part of the Svecofennian orogeny, along the southeastern boundary of the CFGC. It is dominated by plutonic rocks (Fig. 1). A dominant feature in the area is the northeast-trending sinistral Leivonmäki shear zone (LmSZ, Fig. 2, Mikkola et al. 2016, 2018a). South of the LmSZ, the majority of the bedrock consists of rocks belonging to the Pirkanmaa migmatite suite and Pirkanmaa intrusive suite (Luukas et al. 2017), hereafter collectively referred to as the Pirkanmaa suites. The migmatite suite is part of the Western Finland supersuite and mainly consists of variably migmatized greywackes with maximum depositional ages close to 1.91 Ga (Lahtinen et al. 2009, Mikkola et al. 2018b). The minimum age of deposition is 1895 Ma, based on the age of the Pirkanmaa intrusive suite (Kallio et al. 1986, authors' unpublished data), which intrudes into and hosts xenoliths of the Pirkanmaa migmatite suite (Mikkola et al. 2016). The Makkola suite, located in the middle of study area (Fig. 2) and mainly consisting of volcanic units with a limited number of associated plutonic and sedimentary rocks, represents calc-alkaline arc-type magmatism and yields ages varying from 1895 to 1875 Ma (Mikkola et al. 2018c). Most of the occurrences of the Makkola suite are located in the vicinity of the LmSZ.

North of the LmSZ, the bedrock belongs to the CFGC. In the classification scheme of Nironen (2005), all plutonic rocks of the CFGC in our study area belong to the synorogenic group. Nironen further subdivided them into synkinematic (1.89–1.87 Ga) and post-kinematic granitoids (1.88–1.87 Ga). Here, we use the division of Mikkola et al. (2016), in which the ca. 1885–1880 Ma Jyväskylä suite (Rämö et al. 2001, Nikkilä et al. 2016, authors' unpublished data)

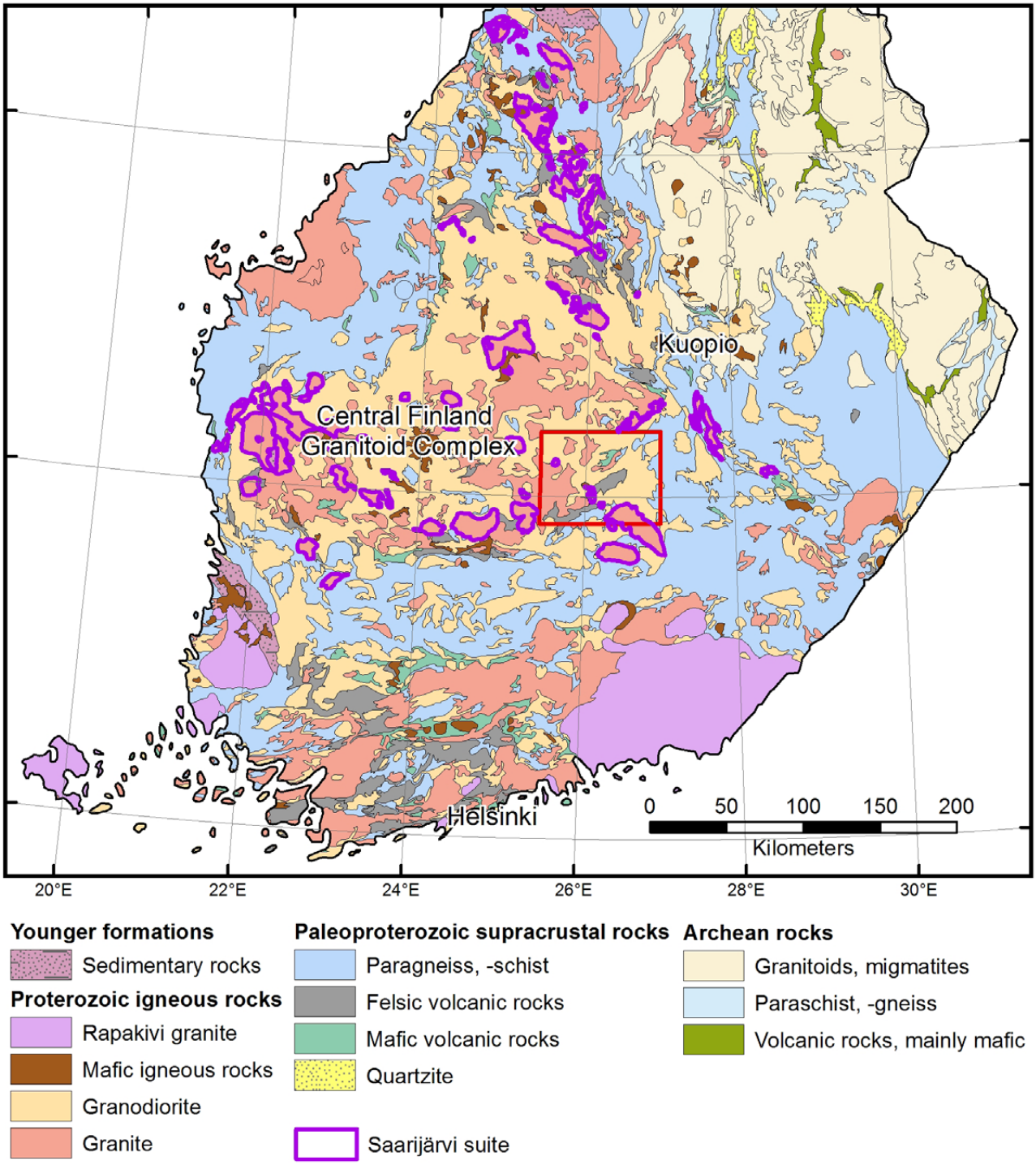

Fig. 1. Location of the study area on the geological map of southern and central Finland. Map modified from Nironen et al. (2016) and Bedrock of Finland – DigiKP.

makes up the bulk of the CFGC and equals the syn-kinematic group of Nironen (2005). The Jyväskylä suite consists of two lithodemes: Vaajakoski quartz diorites and Muurame granitoids, the latter of which include two phases called the Muuratjärvi porphyritic granodiorite and the Muuratsalo porphyritic granite. It should be noted that the rocks interpreted as belonging to the Muurame lithodeme are also present south of the LmSZ, where they intrude into the Pirkanmaa suites.

The post-kinematic granitoids of Nironen (2005), together with the more mafic rocks (typically diorites) that they are commonly associated with, form the bimodal Saarijärvi plutonic suite (Fig. 1, Mikkola

et al. 2016, Luukas et al. 2017, Virtanen & Heilimo 2018). Based on geochronological data, the Saarijärvi suite is partly coeval with the Jyväskylä suite, as it yields ages between ca. 1885 and 1875 Ma (Rämö et al. 2001, Nikkilä et al. 2016, authors' unpublished data). This suite is present on both sides of the LmSZ, varying in size from intrusions tens of kilometres across to 1-metre-wide dykes cross-cutting older rocks. Granitoids of the Saarijärvi suite are commonly porphyritic, and they vary mineralogically from quartz monzonite to granite, display weaker deformation than the rocks of the Jyväskylä suite and are compositionally A-type (Virtanen & Heilimo 2018). The youngest granitoid phase in the study area is the Oittila suite, which is present as small intrusions and locally abundant dykes on both sides of the LmSZ but is more voluminous within the CFGC (Mikkola et al. 2016). The age of this suite is ca. 1875 Ma (authors' unpublished data). In addition to plutonic rocks, the CFGC contains areas of volcanic rocks and paragneisses up to several kilometres in length (Fig. 2), which cannot be correlated with the larger entities based on available data. The main characteristics of the lithological units are summarized in Table 1.

3 MATERIAL AND METHODS

The material used for this study includes 300 samples from both outcrops and drill cores. In addition to the samples taken by the authors, they include 17 samples taken by T. Mutanen in 2005. All samples were analysed in Labtium Ltd with the XRF method (Labtium code 175X) and 231 samples with ICP-MS (Labtium code 308PM) for additional trace element data. A detailed description of the methods can be found in Appendix 1. All geochemical data are provided in the Electronic Appendix. In addition to the new data, 84 analyses published by Rasilainen et al. (2007, n = 45), Mikkola et al. (2016, n = 18) and Kallio et al. (2018, n = 21) were used.

4 DESCRIPTION OF THE STUDIED UNITS

4.1 Kangasniemi granodiorite lithodeme

The Kangasniemi granodiorite lithodeme (hereafter the Kangasniemi granodiorites) belonging to the Pirkanmaa intrusive suite forms the majority of the bedrock southeast of the LmSZ (Fig. 2). Rocks of the lithodeme are ca. 1895 Ma in age (Kallio 1986, authors' unpublished data), equigranular, with a grain size varying from fine to medium grained. In addition to granodiorites and tonalites, the lithodeme also includes smaller areas consisting of quartz diorites, diorites and quartz monzodiorites. These domains of more mafic rocks are less than 4 km in diameter and usually more intensively deformed and foliated. Co-genetic finer-grained dioritic enclaves are a characteristic feature on the outcrop scale (Fig. 3A). Both hornblende and biotite are usually present as mafic minerals in varying proportions. The strength of the foliation varies, being typically moderate. The texture of the rock varies due to deformation. Xenoliths of the Pirkanmaa migmatite suite are abundant, varying in diameter from the centimetre to the kilometre scale.

Table 1. Plutonic units of the study area and their characteristic features. For a description of the Saarijärvi suite, see Virtanen and Heilimo (2018).

Age (Ma)	Unit	Composition	Mineralogy, texture	Other
ca. 1895	Lammuste lithodeme	Mainly intermediate with some outliers SiO_2=45–65 wt%, weak negative Eu anomaly	Deformed, weakly porhyritic quartz diorites, quartz monzonites	Plutonic member of the Makkola suite consisting mainly of volcanic units (Mikkola et al. 2018a).
ca. 1895	Kangasniemi lithodeme of the Pirkanmaa intrusive suite	Mainly intermediate to acid SiO_2=41–72 wt% and K_2O=1–4 wt%, weak negative Eu anomaly	Equigranular, variably deformed granodiorites and tonalites.	
ca. 1885	Vammala suite	Mainly mafic and ultramafic, containing few intermediate samples as fractionates SiO_2 37–58 wt%, MgO = 3–26 wt%	Gabbros and ultramafic plutonic rocks	Intrudes into Pirkanmaa migmatite and intrusive suites
1885–1880	Jyväskylä suite			Bulk of the Central Finland Granitoid Complex in the study area
	Muurame granitoid lithodeme	Mainly acidic SiO_2=60–75 wt%, and slightly enriched K_2O=3.5–9 wt%, negative Eu anomaly	Deformed K-feldspar porphyritic granitoids	
	Vaajakoski lithodeme	Mainly intermediate; SiO_2=43–58 wt%	Deformed quartz diorites, hornblende and biotite as mafic minerals, pyroxenes locally preserved	Commonly gradual contacts with the Muurame lithodeme
1880–1875	Saarijärvi suite	Bimodal suite, felsic members display A-typegeochemical characteristics	Felsic members typically K-feldspar porphyritic quartz monzonites and granites. Mafic members equigranular diorites	Mingling textures between the end members common. Located in the vicinity of major fault zones
ca. 1875	Oittila suite	Mainly elevated SiO_2=64–78 wt%, and K_2O=4–8 wt%, mainly negative Eu anomalies	Equigranular or weakly porpyritic granitoid dykes and small intrusions, relatively undeformed and leucocratic	
	Rutalahti lithodeme	High MgO (up to 32 wt%), Mg#, Ni, and Cr		

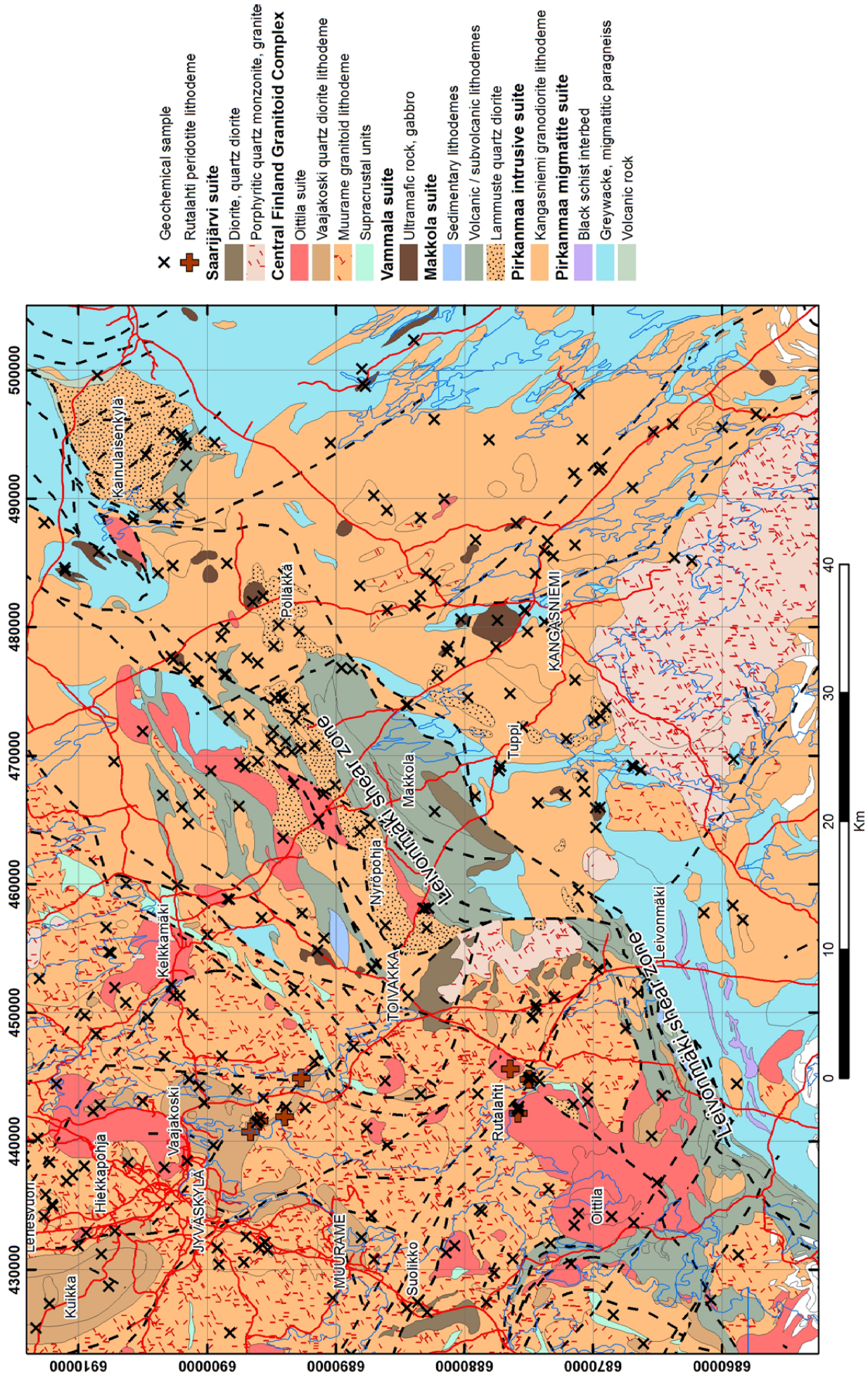

Fig. 2. Geological map of the study area with sample locations. Map modified from Mikkola et al. (2016). Note that the locations of Rutalahti peridotite intrusions are shown as symbols and not as areas due to their small size.

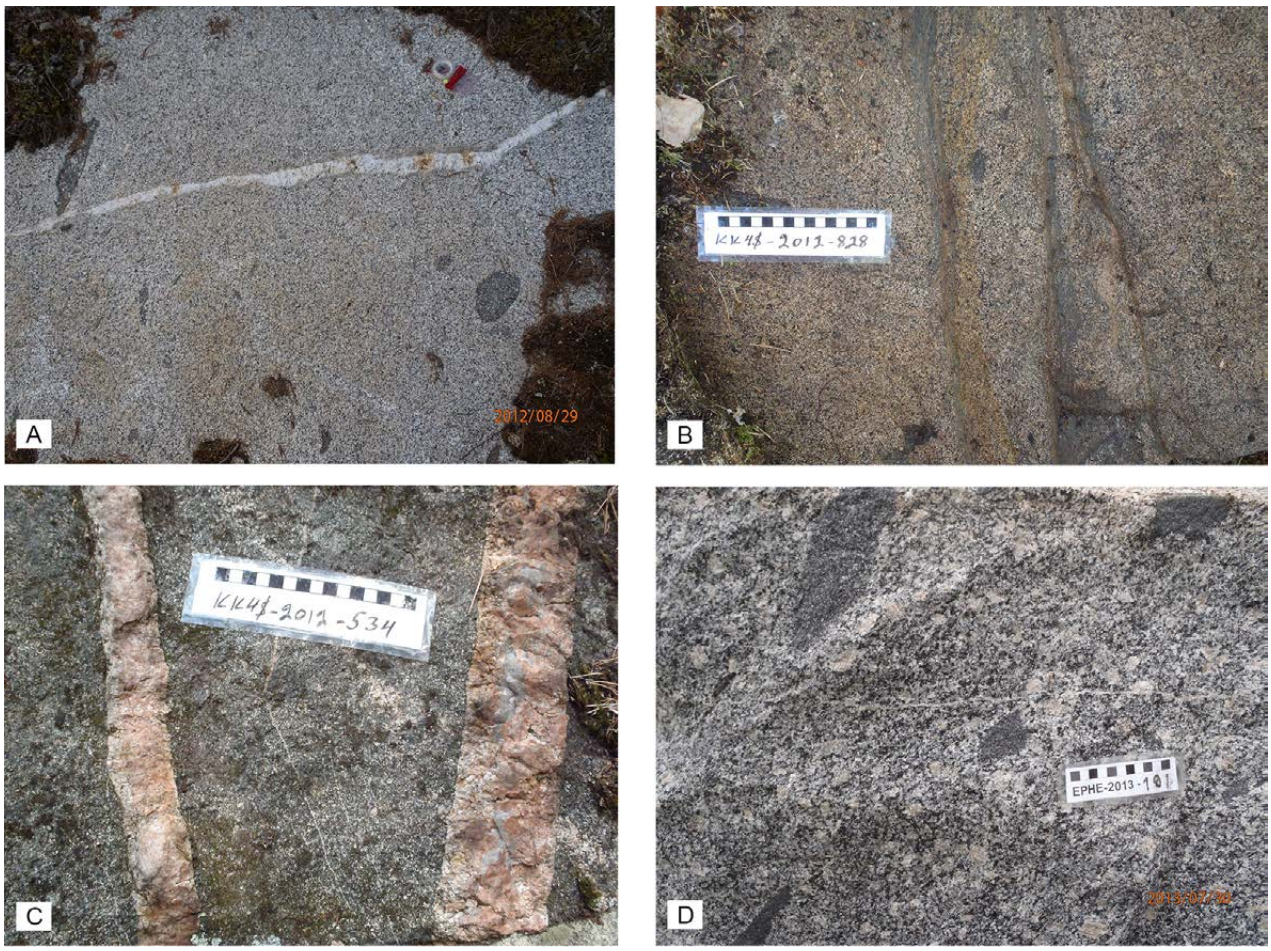

Fig. 3. A) Kangasniemi granodiorite hosting finer-grained and more mafic enclaves and cross-cut by a dyke belonging to the Oittila suite. Length of the compass 12 cm. B) Lammuste quartz diorite with shear seams belonging the Leivonmäki shear zone. C) Gabbro belonging to the Vammala suite and cross-cut by pegmatite dykes representing the most felsic variants of the Oittila suite. D) Porphyritic granodiorite of the Muurame lithodeme with equigranular finer-grained enclaves. The scale bars in B–D have a centimetre scale.

4.2 Lammuste quartz diorite lithodeme

The Lammuste quartz diorite lithodeme (hereafter Lammuste quartz diorites) belongs to the Makkola suite, which otherwise mainly consists of volcanic rocks (Mikkola et al. 2018c). Rocks grouped into the Lammuste quartz diorites are located in the vicinity of the volcanic units in the area (Fig. 2). Based on age determinations, this lithodeme is ca. 1895 Ma in age (authors' unpublished data), and thus coeval with both the Pirkanmaa intrusive suite and the oldest volcanic units of the Makkola suite (Mikkola et al. 2018c). Hybabyssal porphyritic dykes shown to be coeval and compositionally similar to the dykes within the volcanic segments cross-cut the Lammuste quartz diorites (Mikkola et al. 2018c). The unit is composed of three larger intrusions, Kainulaisenkylä, Nyröpohja and Pölläkkä (Fig. 2), and a number of smaller intrusions. Rocks of the lithodeme are hornblende-bearing quartz diorites, quartz monzodiorites and quartz monzonites. At the outcrop scale, the rock is weakly foliated, even-grained or contains only slightly coarser plagioclase phenocrysts (Fig. 3B). The Lammuste lithodeme also contains small areas of gabbros, which have been altered so that pyroxene is only present as small remnants (Ikävalko 1981).

4.3 Vammala suite

The Vammala suite in the study area includes small gabbro and ultramafic intrusions that have intruded into the Pirkanmaa suites. The classification of intrusions in the Vammala suite is largely based on the country rock. Gabbros north of the LmSZ have been included in the CFGC, whereas mafic rocks south of the LmSZ are considered as part of the Vammala suite. However, it should be noted that ultramafic intrusives north of the LmSZ are scarce. Despite being volumetrically small, this suite forms an economically important part of the study area by hosting Ni–Cu mineralizations (e.g. Kohonen 1988). In addition to the intrusions, the rocks of the suite are present as enclaves down to 10 cm in diameter in rocks of the Pirkanmaa suites. The larger intrusions of the suite are mainly intact, but narrow dykes and smaller intrusions have been fragmented by intensive deformation. No direct age data are available for the Vammala suite in the study area. However, as they intrude into the Pirkanmaa suites, which are ca. 1895 Ma in age and are cross-cut by dykes and veins of the Oittila suite (ca. 1875 Ma, Fig. 3C), their age is relatively well constrained at ca. 1885 Ma. Pyroxene has been a primary phase in most cases, albeit often nearly completely altered to hornblende in later stages. The locally observed primary hornblende might represent different phases within an intrusion, e.g. representing a change between a gabbro and a diorite phase or an ultramafic and a mafic phase. However, more detailed study would be required to demonstrate this.

4.4 Jyväskylä suite

4.4.1 Muurame granitoid lithodeme

The Muurame granitoid lithodeme (hereafter Muurame granitoids) consists of two phases: the Muuratjärvi porphyritic granodiorite and Muuratsalo porphyritic granite. These phases only differ in the content of K-feldspar phenocrysts, which in granodiorite is 5–20 wt% and in granite 20–40 wt%. The ground mass is hypidiomorphic and phenocrysts are typically 2–3 cm in diameter (Fig. 3D). The observable variation in the phenocryst content could locally represent magmatic flow structures. However, deformation-induced foliation is common. The common mafic minerals are biotite and hornblende, whereas pyroxenes are only present in small areas in the vicinity of the town of Jyväskylä. When pyroxene is present, the rock is darker and slightly purple at the outcrop scale (Fig. 4A). Abundant finer-grained and more mafic enclaves are, at least partly, fragmented synplutonic dykes representing the Vaajakoski quartz diorite lithodeme. This evidences the concurrent emplacement of these two lithodemes. Occasionally, K-feldspar phenocrysts are fully or partially mantled by recrystalline micrograins of plagioclase and quartz, forming a white ring (Fig. 4B).

In this study, data from undeformed K-feldspar porphyritic granite in the Lehesvuori area (Fig. 2) have been included in the Muurame granitoids due to the lack of other comparable units, although this intrusion yielded an age of 1891 ± 5 Ma (Lahtinen et al. 2016).

4.4.2 Vaajakoski quartz diorite lithodeme

The Vaajakoski quartz diorite lithodeme consists of even-grained, homogeneous and weakly foliated rocks (Fig. 4C) that have gradual contacts with the surrounding Muurame granitoids. The modal composition of the suite varies, including the dominant quartz diorites, but also diorites, gabbros and tonalites. In certain cases, a gabbro core can be observed within the quartz diorite area, e.g. the Kuikka intrusion north of Jyväskylä (Fig. 2), which also has a tonalite outer rim. Characteristic mafic minerals in these equigranular rocks are hornblende and biotite, whereas pyroxenes have only locally been preserved. These enderbite areas are located close to larger shear zones that have concentrated deformation and fluid flow, leaving relatively anhydrous and deformed areas close to the large shear systems. Co-genetic dioritic dykes and boudinaged mafic microgranular enclaves (MMEs) are typical features for the Vaajakoski lithodeme. The lithodeme is recognizable as local highs in both the aeromagnetic and Bouguer anomaly map (Mikkola et al. 2018a). This is most likely due to abundant mafic minerals and weak magnetite dissemination.

Fig. 4. A) Granite of the Muurame lithodeme displaying a sharp contact between dark-coloured pyroxene bearing charnockite on the right and a hydrated paler-coloured variant on the left. Scale bar with a cm scale. B) Rapakivi-like texture caused by microcrystalline plagioclase and quartz formed on boundaries of K-feldspar phenocrysts. Edge of the compass with a mm scale. C) Vaajakoski quartz diorite with finer-grained enclaves, cross-cut by a narrow granite dyke belonging to the Oittila suite. Length of the compass 12 cm. D) Folded granite dyke belonging to the Oittila suite intruded into mafic volcanic rock. Scale bar with a cm scale.

4.5 Oittila suite

The granitoids of the Oittila suite are the youngest voluminous magmatic event in the study area. The suite cross-cuts the other granitoid units as intrusions (<10 km in diameter) and, more characteristically, as locally abundant dykes varying in direction. The majority of the dykes are relatively undeformed, but some have been folded (Fig. 4D). The suite is part of the CFGC, and can be found on both sides of the LmSZ. Based on age determinations, the Oittila suite is ca. 1875 Ma in age, and thus overlaps in age with the Saarijärvi suite (1885–1875 Ma, Rämö et al. 2001, authors' unpublished data). However, based on field observations, the age relationship is clear and the Oittila suite cross-cuts the Saarijärvi suite. Biotite is the most common mafic mineral and hornblende is locally present. In terms of rock types, the suite includes both granites and granodiorites, most of which are equigranular, although some intrusions are characterized by small (<1 cm) K-feldspar phenocrysts. The main difference between the Oittila and Jyväskylä suites is the more leucocratic and less deformed character of the former. The Oittila and Saarijärvi suites differ in the clear bimodality and the A-type chemistry of the granitoids of the latter suite.

4.6 Rutalahti peridotite lithodeme

Peridotites of the Rutalahti lithodeme are located between Rutalahti and Vaajakoski in connection with a major southeast-trending shear system. They form small dyke-like intrusions, the largest ones being 1000 m x 400 m. These intrusions are clearly visible on the aeromagnetic map, and they were briefly described by Mutanen (2011). Based on thin-section studies, these altered rocks were originally olivine-bearing ultramafic rocks. Primary medium-grained olivine and pyroxene can only be observed as remnants, and a variable degree of alternation is abundant. In particular, secondary serpentine and small amounts of iddingsite can be seen.

5 GEOCHEMISTRY

5.1 Kangasniemi granodiorite lithodeme

Samples of Kangasniemi granodiorites span in rock type from gabbros to granites. Thus, the SiO_2 concentration varies from 45.1 wt% to 73.7 wt% (median 63.2 wt%). Of the major elements, MgO, CaO, FeOt and TiO_2 display a good correlation with SiO_2 (Fig. 5), excluding the most basic samples. With respect to trace elements, the correlations with SiO_2 are weak or non-existent. Chondrite-normalised REE patterns display moderate enrichment in LREE with respect to HREE (median $(La/Yb)_N$ = 11.8, Fig. 7) and typically a weakly negative Eu anomaly (median Eu/Eu* = 0.79). On spider diagrams, the analyses display negative anomalies with respect to Nb, P and Ti, in addition to significant scatter in LILE concentrations (Fig. 8).

On the modified alkali-lime index (MALI) diagram of Frost et al. (2001), the majority of the Kangasniemi granodiorites plot in the calc-alkalic field, and on the TAS diagram they span from diorites to granites (Fig. 10). On the classification diagrams of Pearce et al. (1984), the samples plot almost exclusively in the volcanic arc granite field. Excluding one outlier, the samples plot within the volcanic arc array on the Nb/Yb vs. Th/Yb diagram of Pearce and Peate (1995) and cluster in the field of continental arc rocks (Fig. 10D).

5.2 Lammuste quartz diorite lithodeme

Lammuste quartz diorites display a wide compositional spectrum from ultrabasic to felsic compositions (SiO_2 = 39.8–73.1 wt%), but they are on average slightly more mafic than the Kangasniemi granodiorites (median SiO_2 = 58.0 wt%, Fig. 5). Of the major elements, FeOt and CaO show a good correlation with SiO_2, whereas TiO_2, MgO and Na_2O show a moderate correlation with SiO_2. Lanthanum is the trace element displaying the strongest positive correlation with SiO_2, whereas the others scatter (Figs 5, 6). Enrichment of LREE over HREE is similar to the samples representing the Kangasniemi granodiorite lithodeme (median $(La/Yb)_N$ = 11.3 versus 11.8, Fig. 7), as is the Eu anomaly (median Eu/Eu* = 0.85 versus 0.79). On the spider diagram, Nb, P, and Ti display negative anomalies in nearly all samples, and Zr in some of the samples (Fig. 8). Positive Sr anomalies are common.

On the modified alkali-lime index (MALI) diagram of Frost et al. (2001), the majority of the Lammuste quartz diorites plot in the calc-alkalic field and on the TAS diagram in the gabbroic diorite, diorite and monzonite fields (Fig. 10). On the classification diagrams of Pearce et al. (1984), samples from the Lammuste lithodeme plot in the volcanic arc granite field, and within the volcanic arc array and continental arc field of Pearce and Peate (1995).

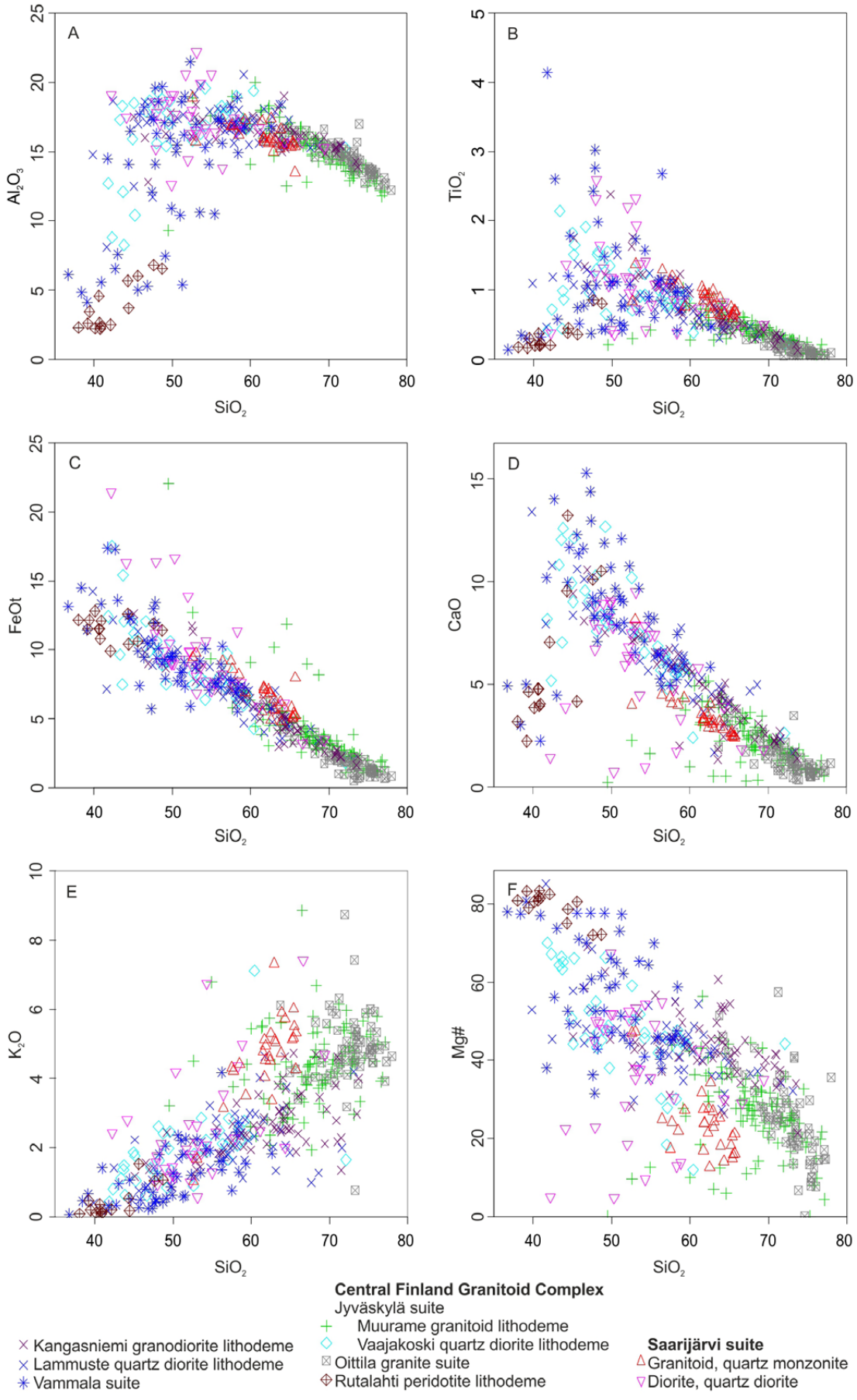

Fig. 5. Harker diagrams of the studied units. Analyses from Virtanen and Heilimo (2018) representing the Saarijärvi suite are included for comparison.

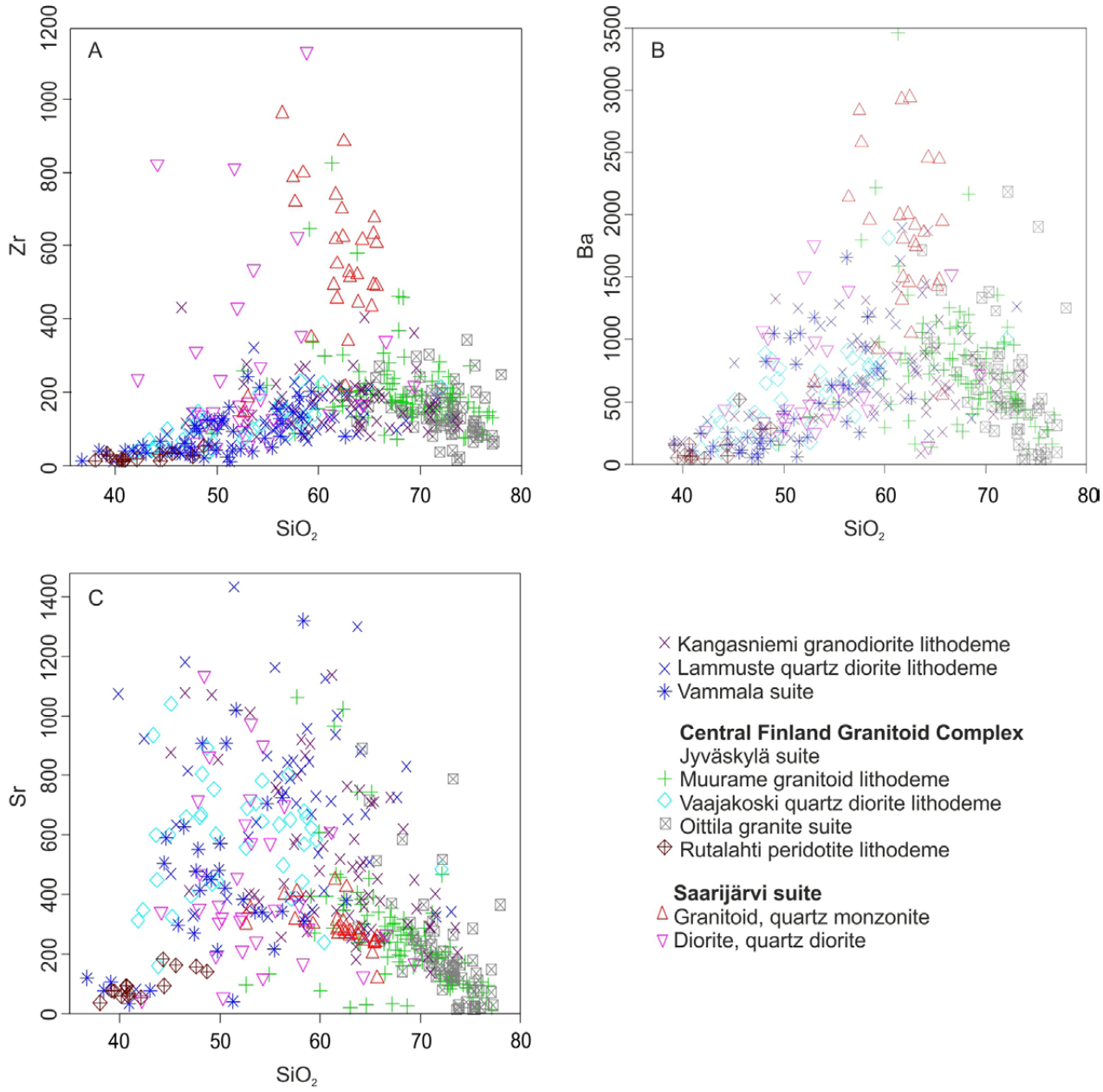

Fig. 6. Harker diagrams of the studied units continued. Analyses from Virtanen and Heilimo (2018) representing the Saarijärvi suite are included for comparison.

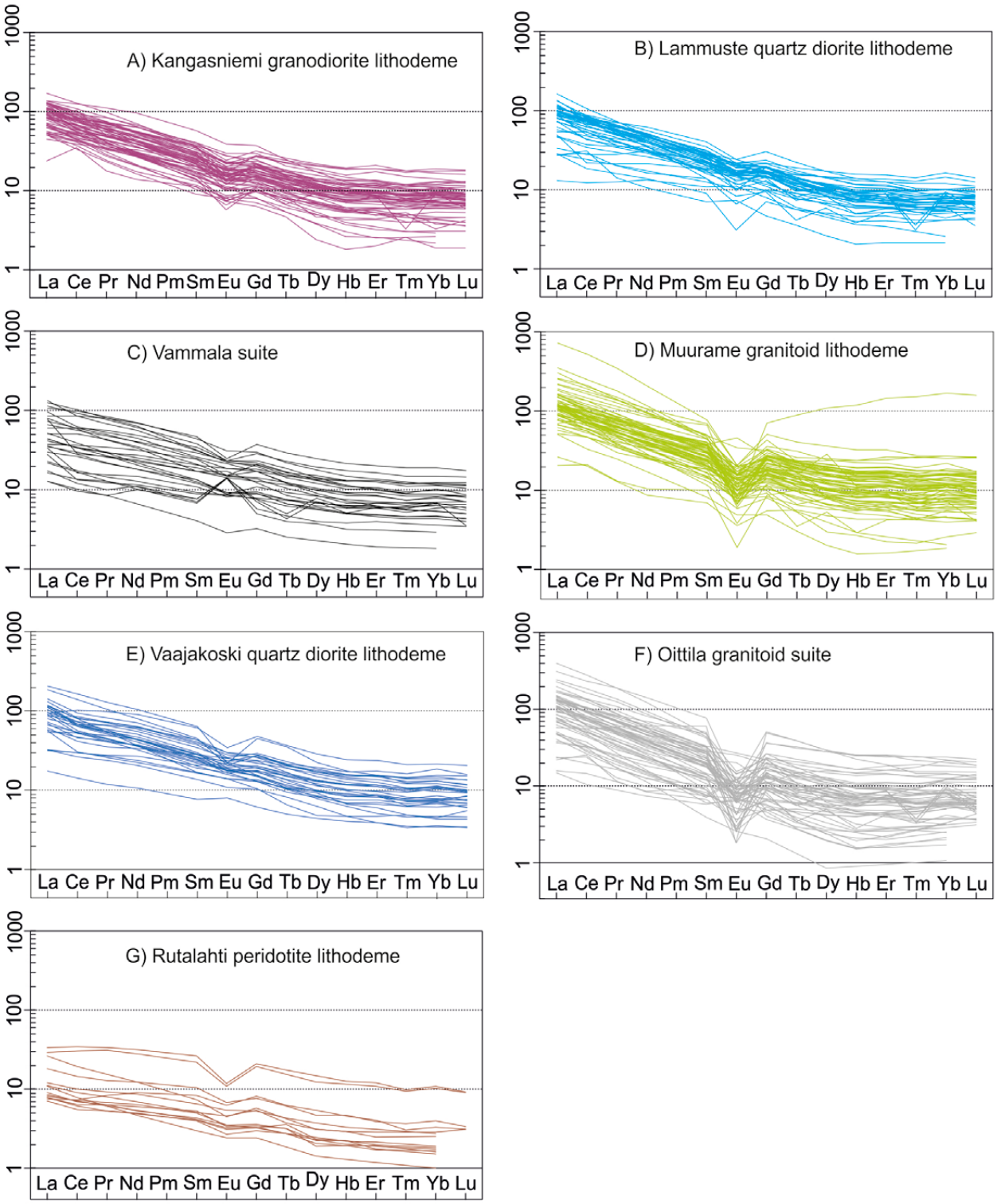

Fig. 7. Chondrite-normalised REE patterns of the studied units. Chondrite values from Boynton (1984).

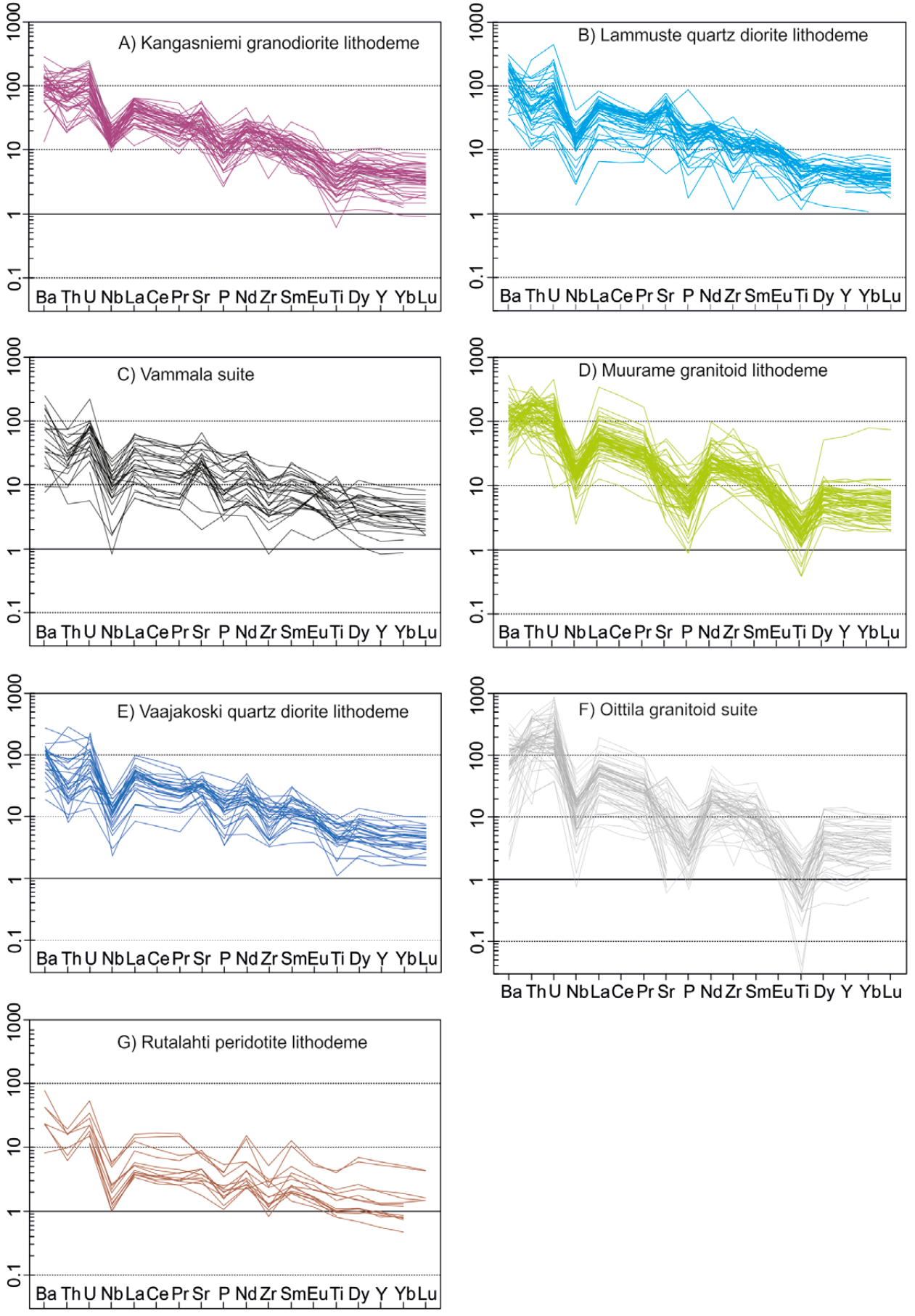

Fig. 8. Spider diagrams of the studied samples normalised with primitive mantle values of McDonough and Sun (1995).

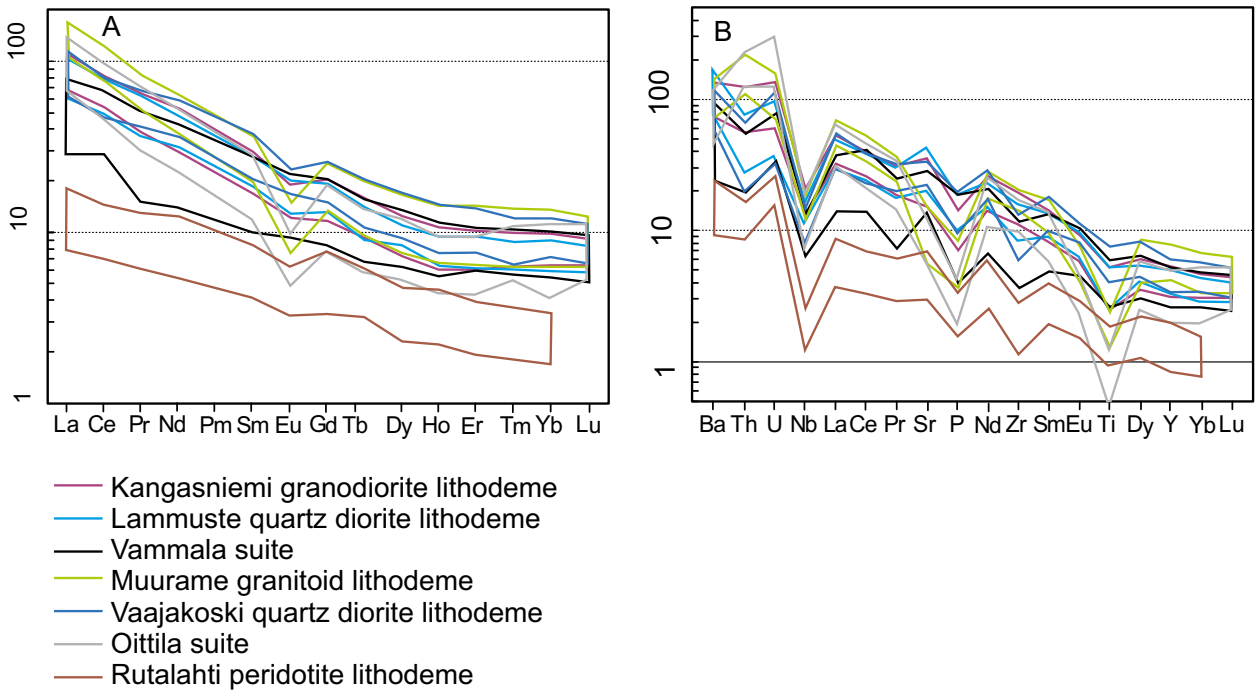

Fig. 9. Comparison of REE patterns and trace element characteristics of the studied units. The area for each unit is based on the median value ± one quartile.

5.3 Vammala suite

Variation in the amounts of minerals, which can be seen as variation in rock types from ultramafic rocks to tonalites in the Vammala suite samples, is reflected by SiO_2 concentrations varying from 36.7 to 62.6 wt%, with a median value of 49.9 wt%. Samples of the Vammala suite do not form clear fractionation patterns with respect to SiO_2, but instead, both the main and trace elements scatter (Figs 5, 6). Some of the scatter may be caused by magmatic accumulation of olivine, i.e. the samples are enriched in MgO, Cr and Ni and depleted in Al_2O_3. REE display moderate fractionation between LREE and HREE (median $(La/Yb)_N$ = 7.2, Fig. 7) and the Eu anomaly varies from negative to positive (Eu/Eu* = 0.59–2.37, median = 0.87). On spider diagrams, the common denominator of the samples is the negative Nb anomaly and overall weaker fractionation than what is observed in granitoid units (Figs 8, 9). Strontium shows a positive anomaly in most of the samples and the negative Ti anomaly is weaker than in the granitoid units. Additionally, some of the samples display clear positive Ti anomalies.

Vammala suite samples mainly plot in the calc-alkalic array on the modified alkali-lime index diagram (MALI) of Frost et al. (2001), and on the TAS diagram they span compositionally from peridote gabbro to diorite (Fig. 10). On the classification diagram of Pearce and Peate (1995), the samples representing the Vammala suite plot within the volcanic arc array and mainly within the continental arc field.

5.4 Jyväskylä suite

5.4.1 Muurame granitoid lithodeme

Samples from the Muurame granitoid lithodeme display a good correlation between SiO_2 (range = 49.5–77.1 wt%, median 68.3 wt%) and all major elements, excluding Na_2O and K_2O (Fig. 5), especially when taking into account that the samples with anomalously high FeOt and depleted in SiO_2, Al_2O_3, CaO, MgO, TiO_2 and P_2O_5 are altered samples from Suolikko and Hiekkapohja mineralization areas (Kallio et al. 2018, Heilimo et al. 2017). When these anomalous samples are excluded, Sr displays a clear correlation with SiO_2 (Fig. 6). The median $(La/Yb)_N$ for the Muurame lithodeme is 10.7, and the group is characterised by a pronounced negative Eu anomaly (median Eu/Eu* = 0.58, Fig. 7). Ti, P

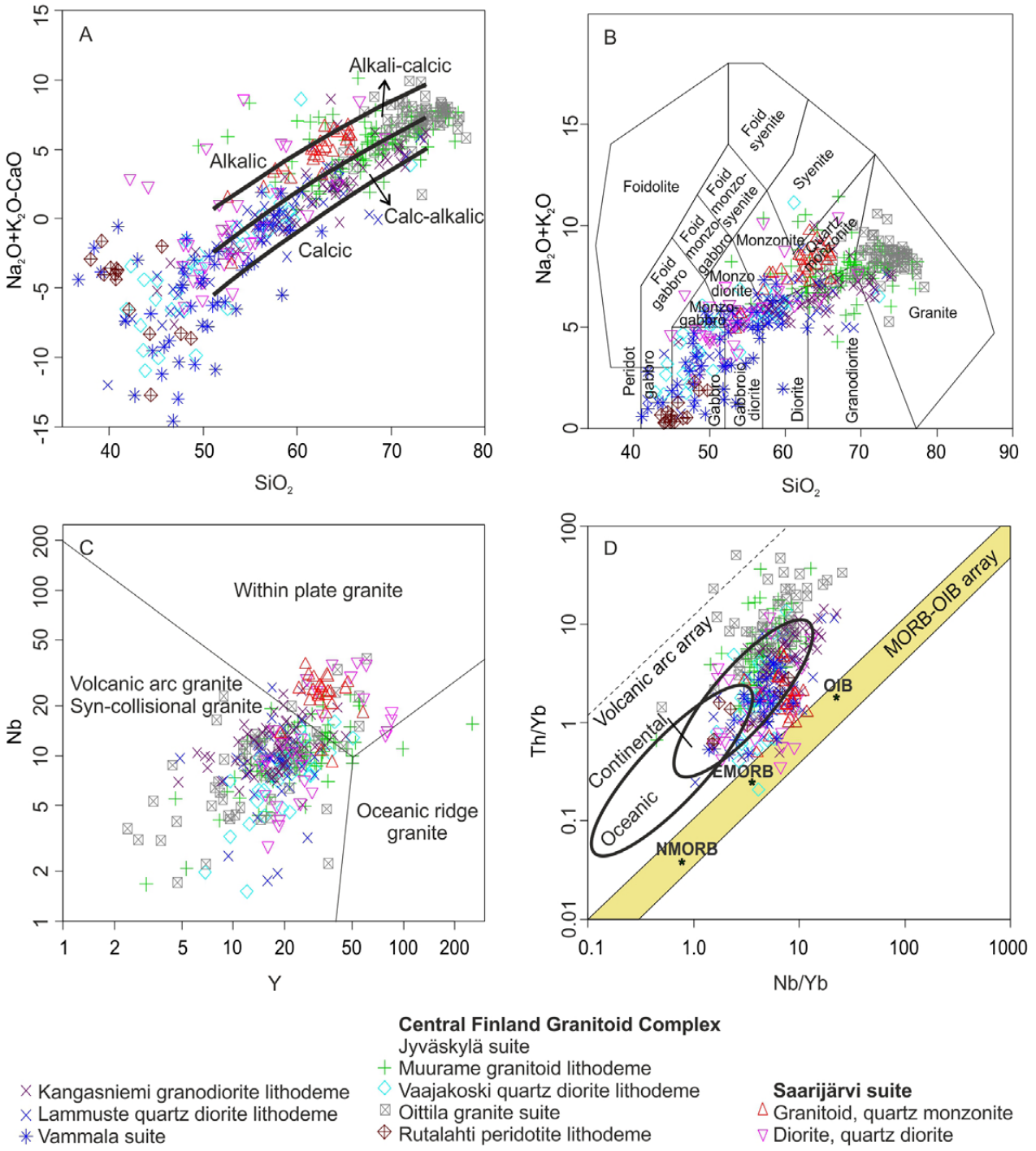

Fig. 10. A) Na_2O+K_2O-CaO classification diagram of Frost et al. (2001). B) TAS diagram with boundaries by Middlemost (1994). C) Y vs. Nb diagram of Pearce et al. (1984) for identifying the environments of granitoid formation. D) Nb/Yb vs. Th/Yb diagram of Pearce and Peate (1995) with the MORB-OIB compositional array and fields of oceanic and continental arcs.

and Nb form negative anomalies on spider diagrams (Fig. 8). LILE scatter can also be observed in samples from the Muurame lithodeme, but less than in the case of the Kangasniemi granodiorite lithodeme, and Ba displays a negative anomaly in most of the samples. Despite their older age, the samples from the Lehesvuori area cannot be separated compositionally from the Muurame suite. Instead, they are compositionally similar to the most felsic variants of the Muurame suite (~74 wt% SiO_2), excluding one dyke sample with an exceptional flat REE pattern (Electronic Appendix, sample MAAH-2014-2.1, $(La/Yb)_N$ = 1.7).

On the modified alkali-lime index diagram, the Muurame granitoid samples straddle the boundary between calc-alkalic and alkali-calcic. On the TAS diagram, most of the samples plot in the granodiorite, quartz monzonite and granite fields (Fig. 10). On both diagrams, the most obvious outliers represent altered samples from or near mineralizations. Most of the samples plot in the field of volcanic arc granites on the diagrams of Pearce et al. (1984), but a small number plot in the field of within-plate granites. On the Nb/Yb vs. Th/Yb diagram (Pearce & Peate 1995), all samples plot in the volcanic arc array and most fall in the continental arc field (Fig. 10D).

5.4.2 Vaajakoski quartz diorite lithodeme

Samples of the Vaajakoski quartz diorites form a compositional spectrum from ultrabasic to intermediate compositions, as SiO_2 varies from 41.8 to 60.4 wt%, excluding an outlier SiO_2 with 72.1 wt%. The outlier is from a trondhjemitic part of a small intrusion regarded as and interpreted to represent the last remaining residue. Out of the main elements, FeOt, MgO, CaO and Na_2O display a good correlation with SiO_2, although scatter exists in the samples poorer in SiO_2 (Fig. 5). Fractionation of REE is moderate, with a median La_N/Yb_N of 8.8, and the negative Eu anomaly is either weak or lacking (median Eu/Eu* = 0.87, Fig. 7). On primitive mantle-normalized spider diagrams, LILE display scatter, but most samples display a negative Th anomaly in addition to positive Sr and negative Nb, P, and Ti anomalies (Fig. 8).

Vaajakoski quartz diorites mainly classify as calc-alkalic on the MALI diagram of Frost et al. (2001) and span from gabbro to diorite on the TAS diagram (Fig. 10). Excluding two outliers, the samples plot in the field of volcanic arc granites on the diagram of Pearce et al. (1984) and within the continental arc field on the diagram of Pearce and Peate (1995).

5.5 Oittila suite

Granitoids of the Oittila suite display SiO_2 concentrations from 63.7 wt% to 78 wt% (median = 73.2 wt%) and a good correlation between SiO_2 and TiO_2, Al_2O_3, FeOt, MgO and CaO, whereas Na_2O and K_2O scatter strongly, similarly to the trace elements (Fig. 5). The REE patterns display significant scatter, although on average they show strong fractionation and enrichment in LREE (La_N/Yb_N = 0.7–96.0, median = 13.4) and a strongly negative Eu anomaly (Eu/Eu* = 0.08–2.18, median = 0.51). All analyses with a clearly positive Eu anomaly display relatively low enrichment in LREE, but the degree of REE fractionation and the size of the Eu anomaly do not correlate with each other. On spider diagrams normalised with primitive mantle, the samples display negative anomalies in Ba, Nb, P and Ti. Most of the samples lack a Sr anomaly, but samples with both positive and negative anomalies are present.

On the MALI diagram, the Oittila granitoid samples plot along the boundary of calc-alkalic and alkali-calcic fields. On the TAS diagram, nearly all of them plot in the granite field (Fig. 10). On the Y vs. Nb diagram, most of the samples plot in the field of volcanic arc granites, and on the Nb/Yb vs. Th/Yb diagram they fall in, or slightly above, the continental arc field (Fig. 10). On the last two diagrams, the samples display significant scatter.

5.6 Rutalahti peridotites lithodeme

The samples from Rutalahti peridotites vary from ultrabasic to basic in composition (SiO_2 = 38.0–48.7 wt%) and form clear differentiation trends with respect to Al_2O_3, MgO, Na_2O, P_2O_5 and TiO_2 (Fig. 5). Out of the trace elements, the total REE concentrations, Ni, Cr, and Y display a clear correlation with SiO_2. Fractionation of REE is moderate (median La/Yb_N = 4.66) and the Eu anomaly is in most cases moderate (median Eu/Eu* = 0.80, Fig. 7), but increases in size towards the more evolved compositions. The two most evolved samples display a strong negative anomaly (Eu/Eu* ~ 0.5). On primitive mantle-normalised spider diagrams, LILE scatter by one to two orders of magnitude and the samples display negative Th, Nb, P and Zr anomalies (Fig. 8). The Ti anomaly is weak or missing. On the TAS diagram, the Rutalahti peridotites plot in peridotite gabbro and gabbro fields. On the diagram of Pearce and Peate (1995), they plot in the continental arc field (Fig. 10).

6 DISCUSSION

6.1 Assessment of alteration and elemental mobility

All of the Svecofennian rocks have been metamorphosed or altered in later stages. The study area mostly metamorphosed in upper amphibole and granulite facies at 1.89–1.88 Ga (Hölttä & Heilimo 2017), but younger, more local elemental mobility, induced by intrusions or major shear systems, is also possible. The majority of the samples in this study were taken from locations that do not show significant signs of alteration. The exception is certain samples, for instance, from the Suolikko and Hiekkapohja areas (Fig. 2), which display distinct alteration related to mineralization including sulphide and hydrothermal processes (Halonen 2015, Heilimo et al. 2017, Kallio et al. 2018). These samples stand out from the main population of the Muurame lithodeme based, for example, on higher FeOt and K_2O and lower CaO concentrations with respect to SiO_2 (Figs 5C, D, E). The most intensive alteration is related to small, structurally favourable seams that cross-cut both the Suolikko and Hiekkapohja targets. The lack of widespread intensive alteration limits the ore potential of the area with respect to porphyry-type deposits typically associated with alteration halos several kilometres across (e.g. Sillitoe 2010).

Although the most intensive alteration is limited to a few target-scale areas, certain signs of weaker widespread post-crystallization alteration are observable. One such sign is the poor correlation between SiO_2 and LILE displayed, for example, by the main population of the Muurame granitoids (Figs 5, 6). The less mobile elements in the same suite, e.g. TiO_2, Al_2O_3 and Sr, display a significantly better correlation, which is likely to reflect some mobility in the composition. Local intensive alteration is associated with shear zones that have been active over an extended period of time under both semi-plastic and brittle conditions (Mikkola et al. 2018a).

6.2 Comparison between the Lammuste quartz diorites and Kangasniemi granodiorites

The compositional differences displayed by the Lammuste quartz diorites and the more voluminous Kangasniemi granodiorites (Fig. 2) are minor and controlled by the given SiO_2 level. Furthermore, based on the available age data (Kallio 1986, authors' unpublished data), these units are coeval (~1895 Ma). Thus, we interpret that both of the units were generated by similar processes during the geological evolution of the area, but the source probably contained variable amounts of crustal and juvenile components. Therefore, the division into separate units is somewhat arbitrary, but can be justified by the close spatial association of the Lammuste quartz diorites with the volcanic units of the Makkola suite (Fig. 2). In the case of the Kangasniemi granodiorites, and the Pirkanmaa intrusive suite as a whole, the association with volcanic units is lacking, as the suite mainly intrudes into the paragneisses of the Pirkanmaa migmatite suite. The composition of both the Lammuste quartz diorites and the Kangasniemi granodiorites is relatively typical for calc-alkaline series formed in an arc environment, including fractionated REE patterns and negative anomalies in Nb and Ti (Figs 7, 8).

6.3 Jyväskylä suite, compositional evolution in a maturing continental arc

Based on the observed compositions, the spatially voluminous Muurame granitoids and the Vaajakoski quartz diorites of the Jyväskylä suite form a series without gaps in the compositional spectrum. The trace element characteristics of the two lithodemes are characteristic of plutonic rocks formed in an arc environment, e.g. with enrichment in LREE and negative Nb and Ti anomalies (Fig. 8, e.g. Tatsumi et al. 1986). The units additionally display gradual contacts indicating coeval emplacement. Based on age data, the units are coeval at 1885–1880 Ma (Rämö et al. 2001, Nikkilä et al. 2016, Kallio et al. 2018, authors' unpublished data). Based on the points above, the units can be taken as co-magmatic.

The Vaajakoski quartz diorites have higher Mg# (27–60) and are poorer in SiO_2 (41.8–60.4 wt%) than the Muurame granitoids. The continuum they form with the Muurame granitoids is similar to that of continental arcs, where compositions span from basic to felsic, but the latter are more abundant (e.g.

Ducea et al. 2015). We propose that the felsic end members, i.e. the Muurame granitoids, were derived from partial melting of pre-existing crust and the more mafic compositions, i.e. the Vaajakoski quartz diorites, represent more juvenile magmas variably contaminated and fractionated during ascent. In the inner parts of the CFGC, rocks that could be regarded as belonging to the Vaajakoski quartz diorites are only present in very limited amounts (Bedrock of Finland – DigiKP). Nikkilä et al. (2016) interpreted based on data from these areas, lacking signs of significant juvenile contribution from mantle, that the Muurame granitoids (their group 2) represent partial melts of the middle crust thickened in collision with in the Savo arc (also known as the Keitele microcontinent) and the Archean craton at ~1.91 Ga. The absence of the Vaajakoski quartz diorites in the central parts of CFGC could be due to two factors: either the larger distance from active subduction or thicker crust that prevented the ascent of mantle-derived melts to the current erosion level. However, possible thrusting observed in the FIRE seismic reflection data in the CFGC area (Sorjonen-Ward 2006) might have stacked crustal sections, making evaluation of the role of the mantle components challenging or even impossible in the region.

The contact of the Jyväskylä suite (and CFGC) with the Kangasniemi granodiorites is tectonic, but small intrusions belonging to the Jyväskylä suite have been identified within the Kangasniemi granodiorites. Therefore, it can be concluded that these two subareas are not exotic with respect to each other (Fig. 2). The Kangasniemi granodiorites and the Muurame granitoids display significant compositional similarities, but closer inspection reveals certain differences between the suites, the latter being on average poorer in MgO, richer in K_2O and REE, and displaying a stronger negative Eu anomaly (Figs 5, 7). All these features are typical with the maturing of an arc (e.g. Ducea et al. 2015), suggesting continuous evolution instead of abrupt changes in magma genesis.

The Lehesvuori granite (Fig. 2), occurring in the middle of an area dominated by Muurame granitoids, provides an example of the dangers of relying on post-crystallisation features to interpret the relationships of plutonic rocks with orogenic phases. This granite has an unfoliated and undeformed appearance on outcrop (Mikkola et al. 2016), but it is nevertheless the oldest known granitoid (1891 ± 5 Ma, Lahtinen et al. 2016) north of the LmSZ in our study area. The likely cause for the undeformed appearance of this granite is its location between major fault zones that have controlled the local distribution of the deformation (Fig. 2).

6.4 Vammala suite versus Vaajakoski lithodeme

Based on available age data, the Vammala suite and the Vaajakoski lithodeme are coeval (Kallio 1986, author's unpublished data). The observed elemental compositions of the units partially overlap, and both units display the effects of cumulation processes in samples with low SiO_2 contents. Scatter in TiO_2 (Fig 5B) can be explained by crystallization of ilmenite, while MgO-rich and CaO-poor samples probably represent orthopyroxene±olivine-rich cumulates. Certain differences can be identified: the Vammala suite is on average richer in MgO, Ni and Cr, whereas the Vaajakoski lithodeme is on average richer in, e.g., Al_2O_3, K_2O, LREE and Zr (Figs 5, 6, 9). The varying degree and type of crustal contamination or fractional processes are probably factors in creating these compositional differences. The Vammala suite mainly intruded into the metagreywackes of the Pirkanmaa migmatite suite, and to lesser extent into the Kangasniemi granodiorites. At the same time, the Vaajakoski quartz diorites intruded into the more felsic plutonic units of the CFGC. The geotectonic setting of the Vammala suite was probably a marginal (or back arc?) basin in the southern boundary of the CFGC at 1.90–1.88 Ga (Makkonen 2015). The tensional setting would have allowed the units to locate above the subduction zone (Peltonen 1995). Based on the above considerations, we interpret that the Vammala and Vaajakoski lithodemes share a common origin and that the subtle differences between them are due to crustal contamination that could be related to the thickness of the crust at time of emplacement. Parental magmas of the Vammala suite have been interpreted as tholeiitic arc basalts (Peltonen 1995), and the trace element characteristics (eg. high Th/Yb ratio, Fig. 10D) of our data support this interpretation, although detailed modelling of the parental magma is beyond the scope of this study

6.5 The truly different Saarijärvi suite

Geochemically, the rocks of the Saarijärvi suite can be distinguished from those of the Jyväskylä suite by, for example, their higher K_2O, Ba and Zr concentrations (Figs 5, 6) and lower Mg#. Virtanen and Heilimo (2018) demonstrated that the granitoids of the Saarijärvi suite are largely A-type in terms of their geochemical fingerprint. Although these intrusions are also easily identifiable in the field (Fig. 2), some of the samples display signs of contamination with crustal material in a high-pressure regime, modifying the composition towards calc-alkaline affinity (Virtanen & Heilimo 2018). This contamination creating eg. higher Ba, Sr, Eu, Al_2O_3 contents, together with available overlapping emplacement ages (Rämö et al. 2001, Nikkilä et al. 2016, authors unpublished data, Table 1), supports coeval emplacement of granitoids with distinctly different chemical characteristics, i.e. the calc-alkaline Jyväskylä suite magmas and the Saarijärvi magmas with A-type affinities.

6.6 Oittila suite, the result of further fractionation of the Muurame granitoids

The youngest granitoid suite, Oittila, based on the authors' unpublished age data, is ca. 1875 Ma in age. It occurs as dykes and intrusions cutting the other units (Fig. 2). The compositional characteristics of the Oittila suite can be produced by either low-degree partial melting of pre-existing felsic crust or highly prolonged magma evolution. As the amount of migmatites at the current erosion level, especially within the CFGC, is very limited or non-existent, the magmas forming the Oittila suite granitoids must originate from deeper crustal levels. Only in the proximity of migmatitic paragneisses of the Pirkanmaa migmatite suite could the granitic dykes represent segregated melts at the current erosion level. However, the neosomes of these paragneisses are trondhjemitic (Mikkola et al. 2018b), and dykes interpreted as belonging to the Oittila suite are typically granitic. Additionally, the neosome formation of the paragneisses occurred at 1885 Ma (Mikkola et al. 2018b) and the age of the Oittila suite is ~1875 Ma (authors' unpublished data).

The Oittila suite and the Muurame granitoids are both K-rich and they display extensive compositional overlap in both major and trace elements (Figs 5, 6). Although the Oittila suite is on average more felsic and richer in K_2O, the separation of the units is strongly based on field observations. The Oittila suite has intrusive contacts with the Muurame granitoids. Most of the granite dykes intruded in relatively brittle crustal conditions, but older ones have been folded (Figs 3C, 4D). Based on compositional similarities and emplacement of the dykes, we interpret that the Oittila granitoids are a further evolved fraction of magmas similar to the Muurame granitoids. These two units form a continuum and the relationships between them can be explained by uplift and erosion between 1880 and 1875. This resulted in a shift in the pooling level of the ascending Muurame-type magmas to depths below the current erosion level. In proportion, the emplacement level of the more fractionated melts shifted from the now eroded parts to the present erosion level. Such a shift in the emplacement depth of the Jyväskylä suite in the central parts of the CFGC was also proposed by Nikkilä et al. (2016) based on the degree of deformation.

The large scatter that the Oittila suite displays in the trace element patterns (Figs 7, 8) may partly be connected with the highly evolved character and small volumes of the intrusive units. In granitoids, 70 wt% to 95 wt% of REE reside in accessory minerals, excluding Eu, which also resides in both feldspars (Bea 1996). Consequently, separation of the remaining melt fraction from the crystallised feldspars results in a negative Eu anomaly and high total REE, whereas the crystal mush left behind exhibits a positive Eu anomaly and low total REE. Both of the aforementioned REE pattern types are present in the analyses of the samples from the Oittila suite. It should be noted that it is possible that some of the Oittila granitoids could belong to the ca. 1800 Ma post-orogenic granites known from areas surrounding the CFGC (Alviola et al. 2001, Andersson et al. 2006, Kontinen et al. 2013). Hitherto, these have not been reported from within the CFGC itself. However, Kallio et al. (2018) tentatively linked the formation of the Suolikko mineralization (Fig. 2) to fluid released from a granitoid intrusion with an age of ca. 1790 Ma.

6.7 Rutalahti peridotites, a message from the mantle

Of the units with more mafic compositions, the one forming a distinct group on a compositional basis is the Rutalahti peridotite lithodeme, which displays consistently high Mg#, Ni, and Cr, as well as low Al_2O_3 and TiO_2 (Figs 5, 6). Some overlap with the MgO-rich cumulate members of the Vammala suite exists, but the mode of occurrence in the field efficiently distinguishes the two units (Fig. 2). The samples with the highest MgO, Cr and Ni are also poor in CaO, and are therefore likely to represent olivine±orthopyroxene cumulates. Precise estimation of the composition of the parental magma would require additional geochemical studies. However, based on the available data, the magma of the Rutalahti peridotites was more mafic than that of the Vammala suite, as even the most evolved compositions of the Rutalahti peridotites are ultramafic. The trace element patterns distinctly differ; the Rutalahti peridotites with their weakly enriched and fractionated REE patterns are more akin to the EMORB-type magmas than the arc-type magmas that form the Vammala suite (Figs 7, 8). However, the Rutalahti peridotite samples also display negative Nb anomalies and relatively high Th/Yb ratio (Fig. 10CD) characteristic of a source modified in an arc environment (e.g. Ducea et al. 2015). The observed variation in the enrichment in LILE could be due to varying degrees of contamination during ascent. The age of the Rutalahti peridotite lithodeme is not well constrained, although based on the field relationships it postdates the other units described here. The peridotites are emplaced in close proximity to major shear zones, and their formation and ascent could thus be related to partial melting of mantle triggered, for example, by delamination of the lower crust and the ascent of magmas via existing weakness zones.

6.8 Crustal evolution with emphasis on the granitoids

The voluminous plutonic units described in this study represent 20 Ma of Paleoproterozoic crustal growth belonging to the younger Svecofennian magmatism in the Central Finland area, i.e. 1900–1870 Ma (a.k.a. Central Ostrobothnia supergroup after Luukas et al. 2017). Magmatism linked to this phase has been interpreted in two fundamentally different ways: subduction-related arc magmatism (e.g. Nironen 2005, 2017, Lahtinen et al. 2009, 2017) or partial melting of crust thickened in the collision of exotic terranes with the Karelia craton at ~1.91 Ga (Nikkilä et al. 2016). The latter model was based on a study from an area with limited amounts of coeval mantle-derived melts at the current erosion level. In our study area, the Muurame granitoids forming the bulk of the CFGC are co-magmatic with more juvenile components, i.e. Vaajakoski quartz diorites, based on field relationships, age data and compositional characteristics. Therefore, we interpret that partial melting of thickened crust alone cannot explain the intrusion of these magmas, which display a similar compositional range to the modern day calc-alkaline arcs. The model of Nikkilä et al. (2016) is also problematic in terms of the location of southernmost Finland (Bergslagen block) as already adjacent to the CFGC at 1.89 Ga. This is contrary to the observation of Peltonen (2005) that the ultramafic-mafic intrusions intruding the Pirkanmaa suites are Vammala-type and differ from those in the Bergslagen block based, for example, on size and the proximity to volcanic units. As the boundary between the two gabbro types strictly follows the terrain boundary, the gabbros must have been emplaced before their amalgamation (Peltonen 2005). Thus, the age of these intrusions (ca. 1885 Ma) defines the maximum age for the collision between the Bergslagen area and the CFGC.

Instead of clear compositional differences between them, the Lammuste quartz diorites, Kangasniemi granodiorites, Muurame granitoids and Oittila granites form a succession towards more felsic compositions and higher LILE concentrations (Figs 5, 6). All units show trace element compositions resembling each other and characteristic of arc magmas, which tend to display a similar evolutionary trend as the arc matures (Ducea et al. 2015). Volcanic units coeval with the plutonic rocks along the southern boundary of the CFGC also have composition characteristics typical of continental arcs (Kähkönen 1989, Heikura 2017, Mikkola et al. 2018c). Based on the above, we connect the majority of the plutonic rocks in the present study area to an active subduction phase proposed, among others, by Nironen (2005, 2017) and Lahtinen et al. (2009, 2017).

The presence of the Saarijärvi suite granitoids with A-type compositional characteristics and

overlapping spatially and temporally with the calc-alkaline suites is somewhat atypical, as A-type granitoids are most often formed in anorogenic settings (Loiselle & Wones 1979). Elliot et al. (1998), Nikkilä et al. (2016) and Virtanen and Heilimo (2018) interpreted that the Saarijärvi suite granitoids are partial melts from the lower crust, forming a bimodal suite with diorites and quartz diorites. As intrusions of this suite are often close to major crustal fault zones, their emplacement is probably related to local transtensional or short-lived extensional settings formed in a predominantly compressional setting (e.g. Elliott et al. 1998, Nironen et al. 2000, Rämö et al. 2001, Virtanen & Heilimo 2018). Although the intrusions of the Saarijärvi suite display sharp boundaries with the Jyväskylä suite, the data of Virtanen and Heilimo (2018) and this study indicate that the two magma types locally mingled.

7 CONCLUSIONS

Instead of abrupt compositional changes, the majority of the units in the present study form a compositional continuum towards more felsic and evolved compositions.

A juvenile component, represented by the Vammala and Vaajakoski suites, as well as the Rutalahti lithodeme, provides evidence that the CFGC did not solely originate from partial melting of thickened pre-exiting crust.

The compositional similarities of the 1895–1875 Ma Svecofennian volcanic and plutonic units indicate that they are part of the same magmatic event.

The majority of the plutonic rocks along the southeastern boundary of the Central Finland Granitoid Complex represent calc-alkaline and alkali-calcic magmatism formed in a Paleoproterozoic continental arc during active subduction.

8 ACKNOWLEDGEMENTS

We kindly acknowledge everybody who has been involved in the field and data processing stages of this study, as well as Drs Jussi Heinonen and Laura Lauri for their reviews.

REFERENCES

Alviola, R., Mänttäri, R., Mäkitie, H. & Vaasjoki, M. 2001. Svecofennian rare-element granitic pegmatites of the Ostrobothnia region, western Finland; their metamorphic environment and time of intrusion. In: Mäkitie, H. (ed.) Svecofennian granitic pegmatites (1.86–1.79 Ga) and quartz monzonite (1.87 Ga), and their metamorphic environment in the Seinäjoki region, western Finland. Geological Survey of Finland, Special Paper 30, 9–29. Available at: http://tupa.gtk.fi/julkaisu/specialpaper/sp_030.pdf

Andersson, U. B., Eklund, O., Fröldö, S. & Konopelko, D. 2006. 1.8 Ga magmatism in the Fennoscandian Shield; lateral variations in subcontinental mantle enrichment. Lithos 86, 110–136

Bedrock of Finland - DigiKP. Digital map database [Electronic resource]. Espoo: Geological Survey of Finland [referred 31.04.2017]. Version 2.0.

Boynton, W. V. 1984. Cosmochemistry of the rare earth elements: meteorite studies. In: Henderson, P. (ed.) Rare earth element geochemistry. Amsterdam: Elsevier, p. 63.

Ducea, M. N., Saleeby, J. B. & Bergantz, G. 2015. The Architecture, Chemistry, and Evolution of Continental Magmatic Arcs. Annual Review of Earth and Planetary Sciences 43, 299–331.

Elliott, B. A. 2003. Petrogenesis of the Post-kinematic Magmatism of the Central Finland Granitoid Complex II; Sources and Magmatic Evolution. Journal of Petrology 44, 1681–1701.

Eskola, P. 1932. On the origin of granitic magmas. Zeitschrift für Kristallographie, Mineralogie und Petrographie 42, 455–481. (in German)

Frost, B. R., Barnes, C. G., Collins, J. W., Arculus, J. R., Ellis, J. D. & Frost C. D. 2001. A Geochemical Classification for Granitic Rocks. Journal of Petrology 42, 2033–2048.

Halonen, S. 2015. Keski-Suomen granitoidikompleksin malmiviitteet Hiekkapohjan alueella. Unpublished master's thesis, University of Oulu, Oulu Mining School. 100 p. (in Finnish). Available at: http://jultika.oulu.fi/files/nbnfioulu-201511242172.pdf

Heikura, A. 2017. The volcanic rocks of the Länkipohja-Jämsä area in the southern part of the Central Finland Granitoid Complex. Unpublished master's thesis, University of Oulu, Oulu Mining School. 81 p. Available at: http://tupa.gtk.fi/opinnayte/heikura_antti_gradu.pdf

Heilimo, E., Mikkola, P., Niemi, S., Luukas, J. & Halonen, S. 2017. Hiekkapohja ore showings in Paleoproterozoic Central Finland Granitoid Complex - a hydrothermal system? Proceedings of the 14th SGA Biennial Meeting, 20–23 August 2017, Québec City, Canada, 359–362.

Hölttä, P. S. & Heilimo, E. 2017. Metamorphic map of Finland. In: Nironen, M. (ed.) Bedrock of Finland at the scale 1:1 000 000 - Major stratigraphic units, metamorphism and tectonic evolution. Geological Survey of Finland, Special Paper 60, 77–127. Available at: http://tupa.gtk.fi/julkaisu/specialpaper/sp_060.pdf

Huhma, H., Claesson, S., Kinny, P. D. & Williams, I. S. 1991. The growth of Early Proterozoic crust: new evidence from Svecofennian zircons. Terra Nova 3, 175–179.

Ikävalko, O. 1981. Makkolan-Kokonkylän suprakrustinen vyöhyke. Unpublished master's thesis, University of Helsinki, Department of Geology and Mineralogy. 119 p. (in Finnish)

Kähkönen, Y. 1989. Geochemistry and petrology of the metavolcanic rocks of the early Proterozoic Tampere Schist Belt, southern Finland. Geological Survey of Finland, Bulletin 345, 1–104. Available at: http://tupa.gtk.fi/julkaisu/bulletin/bt_345.pdf

Kallio, J. 1986. Joutsan kartta-alueen kallioperä. Summary: Pre-Quaternary Rocks of the Joutsa Map-Sheet area. Geological Map of Finland 1:100 000, Explanation to the Maps of Pre-Quaternary Rocks, Sheet 3122. Geological Survey of Finland. 56 p. Available at: http://tupa.gtk.fi/kartta/kallioperakartta100/kps_3122.pdf

Kallio, V., Mikkola, P., Huhma, H. & Niemi, S. 2018. Suolikko Pb-Zn mineralisation and its country rocks in Muurame, Central Finland. In: Mikkola, P., Hölttä, P. & Käpyaho, A. (eds) Development of the Paleoproterozoic Svecofennian orogeny: new constraints from the southeastern boundary of the Central Finland Granitoid Complex. Geological Survey of Finland, Bulletin 407. (this volume). Available at: https://doi.org/10.30440/bt407.10

Kohonen, J. 1988. Salmenkylän gabron Ni-Cu-tutkimukset Kangasniemen kunnassa vuosina 1979–1985. Geological Survey of Finland, archive report M19/3213/-88/2/10. 11p., 12 app. (in Finnish). Available at: http://tupa.gtk.fi/raportti/arkisto/m19_3213_88_2_10.pdf

Kontinen, A., Huhma, H., Lahaye, Y. & O´Brien, H. 2013. New U-Pb zircon age, Sm-Nd isotope and geochemical data on Proterozoic granitic rocks in the area west of the Oulunjärvi Lake, Central Finland. In: Hölttä, P. (ed.) Current Research: GTK Mineral Potential Workshop, Kuopio, May 2012. Geological Survey of Finland, Report of Investigation 198, 70–74. Available at: http://tupa.gtk.fi/julkaisu/tutkimusraportti/tr_198.pdf

Kotilainen, A. K., Mänttäri, I., Kurhila, M., Hölttä, P. & Rämö, O. T. 2016. Evolution of a Palaeoproterozoic giant magmatic dome in the Finnish Svecofennian; New insights from U–Pb geochronology. Precambrian Research 272, 39–56.

Lahtinen, R., Huhma, H., Kähkönen, Y. & Mänttäri, I. 2009. Paleoproterozoic sediment recycling during multiphase orogenic evolution in Fennoscandia, the Tampere and Pirkanmaa belts, Finland. Precambrian Research 174, 310–336.

Lahtinen, R., Huhma, H., Lahaye, Y., Lode, S., Heinonen, S., Sayab, M. & Whitehouse, M. J. 2016. Paleoproterozoic magmatism across the Archean-Proterozoic boundary in central Fennoscandia: Geochronology, geochemistry and isotopic data (Sm-Nd, Lu-Hf, O). Lithos 262, 507–525.

Lahtinen, R., Huhma, H., Sipilä, P. & Vaarma, M. 2017. Geochemistry, U-Pb geochronology and Sm-Nd data from the Paleoproterozoic Western Finland supersuite – A key component in the coupled Bothnian oroclines. Precambrian Research 299, 264–281.

Luukas, J., Kousa, J., Nironen, M. & Vuollo, J. 2017. Major stratigraphic units in the bedrock of Finland, and an approach to tectonostratigraphic division. In: Nironen, M. (ed.) Bedrock of Finland at the scale 1:1 000 000 - Major stratigraphic units, metamorphism and tectonic evolution. Geological Survey of Finland, Special Paper 60, 9–40. Available at: http://tupa.gtk.fi/julkaisu/specialpaper/sp_060.pdf

Loiselle, M. C. & Wones, D. R. 1979. Characteristics and origin of anorogenic granites. Geological Society of America Abstracts with Programs 11, p. 468.

Makkonen, H. V. 2015. Nickel Deposits of the 1.88 Ga Kotalahti and Vammala Belts. In: Maier, W. D., Lahtinen, R. & O´Brien, H. (eds) Mineral Deposits of Finland. Elsevier Science B.V., 253–290.

McDonough, W. F. & Sun, S.-S. 1995. Composition of the Earth. Chemical Geology 120, 223–253.

Middlemost, E. A. K. 1994. Naming materials in magma/igneous rock system. Earth Science Review 37, 215–224.

Mikkola, P., Heilimo, E., Aatos, S., Ahven, M., Eskelinen, J., Halonen, S., Hartikainen, A., Kallio, V., Kousa, J., Luukas, J., Makkonen, H., Mönkäre, K., Niemi, S., Nousiainen, M., Romu, I. & Solismaa, S. 2016. Jyväskylän seudun kallioperä. Summary: Bedrock of the Jyväskylä area. Geological Survey of Finland, Report of Investigation 227. 95 p., 6 apps. Available at: http://tupa.gtk.fi/julkaisu/tutkimusraportti/tr_227.pdf

Mikkola, P., Heilimo, E., Luukas, J., Kousa, J., Aatos, S., Makkonen, H., Niemi, S., Nousiainen, M., Ahven, M., Romu, I. & Hokka, J. 2018a. Geological evolution and structure along the southeastern border of the Central Finland Granitoid Complex. In: Mikkola, P., Hölttä, P. & Käpyaho, A. (eds) Development of the Paleoproterozoic Svecofennian orogeny: new constraints from the southeastern boundary of the Central Finland Granitoid Complex. Geological Survey of Finland, Bulletin 407. (this volume). Available at: https://doi.org/10.30440/bt407.1

Mikkola, P., Huhma, H., Romu, I. & Kousa, J. 2018b. Detrital zircon ages and geochemistry of the metasedimentary rocks along the southeastern boundary of the Central Finland Granitoid Complex. In: Mikkola, P., Hölttä, P. & Käpyaho, A. (eds) Development of the Paleoproterozoic Svecofennian orogeny: new constraints from the southeastern boundary of the Central Finland Granitoid Complex. Geological Survey of Finland, Bulletin 407. (this volume). Available at: https://doi.org/10.30440/bt407.2

Mikkola, P., Mönkäre, K., Ahven, M. & Huhma, H. 2018c. Geochemistry and age of the Paleoproterozoic Makkola suite volcanic rocks in central Finland. In: Mikkola, P., Hölttä, P. & Käpyaho, A. (eds) Development of the Paleoproterozoic Svecofennian orogeny: new constraints from the southeastern boundary of the Central Finland Granitoid Complex. Geological Survey of Finland, Bulletin 407. (this volume). Available at: https://doi.org/10.30440/bt407.5

Mutanen, T. 2011. Alkalikiviä ja appiniitteja. Raportti hankkeen Magmatismi ja malminmuodostus II toiminnasta 2002-2005. Geological Survey of Finland, archive report 9/2011. 627 p. (in Finnish). Available at: http://tupa.gtk.fi/raportti/arkisto/9_2011.pdf

Nikkilä, K., Mänttäri, I., Nironen, M., Eklund, O. & Korja, A. 2016. Three stages to form a large batholith after

terrane accretion – An example from the Svecofennian orogen. Precambrian Research 281, 618–638.

Nironen, M. 1997. The Svecofennian Orogen: a tectonic model. Precambrian Research 86, 21–44.

Nironen, M. 2005. Proterozoic orogenic granitoid rocks. In: Lehtinen, M., Nurmi, P. & Rämö, O. T. (eds) The Precambrian Bedrock of Finland - Key to the evolution of the Fennoscandian Shield. Elsevier Science B.V., 443–479.

Nironen, M. 2017. Guide to the Geological Map of Finland – Bedrock 1:1 000 000. In: Nironen, M. (ed.) Bedrock of Finland at the scale 1:1 000 000 - Major stratigraphic units, metamorphism and tectonic evolution. Geological Survey of Finland, Special Paper 60, 41–76. Available at: http://tupa.gtk.fi/julkaisu/specialpaper/sp_060.pdf

Nironen, M., Kousa, J., Luukas, J. & Lahtinen, R. (eds) 2016. Geological Map of Finland – Bedrock 1:1 000 000. Espoo: Geological Survey of Finland. Available at: http://tupa.gtk.fi/kartta/erikoiskartta/ek_097_300dpi.pdf

Pearce, J. A. & Peate, D. W. 1995. Tectonic implications of the composition of volcanic arc magmas. Annual Reviews Earth and Planetary Sciences 23, 251–285.

Pearce, J. A., Harris, N. B. W. & Tindle, A. G, 1984. Trace element discrimination diagrams for the tectonic interpretation of granitic rocks. Journal of Petrology 25, 956–98.

Peltonen, P. 1995. Petrogenesis of ultramafic rocks in the Vammala Nickel Belt: Implications for crustal evolution of the early Proterozoic Svecofennian arc terrane. Lithos 34, 253–274.

Peltonen, P. 2005. Svecofennian mafic-ultramafic intrusions. In: Lehtinen, M., Nurmi, P. & Rämö, O. T. (eds) The Precambrian Bedrock of Finland - Key to the evolution of the Fennoscandian Shield. Elsevier Science B.V., 407–441.

Rämö, O. T., Vaasjoki, M., Mänttäri, I., Elliott, B. A. & Nironen, M. 2001. Petrogenesis of the Post-kinematic Magmatism of the Central Finland Granitoid Complex I; Radiogenic Isotope Constraints and Implication for Crustal Evolution. Journal of Petrology 42, 1971–1993.

Rasilainen, K., Lahtinen, R. & Bornhorst, T. J. 2007. The Rock Geochemical Database of Finland Manual. Geological Survey of Finland, Report of Investigation 164. 38 p. Available at: http://tupa.gtk.fi/julkaisu/tutkimusraportti/tr_164.pdf

Sillitoe, R. H. 2010. Porphyry Copper System. Economic geology 105, 3–41.

Simonen, A. 1960. Plutonic rocks of the Svecofennides in Finland. In: Simonen, A. Plutonic rocks of the Svecofennides in Finland. Geological Survey of Finland, Bulletin 189, 1–101. Available at: http://tupa.gtk.fi/julkaisu/bulletin/bt_189.pdf

Simonen, A. 1980. The Precambrian in Finland. In: Simonen, A. The Precambrian in Finland. Geological Survey of Finland, Bulletin 304, 1–58. Available at: http://tupa.gtk.fi/julkaisu/bulletin/bt_304.pdf

Sorjonen-Ward, P. 2006. Geological and structural framework and preliminary interpretation of the FIRE 3 and FIRE 3A reflection seismic profiles, central Finland. In: Kukkonen, I. T. & Lahtinen, R. (eds) Finnish Reflection Experiment FIRE 2001–2005. Geological Survey of Finland, Special paper 43, 105–159. Available at: http://tupa.gtk.fi/julkaisu/specialpaper/sp_043.pdf

Tatsumi, Y., Hamilton, D. L. & Nesbitt R. W. 1986. Chemical characteristics of fluid phase released from a subducted lithosphere and origin of arc magmas: Evidence from high-pressure experiments and natural rocks. Journal of Volcanology and Geothermal Research 29, 293–309.

Virtanen, V. & Heilimo, E. 2018. Petrology of the geochemically A-type Saarijärvi suite: evidence for bimodal magmatism. In: Mikkola, P., Hölttä, P. & Käpyaho, A. (eds) Development of the Paleoproterozoic Svecofennian orogeny: new constraints from the southeastern boundary of the Central Finland Granitoid Complex. Geological Survey of Finland, Bulletin 407. (this volume). Available at: https://doi.org/10.30440/bt407.7

Development of the Paleoproterozoic Svecofennian orogeny: new constraints from the southeastern boundary of the Central Finland Granitoid Complex
Edited by Perttu Mikkola, Pentti Hölttä and Asko Käpyaho
Geological Survey of Finland, Bulletin 407, 130–150, 2018

PETROLOGY OF THE GEOCHEMICALLY A-TYPE SAARIJÄRVI SUITE: EVIDENCE FOR BIMODAL MAGMATISM

by

Ville J. Virtanen[1)] and Esa Heilimo[2)]

Virtanen, V. J. & Heilimo, E. 2018. Petrology of the geochemically A-type Saarijärvi suite: evidence for bimodal magmatism. *Geological Survey of Finland, Bulletin 407*, 130–150, 10 figures and 2 tables.

The Central Finland Granitoid Complex is mainly composed of calc-alkaline I-type granitoids and less voluminous cross-cutting A-type Saarijärvi suite granitoids, both formed in the mainly convergent Paleoproterozoic Svecofennian orogeny. The bimodal Saarijärvi suite consists of felsic, often porphyritic, granitoids and quartz monzonites and to lesser extent of equigranular gabbros, diorites, quartz diorites and tonalites. The quartz monzonites and granites are weakly to non-foliated and contain biotite and hornblende as the dominant mafic minerals, while pyroxene is locally present. High FeO, K_2O, Ba and Zr, together with low MgO, CaO and Sr contents, indicate an A-type geochemical affinity. High Al_2O_3, Ba and Eu contents, however, deviate from the typical A-type geochemistry. Furthermore, some of the samples have volcanic arc granite (VAG) characteristics, instead of within-plate granite (WPG) affinity. The geochemistry of the granites and quartz monzonites is similar to such A-type granitoids that formed by differentiation of mantle-derived (juvenile) mafic magma with assimilation of crustal material in a high-pressure regime. Field observations of mafic microgranular enclaves (MMEs) and synplutonic dykes representing the mafic component in granites and quartz monzonites suggest a clear petrogenetic linkage with these rocks. One of the quartz monzonite intrusions hosts a synplutonic dyke and ubiquitous MMEs, pointing to continuous mafic input during the crystallization of the intrusion. Our geochemical modelling suggests mingling with minor chemical exchange between the felsic and mafic magmas during the emplacement.

Appendix 1 is available at: http://tupa.gtk.fi/julkaisu/liiteaineisto/bt_407_appendix_1.pdf

Electronic Appendix is available at: http://tupa.gtk.fi/julkaisu/liiteaineisto/bt_407_electronic_appendix.xlsx

Keywords: Central Finland Granitoid Complex, Paleoproterozoic, geochemistry, A-type, granites, diorites, bimodal, mingling, Svecofennian, Finland

[1)] *Department of Geosciences and Geography, University of Helsinki, P.O. Box 64, FI-00014 Helsinki, Finland*
[2)] *Geological Survey of Finland, P.O. Box 1237, FI-70211 Kuopio, Finland*

VERTAISARVIOITU
KOLLEGIALT GRANSKAD
PEER-REVIEWED
www.tsv.fi/tunnus

https://doi.org/10.30440/bt407.7

Editorial handling by Perttu Mikkola.

Received 30 November 2017; Accepted 15 April 2018

1 INTRODUCTION

A-type granitoids typically form in anorogenic or extensional tectonic settings, and their geochemical features are distinctive from typically syn-collisional I- and S-type granitoids (Loiselle & Wones 1979). Characteristic A-type geochemistry is commonly defined by high (ferroan) Fe/(Fe+Mg), K_2O/Na_2O and Ga/Al ratios, as well as a high concentration of total alkalis, large ion lithophile elements (LILE), high field strength elements (HFSE) and trivalent rare earth elements (REE) (e.g. Loiselle & Wones 1979, Collins et al. 1982, Pearce et al. 1984, Whalen et al. 1987). A-type magmas are depleted in Al_2O_3, MgO, CaO and trace elements that are compatible in mafic silicates (e.g. Sc, Cr, Co, Ni) or in feldspars (Ba, Sr and Eu; Loiselle & Wones 1979). Aluminium saturation ranges from peralkaline to metalumious to mildly peraluminous varieties (e.g. Collins et al. 1982, Eby 1990, Frost & Frost 2011). Many petrogenetic models exist for geochemically different types of A-type granitoids. Differentiation from alkali basalt (Loiselle & Wones 1979) forms alkalic to alkali-calcic peralkaline granitoids (Frost & Frost 2011), whereas differentiation from tholeiitic basalt (Eby 1990, Frost & Frost 1997, Barbarin 1999) generally forms alkalic to alkali-calcic, metaluminous to weakly peraluminous granitoids (Frost & Frost 2011). Low-pressure dehydration melting of biotite- or amphibole-bearing quartzofeldspathic rocks (e.g. Rämö & Haapala 1995, Patiño Douce 1997) forms calc-alkalic metaluminous to peraluminous granitoids (Frost & Frost 2011). Combinations of these petrogenetic processes are not uncommon, and crustal assimilation during basaltic differentiation tends to drive the composition towards a more calcic and aluminium-rich (from peralkaline to metaluminous to peraluminous) direction (Frost & Frost 2011).

Felsic A-type granitoids often form a bimodal system with coeval mafic rocks, and interaction structures are common (e.g. Didier & Barbarin 1991, Barbarin 2005). It has been proposed that in these bimodal settings, mafic magmas could either act as the necessary heat source for crustal melting or that granitic magma could form by differentiation from mafic parental magma (e.g. Bridgwater et al. 1974, Emslie 1978, Eby 1990, Eklund et al. 1994, Rämö & Haapala 1995, Frost & Frost 1997). Many factors control the nature of interactions between mafic and felsic magmas, e.g. the relative proportions of the magmas, magma compositions (especially SiO_2 contents), dissolved volatiles, temperatures, viscosities and the crystallinities of the magmas (e.g. Furman & Spera 1985, Sparks & Marshall 1986, Fernandez & Barbarin 1991, Giordano et al.

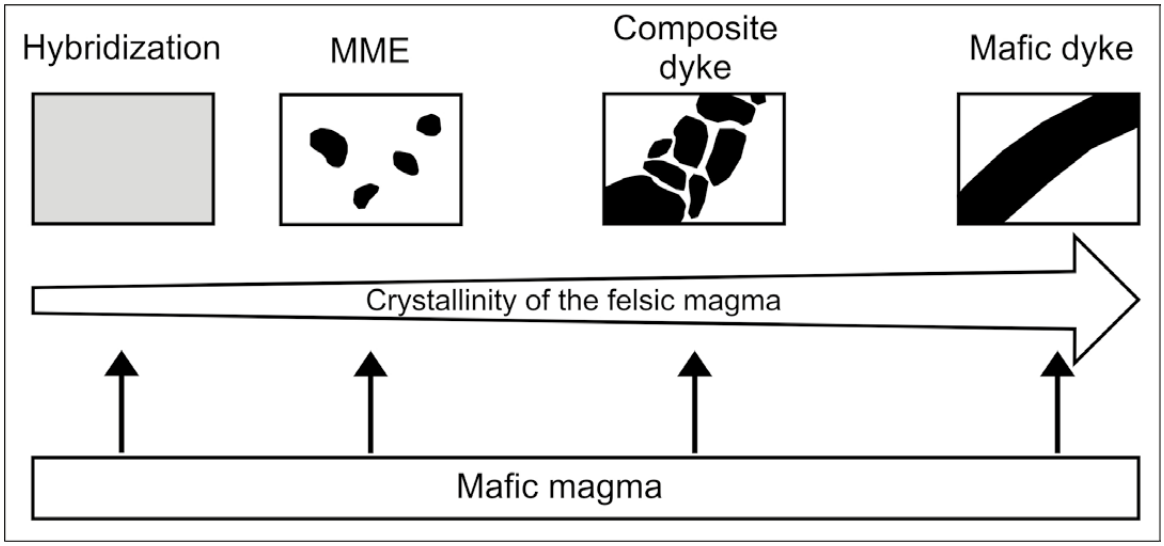

Fig. 1. A schematic diagram showing the effect that the crystallinity of felsic magma (white) has on the behaviour of intruding mafic magma (black). At a low level of crystallinity, the mafic and felsic magmas thoroughly mix, leading to homogeneous hybrid rock. When the crystallinity level increases, the magmas mingle and microgranular mafic enclaves (MMEs) form. A further increase in crystallinity inhibits the efficient transportation of mafic magma and synplutonic dykes form. After Fernandez and Barbarin (1991).

2008). Generally, when the proportion of the hotter mafic magma is relatively large and the crystallinity of the magmas is low, thermal equilibrium may be established between the mafic and felsic magmas. As the mafic magma cools down and heats the felsic magma, their viscosity difference becomes small and they may thoroughly mix to form a hybrid magma (Anderson 1976, Reid 1983, Sparks & Marshall 1986, Fernandez & Barbarin 1991, Andersson & Eklund 1994, Salonsaari 1995, Fig. 1). A smaller proportion of mafic magma cools down and solidifies too rapidly for the thermal equilibrium to be reached, impeding mixing and leading to the formation of mafic microgranular enclaves (MMEs) and synplutonic composite dykes by magma mingling (Sparks & Marshall 1986, Barbarin & Didier 1991, Fernandez & Barbarin 1991, Fig. 1).

The Central Finland Granitoid Complex (CFGC, Fig. 2) formed in the dominantly convergent Svecofennian orogeny, which started at 1.91 Ga (Lahtinen 1994, Nironen 1997). At the current erosion level, it is mainly composed of 1.89–1.88 Ga calc-alkaline I-type granitoids (Front & Nurmi 1987), here the Jyväskylä suite after Mikkola et al. (2016). The volumetrically minor bimodal Saarijärvi suite (Fig. 2) sharply cross-cuts the Jyväskylä suite granitoids, although the ages partly overlap at 1.88–1.87 Ga (Huhma 1986, Elliott et al. 1998, Mikkola et al. 2016). Granitoids of the Saarijärvi suite have A-type geochemical affinity and they are closely associated with coeval minor mafic intrusives of the same suite (Elliott et al. 1998, Mikkola et al. 2016, Nikkilä et al. 2016). It has been proposed that the felsic members of the Saarijärvi suite formed either by differentiation from mafic magma with a minor crustal component (Nironen et al. 2000, Elliott 2003) or by remelting of mafic lower crustal residue after extraction of the Jyväskylä suite parental magmas (Nikkilä et al. 2016). In the literature, the Saarijärvi suite has previously been referred to as a postkinematic suite by Elliott et al. (1998) and Nironen (2003), among others, and as Group 3 by Nikkilä et al. (2016).

The aim of this paper is to petrographically and geochemically characterize the Saarijärvi suite rocks of the southeastern CFGC (Figs 2 & 3) by comparing them with previously studied members of the suite. Classification diagrams for granitoids, based

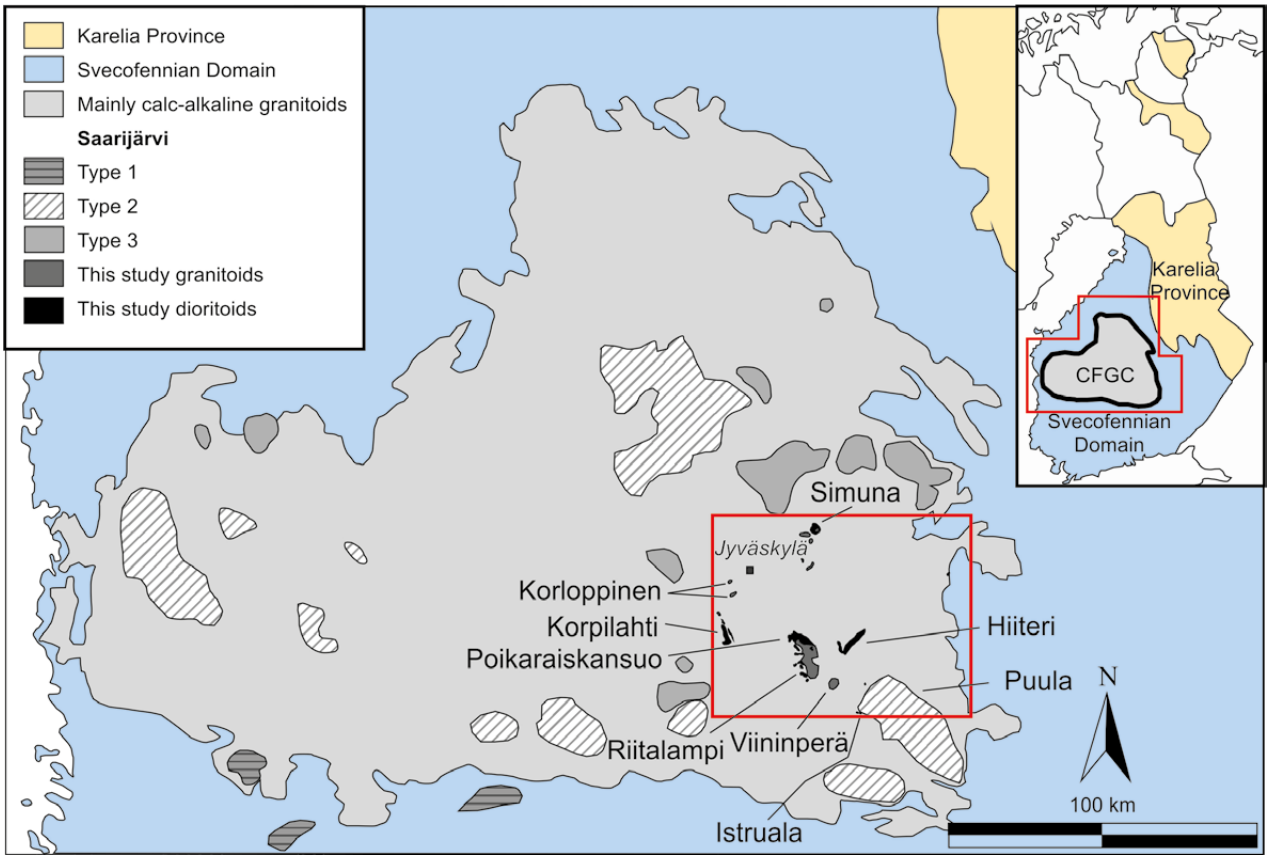

Fig. 2. Geological map of the Central Finland Granitoid Complex showing the locations of the Saarijärvi suite intrusions. The names of the intrusions within the study area, indicated by the red rectangle, are shown in the figure.

on whole-rock geochemistry, are utilized to make petrogenetic interpretations for the rocks of the study area, and the results are compared with more comprehensively studied rocks of the CFGC. In addition, we emphasize the interaction between felsic and mafic magmas of the Saarijärvi suite by presenting petrographic evidence together with a simple geochemical model suggesting mingling between these contrasting magmas.

2 GEOLOGICAL SETTING

The bedrock of Central Finland formed during the Paleoproterozoic convergent Svecofennian orogeny, when crustal material accreted to the Archean Karelia Province (e.g. Lahtinen 1994, Nironen 1997, 2017). The accretion of the well-studied Svecofennian orogeny started ca. 1.91 Ga, when Paleoproterozoic crustal blocks amalgamated to the southeastern edge of the Karelia Province (Lahtinen 1994, Nironen 1997). Subsequent collisions of island arcs caused the peak of the metamorphism mostly in upper amphibolite and granulite facies at 1.89–1.88 Ga (Nironen 1997).

The study area is located in the southeastern CFGC (Fig. 2), in the core part of the Svecofennian orogeny close to the boundary of the Western Finland supersuite (Fig. 3). In our study area, the Western Finland supersuite is represented by the Pirkanmaa migmatite suite, mainly consisting of migmatized greywackes, which were deposited close to 1.91 Ga (Lahtinen et al. 2009, Mikkola et al. 2018b). These metasedimentary rocks are intruded by calc-alkaline and alkaline-calcic, Na-rich I-type ~1895 Ma (Kallio 1986, authors' unpublished data) tonalites and granodiorites of the Pirkanmaa intrusive suite. These medium-grained, granular and foliated plutonic rocks dominate the SE part of the study area and contain xenoliths of the migmatitic paragneiss and MMEs that resemble the diorite and quartz diorite intrusions of the area (Heilimo et al. 2018). Rocks of both of the Pirkanmaa suites are intruded by small mafic to ultramafic intrusions and boudinaged dykes of the Vammala suite with ages close to 1885 Ma (Mikkola et al. 2016).

The central part of study area is transected by a large-scale dextral shear zone trending NE–SW (Mikkola et al. 2018a, Fig. 3). Near this Leivonmäki shear zone, the bedrock mainly consists of the Makkola suite, consisting of supracrustal units and associated plutonic rocks. The Makkola suite represents calc-alkaline arc-type magmatism and yields ages from 1895 to 1875 Ma (Mikkola et al. 2018c). The Makkola suite is preserved at a lower metamorphic stage (amphibolite facies) compared to the rest of the study area (Hölttä & Heilimo 2016).

The bulk of the bedrock northwest of the Leivonmäki shear zone consists of plutonic rocks of the CFGC belonging to the 1885–1880 Ma Jyväskylä suite (Rämö et al. 2001, authors' unpublished data, Fig. 3). The most common rocks of the Jyväskylä suite are K-feldspar porphyritic granitoids of the Muurame lithodeme and equigranular quartz diorites of the Vaajakoski lithodeme (Heilimo et al. 2018, Table 1). Small leucocratic calc-alkaline intrusions and dykes of the 1875 Ma Oittila suite cross-cut the Jyväskylä, Makkola and Saarijärvi suites and the Pirkanmaa lithodeme (Mikkola et al. 2016, Heilimo et al. 2018).

The Saarijärvi suite intrusions can be found throughout the CFCG, and they have usually been emplaced near crustal-scale shear systems (Fig. 2, Nironen et al. 2000, Nikkilä et al. 2016). The previous name, postkinematic, is based on the interpretation that these intrusions record the local termination of compressional deformation within the CFGC, and the initiation of extensional or transtensional regimes in the areas of their occurrence (Elliott et al. 1998, Nironen et al. 2000, Mikkola et al. 2016). In the study area, the largest of these granitoid intrusions is the 40 x 10 km^2 Puula granite, which often contains enclaves of the local country rocks. Smaller Riitalampi and Viiniperä intrusions (Fig. 3) mainly consist of porphyritic quartz monzonites, which locally display a rapakivi-like texture (*sensu lato*) at the macroscopic scale (Fig. 4A, B). Due to mineralogical variation, the term granitoid is used in this paper when referring to the felsic members of the Saarijärvi suite. Approximately ten smaller intrusions included in the Saarijärvi suite granitoids are known from other parts of the study area, and like the larger ones, they are located near large-scale southeast-trending faults (Mikkola et al. 2016).

Four mineralogically and geochemically distinct types (Type 1, 2, 3a, and 3b) of the Saarijärvi suite granitoids have been identified (Elliott et al. 1998,

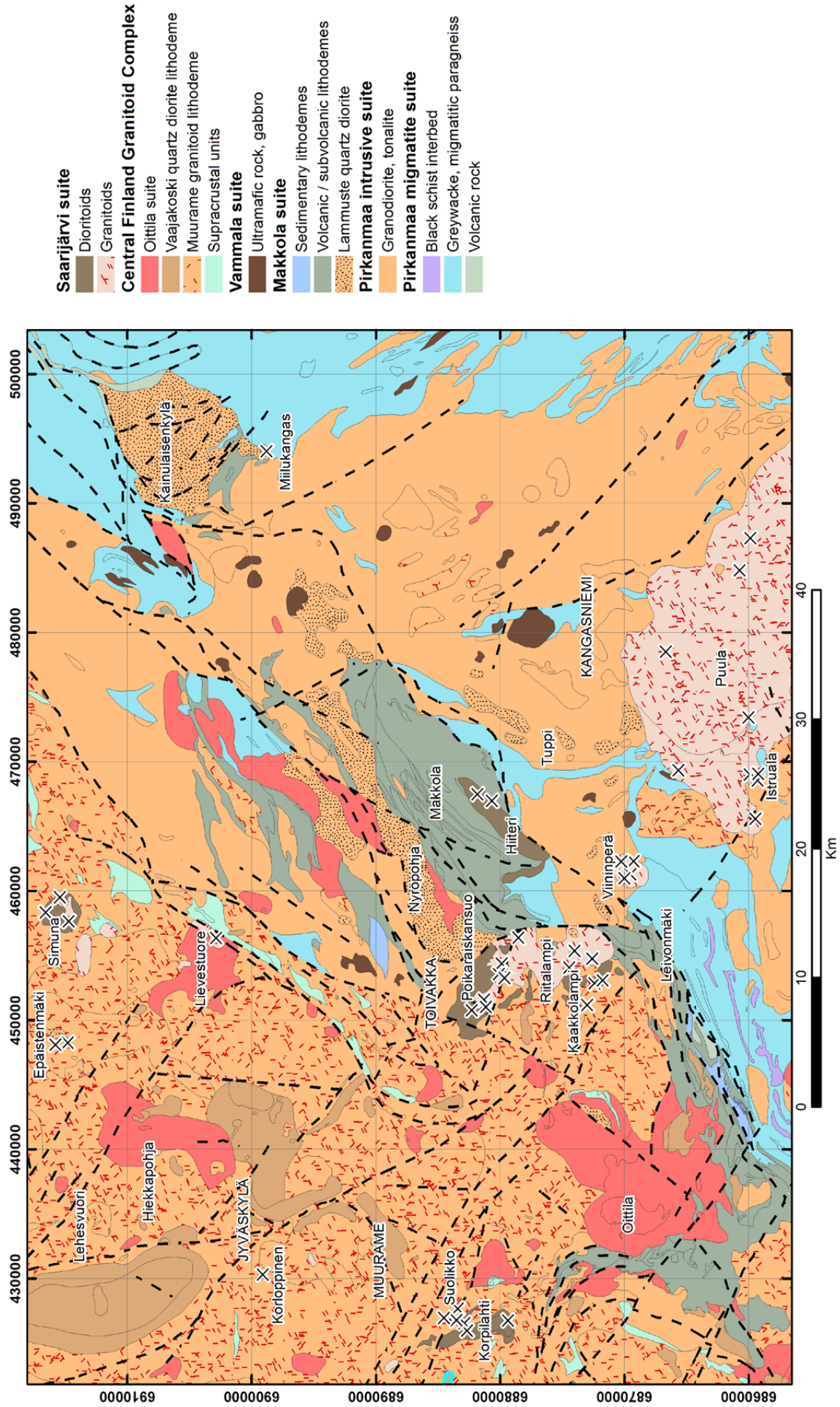

Fig. 3. Geological map of the study area. Sample localities of the studied intrusions (granitoids: Puula, Viininperä, Riitalampi, Korloppinen; dioritoids: Istruala, Hiiteri, Poikaraiskansuo, Korpilahti, Simuna) are indicated by crosses. Stippled lines represent shear zones and the SW–NE-trending Leivonmäki shear zone is marked between Riitalampi and Viininperä intrusions. Map modified from Mikkola et al. (2016).

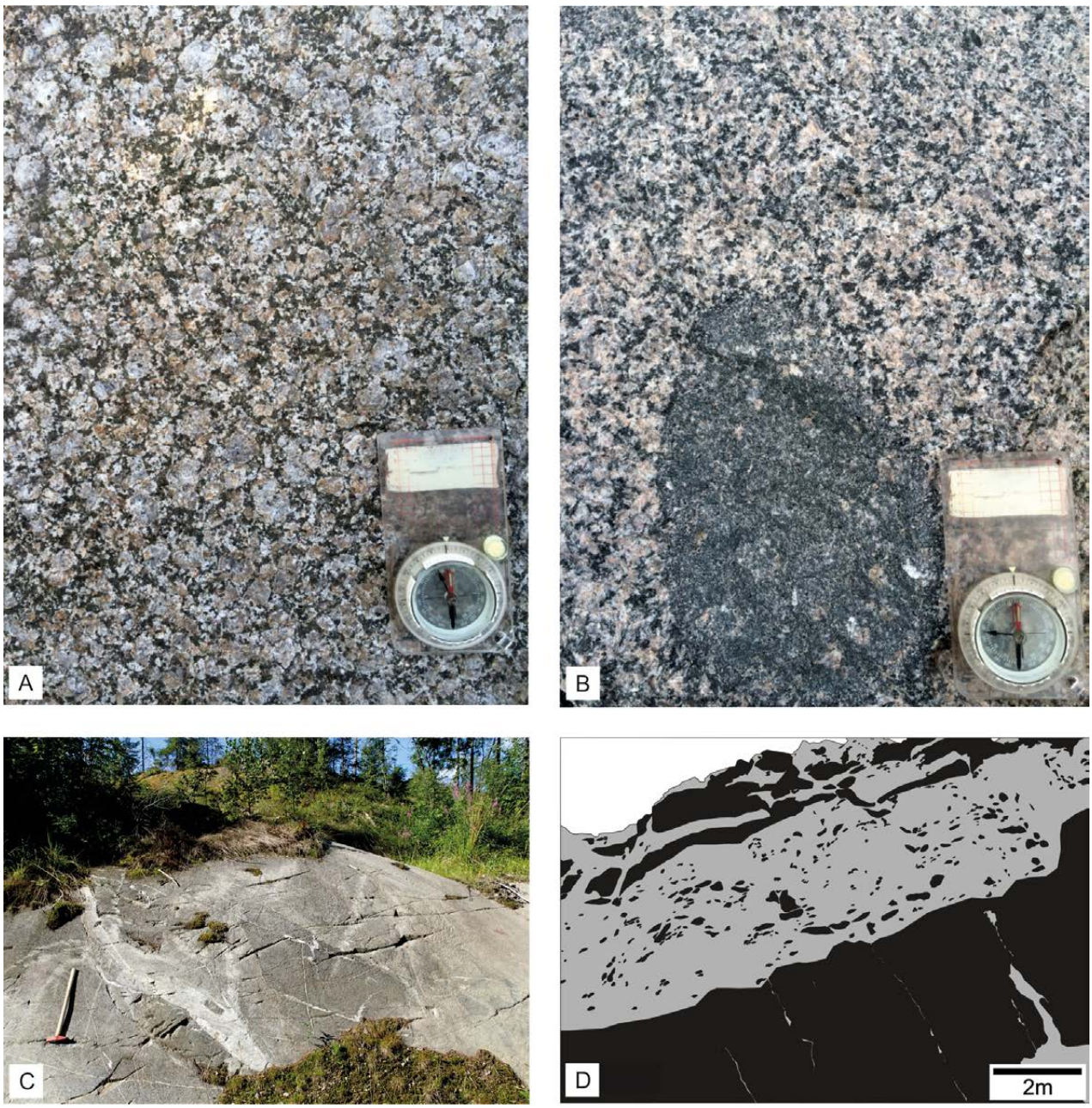

Fig. 4. A) Typical unfoliated quartz monzonite of the Viininperä intrusion, with pinkish subhedral K-feldspar phenocrysts, some of which are partially mantled by white plagioclase and quartz. Mafic silicates, i.e. biotite and hornblende, are mainly present as interstitial grain aggregates. Length of the compass 12 cm. B) A microgranular mafic enclave (MME)-bearing quartz monzonite sample from Viininperä intrusion. Alkali feldspar and plagioclase xenocrysts in the MME are derived from the host quartz monzonite. C) A gabbro outcrop from the Simuna intrusion representing the mafic members of the Saarijärvi suite. Cross-cutting magma pulses are observable as a variable grain size. Length of the hammer 60 cm. Photo by Marjaana Ahven. D) Sketch of the quarry wall at the Riitalampi intrusion showing the synplutonic occurrence of the lithologies and mingling. Grey represents quartz monzonite and black diorite. The black globules are dioritic MMEs that intruded into quartz monzonite, which was in a partially molten state. The synplutonic dyke (at the bottom of the wall) intruded into nearly solid quartz monzonite, after which the quartz monzonite back-veined into diorite.

Nironen et al. 2000). Type 1 rocks are granodiorites and granites with biotite as the only mafic main mineral (Table 1), and they are more strongly peraluminous compared to the other types that range from metaluminous to marginally peraluminous (Elliott et al. 1998, Nironen et al. 2000). Biotite ± hornblende-bearing granites of Type 2 are characterized by accessory fluorite (Table 1), and they are generally more silica-rich than the other types (Elliott et al. 1998, Nironen et al. 2000). Type 3b

Table 1. The rock types and typical mineralogy of granitoids of Jyväskylä and Saarijärvi suites. After Front and Nurmi (1987), Elliott et al. (1998), Rämö et al. (2001).

	Jyväskylä suite	**Saarijärvi suite granitoids**			
		Type 1	**Type 2**	**Type 3a**	**Type 3b**
Rock type	tonalite, granodiorite, and granite	granodiorite and monzogranite	monzogranite	monzogranite, quartz monzonite, and quartz syenite	granodiorite and quartz monzonite
Main mafic silicates	biotite ± hornblende ± pyroxene	biotite	biotite ± hornblende	biotite, hornblende ± pyroxene	biotite, hornblende, pyroxene ± olivine
Typical accessory minerals	apatite, zircon, titanite, magnetite	zircon, apatite, ilmenite ± fluorite	fluorite, zircon, apatite, titanite, allanite, ilmenite	zircon, apatite, titanite, ilmenite ± magnetite	zircon, apatite, titanite, ilmenite ± magnetite

quartz monzonites and granites have a mafic mineral assemblage of biotite, hornblende, pyroxene ± fayalite (Table 1), and they are the most mafic granitoids of the Saarijärvi suite (Nironen et al. 2000, Rämö et al. 2001). Geochemically, Type 3a rocks overlap with Types 2 and 3b, and the intrusions often have pyroxene-bearing margins (Nironen et al. 2000).

Mafic members of the Saarijärvi suite show variation from gabbro to quartz diorite and locally up to tonalites as the most evolved members. Due to this variation, they are referred to as dioritoids in this paper. They are typically spatially and temporally associated with the suite's felsic members, although exceptions exist (Figs 2, 3, 4D). A typical feature of the intrusions is the presence of several magma pulses forming diverse cross-cutting relationships, e.g. in the Simuna (Fig. 4C) and Korpilahti intrusions (Fig. 3). The intrusions are typically equigranular, but some of them, e.g. the Hiiteri intrusion, are plagioclase porphyritic (Mikkola et al. 2016).

3 MATERIALS AND METHODS

Systematic field observations and sampling were carried out in the study area during 2012–2016. A total of 44 samples were included in this study for optical petrography and whole-rock geochemical analysis. The whole-rock geochemical analyses were performed by Labtium Ltd using X-ray fluorescence (XRF) and inductively coupled plasma mass spectrometry (ICP-MS). XRF (Labtium code 175X) was used to determine the major elements as well as certain trace elements and ICP-MS (Labtium code 308PM) was used to determine the rest of the trace elements. Detailed descriptions of the analytical methods are presented in Appendix 1 and the full results in the Electronic Appendix.

4 GEOLOGY OF THE SAARIJÄRVI SUITE

4.1 Granitoids

The following petrographic description is based on the MSc thesis of Virtanen (2017), unless otherwise mentioned. Saarijärvi suite granitoids are dominantly medium-grained alkali feldspar porphyritic quartz monzonites (Fig. 4A) and granites with local plagioclase phenocrysts, although some equigranular varieties have also been identified (Elliott et al. 1998, Mikkola et al. 2016). Subhedral and ovoid alkali feldspar phenocrysts are typically 1–4 cm in diameter and comprise 30–50 vol.% of

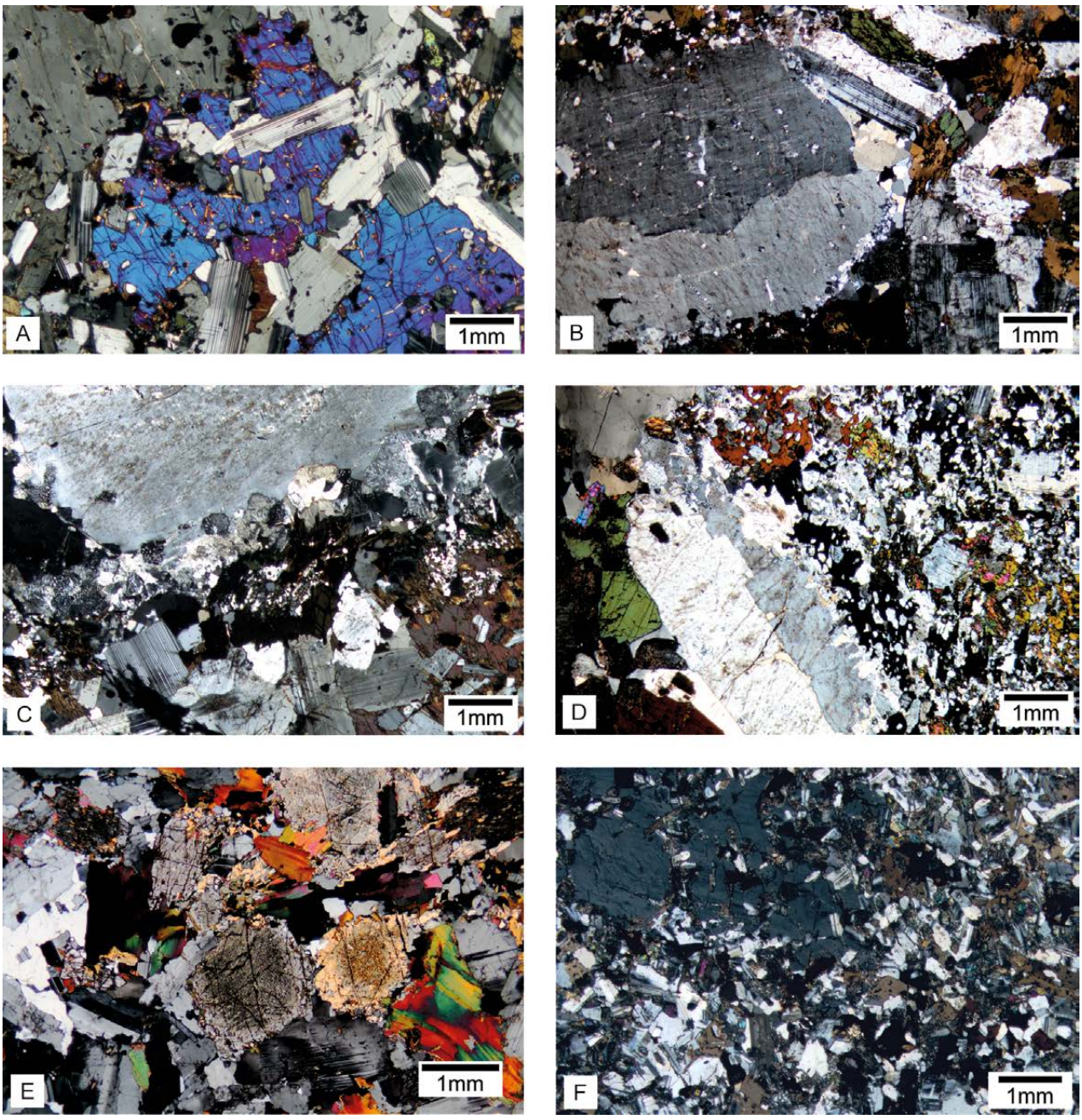

Fig. 5. A) Bluish orthopyroxene subophitically enclosing subhedral to euhedral plagioclase grains in Viininperä monzodiorite. An anhedral alkali feldspar grain in the upper left corner. B) A subhedral perthitic orthoclase phenocryst with partial mantle composed of microcrystalline plagioclase and quartz in a Riitalampi intrusion sample. C) Contact between syenogranite and an intermediate enclave in the Viininperä intrusion. Wart-like myrmekitic bulges replace orthoclase in contact with groundmass plagioclase of the enclave. In the bottom right hand corner of the photo, there is a poikilitic hornblende grain that encloses groundmass grains of the enclave. D) From the same thin section as C). An orthoclase xenocryst inside an MME derived from the host quartz monzonite. A poikilitic biotite grain is present in the top section of the photo. E) Granular unfoliated Simuna gabbro with clinopyroxene and biotite as mafic minerals. There is a thin rim of clinoamphibole around the clinopyroxene. Photo by Marjaana Ahven. F) Poikilitic alkali feldspar xenocryst, in the top left corner, encloses groundmass grains in the mingled Riitalampi MME sample. All photos taken under cross-polarized light.

the rock. They are perthitic orthoclase and often partly or completely mantled by <1 mm composite rims of myrmekitic quartz and plagioclase. In the porphyritic rocks, the groundmass is composed of plagioclase, quartz, alkali feldspar, hornblende and biotite with local ortho- and clinopyroxene (Mikkola et al. 2016, Fig. 5A, B). Groundmass plagioclase is typically weakly altered or unaltered, although some individual grains are strongly altered to sericite. Quartz is present in the interstices between feldspars (Fig. 5B) and as microgranular grains within grain aggregates dominated by mafic silicates. Hornblende in these aggregates is subhedral, altered to secondary amphibole and biotite at the margins, whereas biotite is typically subhedral and unaltered. When present, the pyroxenes are associated with these grain aggregates. Typical accessory minerals in the Saarijärvi suite granitoids are apatite, zircon, allanite and ilmenite that often has a corona of secondary titanite. The minerals generally exhibit undulatory extinction, plagioclase lamellae are occasionally bent and quartz is locally re-crystallized.

Fine-grained dioritic MMEs showing prominent mingling structures (e.g. captured feldspar xenocrysts) are associated with some of the granite and quartz monzonite intrusions (Mikkola et al. 2016, Fig. 4B, D). The MMEs are rounded and typically 5–20 cm in diameter, although their size locally exceeds 1 m. The population of the MMEs is versatile, and both xenocryst-bearing and xenocryst-free MMEs, with or without a visible reaction rim, can be observed on a single outcrop. The groundmass of the MMEs is composed of plagioclase, biotite and clinopyroxene, with minor hornblende (Fig. 5C, D, F). Plagioclase is subhedral and mostly unaltered. Most of the clinopyroxene grains have been strongly altered into colourless amphibole, biotite and chlorite. Biotite is subhedral to anhedral and sometimes sagenitic (contains rutile inclusions). The observed reaction rims around the MMEs are ca. 1 mm thick and composed of biotite and hornblende. Hornblende and biotite poikilitically enclose the groundmass minerals of the MMEs (Fig. 5C, D). The amount of these poikilitic grains rapidly decreases towards the centres of the MMEs. Euhedral to subhedral alkali feldspar and plagioclase, as well as poikilitic alkali feldspar and quartz xenocrysts from host rocks have been identified from many of the MMEs (Mikkola et al. 2016, Fig. 5D, F).

4.2 Dioritoids

The composition of the Saarijärvi suite dioritoids ranges from gabbros and diorites to more evolved quartz diorites and tonalites (Mikkola et al. 2016, Fig. 4C). Diorites and gabbros located in Istruala are structurally diverse, and both even-grained and slightly plagioclase porphyritic types with fine- to coarse-grained groundmass are known (Rämö et al. 2001, Mikkola et al. 2016). The porphyritic varieties are ophitic with clinopyroxene enclosing plagioclase. Close to the contact with the Puula intrusion, feldspar xenocrysts found in Saarijärvi suite dioritoids demonstrate mingling between the magmas. Three types of diorites, namely fine, medium and coarse grained, have been found in Korpilahti. In Poikaraiskansuo, diorites and minor quartz diorites are massive and fine-grained with plagioclase, hornblende and biotite ± quartz as the main minerals. Diorites of Hiiteri are fine to medium grained and generally plagioclase porphyritic. Locally, the diorite grades into structurally similar quartz diorite. Gabbros, norites and diorites exist in the multiphase Simuna intrusion, where the different types cross-cut and brecciate each other (Fig. 4C). The main minerals are plagioclase, orthopyroxene or clinopyroxene, secondary hornblende and biotite (Fig. 5E). Plagioclase and clinopyroxene are present as poikilitic grains. Typical accessory minerals in the Simuna intrusion include apatite, quartz, magnetite and ilmenite (Mikkola et al. 2016). In the Saarijärvi suite dioritoids, subsolidus alteration of pyroxenes to secondary amphiboles is generally pervasive, but not observed close to shear zones.

5 GEOCHEMISTRY

5.1 Granitoids

The geochemical characteristics of the granitoids and quartz monzonites are based on 22 whole-rock geochemical analyses from seven intrusions that are presented in selected compositional diagrams (Fig. 6). Most of the diagrams, excluding the ones showing Ba and Rb, display coherent compositional trends against SiO_2. Negative correlations can be observed in Al_2O_3, FeO*, MgO, CaO, Na_2O, Sr and Zr, whereas K_2O shows a positive correlation (Fig. 6), possibly due to the late accumulation of alkali feldspar. Compared to the Jyväskylä suite, the felsic members of the Saarijärvi suite show enriched characteristics in K_2O, Ba, Zr, $Na_2O + K_2O$ and FeO*/MgO, whereas they are depleted in MgO, CaO and Sr (Fig. 6, Heilimo et al. 2018). In the classifications of Elliott et al. (1998) and Nironen et al. (2000), our samples show the closest resemblance to Type 3a and Type 2 rocks (Fig. 6). The REE patterns of the granitoids are uniform, with the exception of the Korloppinen intrusion. The total REE contents of the coherent samples vary between 142.7–305.8 ppm (mean 199.4 ppm), they show both positive and negative Eu anomalies, with Eu/Eu* between 0.53–1.29 (mean 0.96), and are LREE enriched with $(La/Yb)_N$ between 6.7 and 13.0 (mean 9.9) (Fig. 7). The Korloppinen intrusion has considerably higher total REEs, with 613.5 ppm, and a more pronounced negative Eu anomaly (Eu/Eu* = 0.18). It also shows stronger LREE enrichment with $(La/Yb)_N$ of 17.4 (Fig. 7).

The aluminium saturation of the granitoids and quartz diorites varies from metaluminous to slightly peraluminous (Fig. 6M). They have ferroan (Fig. 8A) and alkali to alkali-calcic compositions (Fig. 8A, B), as well as high Zr+Nb+Ce+Y concentrations (Fig. 8C, D) typical of many A-type granites. In geotectonic classification diagrams (Pearce et al. 1984), the Saarijärvi suite granitoids plot in the fields of within-plate granites (WPG) and volcanic arc granites (VAG) (Fig. 8E, F).

5.2 Geochemistry of the Saarijärvi suite dioritoids

Data for the 11 mafic intrusions and MMEs consist of 20 and 2 whole-rock geochemical analyses, respectively. The rocks are basic to intermediate and the most evolved phases display partial overlapping with the least evolved quartz monzonite samples (Fig. 6). Highly varying Al_2O_3, CaO, MgO, NaO, Ba and Sr compositions are observed among the mafic intrusions (Fig. 6). However, FeOt, K_2O, Rb, Zr, $Na_2O + K_2O$ and FeO*/MgO show relatively coherent trends, with only a few exceptions (Fig. 6). The MME samples show similar whole-rock compositions with the samples from intrusions, reflecting the dominance of dioritic material over felsic xenocrysts in the MMEs (Fig. 6). Mafic rocks generally have lower total REE contents (51.5–406.7 ppm, mean 146.2 ppm) than the granitoids (Fig. 7B). The REE patterns are LREE enriched with $(La/Yb)_N$ of 2.9–17.5 (mean 8.7). Some of the samples show distinct Eu and Ce anomalies, with $(Eu/Eu^*)_N$ and $(Ce/Ce^*)_N$ ranging between 0.60–1.08 and 0.57–1.27, respectively. The MME samples have REE patterns that overlap with some of the samples representing intrusions (Fig. 7C). They show LREE enrichment with $(La/Yb)_N$ of 6.6 and 9.7, as well as slightly negative Eu anomalies with (Eu/Eu*) of 0.71 and 0.82.

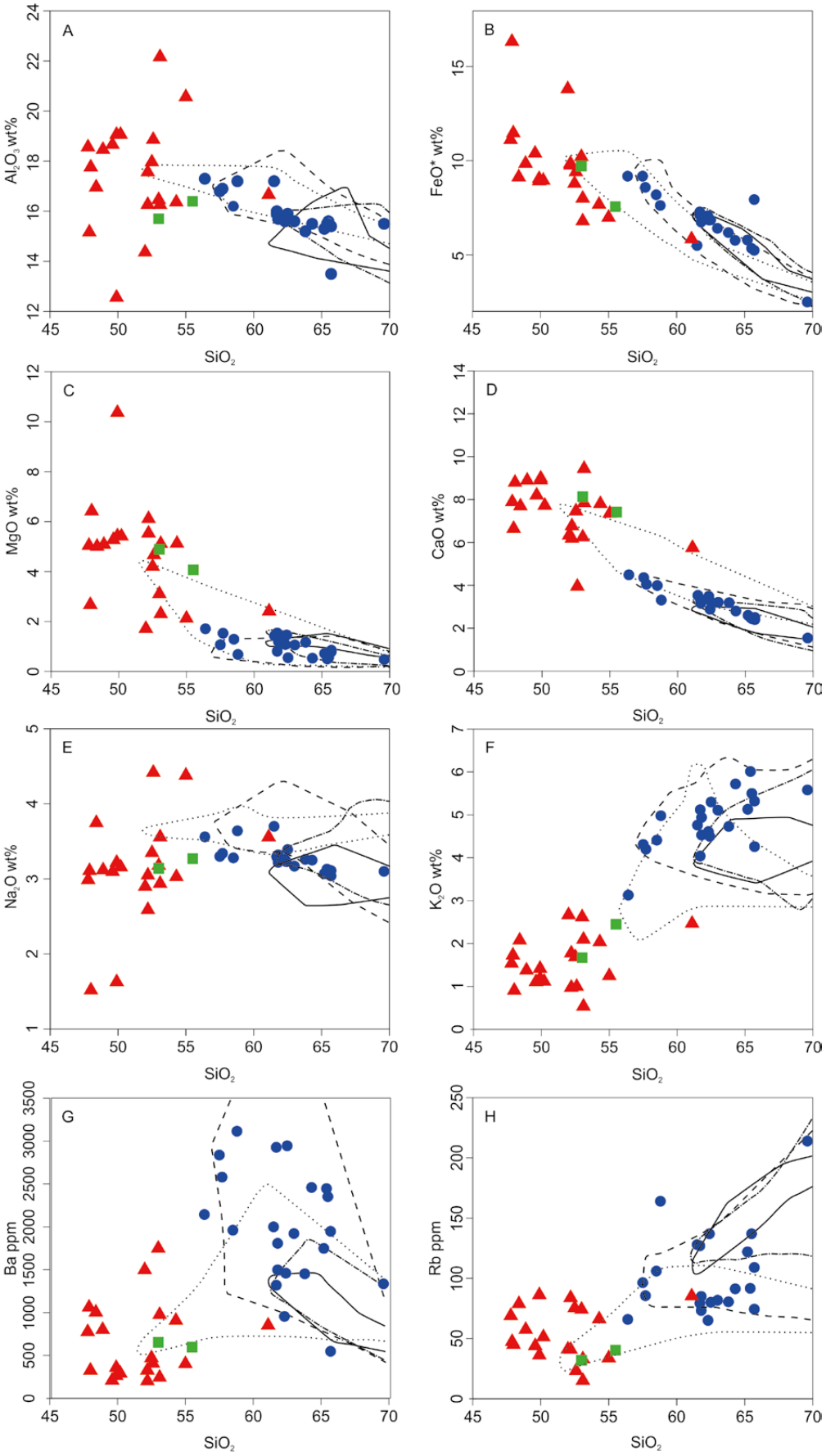

Fig. 6. Harker diagrams of Al_2O_3, FeO* (FeO + 0.8998Fe_2O_3), MgO, CaO, Na_2O, and K_2O, as well as diagrams of Ba, Rb, Sr, Zr, Na_2O + K_2O, and FeO*/MgO versus SiO_2 in weight percent. The fields of different types (1, 2, 3a and 3b) of Saarijärvi suite granitoids have been drawn after Nironen et al. (2000). The aluminium saturation index (M) has been adapted from Shand (1943).

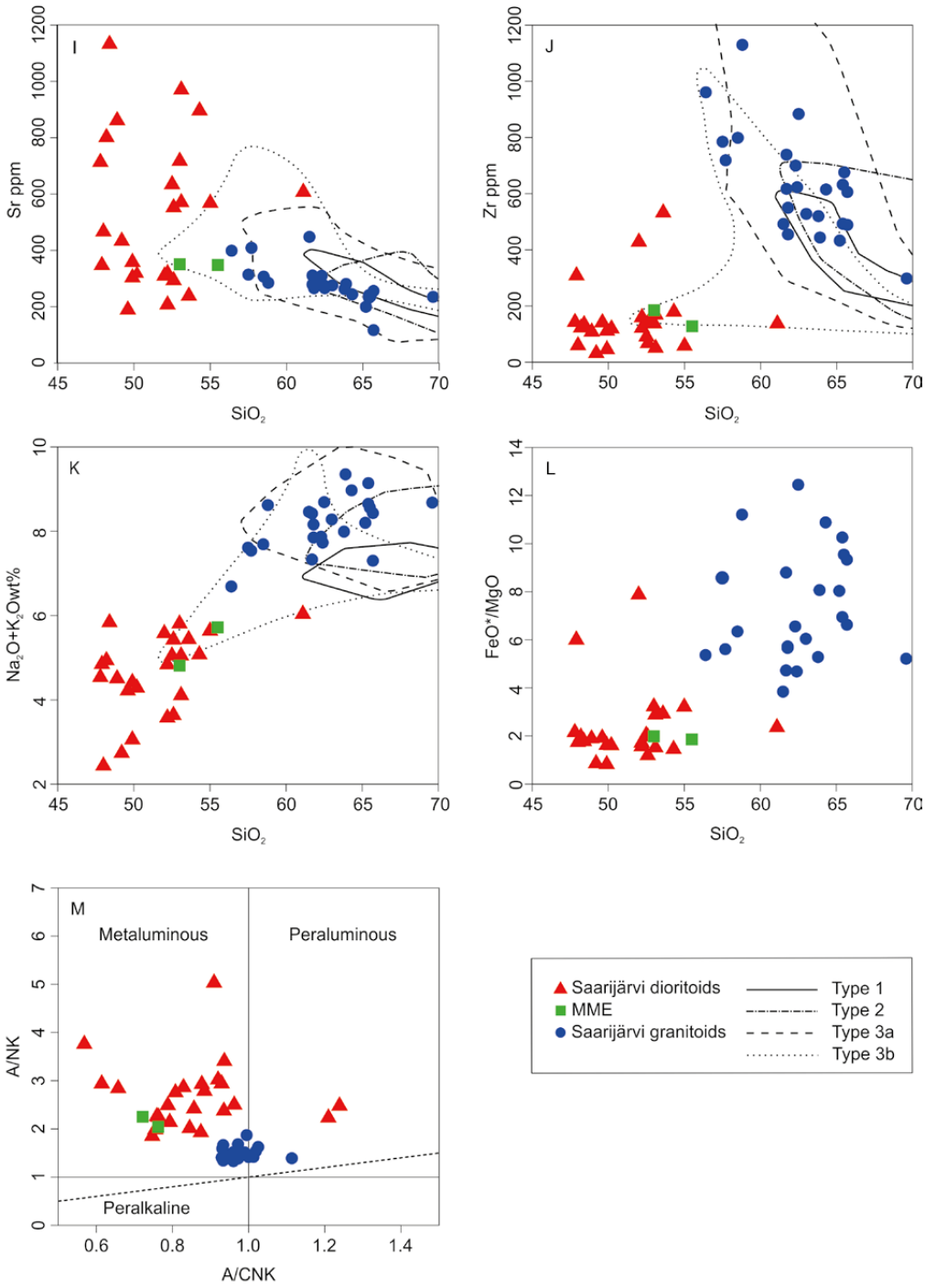
I
Sr ppm
SiO2
J
Zr ppm
SiO2
K
Na2O+K2Owt%
SiO2
L
FeO*/MgO
SiO2
M
Metaluminous
Peraluminous
Peralkaline
A/NK
A/CNK
Saarijärvi dioritoids
MME
Saarijärvi granitoids
Type 1
Type 2
Type 3a
Type 3b

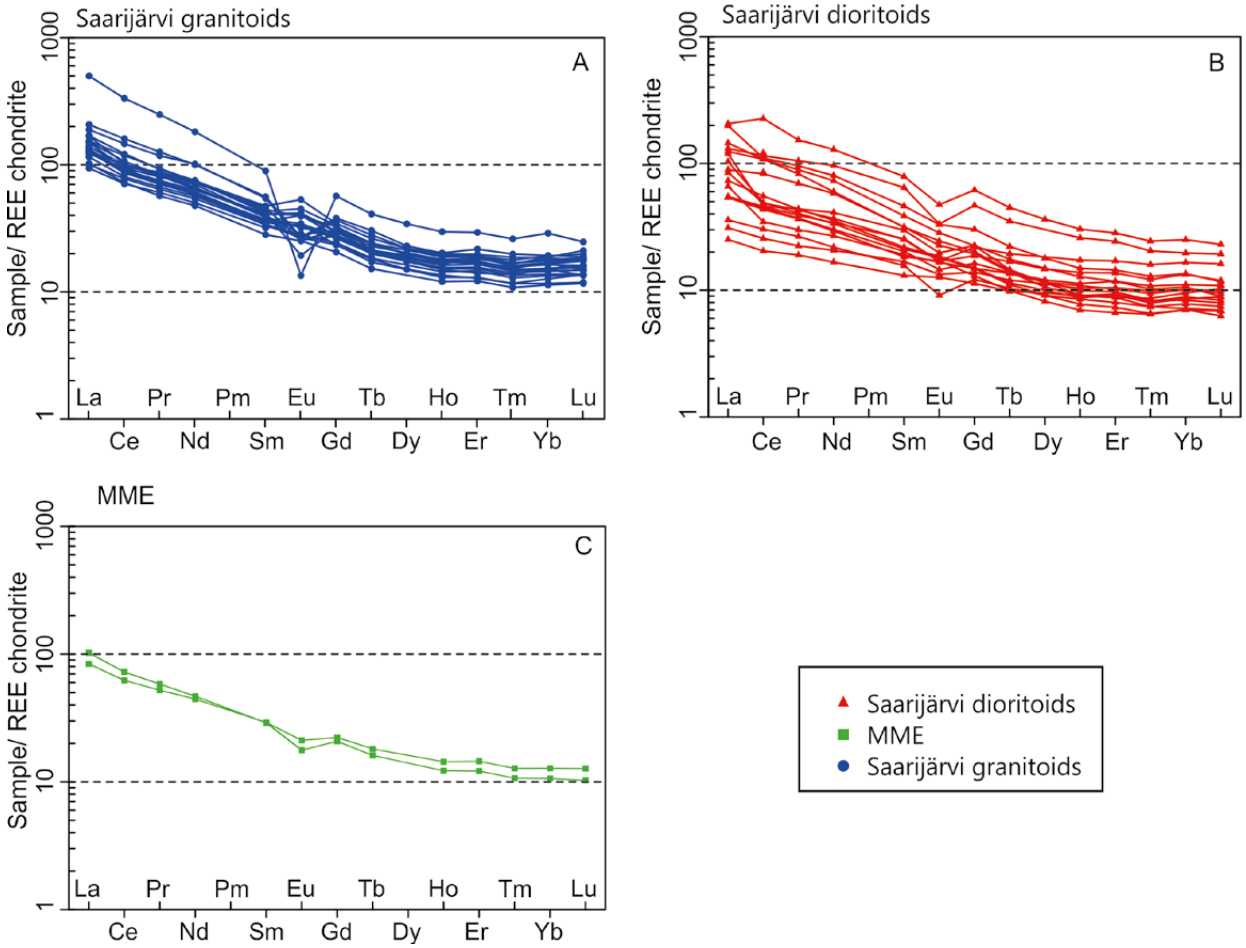

Fig. 7. Rare earth element (REE) patterns of A) granitoids, B) dioritoids of the Saarijärvi suite, and C) mafic microgranular enclave (MME) samples containing K-feldspar xenocrysts. The REE patterns are normalized to the chondritic values of Boynton (1984).

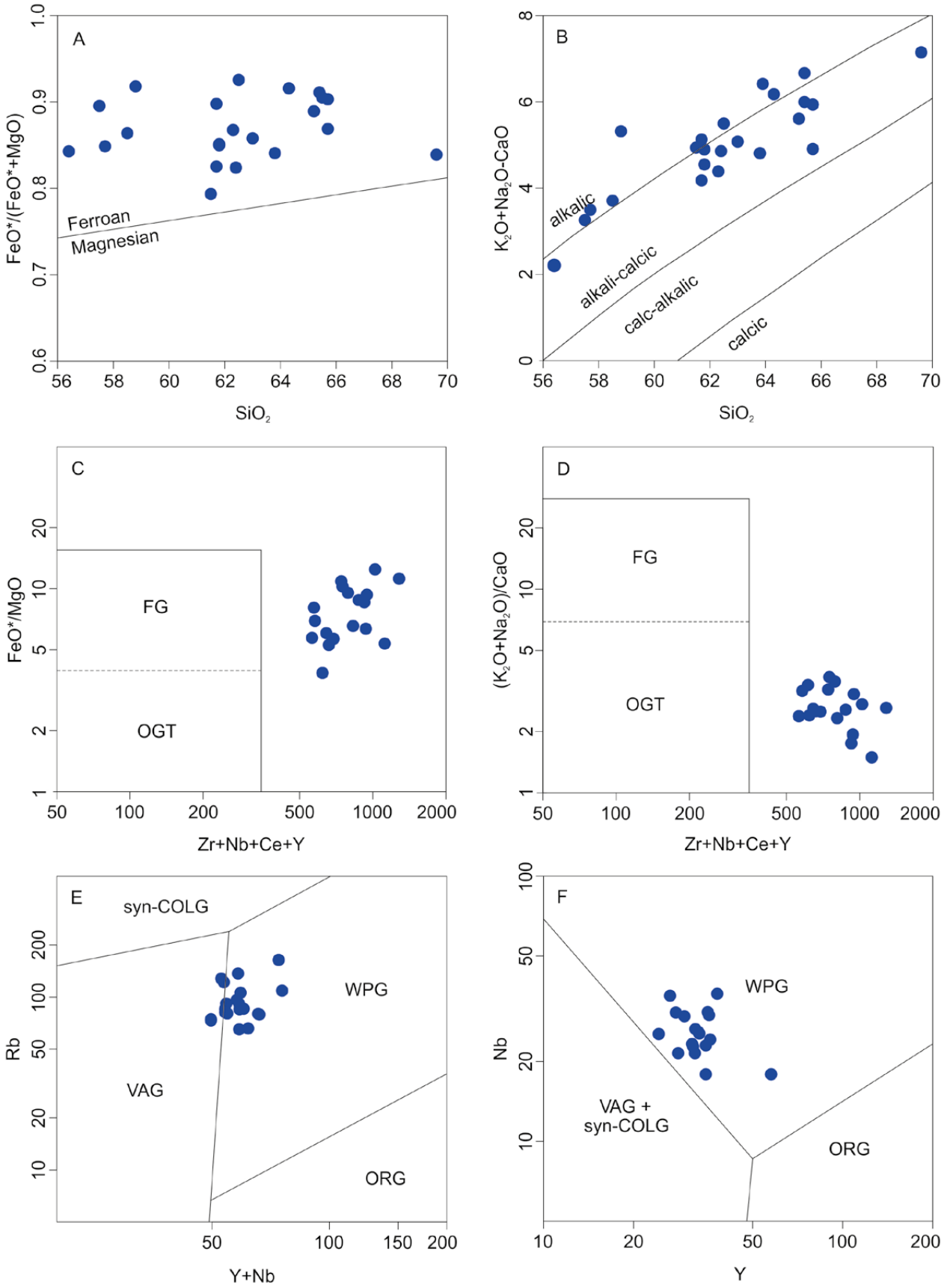

Fig. 8. Compositions of Saarijärvi suite granitoids plotted on selected geochemical classification diagrams. A) the FeO*/(FeO* + MgO), and B) $K_2O + Na_2O - CaO$ versus SiO_2 diagrams of Frost et al. (2001). C) the FeO*/MgO, and D) $(K_2O + Na_2O)/CaO$ versus SiO_2 diagrams of Whalen et al. (1987). Abbreviations as follows: OGT = unfractionated I- S- and M-type granitoids, FG = fractionated felsic granitoids, and unmarked field = A-type granitoids. E) The Rb versus Y + Nb, and F) Nb versus Y diagrams are from Pearce et al. (1984). The fields are as follows: ORG = ocean ridge granites, VAG = volcanic arc granites, WPG = within-plate granites, syn-COLG = syncollision granites.

6 DISCUSSION

6.1 Petrographic evidence of deformation and subsolidus processes

Foliated Jyväskylä suite rocks, the most common rock type in the study area, are easily distinguished from the generally non-foliated Saarijärvi suite rocks in the field. However, petrographic examination also revealed a low degree of deformational features from the Saarijärvi suite granitoids. Common undulatory extinction of minerals, bent plagioclase lamellae and occasional re-crystallization of quartz were observed. The formation of myrmekitic plagioclase and quartz rims around alkali feldspar phenocrysts is related to medium-grade deformation at temperatures of ca. 400–500 °C, in which case the myrmekite systematically forms on those sides of alkali feldspar phenocrysts that are under compression (e.g. Phillips & Carr 1973, Simpson & Wintsch 1989, Passchier & Trouw 1998). However, no systematic distribution of myrmekite is observed in Saarijärvi suite granitoids, probably due to weak compression. The deformational overprint of the structure also makes it difficult to evaluate whether the observed interstitial occurrence of water-bearing mafic silicates results from late saturation of water from crystallizing magma (typical of A-type granitoids; e.g. Clemens et al. 1986) or from a difference in competence between the minerals during deformation. No distinct features related to deformation are present in the more mafic members of the Saarijärvi suite.

6.2 Mineralogical and geochemical comparison between characteristic CFGC granitoids and those of the Saarijärvi suite

Granitoids of the Saarijärvi suite can be distinguished from the prevalent Jyväskylä suite rocks by their distinct geochemical features. The Jyväskylä suite is characterized by I-type geochemistry (Heilimo et al. 2018), whereas those of the Saarijärvi suite have a geochemical affinity to A-type granitoids (Front & Nurmi 1987, Elliott et al. 1998, Nironen et al. 2000, Nikkilä et al. 2016, this study). The most significant geochemical features distinguishing the Jyväskylä and Saarijärvi suites are higher $Na_2O + K_2O$, K_2O, Ba, Zr and total REE contents, lower MgO, CaO and Sr contents, as well as a higher FeO*/MgO ratio at a given SiO_2 content (Fig. 6, Heilimo et al. 2018).

Elliott et al. (1998) and Nironen et al. (2000) recognized four mineralogically and geochemically distinct groups among the granitoids of the Saarijärvi suite: Types 1, 2, 3a and 3b. Geochemically, the here-studied Saarijärvi suite granitoids show a shift from Type 3a to Type 2 rocks with increasing SiO_2 contents (Fig. 6). The presence of biotite + hornblende ± pyroxene as the main mafic minerals, and the absence of fluorite, which is a characteristic accessory mineral in Type 2 rocks (Elliott et al. 1998, Nironen et al. 2000, Table 1), underlines the similarity between the studied Saarijärvi suite granitoids and Type 3a rocks.

6.3 Source constraints of the Saarijärvi suite granitoids based on whole-rock geochemistry

Isotopic compositions together with geochemical modelling have been used to construct a petrogenetic model for the granitoids of the Saarijärvi suite (Rämö et al. 2001, Elliott 2003). In this model, it was proposed that the parental magma of these granitoids formed when partial melts of mantle-derived basaltic rock mixed with anatectic melts of mafic granulitic crust at a pressure of ca. 16 kbar (Elliott 2003, Fig. 9). We suggest that this model can explain some of the whole-rock geochemical features atypical of mantle-derived A-type granitoids, e.g. relatively high Al_2O_3 and high abundances of trace elements compatible in feldspars (Ba, Sr, and Eu) present in the here-studied rocks. In addition, crustal assimilation can shift A-type rocks from the WPG to the VAG field (Pearce et al. 1984), which could explain the VAG affinity of some of the Saarijärvi suite granitoids (Fig. 8E, F).

The source of the Saarijärvi suite granitoids of this study can be qualitatively evaluated with certain whole-rock geochemical features. Ferroan, alkalic to alkali-calcic granitoids with metaluminous to slightly peraluminous aluminium saturation and a typical A-type trace element composition, as

observed in our samples, can be formed by partial melting of mantle-derived basalts with or without crustal input to the melt phase (e.g. Eby 1992, Barbarin 1999, Bonin 2007, Frost & Frost 2011). Examples of geochemically similar A-type granitoids with a mainly mantle-derived origin include the Mesoproterozoic alkalic Sybille intrusion (Scoates et al. 1996) and alkali-calcic San Isabel (Cullers et al. 1992) and Sherman (Frost et al. 1999) batholiths of the southwestern USA, the Mesoproterozoic alkali-calcic Suomenniemi batholith of southeastern Finland (Rämö 1991) and the mainly alkali-calcic Kokshaal intrusions of southeastern Kyrgyzstan (Konopelko et al. 2007). As noted above, the Saarijärvi suite granitoids differ from the typical A-type geochemistry by having high Al_2O_3, Ba, Sr and Eu contents, i.e. elements that are highly concentrated in feldspars, especially plagioclase. The residual mineral assemblage of incongruent dehydration melting of hornblende is strongly controlled by pressure (Patiño Douce 1997). Orthopyroxene and plagioclase dominate the residual mineral assemblage at low pressures (<4 kbar), yielding the typical A-type composition (Patiño Douce 1997). As the pressure increases, the proportion of residual plagioclase decreases, and at high pressures (>8 kbar), clinopyroxene becomes the dominant residual phase, hence enriching the melt phase in elements with affinity for plagioclase. Additionally, with an increasing pressure, the melt phase becomes richer in SiO_2 (>70 wt%) and the FeO*/MgO ratio shifts towards the magnesian field (Patiño Douce 1997, Frost et al. 2001). Hence, a deep crustal source going through incongruent dehydration melting of hornblende is not likely to be the main source for granitoids of the Saarijärvi suite. A mantle-derived mafic melt going through differentiation could explain the A-type geochemical features of the Saarijärvi suite, whereas the assimilation of a hornblende-bearing deep crustal source could introduce the elements otherwise scarce in A-type granitoids (Al_2O_3, Ba, Sr and Eu) to the melt phase. Nevertheless, thermodynamic modelling should be conducted to test whether this mixing process is physically feasible or not.

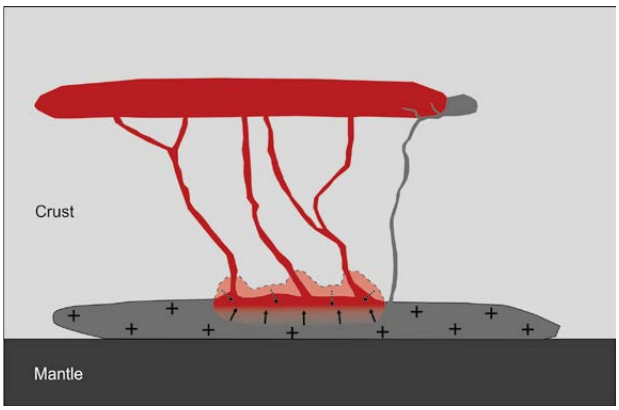

Fig. 9. A schematic illustration of the petrogenesis of Saarijärvi suite granitoids of the Central Finland Granitoid Complex (CFGC) based on Rämö et al. (2001), Elliott (2003) and this study. Mantle-derived basaltic underplate (dark grey with crosses) differentiates (solid arrows), producing parental melt of the granitoids (dark red). This melt is then mixed with anatectic melts (stippled arrows) of the crust (light red) under high pressure. Unmixed melt (dark grey) forms the parental melt of the diorite intrusions that are usually located adjacent to, and mingled with, the granitoid intrusions. The figure is not to scale.

6.4 Source indications for the Saarijärvi suite dioritoids

The mafic members of the Saarijärvi suite are geochemically more heterogeneous than the granitoids. The observed variation can originate from many processes, e.g. source heterogeneity, assimilation, fractionation and hydrothermal alteration. The mafic members have been interpreted as mostly mantle derived (Nironen et al. 2000), but might also contain other minor components from crustal sources or assimilation. Ce anomalies, observed in some of the samples (Fig. 7B), can be caused by variable input from seafloor rocks (Dickin 1987, Neal & Taylor 1989). The REEs (with the exception of Eu) are commonly present in the valence state +3 and hence they tend to behave similarly to each other in geochemical fractionation. In the marine environment, Ce may be present in the oxidized valence state +4 and thus behave differently from the other REEs, leading to negative anomalies in deep ocean water and pelagic sediments and positive anomalies in manganese nodules found on ocean floors (Dickin 1987, Neal & Taylor 1989). During the Svecofennian orogeny, subduction could have provided a variable source of seafloor rocks (e.g. MORB, pelagic sediments, manganese nodules) for the mantle beneath the CFGC. Further studies are required to evaluate whether there really is a recycled ocean-floor component in some of the mafic members of the Saarijärvi suite.

6.5 Coeval mafic-felsic magmatism: a case study from the Riitalampi intrusion

The close spatial and temporal relationship between the mafic and felsic magmas is manifested by abundant, typically dioritic MMEs and occasional synplutonic dykes found in many intrusions of the Saarijärvi suite. A large portion of the MMEs enclose feldspar and quartz xenocrysts derived from the host rock in the magmatic stage. In the Riitalampi intrusion, MMEs and a synplutonic dyke are found on a single outcrop (Fig. 4D), which suggests that at least in some cases the mafic input started when the intrusion was only partly crystalline (MME-forming stage) and continued until the intrusion was nearly completely solid (synplutonic dyke-forming stage).

The extent of the mingling process in the Riitalampi intrusion has been numerically estimated (Virtanen 2017) using a least-squares approximation with the MAGFRAC program (Morris 1984). A xenocryst-free MME (MME1) from the Riitalampi intrusion was chosen to represent the composition of the parental magma of the MME, and a xenocryst-bearing MME (MME2) was chosen to represent the product of the mingling process (Table 2). Variable combinations of measured major mineral compositions of the Riitalampi quartz monzonite (Virtanen 2017) + pure SiO_2 were then mixed with the whole-rock composition of MME1 to produce MME2 (Table 2).

Of the experimented mineral assemblages, the best fit based on both geochemistry and petrography was produced by mixing 78.7% of MME1 with 6.9% of alkali feldspar, 10.7% of plagioclase and 2.7% of quartz from the host rock (Table 2). This model has $r^2 = 0.121$ (Table 2). Even better mathematical fits were achieved by including biotite and hornblende, which would have been removed from MME1 in the model. However, such models are not supported by petrographic observations. Chemical equilibration between the MME and felsic host transports MgO and FeO from the MME and introduces SiO_2 and K_2O to the MME (e.g. Debon 1991, Orsini et al. 1991). We suggest that the chemical diffusion of FeO and MgO occurred from partially molten MME1 to the quartz monzonite (Fig. 10), and as biotite and hornblende are the main hosts for MgO and FeO in this system, models involving their removal from MME1 result in a better mathematical fit. Poikilitic quartz, alkali feldspar (Fig. 5F) and biotite grains (Fig. 5D), like those in some of the MMEs in the Riitalampi intrusion, have in certain cases been interpreted to result from the chemical diffusion of SiO_2 and K_2O to the MMEs (Barbarin & Didier 1991, Hibbard 1991). This indicates that the diffusion also occurred from partially molten quartz monzonite to MME1, as would be expected (Fig. 10).

Table 2. MAGFRAC least-squares approximation sheet (Morris 1984) showing measured whole-rock compositions of mingled MME2 (ASM$-2013-224.2) and xenocryst-free MME1 (PIM$-2012-88.2), measured alkali feldspar (Afs) and plagioclase (Plg) compositions from quartz monzonite (ASM$-2013-224.1), and quartz (Qtz) as pure SiO_2. Mineral compositions are from Virtanen (2017). The r value is the calculated difference between the measured and calculated compositions of the mingled MME2. The model calculates the relative proportions for the selected phases (MME1, Afs, Plg, and Qtz) so that lowest possible r^2 value is achieved for the calculated MME.

	ASM$-2013-224.2	**PIM$-2012-88.1**	**ASM$-2013-224.1**			**ASM$-2013-224.1**		
	Mingled MME2	MME1	Afs	Plg	Qtz	Calculated	r	r^2
SiO_2	55.5	53.0	63.0	58.5	100.0	55.5	-0.000	0.000
TiO_2	1.1	1.4	0.0	0.0	0.0	1.1	-0.017	0.000
Al_2O_3	16.4	15.7	18.0	25.1	0.0	16.4	-0.025	0.001
FeO*	8.4	10.8	0.0	0.0	0.0	8.6	-0.172	0.029
MnO	0.1	0.2	0.0	0.0	0.0	0.2	-0.059	0.003
MgO	4.1	4.9	0.0	0.0	0.0	3.9	0.213	0.045
CaO	7.4	8.1	0.0	7.4	0.0	7.2	0.181	0.033
Na_2O	3.3	3.1	0.9	8.1	0.0	3.4	-0.086	0.007
K_2O	2.5	1.7	15.7	0.1	0.0	2.5	0.034	0.001
P_2O_5	0.3	0.4	0.0	0.0	0.0	0.3	-0.017	0.000
Total	99.1	99.3	97.6	99.3	100.0		Sum r^2	0.121
Proportion		78.7	6.9	10.7	2.7			

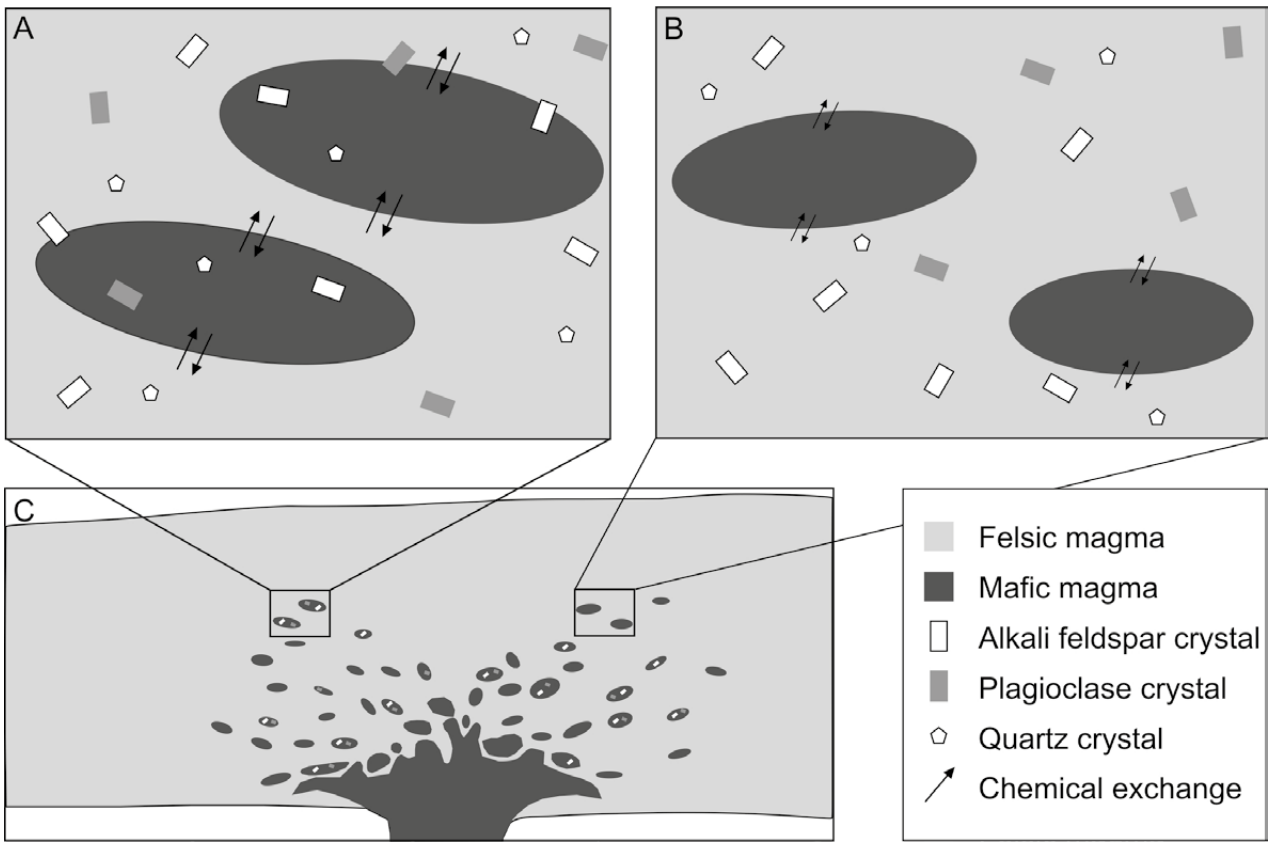

Fig. 10. A schematic illustration of coeval mafic-felsic magmatism in the Riitalampi intrusion. A) Some of the alkali feldspar, plagioclase and quartz crystals of partially crystallized quartz monzonite magma are captured by blobs of mafic magma. Chemical exchange drives compositional equilibrium between the magmas. B) Some of the mafic blobs are crystallized fast enough to prevent crystal entrainment from the quartz monzonite. Faster crystallization of the mafic magma also limits the extent of chemical exchange, leaving the composition of these blobs relatively unchanged. c) As mafic magma intrudes the partially crystalline Riitalampi intrusion, movement of the felsic magma splits it into blobs. These mafic blobs are then crystallized as mafic microgranular enclaves (MMEs).

The results of the mingling model together with petrographic evidence suggest that of the major minerals, alkali feldspar, plagioclase and quartz were captured by the low viscosity MMEs, whereas biotite and hornblende were not (Fig. 10). Whether this resulted from later saturation of the water-bearing mafic silicates or some other physical factor cannot be reliably deduced from the results. In addition to mingling, small-scale chemical diffusion is likely to have taken place between MMEs and the host quartz monzonite. Although there is no definite observation that the Poikaraiskansuo diorite, located at the northern contact of the Riitalampi intrusion (Fig. 3), is the source for the MMEs, the whole-rock geochemical compositions of the two are relatively similar and further examination is encouraged.

6.6 Role of the Saarijärvi suite in the crustal growth

Together with previous studies (Elliott et al. 1998, Nironen et al. 2000, Rämö et al. 2001, Elliot 2003, Nikkilä et al. 2016), we have established that the type of Saarijärvi suite magmatism differs from the main magmatic event of the CFGC. While the granitoids of the Jyväskylä suite are likely to represent the recycling of older crustal material (Heilimo et al. 2018), the geochemistry of the Saarijärvi suite granitoids is similar to well-studied granitoids that formed via the differentiation of juvenile magmas (Frost et al. 2001, Elliott 2003, Fig. 9), and hence Saarijärvi suite granitoids probably represent a minor crustal growth episode during the Svecofennian orogeny.

Members of the Saarijärvi suite sharply cross-cut the Jyväskylä suite rocks and show no evidence of strong deformation during or after the Svecofennian orogeny. However, the U–Pb ages of the Puula (1875 ± 4 Ma; Rämö et al. 2001), Riitalampi (1879 ± 4 Ma; authors' unpublished data) and Viininperä (1882 ± 3 Ma; Virtanen 2017) intrusions of the Saarijärvi suite granitoids show that they formed during the late synorogenic stage of the Svecofennian orogeny and overlap in age with the Jyväskylä suite granitoids. The Saarijärvi suite rocks are often spatially associated both with each other and major fracture zones (Mikkola et al. 2016). Hence, it appears that the formation of the Saarijärvi suite intrusions is associated with local extensional or transtensional settings that were present in the dominantly compressional setting in the CFGC area, as already proposed by previous authors (e.g. Elliott et al. 1998, Nironen et al. 2000, Rämö et al. 2001). The overall geological development of the area is further discussed by Mikkola et al. (2018a).

7 CONCLUSIONS

The Saarijärvi suite rocks of the southeastern CFGC postdate the main deformation event of the Svecofennian orogeny but are synkinematic with respect to the orogeny as whole. Emplacement near shear zones together with weak deformational structures suggest that the intrusions denote local extensional or transtensional tectonic settings, as proposed by previous authors.

The geochemical signature of the Saarijärvi suite granitoids is similar to A-type granitoids that formed via the differentiation of mantle-derived basalts, and the subtle differences could indicate the assimilation of crustal material in a high-pressure regime.

The main source of the mafic component of the suite is mantle-derived magma, with possible input from a recycled ocean-floor component.

Based on field evidence, mingling between the felsic and mafic magmas has taken place. The mafic magma input was continuous during the crystallization of host granitoid, but the effects were restricted to mingling and probably limited chemical diffusion.

ACKNOWLEDGEMENTS

We want to express our gratitude to all those who contributed to the fieldwork during the Ore Potential Project: this study would not have been possible without you. For the study materials, we want to thank the staff of the thin section laboratory at GTK Kuopio. Both authors benefited from discussions with Tapani Rämö, whose knowledge of the subject is impressive. We also want to thank Perttu Mikkola, Marjaana Ahven and Jukka Kousa for their constructive feedback, which improved the contents of the manuscript, as well as for figure handling by Ritva Jokisaari and Riitta Turunen. Aku Heinonen and Olav Eklund are acknowledged for constructive comments that considerably improved the contents of the manuscript.

REFERENCES

Anderson, A. T. 1976. Magma mixing: petrological process and volcanological tool. Journal of Volcanology and Geothermal Research 1, 3–33.

Andersson, U. B. & Eklund, O. 1994. Cellular plagioclase intergrowths as a result of crystal-magma mixing in the Proterozoic Åland rapakivi batholith, SW Finland. Contributions to Mineralogy and Petrology 117, 124–136.

Barbarin, B. 1999. A review of the relationship between granitoid types, their origins and their geodynamic environments. Lithos 46, 605–626.

Barbarin, B. 2005. Mafic magmatic enclaves and mafic rocks associated with some granitoids of the central Sierra Nevada batholith, California: nature, origin, and relations with the hosts. Lithos 80, 155–177.

Bonin, B. 2007. A-type granites and related rocks: Evolution of a concept, problems and prospects. Lithos 97, 1–29.

Boynton, W. V. 1984. Cosmochemistry of the rare earth elements; meteorite studies. In: Henderson, P. (ed.) Rare earth element geochemistry. Amsterdam: Elsevier, 63–114.

Bridgwater, D., Sutton, J. & Watterson, J. 1974. Crustal downfolding associated with igneous activity. Tectonophysics 21, 57–77.

Chappell, B. W. & White, A. J. R. 1974. Two contrasting granite types. Pacific Geology 8, 173–174.

Collins, W. J., Beams, S. D., White, A. J. R. & Chappell, B. W. 1982. Nature and Origin of A-Type Granites with Particular Reference to Southeastern Australia. Contributions to Mineralogy and Petrology 80, 189–200.

Cullers, R. L., Griffin, T., Bickford, M. E. & Lawford Anderson, J. 1992. Origin and chemical evolution of the 1360 Ma San Isabel batholith, Wet Mountains, Colorado: A mid-crustal granite of anorogenic affinities. Geological Society of America Bulletin 104, 316–328.

Debon, F. 1991. Comparative major element chemistry in various "microgranular enclace–plutonic host" pairs. In: Didier, J. & Barbarin, B. (eds) Enclaves and Granite Petrology. Amsterdam: Elsevier, 293–312.

Dickin, A. P. 1987. Cerium isotope chemistry of ocean island basalts. Nature 326, 283–284.

Didier, J. & Barbarin, B. 1991. The different types of enclaves in granites – Nomenclature. In: Didier, J. & Barbarin, B. (eds) Enclaves and Granite Petrology. Amsterdam: Elsevier, 19–23.

Eby, G. N. 1990. The A-type granitoids: A review of their occurrence and chemical characteristics and speculations on their petrogenesis. Lithos 26, 115–134.

Eby, G. N. 1992. Chemical subdivision of the A-type granitoids: Petrogenetic and tectonic implications. Geology 20, 641–644.

Eklund, O., Fröjdö, S. & Lindberg, B. 1994. Magma Mixing, the Petrogenetic Link between Anorthositic Suites and Rapakivi Granites, Åland, SW Finland. Mineralogy and Petrology 50, 3–19.

Elliott, B. A. 2003. Petrogenesis of the Post-kinematic Magmatism of the Central Finland Granitoid Complex II; Sources and Magmatic Evolution. Journal of Petrology 44, 1681–1701.

Elliott, B. A., Rämö, O. T. & Nironen, M. 1998. Mineral chemistry constraints on the evolution of the 1.88–1.87 Ga post-kinematic granite plutons in the Central Finland Granitoid Complex. Lithos 45, 109–129.

Emslie, R. F. 1978. Anorthosite Massifs, Rapakivi Granites, and Late Proterozoic Rifting of North America. Precambrian Research 7, 61–98.

Fernandez, A. N. & Barbarin, B. 1991. Relative rheology of coeval mafic and felsic magmas: Nature of resulting interaction processes. Shape and mineral fabrics of mafic microgranular enclaves. In: Didier, J. & Barbarin, B. (eds) Enclaves and Granite Petrology. Amsterdam: Elsevier, 263–275.

Front, K. & Nurmi, P. A. 1987. Characteristics and geological setting of synkinematic Svecokarelian granitoids in southern Finland. Precambrian Research 35, 207–224.

Frost, B. R., Barnes, C. G., Collins, W. J., Arculus, R. J., Ellis, D. J. & Frost, C. D. 2001. A Geochemical Classification for Granitic Rocks. Journal of Petrology 42, 2033–2048.

Frost, C. D. & Frost, B. R. 1997. Reduced rapakivi-type granites: The tholeiite connection. Geology 25, 647–650.

Frost, C. D. & Frost, B. R. 2011. On Ferroan (A-type) Granitoids: their Compositional Variability and Modes of Origin. Journal of Petrology 52, 39–53.

Frost, C. D., Frost, B. R., Chamberlain, K. R. & Edwards, B. R. 1999. Petrogenesis of the 1.43 Ga Sherman Batholith, SE Wyoming, USA: a Reduced, Rapakivi-type Anorogenic Granite. Journal of Petrology 40, 1771–1802.

Furman, T. & Spera, F. J. 1985. Co-Mingling of acid and basic magma with implications for the origin of mafic I-type xenoliths: field and petrochemical relations of an unusual dike complex at Eagle Lake, Sequoia National Park, California, U.S.A. Journal of Volcanology and Geothermal Research 24, 151–178.

Giordano, D., Russell, J. K. & Dingwell, D. B. 2008. Viscosity of magmatic liquids: A model. Earth and Planetary Science Letters 271, 123–134.

Heilimo, E., Ahven, M. & Mikkola, P. 2018. Geochemical characteristics of the plutonic rock units present at the southeastern boundary of the Central Finland Granitoid Complex. In: Mikkola, P., Hölttä, P. & Käpyaho, A. (eds) Development of the Paleoproterozoic Svecofennian orogeny: new constraints from the southeastern boundary of the Central Finland Granitoid Complex. Geological Survey of Finland, Bulletin 407. (this volume). Available at: https://doi.org/10.30440/bt407.6

Hibbard, M. J. 1991. Textural anatomy of twelve magma-mixed granitoid systems. In: Didier, J. & Barbarin, B. (eds) Enclaves and Granite Petrology. Amsterdam: Elsevier, 431–464.

Hölttä, P. S. & Heilimo, E. 2017. Metamorphic map of Finland. In: Nironen, M. (ed.) Bedrock of Finland at the scale 1:1 000 000 - Major stratigraphic units, metamorphism and tectonic evolution. Geological survey of Finland Special paper 60, 77–127. Available at: http://tupa.gtk.fi/julkaisu/specialpaper/sp_060.pdf

Huhma, H. 1986. Sm-Nd, U-Pb and Pb-Pb isotopic evidence for the origin of the Early Proterozoic Svecokarelian crust in Finland. Geological Survey of Finland, Bulletin 337. 48 p. Available at: http://tupa.gtk.fi/julkaisu/bulletin/bt_337.pdf

Kallio, J. 1986. Joutsan kartta-alueen kallioperä. Summary: Pre-Quaternary Rocks of the Joutsa Map-Sheet area. Geological Map of Finland 1:100 000, Explanation to the Maps of Pre-Quaternary Rocks, Sheet 3122. Geological Survey of Finland. 56 p. (in Finnish). Available at: http://tupa.gtk.fi/kartta/kallioperakartta100/kps_3122.pdf

Konopelko, D., Biske, G., Seltmann, R., Eklund, O. & Belyatsky, B. 2006. Hercynian post-collisional A-type granites of the Kokshaal Range, Southern Tien Shan, Kyrgyzstan. Lithos 97, 140–160.

Lahtinen, R. 1994. Crustal evolution of the Svecofennian and Karelian domains during 2.1–1.79 Ga, with special emphasis on the geochemistry and origin of 1.93–1.91 Ga gneissic tonalites and associated supracrustal rocks in the Rautalampi area, central Finland. In: Lahtinen, R. Crustal evolution of the Svecofennian and Karelian domains during 2.1-1.79 Ga, with special emphasis on the geochemistry and origin of 1.93-1.91 Ga gneissic tonalites and associated supracrustal rocks in the Rautalampi area, central Finland. Geological Survey of Finland, Bulletin 378, 1–128. Available at: http://tupa.gtk.fi/julkaisu/bulletin/bt_378.pdf

Lahtinen, R., Korja, A., Nironen, M. & Heikkinen, P. 2009. Palaeoproterozoic accretionary processes in Fennoscandia. In: Cawood P. A. & Kröner A. (eds) Earth accretionary systems in space and time. Geological Society London, Special publication 318, 237–256.

Loiselle, M. C. & Wones, D. R. 1979. Characteristics and origin of anorogenic granites. Geological Society of America, Abstracts with Programs 11, p. 468.

Mikkola, P., Heilimo, E., Aatos, S., Ahven, M., Eskelinen, J., Halonen, S., Hartikainen, A., Kallio, V., Kousa,

J., Luukas, J., Makkonen, H., Mönkäre, K., Niemi, S., Nousiainen, M., Romu, I. & Solismaa, S. 2016. Jyväskylän seudun kallioperä. Summary: Bedrock of the Jyväskylä area. Geological Survey of Finland, Report of Investigation 227. 113 p. (in Finnish). Available at: http://tupa.gtk.fi/julkaisu/tutkimusraportti/tr_227.pdf

Mikkola, P., Heilimo, E., Luukas, J., Kousa, J., Aatos, S., Makkonen, H., Niemi, S., Nousiainen, M., Ahven, M., Romu, I. & Hokka, J. 2018a. Geological evolution and structure along the southeastern border of the Central Finland Granitoid Complex. In: Mikkola, P., Hölttä, P. & Käpyaho, A. (eds) Development of the Paleoproterozoic Svecofennian orogeny: new constraints from the southeastern boundary of the Central Finland Granitoid Complex. Geological Survey of Finland, Bulletin 407. (this volume). Available at: https://doi.org/10.30440/bt407.1

Mikkola, P., Huhma, H., Romu, I. & Kousa, J. 2018b. Detrital zircon ages and geochemistry of the metasedimentary rocks along the southeastern boundary of the Central Finland Granitoid Complex. In: Mikkola, P., Hölttä, P. & Käpyaho, A. (eds) Development of the Paleoproterozoic Svecofennian orogeny: new constraints from the southeastern boundary of the Central Finland Granitoid Complex. Geological Survey of Finland, Bulletin 407. (this volume). Available at: https://doi.org/10.30440/bt407.2

Mikkola, P., Mönkäre, K., Ahven, M. & Huhma, H. 2018c. Geochemistry and age of the Paleoproterozoic Makkola suite volcanic rocks in central Finland. In: Mikkola, P., Hölttä, P. & Käpyaho, A. (eds) Development of the Paleoproterozoic Svecofennian orogeny: new constraints from the southeastern boundary of the Central Finland Granitoid Complex. Geological Survey of Finland, Bulletin 407. (this volume). Available at: https://doi.org/10.30440/bt407.5

Morris, P. A. 1984. MAGFRAC: a basic program for least-squares approximation of fractional crystallization. Computers and Geosciences 10, 437–444.

Neal, C. R. & Taylor, L .A. 1989. A negative Ce anomaly in a peridotite xenolith: Evidence for crustal recycling into the mantle or mantle metasomatism? Geochimica et Cosmochimica Acta 53, 1035–1040.

Nikkilä, K., Mänttäri, I., Nironen, M., Eklund, O. & Korja, A. 2016. Three stages to form a large batholith after terrane accretion – An example from the Svecofennian orogen. Precambrian Research 281, 618–638.

Nironen, M. 1997. The Svecofennian Orogen: a tectonic model. Precambrian Research 86, 21–44.

Nironen, M. 2003. Keski-Suomen granitoidikompleksi, karttaselitys. Summary: Central Finland Granitoid Complex – Explanation to a map. Geological Survey of Finland, Report of Investigation 157. 45 p. (in Finnish). Available at: http://tupa.gtk.fi/julkaisu/tutkimusraportti/tr_157.pdf

Nironen, M., Elliott, B. A. & Rämö, O. T. 2000. 1.88–1.87 Ga post-kinematic intrusions of the Central Finland Granitoid Complex: a shift from C-type to A-type magmatism during lithospheric convergence. Lithos 53, 37–58.

Orsini, J. B., Cocirta, C. & Zorpi, M. J. 1991. Genesis of mafic microgranular enclaves through differentiation of basic magmas, mingling and chemical exchanges with their host granitoid magmas. In: Didier, J. & Barbarin, B. (eds) Enclaves and Granite Petrology. Amsterdam: Elsevier, 445–464.

Passchier, C. J. & Trouw, R. A. J. 1998. Microtectonics. Berlin: Springer-Verlag. 289 p.

Patiño Douce, A. E. 1997. Generation of metaluminous A-type granites by low-pressure melting of calc-alkaline granitoids. Geology 25, 743–746.

Pearce, J. A., Harris, N. B. W. & Tindle, A. G. 1984. Trace Element Discrimination Diagrams for the Tectonic Interpretation of Granitic Rocks. Journal of Petrology 25, 956–983.

Phillips, E. R. & Carr, G. R. 1973. Myrmekite associated with alkali feldspar megacrysts in felsic rocks from New South Wales. Lithos 6, 245–260.

Rämö, O. T. 1991. Petrogenesis of the Proterozoic rapakivi granites and related basic rocks of the southeastern Fennoscandia: Nd and Pb isotopic and general geochemical constraints. Geological Survey of Finland, Bulletin 355, 1–161. Available at: http://tupa.gtk.fi/julkaisu/bulletin/bt_355.pdf

Rämö, O. T. & Haapala, I. 1995. One hundred years of Rapakivi Granite. Mineralogy and Petrology 52, 129–185.

Rämö, O. T., Vaasjoki, M., Mänttäri, I., Elliott, B. A. & Nironen, M. 2001. Petrogenesis of the Post-kinematic Magmatism of the Central Finland Granitoid Complex I; Radiogenic Isotope Constraints and Implication for Crustal Evolution. Journal of Petrology 42, 1971–1993.

Reid, J. B., Jr., Evans, O. C. & Fates, D. G. 1983. Magma mixing in granitic rocks of the central Sierra Nevada, California. Earth and Planetary Science Letters 66, 243–261.

Salonsaari, P. T. 1995. Hybridization in the subvolcanic Jaala-Iitti complex and its petrogenetic relation to rapakivi granites and associated mafic rocks of southeastern Finland. Geological Society of Finland, Bulletin 67, 1–104. Available at: https://doi.org/10.17741/bgsf/67.1b

Shand, S. J. 1943. Eruptive Rocks: their Genesis, Composition, Classification, and their Relation to Ore-Deposits with a Chapter on Meteorites. New York: John Wiley & Sons. 444 p.

Scoates, J. S., Frost, C. D., Mitchell, J. N., Lindsley, D. H. & Frost, B. R. 1996. Residual-liquid origin for a monzonitic intrusion in a mid-Proterozoic anorthosite complex: The Sybille intrusion, Laramie anorthosite complex, Wyoming. Geological Society of America Bulletin 108, 1357–1371.

Simpson, C. & Wintsch, R. P. 1989. Evidence for deformation-induced K-feldspar replacement by myrmekite. Journal of Metamorphic Geology 7, 261–275.

Virtanen, V. J. 2017. Paleoproterozoic Postkinematic A-type Magmatism of Southeastern Central Finland Granitoid Complex: Petrography, Geochemistry, and Geochronology of the Riitalampi, Viininperä, and Korloppinen Localities. Unpublished Master's Thesis, University of Helsinki, Department of Geosciences and Geography. 93 p. Available at: http://urn.fi/URN:NBN:fi-fe2017112251034]

Whalen, J. B., Currie, K. L. & Chappell, B. W. 1987. A-type granites: geochemical characteristics, discrimination and petrogenesis. Contributions to Mineralogy and Petrology 95, 407–419.

Development of the Paleoproterozoic Svecofennian orogeny: new constraints from the southeastern boundary of the Central Finland Granitoid Complex
Edited by Perttu Mikkola, Pentti Hölttä and Asko Käpyaho
Geological Survey of Finland, Bulletin 407, 151-167, 2018

INDICATIONS OF A Cu-Au MINERALISATION AT LAMMUSTE, CENTRAL FINLAND

by

Soili Solismaa, Sami Niemi, Esa Heilimo, Jari Nenonen and Jukka Kousa

Solismaa, S., Niemi, S., Heilimo, E., Nenonen, J. & Kousa, J. 2018. Indications of a Cu-Au mineralisation at Lammuste, central Finland. *Geological Survey of Finland, Bulletin 407*, 151–167, 16 figures and 2 tables.

The Lammuste study area is located in Central Finland. The dominant geological feature of the area is a 10 x 15 km quartz diorite intrusion easily observable on the aeromagnetic map. As the area is part of a large drumlin field, the number of outcrops is limited.

Lammuste was targeted for exploration after the Geological Survey of Finland (GTK) received layman's samples enriched in Au, Cu and Ag from the area in 2013. The highest concentrations in these boulders were Au 1.9 ppm, Cu 10 wt% and Ag 66 ppm. Both quartz diorite and mafic metavolcanic rock samples displayed ore-grade concentrations. The exploration methods included boulder and bedrock mapping, geophysical measurements, till geochemistry, drilling and petrographic study. The glacial transport distance of the mineralized boulders was examined with boulder exploration and research excavations. Mafic metavolcanic rocks intersected with drilling were comparable to the mineralized boulders, which suggests short glacial transport. The mineralized boulders primarily consist of plagioclase and hedenbergite, but in drill cores, the mafic metavolcanic layers mainly consist of plagioclase and hornblende. On the outcrops in the entire area of the quartz diorite, chalcopyrite frequently occurs as single grains or weak dissemination.

Some similarities with Proterozoic porphyry copper deposits were found, for instance in the formation conditions, the connection to igneous rocks and signs of adequate alteration. Although distinct Cu–Au mineralisation remains undiscovered, the area shows widespread signs of ore-forming processes. More exploration is needed to better evaluate the ore potential of the area.

Appendix 1 is available at: http://tupa.gtk.fi/julkaisu/liiteaineisto/bt_407_appendix_1.pdf

Keywords: mineral exploration, chalcopyrite, copper ores, porphyry copper, copper, gold, quartz diorites, glacial features, geophysics, drilling, Svecofennian, Paleoproterozoic

Geological Survey of Finland, P.O. Box 1237, FI-70211 Kuopio, Finland
E-mail: soili.solismaa@gtk.fi

VERTAISARVIOITU
KOLLEGIALT GRANSKAD
PEER-REVIEWED
www.tsv.fi/tunnus

https://doi.org/10.30440/bt407.8

Editorial handling by Perttu Mikkola.

Received 30 June 2017; Accepted 1 December 2017

1 INTRODUCTION

The Lammuste area is located west of the city of Pieksämäki in central Finland (Fig. 1). The dominant geological feature of the target area is the 15 x 10 km Lammuste quartz diorite intrusion rotated dextrally within the SW–NE-trending Leivonmäki shear zone (Mikkola et al. 2018a). On the aeromagnetic map, the intrusion appears as a magnetic high and its rotation is clearly indicated (Fig. 3 in Mikkola et al. 2018a). Strips of mafic metavolcanic rocks belonging to the Pirkanmaa migmatite suite and well-preserved metagreywackes of the same suite flank the intrusion on the northeastern and eastern side of the intrusion (Mikkola et al. 2018b, Kousa et al. 2018). On the southwestern side, it is flanked by tonalite (Heilimo et al. 2018). The Lammuste quartz diorite, yielding a zircon U–Pb age of 1897 ± 7 Ma (authors' unpublished data), is coeval with the main phase of the Makkola suite, mainly consisting of calc-alkaline volcanic rocks (Mikkola et al. 2018c).

Layman's samples sent by Teuvo Heikkinen in 2013 to the Geological Survey of Finland (GTK) provided the impetus for exploration in the area. The highest concentrations from quartz diorite boulder samples were Au 1.3 ppm, Cu 10 wt% and Ag 66 ppm (sample 20152358). A mafic metavolcanic rock sample (20131969) contained Au 1.9 ppm, Cu 3 wt% and Ag 25 ppm. Comparable earlier findings include a metadiabase boulder (2399/75, Fig. 1) containing 2.26% of Cu sent to Outokumpu Oy in 1975. A quartz diorite sample (19901598) taken from an outcrop in the northern parts of the intrusion containing 0.6 wt% of Cu and 0.16 ppm of Au was sent to GTK in 1990.

Due to its location within a large Quaternary drumlin field, the number of outcrops in the Lammuste area is limited. The objective of this study was to consider the similarities of the study area with known Paleoproterozoic porphyry copper deposits. In the Fennoscandian shield, such deposits have been previously studied, for example, by Nurmi (1984) and Tiainen et al. (2013) in Finland and by Weihed (1990) and Wanhainen (2006) in

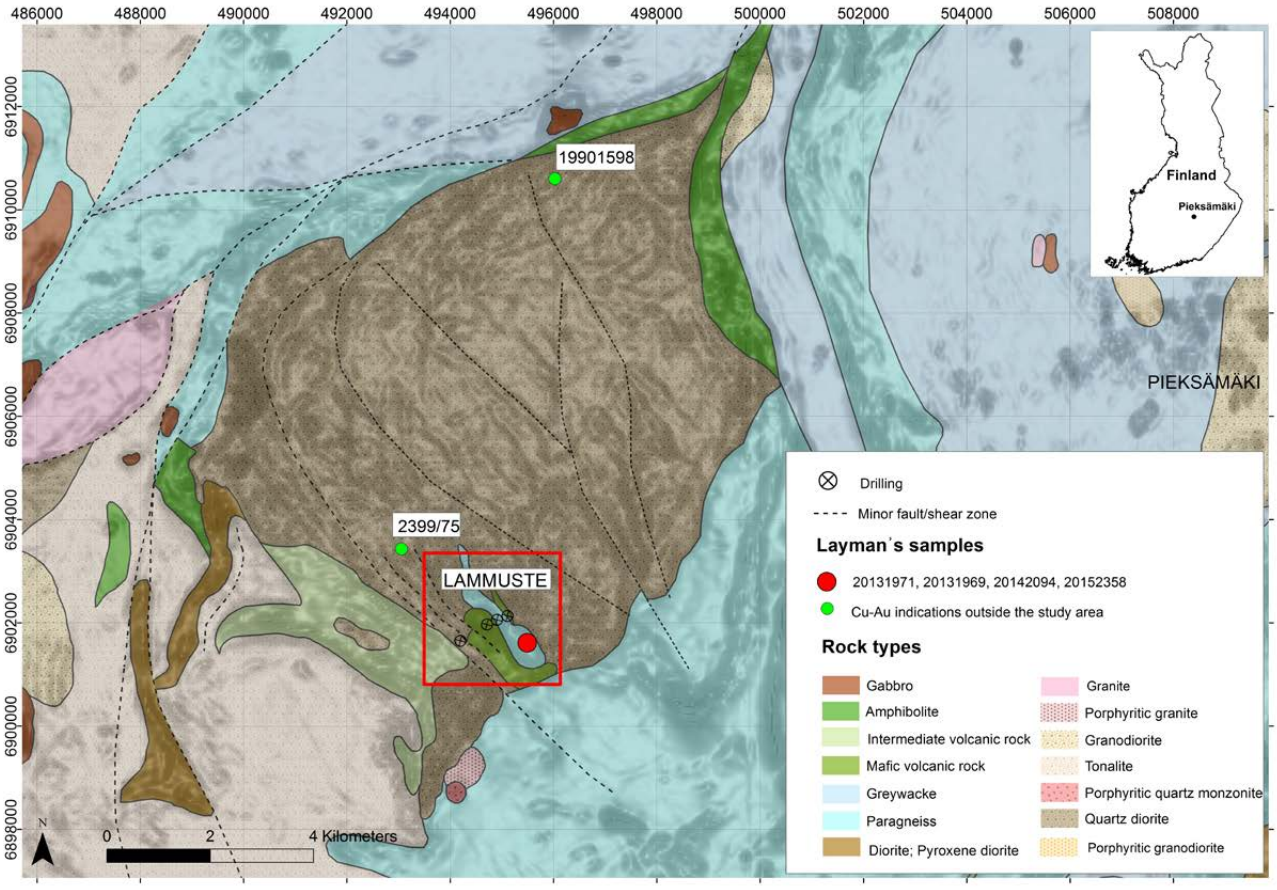

Fig. 1. Geological and magnetic map of the Lammuste area with localities of drilling targets and layman samples. Bedrock map modified from Mikkola et al. (2016) and Bedrock of Finland - DigiKP.

Sweden. Recently, GTK targeted the Hiekkapohja area 60 km eastwest of Lammuste with a similar interest (Heilimo et al. 2017). Proterozoic porphyry-type deposits still remain poorly understood compared with larger and better preserved Phanerozoic deposits (Kirkham & Dunne 2000).

2 EXPLORATION METHODS

Only an overview of the applied exploration methods is provided here, as a more detailed description is given in Solismaa et al. (2016). Boulder mapping was carried out in the vicinity of the layman's samples and upstream from them with respect to glacial flow. At the same time, all the identified outcrops were mapped.

To determine the glacial transport distance of the mineralized boulders, nine research excavations were dug with an excavator. Till stratigraphy observations were made from the walls of these research excavations and bedrock observations from their bottom if the bedrock surface was reached.

Four drill holes totalling 606.8 m were drilled in the area. The rock samples were analysed by Labtium Ltd. The analytical methods used for sulphide-bearing samples were aqua regia leaching with inductively coupled plasma mass spectrometry (ICP-MS) and inductively coupled plasma optical emission spectrometry (ICP-OES) (Labtium code 511PM). Precious metals were examined with the fire assay enrichment method and ICP-MS (Labtium code 705P). Whole-rock analyses from 14 drill core and outcrop samples in addition to one boulder sample were conducted on selected samples with XRF (Labtium code 175X) and total digestion with ICP-MS (Labtium code 308PM). The analytical methods are described in Appendix 1.

Ground-measured magnetic (67 line kilometres) and induced polarization (IP) surveys (22.5 line kilometres) were carried out with 100-m line spacing. A gravity survey (five lines, total 6.6 km) was conducted to identify density variations in the study area. Four lines were surveyed using the horizontal loop electromagnetic method (HLEM) to check whether the conductive anomaly identified in the airborne electromagnetic (AEM) survey originated from bedrock or from a power line.

The rock-forming and ore minerals were identified macroscopically from rock samples and from selected samples with a polarizing microscope from thin sections. Electron microprobe analysis was performed on 3 thin sections in GTK's laboratory to confirm certain optical identifications.

3 RESULTS

3.1 Boulders

Sulphide-rich boulders, up to several metres in diameter, discovered within 100 m of the original layman's sample (Fig. 1) are to date the most promising findings in the Lammuste area. Two main rock types were observed in the mineralized boulders: mafic metavolcanic rock and quartz diorite with mafic enclaves. Sample 20131969 is a mafic metavolcanic rock (Fig. 2A) containing 3% Cu and 1.9 ppm Au. The highest Cu, Au and Ag contents in a quartz diorite sample are 10 wt%, 1.3 ppm and 66 ppm, respectively, from sample 20152358 (Fig. 2B).

Mineralized mafic metavolcanic boulders are mineralogically recrystallized and fine-grained (<2 mm) rock types. Boulders are commonly composed of plagioclase and hedenbergite (Fig. 3). The hedenbergite was identified with microprobe analysis. Accessory minerals are sphene, chalcopyrite, magnetite, chalcosite, apatite and pyrite. Chalcopyrite shows alteration to chalcosite (Fig. 4) and occurs together with hedenbergite clusters.

3.2 Research excavations

Excavation at the site of the mineralized boulders revealed only younger basal till deposited by the Middle and Late Weichselian glaciation phase (Nenonen 1994). This interpretation was confirmed by striations on the surface of the bedrock at the bottom of the pit oriented to 320–325 degrees,

Fig. 2. A) A mineralized mafic metavolcanic boulder (layman's sample 20131969, size 8 x 5 cm) with 2.9% Cu, 1.8 ppm Au and 25 ppm Ag. B) A quartz diorite boulder (20152358), a sample of which contained 10 wt% Cu, 1.3 ppm Au and 66 ppm Ag. Length of the matchbox 5 cm.

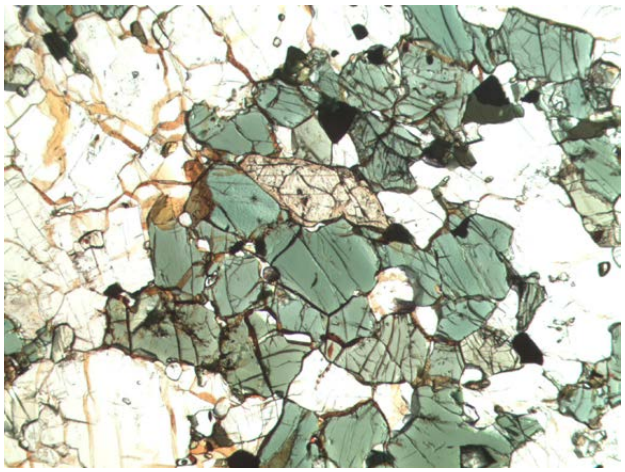

Fig. 3. Granoblastic texture of the mafic metavolcanic rock in a boulder (SMMA-2015-19.1) containing green clinopyroxene (hedenbergite), plagioclase and sphene. Field of vision 3 mm, plane-polarized light.

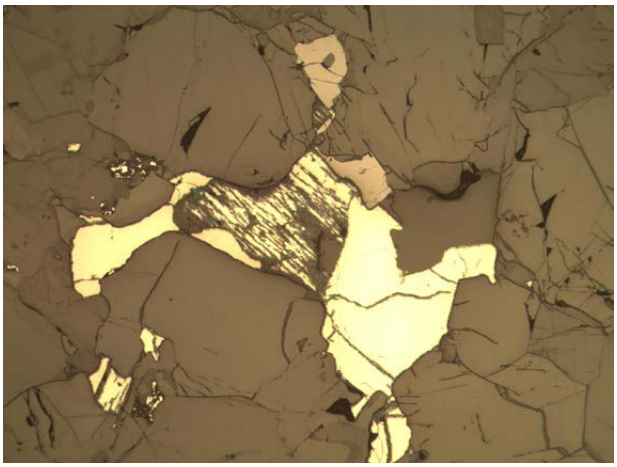

Fig. 4. Chalcopyrite shows alteration to chalcosite in mafic metavolcanic boulder SMMA-2015-19.1. Field of vision 1.5 mm, reflected and plane-polarized light.

which is also the direction of the drumlins. The boulders in the till were rather rounded and mainly mafic metavolcanic rocks and quartz diorites. Mafic metavolcanic rocks and quartz diorite with chalcopyrite grains and weak dissemination were found at the bottom of research excavations SMMA-2015-27, -28, -29 and -34 (Fig. 5).

In research excavations SMMA-2015-30, -31, -32 and -33, north of the drumlin's proximal end, the boulders in the till were rounded and mainly consisted of granodiorite, indicating longer glacial transport, contrary to the boulders representing the local bedrock at the distal end of drumlin (Solismaa et al. 2016).

Based on the results of boulder exploration, till stratigraphic studies and bedrock observations from the bottom of the research excavations, it is likely that the origin of the layman's samples is within 700 m of where they were located in a northwest direction.

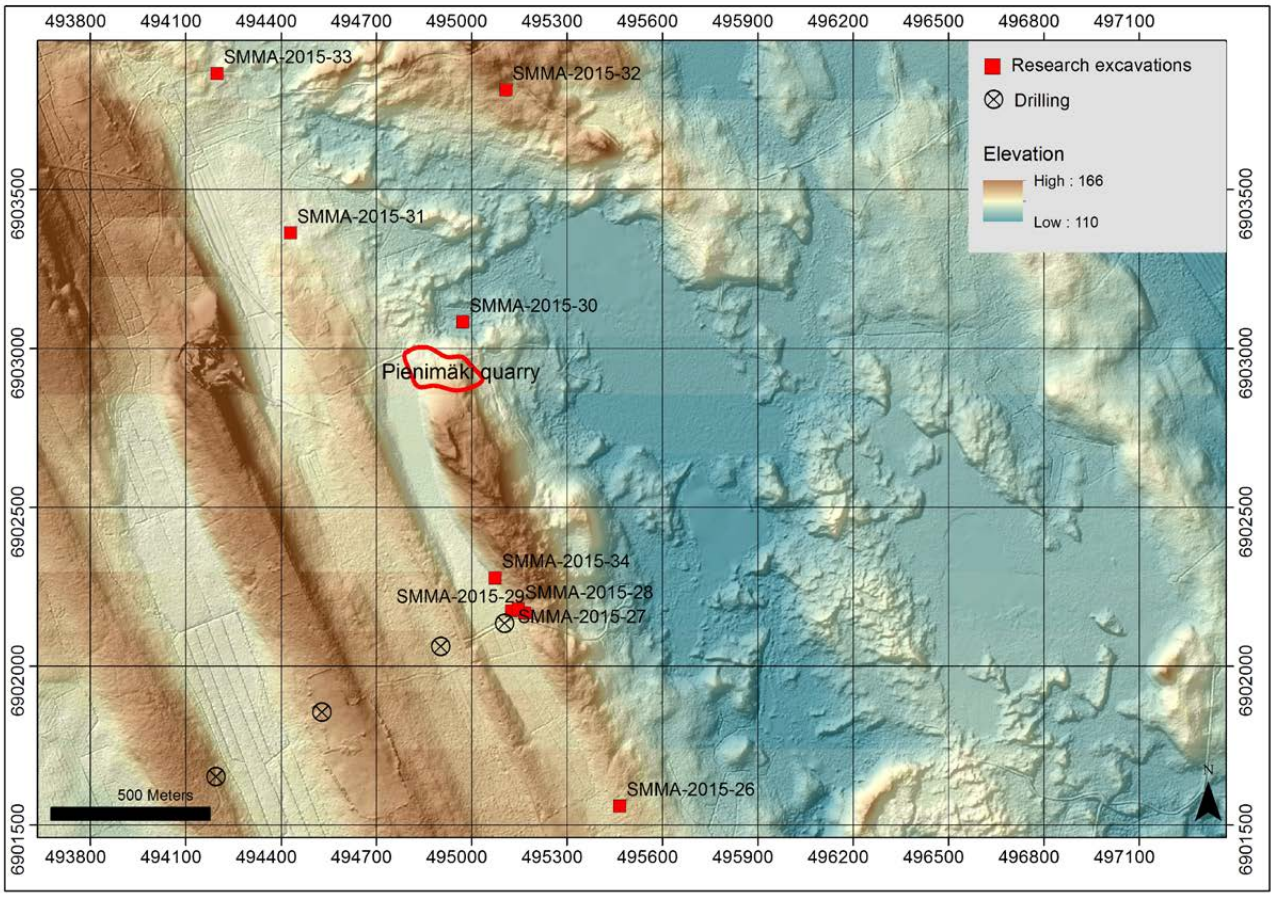

Fig. 5. Research excavation sites and drill holes on top of the airborne laser scanning elevation model.

3.3 Geophysical survey

As the horizontal loop electromagnetic method (HLEM) survey did not indicate any conductors, the anomaly seen in in the airborne electromagnetic survey (AEM) data is interpreted as being caused by the power line. Drilling results showed that the thickness of overburden in the Lammuste area is 15 m in many places (Solismaa et al. 2016). The depth penetration of the IP survey in the dipole-dipole configuration that was used was 15 m or less, so it is possible that in many places, the IP signal is actually received from the overburden instead of the bedrock. Thus, to ensure a signal originating from the bedrock, the IP survey should be carried out in a different configuration.

Two of the drill holes targeted a magnetic high of ~1300 nT about 500 m west of the mineralized boulders (Fig. 6). The other two drill holes targeted magnetic minimum areas northeast of the site of the layman's samples.

3.4 Rock types

The drillings revealed a greater diversity of rock types than the outcrop observations in the Lammuste area. Only the major rock types are described in this chapter. In addition to the quartz diorite typical for the outcrops of the study area, metamorphosed mafic volcanic rocks and pelitic to psammitic gneisses were found to be abundant in the drill cores (Fig. 7).

3.4.1 Mafic metavolcanic rock

In addition to the boulders, mafic metavolcanic rocks were intersected by drill cores N4342015R26 and N4342015R28 (Fig. 8). The composition, texture and grain size vary significantly in these heterogeneous rocks, which occasionally have a porphyritic texture and are often cross-cut by thin, altered

mafic veins. The main minerals are plagioclase, hornblende and biotite. Typical accessory minerals are garnet, epidote, sphene, quartz, pyrite, chalcopyrite, diopside, apatite and alkali feldspar. In the drill cores, hornblende can be seen as phenocryst-like aggregates varying from 1 to 5 mm in diameter. The ground mass is fine to medium grained.

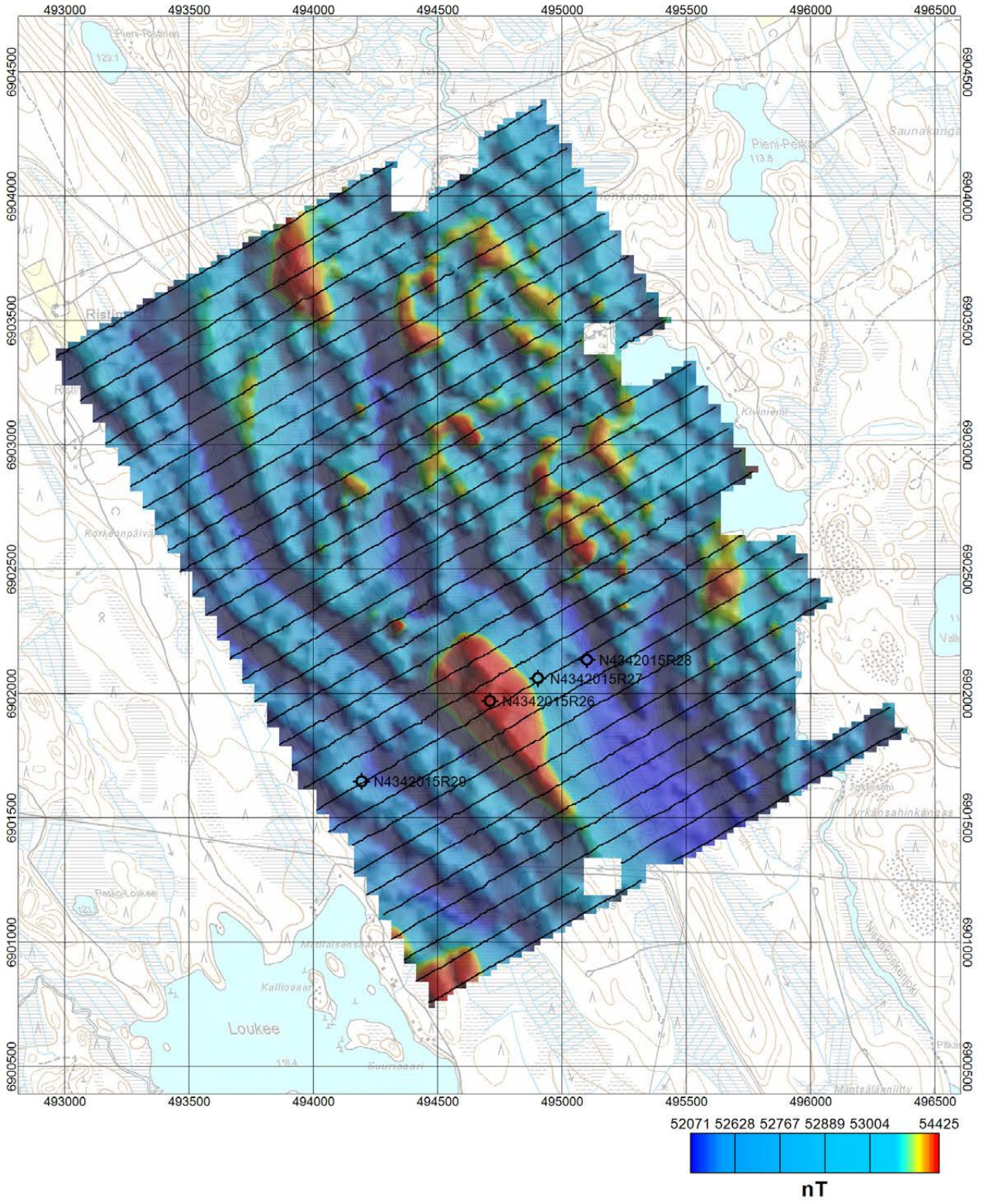

Fig. 6. Ground-measured total magnetic intensity reduced to pole, and location of drill holes in the Lammuste area. Basemap © National Land Survey of Finland

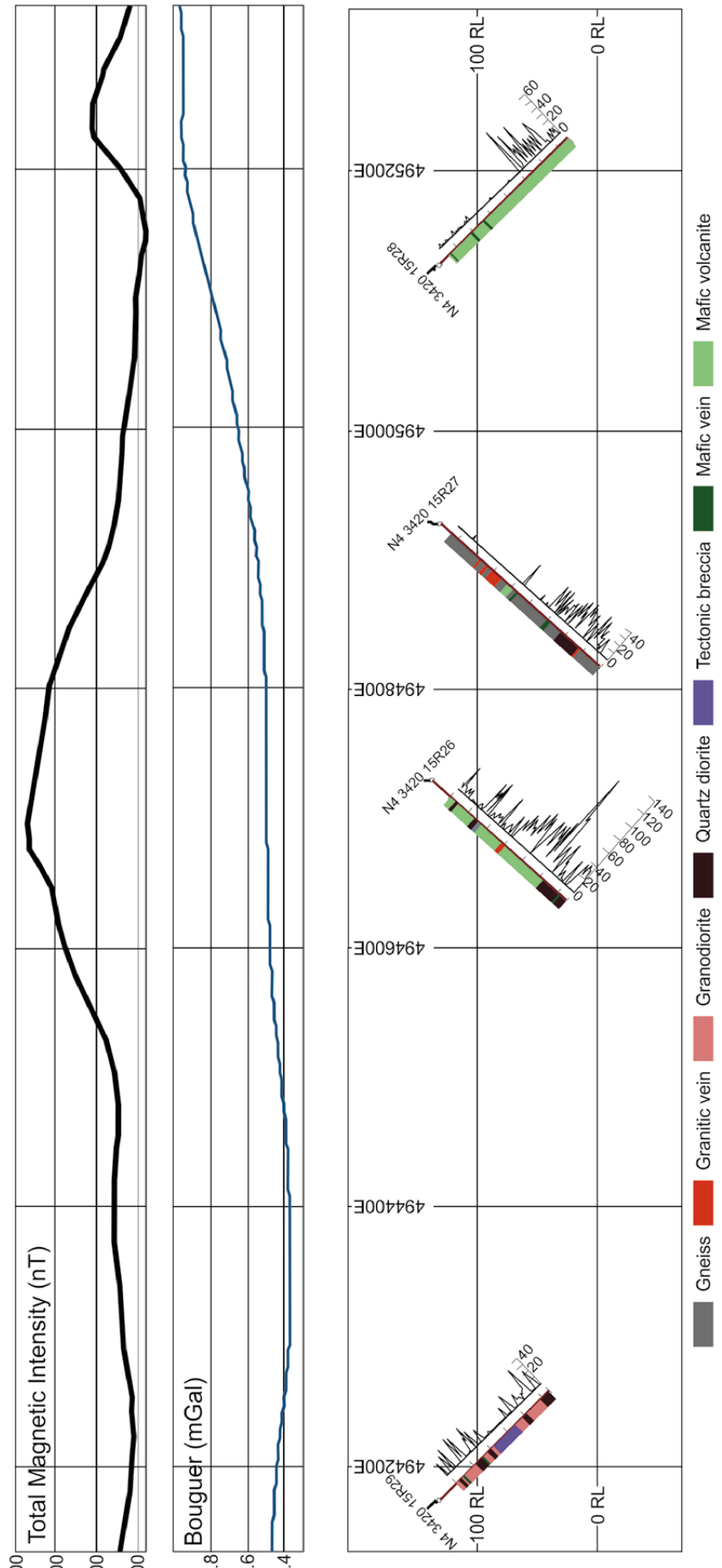

Fig. 7. Drilling profile from Lammuste. On top, profiles sampled from interpolated grids of the ground-surveyed total magnetic field and Bouguer anomaly. Susceptibility (scale k(SI) 10^{-3}) measured at 1-m intervals from the drill core with a hand-held KT-10 meter as a profile next to the rock columns.

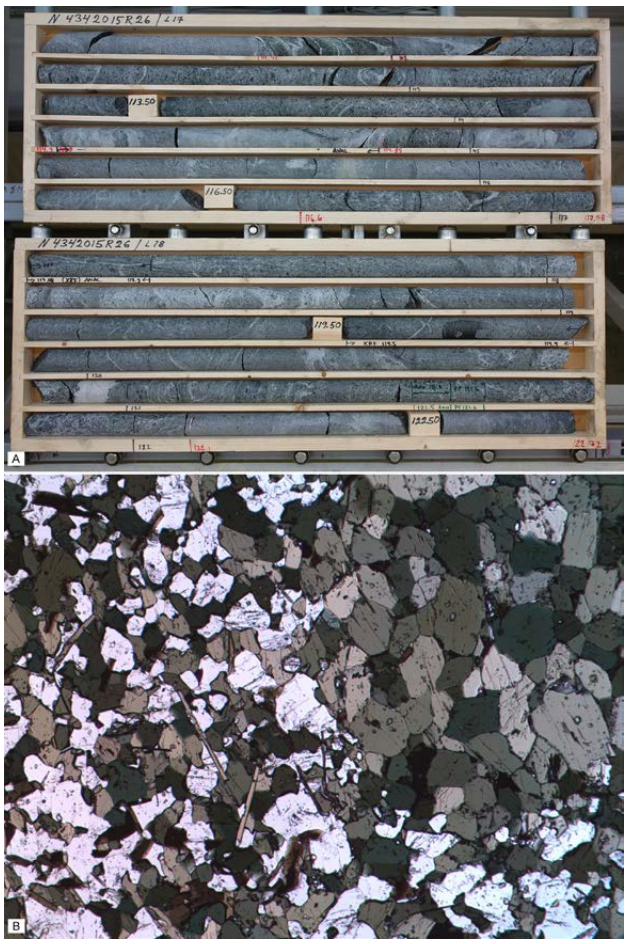

Fig. 8. Typical mafic metavolcanic rock in A) drill core N4342015R26 and B) thin section N4342015R26 121.50, field of vision 5 mm, plane-polarized light. Hornblende can be observed as "dots" in the drill core and in thin section as grain aggregates in plagioclase-hornblende ground mass.

All natural outcrops in the Lammuste area consist of quartz diorite with sporadic mafic inclusions and veins (Figs. 1 and 9). Chalcopyrite was frequently observed from the outcrops, either as single grains or weak dissemination, from the entire area of the intrusion. Detailed observations were made from the aggregate quarry in the Pienimäki area. Typically, the Lammuste quartz diorite is foliated and medium grained, containing plagioclase, hornblende, biotite and quartz as the main minerals. Plagioclase frequently shows medium-grade alteration to sericite. Accessory minerals are chalcopyrite, epidote, apatite, orthopyroxene, alkali feldspar, pyrite and pyrrhotite.

Drill core N4342015R29 consists of porphyritic quartz diorite that grades into granodiorite, which is brecciated and altered from 64 to 89 m in the drill hole. The brecciated part of the drill core is coloured pink, presumably due to hydrothermal hematitization (Fig. 10). The occurrence of thin calcite veins and carbonate alteration characterize this brecciated zone of granodiorite.

3.4.2 Gneiss

Gneisses were especially observed in drill core N4342015R27 (Fig. 11). Psammitic migmatized gneisses dominate the upper part of the drill core, while in the lower part the composition is pelitic. The gneisses are cut by both pegmatite and mafic

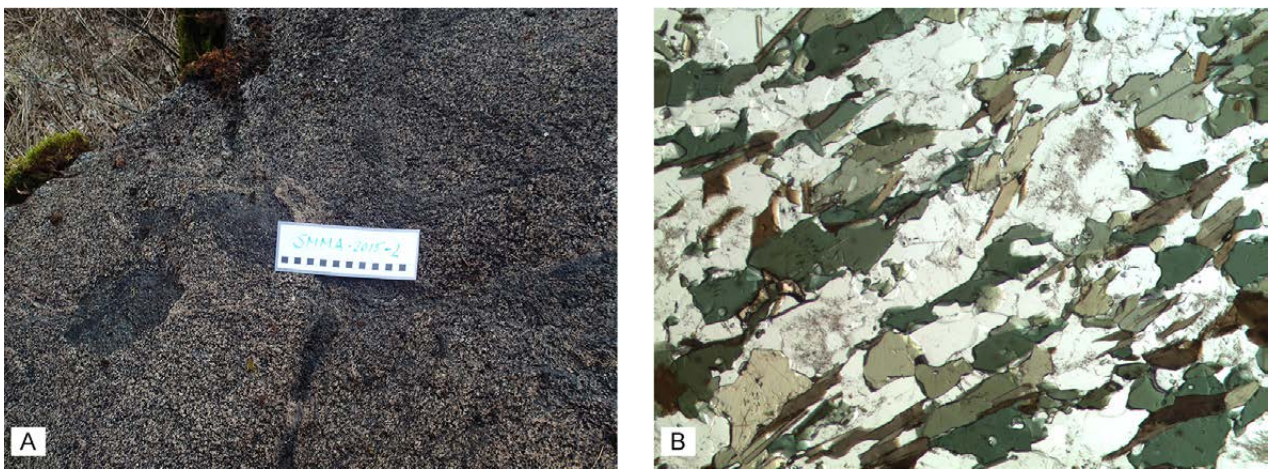

Fig. 9. Typical Lammuste quartz diorite in A) outcrop SMMA-2015-2 with rounded mafic enclaves, scale bar with cm scale, and B) a thin section from drill core N4342015R29, depth 24 m, field of vision 3 mm, plane-polarized light.

Fig. 10. Brecciated, altered and fragmented granodiorite in drill core N4342015R29. Width of the box 1 m.

dykes. From a depth of 88 m to 180 m, sillimanite has been variably altered retrogradely to muscovite. Magnetite dissemination causes elevated susceptibility between 115 and 170 m. The main minerals of the gneiss are plagioclase, quartz and biotite, while garnet, alkali feldspar, muscovite, sillimanite, magnetite, chalcopyrite, and pyrite can be found as accessory minerals.

3.4.3 Altered mafic veins and granitic veins

Mafic veins cross-cutting both mafic volcanic rocks and quartz diorites are a common feature in the Lammuste area. Veins varying in width from 10 to 100 cm were observed from the area of the Pienimäki quarry (Fig. 5), from research excavation SMMA-2015-34 (Fig. 5), and from the drill cores. The degree of alteration is highly variable, with biotite and chlorite after hornblende being character-

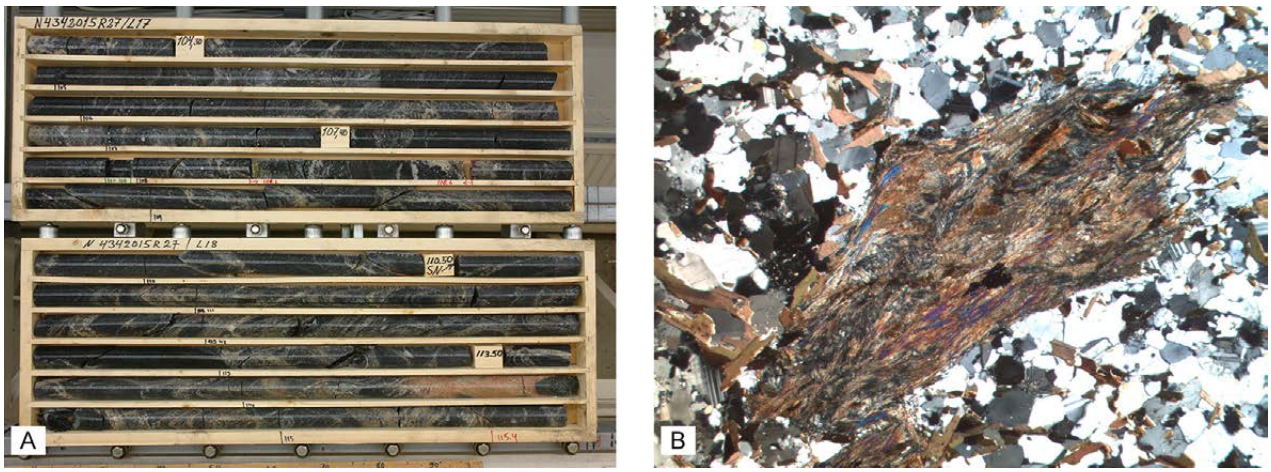

Fig. 11. A) Sillimanite gneiss and a pegmatite vein in drill core N4342015R27 and B) sillimanite in thin section from the drill core, depth 117.60 m, field of vision 5 mm, cross-polarized light.

istic. A mafic altered dyke intruding quartz diorite in the Pienimäki quarry consists of hedenbergite (identified with a polarizing microscope), tremolite, hornblende, plagioclase and chalcopyrite dissemination similar to mineralized boulder SMMA-2015-19.1. A mafic, foliated and altered vein in drill core N4342015R26 at the depth 141.90–142.80 m mainly consists of chlorite and biotite. Accessory minerals are disseminated garnet and calcite, which was observed as thin veins in the lower part of the vein.

The grain size of the granitic veins observed in drill cores N4342015R26, R27 and R28 varies from coarse to fine grained. Veins cross-cut the mafic volcanic rock and the gneiss. The width of the veins varies from 10 cm to three metres.

3.5 Geochemistry

The highest gold and copper contents from the drill cores were found in drill cores N434201526 (114.30–114.85 m; Au 23 ppb and Cu 312 ppm) and N4342015R28 (124.50–125.30 m; Au 17 ppb and Cu 411 ppm). The Au, Ag and Cu content of the rock samples collected during the boulder exploration and the bedrock mapping are presented in Table 1. The locations of samples with the highest Cu contents are presented in Figure 12.

Table 1. Au, Ag and Cu content of boulders (B) and outcrop (O) samples. <10 = below detection limit; n.a. = not analysed.

SAMPLE ID	ROCK TYPE (B/O)	Au ppb	Ag ppm	Cu ppm	X	Y
20152554	Granodiorite (O)	173	5.1	18200	494940	6902921
20152561	Granodiorite (O)	282	2.9	4700	495368	6901882
20152358	Quartz diorite (B)	1320	66.2	100000	495475	6901544
20131971	Sulphide rock (B)	63	17.9	10200	495497	6901595
20142094	Quartz diorite (B)	792	78.0	100000	495497	6901581
20131969	Mafic metavolcanic rock (B)	1850	25.0	29500	495497	6901581
SMMA-2015-7.1	Quartz diorite (O)	<10	n.a	180	494951	6902647
SMMA-2015-7.2	Mafic dyke(O)	<10	0.0	21	494951	6902647
SMMA-2015-9.1	Quartz diorite (O)	<10	0.1	198	496037	6910640
SMMA-2015-10.1	Mafic metavolcanic rock (O)	21	n.a	60	496980	6911578
SMMA-2015-19.1	Mafic metavolcanic rock (B)	704	23.0	14000	495469	6901560
SMMA-2015-22.1	Limestone (O)	<10	n.a	30	494094	6902972
TOS$-2015-11.3	Felsic dyke(O)	<10	0.3	145	492450	6908674
TOS$-2015-11.4	Felsic dyke(O)	<10	n.a	110	492459	6908685
TOS$-2015-14.1	Quartz diorite (O)	15	0.3	421	494944	6902652
TOS$-2015-23.1	Granodiorite (B)	250	3.8	4940	498803	6902528
TOS$-2015-29.1	Granite (O)	<10	n.a	30	494346	6899449
TOS$-2015-3.1	Granodiorite (O)	<10	0.1	56	492318	6906429
TOS$-2015-33.1	Granodiorite (B)	<10	0.1	133	492226	6904265
TOS$-2015-8.1	Quartz diorite (O)	<10	0.1	98	494540	6903207
TOS$-2015-9.1	Granodiorite (O)	<10	0.0	45	493291	6904884
SMMA-2015-24.1	Mafic dyke (O)	11	0.2	329	494966	6902887
TOS$-2014-203.1	Quartz diorite (O)	<5	0.1	43	495855	6901639
TOS$-2014-204.1	Quartz diorite (B)	80.7	5.9	2230	495980	6901543
TOS$-2014-205.1	Quartz diorite (B)	<5	0.1	377	495960	6901415
TOS$-2014-67.1	Quartz diorite (B)	891	16.3	15700	495532	6901470
TOS$-2014-68.1	Quartz diorite (B)	846	10.5	9430	495406	6901723
TOS$-2014-22.1	Quartz diorite (B)	684	n.a.	11960	495497	6901581
TOS$-2014-60.1	Diorite (B)	301	7.6	8760	495501	6901587
TOS$-2014-61.1	Diorite (B)	24	0.9	1170	495480	6901550
EPHE-2012-67.1	Quartz diorite (O)	<10	0.1	77	495040	6902773

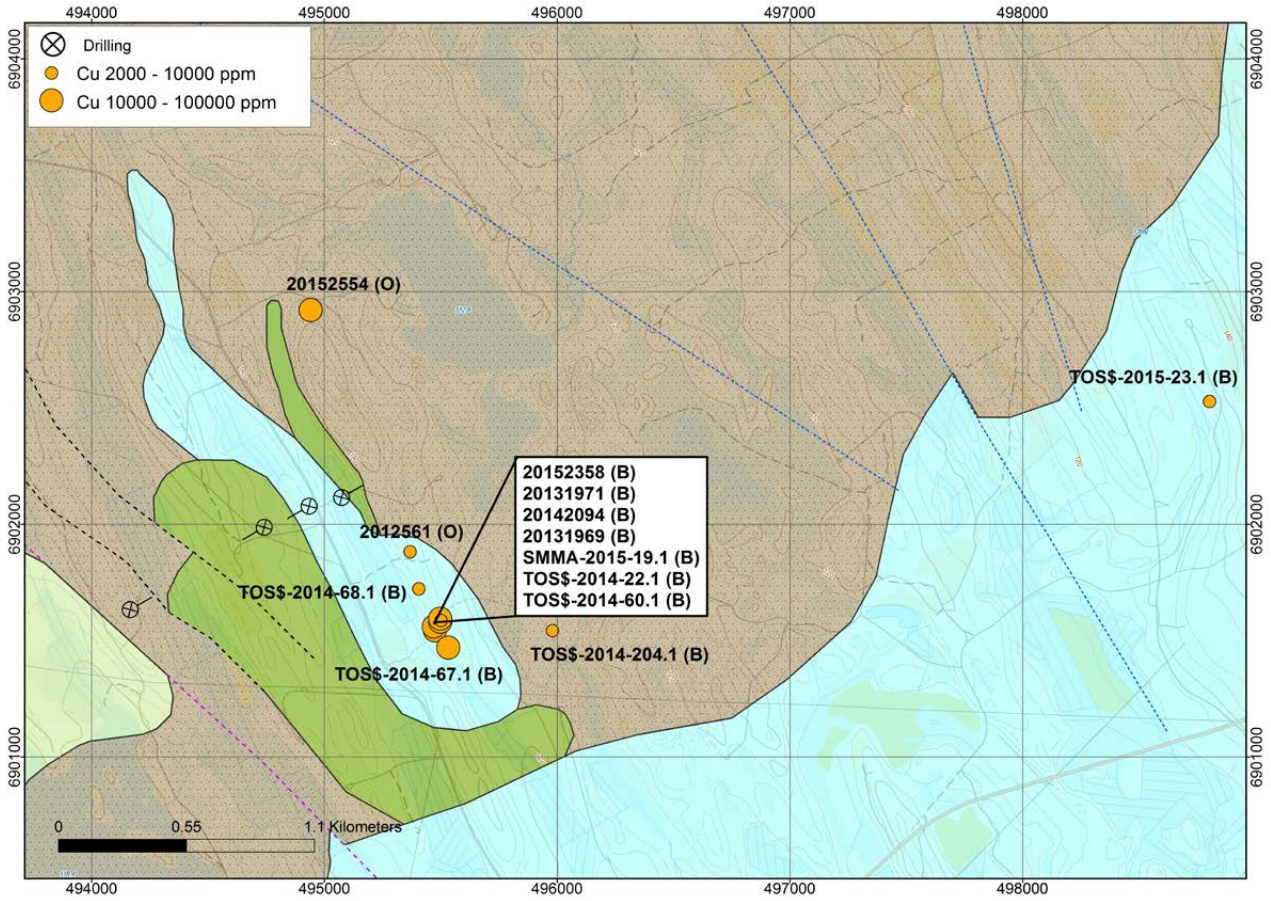

Fig 12. Cu content of boulders and outcrop samples in the study area. Boulders (B) and outcrop (O) samples. See Fig. 1 for a key to the rock types. Basemap © National Land Survey of Finland.

The Ishikawa alteration index (AI = (100*(K_2O+MgO))/(K_2O+MgO+Na_2O+CaO)) was originally used to describe the intensity of sericite and chlorite alteration in volcanic rocks in Kuroko type volcanic-hosted massive sulphide (VHMS) deposits (Ishikawa et al. 1976). The alteration index measures the breakdown of sodic plagioclase and is therefore closely related to Na depletion, and an increasing AI value is a sign of increasing K_2O. The alteration index does not take into account carbonate alteration, which may reduce the calculated value (Large et al. 2001).

The AI index for hydrothermally altered samples varies between 50 and 100 (Large et al. 2001). In Lammuste, the values vary between 14 and 73. Samples with values above 50 (Fig. 13) are a mafic dyke (SMMA-2015-23.1), a mafic vein (N4342015R26 142.00–142.30) and gneiss (N4342015R27 37.60–38.30). The mafic metavolcanic rock boulder with 1.4 wt% Cu and 0.7 ppm Au (SMMA-2015.19.1) has a decreased K_2O and increased Na_2O content and the alteration index is low compared to the other samples (Fig. 13, Table 2). An increasing Na_2O content could be a sign of sodic alteration. Typical minerals related to sodic alteration are Na plagioclase, actinolite, epidote, chlorite and sphene (Dilles 2010).

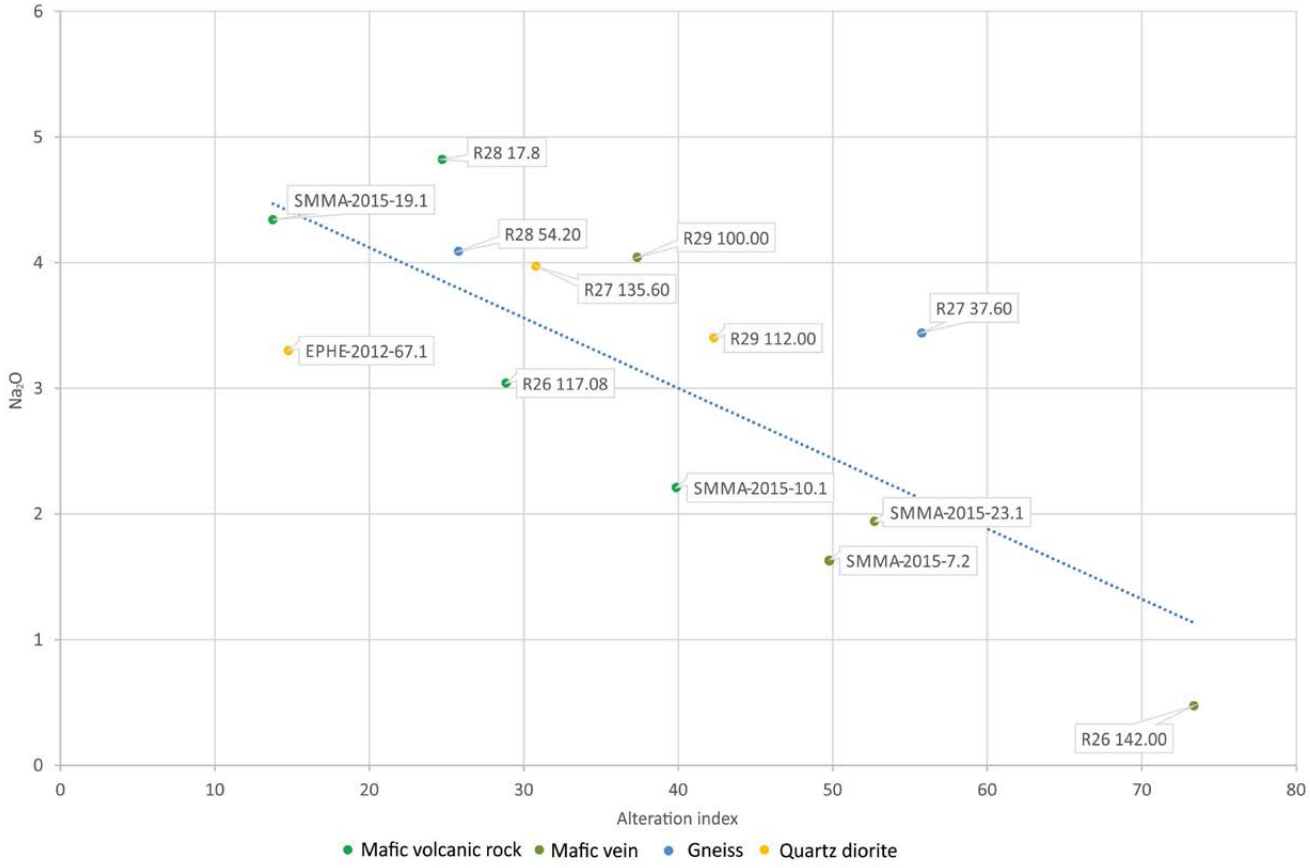

Fig. 13. Alteration index and Na_2O content of the whole-rock-analysed samples. Carbonate alteration may reduce the alteration index value.

Table 2. Main element compositions of 15 samples from the Lammuste area.

Sample ID	ROCK TYPE	SiO	TiO	Al	Fe	MnO	MgO	CaO	Na	K	P
		wt.%	wt.%	wt.%	wt.%	wt.%	wt.%	wt.%	wt.%	wt.%	wt.%
N4342015R26 117.08-117.30	Mafic meta-volcanic rock	48.2	1.09	16.5	12.80	0.21	4.43	10.22	3.04	0.95	0.55
N4342015R28 17.80-18.50	Mafic meta-volcanic rock	56.6	0.62	19.7	7.09	0.15	1.87	6.35	4.82	1.80	0.34
SMMA-2015-10.1	Mafic meta-volcanic rock	45.3	0.61	14.0	11.90	0.20	8.31	12.17	2.21	1.23	0.34
SMMA-2015-19.1 (boulder)	Mafic meta-volcanic rock	53.7	0.41	18.6	7.87	0.16	1.04	10.57	4.34	1.34	0.44
N4342015R26 142.00-142.30	Mafic vein	41.6	0.46	8.1	7.95	0.21	23.00	7.93	0.47	0.17	0.15
N4342015R29 100.00-100.90	Intermediate vein	58.1	0.77	16.1	7.13	0.11	4.39	6.76	4.04	2.05	0.32
SMMA-2015-23.1	Mafic dyke (width >1m)	45.1	1.07	12.5	13.40	0.25	9.23	8.33	1.94	2.22	0.49
SMMA-2015-7.2	Mafic dyke (width >1m)	46.4	1.04	11.4	12.00	0.24	9.22	9.64	1.63	1.95	0.52
N4342015R27 37.60-38.30	Gneiss	65.8	0.57	16.3	4.55	0.04	1.21	1.89	3.44	5.51	0.16
N4342015R28 54.20-54.90	Gneiss	60.9	0.55	18.6	6.03	0.11	1.30	5.64	4.09	2.08	0.31
N4342015R27 135.60-136.30	Quartz diorite	64.0	0.43	18.4	3.95	0.06	0.75	4.75	3.97	3.13	0.23
N4342015R29 112.00-112.80	Quartz diorite	64.5	0.50	15.8	5.29	0.08	1.85	4.22	3.40	3.74	0.23
SMMA-2015-7.1	Quartz diorite (+quartz vein)	75.1	0.39	10.2	4.38	0.08	1.47	4.35	2.42	0.92	0.21
EPHE-2012-67.1	Quartz diorite	56.7	0.75	16.5	8.92	0.16	3.26	6.59	3.30	1.76	0.30
SMMA-2015-22.1	Calcite rich fracture filling	1.5	0.01	0.2	1.29	0.85	0.55	46.76	0.05	0.01	<0.01

4 DISCUSSION

4.1 Alteration textures

Porphyry-type copper deposits frequently occur in volcanic arc environments as a consequence of fluid activity caused by subduction related granitoids. Although Precambrian examples are known, deposits of this type become gradually more abundant in younger geological associations (Kirkham & Dunne 2000, Sinclair 2007). Hydrothermal activity during the crystallization and cooling of the felsic magma creates alteration zones, hydrothermal breccias and vein stockworks. The alteration zones can be broadly divided into potassic, phyllic, argillic and propylitic zones within and around the shallow porphyry intrusion (Lowell and Guilbert 1970). The potassic alteration occurs in the central part of the porphyry deposit and is observable as alteration of amphibole and plagioclase to biotite and K-feldspar. The next zone is characterized by sericitic alteration continuing to argillic (clay minerals and quartz) and outer propylitic zone (chlorite, epidote group, albite and carbonates). Overlapping of the alteration zones is not an uncommon feature and their distribution is unevenly controlled by deformation structures, especially in the small Paleoproterozoic porphyry copper deposits (Nurmi 1984). Additionally, one or

more zones may be lacking or overprinted by later metamorphism.

The alteration zones typical for porphyry copper deposits were not identified in the Lammuste area. In Lammuste, extensive sericitic alteration is uncommon and was only found in one thin section (Fig. 14), while a moderate degree of seritization was more frequent. Propylitic alteration is evidenced by observed epidotization and chloritization (Figs. 14, 15 and 16). Similar epidotization was found in the mineralized boulders and in drill core N4342015R28.

The existence of hedenbergite in the mafic dyke in the Pienimäki quarry and in the mineralized boulders could be related to contact metamorphism. According to Stanton (1972), the addition of silica and iron to carbonate rock as a consequence of contact metamorphism creates the minerals andradite, hedenbergite and iron oxides and/or sulphide minerals. Rocks of this type are often referred to as skarns. However, no primary carbonate rocks have been observed in the target area, excluding occasional calcite fillings in fractures (Table 2, sample SMMA-2015-22.1).

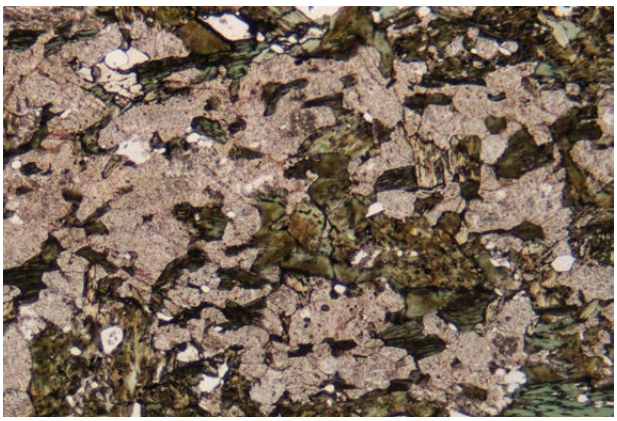

Fig. 14. Pervasive alteration of plagioclase to sericite and chloritization of hornblende in quartz diorite. Sample SMMA-2015-3.1 from the Pienimäki quarry. Plane-polarized light, field of vision 5 mm.

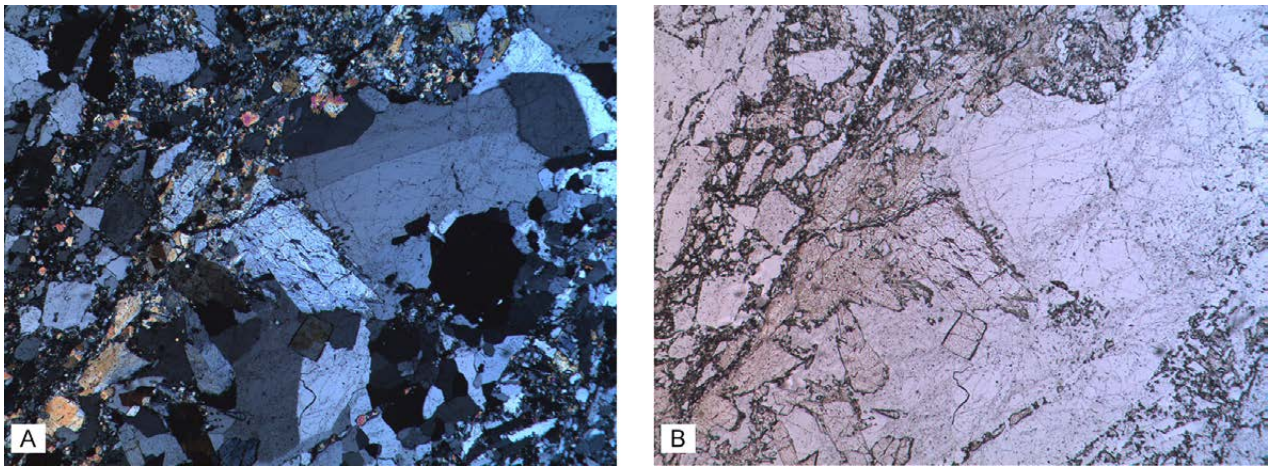

Fig. 15. Fine-grained clinozoisite in quartz diorite. Sample SMMA-2015-3.2 from the Pienimäki quarry. A) Cross-polarized light, B) plane-polarized light. Field of vision 5 mm.

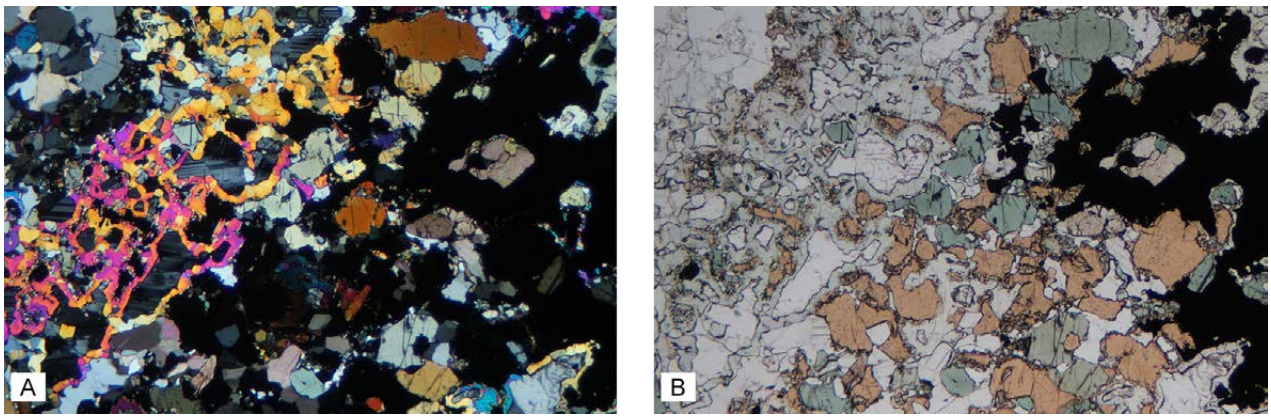

Fig. 16. Epidotization and garnet (andradite) in mafic metavolcanic rock from drill core N4342015R28, depth 123.60 m. A) Cross-polarized light, B) plane-polarized light. Field of vision 5 mm.

4.2 Comparison with some Paleoproterozoic porphyry-type deposits in Fennoscandia

The Lammuste quartz diorite intrusion has certain common features with Paleoproterozoic porphyry Mo, Cu and Au deposits described from the Svecofennian domain of Finland by Nurmi (1984). The deposits are mainly associated with I-type granitoids and have zircon U–Pb ages between 1850 and 1900 Ma. The Lammuste quartz diorite is compositionally a calc-alkaline I-type intrusion, showing Na_2O enrichment compared to K_2O (Chappell & White 1974) and having a zircon U–Pb age of 1897 ± 7 Ma (Heilimo et al. 2018, authors' unpublished data). Minor porphyry-type Mo, Cu, and Au deposits in Finland are hosted by granitoid intrusions, which are related to large batholites and surrounded by supracrustal sequences of variable metamorphic grade (Nurmi 1984). Typically, wall rock alteration occurs besides the veining as propylitic alteration (Nurmi op. cit.). Host granitoids are generally calc-alkaline and contain sphene, hornblende and magnetite, characteristics also displayed by quartz diorites of the Lammuste area. Enrichment in Na and a high Sr/Y ratio characterize the adakitic composition (Moyen 2009), which has been identified in some cases as being related to porphyrite deposits (Thiéblemont et al. 1997). These features are also observed in the Lammuste study area (e.g. EPHE-2012-67.1; Sr/Y ratio 96), although distinct Cu–Au mineralisation is only observed from the boulders. The texture typical for the host rock of porphyrite deposit is also rarely found.

The Kedonojankulma deposit in south Finland is related to a 1.5 x 0.5 km tonalite intrusion aged 1883 ± 5 Ma (Tiainen et al. 2013). Based on geochemical data, the granitoids in the Kedonojankulma area are volcanic arc-type rocks (Tiainen et al. 2012). Cu–Au(–Ag–Mo) mineralisation in the Kedonojankulma is hosted by a porphyritic and strongly altered quartz-plagioclase-rich phase of the intrusion, while in Lammuste, the Cu–Au showings are hosted by volcanogenic mafic hornblende gneiss and quartz diorite based on the observation of mineralized boulders. The outcrop samples studied from the Lammuste area represent an arc environment based on geochemistry (Heilimo et al. 2018).

Aitik, the largest known Proterozoic porphyry Cu–Au–Ag deposit, is located in northern Sweden. The host rock of the deposit is altered and deformed volcaniclastic rock aged 1.9 Ga. The footwall rock of the deposit is a porphyritic quartz monzodiorite aged 1887 ± 8 Ma (Wanhainen 2006). Regional metamorphism, alteration and deformation has disturbed the primary features, as has happened for Lammuste mafic volcanic rocks. Potassic alteration has been detected throughout the intrusion, which provides evidence of the synmagmatic origin of the mineralized zone and quartz monzonite. Potassic alteration occurs as biotite replacing amphibolite and as the growth of secondary K-feldspar.

The Jörn granitoid complex (JGC) in the Skellefte area, northern Sweden (Wilson et al. 1987), shares some features with those of the Lammuste area. It is a Paleoproterozoic subduction-related granitoid intruded into a volcanic arc environment. The JGC occupies a relatively large area of approximately 30 x 30 km. The surrounding bedrock consists of marine metasediments and submarine metavolcanic rocks (Wilson et al. 1987). The JGC is formed by zones of I- and S-type granites. These zones have been divided with the help of the aeromagnetic survey. The method is based on the study of Ishihara (1977) on the usefulness of magnetite and ilmenite for granitoid classification. I-type granitoids are usually magnetite bearing, whereas S-type granitoids show low magnetic susceptibility, because ilmenite is the typical oxide mineral instead of magnetite. The central part of the Lammuste intrusion forms a local magnetic minimum (Fig. 1) and it could represent a magma phase from a different source to that forming the outer rim of the intrusion. Alternatively, the differences in magnetic measurements are caused by later alternation. Due to extensive Quaternary coverage, outcrop observations could not be made from the central parts of the Lammuste area.

Another locality that could be compared to Lammuste is the Tallberg Cu–Au deposit located in the southern part of the JGC (Weihed 1990), in the outer and older zone of the complex. A large mineralized mafic dyke cuts the granodiorite close to the Cu–Au deposit. Minor aplitic dykes are related to the porphyry stocks and sheets found southwest of this dyke. The area was later intruded by mafic dykes, which represent the latest magmatic event. The Tallberg area is characterized by brittle brecciation and the central part of brecciated area is rich of chalcopyrite, pyrite, sphalerite, molybdenite and magnetite. Dissemination of magnetite, pyrite and minor chalcopyrite is common in the host rock of the deposit.

Comparing the Lammuste intrusion and the Jörn granitoid complex leads us to consider the possibility that we have observed only a small part on the top of the intrusion. The fluids enriched in metals and related to a large intrusion might have affected a much larger area than we think. To better understand the size and depth of the possible ore-forming intrusion, additional studies should be carried out.

5 SUMMARY

Despite promising boulder samples, significant Au or Cu mineralisation was not located. However, chalcopyrite was found from practically all quartz diorite outcrops as sporadic grains or weak dissemination, and mafic metavolcanic rock similar to the mineralized boulders was located with drilling. The formation of Cu–Au–Ag-rich boulders is probably related to the quartz diorite intrusion. However, the amount of data is too limited to properly relate them to a well-described ore-forming process.

Nevertheless, the Lammuste quartz diorite intrusion and its surroundings have features typical of porphyry copper deposits, e.g. the formation conditions, igneous host rocks and alterations. The composition indicates that the intrusion is I-type and formed in an arc environment. The observed occurrence of hedenbergite could be related to skarn formation. However, carbonate minerals were only observed as occasional dissemination and fillings in fractures. Overall, the results give the impression of multiple ore-forming processes interacting in the Lammuste area.

6 ACKNOWLEDGEMENTS

Teuvo Heikkinen is acknowledged for sending mineralized boulders and being a great help to us in many ways during the exploration. He also took the photo in Figure 2B, and Jouko Ranua took the sample picture in Figure 2A. The work of experienced research assistants Rauli Lempiänen, Tuomo Stranius and Mauri Luukkonen, GTK's drilling crew and field crew for geophysics, was indispensable for this study. Mia Tiljander is thanked for microprobe analyses and Tapio Halkoaho together with Hannu Makkonen for advice during the thin-section study. We also want to thank Markku Tiainen, Ferenc Molnár and Olavi Kontoniemi for their constructive comments on the manuscript.

REFERENCES

Bedrock of Finland - DigiKP. Digital map database [Electronic resource]. Espoo: Geological Survey of Finland [referred 02.12.2016]. Version 2.0.

Chappel, B. & White, A. 1974. Two contrasting granite types. Pacific Geology 8, 173–174.

Dilles, J. 2010. Hydrothermal alteration. In: John, D. (ed.) Porphyry Copper Deposit Model. USGS Scientific Investigations Report 2010–5070–B, 57–64.

Heilimo, E., Ahven, M. & Mikkola, P. 2018. Geochemical characteristics of the plutonic rock units present at the southeastern boundary of the Central Finland Granitoid Complex. In: Mikkola, P., Hölttä, P. & Käpyaho, A. (eds) Development of the Paleoproterozoic Svecofennian orogeny: new constraints from the southeastern boundary of the Central Finland Granitoid Complex. Geological Survey of Finland, Bulletin 407. (this volume). Available at: https://doi.org/10.30440/bt407.6

Heilimo, E., Mikkola, P., Niemi, S., Luukas, J. & Halonen, S. 2017. Hiekkapohja ore showings in Paleoproterozoic Central Finland Granitoid Complex - a hydrothermal system? Proceedings of the 14th SGA Biennial Meeting, 20-23 August 2017, Québec City, Canada, 359–362.

Ishihara, S. 1977. The magnetite-series and ilmenite-series granitic rocks. Mining Geology 27, 293–305.

Ishikawa, Y., Sawaguchi, T., Iwaya, S. & Horiuchi, M. 1976. Delineation of prospecting targets for Kuroko deposits based on modes of volcanism of underlying dacite and alteration halos: Mining Geology 26, 105–117. (in Japanese with English abstract)

Kirkham, R. & Dunne, K. 2000. World distribution of porphyry, porphyry-associated skarn, and bulk-tonnage epithermal deposits and occurrences. Geological Survey of Canada, Open File 3792a. 26 p.

Kousa, J., Mikkola, P. & Makkonen, H. 2018. Paleoproterozoic mafic and ultramafic volcanic rocks in the South Savo region, eastern Finland. In: Mikkola, P., Hölttä, P. & Käpyaho, A. (eds) Development of the Paleoproterozoic Svecofennian orogeny: new constraints from the southeastern boundary of the Central

Finland Granitoid Complex. Geological Survey of Finland, Bulletin 407. (this volume). Available at: https://doi.org/10.30440/bt407.4

Large, R., Gemmell, J., Paulick, H. & Huston, D. 2001. The alteration box plot: A simple approach to understanding the relationship between alteration mineralogy and lithogeochemistry associated with volcanic-hosted massive sulfide deposits. Economic Geology 96, 957–971.

Lowell, J. & Guilbert, J. 1970. Lateral and vertical alteration-mineralization zoning in porphyry ore deposits. Economic Geology 65, 373–408.

Mikkola, P., Heilimo, E., Aatos, S., Ahven, M., Eskelinen, J., Halonen, S., Hartikainen, A., Kallio, V., Kousa, J., Luukas, J., Makkonen, H., Mönkäre, K., Niemi, S., Nousiainen, M., Romu, I. & Solismaa, S. 2016. Jyväskylän seudun kallioperä. Summary: Bedrock of the Jyväskylä area. Geological Survey of Finland, Report of Investigation 227. 113 p. Available at: http://tupa.gtk.fi/julkaisu/tutkimusraportti/tr_227.pdf

Mikkola, P., Heilimo, E., Luukas, J., Kousa, J., Aatos, S., Makkonen, H., Niemi, S., Nousiainen, M., Ahven, M., Romu, I. & Hokka, J. 2018a. Geological evolution and structure along the southeastern border of the Central Finland Granitoid Complex. In: Mikkola, P., Hölttä, P. & Käpyaho, A. (eds) Development of the Paleoproterozoic Svecofennian orogeny: new constraints from the southeastern boundary of the Central Finland Granitoid Complex. Geological Survey of Finland, Bulletin 407. (this volume). Available at: https://doi.org/10.30440/bt407.1

Mikkola, P., Huhma, H., Romu, I. & Kousa, J. 2018b. Detrital zircon ages and geochemistry of the metasedimentary rocks along the southeastern boundary of the Central Finland Granitoid Complex. In: Mikkola, P., Hölttä, P. & Käpyaho, A. (eds) Development of the Paleoproterozoic Svecofennian orogeny: new constraints from the southeastern boundary of the Central Finland Granitoid Complex. Geological Survey of Finland, Bulletin 407. (this volume). Available at: https://doi.org/10.30440/bt407.2

Mikkola, P., Mönkäre, K., Ahven, M. & Huhma, H. 2018c. Geochemistry and age of the Paleoproterozoic Makkola suite volcanic rocks in central Finland. In: Mikkola, P., Hölttä, P. & Käpyaho, A. (eds) Development of the Paleoproterozoic Svecofennian orogeny: new constraints from the southeastern boundary of the Central Finland Granitoid Complex. Geological Survey of Finland, Bulletin 407. (this volume). Available at: https://doi.org/10.30440/bt407.5

Moyen, J. 2009. High Sr/Y and La/Yb ratios: The meaning of the "adakitic signature". Lithos 112, 556–574.

Nenonen, J. 1994. The Kaituri drumlin and drumlin statigraphy in the Kangasniemi area, Finland. Sedimentary geology 91, 365–372

Nurmi, P. 1984. Applications of lithogeochemistry in the search for Proterozoic porphyry-type molybdenum, copper and gold deposits, southern Finland. In: Nurmi, P. A. Applications of lithogeochemistry in the search for Proterozoic porphyry-type molybdenum, copper and gold deposits, southern Finland. Geological Survey of Finland Bulletin 329, 1–40. Available at: http://tupa.gtk.fi/julkaisu/bulletin/bt_329.pdf

Sinclair, W. 2007. Porphyry deposits. In: Goodfellow, W. (ed.) Mineral Deposits of Canada: A Synthesis of Major Deposit-Types, District Metallogeny, the Evolution of Geological Provinces, and Exploration Methods. Geological Association of Canada, Special Publication 5, 223–243.

Solismaa, S., Nenonen, J., Niemi, S. & Kousa, J. 2016. Pieksämäen Lammusteen malminetsintätutkimukset vuosina 2013–2015. Geological Survey of Finland, archive report 1/2016. 29 p. (in Finnish). Available at: http://tupa.gtk.fi/raportti/arkisto/1_2016.pdf

Stanton, R. 1972. Ore petrology. New York: McGraw-Hill. 713 p.

Thiéblemont, D., Stein, G. & Lescuyer, J. 1997. Epithermal and porphyry deposits: the adakite connection. Comptes Rendus de l´Academie des Science, Series II 325, 103–109

Tiainen, M., Kärkkäinen, N., Lohva, J. Sipilä, P. & Huhta, P. 2012. Discovery of the Kedonojankulma Cu-Au occurrence, hosted by a Svecofennian porphyritic granitoid in Southern Finland. In: Grönholm, S. & Kärkkäinen, N. (eds) Gold in Southern Finland: Results of GTK studies 1998-2011. Geological Survey of Finland, Special Paper 52, 73–90. Available at: http://tupa.gtk.fi/julkaisu/specialpaper/sp_052.pdf

Tiainen, M., Molnár, F. & Koistinen, E. 2013. The Cu-Mo-Au mineralization of the Paleoproterozoic Kedonojankulma intrusion, Häme Belt, Southern Finland. Proceedings of the 12th Biennial SGA Meeting, 12–15 August 2013, Uppsala, Sweden, vol. 2, 892–895.

Wanhainen, C. Billström, K. & Martinsson, O. 2006. Age, petrology and geochemistry of the porphyritic Aitik intrusion, and its relation to the disseminated Aitik Cu-Au-Ag deposit, northern Sweden. Geologiska Föreningens i Stockholm Förhandlingar 128, 273–286.

Weihed, P. 1990. Lithogeochemistry, metal and alteration in the Proterozoic Tallberg porphyry-type deposit, northern Sweden. Journal of Geochemical Exploration 42, 301–325.

Wilson, M., Sehlstedt, S., Claesson, L., Smellie, T., Aftalion, M., Hamilton, J. & Fallick, A. 1987. Jörn: An early Proterozoic intrusive complex in a volcanic-arc environment, north Sweden. Precambrian Research 36, 201–225.

Development of the Paleoproterozoic Svecofennian orogeny: new constraints from the southeastern boundary of the Central Finland Granitoid Complex
Edited by Perttu Mikkola, Pentti Hölttä and Asko Käpyaho
Geological Survey of Finland, Bulletin 407, 168–185, 2018

HARJUJÄRVENSUO GOLD MINERALISATION IN LEIVONMÄKI, CENTRAL FINLAND

by

Perttu Mikkola[1)], Matti Niskanen[1)] and Janne Hokka[2)]

Mikkola, P, Niskanen, M. & Hokka, J. 2018. Harjujärvensuo gold mineralisation in Leivonmäki, Central Finland. *Geological Survey of Finland, Bulletin 407*, 168–185, 10 figures and 2 tables.

Harjujärvensuo gold mineralisation in Leivonmäki, Central Finland, was discovered during fieldwork related to a regional mineral potential mapping project. The mineralisation is hosted by a sedimentary sequence consisting of paraschists, greywackes and conglomerates and intruded by felsic porphyrite dykes. The host rocks are variably sheared, weakly seritized and cut by millimetre-scale carbonate±quartz veins. In Harjujärvensuo, Au shows the strongest positive correlation with As. The gold anomalous zone (>10 ppb) is 160 metres wide and the highest concentration in a one-metre drill core intersection is 4.5 ppm. Harjujärvensuo, like the two other nearby mineralisations, is orogenic in type and related to the sinistral northeast-trending Leivonmäki shear zone.

Appendix 1 is available at: http://tupa.gtk.fi/julkaisu/liiteaineisto/bt_407_appendix_1.pdf

Electronic Appendix is available at: http://tupa.gtk.fi/julkaisu/liiteaineisto/bt_407_electronic_appendix.xlsx

Keywords: arsenopyrite, quartz veins, gold, drilling, boulder trains, mineral exploration, metasedimentary rocks, Svecofennian, Paleoproterozoic, Finland

[1)] *Geological Survey of Finland, P.O. Box 1237, FI-70211 Kuopio, Finland*
[2)] *Geological Survey of Finland, P.O. Box 96, FI-02151 Espoo, Finland*
E-mail: perttu.mikkola@gtk.fi

VERTAISARVIOITU
KOLLEGIALT GRANSKAD
PEER-REVIEWED
www.tsv.fi/tunnus

https://doi.org/10.30440/bt407.9

Editorial handling by Pentti Hölttä.

Received 30 June 2017; Accepted 1 June 2018

1 INTRODUCTION

The history of gold exploration in Leivonmäki and surrounding areas dates back to the 1940s, when the first gold-bearing layman samples from the area were sent to the Geological Survey of Finland (Pääkkönen 1947). These samples led to the location of the southern extensions of the Tammijärvi Cu–W–Au mineralisation in the municipality of Luhanka (Pääkkönen 1951). Since its initial discovery, the Tammijärvi mineralisation, as well as its surroundings, have been targeted by both private companies (e.g. Wennervirta 1973, Mattila 1980, Hurskainen 1989, Pajula 2015) and the Geological Survey of Finland (GTK, e.g. Oivanen 1958, Lindmark 1988), although in certain stages of history, tin, tungsten and copper have been the main focus of the studies. To date, the most significant discovery in the area has been the Vatsa gold deposit, located in the 1990s by Terra Mining (Liikanen 1992). Based on currently available data, the Vatsa deposit hosts at least 1 Mt of ore with an average gold content of 1.73 ppm (Lappland Gold Miners 2015).

During the field work carried out by the Central Finland ore potential mapping project, several Au-bearing glacial boulders were found by research assistants Rauli Lempiäinen and Tuomo Stranius. Based on the morphology of the boulders and the bedrock of the study area, it was anticipated that they were local, i.e. they had not been transported more than a few hundred metres. Thus, in order to locate the starting point of these conglomerate boulders, a ground-measured magnetic survey was carried out in the area, and a profile consisting of six drill holes was drilled. The drilling intersected a 160-m-wide zone anomalous in gold (Au >10 ppb), and the highest analysed concentration in a one-metre sample was 4.5 ppm. The location was named Harjujärvensuo after a bog in the area. This paper briefly describes the Harjujärvensuo mineralisation and evaluates its similarities to and differences from the two other known mineralisations in the same area.

2 GEOLOGICAL SETTING

The Au mineralisation is located near the contact of the calc-alkaline Makkola suite volcanic rocks in the north (Mikkola et al. 2018c) and Pirkanmaa migmatite suite rocks in the south (Mikkola et al. 2018b, Fig. 1). The latter suite mainly consists of metasedimentary rocks, greywackes with conglomerate, black schist and pelite interbeds, but it also contains some picritic volcanic rocks in the vicinity of the contact with the Makkola suite (Kousa et al. 2018). Rocks of the Pirkanmaa migmatite suite are, as the name implies, typically migmatized, but in certain locations, including the area of the mineralisation, rocks of lower metamorphic grade and well-preserved depositional structures can be observed. Based on material that included a conglomerate sample from Harjujärvensuo, the maximum depositional age of the Pirkanmaa migmatite suite in the area is ca. 1920 Ma (Mikkola et al. 2018b), whereas the ages of the Makkola suite volcanic rocks vary from 1895 to 1875 Ma (Mikkola et al. 2018c).

The actual contact between the two suites has been interpreted as tectonic (Mikkola et al. 2018a), and it is part of the sinistral Leivonmäki shear zone trending from southwest to northeast. The Tammijärvi Au mineralisation is located 11 km to the southwest along the Leivonmäki shear zone in the vicinity of the contact between the greywackes and volcanic rocks of the Makkola suite. The Vatsa Au mineralisation, 9 km west–northwest of the Harjujärvensuo Au mineralisation (Fig. 1), is located within an east–west-trending shear zone (Lappland Gold Miners 2015) branching from the main Leivonmäki shear zone.

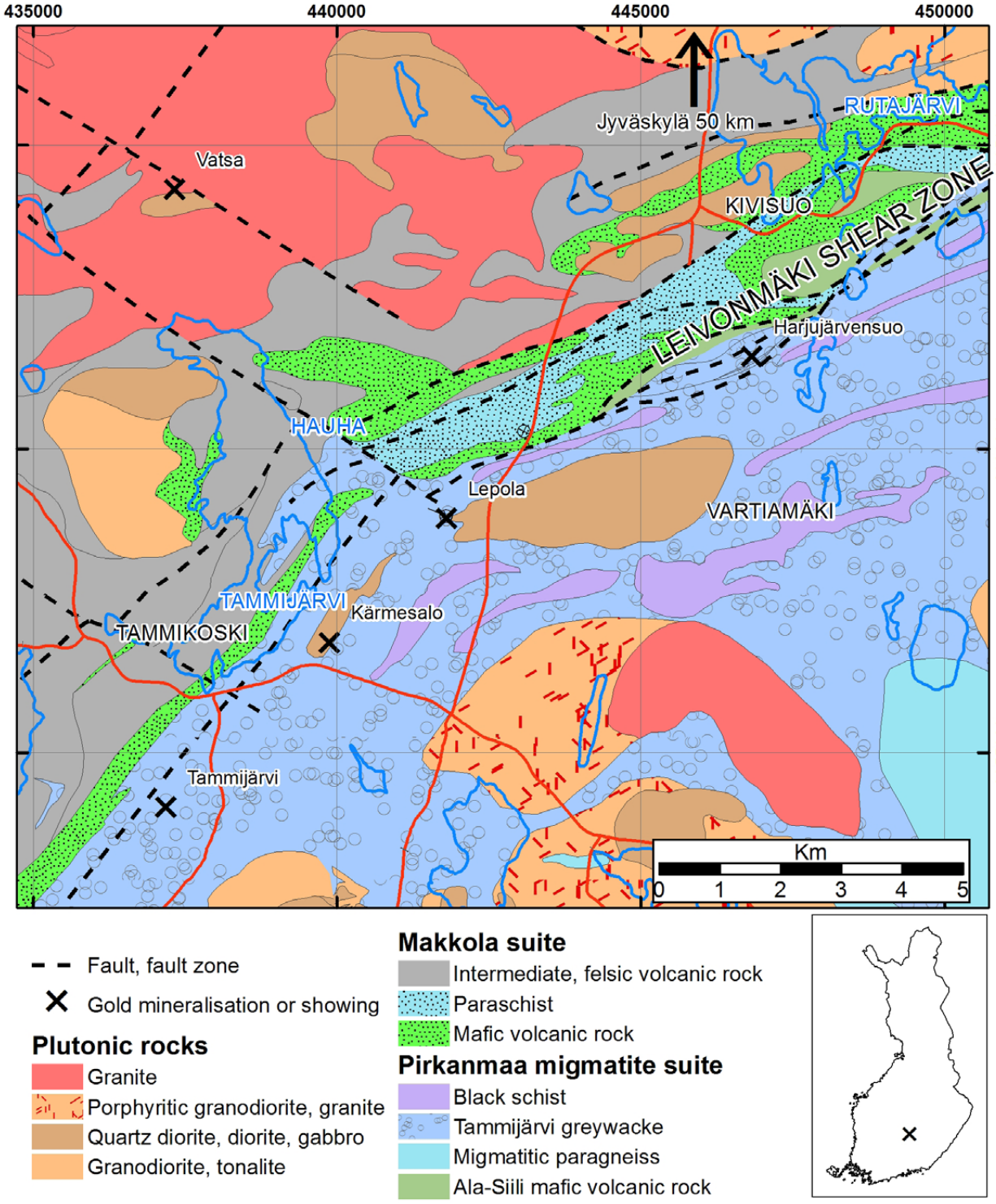

Fig. 1. Geological map of the surroundings of the Harjujärvensuo gold mineralisation. Map modified from Mikkola et al. (2016). Basemap © National Land Survey of Finland.

3 EXPLORATION HISTORY AND METHODS

The first gold-anomalous boulders from the Harjujärvensuo area were located in 2011. The Quaternary coverage in the area is extensive and mainly consists of till variably covered with peat layers. As the ice flow in the area has been from the north (±10°), a search for boulders and possible outcrops was carried out in 2014 north of the initially found boulders. This search resulted in the location of more than ten gold-anomalous boulders and three outcrops (max. 4.8 ppm from a boulder, 1 outcrop and 5 boulders with Au = 100–300 ppb) ca. 1 km northeast of the boulders that were found first (Fig. 2). Based on till morphology, the fact that the gold-anomalous outcrops had similar rock types to the boulders and the overall interpretation of bedrock geology of the area, the boulders were interpreted as relatively local, with transport distances of less than 1000 metres.

Following this interpretation, a systematic magnetic ground survey was conducted in the area using an Overhauser GPS (global positioning system) proton magnetometer. Measurement was carried out twice each second, equalling an approximately one-metre distance between measurement points. The line separation was 50 m in the eastern half of the surveyed area and 100 m in western half. Three of the lines were extended in a NNW direction to obtain more accurate information on the background magnetic anomaly for interpretation.

Based on the structures interpreted from the geophysical data, a drilling programme consisting of a profile of five drill holes and one separate drill hole was planned. The azimuth of the drill holes (155°) was perpendicular to the strike of the anomalies in the geophysical data. In addition to purely explorational motivation, the drilling also aimed at providing information on the complicated contact zone between the Pirkanmaa migmatite suite and volcanic units of the Makkola suite. Drilling at the target was conducted using GTK's own drilling rig (GM-150) and the 6 drill holes totalled 892.90 m in length. The diameter of the drill core was 42 mm.

Altogether, 131 samples from the drill cores were analysed by Labtium Oy. The sample length was typically 1 m, but shorter segments were analysed in the case of narrow rock units. All analyses are listed in the Electronic Appendix and representative ones in Table 1. All samples were analysed for Au using the Pb fire assay method followed by inductively coupled plasma optical emission spectroscopy (ICP-OES, Labtium code 705P, detection limit 10 ppb). The main elements and certain trace elements were analysed from 60 samples using X-ray fluorescence (Labtium codes 175X and 176X). See Appendix 1 for the analytical procedures. The geochemical data were plotted using the Geochemical Data Toolkit (GCDKit) program of Janoušek et al. (2006).

4 RESULTS

4.1 Drill core observations

Drill hole N4312016R12 was planned to test the cause of a strong elongated magnetic anomaly in the northern part of the target area (Fig. 2). To the depth of 165.80 m, the drill hole intersected variably sheared uralite porphyrite containing ca. 1-m-thick greenish grey schist interbeds that lack porphyries and commonly display bedding with a ca. 1-cm thickness (Fig. 4). The size of the uralite porphyries is typically 3–5 mm, the local maximum being 10 mm. Small-scale layered variation in the amount and size of the porphyries suggests that the uralite porphyrite originated as lava flows, and the interbeds are interpreted as finer grained tuffs or tuffites deposited between them. The end of the drill core consists of grey paraschist displaying variably intense layering (Fig. 4) with greenish tuffite interbeds similar to those in the uralite porphyrite. Based on graded bedding observations from the lower part of the drill core, it appears that the uralite porphyrites erupted on the paraschists, but as the whole area is intensively folded and faulted, this observation should be considered as tentative. Susceptibility measurements indicate that the uralite porphyrite is the cause of the observed positive magnetic anomaly, but the correlation between rock types and susceptibility is ambiguous, as the susceptibility of the uralite porphyrite varies by an order of a magnitude over short distances without any correlation, for example, with observed structures.

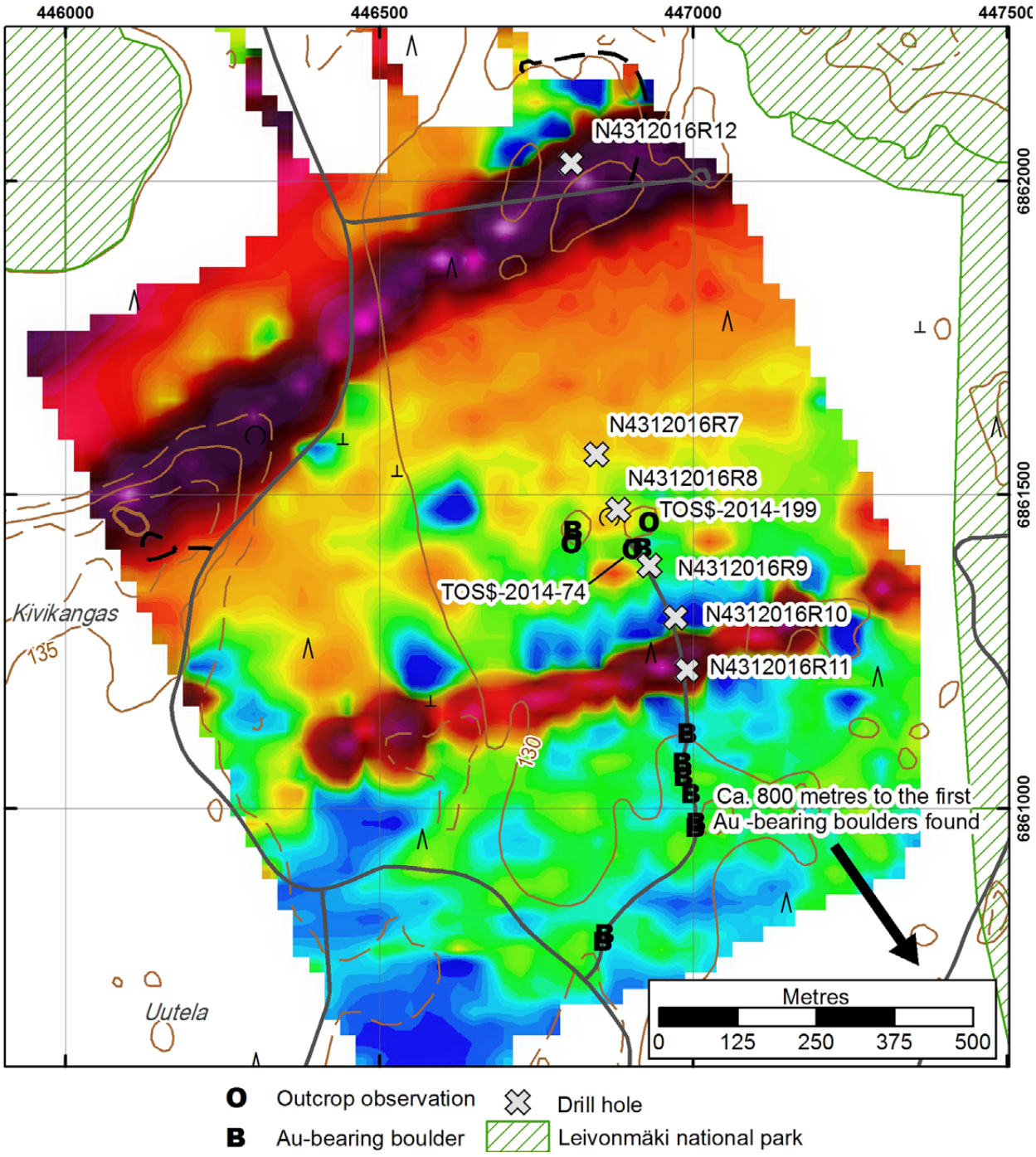

Fig. 2. Ground surveyed magnetic map of the study area. Blue denotes low and red high values. Also shown are the locations of drill holes and gold-bearing boulders and outcrops. Basemap © National Land Survey of Finland.

Drill holes N4312016R7–R11 form a continuous profile and targeted the area that based on glacial morphology, geophysics and the few available outcrop observations was considered as the most likely source area of the gold-enriched boulders. The beginning of drill hole N4312016R7 consists of paraschists with coarser grained and more massive greywacke interbeds (Fig. 5), in addition to felsic porphyrite dykes less than 2 m in thickness and parallel to the bedding and schistosity of the host rock. Greenish grey amphibole schist interlayers, typically less than 30 cm in thickness, similar in appearance to the tuffites in N4312016R12 are present below 100 m. Matrix-supported conglomerate, with pebbles that are heterogeneous in both size and type (Fig. 5), typically forms 1–2-m-thick interbeds

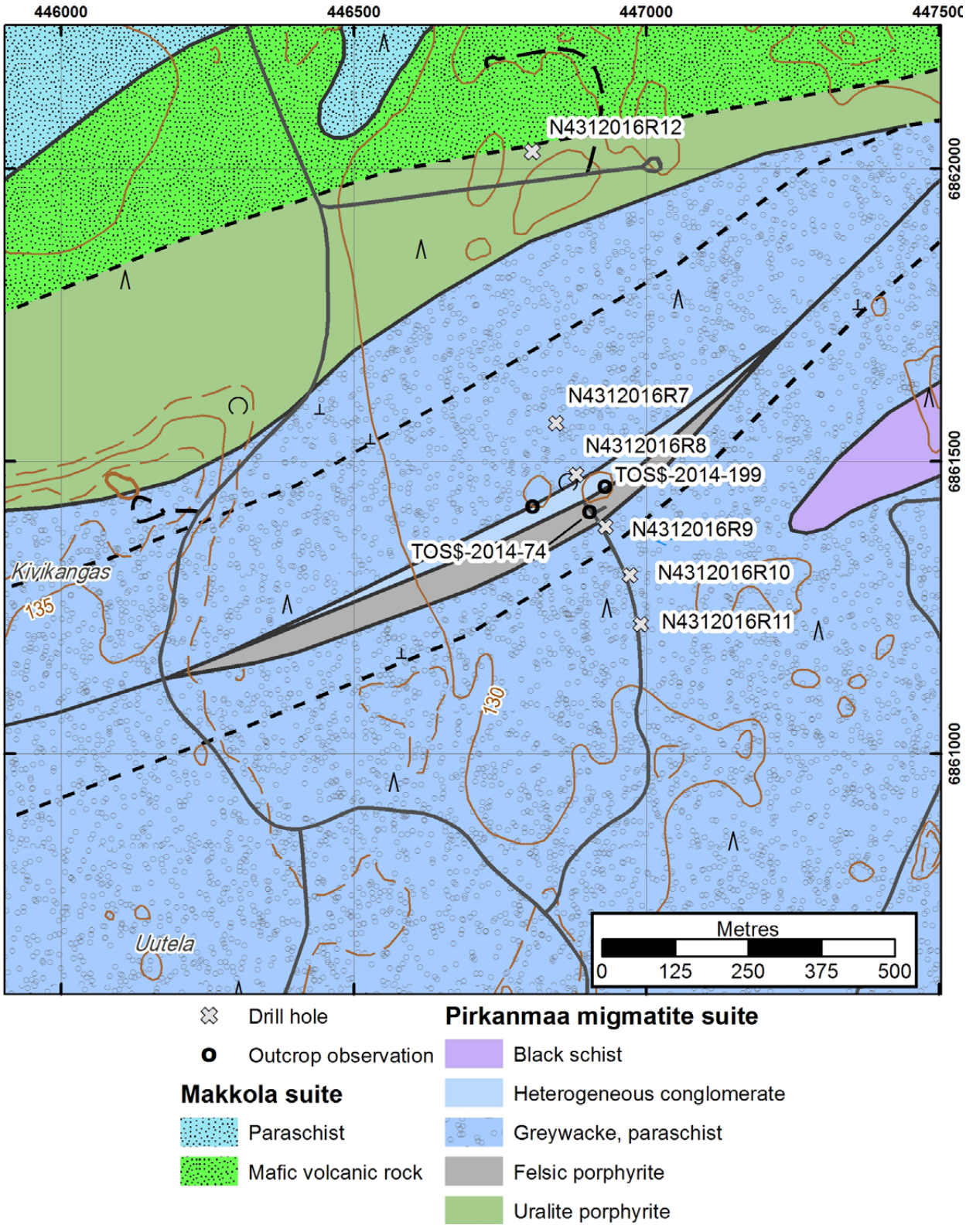

Fig. 3. Bedrock map of the study area, the locations of drill holes and outcrop observations. Basemap © National Land Survey of Finland.

Fig. 4. Samples from drill core N4312016R12. A) A layered greenish grey schist interbed, B) unsheared uralite porphyrite, C) sheared uralite porphyrite and D) grey paraschist from the end of the drill hole. Diameter of the drill core 42 mm.

below 110 m. This conglomerate type, referred to as heterogeneous conglomerate in this study, also crops out at observation location TOS$-2014-199 (Fig. 3). Variably rounded pebbles vary in size from sand-sized particles up to 5 cm. The centimetre-scale pebbles are schist fragments, whereas the smaller sized (~1 mm) ones are quartz grains or quartz aggregates. The beginning of N4312016R8 mainly consists of greywacke and heterogeneous conglomerate, with a limited number of paraschist interbeds. The southern boundary for the heterogeneous conglomerate type is a 40-m-thick felsic porphyrite dyke (depth 60.30–103.25). South of this dyke, which is also visible on outcrop TOS$-2014-74, the drill core contains alternating paraschist and greywacke beds. The thickness of the beds varies from a few centimetres to a few metres, with one thicker quartz vein (118.95–120.10).

Drill holes N4312016R9, R10 and R11 are similar with respect to their lithology, consisting of alternating greywacke and paraschist interbeds with smaller amounts of conglomerates and quartz veins (Fig. 6). The conglomerates clearly differ from those in drill holes N4312016R7 and R8. Pebbles are more uniform in size, smaller (typically ≤1 cm in size) and more felsic in composition, consisting of individual quartz and plagioclase crystals, quartz aggregates and granitoid fragments. The quantity of pebbles correlates with their size and there is a continuum from greywackes through matrix-rich conglomerates with millimetre-scale pebbles to ones with centimetre-scale pebbles and clast support (Fig. 6F). This conglomerate type is referred to as felsic conglomerate in this study. Due to folding, the available younging direction observations, mainly towards the south, do not have stratigraphic significance. The positive magnetic anomaly between drill holes N4312016R11 and R10 is transected by the latter. In a 6-m-long section, from 67 to 73 m, the susceptibility of the paraschist rises by an order of a magnitude without a significant change in the appearance of the drill core. Drill cores N4312016R9 and R11 transect two narrow mafic dykes, 50 and 25 cm wide, respectively, that differ from the amphibole schists in N4312016R7 with slightly weaker foliation and missing layering.

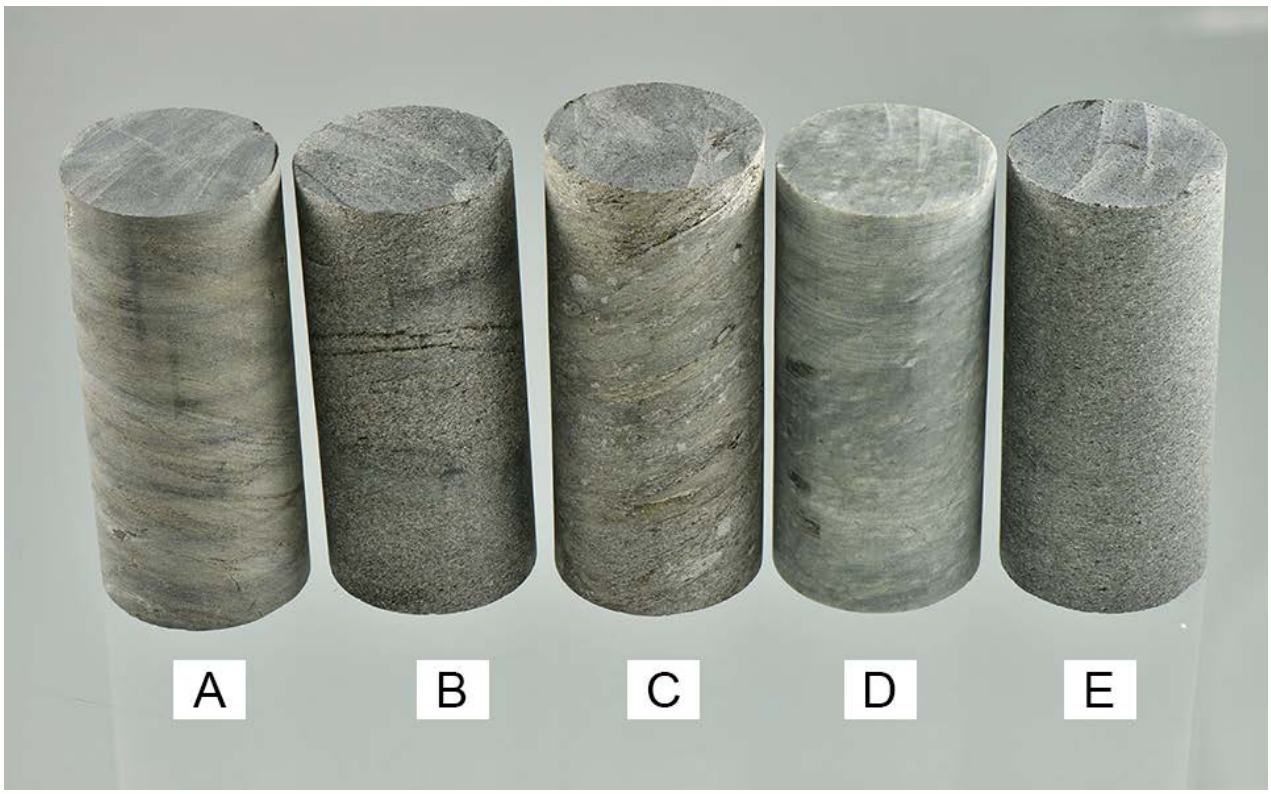

Fig. 5. Samples from drill core N4312016R8. A) Grey paraschist, B) greywacke, C) "heterogeneous" conglomerate, D) a felsic porphyrite dyke and E) greywacke. Diameter of the drill core 42 mm.

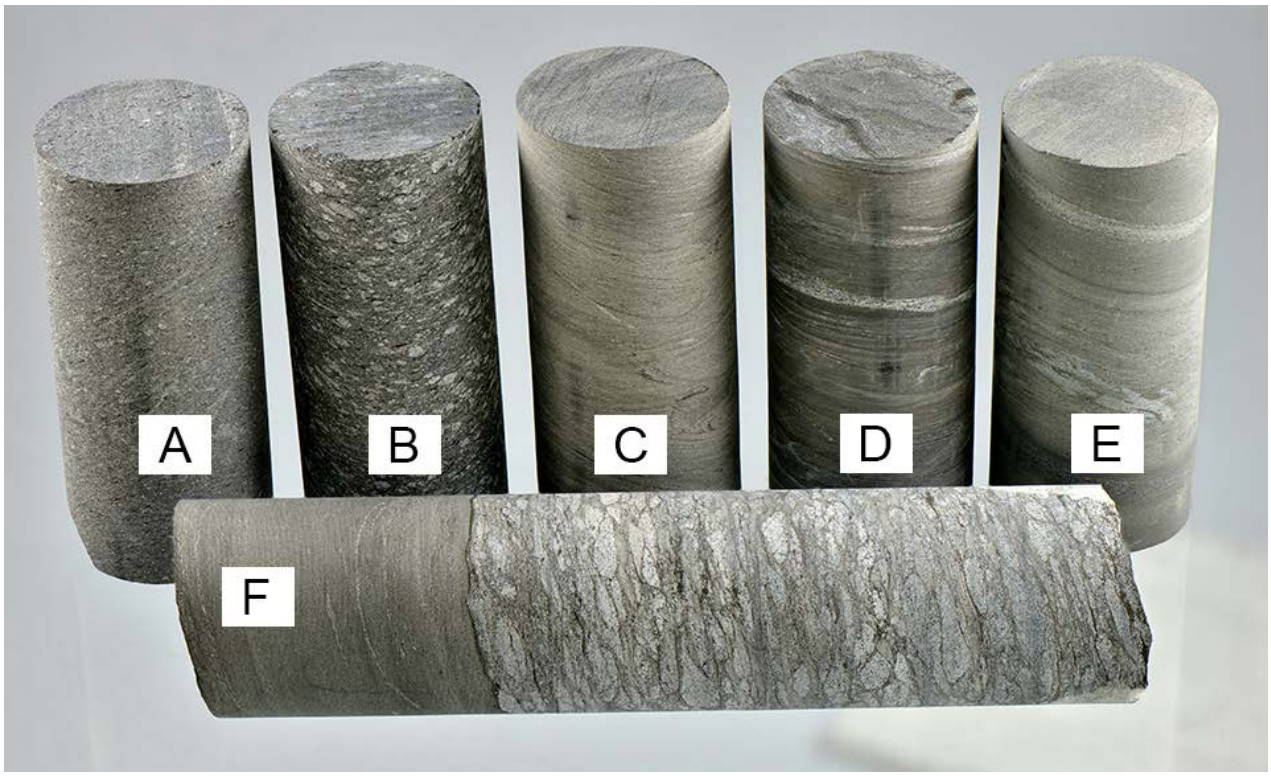

Fig. 6. Samples from drill core N4312016R9. A) Typical greywacke, B) lithic greywacke with coarser clasts, C)–E) samples from paraschist interbeds with quartz±carbonate veins. F) Contact between paraschist and a conglomerate bed. Diameter of the drill core 42 mm.

All rocks intersected by the drill holes, exposed on the outcrops and mineralised boulders, are variably sheared, and folds associated with this shearing are locally visible. Despite the deformation, well-preserved primary textures are commonly observable. The foliation coincides with the bedding and, based on measurements from oriented drill cores, their strike is parallel to the magnetic anomalies in the magnetic data. Planar structures dip consistently in the direction 340–350° at a steep angle (70–75°).

Thin (<2 mm) quartz and/or carbonate veins appear mainly parallel to the foliation, although a smaller number of crosscutting ones are also present. These veins are present in all drill cores but are most common in drill holes N4312016R7 and R8. The most common sulphur minerals are pyrrhotite and arsenopyrite, the former commonly associated with the narrow quartz±carbonate veins, whereas the latter typically occurs as fine-grained dissemination in drill holes N4312016R7 and R8.

4.2 Petrography and mineralogy

The felsic porphyry is weakly to moderately oriented leucocratic rock, with fine-grained (≤0.2 mm) granitic groundmass hosting rounded K-feldspar and plagioclase phenocrysts 1–2 mm across. Sericite alteration of especially the larger phenocrysts is a characteristic feature. Small garnet grains are present in some of the samples.

Amphibole schists and tuffites from drill cores N4312016R7 and R12 are lepidoblastic, mainly fine grained and display layering as variation in both mineralogy and grain size, most likely reflecting the original bedding. The main minerals are biotite, amphibole (hornblende and/or cummingtonite), plagioclase and quartz. Paraschists and the matrix of the greywackes and conglomerates consist of fine-grained (<0.05 mm), strongly oriented biotite, quartz and plagioclase. Paraschists display the primary bedding as variation in grain size and/or relative mineral abundances. Clasts in the greywackes mainly consist of quartz and quartz aggregates, while less abundant lithic fragments are more common in samples with coarser clasts.

Small (≤1 mm) garnets are present in certain thin layers, some of which could originally have been carbonate-richer interlayers. Locally, lens-shaped aggregates ca. 2 mm across and rich in biotite are present, these could be pseudomorphs and/or fragments of sediments richer in clay, as they are locally present in conglomerate interbeds.

Sericite alteration is common, but only locally penetrative. More commonly, it is constrained to narrow seams or has a patchy appearance. Locally, late-stage coarser grained muscovite is also present as aggregates a few millimetres across. Certain paraschist samples contain pale-coloured ca. 1 mm lens-shaped forms, richer in sericite than the groundmass, and possibly pseudomorphs after andalusite. Signs of chloritization are also locally observable, but it is always weaker than the seritization. Based on thin section observations, carbonates are also dispersed in the groundmass of the rocks, in addition to millimetre-scale veins with or without quartz.

The dominant sulphide mineral is pyrrhotite, which is present in all of the sedimentary rock types in variable amounts as small-grained dissemination (<0.2 mm), in addition to the coarser grained variant associated with the quartz±carbonate veins. The second most abundant sulphide mineral is arsenopyrite, which always occurs as small-grained dissemination in the groundmass and is common in samples from N4312016R7 and R8. Pyrite and chalcopyrite are present in small quantities, the latter practically always in connection with pyrrhotite. Ilmenite is the only oxide present in notable quantities. Native gold was not observed in the studied thin sections. Despite large variation, paraschist samples from drill core N4312016R12 are on average poorer in sulphide minerals than the other ones.

4.3 Geochemistry

4.3.1 Host rocks

On Harker diagrams, the paraschist, greywacke and heterogeneous conglomerate samples display scatter in most main and trace elements, but with respect to MgO, Al_2O_3, Fe_2O_3t and P_2O_5, for example, display a good correlation with SiO_2 (Fig. 7). It can be noted that if the wide felsic porphyry dyke in drill hole N4312016R8 is used as a boundary, samples south of it are on average more felsic than those north of it, although overlap exists. On the clas-

sification diagram of Pettijohn et al. (1972), the paraschists, greywackes and conglomerates plot in the greywacke field.

The felsic porphyrite is rich in SiO_2 (72.2–74.8%) and K_2O (3.9–4.4%). Compositionally, it is more felsic than the Makkola suite volcanic rocks (Mikkola et al. 2018c), with a resemblance to the Oittila suite granitoids (Heilimo et al. 2018).

Geochemically, the amphibolite schists and mafic tuffite samples resemble each other and clearly differ from the paraschist, greywacke and conglomerate samples in having, for example, lower Al_2O_3 and higher concentrations of MgO and Cr. One of the amphibolite schist samples is intensively biotite altered, which explains its anomalously high K_2O concentration. The mafic dyke sample compositionally differs from the mafic tuffites and amphibolite schists, as it has significantly lower MgO, Mg# and Cr values associated with higher TiO_2, P_2O_5 and Zr concentrations (Table 1). The uralite porphyrites have distinctly higher MgO and lower Al_2O_3 concentrations than the amphibolite schists and mafic tuffites, and they belong to the picritic Ala-Siili lithodeme (Kousa et al. 2018) of the Pirkanmaa migmatite suite. Regardless of the rock type, the samples from Harjujärvensuo are variably enriched in As (≤6780 ppm, Fig. 10A) and S (≤1.8%).

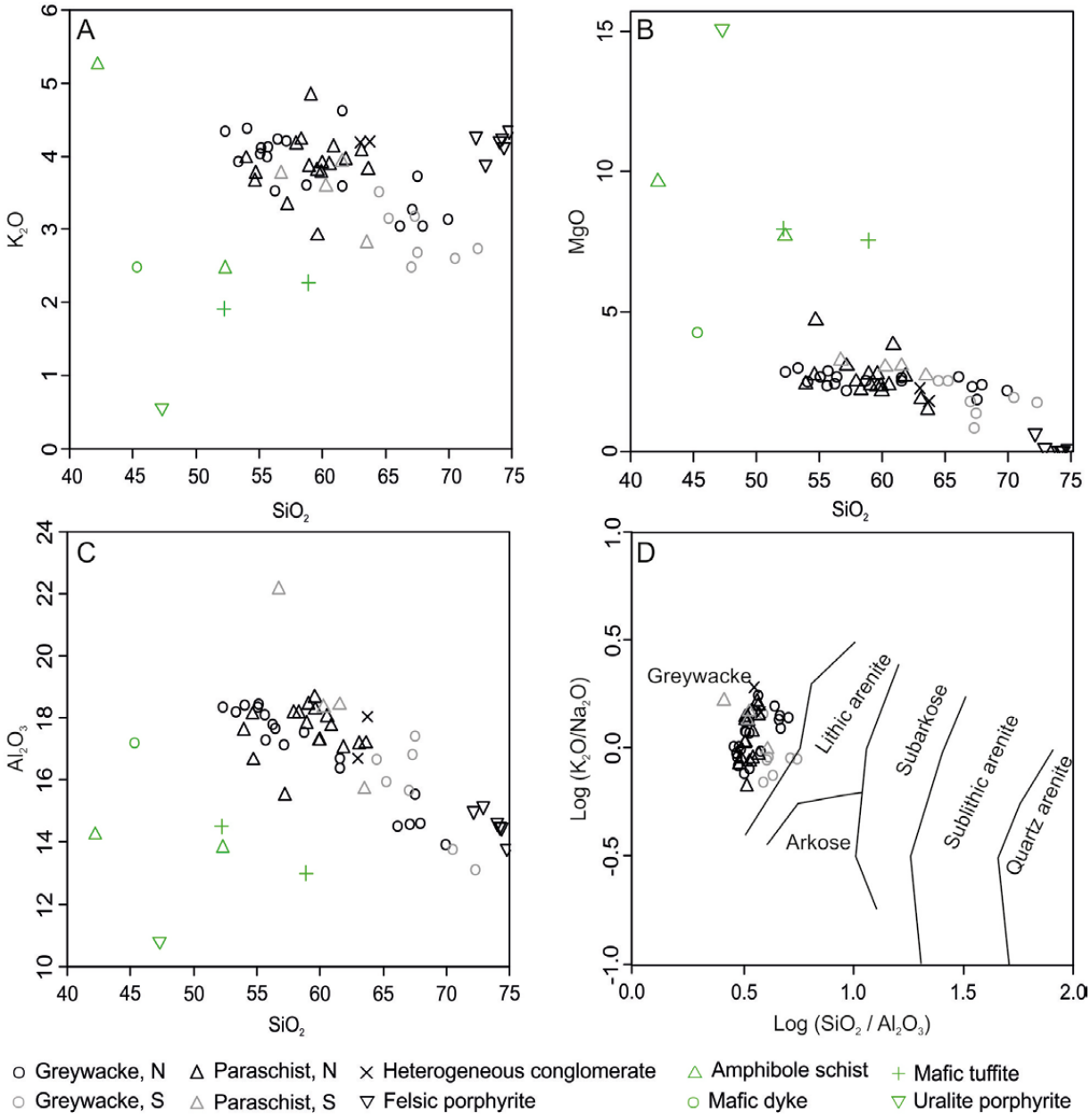

Fig. 7. A–C) Harker diagrams and D) a classification diagram of Pettijohn et al. (1972), with boundaries modified by Herron (1988).

Table 1. Representative whole-rock analyses.

Sample	N4312016R7 43.00-44.00	N4312016R7 47.00-48.00	N4312016R9 58.00-59.00	N4312016R7 50.00-51.00	N4312016R9 25.00-26.00	N4312016R12 73.00-74.00	N4312016R7 117.00-118.00	N4312016R8 60.30-61.00
Rock type	Greywacke	Greywacke	Greywacke	Paraschist	Paraschist	Mafic tuffite	Conglomerate, heterogeneous	Felsic porphyry
SiO	55.59	52.30	67.30	57.92	63.50	52.20	63.00	72.16
TiO	0.67	0.77	0.37	0.73	0.73	0.83	0.67	0.11
Al	18.11	18.35	16.81	18.14	15.70	14.50	16.70	15.00
Fe	7.81	8.78	3.76	7.56	6.00	8.60	5.80	2.45
MnO	2.36	2.86	0.85	2.50	2.71	7.96	2.26	0.66
MgO	0.28	0.21	0.07	0.21	0.08	0.13	0.05	0.09
CaO	4.32	3.59	3.37	3.08	2.64	7.08	3.02	1.12
Na	4.01	4.23	3.59	3.92	2.83	3.29	2.85	3.43
K	4.00	4.34	3.18	4.16	2.81	1.91	4.19	4.27
P	0.42	0.53	0.17	0.43	0.26	0.26	0.36	0.04
Au ppb	4520	62	14	728	<10	<10	118	39
As ppm	3710	280	110	840	<10	<10	796	110
Bi	<30	<30	<30	<30	<30	<30	<30	<30
Cu	120	60	<20	70	50	88	150	<20
Pb	1460	60	<30	70	<30	<30	<30	60
Zn	1350	170	70	300	88	79	50	80
S	18000	4100	3300	8300	2590	1870	12800	7000
Sb	580.0	<50	<50	<50	<100	<100	<100	<50
Ba	1250	1700	700	1420	510	637	1407	230
Cl	<100	200	<100	200	102	<100	118	<100
Cr	40	<20	<20	40	82	617	94	<20
Ga	<10	<10	<10	<10	25	16	24	<10
Mo	<10	<10	<10	<10	<10	<10	<10	<10
Nb	<10	<10	<10	<10	<10	<10	<10	20
Ni	20	<20	<20	<20	38	125	28	<20
Rb	140	140	140	140	143	60	143	140
Sn	<30	<30	<30	<30	<30	<30	<30	<30
Sr	900	720	310	570	213	385	480	110
C	3230	2810	-	1180	1550	870	250	1590
Th	<30	<30	30	<30	23	5	23	<30
U	<10	<10	<10	<10	<10	<10	<10	<10
V	110	130	30	120	130	211	147	20
Y	30	40	20	30	30	25	32	40
Zr	180	150	180	180	185	126	165	100

<30 = below detection limit and the approriate limit

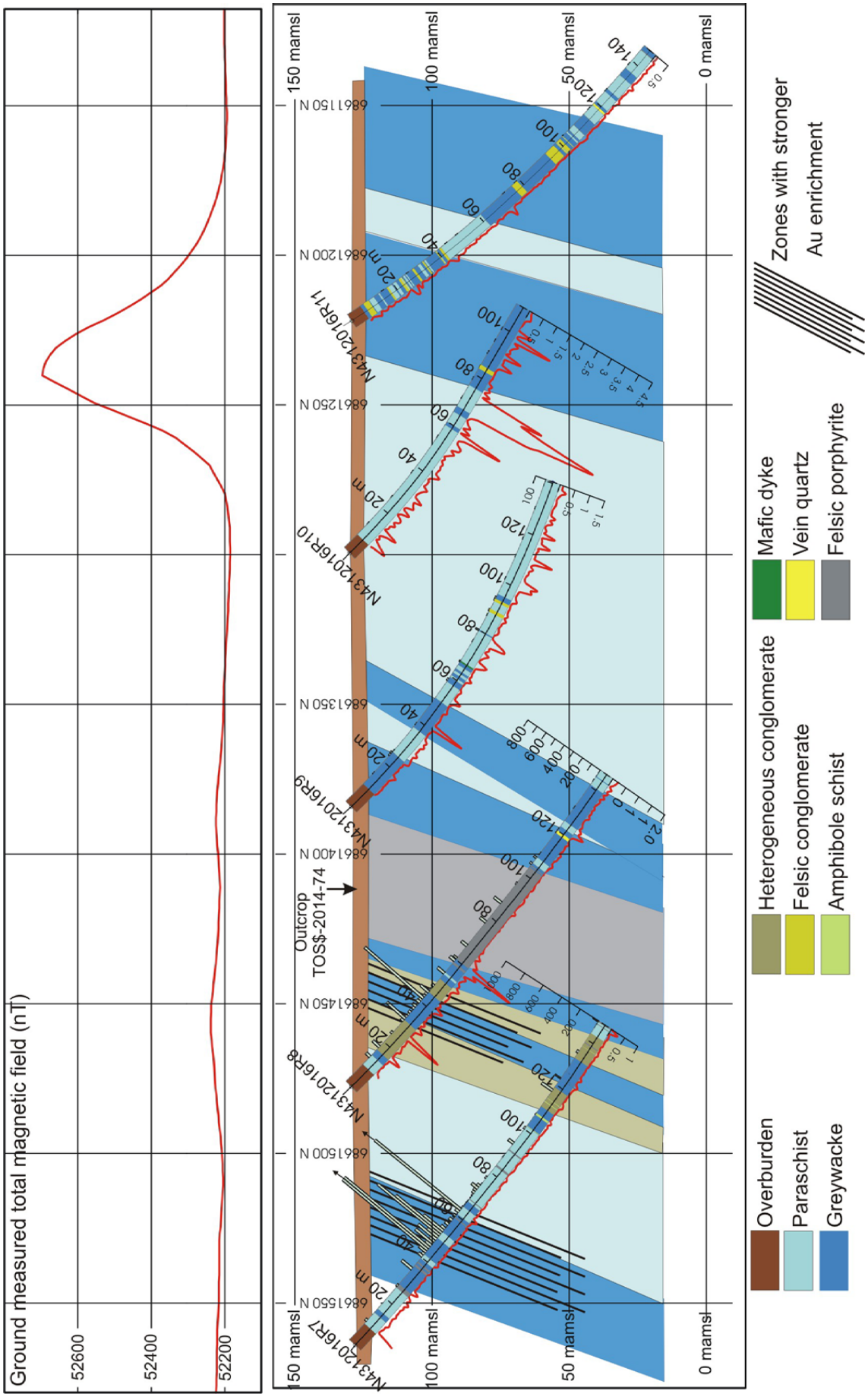

Fig. 8. Drilling profile from Harjujärvensuo with the geological interpretation. On top is the profile sampled from the interpolated grid of the ground-surveyed total magnetic field. Susceptibility (scale for k(SI) 10^{-3}) measured at 1-m intervals from the drill core with a hand-held KT-10 meter is presented as a red profile below the rock columns. Analysed gold concentrations are displayed as bars above the rock columns. Note that the values above 1000 ppb have been cut off and indicated with an arrow on top of the bar.

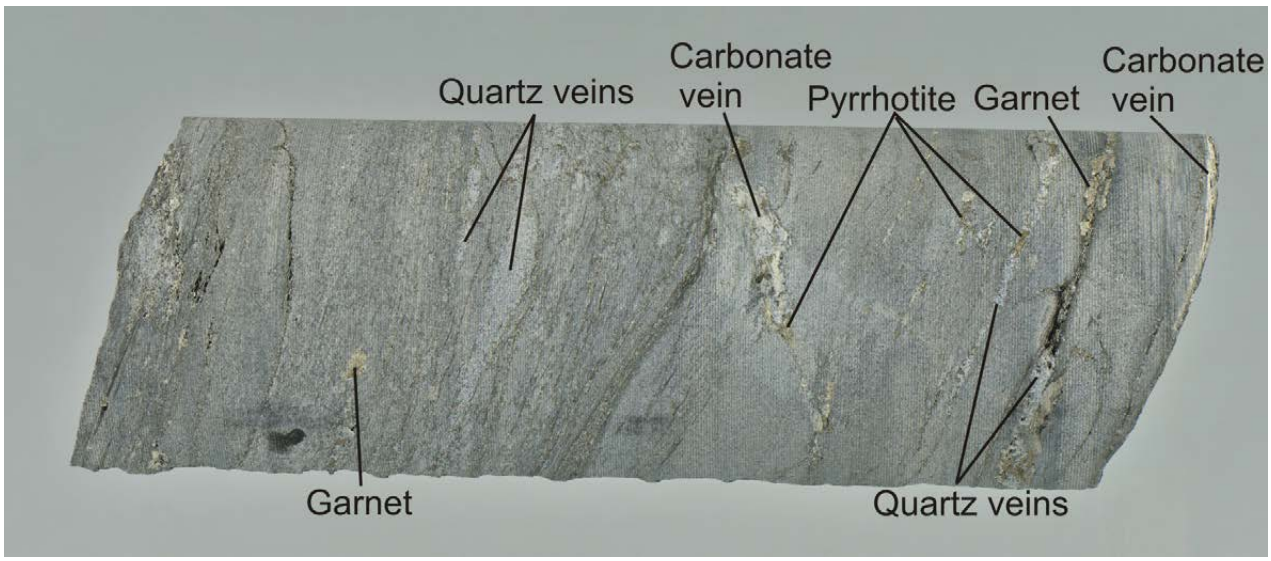

Fig. 9. Sample from drill hole N4312016R7, depth 43.00. Diameter of the drill core 42 mm.

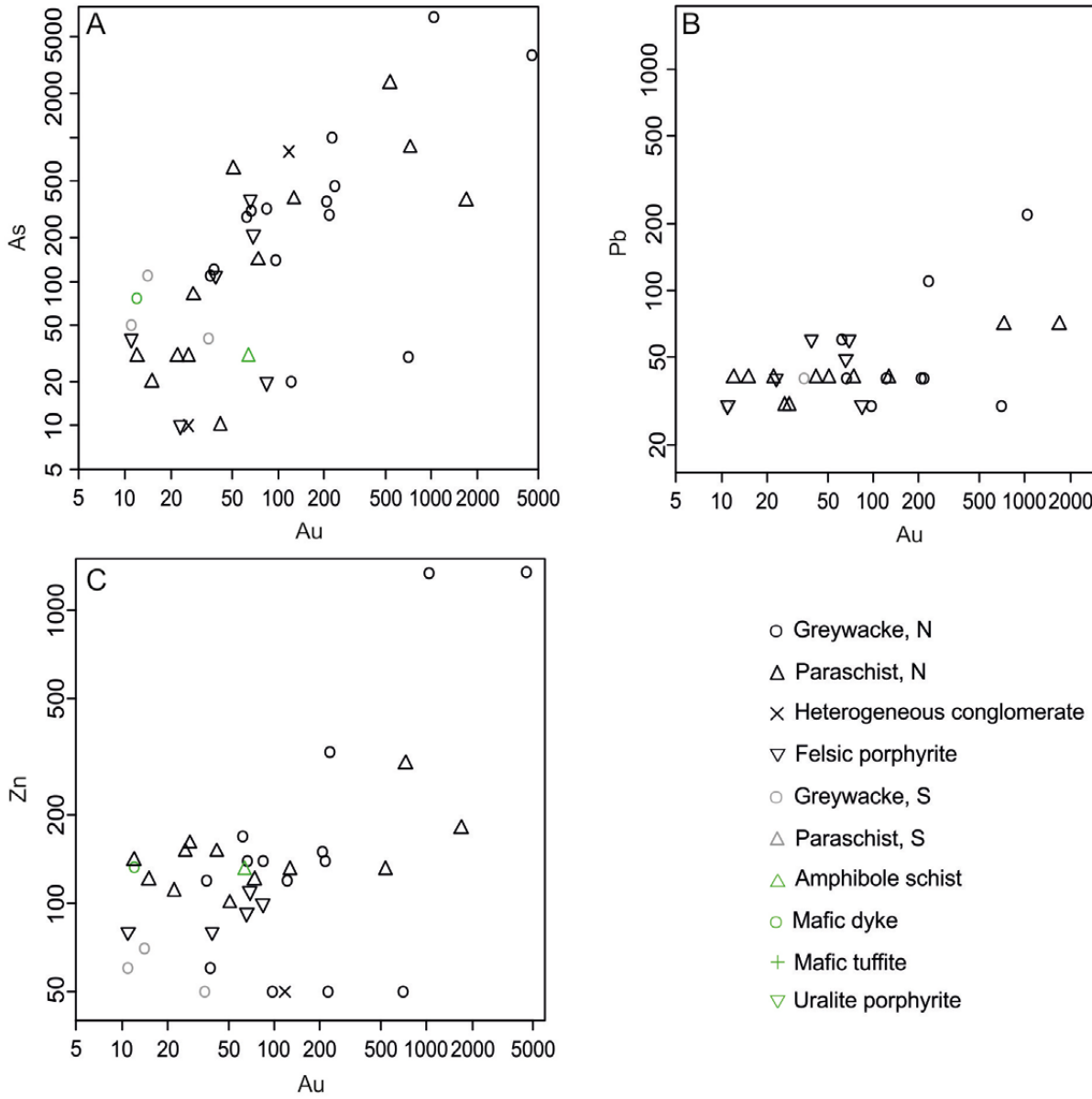

Fig. 10. Au vs. As, Pb and Zn plots for the Harjujärvensuo samples.

4.3.2 Mineralisation

The section continuously enriched in gold extends from beginning of drill hole N4312016R7 and continues to a depth of 108 m in drill hole N4312016R8 (Fig. 8), thus having a width of ca. 160 m. Most of the samples from this section contain a few tens, or a few hundreds of ppb of Au. The best intersection is in drill hole N4312016R7 from 42.00 to 53.00 m, which in addition to having the highest Au content (4.5 ppm, 43.00–44.00, Fig. 9), contains three metres with contents of 0.5–1 ppm and five metres with 100–200 ppb. The second highest Au concentration, 1.7 ppm, is from the analysis interval 62.00–63.00 in the same hole. Drill hole N4312016R9 down to a depth of 100 m is also weakly anomalous in gold (10–35 ppb).

Of the analysed elements, As shows the best correlation with Au (Fig. 10, Table 2). Pb also shows a correlation with Au, but if the Au-richest sample, which is also the one richest in Pb, is discarded, the correlation becomes weak, i.e. Pearson's correlation coefficient is reduced from 0.92 to 0.54. The correlation between Sb and Au cannot be properly evaluated, as only three of the samples contain Sb above the detection limit (50 or 100 ppm, depending on the sample batch), but out of these three samples, two are strongly enriched in Au (1.7 and 4.5 ppm) and additionally in Zn (1340 and 1350 ppm). The gold concentration does not show any correlation with either the Ishikawa alteration index (AI, Ishikawa et al. 1976) or the chlorite-carbonate-pyrite index (CCPI).

5 DISCUSSION

5.1 General geological setting

Based on the available data, the stratigraphy of the Harjujärvensuo area cannot be reliably interpreted, and it is possible that a major tectonic boundary exists between drill holes N4312016R12 and R7. However, there are no signs of this in the magnetic data, and the occurrence of the thin amphibole schist interbeds in drill hole N4312016R7, similar in composition to the mafic tuffites from N4312016R12, also suggests that they are part of the same stratigraphic sequence. The coherent compositional variation shown by the greywackes and paraschists of profile N4312016R7–R11 indicates that they are a part of the same geological unit displaying gradual compositional changes caused by variation in the influx, i.e. grain size, different source areas or variation in volcanic activity. Further support for the interpretation that all rocks encountered in the Harjujärvensuo area belong to the Pirkanmaa migmatite suite are the uralite porphyries that belong to the picritic Ala-Siili lithodeme of the suite. The detrital zircon population of a sample taken from the heterogeneous conglomerate was also typical for the Pirkanmaa migmatite suite, i.e. having a maximum depositional age of 1.92 Ga and a bimodal distribution with peaks at 2.0 Ga and 2.7 Ga (Mikkola et al. 2018b).

5.2 Type of mineralisation and comparison with other mineralisations in the area

No detailed mineralogical studies have been carried out on mineralised samples from Harjujärvensuo, but as the gold clearly correlates with As and arsenopyrite occurs as dissemination in the host rock, it can be argued that the quartz veins represent a younger phase following the main mineralisation event dispersing Au and As in the host rock. The seritization occurred during this mineralisation. The lack of a correlation between the AI quantifying the serizite alteration and Au could be caused by later carbonate alteration and veining modifying the value of the index in the opposite direction than seritization. Based on the available data, the Harjujärvensuo mineralisation can be classified as orogenic in type. It is hosted by a metasedimentary sequence consisting of clastic sediments varying from paraschists to conglomerates in grain size. The quartz±carbonate veining and serizite alterations commonly associated with orogenic gold deposits are not dominant features in Harjujärvensuo, but are present.

The Harjujärvensuo mineralisation is located in a geologically identical location to the Tammijärvi mineralisation (Luukkonen 1994), i.e. within the major Leivonmäki shear zone (Fig. 1) and in the vicinity of the contact between volcanic rocks of the Makkola suite and the Pirkanmaa migmatite suite,

on the side of the latter. Also, the weaker Lepola Au showing is located in the same rocks and contact zone (Fig. 1, Mattila 1980). The Kärmesalo Au showing is also in the same zone, but in this case the gold-enriched rock is quartz diorite (Oivanen 1958). In addition to unprocessed analytical data, only limited information is available from the Vatsa Au mineralisation and practically no data at all on the ore mineralogy (Liikanen 1992, Lehto & Finnäs 1997, Rönnqvist 2013, Lappland Gold Miners 2015). The gold mineralisation is hosted by a quartz-veined east–west-trending sheared contact zone between granite and a gabbro (Lehto & Finnäs 1997), which could be a branch of the Leivonmäki shear zone (Mikkola et al. 2016).

Despite the similar host rocks at Tammijärvi and Harjujärvensuo, the locations differ in numerous ways. Samples from Tammijärvi are enriched in W (<0.92%), Cu (<0.84%) and Sn (<700 ppm), whereas in Harjujärvensuo, Sn is below the detection limit (30 ppm) in all of the drill core samples (<3.5 ppm in the boulder samples), and Cu is only weakly enriched (<450 ppm). The lack of significant enrichment in Sn and Cu also characterizes the Vatsa mineralisation (data attachments of Rönnqvist 2013). Drill core samples from Harjujärvensuo were not analysed for W and Ag, as the analyses from the boulder samples (<1.25 ppm) indicated no significant enrichment in these elements. An important difference is also observable in the mode of occurrence of arsenopyrite; in Harjujärvensuo, it occurs as fine-grained dissemination, more abundant in Au mineralised parts, whereas in Tammijärvi, it occurs as larger aggregates (≤5 mm) in quartz veins (Luukkonen 1994). However, in both locations, a correlation between As and Au concentrations is evident, contrary to the Vatsa target, where As is only slightly enriched (<1000 ppm,

Table 2. Characteristics of the Harjujärvensuo, Tammijärvi and Vatsa gold mineralisations. Data for Harjujärvensuo also include results (Ag, Bi, Mo, Se, Sn, W) from boulder samples that were analysed with a method having a lower detection limit than the drill core samples. Data for Tammijärvi are from Luukkanen (1994) and Lindmark (1988). Note that the Cu, Sn and W concentrations for Tammijärvi are from a 4.55-m-long drilling intersection and values for other elements are from outcrop samples. Data for Vatsa are from the data attachments of Rönnqvist (2013). Pearson's correlation coefficients for Harjujärvensuo and Vatsa were calculated by the authors and those for Tammijärvi are taken from Luukkonen (1994). "Possible" in the column for Harjujärvensuo indicates that the material is too limited (n = 9) and scattered to justify the use of statistical methods, but based on visual inspection, a correlation between the elements could exist.

	Harjujärvensuo		**Tammijärvi**		**Vatsa**	
Host rocks	Sheared metasedimentary rocks, limited quartz±-carbonate veining		Sheared metasedimentary rocks, strong quartz±-carbonate veining		Sheared and quartz veined contact of granite and gabbro	
Arsenopyrite	As dissemination		In quartz veins		In quartz veins	
Enrichment in elements other than Au, and their correlation with Au						
Ag	<1.25 ppm	possible	137 ppm	0.87	b.d.l.	no
As	<7000 ppm	0.60	<4.6%	0.88	<1000 ppm	no
Bi	<2 ppm	possible	<3250 ppm	0.94	<420 ppm	0.83
Cu	<450 ppm	no	<0.84%	0.73	<3000 ppm	no
Mo	<1.5 ppm	no	not reported	---	<4000 ppm	no
Pb	<1460 ppm	0.92*	<50 ppm	no	<650 ppm	no
Sb	<580 ppm	possible	<70 ppm	0.91	<200 ppm	no
Se	<2 ppm	no	<60 ppm	0.86	b.d.l.	no
Sn	<3.5 ppm	no	<700 ppm	0.70	<40 ppm	no
W	<3 ppm	no	<0.92%	0.58	<1200 ppm	no
Zn	<1350 ppm	0.78**	<500 ppm	0.74	<450 ppm	no

* Note that if the Au-richest sample is removed the correlation coefficient is reduced to 0.54

** Note that if the Au-richest sample is removed the correlation coefficient is reduced to 0.50

excluding outliers) and it does not display a correlation with Au (based on the data attachments of Rönnqvist 2013). The Vatsa and Tammijärvi targets both show a good correlation between Bi and Au (Liikanen 1992, Luukkonen 1994). This connection is lacking from Harjujärvensuo, as Bi in all of the drill core samples was below the detection limit of 30 ppm, and below 2 ppm in the boulder samples. Enrichment in molybdenum has been reported from the Vatsa occurrence (Rönnqvist 2013, Mo ≤ 4000 ppm), but not from Tammijärvi (Luukkonen 1994) or Harjujärvensuo, where the Mo concentrations of all analyses were below the detection limit (10 ppm). It should be noted that Mo and Au do not display a significant correlation in Vatsa, either. Thus, it is possible that the local Mo enrichment event is separate from the Au mineralizing one, especially as Mo indications are known from other parts of the granite intrusion hosting the gold mineralisation (Ikävalko 1984).

The observed characteristics of the Vatsa, Tammijärvi and Harjujärvensuo mineralisations are summarised in Table 2. Overall, the only common denominators of these are the sheared character of the host rocks, quartz veins and enrichment in Au. In all locations, the shearing is connected with the large-scale Leivonmäki shear zone transecting the area, and the differences could be caused by variation in the exact timing of mineralisation with respect to the prolonged activity of the deformation zone (Mikkola et al. 2018a). The differences in host rocks could also explain some of the variation in mineralisation styles by creating traps for different elements based on compositional differences.

5.3 Potential of the target

As only one profile has been drilled, the target remains open in all directions. Some indication of extension towards the east is given by the location of the gold anomalous boulders that were first found; as glacial transport has been from due north, these boulders are located too far east to have been derived from the area of the drilling profile. Geochemical sampling of the bottom till could be effective in the area, based on drill-hole data the Quaternary cover in the area is ca. 5 m thick.

When considering the attractiveness of the target for further exploration work, the presence of Leivonmäki National Park 500 m east and 800 m northwest of the drilling profile has to be taken into consideration. The profile itself is, however, located on forestry land, and permitting early stage exploration activities does not therefore pose significant challenges.

Based on petrophysical laboratory measurements and observations from the drill cores, it seems unlikely that neither gravimetric nor electrical methods could be successfully used to directly locate the extensions of the mineralised zones. No significant differences exist in the measured density and conductivity values between rock types and their mineralised versions. With respect to the magnetic measurements, it seems that the highest Au concentrations coincide with a gradient on the magnetic map (Fig. 2) from higher values in the north towards lower values in the south. If this is the case, continuations of the mineralised zones should be searched for along the strike of the bedding/foliation (065-085°). The above is probably an oversimplification, but the drill cores and outcrops do show strong lineation that could correlate with a lens-shaped mineralisation.

6 CONCLUSIONS

The gold anomalous zone in Harjujärvensuo is 160 m wide and open in all directions. Boulder observations indicate continuation at least east of the drilled profile.

Harjujärvensuo is interpreted as orogenic in type. Based on the available data, gold shows a correlation with As and possibly with Ag, Bi, Pb, Sb and Zn.

The three known gold mineralisations in the area differ significantly with respect to the enriched elements and host rocks. Practically the only common denominator is the deformation and sheared nature of the host rocks.

The differences between the mineralisation styles are likely to be caused by mineralisation in different phases of activity of the Leivonmäki shear zone transecting the area.

ACKNOWLEDGEMENTS

Seasoned research assistants Rauli Lempiäinen and Tuomo Stranius are acknowledged for locating the boulders leading to the discovery of the Harjujärvensuo mineralisation. Jouko Ranua is thanked for the drill-core photos used. Riitta Turunen finalised the geochemical diagrams.

REFERENCES

Heilimo, E., Ahven, M. & Mikkola, P. 2018. Geochemical characteristics of the plutonic rock units present at the southeastern boundary of the Central Finland Granitoid Complex. In: Mikkola, P., Hölttä, P. & Käpyaho, A. (eds) Development of the Paleoproterozoic Svecofennian orogeny: new constraints from the southeastern boundary of the Central Finland Granitoid Complex. Geological Survey of Finland, Bulletin 407. (this volume). Available at: https://doi.org/10.30440/bt407.6

Herron, M. M. 1988. Geochemical classification of terrigenous sands and shales from core or log data. Journal of Sedimentary Petrology 58, 820–829.

Hurskainen, V. 1989. Malmitutkimukset Luhangan Tammijärven alueella 1989. Outokumpu exploration, report 001/3122 06/VIH/1989. 4 p., 14 app. (in Finnish). Available at: http://tupa.gtk.fi/raportti/arkisto/001_3122_06_vih_89.pdf

Ikävalko, O. 1984. Oittilan graniittiin liittyvät molybdeenitutkimukset Korpilahdella 1983. Geological survey of Finland, archive report M19/3211/-83/1/30. 15 p., 4 app. (in Finnish). Available at: http://tupa.gtk.fi/raportti/arkisto/m19_3211_83_1_30.pdf

Ishikawa, Y., Sawaguchi, T., Iwaya, S. & Horiuchi, M. 1976. Delineation of prospecting targets for Kuroko deposits based on models of volcanism of underlying dacite and alteration halos. Mining Geology 26, 103–117.

Janoušek, V., Farrow, C. M. & Erban, V. 2006. Interpretation of whole-rock geochemical data in igneous geochemistry: introducing Geochemical Data Toolkit (GCDkit). Journal of Petrology 47, 1255–1259.

Kousa, J., Mikkola, P. & Makkonen, H. 2018. Paleoproterozoic mafic and ultramafic volcanic rocks in the South Savo region, eastern Finland. In: Mikkola, P., Hölttä, P. & Käpyaho, A. (eds) Development of the Paleoproterozoic Svecofennian orogeny: new constraints from the southeastern boundary of the Central Finland Granitoid Complex. Geological Survey of Finland, Bulletin 407. (this volume). Available at: https://doi.org/10.30440/bt407.4

Lappland Gold Miners 2015. Vatsa project, Hopeavuori project, Tampere district. Mining claim report 6702/1-2. 4 p. Available at: http://tupa.gtk.fi/raportti/valtaus/6702_1_2.pdf

Lehto, T. & Finnäs, P. 1997. Vatsa 1996 Malminetsintätutkimukset. Mining claim report 4655/1, 4695/1. 3 p., 3 app. (in Finnish). Available at: http://tupa.gtk.fi/raportti/valtaus/4655_1_4695_1.pdf

Liikanen, J. 1992. Vatsa 1991. Rapport om geologiska undersökningar i Korpilahti. Mining claim report 4665/1. 7 p., 8 app. (in Swedish). Available at: http://tupa.gtk.fi/raportti/valtaus/4665_1.pdf

Lindmark, B. 1988. Tina- ja volframitutkimukset Luhangan Tammijärvellä vuosina 1978 - 1986. Geological survey of Finland, archive report M19/3122/-87/1/10. 41 p., 3 app. (in Finnish). Available at: http://tupa.gtk.fi/raportti/arkisto/m19_3122_87_1_10.pdf

Luukkonen, A. 1994. Main geological features, metallogeny and hydrothermal alteration phenomena of certain gold and gold-tin-tungsten prospects in southern Finland. Geological Survey of Finland, Bulletin 377. 153 p. + 8 app. Available at: http://tupa.gtk.fi/julkaisu/bulletin/bt_377.pdf

Mattila, E. 1980. Luhanka Lepola, tunnustelukairaus. Rautaruukki Oy, exploration report OU 27/80. 1 p., 4 app. (in Finnish). Available at: http://tupa.gtk.fi/raportti/arkisto/ou_27_80.pdf.

Mikkola, P., Heilimo, E., Aatos, S., Ahven, M., Eskelinen, J., Halonen, S., Hartikainen, A., Kallio, V., Kousa, J., Luukas, J., Makkonen, H., Mönkäre, K., Niemi, S., Nousiainen, M., Romu, I. & Solismaa, S. 2016. Jyväskylän seudun kallioperä. Summary: Bedrock of the Jyväskylä area. Geological Survey of Finland, Report of Investigation 227. 95 p., 6 apps. Available at: http://tupa.gtk.fi/julkaisu/tutkimusraportti/tr_227.pdf

Mikkola, P., Heilimo, E., Luukas, J., Kousa, J., Aatos, S., Makkonen, H., Niemi, S., Nousiainen, M., Ahven, M., Romu, I. & Hokka, J. 2018a. Geological evolution and structure along the southeastern border of the Central Finland Granitoid Complex. In: Mikkola, P., Hölttä, P. & Käpyaho, A. (eds) Development of the Paleoproterozoic Svecofennian orogeny: new constraints from the southeastern boundary of the Central Finland Granitoid Complex. Geological Survey of Finland, Bulletin 407. (this volume). Available at: https://doi.org/10.30440/bt407.1

Mikkola, P., Huhma, H., Romu, I. & Kousa, J. 2018b. Detrital zircon ages and geochemistry of the metasedimentary rocks along the southeastern boundary of the Central Finland Granitoid Complex. In: Mikkola, P., Hölttä, P. & Käpyaho, A. (eds) Development of the Paleoproterozoic Svecofennian orogeny: new constraints from the southeastern boundary of the Central Finland Granitoid Complex. Geological Survey of Finland, Bulletin 407. (this volume). Available at: https://doi.org/10.30440/bt407.2

Mikkola, P., Mönkäre, K., Ahven, M. & Huhma, H. 2018c. Geochemistry and age of the Paleoproterozoic Makkola suite volcanic rocks in central Finland. In: Mikkola, P., Hölttä, P. & Käpyaho, A. (eds) Development of the Paleoproterozoic Svecofennian orogeny: new constraints from the southeastern boundary of the Central Finland Granitoid Complex. Geological Survey of Finland, Bulletin 407. (this volume). Available at: https://doi.org/10.30440/bt407.5

Oivanen, P. 1958. Raportti malmitutkimuksista Luhangan Tammijärvellä kesäkuussa 1956. Geological survey of Finland, archive report M17/Lhk-56/2. 2 p. (in Finnish). Available at: http://tupa.gtk.fi/raportti/arkisto/m17_lhk_56_2.pdf

Pääkkönen, V. 1947. Geologisen tutkimuslaitoksen malmitutkimukset Luhangalla kesällä 1947. Geological survey of Finland, archive report M17/Lhk-47/1. 3 p.,

1 app. (in Finnish). Available at: http://tupa.gtk.fi/raportti/arkisto/m17_lhk_47.pdf

Pääkkönen, V. 1951. Loppuselostus malmitutkimuksista Luhangan Sydänmaan alueella. Kivipuro 1-6 nimisten valtausalueiden hylkääminen. Mining claim report 0679/1-6. 4 p., 25 app. (in Finnish). Available at: http://tupa.gtk.fi/raportti/arkisto/m17_lhk_51_1.pdf

Pajula, O. 2015. Loppuraportti valtauksilla "Lepola, Tammijärvi ja Sydänmaa 1-2, 8004/1-4" suoritetuista tutkimuksista. Mining claim report 8004/1-4. 17 p. (in Finnish). Available at: http://tupa.gtk.fi/raportti/valtaus/8004_1_4.pdf

Pettijohn, F. J., Potter, P. E. & Siever, R. 1972. Sand and Sandstone. Berlin: Springer-Verlag. 600 p.

Rönnqvist, J. 2013. Redogörelse för undersökningsarbeten samt infromationsmaterial som gäller undersökning enligt Gruvlagen 10.6.2011/621 15 1 mom. 2 inom inmutningsområde Vatsa nr 1 reg nr 7672/1, Vatsa nr 2 reg nr 7672/2, Vatsa nr 3 reg nr 7672/3, Vatsa nr 4 reg nr 7672/4 samt Vatsa nr 5 reg nr 7672/5. Mining claim report 7672/1-5. 11 p. (in Swedish). Available at: http://tupa.gtk.fi/raportti/valtaus/7672_1_5.pdf

Wennervirta, H. 1973. Soijan pohjatutkimus Luhanka Tammijärvi. Outokumpu exploration, report 062/3122/HW/73. 3 p., 9 app. (in Finnish). Available at: http://tupa.gtk.fi/raportti/arkisto/061_3122_06_hw_73.pdf

Development of the Paleoproterozoic Svecofennian orogeny: new constraints from the southeastern boundary of the Central Finland Granitoid Complex
Edited by Perttu Mikkola, Pentti Hölttä and Asko Käpyaho
Geological Survey of Finland, Bulletin 407, 186–208, 2018

SUOLIKKO Pb-Zn MINERALISATION AND ITS COUNTRY ROCKS IN MUURAME, CENTRAL FINLAND

by

Ville Kallio[1)], Perttu Mikkola[2)], Hannu Huhma[3)] and Sami Niemi[2)]

Kallio, V., Mikkola, P., Huhma, H. & Niemi, S. 2018. Suolikko Pb-Zn mineralisation and its country rocks in Muurame, Central Finland. *Geological Survey of Finland, Bulletin 407*, 186–208, 10 figures and 4 tables.

The Suolikko Pb–Zn mineralisation in southern parts of the Central Finland Granitoid Complex is associated with a narrow shear zone predating the hydrothermal mineralisation event. In addition to Pb (≤1.7%) and Zn (≤1.7%), the mineralisation is variably enriched in Cu (≤0.2%), Sn (≤900 ppm) and Ag (≤50 ppm). Dominant sulphides are sphalerite, chalcopyrite, galena, pyrrhotite and pyrite. Gahnite is abundant. The mineralised rocks are garnet-bearing porphyritic granites and diorites. The actual mineralisation is surrounded by a narrow halo of amazonite granite, the genesis of which is related to the mineralisation process. The known width of the mineralisation is ≤10 m and potential length ~400 m. Based on single-grain dating of zircon, the porphyritic granites surrounding the mineralisation crystallised at 1881 ± 4 Ma. Monazite and zircon analyses from a mineralised sample suggest that the mineralisation event took place at around 1785 Ma. The proposed fluid source was a post-tectonic granite.

Appendix 1 is available at: http://tupa.gtk.fi/julkaisu/liiteaineisto/bt_407_appendix_1.pdf

Electronic Appendix is available at: http://tupa.gtk.fi/julkaisu/liiteaineisto/bt_407_electronic_appendix.xlsx

Keywords: copper, lead, zinc, silver, sphalerite, galena, gahnite, chalcopyrite, amazonite, zircon, monazite, hydrothermal alteration, U/Pb, absolute age, granites, Svecofennian, Paleoproterozoic, Finland

[1)] *Oulu Mining School, University of Oulu, P.O. Box 3000, FI-90014 Oulun Yliopisto, Finland*
[2)] *Geological Survey of Finland, P.O. Box 1237, FI-70211 Kuopio, Finland*
[3)] *Geological Survey of Finland, P.O. Box 96, FI-02151 Espoo, Finland*

E-mail: villekallio83@gmail.com

VERTAISARVIOITU
KOLLEGIALT GRANSKAD
PEER-REVIEWED
www.tsv.fi/tunnus

https://doi.org/10.30440/bt407.10

Editorial handling by Pentti Hölttä and Asko Käpyaho.

Received 30 June 2017; Accepted 3 September 2018

1 INTRODUCTION

Core of the Svecofennian domain in Finland, the Central Finland Granitoid Complex (CFGC) has been considered as mainly uninteresting with respect to ore prospecting (e.g. Eilu et al. 2012). However, several mineralisations of different types are known and have been studied to uneven extent. Several of these contain variable amounts of Zn–Pb–Cu–Sn and include the mineralisations in the Hiekkapohja and Muittari areas (Fig. 1). In the Hiekkapohja area, several small mineralisations are known, and as an entity, the system has some features common to modern large-scale porphyry systems (Halonen 2015, Heilimo et al. 2017). In the Muittari area, the mineralisations occur in shear zones (Sipilä 1985). One of the Pb–Zn indications known since the 1960s is the Suolikko mineralisation 20 km southwest of Jyväskylä (Fig. 1). This mineralisation is readily observable in a road cut along highway 9 and the Geological Survey of Finland (GTK) has received layman samples from and studied it on several occasions (Oivanen 1962, Hartikainen 1978, Nikander 2004). This location is referred to as "Road cut" in this study. Vaasjoki (1981) presented lead isotope data for one sample from the Suolikko mineralisation and for another ca. 1 km to the west.

The purpose of this paper is to describe in detail the long-known Suolikko mineralisation occurring in a granitoid-dominated area and to evaluate its age and genesis. The material includes outcrop and drill-core observations, ground surveyed geophysical measurements, thin sections, compositional data from minerals and whole-rock samples, as well as age determinations of zircon and monazite from a mineralised and country rock sample. This paper is mainly based on the unpublished Master's thesis of the first author (Kallio 2017), which contains more detailed field and petrographic descriptions.

2 GEOLOGICAL SETTING

Most of bedrock in Central and South Finland formed during the Paleoproterozoic accretionary Svecofennian orogeny which culminated close to 1.9 Ga ago (e.g. Nironen 2017). Core of the Svecofennian domain in Finland is the CFGC, surrounded by intermittent volcanic belts and voluminous paragneisses (Nironen et al. 2016). Suolikko mineralisation is situated in south-eastern part of the CFGC (Fig. 1) and the bedrock surrounding it mainly consists of porphyritic granitoids belonging to the ca. 1885 Ma Muurame lithodeme (e.g. Mikkola et al. 2016, Heilimo et al. 2018), which together with coeval quartz diorites of the Vaajakoski lithodeme form the Jyväskylä suite. Calc-alkaline rocks of the Jyväskylä suite form the bulk of the CFGC and have been linked alternatively to continental arc setting (e.g. Mikkola et al. 2018a) or thermal relaxation of crust thickened in collisional processes (Nikkilä et al. 2016).

Rocks of the Jyväskylä suite contain small enclaves of older supracrustal rocks and are intruded by rocks belonging to the bimodal Saarijärvi suite aged ca. 1880 Ma (Mikkola et al. 2016, Virtanen & Heilimo 2018 and references therein). The felsic members of this suite are typically K-feldspar porphyritic quartz montzonites with A-type geochemical affinity, and the basic members display mineralogical variation from gabbro to quartz diorite (ibid.). The youngest widespread geological unit in the area comprises the often leucocratic granitoids of the Oittila suite (~1875 Ma), which are found as small intrusions and locally abundant dykes in all of the above-mentioned units. Important structures in the area are the large-scale faults and shear zones trending southeast (Fig. 1) and showing signs of prolonged activity, first under ductile and later under brittle conditions (Nironen 2003, Mikkola et al. 2018a).

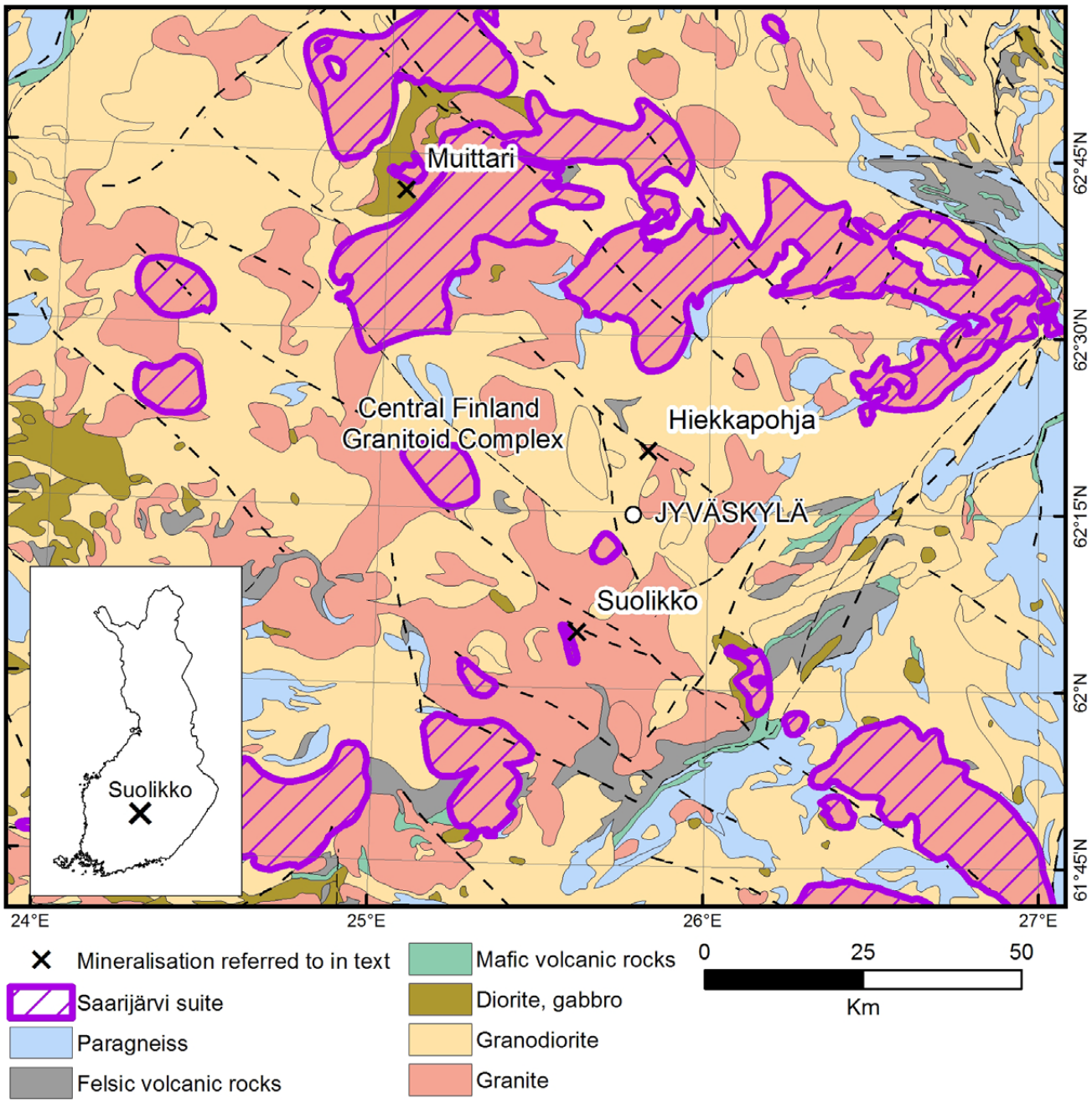

Fig. 1. General geological map of the areas surrounding Suolikko. Bulk of the granitoids and diorites in the area belong to the calc-alkaline Jyväskylä suite. Those interpreted as belonging to the Saarijärvi suite displaying A-type geochemical affinities have been separated with a raster. Map modified from Nironen et al. 2016. The inset shows the location of the area in Finland.

3 MATERIAL

In addition to outcrop mapping, a ground-measured geophysical survey was carried out in the Suolikko area and four drill holes were drilled. The geophysical methods applied were magnetic, induced polarity and electromagnetic Max-Min. All analytical methods are described in Appendix 1. Altogether, 33 whole-rock samples were analysed by Labtium Ltd, all of them with the XRF method (Labtium code 175X), 17 with ICP-MS using total leaching (Labtium code 308PM) and 29 with ICP-MS using partial leaching (Labtium code 511PM). Out of the results from partial leaching, only Ag concentrations are included in this paper and the electronic appendix, as it is not included in the other two

methods. The geochemical data were plotted using the Geochemical Data Toolkit (GCDkit) program by Janoušek et al. (2006). Thin sections were prepared from 50 samples and selected mineral compositions were determined from 13 of these using an electron probe microanalyser (EPMA) at the Center of Microscopy and Nanotechnology of the University of Oulu. One sample weighing ca. 10 kg was taken for U-Pb age determination, and separated zircons were dated using a Nu Plasma HR multicollector ICP-MS. Monazite and zircon from one thin section were analysed for U–Pb age determinations using a Nu Plasma AttoM single collector ICPMS connected to a laser ablation system at the Geological Survey of Finland in Espoo.

4 RESULTS

4.1 Field and drill-core observations

4.1.1 Country rocks

The immediate host rocks of the Suolikko mineralisation mainly consist of porphyritic granite and granodiorite, which are typical representatives of the Muurame lithodeme granitoids (Mikkola et al. 2016, Heilimo et al. 2018). The compositional heterogeneity is visible as varying abundance of K-feldspar. The term porphyritic granite is used in this paper to refer to all porphyritic samples, as they represent the majority of the porphyritic granitoids. The colour of the porphyritic granite varies from reddish grey to grey and the size of the porphyries is typically 5–30 mm. The groundmass is medium grained (1–5 mm) and the texture is variably deformation oriented, often with a sheared augen gneiss appearance (Fig. 3A). Biotite is the most abundant mafic mineral, accompanied by variable amounts of hornblende in some of the samples.

In most places, a zone of amazonite (Pb-bearing K-feldspar) granite with light green – turquoise K-feldspar phenocrysts (Fig. 3C) is located between the garnet-bearing mineralised rocks and the normal porphyritic granites. These amazonite granites locally contain small amounts of sulphides, but do not represent the actual mineralised rocks in the area. The colour of the K-feldspar and on average stronger shearing are the only distinct differences between amazonite and the normal porphyritic granite of the area. Contacts between the two colour variants are gradual.

The porphyritic granite contains fine grained xenoliths up to few metres in size consisting of variable amounts of plagioclase, biotite and hornblende, which could be supracrustal in origin. Mineralogically similar, but coarser grained, xenoliths are likely to belong to the Vaajakoski quartz diorite lithodeme, in some cases these appear migmatitic (Fig. 3B). The latter xenolith type is referred to as diorite in this paper.

The unoriented fine-grained pyroxene-bearing quartz diorite in the southern part of the Suolikko area has been interpreted as belonging to the Saarijärvi suite and is thus younger than the main porphyritic granite in the area (Mikkola et al. 2016, Heilimo et al. 2018). The intrusion is clearly visible as a local maximum on the magnetic map (Fig. 2C).

Equigranular, relatively leucocratic and unoriented granite dykes varying in width from a few centimetres to several metres cross-cut the porphyritic granites and their deformation orientation (Fig. 3A). As is typical for the southern part of the CFGC, the orientation of the dykes does not form distinct patterns. The grain size varies from small grained to pegmatitic. Biotite is the most common mafic mineral, accompanied by hornblende in some of the samples. Based on their age relationships and appearance, these dykes belong to the Oittila suite (Mikkola et al. 2016, Heilimo et al. 2018).

4.1.2 Mineralisation

The mineralised garnet-bearing rocks are known from two outcrops and intersected by two drill holes. In addition to the Road cut, the other outcrop with garnet bearing rocks, referred to as "East End", is located 50 m south–southeast from the Road cut. This outcrop represents the easternmost known location with garnet-bearing rocks and anomalous Zn and Pb concentrations (Fig. 2A). All of the four locations occur on a straight line trending 105°, a direction that coincides with the large-scale faulting observable over the whole area of the CFGC (Figs 1, 2, Nironen 2003, Mikkola et al. 2018a). In ground-surveyed IP data, the mineralised locations coincide with a zone of anomalous chargeability

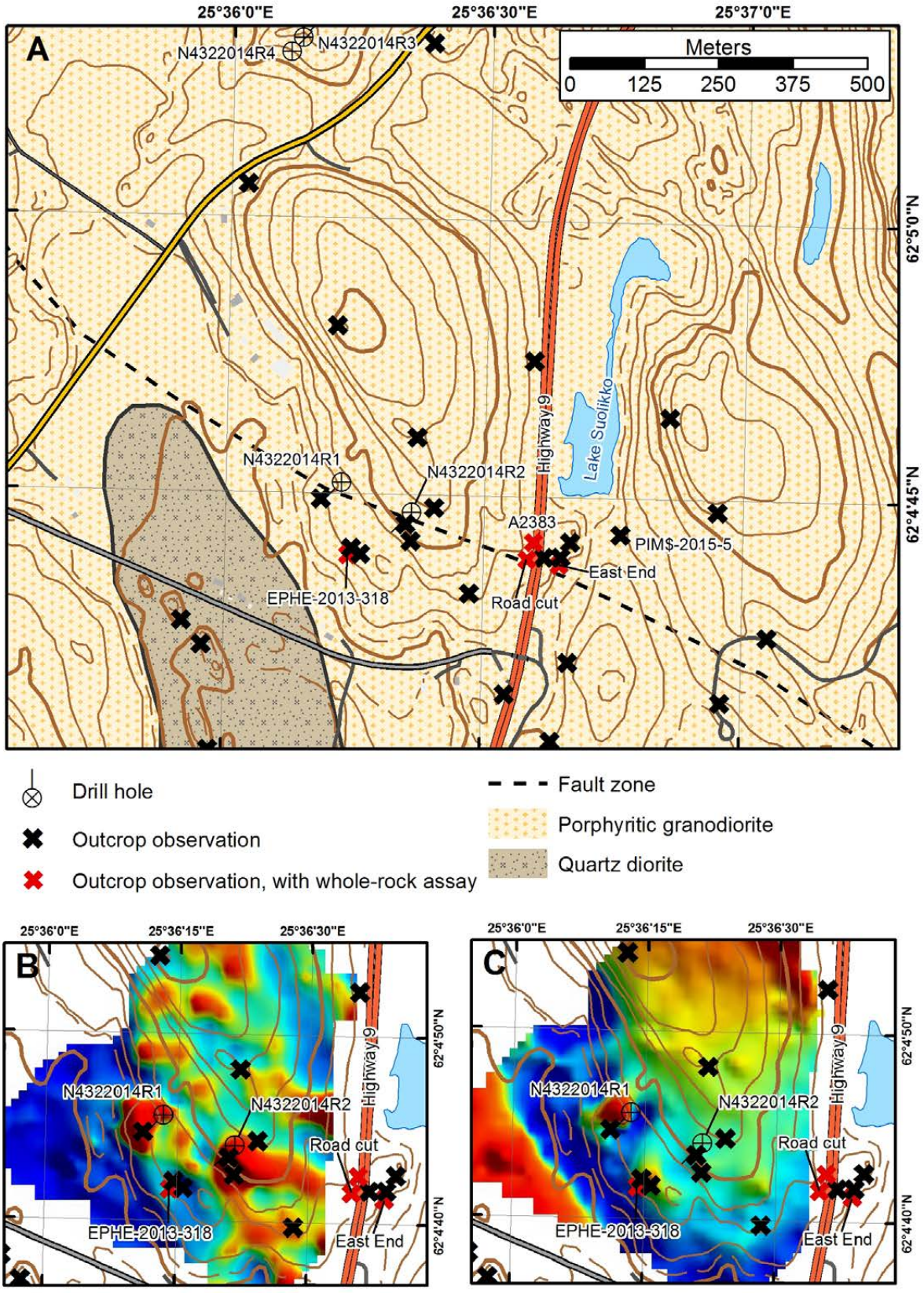

Fig. 2. A) Geological map of the Suolikko area with the locations of drill holes and outcrop observations. Map modified from Mikkola et al. (2016). B) Ground-surveyed chargeability map and C) magnetic map. In B) and C), blue indicates low values and red high values. Basemap © National Land Survey of Finland.

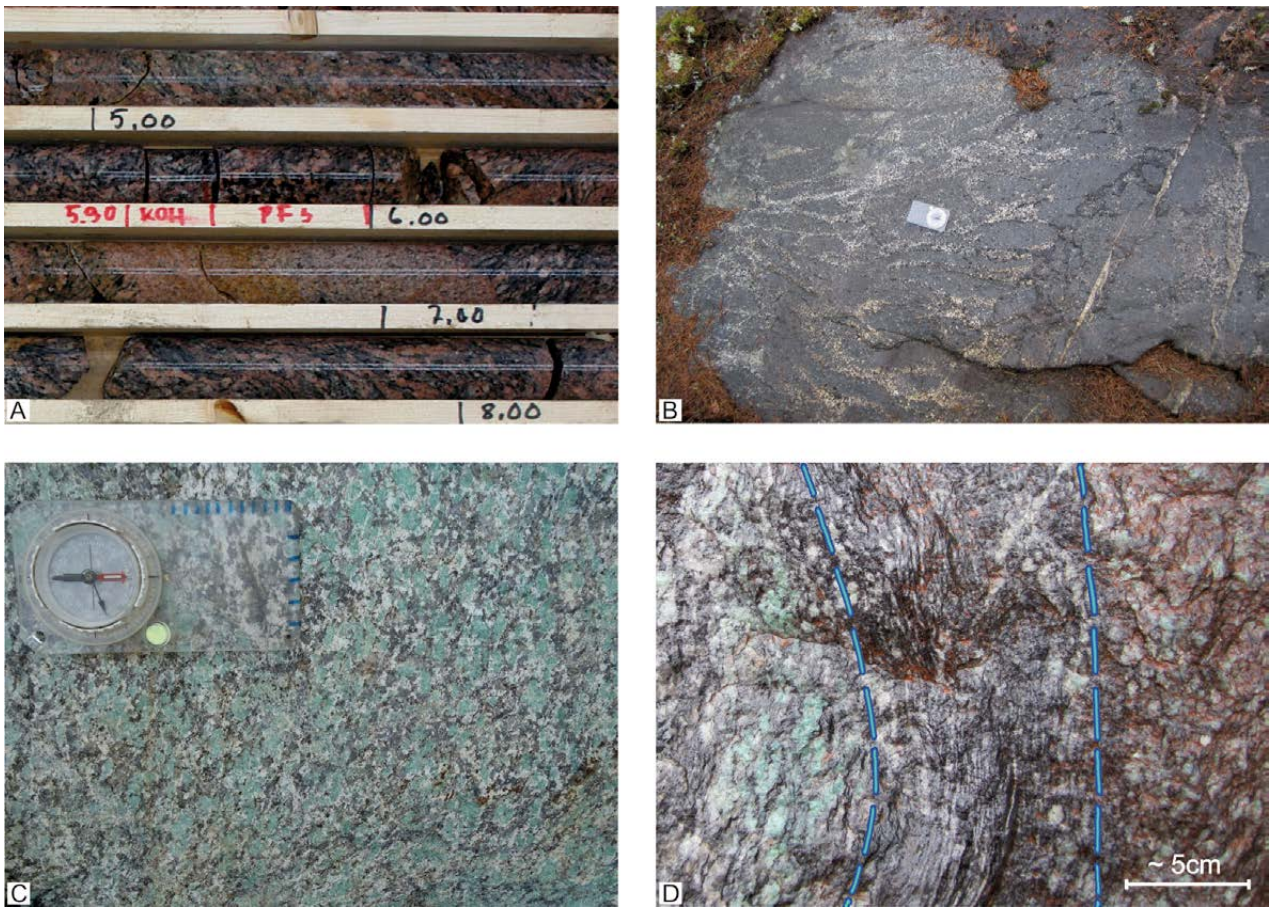

Fig. 3. A) Typical sheared augen gneiss appearance of the porphyritic granite from the Suolikko area and an equigranular granite dyke cross-cutting its orientation. Drill hole N4322014R4, diameter of the drill core 42 mm. B) Diorite with a vein network of diorite that is coarser grained and plagioclase richer than the host rock. Outcrop EPHE-2013-318. Length of the compass 12 cm. C) Amazonite granite from East End. Length of the compass 12 cm. D) A narrow section of the mineralisation from the Road cut, with green amazonite adjacent to the mineralised shear zone. Borders of mineralised zone highlighted with dashed lines.

(Fig. 2B) terminating ca. 70 m northwest of drill hole N4322014R1. Based on petrophysical measurements from drill core samples, the chargeability anomaly is caused by the mineralisation. Based on this, significant extensions of the mineralisation in a northwest direction are unlikely. In the magnetic data, the mineralisation is located in a low area (Fig. 2C), and only one point-like area of high magnetic intensity is present next to drill hole N4322014R1, but based on petrophysical measurements, the drill hole did not intersect its source. Apparent resistivity values in the area of the mineralisation were constantly high and the electromagnetic survey did not reveal any conductivity anomalies related to bedrock.

The distance from East End to drill hole N4322014R1, and thus the potential length of the mineralisation, is ca. 400 m (Fig. 2). The composition and mineralogy of the mineralised parts vary between the four known locations. Table 1 summarises each location's properties. Approximately 100 m north of the mineralised zone, a single outcrop (Fig. 2A, PIM$-2015-5) of porphyritic granite was found with narrow biotite-rich seams trending 105°. These seams also contain chalcopyrite and sphalerite. This is the only known indication of mineralisation processes outside the main mineralised zone in the Suolikko area.

The mineralised rocks are garnet granites (East End, Road cut and N4322014R2) and garnet diorites (N4322014R1). The mineralised parts are often, but not always (Figs 3D, 4), intensively ductilely sheared. The garnet grains do not display signs of significant deformation during or after crystallisation, and late brittle fracturing can only locally be observed in them. All sulphide-rich samples contain garnet, but not all garnet-bearing samples contain significant amounts of sulphides. However, as all of

Table 1. Summary of the different parts of the Suolikko mineralisation and East End location which is only anomalous. The length of drill-core samples was normally 1 m, while shorter samples were used in connection with narrow rock units.

Location	Host rock Comments	Sulphides	Gahnite	Garnet	Width of mineralization	Grade
N4322014R1	Garnet diorite	5–20%	Anhedral, "patchy"	10–20%	~10 metres	Zn ≤1.5%
		Sphalerite	Only in upper part of	Large		Pb ≤0.1%
	Late brittle deformation	Pyrrhotite	the drill core	Poikilo-blastic		Cu ≤0.1%
	in the upper part of drill core	Chalcopyrite		Locally altered to biotite,		Ag ≤4 ppm
		Pyrite		carbonate and pyrite		
N4322014R2	Garnet granite	5–20%	5–25%	5–50%	~10 metres	Zn ≤1.7%
		Chalcopyrite	Small	Small		Pb ≤0.7%
		Pyrrhotite	Subhedral	Euhedral to subhedral		Cu ≤0.2%
		Sphalerite				Ag 5–50 ppm
		Galena				Sn ≤900 ppm
Road cut	Garnet granite	~5%	None	<10%	~2 metres	Pb ≤1.7%
		Sphalerite		Small		Zn ≤1.1%
	Mylonitic texture in host rock	Pyrrhotite		Anhedral		Cu ≤0.1%
	Late brittle deformation	Galena		Fractured		Ag 3–30 ppm
		Pyrite, after pyrrhotite				Sn ≤900 ppm
East End	Garnet granite	<1%	<5%	20–30%	~1 metre	Zn ≤0.1%
		Sphalerite	Small	Small		Pb ≤0.1%
		Pyrite	Subhedral	Euhedral subeuhedral		Cu ≤0.01% Ag ≤0.5 ppm

the garnet granites are anomalous with respect to Zn and Pb, the term garnet granite is used to refer to mineralised variants. Garnet can locally make up nearly 50% of the rock, and it forms slightly varying textures in different parts of the mineralisation. In some places, it is present as small (~1 mm) idiomorphic crystals, whereas in other locations it appears massive or forms a network-like structure. Some of the amazonite granites flanking the mineralisation also contain small amounts of garnet. The most common sulphides are sphalerite, galena, chalcopyrite, pyrrhotite and pyrite, which occur variably as dissemination and elongated pockets.

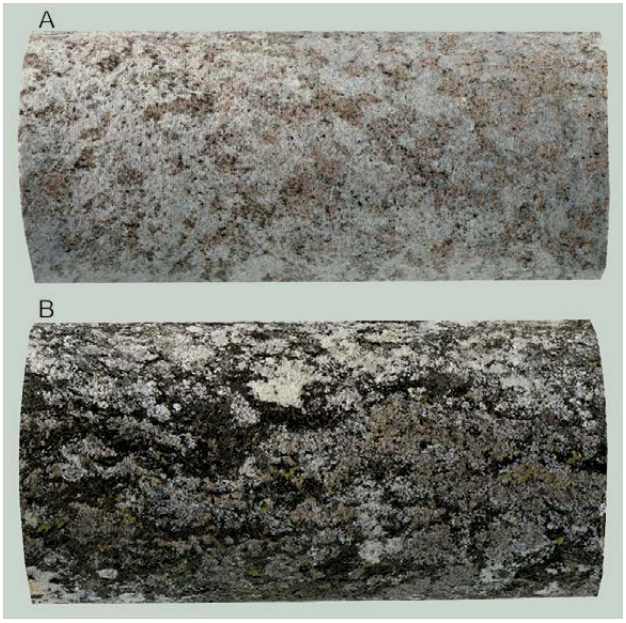

Fig. 4. A) Mineralised garnet granite from drill hole N4322014R2. B) Mineralised garnet diorite from drill hole N432214R1. Diameter of the drill core 42 mm.

4.2 Petrography

4.2.1 Amazonite granites

Amazonite granites and "normal" porphyritic granites cannot be separated in thin section studies, and both are deformed porphyritic biotite granites. Only one of the amazonite granite samples (from N4322014R2) also contained garnet. This sample is also the only one of the group containing small amounts of disseminated sulphides: pyrrhotite, chalcopyrite, sphalerite and galena. In all other amazonite granite samples, opaque minerals only consist of iron oxides, most commonly magnetite that is variably altered to hematite.

4.2.2 Garnet diorites and granites

Based on thin section studies, the garnet diorites and granites typically also contain significant amounts of gahnite (Zn spinel, end member $ZnAl_2O_4$). All gahnite-bearing samples also contain garnet, but not all garnet-bearing samples contain gahnite. The morphology of these two minerals is similar, as both occur either as large poikiloblastic anhedral crystals (N4322014R1) or as small (<1 mm) subhedral to euhedral crystals (other mineralised locations). The presence of garnet is connected with the sulphides in similar way; all samples containing significant amounts of sulphides contain garnet, but not all garnet-bearing samples are enriched in sulphides.

The content of sulphides in garnet-bearing rocks varies from 1% to 20%. They occur variably as interstitial dissemination or as larger patches or narrow veins, the latter two being typical for samples from drill hole N4322014R1. In some samples garnet contains sulphide inclusions. Sphalerite is in some cases in contact with gahnite or occurs as inclusion in it. Overall, the sulphides are most often located in connection with garnet, gahnite, biotite and amphibole, the most enriched locations being strongly oriented biotite ± amphibole bands.

Major minerals of garnet granites are garnet, plagioclase, biotite, K-feldspar, quartz and in most cases also gahnite (Fig. 5A). In addition to the presence of garnet and gahnite, the major difference compared to porphyritic granites is the absence of amphiboles from, and smaller proportion of biotite in, the garnet-bearing samples. Garnet granites display signs of ductile shear, e.g. a decrease in grain size and bending of plagioclase lamellas predating the crystallisation of garnet. Garnet shows no correlation with the strength of deformation of the host rock, as some of the garnet-bearing samples are only weakly oriented, whereas some of the intensively sheared samples do not contain garnet.

Major minerals of garnet diorites are plagioclase, biotite, amphibole and garnet (Fig. 5B). The proportion of garnet (5–20%) is significantly lower in garnet diorites than in garnet granites (up to 50%), and the latter also show stronger overall signs of deformation and shearing. The majority of the amphiboles are hornblende, but some samples also contain ortohoamphibole in connection with hornblende agglomerates and garnet.

In the mineralised samples the reaction in which garnet replaces biotite and hornblende, either completely or partially, is readily observable. Garnet-bearing samples also contain small amounts of sericite and chlorite, but these features are typical for all rocks in the area and unlikely to be connected with mineralisation processes. The same applies for the potassic alteration observed in some of the samples. Locally, garnet has been replaced by ortoamph ibole+quartz+plagioclase (in garnet diorites), and in one sample, garnet has been replaced by carbonate minerals and pyrite.

4.3 Mineral chemistry

Most of the analysed garnet grains are compositionally almandine rich (X_{Fe}=0.80–0.85), containing variable amounts of other end members (Table 2): pyrope (X_{Mg} = 0.01–0.07), grossular (X_{Ca} = 0.02–0.06) and spessartine (X_{Mn} = 0.04–0.15). In some analysed spots, both grossular and spessartine end members exceed 20%. These spots are from the rims of garnet in two samples (from Road cut and N4322014R1) and from the core in a garnet diorite sample from N4322014R1. However, as the number of analysed spots (18 spots from 8 samples) is limited, evaluation of possible zonings or differences between mineralised localities is not possible. Some of the analysed garnet grains also contain traces of ZnO (≤0.24%) and PbO (≤0.10%).

Compositionally, the gahnite grains form a homogeneous group (Table 2) varying from $Zn_{0.58}Fe_{0.38}Mg_{0.04}Al_2O_4$ to $Zn_{0.72}Fe_{0.25}Mg_{0.03}Al_2O_4$.

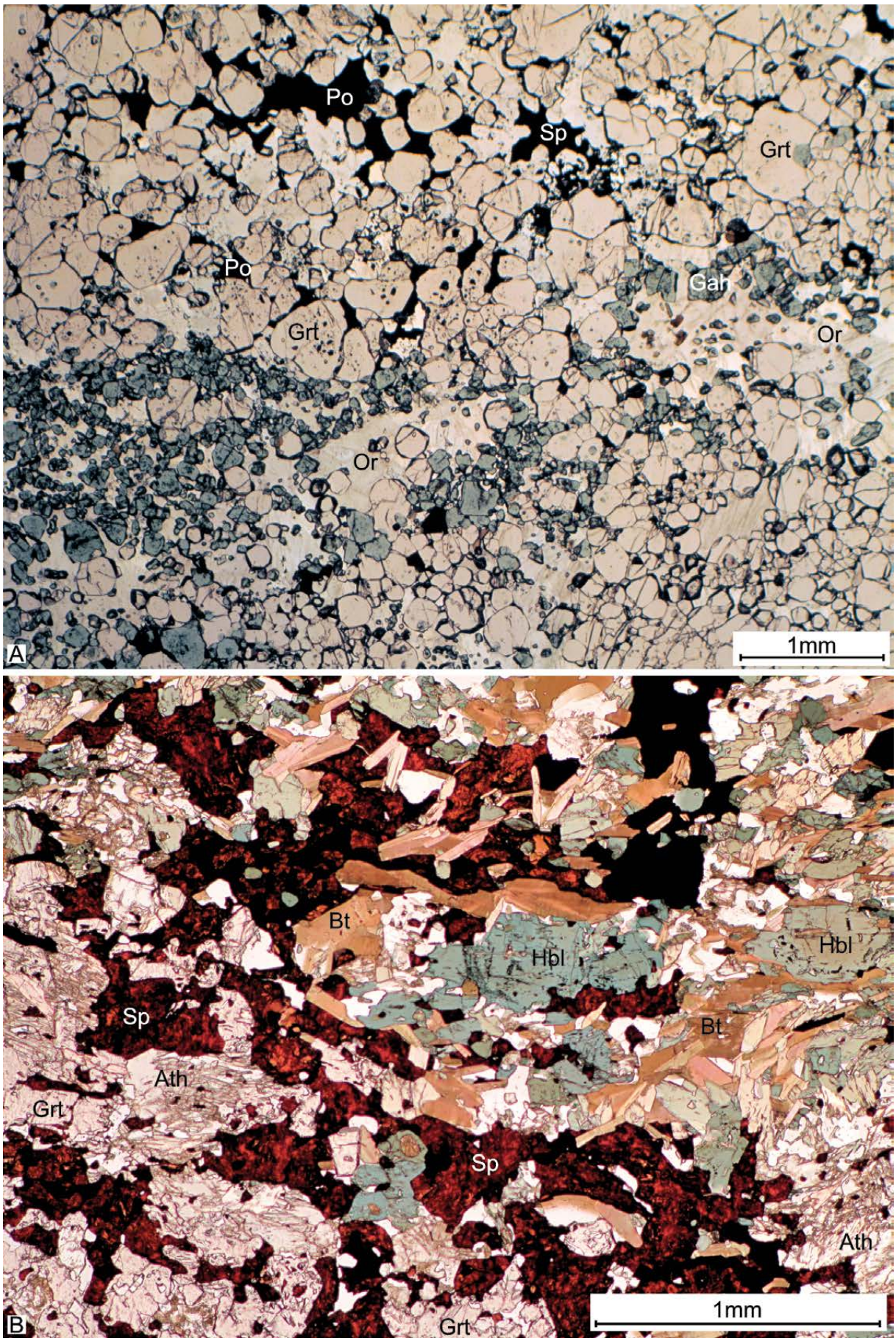

Fig. 5. A) Garnet granite from drill hole N4322014R2. B) Garnet diorite from drill hole N4322014R1. Grt = garnet, Bt = biotite, Hbl = hornblende, Ath = antophyllite, Sp = sphalerite, Or = orthoclase, Gah = gahnite, Po = pyrrhotite.

Table 2. Representative gahnite, garnet and K-feldspar analyses from Suolikko.

	Gahnite			Garnet			K-feldspar		
Sample	**N4322014R1 17.60 Garnet diorite**	**N4322014R2 66.35 Garnet granite**		**N4322014R1 17.60 Garnet diorite**	**N4322014R2 59.80 Garnet granite**	**TOS$-2013-4.3 Garnet granite**	**N4322014R1 56.40 Porphyritic granite**	**PIM$-2015-11.3 Amazonite granite**	**N4322014R2 63.30 Amazonite granite**
SiO_2 wt.-%	b.d.l.	0.02		37.81	37.03	37.47	64.77	64.10	63.67
TiO_2	0.01	b.d.l.		0.02	0.04	0.05	b.d.l.	0.02	b.d.l.
FeO	12.45	12.58		26.22	36.75	33.49	0.08	b.d.l.	0.08
MgO	0.81	0.68		0.72	0.98	0.74	b.d.l.	b.d.l.	b.d.l.
MnO	0.18	0.13		6.60	4.05	5.70	0.05	b.d.l.	0.02
CaO	b.d.l.	b.d.l.		7.76	1.31	1.94	0.02	b.d.l.	b.d.l.
Na_2O	0.93	0.64		b.d.l.	0.01	b.d.l.	1.61	0.51	1.58
ZnO	31.75	30.40		0.09	b.d.l.	0.12	0.21	0.23	0.23
K_2O	0.03	0.01		b.d.l.	b.d.l.	b.d.l.	15.13	16.17	14.55
BaO	b.d.l.	0.02		b.d.l.	b.d.l.	b.d.l.	0.16	0.08	0.18
Al_2O_3	57.68	58.94		20.97	21.55	21.34	18.31	18.33	18.48
Cr_2O_3	b.d.l.	0.02		b.d.l.	b.d.l.	0.02	0.03	0.02	b.d.l.
PbO	b.d.l.	0.05		b.d.l.	0.10	0.03	0.06	0.42	1.67
Total	103.83	103.50		100.18	101.83	100.89	100.40	99.89	100.45
Si p.f.u.	0.00	0.00		3.03	2.98	3.02	2.99	2.99	2.97
Al	1.97	2.00		1.98	2.04	2.03	0.99	1.01	1.02
Fe	0.30	0.30		1.76	2.47	2.26	0.00	0.00	0.00
Mg	0.04	0.03		0.09	0.12	0.09	0.00	0.00	0.00
Mn	0.00	0.00		0.45	0.28	0.39	0.00	0.00	0.00
Ca	0.00	0.00		0.67	0.11	0.17	0.00	0.00	0.00
Na	0.05	0.04		0.00	0.00	0.00	0.14	0.05	0.14
Zn	0.68	0.65		0.01	0.00	0.01	0.01	0.01	0.01
Cr	0.00	0.00		0.00	0.00	0.00	0.00	0.00	0.00
Pb	0.00	0.00		0.00	0.00	0.00	0.00	0.01	0.02
Ba	0.00	0.00		0.00	0.00	0.00	0.00	0.00	0.00
K	0.00	0.00		0.00	0.00	0.00	0.89	0.96	0.87
b.d.l. = below detection limit			Alm	59.4	83.0	77.8	Or 86.0	95.5	85.8
p.f.u. = per formula unit			Prp	2.9	3.9	3.1	Ab 13.9	4.5	14.2
			Sps	15.1	9.3	13.4	An 0.1	0.0	0.0
			Grs	22.5	3.8	5.8			

The zoning readily observable under an optical microscope (dark core, light rim) does not correlate with the compositions.

Analysed K-feldspars included both amazonite (12 spots) and the normal type for reference (2 spots). The concentration of PbO varied from 0.06 to 1.67% (Table 2, Electronic Appendix), the lowest values (which are also elevated) being from pink K-feldspar. The highest values (PbO = 1.28–1.67%) were from a mineralised garnet granite from drill hole N4322014R2. Both microcline and orthoclase contained elevated PbO concentrations and, at least with the current data set, no clear zoning patterns could be identified. In addition to Pb, most of the analysed K-feldspars also contained Zn (ZnO = 0.17–0.40%).

Out of the analysed sulphides (Table 3, Electronic Appendix), galena contained <1% of cations other than Pb. In addition to Cu and Fe, some of the chalcopyrites contained up to 1% of As and Hg. In addition to Zn (51–62%) and Fe (3–12%), some of the sphalerites contained significant amounts of Hg (<2.6%) and Cd (<3.9%), and traces of Mn, Co and Cu. The iron rich composition of the sphalerites indicates relatively high temperatures (Scott & Barnes 1976). The only cation other than Fe present in significant amounts in pyrite and pyrrhotite is Hg (<0.8%) in the latter. Silver was detected in some of the sphalerites and chalcopyrite with concentrations of up to 500 ppm, an outlier in this aspect being one covellite grain from a sample from Road cut that contained 6930 ppm of Ag.

Table 3. Representative sulphide analyses from Suolikko.

	Chalcopyrite		Galena			Sphalerite	
Sample	**N4322014R1 17.60 Garnet diorite**	**N4322014R2 59.80 Garnet granite**	**N4322014R2 59.80 Garnet granite**	**TOS$-2013-4.5 Garnet granite**	**TOS$-2013-4.5 Garnet granite**	**N4322014R1 17.60 Garnet diorite**	**TOS$-2013-4.3 Garnet granite**
S wt.-%	34.36	34.77	13.15	13.18	13.19	32.98	33.33
Fe	29.73	40.27	b.d.l.	0.10	0.14	8.05	3.74
Zn	0.06	0.41	b.d.l.	0.24	0.13	55.60	61.60
Pb	b.d.l.	b.d.l.	86.22	85.60	86.64	b.d.l.	b.d.l.
Cu	33.57	22.58	0.06	0.02	b.d.l.	b.d.l.	b.d.l.
Se	0.07	b.d.l.	b.d.l.	b.d.l.	b.d.l.	0.13	0.04
V	b.d.l.	b.d.l.	0.01	0.01	b.d.l.	b.d.l.	b.d.l.
As	b.d.l.	0.02	b.d.l.	b.d.l.	b.d.l.	b.d.l.	b.d.l.
Mn	b.d.l.	b.d.l.	0.03	0.03	b.d.l.	0.06	b.d.l.
Bi	b.d.l.	b.d.l.	b.d.l.	b.d.l.	b.d.l.	b.d.l.	b.d.l.
Co	0.06	0.07	b.d.l.	b.d.l.	0.02	0.03	0.03
Ag	b.d.l.	0.02	b.d.l.	b.d.l.	b.d.l.	0.02	b.d.l.
Hg	b.d.l.	0.86	b.d.l.	b.d.l.	b.d.l.	0.27	0.27
Ni	b.d.l.	b.d.l.	0.05	b.d.l.	0.05	b.d.l.	0.05
Cd	0.03	0.02	0.16	0.15	0.11	1.17	0.70
Sb	b.d.l.	b.d.l.	b.d.l.	b.d.l.	b.d.l.	b.d.l.	0.05
Ti	b.d.l.	b.d.l.	0.01	0.03	b.d.l.	b.d.l.	b.d.l.
Total	97.88	99.02	99.69	99.36	100.29	98.29	99.81

b.d.l. = below detection limit

4.4 Whole-rock geochemistry

The porphyritic granites from the Suolikko area are chemically typical representatives of the Muurame granitoid lithodeme with respect to both the main and trace element composition (Table 4, Figs 5, 6). The differences between porphyritic and amazonite granites are subtle, the most significant ones being the higher Pb and Zn concentrations of the latter (Fig. 6F). Garnet granites, including the mineralised samples, display a lower level and wider spread in SiO_2 concentrations, and they are also enriched, for example, in FeOt, MnO, Zn and Pb with respect to the porphyritic granites. The amount of garnet correlates with the FeOt concentration. Garnet granites are also more strongly peraluminous than both amazonite and porphyritic granites, and display elevated MnO/FeOt ratios (Fig. 6E). Some of the garnet granite samples display lower Na_2O concentrations. The three granite types display certain differences in the REE pattern, although the overall shape of the distribution curves is similar, i.e. enrichment in LREE over HREE and a negative Eu anomaly. Concentrations of LREE are on average slightly higher in mineralised garnet granites than in amazonite granites, but with respect to HREE, the difference is more pronounced (Fig. 7). One of the mineralised garnet granite samples displays a distinctly differing HREE distribution pattern, i.e. Lu_N higher than Gd_N. The one amazonite granite sample analysed for REE has the lowest total REE concentrations. All granite types also display similar primitive mantle-normalised patterns with negative anomalies in Nb, Sr, P, Eu and Ti (Fig. 7).

The five diorite samples form two groups, one with high MgO and CaO and low TiO_2 and P_2O_5, and the other with the opposite pattern. Samples of the latter type have a plutonic appearance (Fig. 3B), whereas those of the first group are slightly finer-grained with subabyssal appearance. Both of these types display enrichment in LREE over HREE, but without a negative Eu anomaly. The garnet diorites form a coherent group, despite SiO_2 concentrations varying from 44 to 58%. In particular, the REE and trace element patterns are uniform and display patterns resembling those of the granites, not the diorite. Garnet diorites have lower MgO than the diorites, but the differences in the main elements are otherwise less pronounced. Especially noteworthy is the strong enrichment of garnet diorites in REE, particularly LREE (Fig. 7A) and Zr (624–824 ppm), compared to the diorites.

The four mineralised locations display differences in the relative proportions of Zn and Pb (Table 1). The mineralised section of drill core N4322014R1 is rich in Zn (≤1.5% in a 1-m sample), but only weakly enriched in Pb (≤0.1%). Samples from drill core N4322014R2 and Road cut contain approximately equal amounts, ca. 1%, of both Zn and Pb. In samples from East End, the concentrations of Zn and Pb are also equal, but only anomalous (≤0.1%). Concentrations of Cu are below 0.2% in all samples, but the ones from N4322014R2 are on average slightly more enriched than those from other locations. Variable enrichment in Ag can be observed at all four mineralised locations, the highest concentrations being in samples from drill hole N4322014R2 and Road cut, with up to 50 ppm in the latter. Concentrations of Ag display positive correlations with Pb and Cu. Enrichment in Sn is evident in all analysed samples, typical values being 20–100 ppm, and the highest concentrations of 800–900 ppm being from Road cut and drill hole N4322014R2 (Table 4, Electronic Appendix).

Table 4. Representative whole-rock analyses from Suolikko.

Sample	MAAH-2014-27.1	TOS$-2013-4.4	PIM$-2015-11.5	TOS$-2013-4.3	N4322014R2 60.00-61.00	N4322014R4 24.65-24.95	N4322014R1 16.00-17.00
Rock type	Porphyritic granite	Amazonite granite	Garnet granite	Garnet granite	Garnet granite	Diorite	Garnet diorite
	A2383	Road cut	East end	Road cut			
SiO	72.0	73.1	52.6	54.9	42.2	49.2	44.1
TiO	0.28	0.26	0.30	0.42	0.38	0.65	1.37
Al	14.40	13.60	18.90	17.60	19.10	15.40	17.50
FeOt	2.74	2.44	12.70	9.37	21.44	7.49	16.31
MnO	0.03	0.05	2.31	0.41	2.10	0.14	0.45
MgO	0.46	0.37	0.76	0.75	0.63	8.28	2.64
CaO	1.56	1.43	2.26	1.61	1.43	12.66	3.88
Na	3.22	3.27	3.68	3.17	1.92	1.93	3.45
K	4.76	4.81	4.50	6.79	2.42	0.83	2.79
P	0.07	0.08	0.11	0.13	0.08	0.07	0.19
Zn ppm	72	342	1070	8452	28980	123	15470
Pb	<20	453	1211	1489	7339	34	472
Cu	<20	<20	<20	630	1735	77	942
Ag	n.a.	0.21	0.54	2.55	24.31	0.22	3.09
Sn	<20	<20	133	53	814	26	66
S	80	184	282	10590	19090	1534	19210
Ba	446	502	379	484	271	165	442
Rb	180	140	112	249	104	28	127
Sr	110	112	96	131	45	437	341
Th	12.20	8.44	23.20	14.80	28.70	2.79	69.50
U	2.42	1.35	2.39	3.08	3.88	0.86	4.29
Hf	4.77	4.75	8.30	6.92	8.90	1.95	28.10
Zr	160	173	258	218	236	35	824
Nb	9.3	12.7	15.6	23.3	16.7	4.3	30.3
Ta	0.43	0.29	0.89	1.00	1.00	0.26	1.56
Y	26.2	15.2	254	48.6	84.6	15.2	48.9
Sc	9.2	7.2	26.7	14.2	16.3	54.0	31.0
V	20.5	16.7	26.2	22.7	31.3	221	131
Cr	<20	<20	<20	<20	<20	413	41
Co	<5	1.79	3.63	5.40	7.87	28.20	23.30
Ni	<20	<20	<20	<20	<20	63	<20
Ga	<20	21	29	28	50	<20	36
Cl	372	347	338	679	152	276	536
La	36.2	28.0	51.2	37.4	61.4	17.4	186.0
Ce	78.0	57.1	108.0	77.8	127.0	24.9	362.0
Pr	9.1	6.7	12.9	9.2	15.1	3.2	39.0
Nd	34.1	24.4	49.9	34.1	58.2	13.6	141.0
Sm	6.97	4.80	13.00	7.03	12.70	3.21	22.80
Eu	0.71	0.58	0.62	0.51	0.59	1.02	1.30
Gd	6.52	4.29	18.50	6.82	13.50	3.32	17.90
Tb	0.95	0.54	4.22	1.12	2.36	0.51	2.11
Dy	5.72	2.88	35.00	7.67	15.70	3.17	10.60
Ho	1.10	0.52	8.57	1.72	3.29	0.60	1.93
Er	3.10	1.42	30.70	5.54	10.10	1.72	5.72
Tm	0.38	0.18	4.90	0.85	1.48	0.24	0.83
Yb	2.46	1.11	35.00	5.68	9.86	1.55	5.74
Lu	0.33	0.17	5.07	0.84	1.45	0.23	0.93

n.a. = not analysed
<20 = below detection limit and the approriate limit

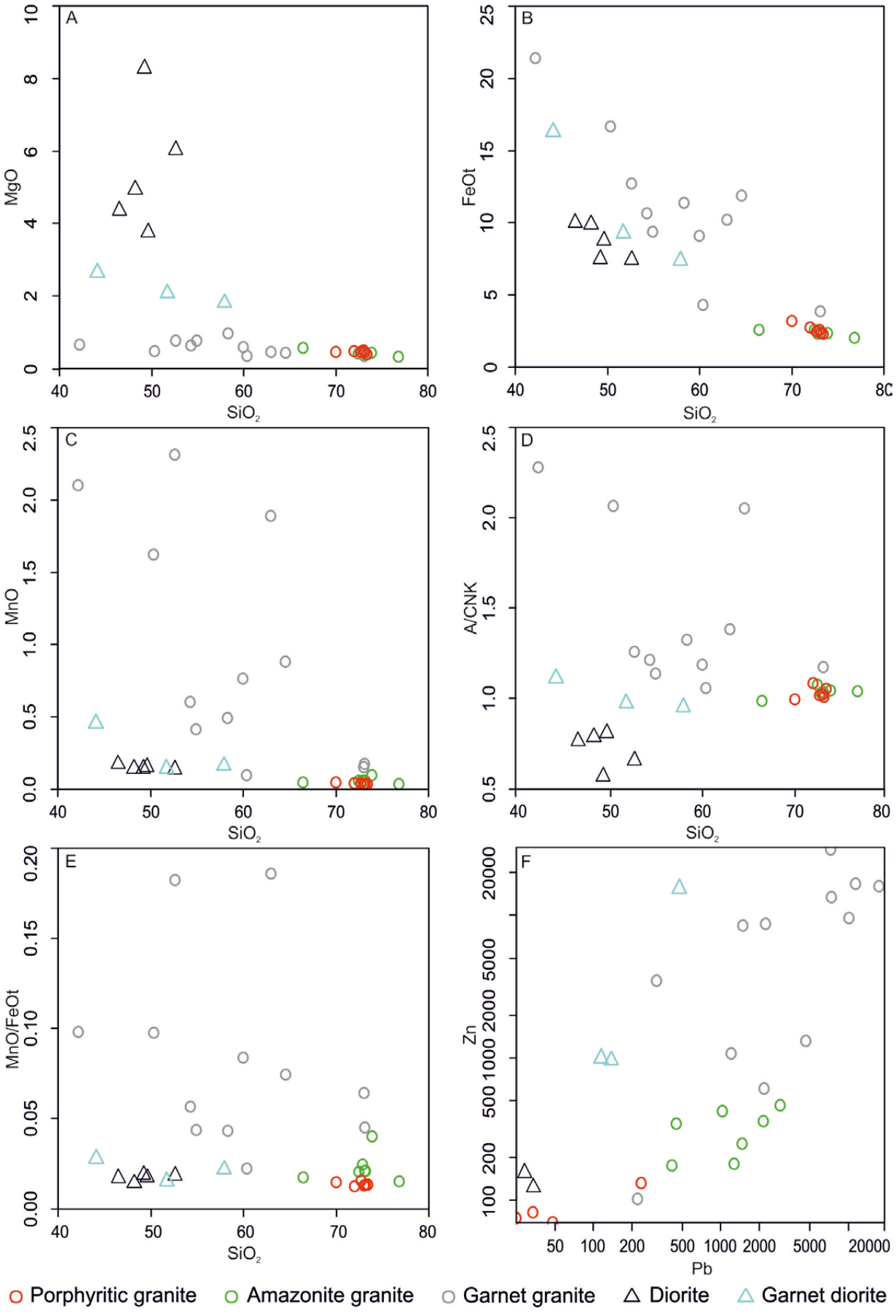

Fig. 6. Selected Harker diagrams (A–E) and a Zn vs. Pb plot (F) for samples from Suolikko. Samples labelled as garnet diorites and garnet granites represent the mineralisation. Note the use of a logarithmic scale in F.

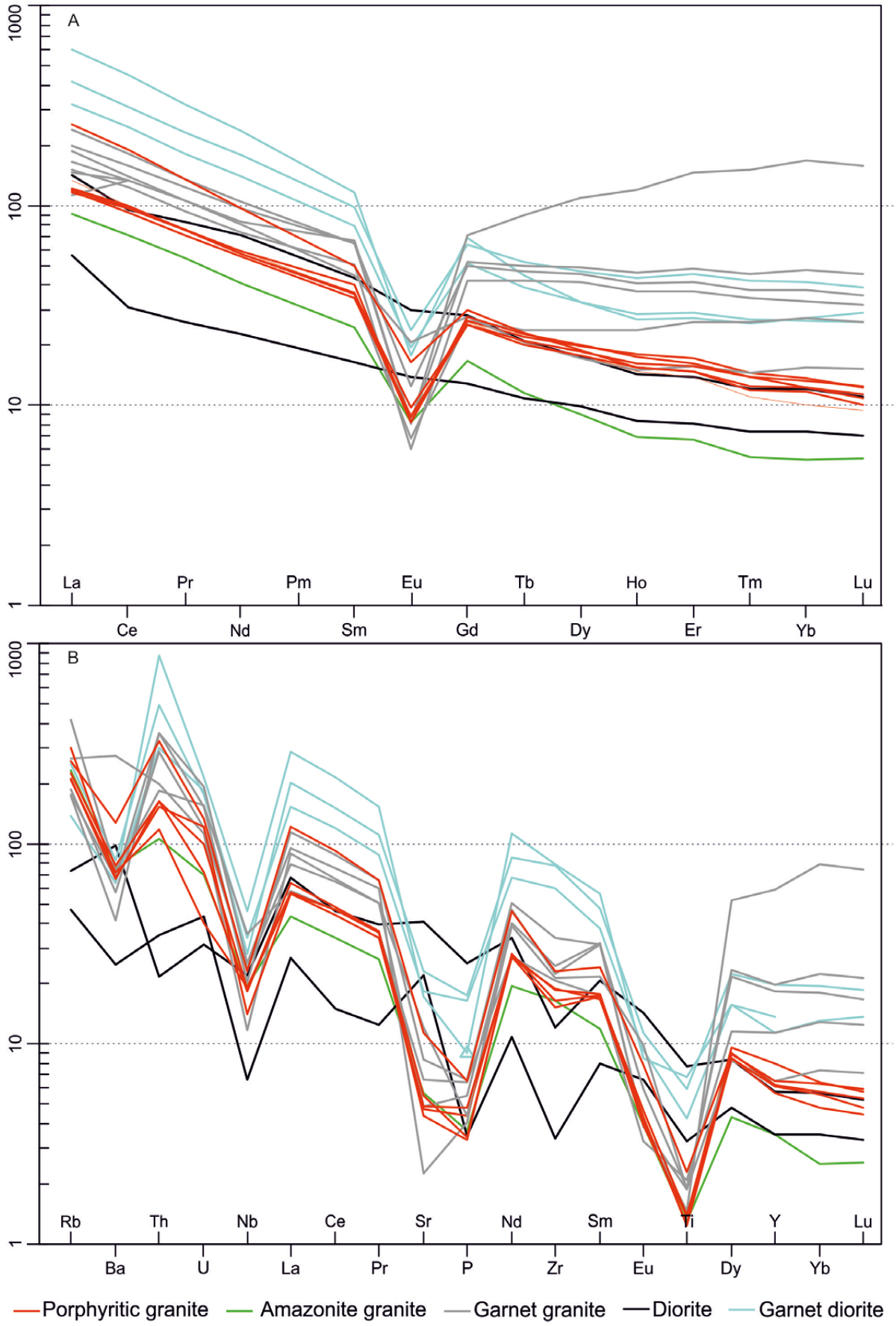

Fig. 7. Samples from Suolikko plotted on a chondrite-normalised REE diagram (A) and spider diagram normalised with primitive mantle (B). Chondrite values from Boynton (1984) and primitive mantle values from McDonough and Sun (1995).

4.5 Age determinations

4.5.1 Porphyritic granite, sample A2383

Porphyritic granite sampled 30 m north of Road cut represents the main rock type in the vicinity of the mineralisation. Separated zircon grains are euhedral and display oscillatory zoning typical for magmatic rocks . Inclusions are common, and some crystals have metamict rims. Altogether, 14 spots were analysed from 12 crystals (Electronic Appendix). Out of these, one analysis was discarded based on high common lead. All remaining 13 analyses are concordant and a concordia age of 1881 ± 4 Ma can be calculated (Fig. 8). We interpret this as the crystallisation age of this porphyritic granite sample.

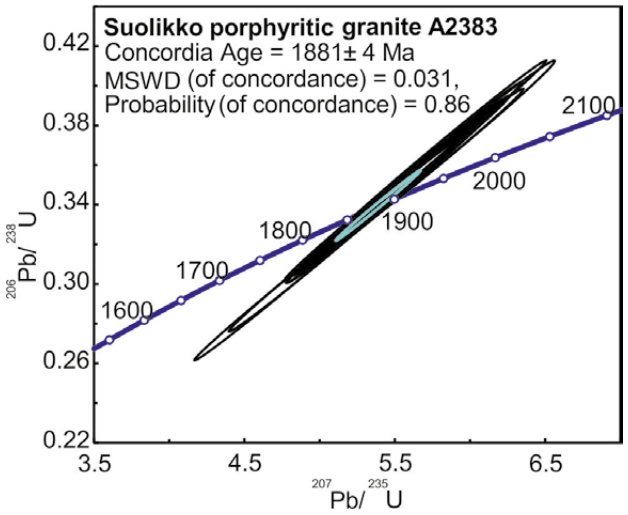

Fig. 8. Concordia diagram of the age determination sample A2383. All errors are drawn at the 2σ level.

4.5.2 Garnet diorite, sample A2462

Thin section N4322014R1 17.60 was used for *in situ* age determination. It is a weakly oriented garnet diorite with abundant pyrrhotite, sphalerite and gahnite. Zircon and monazite typically occur within the biotite mass as inclusions (Fig. 9). Based on the optical properties, zircon crystals form two populations: one population with well-developed zoning and normal interference colours and other with low interference colours, poorly developed zoning and more abundant metamict domains. In some crystals, low interference colours form a rim around "normal" zircon (Fig. 9A).

Altogether, 18 spots from 11 zircon grains were dated (Electronic Appendix); 14 of the analyses are concordant, one is normally discordant and three are reversely discordant (Fig. 10). The lead-lead ages of the concordant and reversely concordant zircon data vary from 1756 to 1876 Ma. The ages do not form distinct groups, but a continuum of ages. No correlation between zircon morphology and age was observed. Moreover, no connection between U or Th concentrations and age was observed.

Monazite is always surrounded by fine-grained alteration products and does not display internal structures (Fig. 9B). The U–Pb analyses on monazite are either concordant or reversely discordant and their $^{207}Pb/^{206}Pb$ ages ages vary from 1771 to 1880 Ma (11 spots from 5 monazite grains). The data form a bimodal population clustering at ca. 1790 and 1870 Ma (Fig. 10). Analyses belonging to

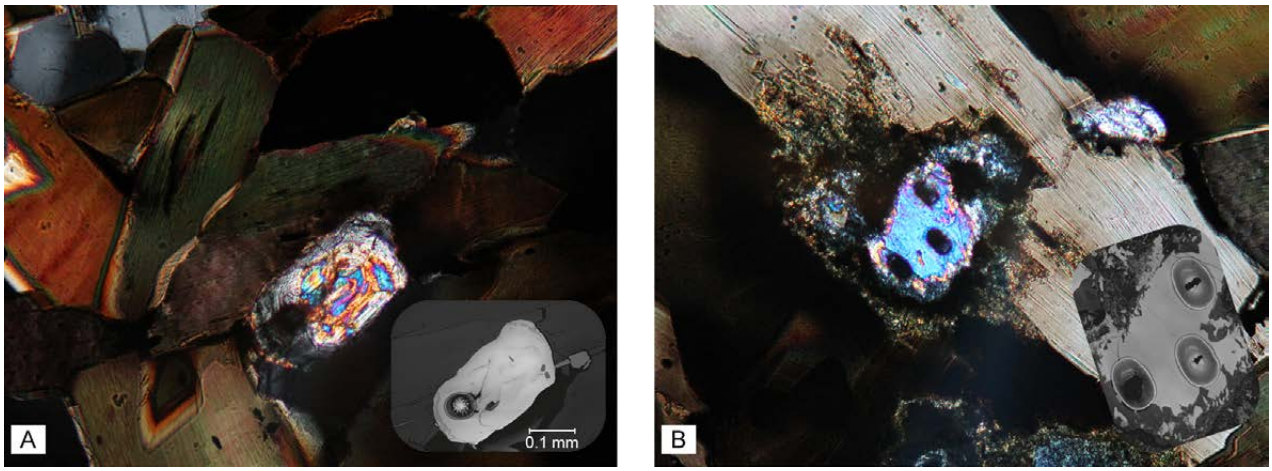

Fig. 9. Microscope images of dated minerals. A) Zircon with a core of typical and a rim of anomalously low interference colours and B) monazite crystal yielding ages of both age groups, although no internal structure can be observed. Insets display the same crystals in BSE images.

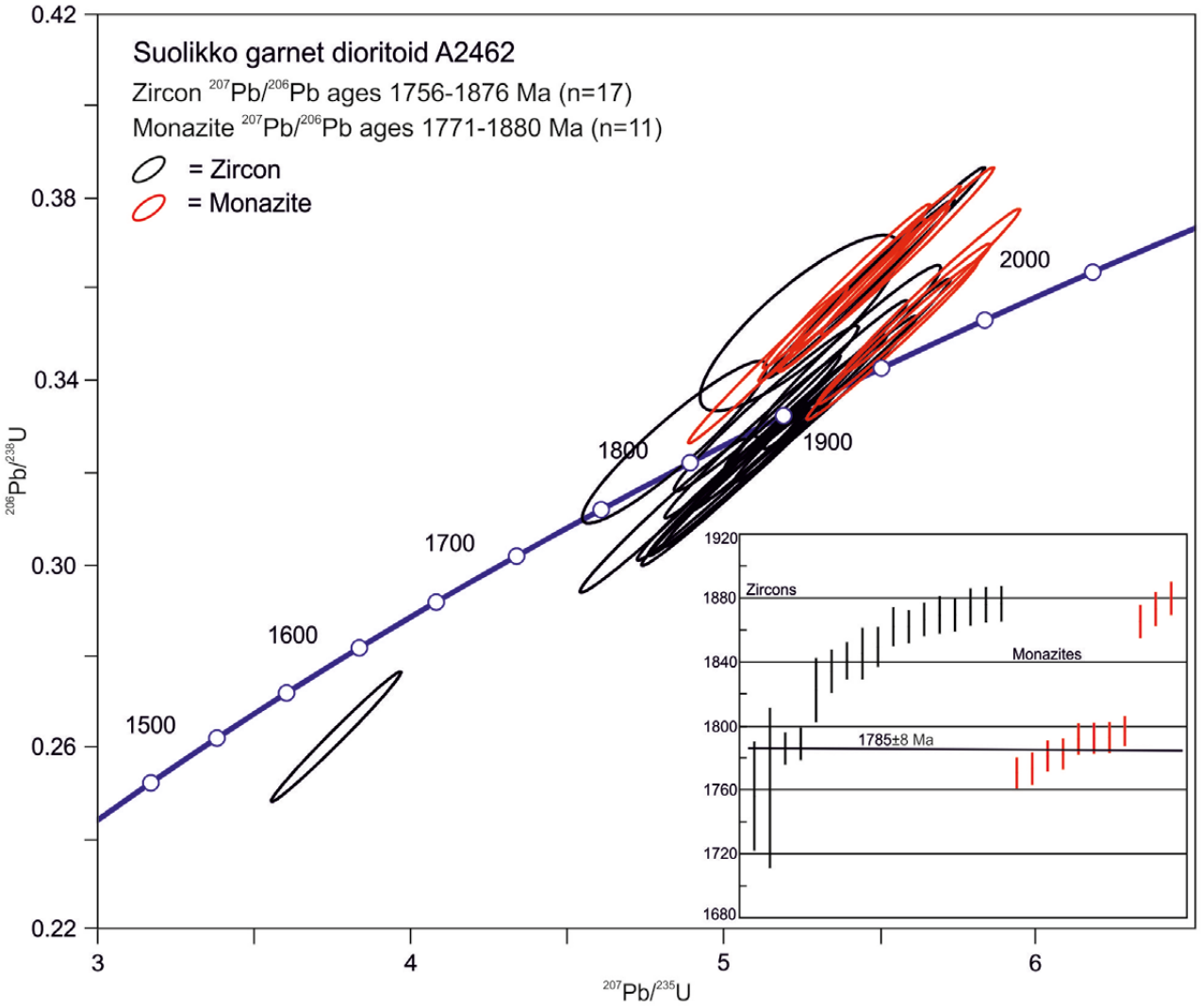

Fig. 10. Concordia diagram of the age determination sample A2462. Inset: $^{207}Pb/^{206}Pb$ ages of concordant or reversely concordant analyses and the weighted average of 1785 ± 8 Ma calculated using the younger age cluster of monazite analyses. All errors are drawn at the 2σ level.

the older group are poorer in U than the younger ones, being 701–863 ppm vs. 1624–3685 ppm, respectively. However, the populations cannot be distinguished optically or using back-scatter electron (BSE) images, and one of the analysed crystals provides ages falling into both groups (Fig. 9B). The weighted average of $^{207}Pb/^{206}Pb$ ages from the younger population is 1785 ± 8 Ma (n = 8).

Our interpretation is that the oldest ages close to 1880 Ma represent the original crystallisation age of the diorite and the younger monazite ages are correlated with a thermal event at 1785 Ma. The zircons of the sample also record this event as lead loss varying from partial to complete.

5 DISCUSSION

5.1 Geological setting

With respect to bedrock geology, the immediate surroundings of the mineralisation can be regarded as typical for the southeast CFGC. It mainly consists of porphyritic granitoids of the Muurame lithodeme. The age of sample A2383, 1881 ± 4 Ma, is also typical for this lithodeme (Heilimo et al. 2018). Also typical for both Suolikko and the CFGC in general are the granite dykes cross cutting the porphyritic granite

(Fig. 3A) belonging to the Oittila suite aged 1875 Ma. Based on cross-cutting relationships, these dykes are also younger than the main deformation phase of the porphyritic granite. The strike of the general schistosity (~105°) in the area coincides with the strike of the shear zone that the mineralisation is spatially connected to. Deformation in the shear zone has been mainly ductile in nature, only locally weaker signs of brittle deformation can be observed. Based these characteristics, the shear zone in Suolikko can be correlated with the large-scale shear zones of the CFGC, which have been active over an extended period of time and experienced both plastic and brittle deformation (Nironen 2003, Mikkola et al. 2018a).

5.2 Amazonite

The turquoise colour of amazonite is connected with the replacement of K^{+} and Si^{4+} with Pb^{2+} and Al^{3+}. The minimum Pb concentration required for an observable change in colour is ca. 60 ppm (Hofmeister & Rossman 1985). In addition to the Pb concentration of K-feldspar, the strength of the colour change also depends on the charge and location of the Pb ion in the crystal structure (ibid.), the former being affected by radioactive radiation and the presence of water. The lack of a correlation between the colour and Pb concentration is also observable in Suolikko, as the amazonites with the strongest colours contain "only" 0.4% of Pb, whereas the crystals richest in lead (~1.5% of Pb) are only weakly coloured. In Suolikko, the lowest Pb concentration in amazonites is ca. 150 ppm, but "normal" K-feldspars can contain up to 500 ppm of lead. The close chemical and petrographical resemblance, as well as the gradual contacts between porphyritic and amazonite granites indicates that the latter is a metasomatically altered variant of the former. The timing of this alteration cannot be constrained, but the proximity to the mineralisation favours contemporary formation of both.

5.3 Garnet-bearing rocks

Based on the observed compositional continuum from garnet granites via amazonite granites to porphyritic granites, similar trace element patterns and gradual contacts between them, we interpret that the three rock types share a common origin and the mineralisation is a product of intensive post-crystallisation alteration. The observed clear change in the MnO/FeOt ratio between porphyritic granites and garnet granites could indicate that the garnet crystallised during alteration, as crystallising garnet favours Mn over Fe (Kontak & Corey 1988). The anomalous Zn and Pb concentrations observed in garnet indicate that the whole-rock enrichment in these elements was either coeval or predated the garnet crystallization. As the garnet grains have not experienced significant deformation during or after crystallisation, they postdate the main deformation phase along the shear zone. Although the mineralisation and shear zone are spatially closely associated, the amount of garnet and grade of the mineralisation do not correlate with the strength of deformation. Based on the above it seems that the shear zone predating the alteration and garnet crystallisation provided pathways for fluids, which in addition to Zn and Pb enriched the mineralisation in MnO, FeOt, Al_2O_3 and depleted it in SiO_2.

As the peak of the regional metamorphism (ca. 1875 Ma) is coeval or predates the ductile deformation phase along the shear zones parallel to the one in Suolikko (e.g. Nironen 2017, Mikkola et al. 2018a), the garnet crystallisation postdating the main ductile deformation must also postdate the peak of the regional metamorphism. However it is possible that the garnet crystallised, at least partially, during the regional late Svecofennian ~1.8 Ga metamorphism (e.g. Ahtonen et al. 2007, Saalmann et al. 2009, Kurhila et al. 2011). This is especially true for samples with limited amounts of volatile bearing minerals (e.g. Fig. 5A), which are unlike to represent assemblages crystallised during hydrothermal alteration.

The three mineralised garnet diorite samples form a homogeneous group that especially with respect to trace element patterns deviates from other diorites, e.g. higher REE and Zr. Among the main elements, the differences are more difficult to deduct, but the garnet diorites have lower MgO and slightly higher FeOt concentrations than the diorites, resulting in significantly lower Mg# (22–30 vs. 40–66) in the former. In the MnO/FeOt ratio, the diorites and garnet diorites do not

deviate. The elevated REE and Zr concentrations of the garnet diorites could in theory be linked to the mineralising alteration, especially as the garnet granites display elevated REE concentrations compared to the porphyritic granites. Additionally, the HREE pattern of one of the garnet granites clearly deviates from the normal gently sloping magmatic pattern of the other samples. A problem with this explanation is that the garnet granites do not show enrichment in Zr (Fig. 7), which would be expected if Zr enrichment in garnet diorites resulted from metasomatic alteration. Similar Zr- and REE-rich diorites with low Mg# have been reported from the Istruala lithodeme (Virtanen & Heilimo 2018). Based on the above and the fact that Zr is regarded as immobile in most hydrothermal systems, the REE and especially Zr enrichment of garnet diorites is likely to be a primary feature. If this is the case garnet diorites are altered members of the Saarijärvi suite and not the Vaajakoski lithodeme that the sampled diorites belong to.

Based on the limited number of compositional analyses from garnet, some of the samples appear to have spessartine- and grossular-richer rims over almandine-richer cores. This could indicate decreasing temperature and higher pressure during the crystallisation of garnet (Tracy 1982). The two textural modes of garnet, small euhedral (Fig. 5A) and larger poikiloblastic anhedral to subhedral crystals (Fig. 5B), have a number of possible explanations. It is possible that the euhedral crystals represent the early stages of garnet formation when conditions favoured nucleation over growth. The anhedral crystals could be a result of continued growth resulting in the intergrowth of separate crystals and capture of interstage minerals as inclusions. This explanation is supported by the observation that the larger garnet grains are typically intergrowths of originally separate crystals. As small euhedral crystals are typical for garnet granites and larger anhedral crystals for garnet diorites, it is also possible that the differences in garnet texture only reflect differences in the original host rock textures or differences in reaction kinematics caused by differing compositions.

5.4 Gahnite

Gahnite can be formed in several geological processes: metamorphism of Zn oxides (Segnit 1962), desulphurisation of sphalerite (Spry 2000), crystallisation from metamorphic-hydrothermal fluids (Wall 1977) or the breakdown of Zn-bearing silicates, e.g. biotite (Dietworst 1980). In Suolikko, gahnite is most typically associated with garnet and biotite, but the sheer volume of gahnite (<25%) with ZnO ~30 wt% proves that the silicate breakdown reactions are not important. Furthermore, the amount of chlorite, which should be formed in the biotite breakdown reaction, is limited in Suolikko.

In samples from drill core N4322014R1, the gahnite often has sphalerite cores and the gahnite itself contains numerous inclusions. This texture is most readily explained by desulphurisation of sphalerite. Especially in samples from N4322014R2, gahnite is not spatially associated with garnet, biotite or sphalerite, but instead form aggregates of small crystals. This could indicate crystallisation directly from the fluid, although some of the grains contain abundant small inclusions, too small for reliable indentification, and could be a result of the complete desulphurisation of sphalerite.

On the classification diagram of Heimann and Spry (2005), the gahnites from Suolikko have compositions typical for either metamorphosed massive sulphide ores or granite pegmatites (see Kallio 2017 for the diagram). The first option is ruled out by the observation that the mineralised garnet granites are altered granites and not metamorphosed sulphide ores. This is also supported by the lead isotope composition of the mineralisation, which clearly deviates from the sulphide ores in central Finland and is instead characteristic of the CFGC (Vaasjoki 1981). It is also obvious that the gahnite in Suolikko did not crystallise from a pegmatite, but a hydrothermal system driven by and fluids released from crystallising granitic magma could be responsible for the mineralisation process. The observed desulphurisation of sphalerite suggests a reduction in sulphur fugacity during mineralisation or later metamorphism.

5.5 Sulphides

The majority of the sulphides are located as interstatial dissemination (commonly pyrrhotite and chalcopyrite) or as vein-like pockets (commonly sphalerite), some of which intrude into garnet. In some cases, sulphides are present as inclusions in larger garnet grainss. Based on the above, it appears that sulphides crystallised both during and following the main phase of garnet growth. Sphalerite typically contains pyrrhotite and chalcopyrite inclusions. The dominance of pyrrhotite over pyrite and the coexistence of garnet and sphalerite indicate low sulphur and oxygen fugacity during the main phase of the mineralisation (Spry & Scott 1986). Based on locally observable late-stage alteration of pyrrhotite to pyrite, sulphur fugacity rose at some point during the cooling of the system, observation which is contrary to the desulphurisation of sphalerite. Differences in the distribution of Pb and Zn could be linked to the composition of the host rocks; as amazonite contains a significant proportion of Pb, it would have been more readily absorbed by granite protoliths than the diorites lacking K-feldspar.

5.6 Timing of mineralisation and fluid source

Based on sample A2383, the age of the porphyritic granites hosting the Suolikko mineralisation, and thus the maximum age of the mineralisation, is 1881 ± 4 Ma. The ages obtained from zircons and monazites of the mineralised garnet diorite A2462 also indicate that it crystallised at approximately the same time. Both minerals were affected by thermal overprint at 1780–1790 Ma, and our interpretation is that this is the age of the mineralisation event. Alternatively it could be interpreted as the age of the younger ca. 1.8 Ga regional metamorphism. But as sample A2383 only 30 meters from the mineralisation and none of the other age determination samples from areas surrounding Suolikko have provided any indications of this late overprint (Mikkola et al. 2018b, c, Heilimo unpublished data), it is in our opinion an unlikely option. In addition to widespread metamorphism (Ahtonen et al. 2007, Saalmann et al. 2009, Kurhila et al. 2011) the 1790–1780 Ma age coincides also with the ages postorogenic granites and pegmatites known south (Eklund et al. 1998), west (Alviola et al. 2001) and north of the CFGC (Kontinen et al. 2013), but not from the CFGC itself. The nearly complete resetting of the monazite ages, or crystallisation of new monazite, and partial resetting of zircon ages suggests relatively high temperatures. As Sn mineralisations are often associated with hydrothermal systems related to granite intrusions (e.g. Reed 1982), the observed enrichment in it can be taken as tentative evidence for a hydrothermal system associated with late intrusion belonging to the group of postorogenic granites.

Although the postorogenic granite as a fluid source is rather speculative the other options contain similar or greater challenges. For example, fluid flow during active movement along the shear zone is not plausible, as according to the observations, mineralisation occurred after ductile deformation phase(s) and before local late brittle deformation. A third possible explanation of metamorphic fluid being released from deeper in the crust and conveyed through an existing weakness zone is problematic, as similar shear and weakness zones exist over a wide area, but only a limited number of mineralisations related to them have been reported. One exception is the Muittari Zn–Pb mineralisation 75 km northwest of Suolikko (Sipilä 1985). However, in the Muittari area, the mineralisation is related to propylitic alteration and the ore minerals mainly occur as narrow dykes, thus differing from the Suolikko mineralisation.

The mineralisations from the Hiekkapohja area 30 km north of Suolikko display certain resemblance in mineralisation style with the here studied mineralisation (Halonen 2015, Heilimo et al. 2017). Both localities display variable enrichment in Zn, Pb and Ag. The Hiekkapohja area also displays strong enrichment in As, a feature missing from Suolikko. Other differentiating factors are the lack of gahnite in Hiekkapohja area and significantly lower proportion of pyrite and pyrrhotite in mineralised samples from Suolikko. Also the interpreted ages of the two localities differ significantly as the age of the mineralisations in Hiekkapohja has been interpreted as 1875 Ma (ibid.). In the Hiekkapohja area, the mineralising fluid originated from crystallising granitoid magma, which reduced the susceptibility of the area of country rocks, producing a clearly detectable aeromagnetic low in the area surrounding the mineralisations (ibid.). In the Suolikko area, no such aeromagnetic low can be identified. However,

the observed similarities between Suolikko and Hiekkapohja and open questions related to both warrant further studies to more precisely define the timing of the mineralisation processes and especially the fluid sources in order to more definitively determine the similarities between the two localities.

6 SUMMARY AND CONCLUSIONS

The Suolikko Pb–Zn mineralisation is less than 10 m wide and possibly up to 400 m long. It is spatially associated with a shear zone that is interpreted to predate the mineralisation event.

Sulphides are hosted by garnet granites and garnet diorites. The mineralisation is typically surrounded by a few metres wide halo of porphyritic amazonite granite.

The main sulphides of the mineralisation are sphalerite, chalcopyrite and galena. Locally, over 50% of Zn and Pb is hosted by gahnite and amazonite, respectively.

We interpret that the host rocks of the mineralisation crystallised ca. 1880 Ma ago. Based on the obtained monazite ages, the mineralisation event most likely occurred at ~1785 Ma.

The mineralisation was likely caused by alteration related to fluid flow. Local alteration of sphalerite to gahnite indicates changes in sulphur fugacity. We tentatively suggest magmatic fluid released from crystallising post-tectonic granite as the cause of the mineralisation.

7 ACKNOWLEDGEMENTS

Jouko Ranua and Mauri Luukkonen are acknowledged for the drill core photos. Riitta Turunen and Ritva Jokisaari finalised the figures. The staff of the GTK's isotope laboratory are thanked for sample preparation and keeping the machines running. Reviews by Drs Tero Niiranen, Hannu Makkonen and an anonymous reviewer helped in improving the manuscript.

REFERENCES

Ahtonen, N., Hölttä, P. & Huhma, H. 2007. Intracratonic Palaeoproterozoic granitoids in northern Finland: prolonged and episodic crustal melting events revealed by Nd isotopes and U-Pb ages on zircon. Bulletin of the Geological Society of Finland 79, 143–174.

Alviola, R., Mänttäri, R., Mäkitie, H. & Vaasjoki, M. 2001. Svecofennian rare-element granitic pegmatites of the Ostrobothnia region, western Finland; their metamorphic environment and time of intrusion. In: Mäkitie, H. (ed.) Svecofennian granitic pegmatites (1.86–1.79 Ga) and quartz monzonite (1.87 Ga), and their metamorphic environment in the Seinäjoki region, western Finland. Geological Survey of Finland, Special Paper 30, 9–29. Available at: http://tupa.gtk.fi/julkaisu/specialpaper/sp_030.pdf

Boynton, W. V. 1984. Cosmochemistry of the rare earth elements; meteorite studies. In: Henderson, P. (ed.) Rare earth element geochemistry. Amsterdam: Elsevier, 63–114.

Connonly, J. A. D. 2005. Computation of phase equilibria by linear programming: A tool for geodynamic modeling and its application to subduction zone decarbonation. Earth and Planetary Science Letters 236, 524–541.

Dietworst, J. L. 1980. Biotite breakdown and the formation of gahnite in metapelitic rocks from Kemio, Southwest Finland. Contributions to Mineralogy and Petrology 75, 327–337.

Eilu, P., Ahtola, T., Äikäs, O., Halkoaho, T., Heikura, P., Hulkki, H., Iljina, M., Juopperi, H., Karinen, T., Kärkkäinen, N., Konnunaho, J., Kontinen, A., Kontoniemi, O., Korkiakoski, E., Korsakova, M., Kuivasaari, T., Kyläkoski, M., Makkonen, H., Niiranen, T., Nikander, J., Nykänen, V., Perdahl, J.-A., Pohjolainen, E., Räsänen, J., Sorjonen-Ward, P., Tiainen, M., Tontti, M., Torppa, A. & Västi, K. 2012. Metallogenic areas in Finland. In: Eilu, P. (ed.) Mineral deposits and metallogeny of Fennoscandia. Geological Survey of Finland, Special Paper 53, 207–342. Available at: http://tupa.gtk.fi/julkaisu/specialpaper/sp_053.pdf

Eklund, O., Konopelko, D., Rutanen, H., Fröjdö, S. & Shebanov, A. D. 1998. 1.8 Ga Svecofennian post-collisional shoshonitic magmatism in the Fennoscandian Shield. Lithos 45, 87–108.

Halonen, S. 2015. Keski-Suomen granitoidikompleksin malmiviitteet Hiekkapohjan alueella. Unpublished master's thesis, University of Oulu, Oulu Mining

School. 100 p. Available at: http://jultika.oulu.fi/files/nbnfioulu-201511242172.pdf

Hartikainen, J. T. 1978. Raportti Korpilahden ympäristön malmitutkimuksista kesällä 1978. Geological Survey of Finland, archive report M17/JTH-78/1. 3 p. (in Finnish)

Heilimo, E., Ahven, M. & Mikkola, P. 2018. Geochemical characteristics of the plutonic rock units present at the southeastern boundary of the Central Finland Granitoid Complex. In: Mikkola, P., Hölttä, P. & Käpyaho, A. (eds) Development of the Paleoproterozoic Svecofennian orogeny: new constraints from the southeastern boundary of the Central Finland Granitoid Complex. Geological Survey of Finland, Bulletin 407. (this volume). Available at: https://doi.org/10.30440/bt407.6

Heilimo, E., Mikkola, P., Niemi, S., Luukas, J. & Halonen, S. 2017. Hiekkapohja ore showings in Paleoproterozoic Central Finland Granitoid Complex – a hydrothermal system? Proceedings of the 14th SGA Biennial Meeting, 20–23 August 2017, Québec City, Canada, 359–362.

Heimann, A. & Spry, P. G. 2005. Zincian spinel associated with metamorphosed Proterozoic base-metal sulfide occurrences, Colorado: A Re-Evaluation of gahnite composition as a guide in exploration. Canadian Mineralogist 43, 601–622.

Hofmeister, A. M. & Rossman, G. R. 1985. A spectroscopic study of irradiation coloring of amazonite: structurally hydrous Pb-bearing feldspar. American Mineralogist 70, 794–804.

Janoušek, V., Farrow, C. M. & Erban, V. 2006. Interpretation of whole-rock geochemical data in igneous geochemistry: introducing Geochemical Data Toolkit (GCDkit). Journal of Petrology 47, 1255–1259.

Kallio, V. 2017. Muuramen Suolikon Pb-Zn-mineralisaation ja sen sivukivien geologia, mineralogia ja geokemia Keski-Suomen granitoidikompleksin kaakkoisosassa. Unpublished master's thesis, University of Oulu, Oulu Mining School. 136 p. (in Finnish). Available at: http://jultika.oulu.fi/files/nbnfioulu-201704251578.pdf

Kontak, D. J. & Corey, M. 1988. Metasomatic origin of spessartine-rich garnet in the South Mountain Batholith, Nova Scotia. Canadian Mineralogist 26, 315–334.

Kontinen, A., Huhma, H., Lahaye, Y. & O´Brien, H. 2013. New U-Pb zircon age, Sm-Nd isotope and geochemical data on Proterozoic granitic rocks in the area west of the Oulunjärvi Lake, Central Finland. Geological Survey of Finland, Report of Investigation 198. 70–74. Available at: http://tupa.gtk.fi/julkaisu/tutkimusraportti/tr_198.pdf

Kurhila, M., Mänttäri, I., Vaasjoki, M., Rämö, O. T. & Nironen, M. 2011. U–Pb Geochronological constraints of the late Svecofennian leucogranites of southern Finland. Precambrian Research 190, 1–24.

McDonough, W. F. & Sun, S.-S. 1995. Composition of the Earth. Chemical Geology 120, 223–253.

Mikkola, P., Heilimo, E., Aatos, S., Ahven, M., Eskelinen, J., Halonen, S., Hartikainen, A., Kallio, V., Kousa, J., Luukas, J., Makkonen, H., Mönkäre, K., Niemi, S., Nousiainen, M., Romu, I. & Solismaa, S. 2016. Jyväskylän seudun kallioperä. Summary: Bedrock of the Jyväskylä area. Geological Survey of Finland, Report of Investigation 227. 95 p., 6 apps. Available at: http://tupa.gtk.fi/julkaisu/tutkimusraportti/tr_227.pdf

Mikkola, P., Heilimo, E., Luukas, J., Kousa, J., Aatos, S., Makkonen, H., Niemi, S., Nousiainen, M., Ahven, M., Romu, I. & Hokka, J. 2018a. Geological evolution and structure along the southeastern border of the Central Finland Granitoid Complex. In: Mikkola, P., Hölttä, P. & Käpyaho, A. (eds) Development of the Paleoproterozoic Svecofennian orogeny: new constraints from the southeastern boundary of the Central Finland Granitoid Complex. Geological Survey of Finland, Bulletin 407. (this volume). Available at: https://doi.org/10.30440/bt407.1

Mikkola, P., Huhma, H., Romu, I. & Kousa, J. 2018b. Detrital zircon ages and geochemistry of the metasedimentary rocks along the southeastern boundary of the Central Finland Granitoid Complex. In: Mikkola, P., Hölttä, P. & Käpyaho, A. (eds) Development of the Paleoproterozoic Svecofennian orogeny: new constraints from the southeastern boundary of the Central Finland Granitoid Complex. Geological Survey of Finland, Bulletin 407. (this volume). Available at: https://doi.org/10.30440/bt407.2

Nikander, J. 2004. Kansannäytteen käyntiraportti, näytteet 20044042/1&3. Geological Survey of Finland, archive report M13/3211/20044042. 3 p. (in Finnish)

Nikkilä, K., Mänttäri, I., Nironen, M., Eklund, O. & Korja, A. 2016. Three stages to form a large batholith after terrane accretion – An example from the Svecofennian orogen. Precambrian Research 281, 618 – 638.

Nironen, M. 2003. Keski-Suomen granitoidikompleksi, Karttaselitys. Summary: Central Finland Granitoid Complex – Explanation to a map. Geological Survey of Finland, Report of Investigation 157. 45 p. Available at: http://tupa.gtk.fi/julkaisu/tutkimusraportti/tr_157.pdf

Nironen, M. 2017. Guide to the Geological Map of Finland – Bedrock 1:1 000 000. In: Nironen, M. (ed.) Bedrock of Finland at the scale 1:1 000 000 – Major stratigraphic units, metamorphism and tectonic evolution. Geological Survey of Finland, Special Paper 60, 41–76. Available at: http://tupa.gtk.fi/julkaisu/specialpaper/sp_060.pdf

Nironen, M., Kousa, J., Luukas, J. & Lahtinen, R. (eds) 2016. Geological Map of Finland – Bedrock 1:1 000 000. Espoo: Geological Survey of Finland. Available at: http://tupa.gtk.fi/kartta/erikoiskartta/ek_097_300dpi.pdf

Oivanen, P. 1962. Selostus malmi- ja kansanaihetutkimuksista Korpilahdella ja Muuramessa v. 1961. Geological Survey of Finland, archive report M17/Kor,Mu-62. 8 p. (in Finnish)

Reed, B. L. 1982. Tin greisen model. In: Erickson, R. L. (ed.) Characteristics of mineral deposit occurrences. U.S. Geological Survey, Open-File Report 82-795, 55–61.

Saalmann, K., Mänttäri, I., Ruffet, G. & Whitehouse, M. J. 2009. Age and tectonic framework of structurally controlled Palaeoproterozoic gold mineralization in the Häme belt of southern Finland. Precambrian Research 174, 53–77.

Scott, S. D. & Barnes, H. L. 1971. Sphalerite geothermometry and geobarometry. Economic Geology 33, 653–669.

Segnit, E. R. 1962. Petrology of the zinc lode, New Broken Hill Consolidated Ltd., Broken Hill, New South Wales. Proceedings of The Australasian Institute of Mining and Metallurgy 199, 87–112.

Sipilä, E. 1985. Kupari-lyijy-sinkki- ja tina-aiheiden tutkimukset Saarijärven Muittarissa 1980–1984. Geological Survey of Finland, archive report M19/2244/85/1/10. 21 p., 26 app. (in Finnish). Available at: http://tupa.gtk.fi/raportti/arkisto/m19_2244_85_1_10.pdf

Spry, P. G. & Scott, S. D. 1986. The stability of zincian spinels in sulphide systems and their potential as exploration guides for metamorphosed massive sulphide deposits. Economic Geology 81, 1446–1463.

Tracy, R. J. 1982. Compositional zoning and inclusions in metamorphic minerals. Reviews in Mineralogy 10, 355–397.

Vaasjoki, M. 1981. The lead isotopic composition of some Finnish galenas. Geological Survey of Finland, Bulletin 316. 25 p. + 1 app. Available at: http://tupa.gtk.fi/julkaisu/bulletin/bt_316.pdf

Virtanen, V. J. & Heilimo, E. 2018. Petrology of the geochemically A-type Saarijärvi suite: evidence for bimodal magmatism. In: Mikkola, P., Hölttä, P. & Käpyaho, A. (eds) Development of the Paleoproterozoic Svecofennian orogeny: new constraints from the southeastern boundary of the Central Finland Granitoid Complex. Geological Survey of Finland, Bulletin 407. (this volume). Available at: https://doi.org/10.30440/bt407.7

Wall, V. J. 1977. Non-sulphide zinc bearing phases and the behaviour of zinc during metamorphism. 2nd Australian Geological Convention, Abstracts, p. 70.

Development of the Paleoproterozoic Svecofennian orogeny: new constraints from the southeastern boundary of the Central Finland Granitoid Complex
Edited by Perttu Mikkola, Pentti Hölttä and Asko Käpyaho
Geological Survey of Finland, Bulletin 407, 209–221, 2018

LITHOGEOCHEMICAL pXRF STUDY ON THE VIRTASALMI Cu DEPOSIT, EASTERN FINLAND

by

Janne Hokka[1)] and Lauri Virnes[2)]*

Hokka, J. & Virnes, L. 2018. Lithogeochemical pXRF study on the Virtasalmi Cu deposit, eastern Finland. *Geological Survey of Finland, Bulletin 407*, 209–221, 7 figures.

Field-portable X-ray fluorescence (pXRF) analysers have become widely used tools, for example, in collecting primary exploration data and distinguishing different minerals. In brownfield exploration targets, where pre-existing drill-core data can be re-measured with a high density and in a relatively reliable manner using pXRF, it can help in improving the understanding of local geology and exploration targeting.

In this study, historical drill cores were re-examined to test the use of a pXRF analyser in detecting the geochemical halos around the Virtasalmi Cu deposit and to demonstrate that the analyser characterizes the mineralization intercepted in drill cores. A total of 304 in situ, non-destructive measurements from five drill holes were conducted to observe the elemental dispersion from distal to proximal zones. From the results, the main lithological units can be discriminated. The data display a gradual increase in CaO, and high concentrations of chalcophile elements, such as Cu, were detected with pXRF. pXRF data were shown to be reliable and can be used for different modelling purposes, as well as in mineral systems studies.

Electronic Appendix is available at: http://tupa.gtk.fi/julkaisu/liiteaineisto/bt_407_electronic_appendix.xlsx

Keywords: volcanic rocks, field-portable X-ray fluorescence analyser, lithogeochemistry, Paleoproterozoic, Svecofennian, Finland

[1)] *Geological Survey of Finland, P.O. Box 96, Betonimiehenkuja 4, FI-02151 Espoo, Finland*
[2)] *Oulu Mining School, P.O. Box 3000, FI-90014 Oulu, Finland*
E-mail: janne.hokka@gtk.fi

VERTAISARVIOITU
KOLLEGIALT GRANSKAD
PEER-REVIEWED
www.tsv.fi/tunnus

https://doi.org/10.30440/bt407.11

Editorial handling by Perttu Mikkola.

Received 8 September 2017; Accepted 19 May 2018

1 INTRODUCTION

Field-portable X-ray fluorescence analysers (pXRF) have clear benefits due to their portability and ease of use, real-time data acquisition with minimal processing, immediate availability and analysis of a reasonably large amount of elemental data in the field in a relatively reliable manner. All these aspects have made pXRF an essential tool in many geological environments.

In recent years, the number of scientific publications in mineral exploration related to pXRF has increased (e.g. Kalnicky & Singhvi 2001, Glanzman & Closs 2007, Goodale et al. 2012, Sarala 2012, Somarin 2012, Sack & Lewis 2013, Durance et al. 2014, Hall et al. 2014, Ross et al. 2014a, Ross et al. 2014b, Sarala et al. 2015, Bourke & Ross 2016). pXRF studies have been conducted in a variety of geological environments and different deposit types. It has been shown that a portable XRF analyser provides an effective tool in exploration lithogeochemistry and chemostratigraphy and can assist in distinguishing between different volcanic units, especially in the pervasively hydrothermal altered lithologies related to volcanogenic massive sulphide deposits, where the primary protolith is visually unrecognisable (Peter et al. 2009, Sack & Lewis 2013, Ross et al. 2014b).

Recently, a 3D model of the historical Virtasalmi Cu deposit was constructed as part of an MSc thesis project (Virnes 2018) using pre-existing geological and mining data with modern state-of-art modelling tools. This has provided new insights into the local Virtasalmi geology and provides an attractive dataset for further exploration and ore research. Lawrie (1988) used immobile element geochemistry to subdivide volcanic rocks in the Virtasalmi region into chemostratigraphic groups according to their similar geochemical signature and spatial distribution. In the proximity of the Virtasalmi mine, mafic volcanic rocks were characterized as suite IIIa amphibolites, which mainly consist of massive flow units that were altered to massive calc-silicate lithologies in the proximity of mineralization. These altered calc-silicate skarn lithologies are interpreted to represent the widespread syn-volcanic hydrothermal alteration in the Virtasalmi volcanic suite, which is coeval with the Virtsasalmi mineralization (Lawrie 1988 & Lawrie 1992).

Nevertheless, only a few samples have been collected from the Virtasalmi deposit to confirm the chemostratigraphic groups, and no systematic sampling has been conducted from the drill cores. In this study, non-destructive, in situ pXRF measurements were conducted using unprepared core samples to examine whether pXRF results can detect the mineralization-related geochemical signatures from distal to proximal zones in the Virtasalmi deposit. This could provide an effective exploration tool in the Virtasalmi volcanic suite.

2 GEOLOGICAL SETTING

Virtasalmi belongs to the Jäppilä-Virtasalmi block, which forms the southeast end point of the older Svecofennian magmatic rocks and is part of the supracrustal rocks of the Svecofennian Raahe–Ladoga zone (RLZ) (Kousa et al. 2018, Fig. 1).

This primitive arc complex is economically important due to several volcanogenic massive sulphide deposits, such as the Vihanti-Pyhäsalmi VMS belt (Mäki et al. 2015 and references therein). Supracrustal rocks of Virtasalmi region, 1.920–1.906 Ga in age (Huhma 1986, Vaasjoki & Sakko 1988, Korsman et al. 1997, Pekkarinen 2002, Kousa et al. 2018), are dominated by different amphibolites, which are mostly submarine subalkaline mafic volcanic rocks, mainly composed of medium-K tholeiitic basalts and andesites (Lawrie 1992, Pekkarinen 2002). All the lithologies have been cut by synkinematic intrusions, which are the most abundant lithology in the district (~60% of the rocks in the area are intrusive rocks) and which in Virtasalmi consists of a gabbro-diorite-quartz-diorite-tonalite-trondhjemite suite of intrusive rocks (Lawrie 1988, Nironen 1989, Kähkönen 2005). The peak metamorphism occurred at Virtasalmi in granulite facies during D1 and went through subsequent retrogression during D2 to lower amphibolite facies conditions (Lawrie 1988). Incomplete retrogression has created a polymetamorphic mineral assemblage where the textures of the granulite fasies minerals range from complete amphibolisation to corona textures (Lawrie 1988, Lawrie 1992).

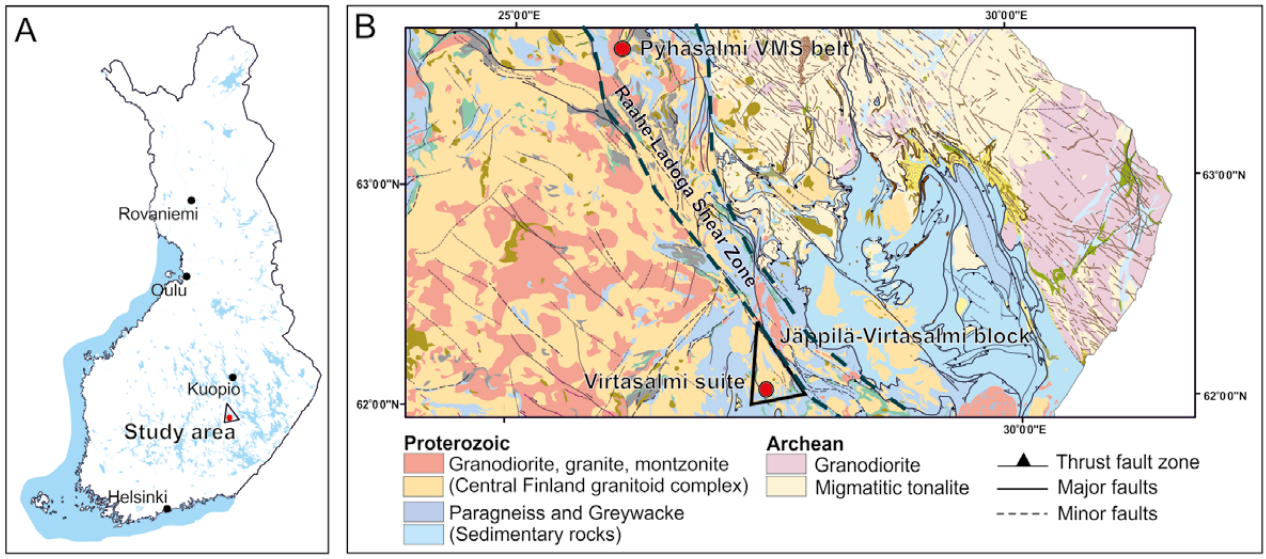
A
Rovaniemi
Oulu
Kuopio
Study area
Helsinki
B
25°00"E
30°00"E
63°00"N
62°00"N
Pyhasalmi VMS belt
Raahe-Ladoga Shear Zone
Jäppilä-Virtasalmi block
Virtasalmi suite
Proterozoic
Granodiorite, granite, montzonite
(Central Finland granitoid complex)
Paragneiss and Greywacke
(Sedimentary rocks)
Archean
Granodiorite
Migmatitic tonalite
Thrust fault zone
Major faults
Minor faults

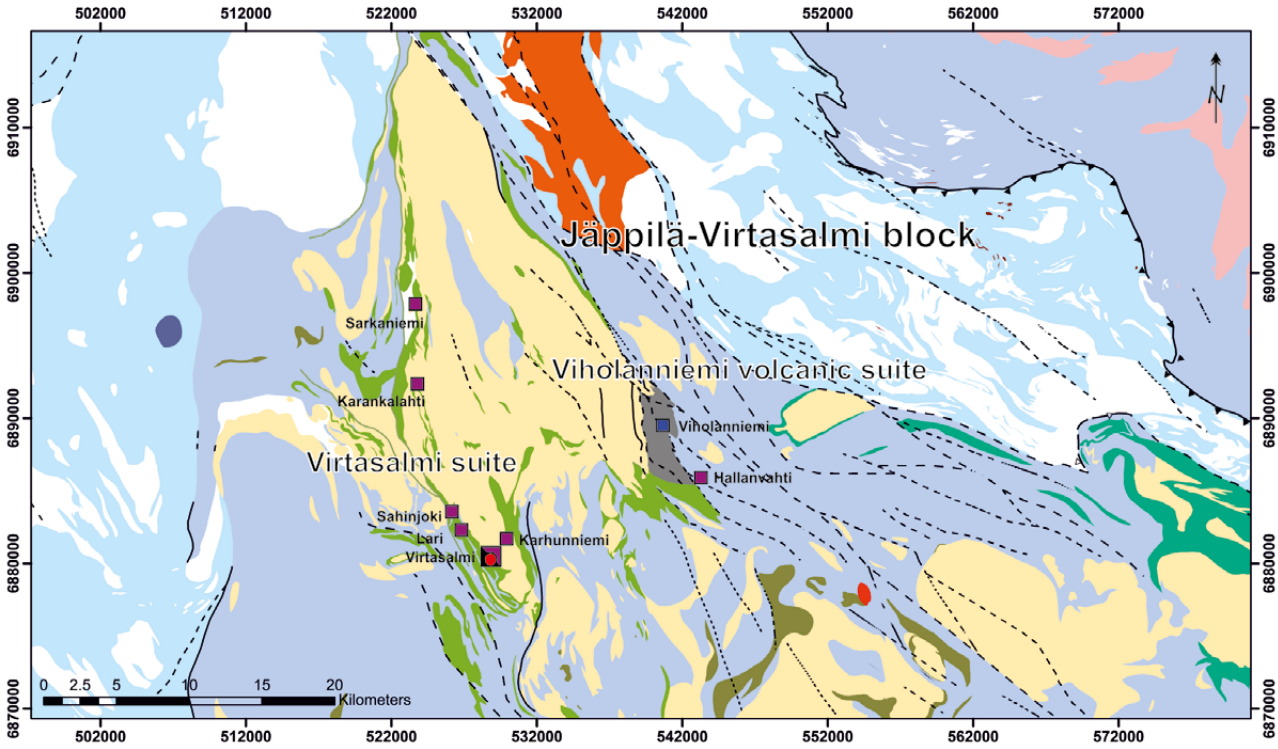
502000
512000
522000
532000
542000
552000
562000
572000
6910000
6900000
6890000
6880000
6870000
N
Jäppilä-Virtasalmi block
Viholanniemi volcanic suite
Virtasalmi suite
Sarkaniemi
Karankalahti
Viholanniemi
Hallanvahti
Sahinjoki
Lari
Virtasalmi
Karhunniemi
0 2.5 5 10 15 20
Kilometers

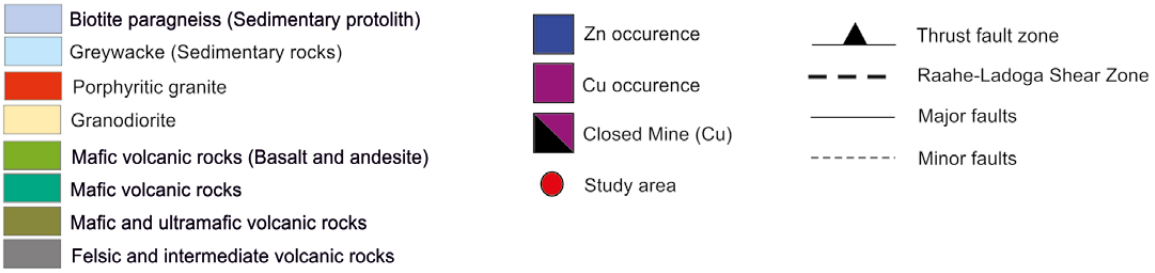
Biotite paragneiss (Sedimentary protolith)
Greywacke (Sedimentary rocks)
Porphyritic granite
Granodiorite
Mafic volcanic rocks (Basalt and andesite)
Mafic volcanic rocks
Mafic and ultramafic volcanic rocks
Felsic and intermediate volcanic rocks
Zn occurence
Cu occurence
Closed Mine (Cu)
Study area
Thrust fault zone
Raahe-Ladoga Shear Zone
Major faults
Minor faults

The Virtasalmi deposit (also known as the Hällinmäki mine) is a polydeformed, prominently lower amphibolite facies metamorphosed, strata-bound syn-volcanic hydrothermal exhalative deposit. The deposit is located within a ca. 1-km-wide and several-kilometres-long, large, northerly dipping F2 antiform structure (Lawrie 1992). The mineralized zone is ca. 650 m long and 16–30 m wide, and under the open pit it continues at least ca. 350 m below the surface (218 m below sea level). The Virtasalmi deposit is comprised of several 2- to 30-m-wide, steeply ~80° NE dipping (Fig. 2) disseminated and network textured chalcopyrite ore lenses within amphibolite and calc-silicate skarn lithologies, respectively (Hyvärinen 1969, Lawrie 1988 & Pekkarinen 2002). High-grade ore is located within unevenly distributed skarnified rocks (Fig. 3), which were formed through intense hydrothermal alteration of the amphibolites. The skarn alteration, which is present in the amphibolites, is most evident in a gradual increase in the proportion of calcic andradite garnet, which can locally form up to 90% of the rock. Typically, scapolite replaces plagioclase in more intensively altered rocks (Lawrie 1988). The main ore minerals in Virtasalmi are chalcopyrite, with minor cubanite as lamellae as well as pyrrhotite, pyrite and magnetite with minor bornite, mackinawite, pentlandite, bravoite, sphalerite, molybdenite, linneite minerals, gersdorffite and millerite (Hyvärinen 1966, 1969).

The Virtasalmi deposit was discovered by the Geological Survey of Finland in 1964. The Virtasalmi mine was operated by Outokumpu Oy during 1966–1983. A total of 4.2 Mt of ore was mined with an average grade of 0.73% Cu and total production reaching 31717.5 tonnes of copper (Puustinen 2003).

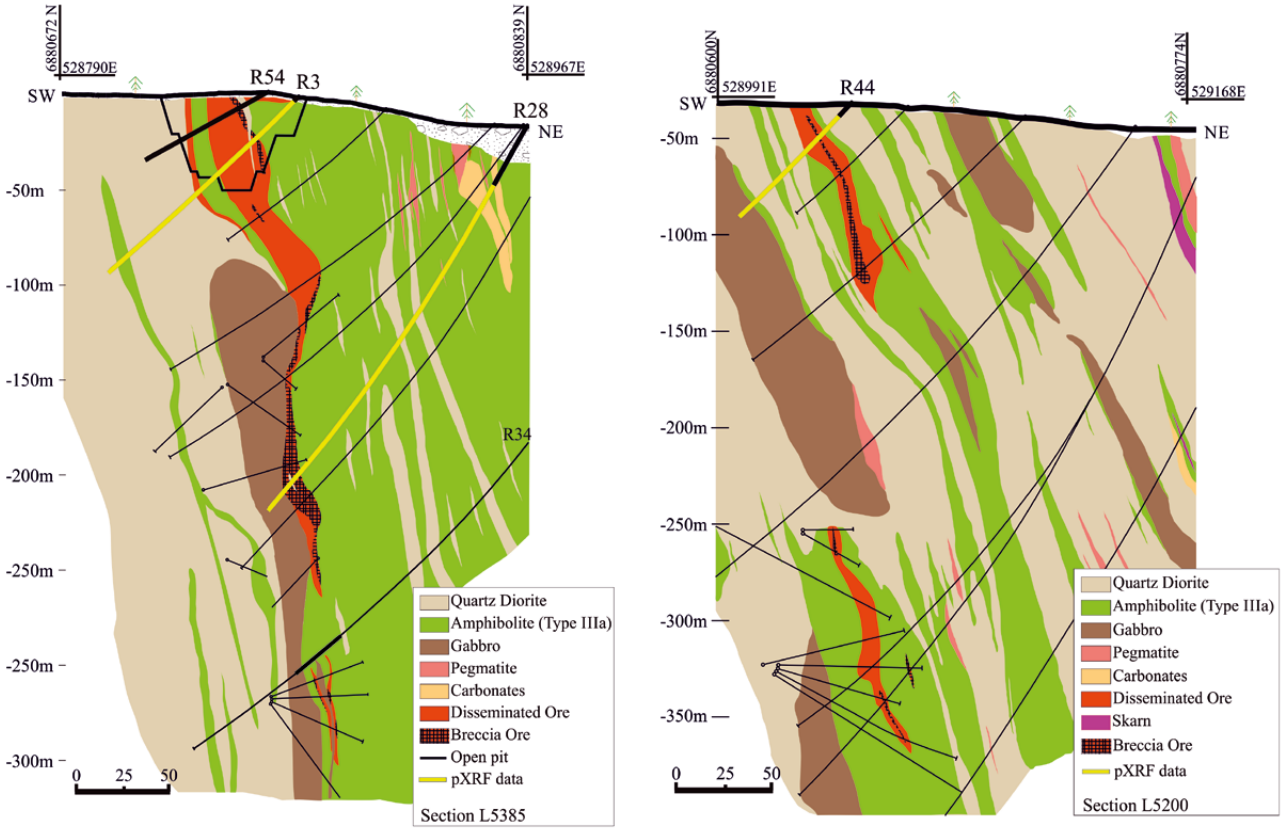

Fig. 2. A simplified cross-section through the Virtasalmi deposit (modified after Vaajoensuu et al. 1978). The yellow-coloured bolding in drill holes represents the portable XRF measurements conducted from drill cores presented in this study. The black-coloured bolded drill holes were also measured during the programme.

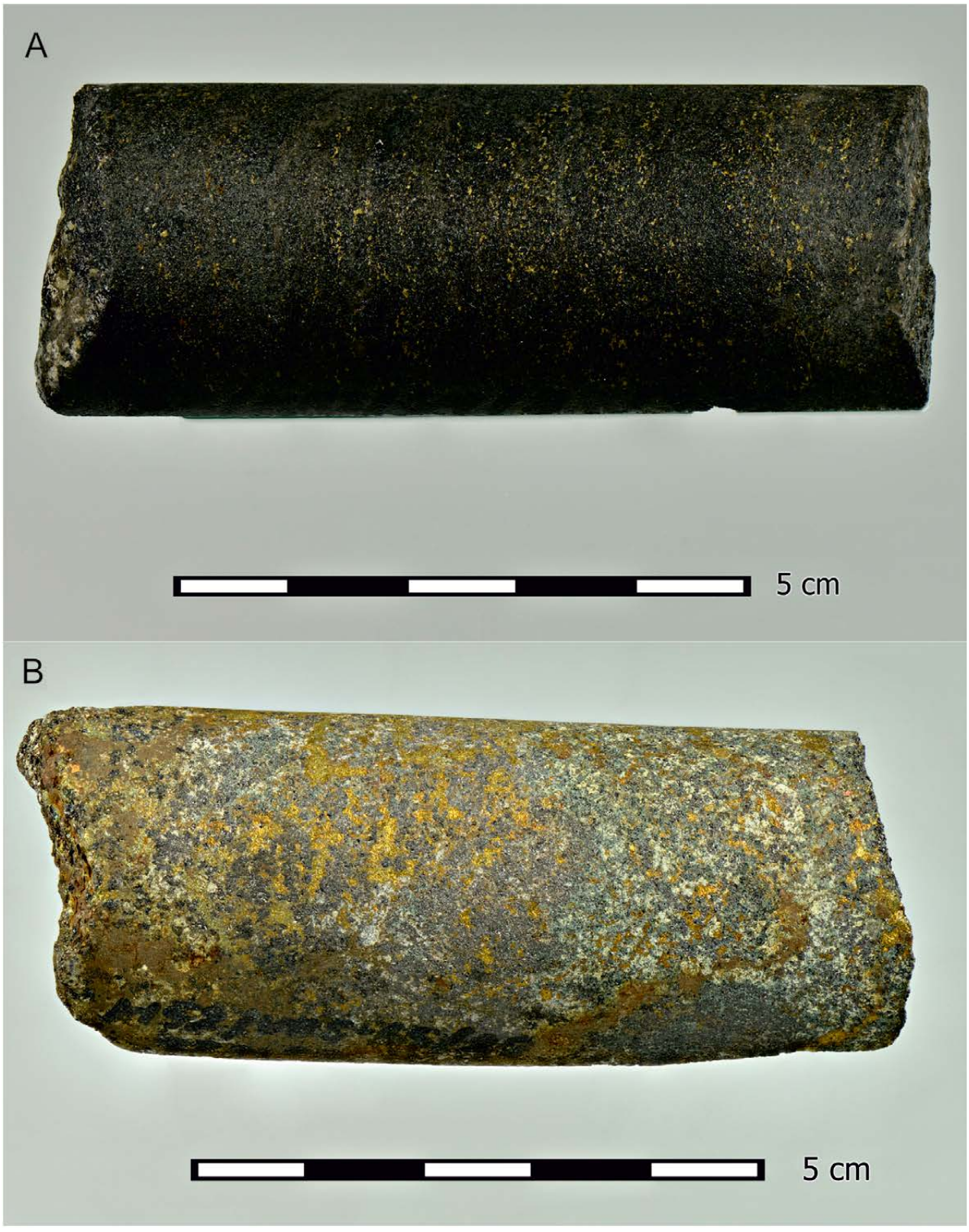

Fig. 3. The Virtasalmi ore types. A) The disseminated ore is of low to medium grade (0.2–0.7% Cu), and either homogeneously distributed or forming sulphide bands in diopside-rich amphibolite. The average grain size of the disseminated ore is between 0.1–0.4 mm. B.) The network texture ore is of high grade (0.7–8% Cu). It commonly forms as network textures around skarn and amphibolite fragments, but sometimes as massive 5–10-cm-long and 1–3-cm-wide lenticular shapes. The average grain size of the main ore minerals is much greater than in the disseminated ore and the grain width can be up to 4 cm.

3 METHODS

3.1 Data collection

The study was conducted with a handheld Delta Premium analyser from Olympus Corporation. The instrument is owned by Geological Survey of Finland. The device is equipped with a 4 W optimized Ta X-ray tube with a maximum tube voltage of 40 kV and a silicon drift detector. The instrument was provided with a mining plus mode (2-beam) and a soil mode (3-beam). Only the mining mode was used in this study. In addition, KT-10 susceptibility measurements were taken from the same measurement points as pXRF readings.

The analyser was placed in a portable workstation with an integrated safety lock to prevent any movement during measurements. The pXRF analyser was set to the mining mode and the final result was an average of three spatially separate point measurements taken from the same depth interval. Due to time constraints, the measurement spacing was optimized according to the lithological units as follows: the mafic volcanic rocks were measured with ca. 1 m spacing, calc-silicate altered units with ca. 0.5 m spacing and the cross-cutting, barren, quartz diorite intrusive rocks with 3 m spacing. The integration time was 60 seconds, i.e. 30 seconds per beam.

The raw data were converted from elemental form to oxide form for the elements Mg, Al, Si, P, K, Ca, Mn, Ti and Fe, while the rest of the elements were left in elemental form. In addition, the alteration index (AI) and chlorite-carbonate-pyrite index (CCPI) after Ishikawa et al. (1976) and Large et al. (2001) were calculated using the modified formula of Sack & Lewis (2013). Moreover, the ratios of immobile elements Ti/Zr and Al/Zr were calculated.

A single point calibration was applied to level the data (Piercey & Devine 2014). A single point calibration was applied to level the data (Piercey & Devine 2014). The calibration standard used for this study was an basaltic andesite (N5122014R19 26.9-27.2). This standard were chosen as it has similar consentrations and matrix as the samples analyzed in this study. Correction was only applied to following elements: Al_2O_3, SiO_2, P_2O_5, CaO, TiO_2, MnO, Fe_2O_3, Cr, Ni and Zr having performed well in matrix-matched precision and accuracy test.

3.2 Data verification and quality control

At the beginning, the instrument was tested for short-term variations using a single NIST 2710A standard (Montana 1 Soil; https://www-s.nist.gov/srmors/view_cert.cfm?srm=2710A) for a one-hour continuous measurement time. This was conducted to test the instrumental drift for the pXRF analyser used in this study. One hour was selected to examine whether there was variation in the first 30–60 minutes of measurement after the instrument had been turned on. The results of the short-term one-hour drift test on a NIST standard for the selected elements showed some variation for all elements, but within the instrument precision for each element.

Instrumental performance was monitored throughout the measuring programme using an in-house field reference sample, which consisted of laboratory pulp (returns) from a fine-grained felsic volcanic rock placed in an XRF sampling cup with prolene (4 µm) thin film. The sample was previously determined by Labtium Oy, Rovaniemi, Northern Finland (WD-XRF, method code 175X). The verification procedure also included internal calibration and a quartz blank measured at a constant interval to check the contamination. The instrument's internal calibration check was performed with a 316 stainless steel calibration check reference coin provided by the manufacturer.

A matrix-matched precision and accuracy test was conducted using a homogeneous basaltic andesite core slab (N5122014R19 26.9-27.2) that had previously been analysed by Labtium Oy from a pressed pellet and using an XRF analyser. The core slab was shot a total of 30 times to obtain measurements covering the whole cut surface. The test was performed using mining plus mode and the pXRF analyser was installed in the portable workstation during measurement. Measurements were then averaged for each sample, giving a representative pXRF composition, and compared with the whole-rock assay results determined by the laboratory.

The calculation was based onconcentration data from multiple analyses (n = 30) taken from the rock slab using Equation (1).

The same results were also used to determine the sample precision or reproducibility, which were reported as the relative standard deviation (RSD%) after measuring the sample 30 times and comparing the results to determine the mineralogical heterogeneity of in situ pXRF measurements (Bourke & Ross 2016).

$$RSD\% = (stdv_i \div mean_i) \times 100 \quad (1)$$

Accuracy was determined by assessing the degree to which the pXRF measurement of an element in a sample matched the reference value from the rock slab. The Labtium laboratory-based concentrations were used as reference values for this test. Differences between the data sets were assessed according to the relative percentage difference (equation (2).

$$\%Difference = \frac{(Mean_{isample} - Certified_{isample})}{Certified_{isample}} \times 100 \quad (2)$$

The mafic rock sample results indicated poor results for K_2O, while a few elements had precision values between 11% and 21%, including MgO, P_2O_5 and V, and the rest had good to excellent precision. Generally, the accepted level for field-portable XRF is 20% RSD. When comparing the accuracy or bias value with the laboratory assay results, significant variability was observed, and the accuracy for most elements was poor (> ±20%). The most reliable elements were P_2O_5, CaO, MnO, Fe_2O_3, Cr and Zr, which all had good accuracy (< ±6%).

4 RESULTS

A total of 304 pXRF measurements, all listed in the Electronic Appendix, were conducted from five representative drill holes (R54, R3, R28, R34 and R44) from two sections, 5385 and 5200, respectively. The drill holes R3, R28, R44 are presented as the main results in this study (Figs 4, 5 and 6). It was demonstrated that pXRF measurements can discriminate the main lithological units of amphibolites, mineralized hedenbergite-garnet skarn and gabbro-diorite.

The pXRF results show the proximal ore zone as a gradual increase in CaO, representing the diopside amphibolite and calcic garnet-hedenbergite skarn altered lithologies, which are the predominant host rocks of Virtasalmi ore. The correlation with the Cu value is also distinctive (Fig. 7).

Chalcophile elements such as Cu, Zn, Fe and Pb are mainly elevated in calc-silicate altered rocks, which indicates that they were introduced from an external hydrothermal fluid source. Pb values are high in the ore zone, but also in adjacent intrusive rocks. The ore typically contains magnetite, pyrite and pyrrhotite, which is seen as elevated Fe and S contents, as well as higher susceptibility readings. The CCPI displays relatively high values in these altered rock units (CCPI 60–90), whereas the AI values are low for all data points (AI 0–30).

The Virtasalmi pXRF dataset was also compared with previously published immobile element geochemistry published in Lawrie (1988). When comparing least-altered amphibolite units of pXRF data against type III amphibolites in the Zr-TiO_2 diagram, a relatively similar trend can be seen with slightly more scatter (Fig. 7). When examining calc-silicate skarn altered lithologies, they plot with a different trend, having a lower TiO_2 concentration and elevated Zr.

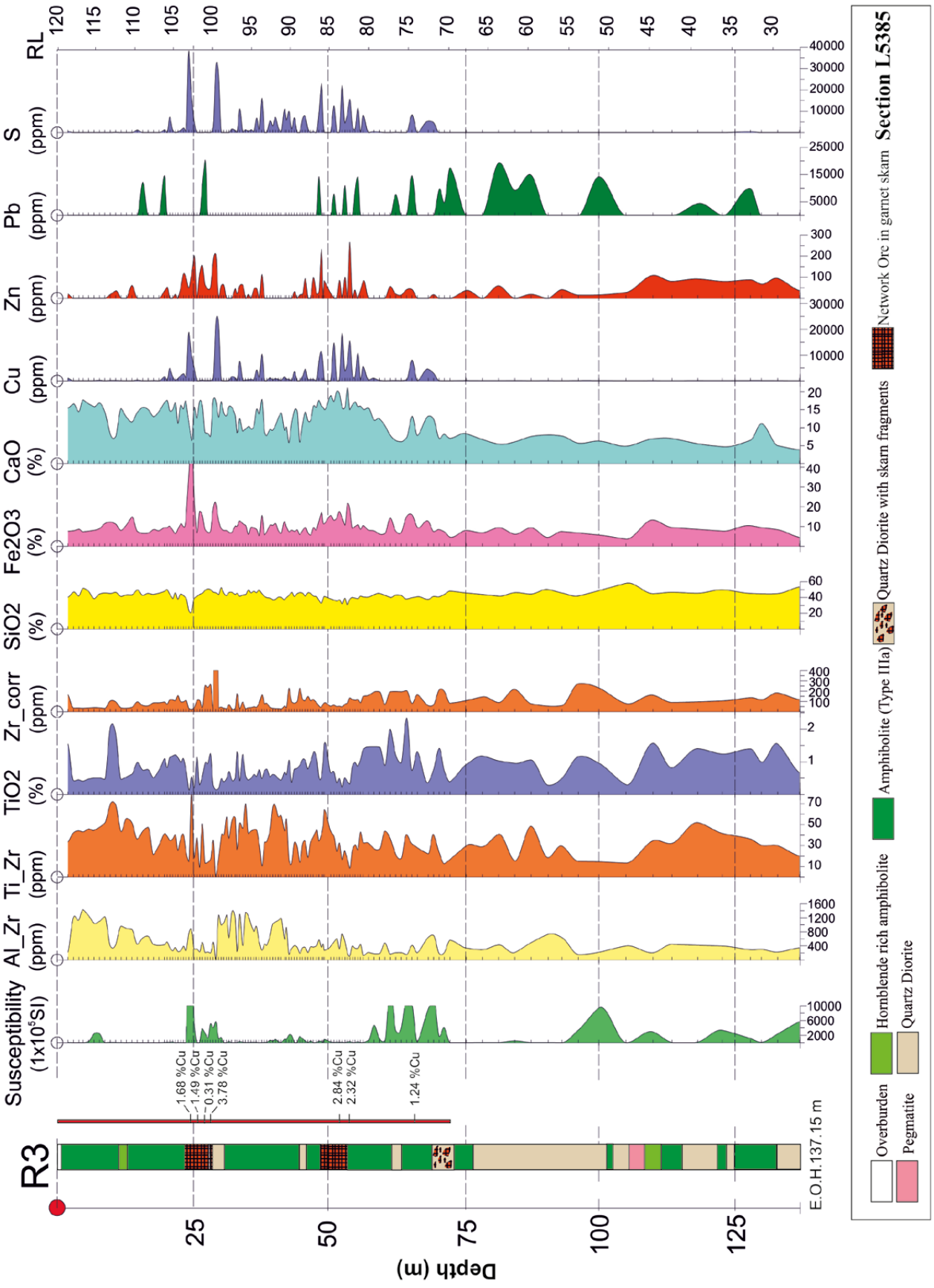

Fig. 4. Non-destructive measurements conducted on the drill core from distal to proximal zones of known mineralization from drill hole R3, together with the simplified original lithological log. The solid red line represents the original continuous sampling intervals. Only ≤1% Cu assay results are presented in this log. The portable XRF measurements clearly indicate the main lithological units of amphibolites, hedenbergite-garnet skarn and gabbro-diorite and sulphide ore.

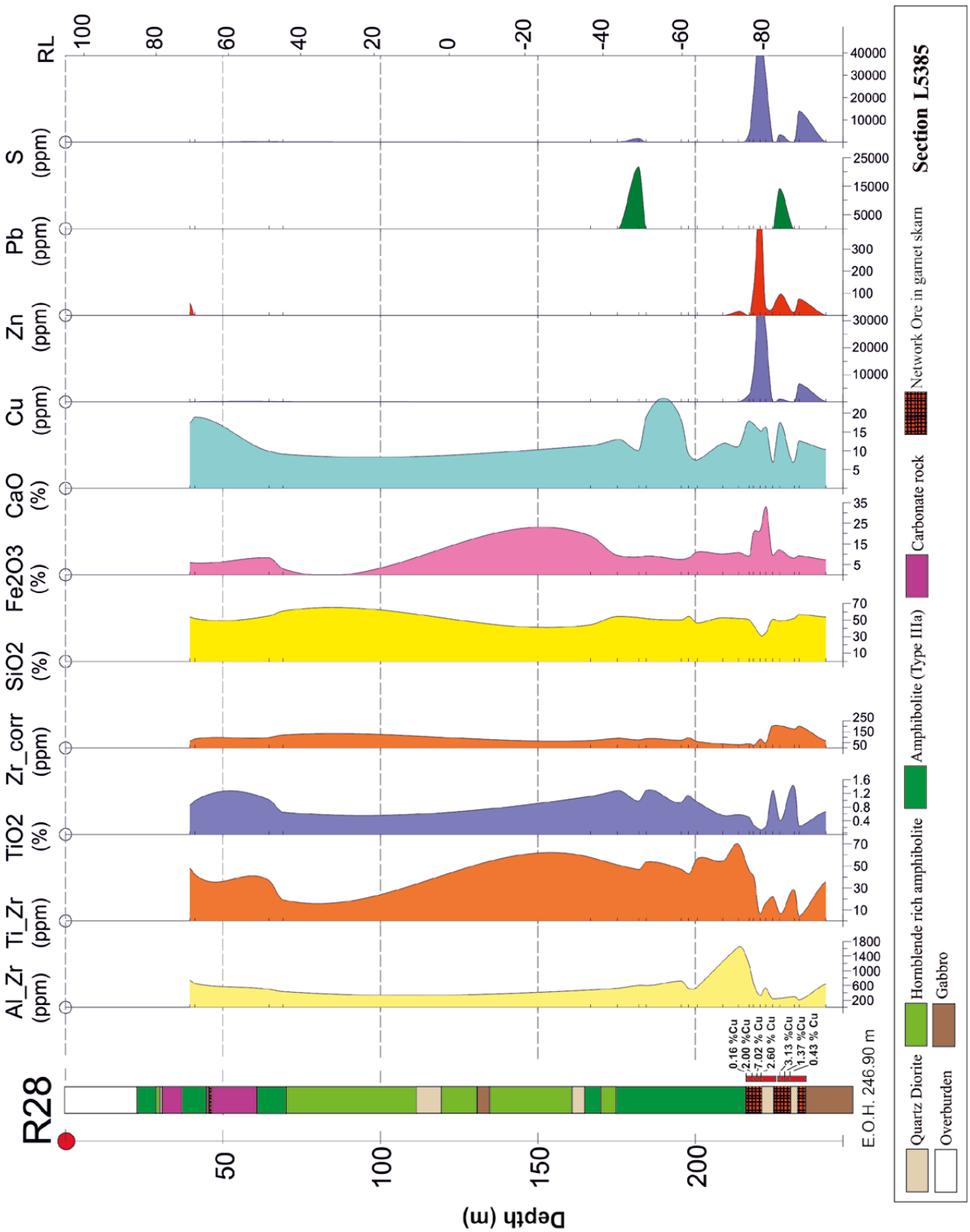

Fig. 5. Non-destructive measurements conducted on the drill core from distal to proximal zones of known mineralization from drill hole R28, together with the simplified original log and Cu assay results.

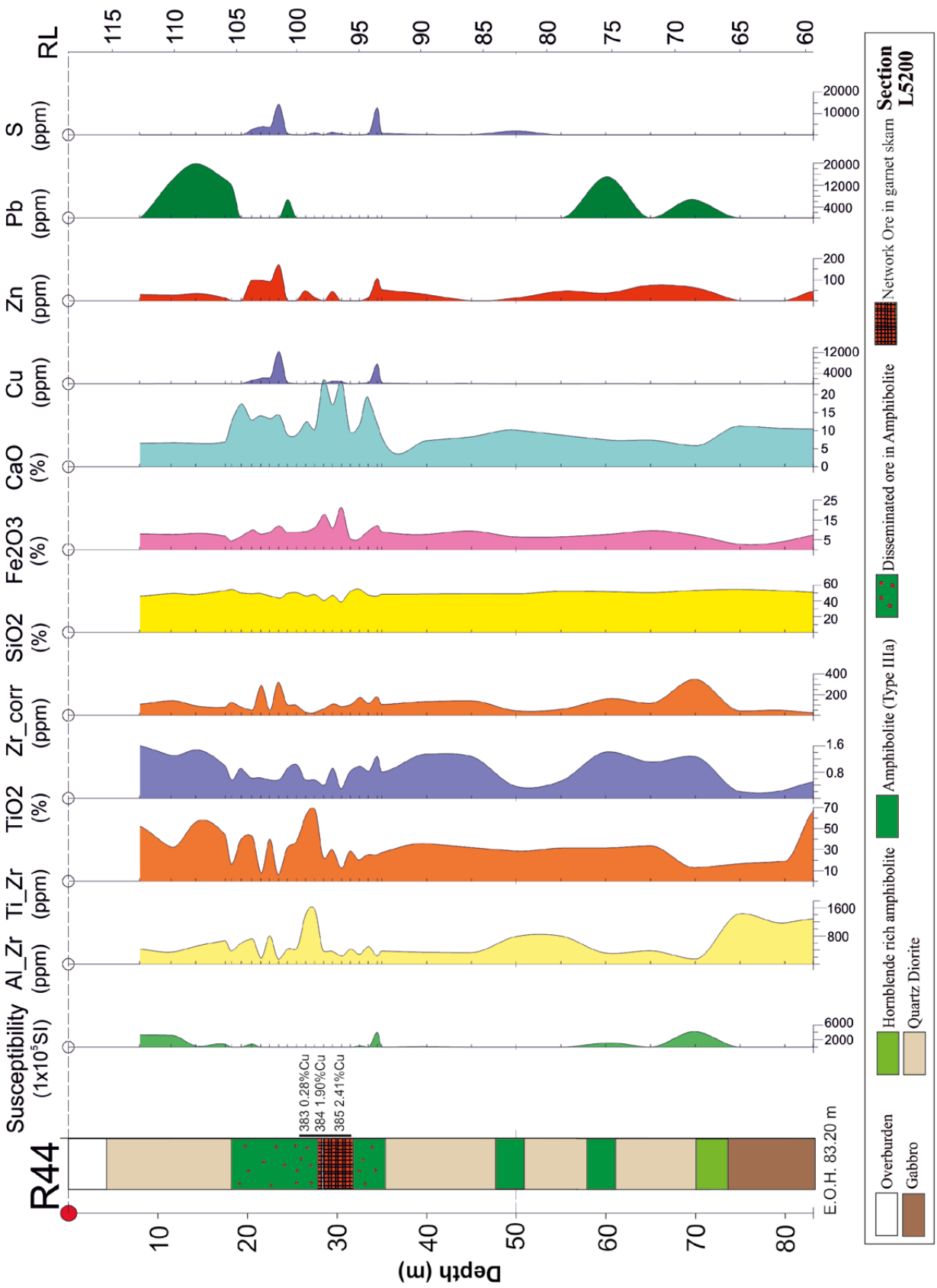

Fig. 6. Non-destructive measurements conducted on the drill core from distal to proximal zones of known mineralization from drill hole R44, together with the simplified original log and Cu assay results.

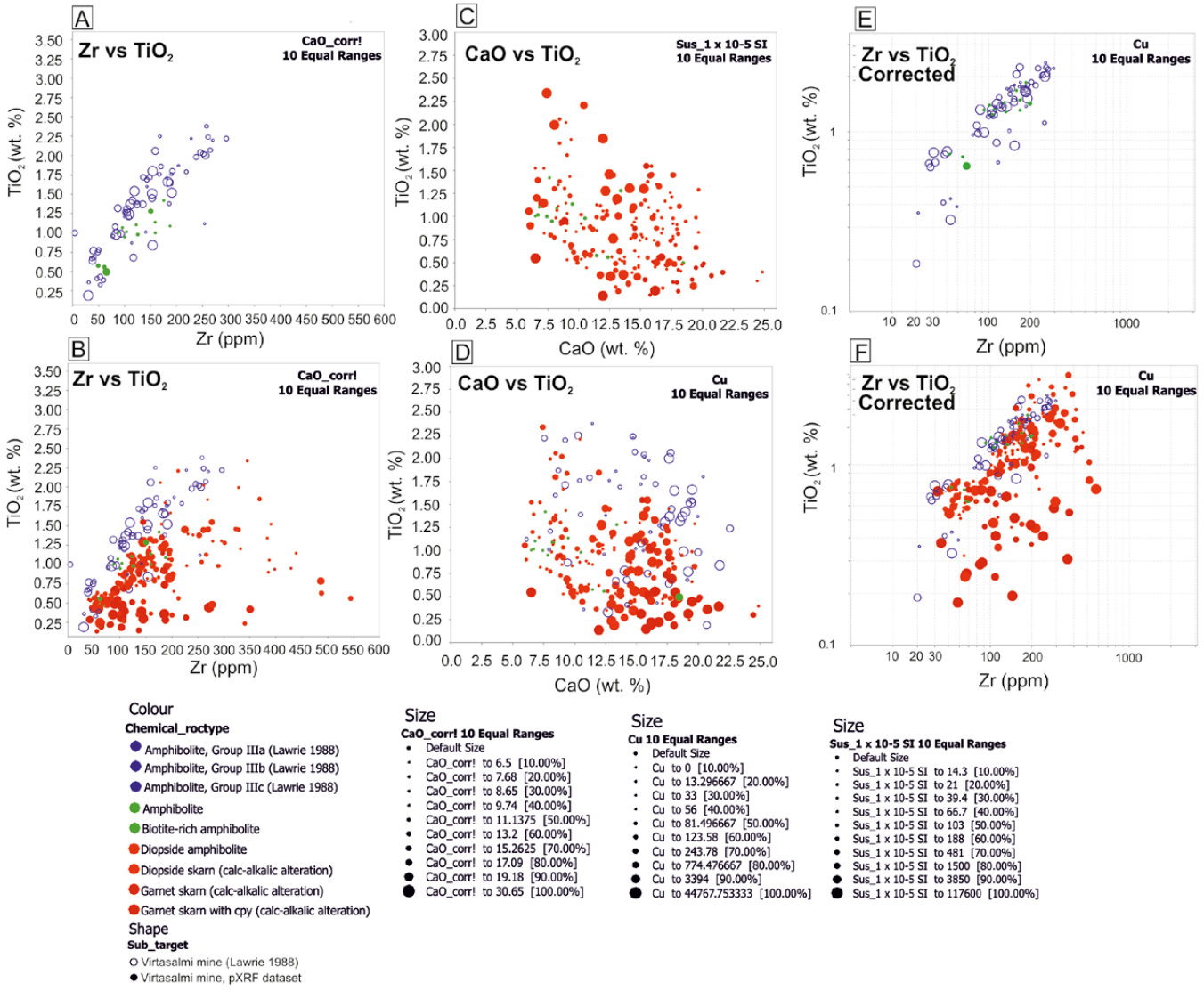

Fig. 7. A) Comparison of least-altered amphibolite units from pXRF data with group III amphibolites in and around the Virtasalmi mine shows a similar trend in the Zr-TiO_2 plot. B) The red-coloured circles represent calc-silicate skarn altered lithologies measured with pXRF, which can be interpreted as alteration trends. The high CaO content is concentrated in calc-silicate skarn altered lithologies due to hedebergite and diopside minerals (red-coloured circles). C) A CaO-TiO_2 diagram in which calc-silicate skarn altered lithologies are plotted according to susceptibility readings. Most of the high readings are in altered sequences due to the presence of magnetite and pyrrhotite minerals. D) A CaO-TiO_2 diagram in which calc-silicate skarn altered lithologies are plotted according to Cu values, clearly showing the correlation between Cu and CaO values. E–F) The corrected values in Zr-TiO_2 plot show several co-genetic trends for amphibolites and calc-silicate skarn altered lithologies. This can be seen in both conventional whole rock (Lawrie 1988) and pXRF data.

5 DISCUSSION AND CONCLUSION

The portable XRF results correlate relatively well with previously analysed intervals and visual logging. However, the results should not be interpreted as true elemental concentrations, but rather as providing a tool for identifying trends. For example, the Pb results are extremely high across the lithologies in all measured drill cores (Figs 4, 5 and 6). Although sphalerite is widely distributed in the Virtasalmi deposit, it is always present at low concentrations, mainly as lamellae in chalcopyrite, pyrrhotite and cubanite (Hyvärinen 1966, 1969). The extremely high readings measured with pXRF could be caused by many different factors, such as the matrix effect, and high readings should always be interpreted carefully. This also emphasizes the importance of reference samples and background information on mineralogy.

The comparison with previously reported immobile element geochemistry published in Lawrie (1988) revealed a difference in the trend, with a lower TiO_2 concentration and elevated Zr (Figs 7A, B). This could be caused by the accuracy of the pXRF device, producing more spread out trends than the original laboratory whole-rock results. Nevertheless, after correction applied the pXRF results in the Zr-TiO_2 diagram also display different trend, which could be interpreted as different cogenetic trends between amphibolite and calc-silicate altered lithologies (Fig.7 E–F). According to Lawrie (1992), HFSE elements in the Virtasalmi amphibolite reflect the original magmatic processes, with limited secondary redistribution. Moreover, it is mentioned that in the Virtasalmi mine, the inter-element ratios of the HFSE elements change in a non-systematic manner in samples taken across the irregular and gradational contacts from amphibolite to calc-silicate rock. Nevertheless, in high metamorphic environments, TiO_2 can be mobile to some extent, and this needs to be taken into consideration and further investigated. Moreover, this could be interpret as indication of strong mass change in altered lithologies. Also the carbonate rocks (Fig.5) show very similar trends in elemental concentrations compared to calc-silicate altered rocks related to the ore zone.

pXRF illustrates the alteration intensity and characterizes the base metal contents of mineralized intercepts in a drill core. In situ pXRF measurements enable unprepared rock samples to be examined with a high density in a relatively rapid manner and provide very detailed results for lithological units, making pXRF a powerful tool in volcanic chemostratigraphy. Although pXRF cannot achieve the accuracy and precision of laboratory whole-rock analysis, it can be used to detect trends and populations critical to the ore zone. In the case of further study and drilling in the Virtasalmi area, pXRF data could confirm the ore sequence and help to make correct decisions in exploration drilling. It could also provide a low-cost data set for further modelling with, for example, multivariate analysis. This could be further used in understanding genetic aspects of the Virtasalmi mineral system.

ACKNOWLEDGEMENTS

We are grateful to reviewers Dr. Pertti Sarala and M.Sc. Marko Moilanen for constructive comments and suggestions that led to improvements of the manuscript. Similar comments on earlier versions were provided by Dr. Juhani Ojala and M.Sc. Helena Hulkki. We wish to also express our gratitude to Eija Vallimies for her efforts in searching the Virtasalmi historical data and the staff of National drill core archive of the Geological Survey of Finland. Finally a warm thank you to our loved ones for their support.

REFERENCES

Bourke, A. & Ross, P.-S. 2016. Portable X-ray fluorescence measurements on exploration drill-cores: comparing performance on unprepared cores and powders for 'whole-rock' analysis. Geochemistry: Exploration, Environment, Analysis 16, 147–157.

Durance, P., Jowitt, S. M. & Bush, K. 2014. An assessment of portable X-ray fluorescence spectroscopy in mineral exploration, Kurnalpi Terrane, Eastern Goldfields Superterrane, Western Australia, Applied Earth Science 12, 150–163.

Hall, G. E. M., Bonham-Carter, G. F. & Buchar, A. 2014. Evaluation of portable X-ray fluorescence (pXRF) in exploration and mining: Phase 1, control reference materials. Geochemistry: Exploration, Environment, Analysis 14, 99–123.

Glanzman, R. K. & Closs, L. G. 2007. Field Portable X-Ray Fluorescence Geochemical Analysis- Its Contribution to Onsite Real-time Project Evaluation. In: Milkereit, B (ed.) Proceedings of Exploration 07: Fifth Decennial International Conference on Mineral Exploration, 291–301.

Goodale, N., Bailey, D. G., Jones, G. T., Prescott, C., Scholz, E., Stagliano, N. & Lewis, C. 2012. Comparison of Sr and Zr data obtained using Olympus Innov-X PXRF models Delta and Omega with WDXRF analyses of the same samples. Journal of Achaeological Science 39, 875–883.

Huhma, H. 1986. Sm-Nd, U-Pb and Pb-Pb isotopic evidence for the origin of the Early Proterozoic Svecokarelian crust in Finland. Geological Survey of Finland, Bulletin 337. 48 p. Available at: http://tupa.gtk.fi/julkaisu/bulletin/bt_337.pdf

Hyvärinen, L. 1966. Karsikummun kupariesiintymän geologiasta, Geological Survey of Finland, archive report M17/Vrs-/66/1. 56 p. (in Finnish). Available at: http://tupa.gtk.fi/raportti/arkisto/m17_vrs_66_1.pdf

Hyvärinen, L. 1969. On the geology of the copper ore field in the Virtasalmi area, eastern Finland. Geological

Survey of Finland, Bulletin 240. 82 p. Available at: http://tupa.gtk.fi/julkaisu/bulletin/bt_240.pdf

Ishikawa, Y., Sawaguchi, T., Ywaya, S. & Horiuchi, M. 1976. Delineation of prospecting targets for Kuroko deposits based on modes of volcanism of underlying dacite and alteration haloes; Mining Geology 26, 105–117.

Kähkönen, Y. 2005. Svecofennian supracrustal rocks. In: Lehtinen, M., Nurmi P. A. & Rämö O. T. (eds) Precambrian Geology of Finland – Key to the Evolution of the Fennoscandian Shield. Amsterdam: Elsevier B.V., 343–406.

Kalnicky, D, J. & Singhvi, R. 2001. Field portable XRF analysis of environmental samples. Journal of Hazardous Materials 83, 93–122.

Korsman, K., Koistinen, T., Kohonen, J., Wennerström, M., Ekdahl, E., Honkamo, M., Idman, H. & Pekkala, Y. (eds) 1997. Suomen kallioperäkartta – Berggrundskarta över Finland – Bedrock map of Finland 1:1 000 000. Espoo: Geological Survey of Finland.

Kousa, J., Huhma, H., Hokka, J. & Mikkola, P. 2018. Extension of Svecofennian 1.91 Ga magmatism to the south, results of the reanalysed age determination samples from Joroinen, central Finland. In: Mikkola, P., Hölttä, P. & Käpyaho, A. (eds) Development of the Paleoproterozoic Svecofennian orogeny: new constraints from the southeastern boundary of the Central Finland Granitoid Complex. Geological Survey of Finland, Bulletin 407. (this volume). Available at: https://doi.org/10.30440/bt407.3

Large, R. R., Gemmell, J. B., Paulick, H. & Herrmann, W. 2001. The alteration box plot; a simple approach to understanding the relationship between alteration mineralogy and lithogeochemistry associated with volcanic-hosted massive sulfide deposits. Economic Geology and the Bulletin of the Society of Economic Geologists 96, 957–971.

Lawrie, K. C. 1988. The origin, nature and tectonic significance of the Hällinmäki Cu-deposit,Virtasalmi District, South-central Finland. Unbup. PhD thesis, Glasgow University. 297 p.

Lawrie, K. C. 1992. Geochemical characterisation of a polyphase deformed, altered and high grade metamorphosed volcanic terrane: implications for the tectonic setting of the Svecofennides, south-central Finland. Precambrian Research 59, 171–205.

Mäki, T., Kousa, J. & Luukas, J. 2015. The Vihanti-Pyhäsalmi VMS belt. In: Maier, W. D., Lahtinen, R. & O'Brien, H. (eds) Mineral deposits of Finland. Amsterdam: Elsevier, 507–530.

Nironen, M. 1989. Emplacement and structural setting of granitoids in the early proterozoic Tampere and Savo schist belts, Finland - Implications for contrasting crustal evolution, Geological Survey of Finland, Bulletin 346. 83 p. Available at: http://tupa.gtk.fi/julkaisu/bulletin/bt_346.pdf

Pekkarinen, L. 2002. Haukivuoren ja Pieksämäen kartta-alueiden kallioperä. Summary: Pre-Quaternary Rocks of the Haukivuori and Pieksämäki Map-Sheet areas. Geological Map of Finland 1:100 000, Explanation to the Maps of Pre-Quaternary Rocks, Sheets 3231 and 3232. Geological Survey of Finland. 98 p. Available at: http://tupa.gtk.fi/kartta/kallioperakartta100/kps_3231_3232.pdf

Peter, J., Mercier-Langevin, P. & Chapman, J. B. 2009. Application of field-portable X-ray fluorescence spectrometers in mineral exploration, with examples from the Abitibi Greenstone Belt. Proceedings of the 24th International Applied Geochemistry Symposium, Fredericton, New Brunswick 1, 83–86.

Piercey, S. J. & Devine, M. C. 2014. Analysis of powdered reference materials and known samples with a benchtop, field portable x-ray fluorescence (pXRF) spectrometer: evaluation of performance and potential applications for exploration lithogeochemistry. Geochemistry: Exploration, Environment, Analysis, 14, 139–148.

Puustinen, K. 2003. Suomen kaivosteollisuus ja mineraalisten raaka-aineiden tuotanto vuosina 1530–2001, historiallinen katsaus erityisesti tuotantolukujen valossa. Geological Survey of Finland, archive report M10.1/2003/3. 578 p. (in Finnish). Available at: http://tupa.gtk.fi/raportti/arkisto/m10_1_2003_3.pdf

Ross, P.-S., Bourke, A. & Fresia, B. 2014a. Improving lithological discrimination in exploration drill-cores using portable X-ray fluorescence measurements: (1) testing three Olympus Innov-X analysers on unprepared cores. Geochemistry: Exploration, Environment, Analysis, 14, 171–185.

Ross, P.-S., Bourke, A. & Fresia, B. 2014b. Improving lithological discrimination in exploration drill-cores using portable X-ray fluorescence measurements: (2) applications to the Zn-Cu Matagami mining camp, Canada. Geochemistry: Exploration, Environment, Analysis 14, 187–196.

Sack, P. J. & Lewis, L. 2013. Field-portable x-ray fluorescence spectrometer use in volcanogenic massive sulphide exploration with examplesfrom the Touleary occurrence (MINFILE Occurrence 115O 176) in west-central Yukon. In: MacFarlane, K. E., Nordling, M. G. & Sack, P. J. (eds) Yukon Geological Survey, Yukon Exploration and Geology 2012, 115–131.

Sarala, P. 2016. Comparison of different portable XRF methods for determining till geochemistry, Geochemistry: Exploration, Environment, Analysis 16, 181–192.

Sarala, P., Taivalkoski, A. & Valkama, J. 2015. Portable XRF – Advanced on-site analysis method in till geochemical exploration. In: Sarala, P. (ed.) Novel technologies for greenfield exploration. Geological Survey of Finland, Special Paper 57, 63–86. Available at: http://tupa.gtk.fi/julkaisu/specialpaper/sp_057.pdf

Somarin, A. K., Lopez, R., Herrera, M. & Güiza-González, S. 2012. Application of the Thermo Scientific Portable XRF Analyzer in Geochemical Exploration: And Example from the Francisco I. Madero Zn-Pb-Cu-(Ag) Deposit, Zacatecas, Mexico. Thermo Scientific Inc. (Poster presentation)

Vaajoensuu, K., Grundström, L. & Astorga, T. 1978. Virtasalmi mine, mining technique. Outokumpu Oy, Finland, mining, milling and metallurgical division, Unpublished company report. 15 p.

Vaasjoki, M. & Sakko, M. 1988. The U-Pb mineral chronology of the Raahe-Ladoga zone. In: Pajunen, M. (ed.) Project No. 235 Metamorphism and geodynamics excursion in Finland 15.6.-19.6.1988. Geological Survey of Finland, Guide 21, 23–24. Available at: http://tupa.gtk.fi/julkaisu/opas/op_021.pdf

Virnes, L. 2018. Geological 3D-modeling of the Virtasalmi Cu deposit in eastern Finland. Unpublished master's thesis, University of Oulu, Oulu Mining School. 52 p. Available at: http://jultika.oulu.fi/files/nbnfioulu-201802271268.pdf

APPENDIX 1: ANALYTICAL METHODS

1 GEOCHEMICAL METHODS

The majority of the whole-rock analyses were carried out by Labtium Ltd. All of these samples were analysed using X-ray fluorescence (XRF) (Labtium codes 175X and 176X) on pressed pellets. Methods 175X and 176X differ in the automatic sample preparation of the latter, contrary to the manual preparation used in 175X. Samples were first crushed with a jaw crusher (Mn-steel jaws) and ground using a tungsten carbide vessel. In XRF, samples are analysed for the following: major elements Si, Ti, Al, Fe, Mn, Mg, Ca, Na, K, P and trace elements As, Ba, Bi, Ce, Cl, Cr, Cu, Ga, La, Mo, Nb, Ni, Pb, Rb, S, Sb, Sc, Sn, Sr, Th, U, V, Y, Zn and Zr. According to the normal convention, the main elements are listed as wt% of oxides and trace elements as elements in ppm in the Electronic Appendix. Total carbon was analysed with a carbon analyser (Labtium method 811L).

In certain samples, additional trace elements (Ce, Co, Dy, Er, Eu, Gd, Hf, Ho, La, Lu, Nb, Nd, Pr, Rb, Sc, Sm, Ta, Tb, Th, Tm, U, V, Y, Yb and Zr) were analysed by inductively coupled plasma mass spectrometry (ICP-MS) using Labtium method 308PM. For this method, the grinding was carried out using a carbide steel vessel. Total dissolution of the samples was performed using perchloric acid.

Aqua regia partial leaching followed by analysis with inductively coupled plasma optical emission spectroscopy (ICP-OES) (Labtium code 511PM) was carried out on a limited number of sulphide-bearing samples. The elements analysed were Ag, Al, As, B, Ba, Be, Bi, Ca, Cd, Ce, Co, Cr, Cu, Fe, K, La, Li, Mg, Mn, Mo, Na, Ni, P, Pb, S, Sb, Sc, Se, Sn, Sr, Te, Th, Ti, U, V, W, Y and Zn.

Gold, platinum and palladium analysis was performed w ith Labtium methods 703P, 704P and 705P, respectively, with the methods differing in the size of the sample (10 g, 25 g and 50 g, respectively). In this method, samples are prepared with the Pb-fire assay method and analysed using ICP-OES. For a detailed description of the analytical methods, see Rasilainen et al. (2007) and the website of Labtium Ltd (www.labtium.fi).

For those samples in which REE elements were determined in the Reactor Laboratory of the Technical Research Centre of Finland (VTT), the instrumental neutron activation analysis (INAA) method was applied following the procedure of Rosenberg et al. (1982).

2 MINERAL CHEMISTRY

A Jeol JXA-8200 electron microprobe analyser (EPMA) at the Centre of Microscopy and Nanotechnology of the University of Oulu, in wavelength dispersive X-ray spectrometer mode, was used to determine mineral compositions from thin sections. The acceleration voltage was 15 kV and the current of the electron beam 15 nA. The diameter of the beam was normally 10 µm, and 5 µm when analysing the finest grained minerals. Oxide minerals were analysed for the following components: SiO_2, TiO_2, Al_2O_3, Cr_2O_3, Fe_2O_3, MgO, CaO, MnO, FeO, Na_2O, K_2O, BaO, PbO and ZnO. Sulphide minerals were analysed for Se, S, Co, As, Cd, Ni, Pb, Fe, Cu, Ag, Zn, Bi, Sb, Ti, V, Mn and Hg. Excel spreadsheets of AGTSoft and GabbroSoft© were utilised in processing the analytical data.

3 U–PB GEOCHRONOLOGY

3.1 Sample preparation

Samples weighting 5–20 kg were washed, crushed, washed using a Wilfley table, and treated with methylene iodide and Clerici® solutions for the separation of the heavy minerals. Non-magnetic heavy fractions were separated using a Frantz isodynamic separator, and zircons were finally selected by hand-picking for analyses. The grains were mounted in epoxy resin and sectioned approximately in half and polished. Back-scattered electron images (BSE) and/or cathodoluminescence (CL) images were prepared for the zircons to select the spot analysis sites. For certain samples, U–Pb dating was carried out *in situ* from thin sections. For these analyses, the samples were initially scanned using a secondary electron microscope (SEM) to locate the zircons and monazites.

3.2 TIMS

The decomposition of minerals and extraction of U and Pb for multigrain TIMS (thermal ionisation decoupled multicollector mass spectrometer) analyses followed the procedure described by Krogh (1973, 1982). Before analysis, zircons were treated using the chemical abrasion (CA) method of Mattinson (2005). ^{235}U–^{208}Pb-spiked and unspiked isotopic ratios were measured using GTK's VG Sector 54 TIMS in Espoo. The measured lead and uranium isotopic ratios were normalized to the accepted values of SRM 981 and U500 standards. Common lead corrections were carried out using the age-related Pb isotope composition of the model of Stacey and Kramers (1975) and errors of 0.2 (for $^{206}Pb/^{204}Pb$ and $^{208}Pb/^{204}Pb$) and 0.1 ($^{207}Pb/^{204}Pb$). The U–Pb age calculations were performed using the PbDat program (Ludwig 1991) and the fitting of the discordia line using the Isoplot/Ex program (Ludwig 2003).

3.3 Nu Plasma HR multicollector ICPMS

U–Pb dating analyses were performed using a Nu Plasma HR multicollector ICPMS at the Geological Survey of Finland in Espoo. The technique was very similar to that of Rosa et al. (2009), except that a Photon Machine Analyte G2 laser microprobe was used. Samples were ablated in He gas (gas flows = 0.4 and 0.1 l/min) within a HelEx ablation cell (Müller et al. 2009). The He aerosol was mixed with Ar (gas flow = 0.8 l/min) prior to entry into the plasma. The gas mixture was optimized daily for maximum sensitivity. All analyses were carried out in static ablation mode. Normal ablation conditions were: beam diameter 20 µm, pulse frequency 5 Hz and beam energy density 0.55 J/cm^2. A single U–Pb measurement included 30 s of on-mass background measurement, followed by 60 s of ablation with a stationary beam. Masses 204, 206 and 207 were measured in secondary electron multipliers, and 238 in an extra high mass Faraday collector. The geometry of the collector block does not allow simultaneous measurement of ^{208}Pb and ^{232}Th. Ion counts were converted and reported as volts by the Nu Plasma time-resolved analysis software. ^{235}U was calculated from the signal at mass 238 using a natural $^{238}U/^{235}U = 137.88$. Mass number 204 was used as a monitor for common ^{204}Pb. In ICPMS analysis, ^{204}Hg mainly originates from the He supply. The observed background counting rate on mass 204 was ca. 1200 (ca. 1.3×10^{-5} V) and had been stable at that level over the year before the analysis reported here. The contribution of ^{204}Hg from the plasma was eliminated by on-mass background measurement prior to each analysis. Age-related common lead (Stacey & Kramers 1975) correction was used when the analysis showed common lead contents above the detection limit. Signal strengths on mass 206 were typically $>10^{-3}$ V, depending on the uranium content and age of the zircon. Two calibration standards were run in duplicate at the beginning and end of each analytical session, and at regular intervals during the sessions. Raw data were corrected for the background, laser-induced elemental fractionation, mass discrimination and drift in ion counter gains and reduced to U–Pb isotope ratios by calibration to concordant reference zircons of known age, using protocols adapted from Andersen et al. (2004) and Jackson et al. (2004).

Standard zircons GJ-01 (609 ± 1 Ma; Belousova et al. 2006) and an in-house standard A1772 (2712 ± 1 Ma; Huhma et al. 2012) were used for calibration. The

calculations were performed off-line using an interactive spreadsheet program written in Microsoft Excel/VBA by T. Andersen (Rosa et al. 2009). To minimize the effects of laser-induced elemental fractionation, the depth-to-diameter ratio of the ablation pit was kept low, and isotopically homogeneous segments of the time-resolved traces were calibrated against the corresponding time interval for each mass in the reference zircon. To compensate for drift in instrument sensitivity and Faraday vs. electron multiplier gain during an analytical session, a correlation of signal vs. time was assumed for the reference zircons. The algorithms used are described in Rosa et al. (2009). The concordant age offset from ID-TIMS ages for several samples including zircon 91500 (1066 Ma) and A382 (1877 ± 2 Ma; Patchett & Kouvo 1986, Huhma et al. 2012) does not exceed 0.5%.

3.4 Nu Plasma AttoM single collector ICPMS

U–Pb dating analyses were performed using a Nu Plasma AttoM single collector ICPMS at the Geological Survey of Finland in Espoo connected to a Photon Machine Excite laser ablation system. Samples were ablated in He gas (gas flows = 0.4 and 0.1 l/min) within a HelEx ablation cell (Müller et al. 2009). The He aerosol was mixed with Ar (gas flow = 0.8 l/min) prior to entry into the plasma. The gas mixture was optimized daily for maximum sensitivity. Typical ablation conditions were: beam diameter 25 µm, pulse frequency 5 Hz and beam energy density 2 J/cm^2. A single U–Pb measurement included a short pre-ablation, 10 s of on-mass background measurement, followed by 30 s of ablation with a stationary beam. 235U was calculated from the signal at mass 238 using a natural 238U/235U = 137.88. Mass number 204 was used as a monitor for common 204Pb. In ICPMS analysis, 204Hg mainly originates from the He supply. The observed background counting rate on mass 204 was 150–200 cps and had been stable at that level over the previous two years. The contribution of 204Hg from the plasma was eliminated by on-mass background measurement prior to each analysis. Age-related common lead (Stacey & Kramers 1975) correction was used when the analysis showed common lead contents significantly above the detection limit (i.e., >50 cps). Signal strengths on mass 206 were typically 100 000 cps, depending on the uranium content and age of the zircon.

Calibration standard GJ-1 (609 ± 1 Ma; Belousova et al. 2006) or in-house standard A382 (1877±2 Ma; Huhma et al. 2012) was run at the beginning and end of each analytical session, and at regular intervals during the sessions. Raw data were corrected for the background, laser-induced elemental fractionation, mass discrimination and drift in ion counter gains and reduced to U–Pb isotope ratios by calibration to concordant reference zircons, using the program Glitter (Van Achterbergh et al. 2001). Further data reduction, including common lead correction and error propagation, was performed using an Excel spreadsheet written by Y. Lahaye and H. O'Brien. Errors include measured within-run errors (SD) and quadratic addition of reproducibility of the standard (SE). To minimize the effects of laser-induced elemental fractionation, the depth-to-diameter ratio of the ablation pit was kept low, and isotopically homogeneous segments of the time-resolved traces were calibrated against the corresponding time interval for each mass in the reference zircon. The concordant age offset from ID-TIMS ages for several samples, including zircon 91500 (1066 Ma) and A382 (1877 ± 2 Ma; Patchett & Kouvo 1986, Huhma et al. 2012), did not exceed 0.5%.

3.5 Nordic Cameca IMS 1270 secondary ion mass spectrometer (SIMS)

Single-grain analyses of zircons were performed with a Nordic Cameca IMS 1270 secondary ion mass spectrometer (SIMS) at the Swedish Museum of Natural History in Stockholm (NORDSIM facility). The spot diameter of the primary O_2^- beam was 20 µm. The instrument was operated in monocollection peak-hopping mode using an ion-counting electron multiplier detector. Pb, Th and U isotopes from each spot were measured for 12 cycles following automated centring, mass calibration and adjustment of energy offset. Pb/U ratios were calibrated against regularly interspersed analyses of the 1065 Ma Geostandards zircon 91500 (Wiedenbeck et al. 1995). Correction for modern common lead was carried out using the isotope composition model of Stacey and Kramers (1975) assuming modern

surface contamination. The detailed analytical procedures are essentially the same as those described by Whitehouse et al. (1999) and Whitehouse & Kamber (2005).

3.6 Data plotting

Plotting of the U–Pb isotopic data and age calculations were performed using the Isoplot/Ex program version 4.15 (Ludwig 2003). All the ages were calculated with 2σ errors and without decay constants errors. Data-point error ellipses in the figures are at the 2σ level.

REFERENCES

Andersen, T., Griffin, W. L., Jackson, S. E., Knudsen, T.-L. & Pearson, N. J. 2004. Mid-Proterozoic magmatic arc evolution at the southwest margin of the Baltic Shield. Lithos 73, 289–318.

Belousova, E. A., Griffin, W. L. & O'Reilly, S. Y. 2006. Zircon crystal morphology, trace element signatures and Hf isotope composition as a tool for petrogenetic modeling: examples from Eastern Australian granitoids. Journal of Petrology 47, 329–353.

Huhma, H., Mänttäri, I., Peltonen, P., Kontinen, A., Halkoaho, T., Hanski, E., Hokkanen, T., Hölttä, P., Juopperi, H., Konnunaho, J., Layahe, Y., Luukkonen. E., Pietikäinen. K., Pulkkinen, A., Sorjonen-Ward, P., Vaasjoki, M. & Whitehouse, M. 2012. The age of the Archaean greenstone belts in Finland. In: Hölttä, P. (ed.) The Archaean of the Karelia Province in Finland. Geological Survey of Finland, Special Paper 54, 74-175. Available at: http://tupa.gtk.fi/julkaisu/specialpaper/sp_054.pdf

Jackson, S. E., Pearson, N. J., Griffin, W. L. & Belousova, E. A. 2004. The application of laser ablation-inductively coupled plasma-mass spectrometry to in-situ U–Pb zircon geochronology. Chemical Geology 211, 47–69.

Krogh, T. 1973. A low-contamination method for hydrothermal decomposition of zircon and extraction of U and Pb for isotopic age determinations. Geochimica et Cosmochimica Acta 37, 485–494.

Krogh, T. E. 1982. Improved accuracy of U-Pb zircon ages by the creation of more concordant systems using an air abrasion technique. Geochimica et Cosmochimica Acta 46, 637–649.

Ludwig, K. R. 1991. PbDat 1.21 for MS-dos: A computer program for IBM-PC Compatibles for processing raw Pb-U-Th isotope data. Version 1.07. U.S. Geological Survey, Open File Report 88–542. 35 p.

Ludwig, K. R. 2003. User's manual for Isoplot/Ex, Version 3.00. A geochronological toolkit for Microsoft Excel. Berkeley Geochronology Center Special Publication No.4.

Mattinson, J. M. 2005. Zircon U-Pb chemical abrasion ("CA-TIMS") method: Combined annealing and multi-step partial dissolution analysis for improved precision and accuracy of zircon ages. Chemical Geology 220, 47–66.

Müller, W., Shelley, M., Miller, P. & Broude, S. 2009. Initial performance metrics of a new custom-designed ArF excimer LA-ICPMS system coupled to a two-volume laser-ablation cell. Journal of Analytical Atomic Spectrometry 24, 209–214.

Patchett, J. & Kouvo, O. 1986. Origin of continental crust of 1.9-1.7 Ga age: Nd isotopes and U-Pb zircon ages in the Svecokarelian terrain of south Finland. Contributions to Mineralogy and Petrology 92, 1-12.

Rasilainen, K., Lahtinen, R. & Bornhorst, T. J. 2007. The Rock Geochemical Database of Finland Manual. Geological Survey of Finland, Report of Investigation 164. 38 p. Available at: http://tupa.gtk.fi/julkaisu/tutkimusraportti/tr_164.pdf

Rosa, D. R. N., Finch, A. A., Andersen, T. & Inverno, C. M. C. 2009. U-Pb geochronology and Hf isotope ratios of magmatic zircons from the Iberian pyrite belt. Mineralogy and Petrology 95, 47–69.

Rosenberg, R. J., Kaistila, M. & Zilliacus, R. 1982. Instrumental epithermal neutron activation analysis of solid geochemical samples. Journal of Radioanalytical Chemistry 71, 419–428.

Sircombe, K. N. 2004. AgeDisplay: an excel workbook to evaluate and display univariante geochronological data using binned frequency histograms and probability density distributions. Chemical. Geology 30, 21–31.

Slama, J., Košler, J., Condon, D. J., Crowley, J. L., Gerdes, A., Hanchar, J. M., Horstwood, M. S. A., Morris, G. A., Nasdala, L., Norberg, N., Schaltegger, U., Schoene, B., Tubrett, M. N. & Whitehouse, M. J. 2007. Plesovice zircon – a new natural reference material for U-Pb and Hf isotopic microanalysis. Chemical Geology, 249, 1–35.

Stacey, J. S. & Kramers, J. D. 1975. Approximation of terrestrial lead isotope evolution by a two-stage model. Earth and Planetary Science Letters 26, 207–221.

Van Achterbergh, E., Ryan C., Jackson, S. & Griffin W. 2001. Data reduction software for LA-ICP-MS. In: Sylvester, P. (ed.) Laser-Ablation ICPMS in the Earth Sciences – Principles and applications. Mineralogical Association of Canada short course series 29, 239–243.

Whitehouse, M. J. & Kamber, B. S. 2005. Assigning dates on thin gneissic veins in high-grade metamorphic terranes; a cautionary tale from Akilia, southwest Greenland. Journal of Petrology 46, 291–318.

Whitehouse, M. J., Kamber, B. S. & Moorbath, S. 1999. Age significance of U-Th-Pb zircon data from early Archaean rocks of West Greenland; a reassessment based on combined ion-microprobe and imaging studies. Chemical Geology 160, 201–224.

Wiedenbeck, M., Alle P., Corfu, F., Griffin, W. L., Meier, M., Oberli, F., Von Quadt, A., Roddick, J. C. & Spiegel, W. 1995. Three natural zircon standards for U-Th-Pb, Lu-Hf, trace element and REE analyses. Geostandards Newsletter 19, 1–23

All GTK's publications online at hakku.gtk.fi

The eleven papers forming this volume of the Bulletin of the Geological Survey of Finland summarize the results of the Central Finland ore potential estimation project. The articles are based on extensive field work and analytical data obtained from samples collected during it. The individual papers vary from target-scale studies of different types of mineralisations to summaries of different rock associations and a synthesis of the new data with earlier interpretations.

With this publication, the basic geological understanding of the area is updated to a level allowing reliable ore potential estimation and the identification of problems for further scientific studies. The work presented also provides keys to improved understanding of the development of the whole Svecofennian domain.

gtk.fi

ISBN 978-952-217-397-3 (pdf)
ISSN 0367-522X (print)
ISSN 2489-639X (online)